GEOLOGICAL SURVEY OF CANADA
COMMISSION GÉOLOGIQUE DU CANADA



# Current Research 1999-C
# Recherches en cours 1999-C

# CANADIAN SHIELD
# BOUCLIER CANADIEN

Natural Resources Canada
Ressources naturelles Canada

## NOTICE TO LIBRARIANS AND INDEXERS

The Geological Survey's Current Research series contains many reports comparable in scope and subject matter to those appearing in scientific journals and other serials. Most contributions to Current Research include an abstract and bibliographic citation. It is hoped that these will assist you in cataloguing and indexing these reports and that this will result in a still wider dissemination of the results of the Geological Survey's research activities.

## AVIS AUX BIBLIOTHÉCAIRES ET PRÉPARATEURS D'INDEX

La série Recherches en cours de la Commission géologique contient plusieurs rapports dont la portée et la nature sont comparables à celles des rapports qui paraissent dans les revues scientifiques et autres périodiques. La plupart des articles publiés dans Recherches en cours sont accompagnés d'un résumé et d'une bibliographie, ce qui vous permettra, on l'espère, de cataloguer et d'indexer ces rapports, d'où une meilleure diffusion des résultats de recherche de la Commission géologique.

GEOLOGICAL SURVEY OF CANADA
COMMISSION GÉOLOGIQUE DU CANADA

# CURRENT RESEARCH 1999-C

# CANADIAN SHIELD

---

# RECHERCHES EN COURS 1999-C

# BOUCLIER CANADIEN

**1999**

Catalogue No. M44-1999/3
ISBN 0-660-17695-5

Available in Canada from
Geological Survey of Canada offices:

601 Booth Street
Ottawa, Ontario K1A 0E8

3303-33rd Street N.W.
Calgary, Alberta T2L 2A7

101-605 Robson Street
Vancouver, B.C. V6B 5J3

or from

Canadian Government Publishing
Public Works and Government Services Canada
Ottawa, Ontario K1A 0S9

A deposit copy of this publication is also available for reference
in selected public libraries across Canada

Price subject to change without notice

**Cover illustration**

Cognate lonestone interpreted as a volcanic ejecta fragment in coarse pebbly sandstone of the ca. 1.83 Ga Christopher Island Formation, eastern Baker Lake basin, Northwest Territories (Nunavut). *See* paper by Rainbird et al., this volume. Photograph by R. Rainbird. GSC 1998-070

**Photo en page couverture**

Caillou délesté de provenance locale qui serait un fragment d'éjecta volcanique dans du grès caillouteux à grain grossier de la Formation de Christopher Island (environ 1,83 Ga), dans l'est du bassin de Baker Lake, Territoires du Nord-Ouest (Nunavut). Voir l'article de Rainbird et al. dans le présent volume. Photo : R. Rainbird. GSC 1998-070

## Separates

A limited number of separates of the papers that appear in this volume are available by direct request to the individual authors. The addresses of the Geological Survey of Canada offices follow:


Geological Survey of Canada
601 Booth Street
Ottawa, Ontario
K1A 0E8
(FAX: 613-996-9990)

Geological Survey of Canada (Calgary)
3303-33rd Street N.W.
Calgary, Alberta
T2L 2A7
(FAX: 403-292-5377)

Geological Survey of Canada (Pacific)
101-605 Robson Street
Vancouver, British Columbia
V6B 5J3
(FAX: 604-666-1124)

Geological Survey of Canada (Pacific)
P.O. Box 6000
9860 Saanich Road
Sidney, British Columbia
V8L 4B2
(FAX: 604-363-6565)

Geological Survey of Canada (Atlantic)
Bedford Institute of Oceanography
P.O. Box 1006
Dartmouth, Nova Scotia
B2Y 4A2
(FAX: 902-426-2256)

Geological Survey of Canada (Quebec)
2535, boulevard Laurier
C.P. 7500
Sainte-Foy (Québec)
G1V 4C7
(FAX: 418-654-2615)


## Tirés à part

On peut obtenir un nombre limité de «tirés à part» des articles qui paraissent dans cette publication en s'adressant directement à chaque auteur. Les adresses des différents bureaux de la Commission géologique du Canada sont les suivantes :


Commission géologique du Canada
601, rue Booth
Ottawa (Ontario)
K1A 0E8
(Télécopieur : 613-996-9990)

Commission géologique du Canada (Calgary)
3303-33rd Street N.W.,
Calgary, Alberta
T2L 2A7
(Télécopieur : 403-292-5377)

Commission géologique du Canada (Pacifique)
101-605 Robson Street
Vancouver, British Columbia
V6B 5J3
(Télécopieur : 604-666-1124)

Commission géologique du Canada (Pacifique)
P.O. Box 6000
9860 Saanich Road
Sidney, British Columbia
V8L 4B2
(Télécopieur : 604-363-6565)

Commission géologique du Canada (Atlantique)
Institut océanographique Bedford
P.O. Box 1006
Dartmouth, Nova Scotia
B2Y 4A2
(Télécopieur : 902-426-2256)

Commission géologique du Canada (Québec)
2535, boulevard Laurier
C.P. 7500
Sainte-Foy (Québec)
G1V 4C7
(Télécopieur : 418-654-2615)

# CONTENTS

# Glacial dispersal patterns and postglacial marine overlap in the Longstaff Bluff area, central Baffin Island[1]

L.A. Dredge
Terrain Sciences Division, Ottawa

*Dredge, L.A., 1999: Glacial dispersal patterns and postglacial marine overlap in the Longstaff Bluff area, central Baffin Island;* in *Current Research 1999-C; Geological Survey of Canada, p. 1–8.*

**Abstract:** The Quaternary geology component of the Central Baffin Project was part of a program designed to provide information for resource development. This report provides a summary of surface materials and glacial history in four areas: Longstaff Bluff, Rushmore Bay, Astarte River, and Flint Lake. The results of this study affect the interpretation of geochemical data derived from lake sediment sampling and till sampling. Ice-flow indicators establish that materials have been transported south and west of their source areas by glaciers. Glacial materials below an elevation of 100 m have been admixed with, or overlain by, postglacial marine sediments. Some postglacial weathering of sulphide minerals in till and bedrock has occurred. Marble-derived carbonate in till in some areas may act as a buffer to limit sulphide leaching, and may explain some geochemical anomalies.

**Résumé :** Le volet «géologie du Quaternaire» du projet du centre de l'île de Baffin fait partie d'un programme visant à fournir des renseignements en vue de la mise en valeur des ressources. Le présent rapport décrit brièvement les sédiments superficiels et l'histoire glaciaire de quatre régions : la falaise Longstaff, la baie Rushmore, la rivière Astarte et le lac Flint. Les résultats de l'étude influe sur l'interprétation des données géochimiques provenant de l'échantillonnage des sédiments lacustres et du till. Les marques d'écoulement glaciaire indiquent que des glaciers ont transporté les sédiments vers le sud et l'ouest depuis leurs sources. Les débris glaciaires rencontrées à une altitude inférieure à 100 m sont recouverts de sédiments marins postglaciaires ou y sont mélangés. Il y a eu une certaine altération postglaciaire de minéraux sulfurés dans le till et le substratum rocheux. À certains endroits, des carbonates dérivés du marbre et rencontrés dans du till pourraient agir de tampon et limiter le lessivage des sulfures, ce qui expliquerait certaines anomalies géochimiques.

[1] Contribution to the 1998-1999 Central Baffin Partnership Project

## INTRODUCTION

The Quaternary geology component of the Central Baffin Project was part of a program designed to provide information for resource development (A. Rencz, unpub. report, 1998). The study area lies in the central part of Baffin Island near Foxe Basin, in the vicinity of Longstaff Bluff (Fig. 1). Within this region, four smaller areas were chosen for detailed ground traverses (Fig. 2): A) Longstaff Bluff, B) Rushmore Bay, C) Astarte River, and D) Flint Lake. These areas contained sites that had previously been identified as having elevated concentrations of sulphide minerals in lake sediments (Hornbrook and Lynch, 1979; Coker et al., 1981). Fieldwork for the Quaternary geology component focused on studying the surface materials in these four areas, determining glacial history, collecting till samples spaced 100–500 m apart for geochemical comparison with vegetation and lake sediment samples, and comparing ground observations with remotely sensed images. This report provides a summary of surface materials, and those aspects of glacial history which affect the interpretation of geochemical data. It focuses on ice-flow indicators and glacial events, and on the extent and effect of the postglacial marine transgression. The results of goechemical analysis of glacial materials will be dealt with in a separate report, as will the broader ramifications of the ice-flow history presented here, and the testing of satellite imagery.

## LOCATION, TOPOGRAPHY, AND SURFACE MATERIALS

The areas investigated lie on the northeastern side of Foxe Basin and extend from the coast inland for a distance of about 50 km. The main materials are bedrock outcrop, till, and raised marine sediments (Fig. 3). Quaternary deposits cover about half the area. A gentle escarpment that overlooks the coastal lowlands, and the cliffed sides of the Flint Lake valley, are major topographic features more than 100 m high. Elsewhere, relief is more subdued. Local relief is 5–10 m on till plains containing small rock outcrops, and in areas of uniformly bedded outcrops, and less than 5 m on coastal lowlands. Relief of 25–50 m is common where there has been differential erosion of folded rocks, resulting in cliff faces and ridge and valley topographies.

Paleozoic dolomite and limestone form the lowlands of Baird Peninsula to the west of the study area, but the study area itself lies within Archean granitic gneiss, together with Proterozoic metasedimentary rocks of the Piling Group (Morgan, 1981; Scott et al., 1997). The Piling Group consists mainly of greywacke-derived schist of the Longstaff Bluff Formation, as well as less extensive rusty sulphide-bearing schist of the Astarte River Formation, and bands of marble and quartzite of the Flint Lake and Dewar Lake formations respectively. These rocks have been complexly folded. Quartzite, feldspar pegmatite, and granitic bodies, additional to these formations, were noted during foot traverses. Rock outcrop is exposed over about half of the area investigated.

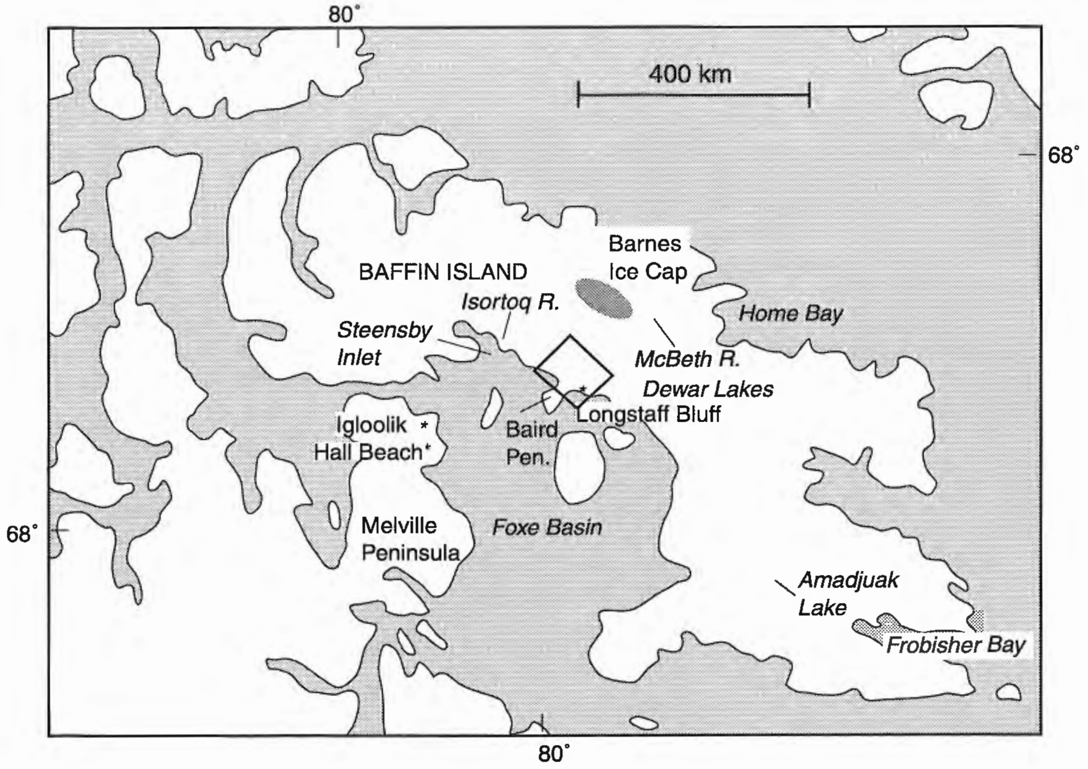


*Figure 1. Regional setting or the study area.*

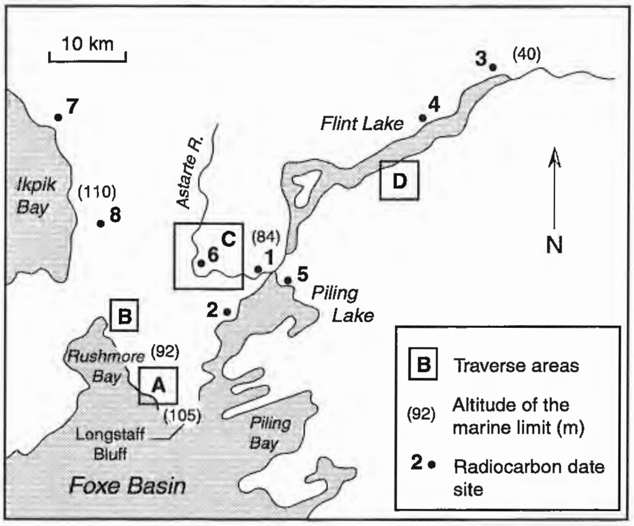


***Figure 2.*** *Map of the study area and traverse areas discussed in the paper.*

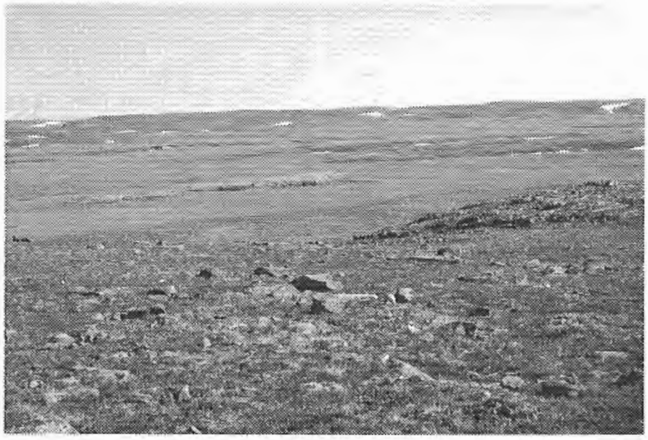

***Figure 3.*** *Upland till plains, and marine deposits in lowlands. Foreground shows gneissic rock knobs; middle ground has marble outcrops, and hills in the background are composed of the Longstaff Bluff schist.*

***Figure 4.*** *Flights of raised beaches at Longstaff Bluff consist of cobbles and boulders. Rock outcrop is greywacke-schist.*

Quaternary deposits consist of glacial and postglacial sediments. Till veneers are less than 1 m thick and contain small rock outcrops. The surface of the terrain in areas of till veneer mimics the structure of the bedrock, producing a prominent linear grain in areas underlain by rocks of the Piling Group. The till veneers are derived principally from nearby rocks, and tend to be bouldery or rubbly. Till blankets, less prevalent in the areas investigated, are 1–5 m thick, and form rolling till plains. The till blankets consist principally of material comminuted from the Longstaff Bluff schist, and hence tend to consist of small abraded pebbles and subangular cobbles in a silty, micaceous, fine sand matrix. Tills derived principally from the schistose rocks in this area are yellow-brown (10YR 4/4), while those derived primarily from marble tend to be olive-grey (5Y 3/2). Marble-derived tills react weakly with hydrochloric acid after they have been dried. Carbonate contents in the marble-derived till from Central Baffin Island were about 9%, as determined by the Leco method. All carbonate determinations were systematically about 4% lower when determined by the Chittick method (Terrain Sciences Division, unpub. lab report, 1998).

A large, flat-surfaced kame delta with ice block depressions lies between Longstaff Bluff and the Rushmore Bay study areas, at an elevation of about 100 m. Beach ridges flank the north and south sides of the feature, but are absent on the eastern side, which is an ice-contact face. Raised deltas of much more limited extent than the kame delta are common along the sides of the Flint Lake valley. These features form coalescing sand pads and terraces at the mouths of streams that emptied into the regressing postglacial sea.

Postglacial marine deposits form plains that consist of sand, underlain by fossiliferous silty sand and clay in the vicinity of Piling Lake and Astarte River. Ice-wedge polygons are prevalent in this type of terrain west of Piling Lake. Flights of raised beaches, consisting of rounded boulder and cobble gravel, ascend from sea level to an elevation of about 100–105 m along the escarpment that forms the contact between Paleozoic and Precambrian rocks (Fig. 4). Most of the boulders are derived from nearby granite or greywacke schist outcrop, but limestone clasts are present below an elevation of 30 m. At higher elevations, the flights of beaches are more steeply sloped, and individual ridges are more closely spaced, than those near present sea level. A zone of bare, wave-washed rock commonly separates the marine deposits from the till blankets, and marks the maximum altitudinal extent of the postglacial sea. Low plains of washed till and rock, interspersed by patches of fine-grained marine sediment lie southeast of Piling Lake; broadly spaced beach ridges extend inland for distances of up to 30 km.

## ICE-FLOW INDICATORS

The main indicators of ice flow in the study area are large ice-scoured crags with either rock or till tails, small erosional bedrock forms such as roches moutonées, and striations. While the orientation of glacial landforms provides azimuths for ice flow, the directional sense of the flow can be determined by crag-and-tail relationships, and ice-plucked forms. The composition of the till can also be used to determine provenance where distinctive rock types have been crossed: in this area, the presence of Paleozoic carbonate clasts in till can be used to infer an ice flow from Foxe Basin.

The relative age of ice flow events has been determined by crossed striations in some places, and by striation sets on sequentially created glacial facets on small outcrops. Because none of the facets are more weathered than others, it is assumed that they all belong to the same glaciation.

### *Longstaff Bluff*

In the Longstaff Bluff area (Fig. 2) most rocks have been glacially polished. Striae are abundant on low rock outcrops of the Longstaff Bluff Formation, both above and below the limit of postglacial marine submergence. Most have azimuths that vary between 220° and 230°. An abundance of small roche moutonée forms indicates that glacial flow was towards the southeast. Till in the area reflects the composition of underlying rocks, and consists of silty sand material, together with numerous greywacke schist clasts. Limestone cobbles are present in the till, but constitute less than 1% of the clasts, and less than 3% of the matrix (Leco method). Sim (1964) also reported limestone clasts in till near the coast in this vicinity, and till with carbonate contents of up to 1.7% of the matrix weight (Chittick method) (Andrews and Sim, 1964). By contrast, Andrews and Sim found that the carbonate content of sediments below marine limit along Piling Bay to be up to 26%, although typical values were less than 2%.

The ice contact kame-outwash delta lying north of Longstaff Bluff has esker segments aligned towards the southwest. The orientation of the esker segments and the ice contact face suggests that, at the time of deglaciation, the hydraulic gradient in the ice sheet, which generally trends parallel to ice flow, was towards 230°.

### *Rushmore Bay*

Directly inland from Rushmore Bay (Fig. 2), a few large, streamlined rock bosses appear to have been glacially abraded on their southern sides, and taper gently towards the north, suggesting ice movement inland from a source in Foxe Basin. Most other outcrops of similar size, however, appear to be oriented in the opposite direction, and some have till tails on their south sides. A small percentage of the striations measured are oriented to 180°–190°, or its reciprocal 000°–010°. Small dispersal trains from a rusty outcrop near the coast indicate southward transport of glacial material, which suggests that the north-south-oriented striations record a southerly ice flow. Small streamlined rock forms with plucked faces, as well as sets of striae on many surfaces, indicate a major ice flow towards 270°, and less commonly, towards 225–235°. Where there are crossing striae, the west- and southwest-trending features postdate the north-south features. Similarly, striated, glacially faceted outcrops have south-trending striae preserved only on sufaces that would have been on the sheltered lee side of the 270° ice flow; therefore, they predate the westward flow.

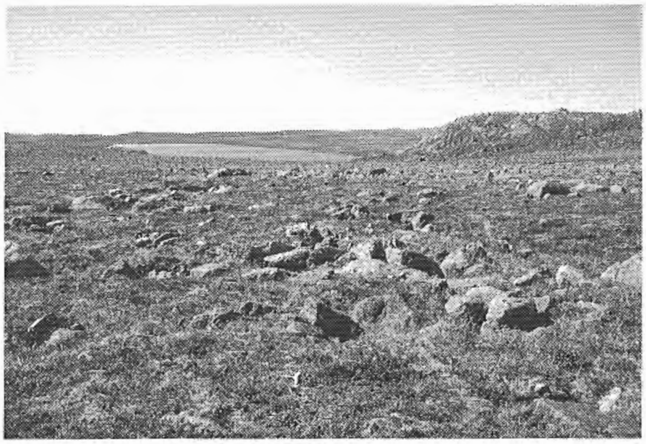

***Figure 5.*** *Till veneer and rock outcrop, Rushmore Bay traverse. Boulders of granite, gneiss, marble, and schist are common. Bedrock at the site of the photograph is schist.*

This area is underlain by marble, schist of the Longstaff Bluff Formation, gneiss, and granite, and is crossed by diabase dykes. Unmapped feldspar pegmatite intrusions are also common. Till cover tends to be thin and bouldery (Fig. 5). Subangular gneissic and schist boulders are prevalent; marble and small dyke clasts are also common at some sites. The till matrix is a stony, gritty, silty sand. No limestone clasts were seen, despite the proximity of extensive limestone bedrock on Baird Peninsula to the south and west. However, the tills reacted to hydrochloric acid at several sites. Laboratory analyses (Leco method) show that carbonates constitute between 3% and 7% of the till matrix. Because there are no limestone clasts, the carbonate is thought to be derived from the underlying marble formations and from the dyke rocks, both of which react to hydrochloric acid.

### *Astarte River*

Two traverses cross the Astarte River area (Fig. 2). The northerly traverse lies entirely within the Longstaff Bluff Formation, while the southerly traverse crosses granite gneiss upland terrain, with marble and schist outcropping in lowland areas. The till ranges from a boulder veneer, which generally reflects the lithology of the underlying schist, to rolling till plains (Fig. 6) with more clast variation, including white and pink granite from outcrops lying northwest of the area. The carbonate content of the till matrix varies from 3% to 6% (Leco method), but is nonreactive with HCl. The higher carbonate values occurred near sites that were closer to, and down-ice from, marble outcrop. No limestone clasts were seen. Fine-grained marine sediments near Astarte River along the southerly traverse contain 7% carbonate, and have a moderate reaction with HCl, although again, no limestone clasts were observed.

Most outcrops are striated and highly polished. On the northern traverse, striae and small plucked or stossed bedrock forms suggest ice flow towards 260°–270°, parallel to the strike of the schistose rocks. Fine striae on granite bodies indicate an additional later flow oriented 230°–250°. At one

*Figure 6. Rolling till plains on the northern Astarte River traverse.*

*Figure 7. Glacially polished and striated rock surface at Astarte River. Main ice flow is shown by a solid arrow, and earlier ice flow on a protected rock facet is shown by a dashed arrow.*

*Figure 8. Till plains, with marble cliff faces in the background, Flint Lake traverse.*

site, striae and small streamlined forms indicating ice flow towards 290° lie atop a larger rock boss that was created by a major westwards flow. On the southerly traverse, most granite outcrops are highly polished, and are covered with striae and centimentre-scale ice-plucked forms indicating ice flow towards 265°–270°. Fine striae and minute plucked forms are superposed on larger features at a number of sites, and indicate a later flow towards 300°, or less commonly, towards 285° or 105°. At Astarte River several low, highly polished, faceted outcrops have iron- or manganese-stained surfaces. These outcrops have been striated and shaped by ice flowing towards 265°, but striae on lee-side facets indicate an earlier flow that was oriented 335° or 155° (Fig. 7). On some parts of the outcrop a third set of striations records an ice flow towards 190°.

### *Flint Lake*

East of Flint Lake, large-scale rock knobs with till tails up to 500 m long are indicative of ice flow towards the southwest, roughly parallel to the orientation of the lake. Nailhead striae, other striae, and minute plucked forms are oriented 235°–240° on schist outcrops near the lake, and also towards 200° elsewhere. Both orientations correspond to local strikes of the rocks and broad structural trends in the area, and to the orientation of most small roche moutonée forms. Crossing striae and roches moutonées at 220° occur with increasing distance from Flint Lake.

The till is shallow over the highest schistose rocks, where outcrops are prevalent. Till in these higher areas is a rubbly, stony, micaceous silty sand that is dark yellow-brown, a product of comminution of the subjacent schist (Astarte River Formation). Elsewhere the till is more than 5 m thick, is less rubbly, and contains more silt (Fig. 8). In all cases, the predominant clast lithology is schist, although resistant granite boulders are abundant, and sulphide-bearing black pelitic schist, marble, and quartz clasts are also present. No limestone clasts were observed. The marble, schist, and sulphide-bearing pelite form outcrops in the area traversed, as do pegmatitic intrusions; granite bodies and Dewar Lake quartzite bands lie to the east and southeast. Carbonate contents of the till matrix varied from 3% to 9% (Leco method), and were highest in till veneers that overlie marble.

## GLACIAL EVENTS AND ICE-FLOW CENTRES

The presence of well developed till containing comminuted local and more distantly travelled rock types, together with glacial erosion surfaces on bedrock, suggest that warm-based, active ice flowed over the areas traversed. Ice-flow indicators suggest the following sequence of glacial events on central Baffin Island: 1) an early ice flow to the south (180°) preserved on outcrop facets; 2) a main flow to the west (270°); 3) subsequent flow to the southwest (230°); and 4) late, minor local flow to the northwest in the area west of the Flint Lake trough. These flows are indicative of Baffin Island ice sources. Limestone erratics and possible rock drumlins at Longstaff Bluff suggest that ice flow from Foxe Basin

**Table 1.** Radiocarbon dates from Flint Lake area, central Baffin Ialand.

| Site | Elevation (m) | Date (BP) | Lab number | Shell species | Location | Reference |
|---|---|---|---|---|---|---|
| 1 | 3 | 1950 ± 100 | I-1830 | *Mya truncata* | Piling Lake | Andrews and Drapier, 1967 |
| 2 | 9 | 2050 ± 170 | I-489 | shells | Piling Lake | Sim, 1964 |
| 3 | 16 | 3100 ± 150 | GSC-564 | *Mya truncata* | Flint Lake | Andrews and Drapier, 1967 |
| 4 | 19 | 3585 ± 140 | I-2830 | shells | Flint Lake | Andrews and Drapier, 1967 |
| 5 | 3 | 4000 ± 140 | GSC-557 | *Mya truncata* | Piling Lake | Andrews and Drapier, 1967 |
| 6 | 64 | 5570 ± 130 | I-1831 | *Mya truncata* | Astarte River | Andrews and Drapier, 1967 |
| 7 | 73 | 6050 ± 250 | I-405 | *Macoma calcarea* | Ikpik Bay | Sim, 1964 |
| 8 | 89 | 6750 ± 250 | I-406 | *Mya truncata* | Ikpik Bay | Sim, 1964 |

reached the coast but did not penetrate inland. In the scenario presented above, the carbonate in the till matrix at Rushmore Bay, Astarte River, and Flint Lake is attributed to nearby marble outcrop.

Where faceted outcrops indicate multiple ice-flow events, both facets are equally weathered; on granite outcrops, weathering is minimal, and on rusty schist outcrops, both facets have Fe-Mn staining that postdates the imposition of the striae. Therefore, all ice flows are attributed to the same major glaciation — the Foxe Glaciation. The earlier ice flow recorded on small facets is thought to relate to the early Foxe Glaciation (possible Clyde phase of Ives and Andrews, 1963; Ayr Stade of Andrews, 1989). The main westward flow is probably of middle or late Foxe Glaciation age, while the southwest flow is most likely late Foxe Glaciation. The co-orientation of the kame delta with the southwestern striae indicates that the southwest ice flow was active at the time of deglaciation, and that sea level was roughly 100 m above present at the time. The flow thus extends into late glacial time, possibly the Cockburn II phase (ca. 7000 a) of Ives and Andrews (1963). The last flow is thought to relate to local splaying at the front of a recessional ice tongue flowing down the Flint Lake trough. It may correspond to the Isortoq phase of Andrews (1970), in which outlet glaciers flowed in valleys after upland areas were deglaciated.

Most evidence from ice-flow indicators, where the directional sense as well as the azimuth can be determined, points to major ice-flow centres that lay on Baffin Island during the last glaciation. The divide probably followed the central spine of the island, as there is little evidence of active glaciation on the upland surfaces of the eastern highland rim (Ives and Andrews, 1963). The ice-flow sequence affecting central Baffin Island near Foxe Basin suggests an early outflow centre on the plateau northwest of the Barnes Ice Cap. Later, the centre of ice flow shifted to an area southeast of the Barnes Ice Cap, possibly in the headwaters of McBeth River. The last ice flow reflected a shift in the ice divide back towards the present ice cap.

The glacial interpretation presented here differs somewhat from that proposed by Ives and Andrews (1963), Sim (1964), and Andrews and Sim (1964), who suggested that the southwest-northwest oriented rock forms and carbonate in the till were a result of a major ice sheet that was centred in Foxe Basin and that ice flowed outwards across central and southern Baffin Island. It was thought that this ice sheet reached the northeast and east coasts, and covered all but the coastal highlands, which remained as nunataks. This ice flow was thought to have persisted from Early Foxe time until the mid-Holocene (7000 years ago), at which time the ice divide shifted onto Baffin Island. The absence of limestone clasts in till, low quantities of carbonate in the till matrix, and ice abrasion forms on bedrock described in this report, argue instead for a major Baffin Island ice sheet.

## POSTGLACIAL EVENTS

### *Marine limits and postglacial sea-level changes*

The elevations of raised beaches and wave-washed bedrock suggest that, at the time of deglaciation, when Baffin Ice had receded from some unknown maximum position in Foxe Basin, to a position near the present coast, relative sea level stood about 105 m above present (Sim, 1964) at Longstaff Bluff. By the time the ice had receded 2 km inland, to the position of the kame delta, sea level had dropped to about 90 m. When it had reached the inner end of Piling Lake, it had fallen to 85 m, and to 40 m when the ice tongue finally withdrew from the head of Flint Lake, 40 km farther northeast. Radiocarbon dates on marine shells in raised marine and deltaic sediments give a first approximation of the rate and style of postglacial emergence, as shown on Figure 9 and Table 1. Shells from sites 1 and 7 were taken from nearshore sands; their elevations approximate the elevation of the marine sea level when they lived. Shells from other sites were collected from silts that represent deeper water environments; for these, sea level was higher than the elevations of the shells. The shells at site 5 are from deltaic deposits that relate to a sea level that stood about 26 m above present. The oldest shells dated in the area gave an age of 6750±250 BP (GSC-291; I-406; Sim, 1964). These shells were collected from a site near the coast at an elevation of 88 m. Although they are somewhat below the marine limit, their age gives a first approximation for the time of deglaciation, because the initial rate of crustal rebound-emergence is rapid (Fig. 9). Although the rate of emergence has decreased over the last 6700 a, the land continues to rise, and is presently rebounding at a rate of between 30 and 45 cm/century. The time of deglaciation, when sea level was about 100 m higher than present, is similar to that for eastern Melville Peninsula (Dredge, 1995). The rate of present-day rebound is similar to the rate of 45 cm/century determined for western Baffin Island (Ives, 1964) and 30 cm/century in the Kingora River area southwest of Hall

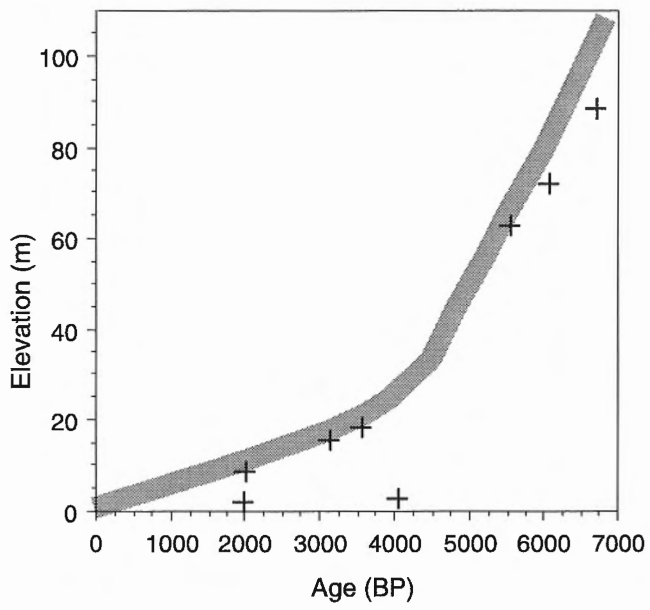


***Figure 9.*** *Sea-level changes, Flint Lake area, based on data from Table 1.*

Beach on Melville Peninsula (Dredge, 1991), but is less than the rate of emergence of 70 cm/century for Hall Beach and Igloolik.

Although Paleozoic limestone boulders and pebbles are present at all sites with marine deposits, they occur in concentrations of much less than 1% at elevations above 30 m, and in concentrations of 1–5% at lower elevations. Their distribution suggests that they have not been derived from the reworking of the till or by early glaciomarine processes involving Foxe Basin-centred glacier ice, but rather, they have been emplaced by rafts of sea ice, carrying debris from Paleozoic outcrops in Foxe Basin, that have been stranded at low tide along gently sloping parts of the coast. Matrix carbonate contents mirror the distibutions of limestone clasts, being greatest in the Piling Lake area (26% (Chittick method); Andrews and Sim, 1964), where slopes are gentlest. Matrix carbonate concentrations are relatively low along the coastal escarpment (<3%; Chittick method), despite the proximity of carbonate source rocks.

### *Postglacial weathering of rock and sediments*

Despite the absence of soil profiles in this Arctic landscape, some weathering of materials has occurred in postglacial time. Glaciated marble outcrops have been roughened by differential weathering of minerals, and fine striae have been weathered off, although larger grooves are still visible. On some surfaces, feldspar crystals now protrude 0.5 cm to 2 cm above the surrounding carbonate groundmass. A dark ferrugenous stain that postdates the creation of striae is another example of postglacial weathering on sulphide-bearing rocks. The vuggy nature of some black schists bearing pyrite, arsenopyrite, and chalcopyrite also suggests that sulphides have been weathered out of some of the rocks. At Flint Lake, bright orange-brown solifluction lobes downslope from these deposits indicate that at least some of the weathering occurred in postglacial time. Low pH values (<4.0) of lake waters in some areas with multi-element anomalies (P. Friske, unpub. data, 1998) further indicate postglacial alteration of sulphides in both till and adjacent rock.

## CONCLUSIONS

Ice-flow indicators from central Baffin Island near the Foxe Basin coast suggest that ice from a centre of outflow in Foxe Basin may have touched the island at Longstaff Bluff, but did not penetrate inland. The timing of this event is uncertain. Most ice-flow features indicate active flow from a divide on the plateau forming the spine of the island, whose outflow centre shifted from a position northwest of the Barnes Ice Cap, then southwest of the cap, and finally to a position on the ice cap itself. Ice from the Baffin Island ice centre extended some unknown distance into Foxe Basin, and subsequently receded to the present coast by about 6800 years ago. During later recessional phases, an ice tongue flowed down the Flint Lake trough. Minor variations in the orientations of striae of up to 15° from regional trends occur from deflection of basal ice along structurally controlled topographic irregularities. These variations are particularly apparent where ice crossed the structural grain of the Longstaff Bluff Formation.

Deglaciation of central Baffin Island began about 6800 years ago. Since then, the land has risen by 100–105 m, at an exponentially decreasing rate, and is continuing to rise at a rate of about 30–45 cm/century. Considerable weathering of sulphide minerals in rock and till has occurred since glaciation.

The results of this study affect the interpretation of geochemical data derived from lake sediment sampling and till sampling. Ice-flow indicators establish that materials have been transported south and west of their source areas by glaciers. Glacial materials below an elevation of 100 m have been admixed with, or overlain by, postglacial marine sediments. Some postglacial weathering of sulphide minerals in till and bedrock has occurred. Marble-derived carbonate in till in some areas may act as a buffer to limit sulphide leaching, and explain some geochemical anomalies.

## ACKNOWLEDGMENTS

Other participants in this integrated project include A. Rencz (party chief), P. Friske, M. McCurdy, S. Day, J. Harris, and H. Iyerak.

## REFERENCES

**Andrews, J.T.**
1970: Differential crustal recovery and glacial chronology, west Baffin Island; Arctic and Alpine Research, v. 2, p. 115–134.
1989: Quaternary geology of the northeastern Canadian Shield; *in* Chapter 3 of Quaternary Geology of Canada and Greenland, (ed.) R.J. Fulton; Geological Survey of Canada, Geology of Canada, no. 1 (*also* Geological Society of America, The Geology of North America, v. K-1), p. 276–302.

**Andrews, J.T. and Drapier, L.**
1967: Radiocarbon dates obtained through Geographical Branch field observations; Geographical Bulletin, v. 9, p. 115–162.

**Andrews, J.T. and Sim, V.W.**
1964: Examination of the carbonate content of drift in the area of Foxe Basin, NWT; Geographical Bulletin, v. 8, p. 174–193.

**Coker, W.B., Ellwood, D.J., and Maurice, Y.T.**
1981: National Geochemical Reconnaissance, Baffin Island, NWT; Geological Survey of Canada, Open File 737.

**Dredge, L.A.**
1991: Raised marine features, radiocarbon dates, and sea level changes, eastern Melville Peninsula, Arctic Canada; Arctic, v 44, p. 63–73.

**Dredge, L.A.** (cont.)
1995: Quaternary geology of northern Melville Peninsula, District of Franklin, NWT; Geological Survey of Canada, Bulletin 484, 114 p.

**Hornbrook, E.H. and Lynch, J.J.**
1979: Geochemical lake sediment and water samples, central Baffin Island, District of Franklin; Geological Survey of Canada, Open File 568, and NGR map 48-1978.

**Ives, J.D.**
1964: Deglaciation and land emergence in northeastern Foxe Basin, NWT; Geographical Bulletin, v. 21, p. 54–65.

**Ives, J.D. and Andrews, J.T.**
1963: Studies in the physical geography of north central Baffin Island. Geographical Bulletin, v 19, p 5–48.

**Morgan, W.C.**
1981: Geology, Lake Gillian, District of Franklin; Geological Survey of Canada, Map 1560A, scale 1:250 000.

**Scott, D.J., St-Onge, M.R., Wodicka, N., and Hanmer, S.**
1997: Geology of the Markham Bay–Crooks Inlet area, southern Baffin Island; *in* Current Research 1997-C; Geological Survey of Canada, p. 157–166.

**Sim, V.W.**
1964: Terrain analysis of west-central Baffin Island; Geographical Bulletin, v. 21, p. 66–92, with map at scale 1:500 000.

Geological Survey of Canada Project 950033-03

# Komatiitic and felsic volcanic rocks overlain by quartzite, Woodburn Lake group, Meadowbank River area, western Churchill Province, Northwest Territories (Nunavut)[1]

E. Zaleski, R. L'Heureux[2], N. Duke[2], L. Wilkinson, and W.J. Davis
Continental Geoscience Division, Ottawa

*Zaleski, E., L'Heureux, R., Duke, N., Wilkinson, L., and Davis, W.J., 1999: Komatiitic and felsic volcanic rocks overlain by quartzite, Woodburn Lake group, Meadowbank River area, western Churchill Province, Northwest Territories (Nunavut);* in *Current Research 1999-C; Geological Survey of Canada, p. 9–18.*

**Abstract:** In an upward-younging stratigraphic succession in the Archean Woodburn Lake group, interbedded spinifex-textured komatiite flows and quartz-eye felsic volcanic rocks are unconformably overlain by basal conglomerate and orthoquartzite. The conglomerate grades upward from polymictic to oligomictic toward the quartzite, and crossbedding in the quartzite youngs away from the unconformable contact. The unconformity is repeated by upright folds, and both the folds and the unconformity are truncated by granite which is involved in a later phase of folding. A more varied package of mafic, intermediate, and felsic volcanic rocks, iron-formation, and minor greywacke structurally overlies the quartzite, in what may also be a stratigraphic relationship. The upper volcanic package also includes ultramafic rocks, but recrystallization to amphibolite-facies assemblages has obliterated primary textures. The relationships suggest that the Woodburn Lake group includes at least two ages of volcanic rocks, and that volcanic rocks stratigraphically underlie and overlie quartzite.

**Résumé :** Dans une succession stratigraphique se rajeunissant vers le haut du groupe archéen de Woodburn Lake, des coulées de komatiite à texture spinifex et des roches volcaniques felsiques à oeil de quartz interstratifiées sont recouvertes en discordance par un conglomérat de base et un orthoquartzite. La nature du conglomérat passe vers le haut de polygénique à oligomictique en direction du quartzite, dans lequel la stratification croisée se rajeunit en s'éloignant du contact discordant. Cette discordance est répétée par des plis droits; ces derniers ainsi que la discordance sont tronqués par du granite qui a subi une phase ultérieure de plissement. Un assemblage plus varié de roches volcaniques mafiques, intermédiaires et felsiques, de formation de fer et de grauwacke en quantités mineures repose structuralement et possiblement stratigraphiquement sur le quartzite. La partie supérieure de l'assemblage volcanique comprend aussi des roches ultramafiques dans lesquelles les textures primaires ont été effacées par suite d'une recristallisation en assemblages du faciès des amphibolites. Les liens portent à croire que le groupe de Woodburn Lake renferme des roches volcaniques d'au moins deux âges différents et que des roches volcaniques sont stratigraphiquement sous-jacentes et sus-jacentes au quartzite.

[1] Contribution to the Western Churchill NATMAP Project
[2] University of Western Ontario, London, Ontario N6A 5B7

## INTRODUCTION

The Woodburn Lake group comprises a deformed sequence of Archean supracrustal rocks in the Rae Province (Western Churchill Province, Fig. 1) north of the regional geophysical anomaly that defines the Snowbird tectonic zone (Hoffman, 1988). The Woodburn Lake group includes several lithological associations typical of Archean cratons, i.e. komatiite-quartzite assemblages, greenstone-type volcanic and sedimentary sequences (Taylor, 1985; Ashton, 1988; Annesley, 1989), and, to the northeast, granulite gneiss units that have been correlated with the supracrustal rocks (Fraser, 1988). Similar Archean assemblages define a discontinuous zone that extends northeasterly for at least 1000 km and includes the Prince Albert group in the Committee Fold Belt (Frisch, 1982; Schau, 1982), and the Mary River group on northern Baffin Island (Bethune and Scammell, 1997). In the Western Churchill Province, interpretation of Archean assemblages is complicated by overprinting of variable intensity during the Paleoproterozoic, and by the presence of Paleoproterozoic supracrustal successions that, in some cases, are difficult to distinguish from Archean successions. The Woodburn Project is focused on the following two principal themes that will contribute to the broader understanding of the geological evolution of the region: 1) the stratigraphy, tectonic setting, petrogenesis, metallogeny, metamorphism, and deformation of the Archean supracrustal rocks of the Woodburn Lake group, and 2) the relationship of the Woodburn Lake group to Paleoproterozoic supracrustal rocks and to the tectonothermal events that affected them. Additional impetus from an economic perspective is provided by the presence of significant gold mineralization hosted by iron-formation at the Cumberland Resources Meadowbank deposits, with a resource base currently estimated at 46.7 t (1.5 million oz., The Northern Miner, v. 24, no. 29, p. 1, 12, September 14–20, 1998).

The Woodburn Project is a part of the Western Churchill NATMAP Project, a collaborative mapping initiative by the Geological Survey of Canada in the Northwest Territories (Nunavut). The Project was initiated in 1996 with 1:50 000 scale mapping (Zaleski et al., 1997a, b), mineral deposit studies (Kjarsgaard et al., 1997, Kerswill et al., 1998), and geochronological studies (Davis and Zaleski, in press) in the area of Pipedream lake and north of Third Portage lake, including the Meadowbank gold deposits (66 H/1, 56 E/4) (Fig. 1). During the 1998 field season, mapping and sampling were extended to the north (NTS 66 H/2, H/7, H/8; 56 E/5) and south (66 A/16, 56 D/13, *see* Zaleski et al., 1999). This paper reports on the preliminary results of fieldwork in the northern map area along the Meadowbank River.

## REGIONAL GEOLOGY

The informal name 'Woodburn Lake group' was originally applied to a sequence of supracrustal rocks (metavolcanic and metasedimentary rocks including iron-formation and quartzite) mapped in the southern Amer Lake map area (NTS 66 H) (Ashton, 1981). To the south, Schau (1983) called the supracrustal rocks in the Whitehills Lake area and to the east (Fig. 1) the 'Ketyet River group', and these rocks have been correlated with and incorporated into the Woodburn Lake group (Schau, 1983; Taylor, 1985; Henderson and Henderson, 1994). Similar supracrustal rocks extend continuously to south of Schultz Lake, and intermittently as inclusions or septa in the dominantly plutonic terrane between Schultz Lake and the Paleoproterozoic Amer group (Tella, 1994). To the east, supracrustal rocks of the Woodburn Lake group form long, northeasterly trending septa extending into the Tehek Lake plutonic complex (Schau, 1983) and toward the granulite terrane northeast of Woodburn Lake (Fraser, 1988).

Definition of the stratigraphic sequence and correlation of lithological units of the Woodburn Lake group have been persistent problems. Quartzite forms a regional marker unit, and much effort has been directed at determining their stratigraphic position(s). Ashton (1988), Fraser (1988) and Annesley (1989) placed quartzite at the top of the sequence, overlying volcanic rocks and interbedded iron-formation. This interpretation was partly based on high abundances of Cr and Ni, and on the presence of fuchsite in the quartzite, which suggested a detrital component derived from mafic or ultramafic rocks. Ashton proposed an unconformity at the base of the quartzite, and interpreted intermittant occurrences of oligomictic conglomerate near the contact as a basal conglomerate. Taylor (1985) interpreted a stratigraphic succession north of Whitehills Lake from greywacke to volcanic rocks (including mafic and komatiitic rocks) and iron-formation, to quartzite overlain by younger volcanic rocks at the top of the sequence (Fig. 1). In contrast, Kjarsgaard et al. (1997) proposed a sequence for the Pipedream and Third Portage lakes area with quartzite at the base, overlain by komatiite and intermediate to felsic volcanic and sedimentary rocks. Zaleski et al. (1997a, b) considered it likely that quartzite lies at the stratigraphic base of the sequence, and proposed that oligomictic conglomerate along quartzite contacts was more consistent with an unconformable surface developed on top of quartzite. This interpretation was supported by the presence of quartz-rich clasts, interpreted as quartzite, in debris-flow deposits in felsic volcanic rocks northeast of Third Portage lake, and by the presence in quartzite of foliated quartz-feldspar porphyry dykes, thought to be possible volcanic feeder dykes. The dykes have since been shown to be 2620+3/-2 Ma, and hence considerably younger than any dated volcanic rocks and coeval with some of the granitic rocks in the area (Davis and Zaleski, in press).

Uranium-lead zircon dating of felsic lapilli tuff north of Third Portage lake identified the youngest rocks known thus far in the Woodburn Lake group (2710+3.5/-2.1 Ma, Davis and Zaleski, in press). The felsic volcanic rocks were interpreted to stratigraphically overlie quartzite, based on sporadic younging indicators, including the presence of possible quartzite clasts (Zaleski et al., 1997a, b; Davis and Zaleski, in press). The detrital zircon population in the quartzite is dominated by ca. 2.96 Ga grains, and the youngest zircon poorly constrains the maximum age of deposition to be at least 2.81 Ga (Davis and Zaleski, in press). To the north near the Meadowbank River, and to the south between Whitehills and

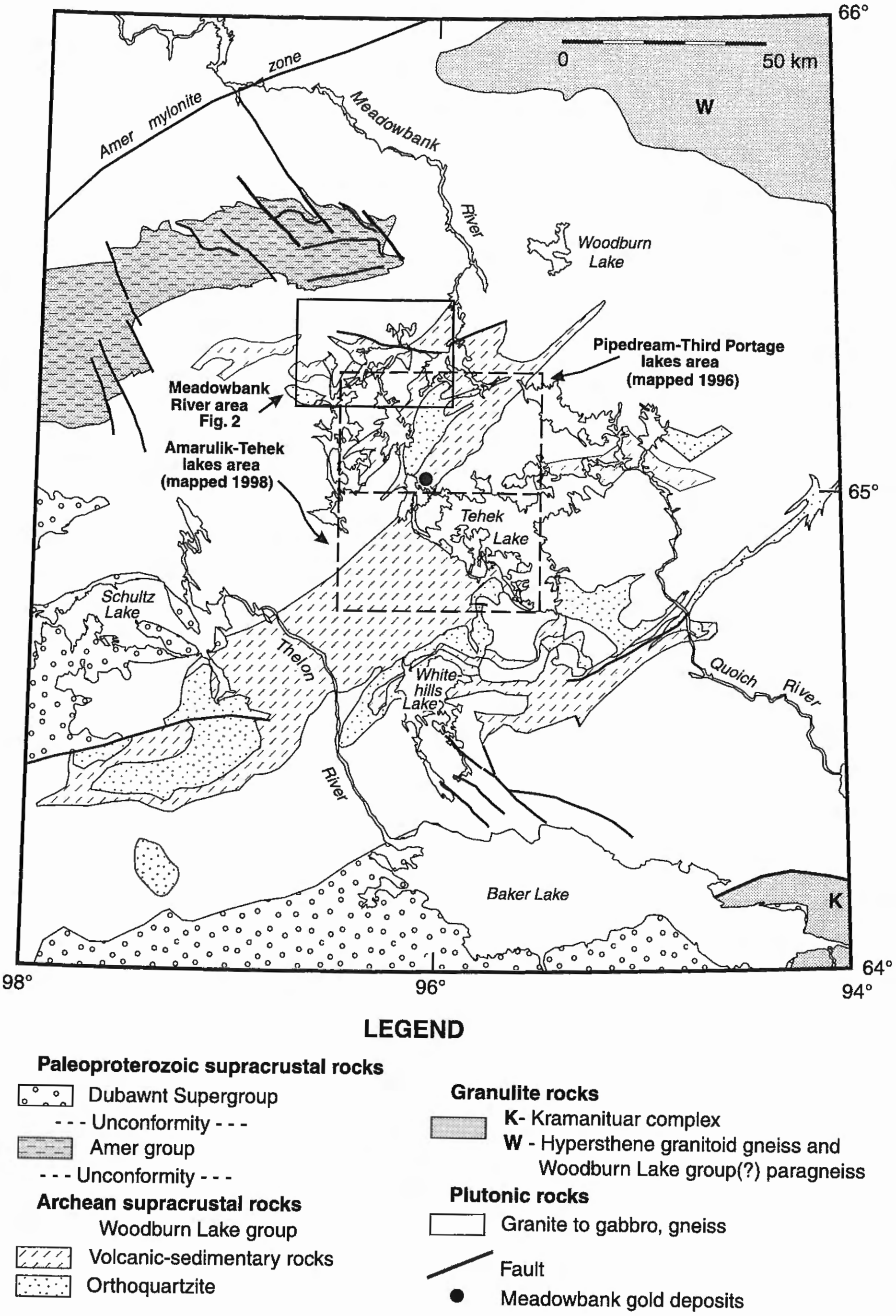


***Figure 1.** Regional setting of the Woodburn Lake group in the Amer Lake (NTS 66 H), Woodburn Lake (NTS 56 E), Baker Lake (NTS 56 D), and Schultz Lake (NTS 66 A) areas. The Pipedream–Third Portage lakes area mapped in 1996 (Zaleski et al., 1997a, b) encompassed the Meadowbank gold deposits. In 1998, mapping was extended to the Meadowbank River area outlined to the north (Fig. 2) and the Amarulik–Tehek lakes area to the south. The regional map is adapted from an unpublished compilation (L. Wilkinson, 1997) based on Donaldson (1966), Schau (1983), Fraser (1985), Taylor (1985), Tella (1994), and a compilation map in progress for the Schultz Lake area based on unpublished mapping by GSC geologists. The fault bounding the northern margin of the Kramanituar complex is based on Sanborn-Barrie (1994).*

Amarulik lakes (Fig. 1), imprecise ages of 2.8 Ga have been reported for felsic volcanic rocks (Tella et al., 1985; Roddick et al., 1992).

Northwest of the Woodburn Lake group, the Paleoproterozoic Amer group has been interpreted as the remnant of a northwesterly verging fold-and-thrust belt (Patterson, 1986). The regional significance of the deformation affecting the Amer group and its relationship to the Woodburn Lake group are major unanswered questions in the tectonic evolution of this part of the Western Churchill Province. Ashton (1988) and Davis and Zaleski (in press) showed that ca. 2.62-2.60 Ga granitic rocks were involved in deformation of Woodburn Lake group, at least 90 Ma after the extrusion of ca. 2.71 Ma volcanic rocks. In the Deep Rose Lake area, 100 km to the west-northwest of the Meadowbank River, the Amer group unconformably overlies ca. 2610 Ma granite which locally contains a foliation that was interpreted to predate the unconformity (Tella et al., 1984; Lecheminant and Roddick, 1991; S. Tella, pers. comm., 1997). This raises the possibility that deformation, synchronous with or postdating 2.61 Ga, predated deposition of the Amer group. Along the southern margin of the Amer group north of the Meadowbank River, structurally interleaved volcanic rocks have been variably interpreted as part of the Amer group (Patterson, 1986) or as part of the Archean sequences (Tella and Heywood, 1983; Tella, 1994).

## TECTONOSTRATIGRAPHY

The Meadowbank River area (Fig. 2) lies north of the Pipedream lake-Third Portage lake area mapped in 1996 (Zaleski et al., 1997a, b), and overlaps with previous mapping by Heywood (1977), Tella and Heywood (1983), Ashton (1988), Fraser (1988), and Tella (1994). The supracrustal rocks in the area can be subdivided into two major associations, interlayered komatiites and felsic volcanic rocks overlain by orthoquartzite, and a volcanic sequence with iron-formation and minor greywacke.

### *Komatiitic and felsic volcanic rocks overlain by orthoquartzite*

On the north shore of the Meadowbank River and to the west, komatiitic and quartz-eye felsic rocks are intercalated in layers from 1 m to hundreds of metres in width (Fig. 2, 3a), with minor thin layers of iron-formation. The layering defines an east-west structural grain. Penetrative fabrics are mostly confined to high-strain domains, and are weak or absent elsewhere. Primary volcanic structures and textures are preserved in komatiitic rocks, including spinifex textures (Fig. 3b), polyhedral jointing, breccia zones, possible pillows, and massive to layered flows. The felsic rocks contain quartz eyes that vary from 0.5–1 cm ellipsoidal lenses of dark monocrystalline quartz to 0.5–5 mm euhedral quartz crystals. Plagioclase phenocrysts are common. The matrix is massive, white to grey, and very fine grained to aphanitic. In view of the low-strain state in much of the area, the interlayering of komatiitic and felsic volcanic rocks is interpreted as volcanic stratigraphy.

Two kilometres northwest of Almost island on the Meadowbank River (Fig. 2), a large outcrop area of multiphase felsic breccias is partly encircled by a layer of komatiite that dips steeply outward. The felsic breccias are characterized by subtle internal contacts between different phases with a high proportion of monolithic angular felsic fragments, including fragments of previously brecciated material. They were interpreted as part of a felsic dome or volcanic centre either intrusive into komatiitic rocks, or onlapped by komatiite flows.

West of the Meadowbank River, quartz-eye felsic rocks and komatiite are overlain by white, locally pyritic and rusty, quartzite (Fig. 2). Observations suggest that the contact is an unconformity and that, despite folding, the sequence youngs upward. Bedding in the quartzite is well defined by prominent jointing along bedding planes typically at 1 cm to 1 m intervals, and schistosity is locally present at a low angle to bedding. The southern contact of the northernmost lens of quartzite (Fig. 2, locality A) is marked by conglomerate which grades from polymictic to oligomictic toward the quartzite (Fig. 3c). A few metres north of the conglomerate, crossbedding in the quartzite shows upright younging toward the north away from the contact (Fig. 3d). Near the northern contact of the quartzite lens, schistosity (bedding not recognized) in quartzite dips moderately toward the south, subparallel to flow layering in komatiite immediately to the north (Fig. 2, locality A). Spinifex sheaves in the komatiite show southward younging toward the quartzite contact.

The same unconformable contact is repeated to the south across a kilometre or more of mostly felsic volcanic rocks (Fig. 2, locality B). This interpretation is supported by a change to southward-dipping bedding and schistosity in quartzite, by local outcrops of conglomerate near the contact, and by southward-younging crossbedding in quartzite (Tella and Heywood, 1983). To the east, polymictic conglomerate on Almost island in the Meadowbank River may be part of the basal conglomerate marking the unconformity (Fig. 2, locality C). However, in this location, the conglomerate is in possible transitional contact with debris-flow deposits that show an overall northward decrease in fragment sizes and proportion of epiclastic components and grade into crystal and lapilli tuffs. Quartzite also outcrops on the north side of Almost island, but primary features are obscure.

West of the Meadowbank River, mafic layers are present in the quartzite in two areas (Fig. 2, east of locality B, and locality D). The more northerly occurrence comprises mafic schist possibly related to the komatiite and the relationships suggest exposure of ultramafic-mafic rocks by a fault. In the southern occurrence, the mafic rocks are coarse grained and massive, resembling a gabbroic sill or dyke intruded into the quartzite.

### *Volcanic rocks with iron-formation and minor greywacke*

South of the Meadowbank River and to the northeast (Fig. 2), a more varied volcanic and sedimentary sequence is present comprising ultramafic, mafic, intermediate, and felsic

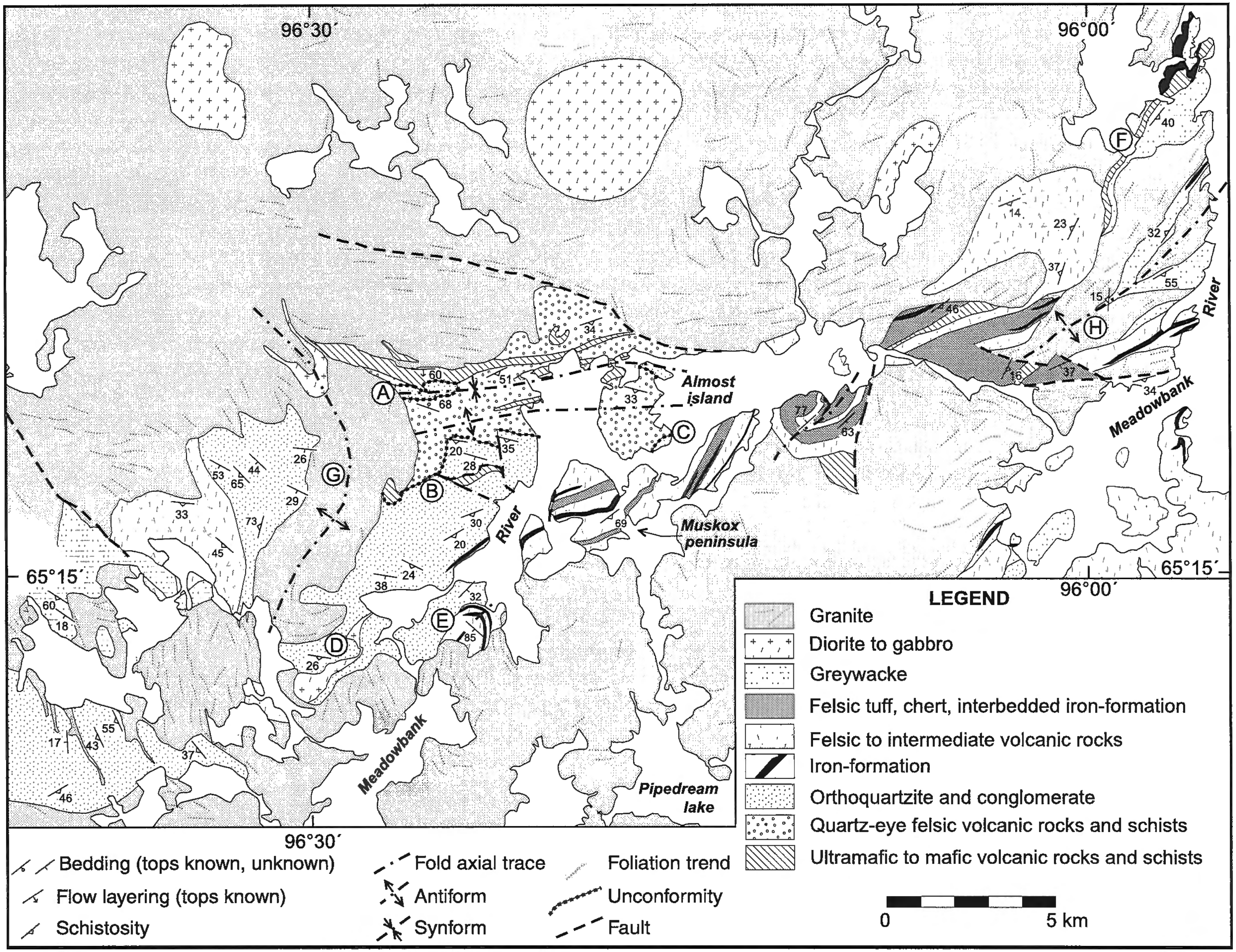


***Figure 2.*** *Generalized geology of the Woodburn Lake group in the area of the Meadowbank River. Locations marked A to H are discussed in the text.*

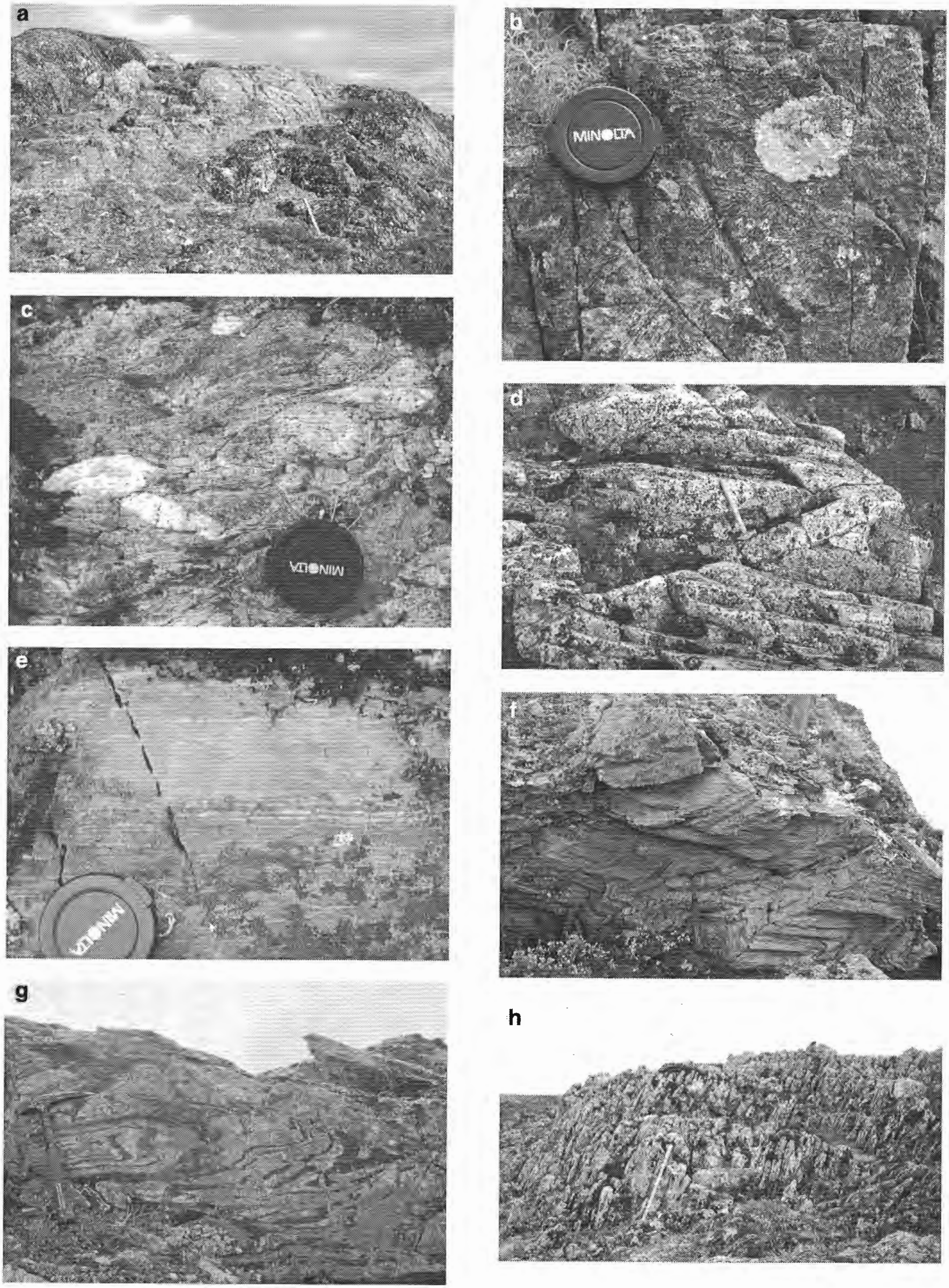
a
b
MINOLTA
c
d
e
f
g
h

volcanic rocks; iron-formation; and cherty tuffs interbedded with iron-formation and minor greywacke. The stratigraphic sequence is uncertain, but along the Meadowbank River near the southwestern margin of the sequence, bedding in quartzite dips toward the southeast, apparently underneath felsic to intermediate rocks interbedded with iron-formation (Fig. 2, locality E). The presence of quartz-rich (possibly quartzite) clasts in a debris-flow deposit in the volcanic rocks also suggests that the sequence overlies quartzite.

The sequence itself is interrupted by plutonic rocks and by faults, and discontinuities across the Meadowbank River suggest that the river may in part follow fault zones. Muskox peninsula and the area to the east is dominated by mafic to intermediate volcanic rocks intercalated with thin (centimetre) to thick (hundreds of metres) units of layered felsic tuff, chert, and iron-formation. The mafic to intermediate rocks are typically massive flows, commonly porphyritic with coarse (5–8 mm) plagioclase and amphibole phenocrysts (or possibly amphibole pseudomorphs) in a dark, fine-grained matrix. Felsic tuffs or chert are typically thinly bedded, and interbedded with banded chert-magnetite iron-formation (Fig. 3e).

Fabric development and metamorphic grade increase toward the northeast, and metamorphic recrystallization makes the identification of protoliths more difficult. Intermediate to felsic plagioclase-porphyritic volcanic rocks are abundant; however, near the northern margin of the supracrustal rocks, recrystallized felsic to intermediate volcanic rocks may be confused with deformed, medium-grained granite. Ultramafic rocks are present in a single zone, 30–250 m in width, traced for about 7 km (Fig. 2, locality F). The ultramafic rocks are characterized by amphibole-garnet-magnetite assemblages indicating amphibolite-facies metamorphic grade. Primary features are obscure or obliterated.

***Figure 3. a)*** *Komatiite flow, about 2–3 m in width, interlayered with quartz-porphyritic felsic rocks along the Meadowbank River. The komatiitic rocks are the light-coloured units, due to weathering and relatively thin lichen cover, whereas the felsic rocks have a heavy growth of black lichen and so appear dark.* ***b)*** *Coarse spinifex blades in komatiite.* ***c)*** *Polymictic conglomerate along the unconformable contact between orthoquartzite and felsic rocks.* ***d)*** *Crossbedded orthoquartzite younging north away from the contact with quartz-porphyritic felsic rocks (in the direction of the hammer handle). The outcrop lies about 20 m north of the conglomerate in c).* ***e)*** *Interbedded felsic tuffs and banded chert-magnetite iron-formation on Muskox peninsula.* ***f)*** *Asymmetric chevron folds in schist developed from ultramafic and felsic volcanic protoliths.* ***g)*** *Overturned isoclinal folds in iron-formation in a high-strain zone along the Meadowbank River.* ***h)*** *Strong pencil cleavage in quartz-porphyritic felsic rocks near the contact with orthoquartzite. The pencils result from the intersection of the dominant subvertical schistosity with a strong, steeply dipping jointing, apparently developed along a spaced crenulation cleavage.*

The ultramafic rocks are associated with banded magnetite-chert iron-formation and silicate-facies amphibole-garnet-magnetite iron-formation, biotitic greywacke, and plagioclase-crystal tuff, an association quite different from that of the interbedded komatiitic rocks and quartz-eye felsic volcanic rocks.

In the western map area, quartzite dips toward the southwest underneath felsic to intermediate volcanic rocks and mafic to intermediate schists interpreted as greywackes. The rocks could be equivalent to the volcanic and sedimentary sequence to the east, although some units typical of the eastern sequence such as iron-formation and interbedded chert, tuff, and iron-formation have not been observed.

## STRUCTURE

The unconformable contact between the interbedded komatiite-felsic volcanic sequence and quartzite is repeated by upright, upward-facing, east-trending folds, consisting of a syncline-anticline pair (Fig. 2, locality A). To the south of the anticlinal trace, bedding in the quartzite consistently dips moderately to shallowly toward the south, until the quartzite abuts against a large, near-massive granite. The syncline apparently plunges to the west; however, the simplest way to account for the occurrence of quartzite on northern Almost island to the east is by a ‘porpoising’ or doubly-plunging fold axis.

West of the Meadowbank River, the large granite body appears to truncate the unconformable contact (Fig. 2, locality A) and divides the quartzite into two main outcrop areas. The granite is mainly massive with weak to moderate foliation locally developed near contacts, consistent with an intrusive relationship. The granite-quartzite contact, and a diorite body intruded by and engulfed by granite, define a macroscopic fold with a curved axial surface trace (Fig. 2, locality G). The fold deforms the dominant schistosity in the supracrustal rocks, and stereographic projection shows that poles to schistosity and bedding define a girdle about an axis that plunges moderately toward the south (Fig. 4a). The nearly isoclinal appearance of the fold in map view is partly due to the moderate plunge. Preliminary interpretation suggests that the curvature of the axial trace is not related to the easterly trending folds of the unconformable contact (Fig. 2, locality A). Bedding in the quartzite on the west side of the granite consistently strikes northwest to west-northwest and dips moderately toward the south and southwest, suggesting that the quartzite lies entirely south of the anticlinal fold trace and that the granite intrudes across both the unconformity and the fold.

In the interlayered komatiitic and felsic volcanic rocks northwest of the Meadowbank River, penetrative fabrics (schistosity and crenulation cleavage) increase south toward the river and, in general, toward contacts with quartzite. In areas of high strain, felsic rocks are transitional to quartz-eye muscovite schists, and komatiitic units are pervaded by carbonate and grade to ultramafic schists characterized by talc, tremolite, serpentine, magnetite, and iron-carbonate. Felsic and ultramafic interlayering in schistose rocks is strongly

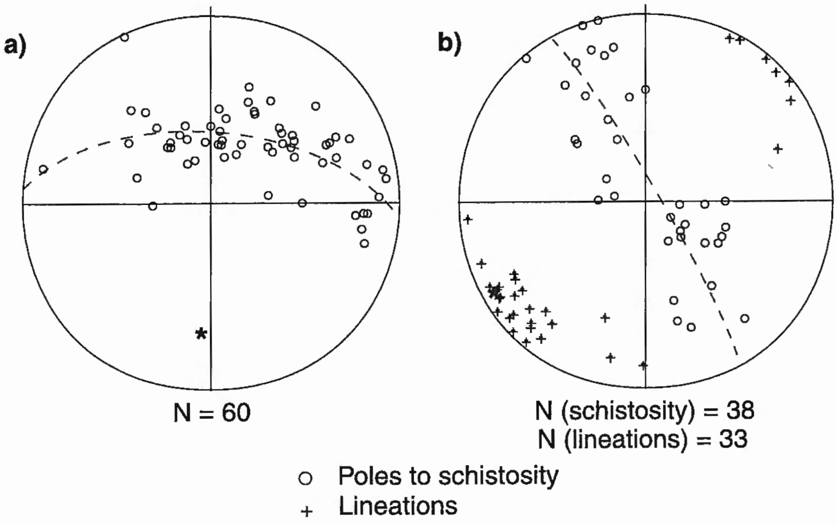


***Figure 4.*** *Equal-area stereographic projections.* ***a)*** *Poles to schistosity and bedding in supracrustal rocks around the granite-cored anticline west of the Meadowbank River (Fig. 2, locality G). The poles define a best-fit girdle about a rotational axis (asterisk) of 184°/31°.* ***b)*** *Poles to schistosity and bedding, and lineations in the area of the antiform in the northeastern map area (Fig. 2, locality H). The poles define a best-fit girdle about a rotational axis (asterisk) of 240°/06°, and the lineations define a maximum distribution of 231°/08°.*

transposed and attenuated and, in many cases, the two are not recognizable as separate components (Fig. 3f). Strongly layered rocks such as iron-formation show isoclinal folds of layering and schistosity (Fig. 3g). Penetrative crenulation cleavages and pencil cleavages are locally present, suggesting intersection of multiple foliations (Fig. 3h).

The high strain along the shore of the Meadowbank River north of Almost island (Fig. 2) is apparently not associated with any major displacement of lithological units and it seems to be primarily due to flattening. The intense fabric development does not obviously continue inland to the west. However, several crudely east-trending lamprophyre and diabase dykes in this area may have intruded along faults or pre-existing zones of weakness. Macroscopic folds of the unconformable contact between the komatiite-felsic sequence and quartzite tighten toward the projected high strain zone, as does the fold of granite and diorite to the west (Fig. 2, localities A, G). This observation suggests that flattening affected the area, and that it postdated the intrusion of granite and development of both sets of folds.

In the volcanic sequence and iron-formation south of the Meadowbank River, macroscopic folds are defined by the map pattern of interlayered lithological units. The rocks are commonly massive, and the dips of bedding and contacts are poorly known. The fold traces trend northeasterly, broadly parallel to the southern part of the trace of folded granite and quartzite.

In contrast, to the northeast, subhorizontal to shallowly southwest-plunging, L>S fabrics are nearly ubiquitous in granitic rocks and supracrustal rocks (Fig. 2, localities F, H). In granite, strong lineations are defined by alignment of elongate minerals and mineral aggregates, whereas planar fabrics are weak or undetectible. The lineations are coaxial or nearly coaxial with a macroscopic fold that deforms the contacts of granite and supracrustal rocks, as well as schistosity (Fig. 2, locality H). Stereographic projection shows that poles to schistosity and bedding define a girdle about an axis that is nearly coaxial with the peak distribution of lineations (Fig. 4b). The relationships suggest that the fold is at least a second generation fold ($F_2$), and that the dominant lineation is associated with the fold.

Plutonic rocks in the area, including granite, diorite, and gabbro, commonly have well developed tectonic fabrics. Formlines based on foliation trends outline regional circular to curvilinear patterns which, in some cases, are broadly conformable to the contacts of dioritic and gabbroic bodies (Fig. 2). The patterns suggest a sheeted plutonic complex with domes or interfering folds exposing plutonic rocks from different levels.

## SUMMARY

There are three main areas of komatiitic rocks known in the Woodburn Lake group, north of Whitehills Lake (Taylor, 1985), west of Pipedream lake (Kjarsgaard et al., 1997; Zaleski et al., 1997a), and the Meadowbank River area described here. Minor occurrences of komatiitic and felsic volcanic rocks, dated at 2710+3.5/-2.1 Ma, overlie quartzite north of Third Portage lake (Zaleski et al., 1997a, b; Davis and Zaleski, in press). Primary features suggest that this is an upright sequence; however, it may be interrupted by an unconformity or a fault. Ultramafic rocks in the Whitehills Lake area are of unknown age; however, their geochemical signature is significantly different from those west of Pipedream lake, suggesting that they are not cogenetic (B. Kjarsgaard, pers. comm., 1998; G. Jenner, pers. comm., 1998).

In the Meadowbank River area, a volcanic stratigraphic sequence comprising interbedded komatiite and felsic volcanic rocks is unconformably overlain by conglomerate and orthoquartzite. Quartz-eye felsic volcanic rock that underlies the quartzite has been previously dated giving a U-Pb zircon age of 2798+24/-21 Ma (Tella et al., 1985), significantly older than the 2710 Ma volcanic rocks in the Pipedream and Third Portage lakes area. This implies that there are two sequences of komatiite-felsic volcanic rocks in the Woodburn Lake group, differing in age by about 110–65 Ma. However, the accuracy of the older age needs to be re-evaluated using modern U-Pb dating methods (W.J. Davis, work in progress).

Mafic, intermediate, and felsic volcanic rocks, associated with iron-formation and greywacke, overlie quartzite along the Meadowbank River and, in the simplest scenario consistent with field observations, this is a stratigraphic relationship. In the east, this sequence also includes a unit of ultramafic rocks, although recrystallized to an amphibolite-facies assemblage. This again implies the presence of a second ultramafic-bearing sequence, in this case comprising rocks of sedimentary origin.

## ACKNOWLEDGMENTS

The Woodburn Project was initiated by Jack and Mariette Henderson. Collaborators in the broader mapping and research program include John Kerswill and Bruce Kjarsgaard, Mineral Resources Division, and George Jenner, Memorial University. Field notes and station locations from the reconnaissance mapping program of W.W. Heywood, S. Tella, and I. Annesley supplied by Subhas Tella were very helpful in directing the present mapping. Gerry Harron and McChip Resources Ltd. made available the results of a high-resolution aeromagnetic survey and detailed mapping on claims held by McChip Resources. The field program was operated out of the Meadowbank camp of Cumberland Resources Ltd., and Brian Alexander, Roger March, and Ewald Gossner of Cumberland Resources Ltd. are gratefully acknowledged for their co-operation and logistical help during the field season. Subhas Tella and Simon Hanmer are thanked for reviewing the manuscript.

## REFERENCES

**Annesley, I.R.**
1989: Petrochemistry of the Woodburn Lake Group komatiite suite, Amer Lake, N.W.T., Canada; Ph.D. thesis, University of Ottawa, Ottawa, Ontario, 406 p.

**Ashton, K.E.**
1981: Preliminary report on geological studies of the ''Woodburn Lake Group'' northwest of Tehek Lake, District of Keewatin; in Current Research, Geological Survey of Canada, Paper 81-1A, p. 269–274.

**Ashton, K.E.** (cont.)
1988: Precambrian geology of the southeastern Amer Lake area (66H/1), near Baker Lake, N.W.T.; Ph.D. thesis, Queen's University, Kingston, Ontario, 335 p.

**Bethune, K.M. and Scammell, R.J.**
1997: Legend and descriptive notes, Koch Island area, District of Franklin, Northwest Territories, (part of NTS 37C); Geological Survey of Canada, Open File 3391, Sheet 4 of 4.

**Davis, W.J. and Zaleski, E.**
in press: Geochronological investigations of the Woodburn Lake group, Western Churchill Province: preliminary results; *in* Radiogenic Age and Isotopic Studies: Report 11, Geological Survey of Canada, Paper 98-2.

**Donaldson, J.A.**
1966: Geology, Schultz Lake, District of Keewatin; Geological Survey of Canada, Preliminary Map 7-1966, scale 1:253 440.

**Fraser, J.A.**
1988: Geology of the Woodburn Lake map area, District of Keewatin; Geological Survey of Canada, Paper 87-11, 12 p.

**Frisch, T.**
1982: Precambrian geology of the Prince Albert hills, western Melville Peninsula, Northwest Territories; Geological Survey of Canada, Bulletin 346, 70 p.

**Henderson, J.R. and Henderson, M.N.**
1994: Geology of the Whitehills-Tehek Lakes area, District of Keewatin, Northwest Territories (parts of 56D, 56E, 66A, and 66H); Geological Survey of Canada, Open File 2923, scale 1:100 000.

**Heywood, W.W.**
1977: Geology of the Amer Lake map-area, District of Keewatin; *in* Report of Activities, Part A, Geological Survey of Canada, Paper 77-1A, p. 409–410.

**Hoffman, P.F.**
1988: United plates of America, the birth of a craton: early Proterozoic assembly and growth of Laurentia; Annual Reviews of Earth and Planetary Sciences, v. 16, p. 543–603.

**Kerswill, J.A. Goff, S.P., Wilkinson, L., Jenner, G.A., Kjarsgaard, B.A., Bretzlaff, R., and Samaris, C.**
1998: An update on the metallogeny of the Woodburn Lake group, western Churchill Province, Northwest Territories; *in* Current Research 1998-C, Geological Survey of Canada, p. 29–41.

**Kjarsgaard, B.A., Kerswill, J.A., and Jenner, G.A.**
1997: Lithostratigraphy and metallogenic implications of komatiite-banded iron-formation - felsic volcanic rocks of the Archean Woodburn Lake group, Pipedream lake, central Churchill Province, Northwest Territories; *in* Current Research 1997-C; Geological Survey of Canada, p. 101–110.

**LeCheminant, A.N. and Roddick, J.C.**
1991: U-Pb zircon evidence for widespread 2.6 Ga felsic magmatism in the central District of Keewatin, N.W.T.; in Radiogenic Age and Isotopic Studies: Report 4; Geological Survey of Canada, Paper 90-2, p. 91–99.

**Patterson, J.G.**
1986: The Amer belt: remnant of an Aphebian foreland fold and thrust belt; Canadian Journal of Earth Sciences, v. 23, p. 2012–2023.

**Roddick, J.C., Henderson, J.R., and Chapman, H.J.**
1992: U-Pb ages from the Archean Whitehills-Tehek lakes supracrustal belt, Churchill Province, District of Keewatin, Northwest Territories; *in* Radiogenic Age and Isotopic Studies: Report 6; Geological Survey of Canada, Paper 92-2, p. 31–40.

**Sanborn-Barrie, M.**
1994: Structural investigation of high-grade rocks of the Kramanituar complex, Baker Lake area, Northwest Territories; *in* Current Research 1994-C, Geological Survey of Canada, p. 121–133.

**Schau, M.**
1982: Geology of the Prince Albert group in parts of Walker Lake and Laughland Lake map areas, District of Keewatin; Geological Survey of Canada, Bulletin 337, 62 p.
1983: Baker Lake map sheet (56D); Geological Survey of Canada, Open File 883, scale 1:250 000.

**Taylor, F.C.**
1985: Precambrian geology of the Half Way Hills area, District of Keewatin; Geological Survey of Canada, Memoir 415, 19 p.

**Tella, S.**
1994: Geology, Amer Lake (66H), Deep Rose Lake (66G), and parts of Pelly Lake (66F), District of Keewatin, Northwest Territories, Geological Survey of Canada, Open File 2969, scale 1:250 000.

**Tella, S. and Heywood, W.W.**
1983: Geology of the Amer Lake (NTS 66H) map-area, District of Keewatin, Northwest Territories; Geological Survey of Canada, Open File 942, scale 1:250 000.

**Tella, S., Thompson, D.L., and James, D.T.**
1984: Geology of parts of the Deep Rose Lake and Pelly Lake map areas, District of Keewatin; *in* Current Research, Part A; Geological Survey of Canada, Paper 84-1A, p. 313–322.

**Tella, S., Heywood, W.W., and Loveridge, W.D.**
1985: A U-Pb age on zircon from a dacite porphyry, Amer Lake map area, District of Keewatin, NWT; *in* Current Research, Part B; Geological Survey of Canada, Paper 85-1B, p. 371–374.

**Zaleski, E., Corrigan, D., Kjarsgaard, B.A., Jenner, G.A., Kerswill, J.A., and Henderson, J.R.**
1997a: Preliminary results of mapping and structural interpretation from the Woodburn project, western Churchill Province, Northwest Territories; *in* Current Research 1997-C; Geological Survey of Canada, p. 91–100.

**Zaleski, E., Corrigan, D., Kjarsgaard, B.A., Kerswill, J.A., Jenner, G.A., and Henderson, J.R.**
1997b: Geology, Woodburn Lake group, Meadowbank River to Tehek Lake (66H/1, 56E/4), District of Keewatin (Nunavut), Northwest Territories; Geological Survey of Canada, Open File 3461, scale 1:50 000.

**Zaleski, E., Duke, N., L'Heureux, R., Davis, W.J., and Wilkinson, L.**
1999: Clastic and chemical sedimentary sequences, Woodburn Lake group, Amarulik Lake to Tehek Lake, western Churchill Province, Northwest Territories (Nunavut); *in* Current Research 1999-C, Geological Survey of Canada.

Geological Survey of Canada Project 970006

# Clastic and chemical sedimentary sequences, Woodburn Lake group, Amarulik Lake to Tehek Lake, western Churchill Province, Northwest Territories (Nunavut)[1]

E. Zaleski, N. Duke[2], R. L'Heureux[2], W.J. Davis, and L. Wilkinson
Continental Geoscience Division, Ottawa

*Zaleski, E., Duke, N., L'Heureux, R., Davis, W.J., and Wilkinson, L., 1999: Clastic and chemical sedimentary sequences, Woodburn Lake group, Amarulik Lake to Tehek Lake, western Churchill Province, Northwest Territories (Nunavut);* in *Current Research 1999-C; Geological Survey of Canada, p. 19–28.*

**Abstract:** In the Amarulik–Tehek lakes area, the Archean Woodburn Lake group comprises psammitic greywacke interlayered with iron-formation and amphibole hornfels, the latter interpreted as metamorphosed rocks of mixed chemical and clastic sedimentary parentage. Amphibole hornfels extends northward to the Meadowbank gold deposits and includes rocks previously mapped as intermediate volcanic rocks. New mapping implies that a reported age of ca. 2.8 Ga for volcanic rocks is invalid, as the area is underlain by greywacke, albeit with volcanogenic components. A structural dome, centred on Amarulik Lake, is defined by outward-dipping bedding and schistosity, and encompasses smaller scale structural complexities such as concentric dip reversals. Orthoquartzite and metacarbonate lie near the eastern margin of the dome and the distribution of units suggests fold interference patterns. Mineral assemblages are typical of amphibolite-facies metamorphic grade, whereas to the north, chloritoid-bearing greenschist-facies assemblages prevail, suggesting that the Meadowbank gold deposit lies near the greenschist-amphibolite transition.

**Résumé :** Dans la région des lacs Amarulik et Tehek, le groupe archéen de Woodburn Lake comporte des grauwackes arénacés intercalés avec de la formation de fer et des cornéennes à amphibole, ces dernières étant interprétées comme des roches métamorphisées de filiation chimique et sédimentoclastique mixte. Les cornéennes à amphibole se prolongent vers le nord jusqu'aux gîtes d'or de Meadowbank et comprennent des roches cartographiées antérieurement comme roches volcaniques intermédiaires. Une nouvelle cartographie indiquerait que l'âge des roches volcaniques déterminé antérieurement à environ 2,8 Ga est faux, car des grauwackes, bien que comprennant des composantes volcanogéniques, leur sont sous-jacents. Un dôme centré sur le lac Amarulik est défini par un litage et une schistosité à pendage vers l'extérieur et englobe des éléments structuraux de moindre étendue, tels que des inversions de pendage concentriques. Des orthoquartzites et des roches carbonatées métamorphisées se rencontrent à proximité de la bordure est du dôme; la répartition des unités porte à croire à des figures d'interférence de plis. Les associations de minéraux sont typiques du métamorphisme au faciès des amphibolites alors que vers le nord, les paragenèses du faciès des schistes verts à chloritoïdes prédominent, ce qui laisserait supposer que le gîte d'or de Meadowbank se trouve à proximité de la transition du faciès des schistes verts au faciès des amphibolites.

[1] Contribution to the Western Churchill NATMAP Project
[2] University of Western Ontario, London, Ontario N6A 5B7

## INTRODUCTION

The Woodburn Lake group comprises a deformed sequence of Archean supracrustal rocks in the Rae Province (Churchill Province) (Fig. 1), north of the regional geophysical anomaly interpreted by Hoffman (1988) as the northeastern extension of the Snowbird tectonic zone. Several lithological associations typical of Archean cratons are represented in the Woodburn Lake group, i.e. komatiite-quartzite assemblages, greenstone-type volcanic and sedimentary sequences (Taylor, 1985; Ashton, 1988; Annesley, 1989), and, to the northeast, granulite gneiss units that have been correlated with the supracrustal rocks (Fraser, 1988). The volcanic and sedimentary rocks are interlayered with iron-formation that represent a variety of facies, including sulphide-, oxide-, and silicate-facies iron-formation (Kerswill et al., 1998). In the Third Portage lake area, iron-formation at the Cumberland Resources Meadowbank deposits is host to significant gold mineralization, with a resource base recently estimated at 46.7 t (1.5 million oz., The Northern Miner, v. 24, no. 29, p. 1, 12, September 14–20, 1998). The western Churchill Province is variably affected by Archean and Paleoproterozoic deformation and metamorphism. The significance and timing of tectonothermal events remains a major question which also applies to the nature and timing of gold mineralization in the Woodburn Lake group (Armitage et al., 1996).

The Woodburn Project is part of the Western Churchill NATMAP Project, a collaborative mapping initiative by the Geological Survey of Canada and Indian and Northern Affairs Canada in the Northwest Territories (Nunavut). The Woodburn Project is focused on the following two principal themes: 1) the stratigraphy, tectonic setting, petrogenesis, metallogeny, metamorphism, and deformation of the Archean supracrustal rocks of the Woodburn Lake group, and 2) the significance and character of Paleoproterozoic tectonothermal events affecting the Woodburn Lake group. The project was initiated in 1996 with 1:50 000 scale mapping (Zaleski et al., 1997a, b), mineral deposit studies (Kjarsgaard et al., 1997, Kerswill et al., 1998), and geochronological studies (Davis and Zaleski, in press) in the area of Pipedream lake and north of Third Portage lake encompassing the Meadowbank gold deposits (66 H/1, 56 E/4). During the 1998 field season, mapping and sampling were extended to the north (NTS 66 H/2, H/7, H/8; 56E/5; *see* Zaleski et al., 1999) and south (66 A/16, 56 D/13). This paper presents the preliminary results of fieldwork in the southern map area between Amarulik Lake and Tehek Lake (Fig. 1).

## REGIONAL GEOLOGY

The Woodburn Lake group comprises deformed Archean supracrustal rocks extending northeasterly from Schultz Lake to beyond the Quoich River (Fig. 1). Supracrustal rocks from the Whitehills Lake area to the Quioch River, the 'Ketyet River group' of Schau (1983), have been correlated with the Woodburn Lake group (Schau, 1983; Taylor, 1985) and subsequent workers considered them to be part of the Woodburn Lake group (Henderson et al., 1991; Henderson and Henderson, 1994). Similar supracrustal rocks extend continuously to south of Schultz Lake (Donaldson, 1966), and intermittantly as inclusions or septa in the dominantly plutonic terrane between Schultz Lake and the Amer group (Tella, 1994).

Definition of the stratigraphic sequence and correlations of lithological units of the Woodburn Lake group have been persistent problems throughout the region. In particular, quartzite units have been used as regional markers and much effort has been focused on determining their stratigraphic position(s) and possible correlations. Ashton (1988), Fraser (1988) and Annesley (1989) placed quartzite at the top of the sequence, overlying volcanic rocks and interbedded iron-formation. Ashton proposed an unconformity at the base of the quartzite, marked intermittantly by the presence of oligomictic conglomerate. Taylor (1985) interpreted the stratigraphy north of Whitehills Lake as a succession from greywacke to volcanic rocks (including mafic and komatiitic rocks) and iron-formation, to quartzite overlain by younger volcanic rocks at the top of the sequence. Henderson et al. (1991) and Henderson and Henderson (1994) considered the stratigraphic succession to be uncertain; however, they noted that quartzite typically occupies a structurally high position. They documented the presence of an elliptical structural dome centred on Amarulik Lake and considered the rocks in the core of the dome to lie at the structural base of the sequence. Kjarsgaard et al. (1997) proposed a stratigraphic sequence for the Pipedream and Third Portage lakes area with quartzite at the base, overlain by komatiite, intermediate to felsic volcanic rocks, and volcaniclastic sedimentary rocks. Zaleski et al. (1997a, b) considered it likely that quartzites lay at the stratigraphic base of the sequence, and proposed that oligomictic conglomerate along quartzite contacts was consistent with an unconformable surface developed on top of quartzite.

Uranium-lead zircon dating of felsic lapilli tuff north of Third Portage lake identified the youngest rocks known thus far in the Woodburn Lake group (2710+3.5/-2.1 Ma, Davis and Zaleski, in press). The felsic rocks were interpreted to stratigraphically overlie quartzite, based on sporadic younging indicators including quartz-rich (possibly quartzite) clasts in volcanogenic debris-flow deposits (Zaleski et al., 1997a, b; Davis and Zaleski, in press). The detrital zircon population in the quartzite is dominated by 2.97-2.95 Ga grains, and the youngest zircon poorly constrains the maximum depositional age to be at least 2.81 Ga (Davis and Zaleski, in press). To the north near the Meadowbank River, and to the south between Whitehills and Amarulik lakes (Fig. 1), imprecise ages of 2.8 Ga have been reported for felsic volcanic rocks (Tella et al., 1985; Roddick et al., 1992).

The supracrustal rocks are intruded by Archean granitic rocks ranging from ca. 2.62–2.60 Ga (Ashton, 1988; Roddick et al., 1992; Davis and Zaleski, in press). Significant deformation postdated the emplacement of the granite bodies (Ashton, 1988; Davis and Zaleski, in press). Regional metamorphic grade increases toward the east and northeast. Upper greenschist- to lower amphibolite-facies assemblages have been reported south of Whitehills Lake (chloritoid-staurolite, Schau, 1983) and north of Third Portage lake (chloritoid-kyanite-muscovite, Ashton, 1988; Zaleski et al., 1997a), and

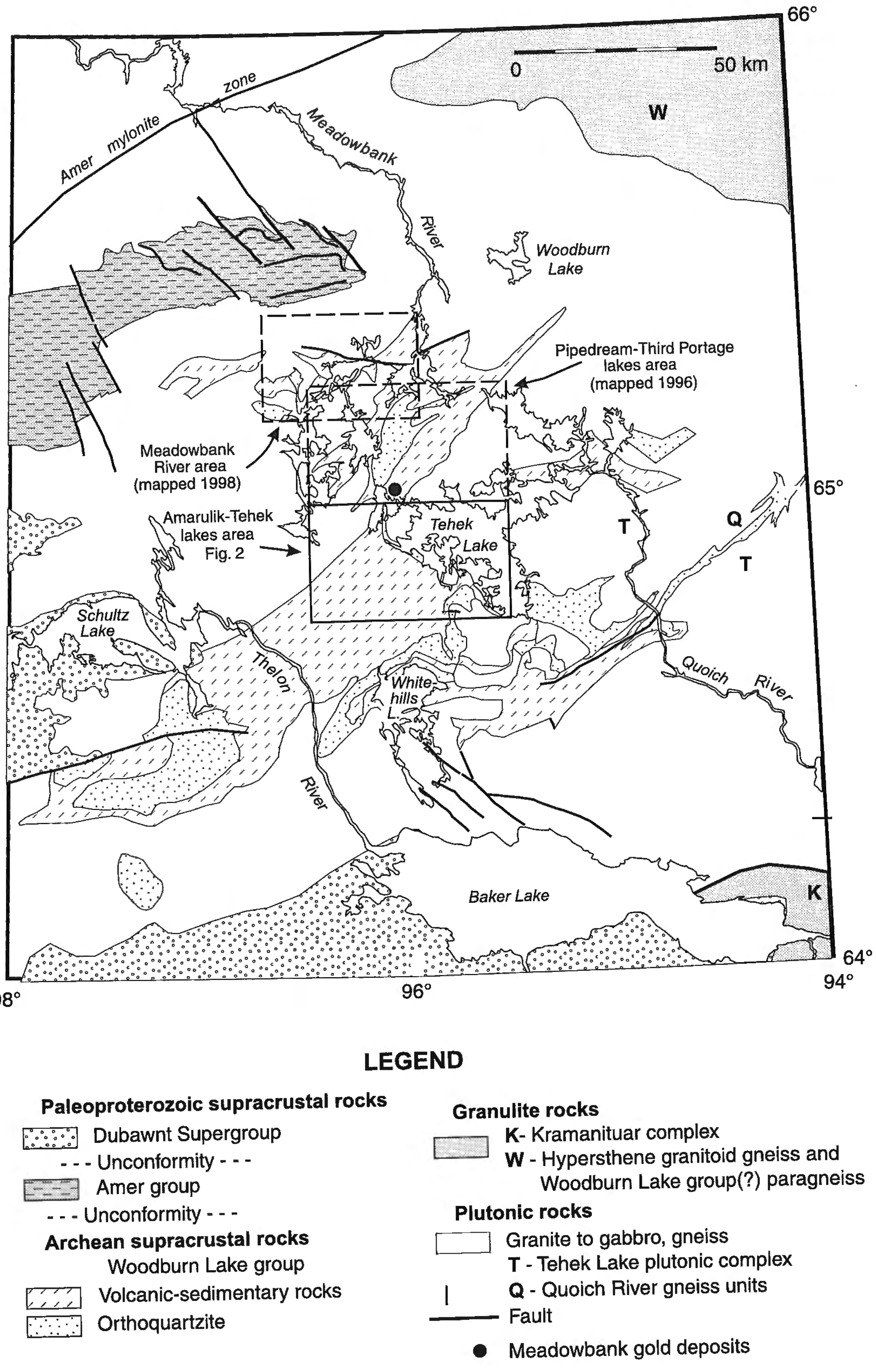


***Figure 1.*** *Regional setting of the Woodburn Lake group in the Amer Lake (NTS 66 H), Woodburn Lake (NTS 56 E), Baker Lake (NTS 56 D), and Schultz Lake (NTS 66 A) areas. The Pipedream–Third Portage lakes area mapped in 1996 (Zaleski et al., 1997a, b) encompassed the Meadowbank gold deposits. In 1998, mapping was extended to the Meadowbank River area outlined to the north and the Amarulik–Tehek lakes area to the south (Fig. 2). The regional map is adapted from an unpublished compilation (L. Wilkinson, 1997) based on Donaldson (1966), Schau (1983), Taylor (1985), Fraser (1988), Tella (1994), and a compilation map in progress for the Schultz Lake area based on unpublished mapping by GSC geologists.*

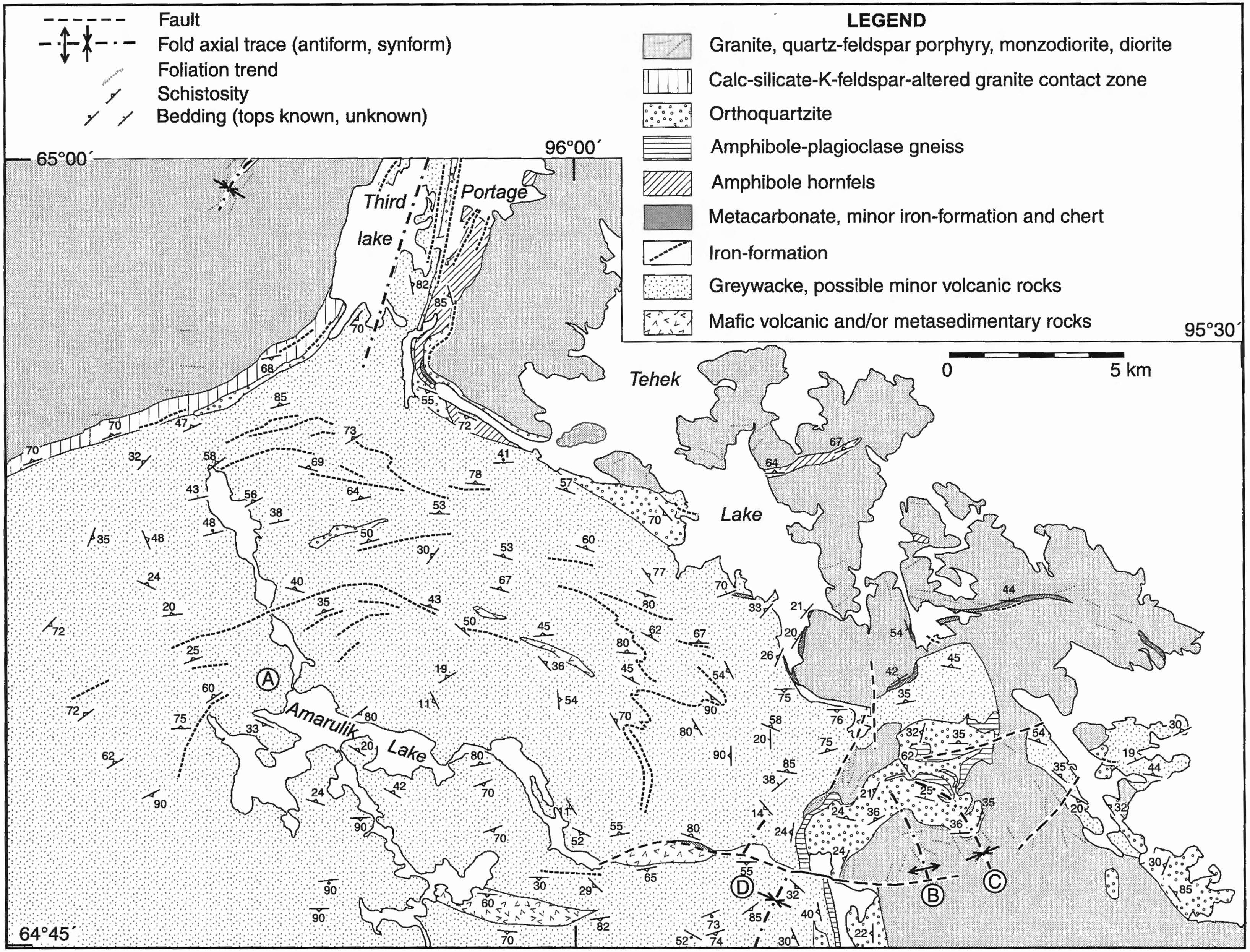


*Figure 2. Generalized geology of the Woodburn Lake group from Amarulik Lake to Tehek Lake. Locations labelled A to D are discussed in the text. The distribution of iron-formation is shown schematically, based on field observations and aeromagnetic data. Some structural measurements west of Amarulik Lake were compiled from the unpublished field notes of J.R. Henderson.*

upper amphibolite-facies assemblages (sillimanite-K-feldspar-muscovite, Schau, 1982) near Tehek Lake. Septa of supracrustal rocks extend into the high-grade terrane of the Tehek Lake plutonic complex and the Quoich River gneiss (Fig. 1), the latter interpreted as high-grade equivalents of the Woodburn Lake group (Heywood and Schau, 1981; Schau et al., 1982). Fraser (1988) considered the granulite terrane northeast of Woodburn Lake to contain paragneiss correlative with the Woodburn Lake group.

Patterson (1986) interpreted the Paleoproterozoic Amer group as a foreland fold-and-thrust belt, and the Tehek Lake plutonic complex and intervening Archean rocks as the metamorphic and plutonic internides of a 'cryptic Hudsonian orogen' (Fig. 1). The Kramanituar complex, which coincides with the geophysical anomaly that defines the Snowbird tectonic zone, underwent high pressure (12–15 kbar), granulite-facies metamorphism at ca. 1.91–1.90 Ga, and rapid exhumation and cooling by 1.89 Ga (Sanborn-Barrie et al., 1997). Both the Amer group and the Kramanituar complex are unconformably overlain by undeformed rocks of the post-Hudsonian (younger than ca. 1.85 Ga) Dubawnt Supergroup (Lecheminant et al., 1984; Gall et al., 1992; Sanborn-Barrie, 1994). Continuing magmatic and low-grade thermal activity are documented by 1.84 Ga igneous monazite from an undeformed granite dyke south of Third Portage lake (Roddick et al., 1992), and by 1.80–1.75 Ga K-Ar ages of micas in the area of Third Portage and Pipedream lakes (Ashton, 1988). At the Meadowbank deposits, Armitage et al. (1996) favoured an epigenetic model for the gold mineralization and, while they viewed the timing to be uncertain, 1.79 Ga K-Ar age for biotite from the Main zone (*in* Armitage et al., 1996, attributed to A. Miller, pers. comm., 1993) led them to consider the possibility of a Proterozoic mineralizing event.

## TECTONOSTRATIGRAPHY

The Amarulik–Tehek lakes area (Fig. 2) lies south of the Pipedream lake–Third Portage lake area mapped in 1996 (Zaleski et al., 1997a, b), and partly in the area of the 1:100 000 scale map of Henderson and Henderson (1994). Previous reconnaissance mapping east of longitude 96°W was carried out by Heywood and Schau (1981) and Schau (1983). The Meadowbank gold deposits lie 1–3 km north of the northern margin of the Amarulik–Tehek lakes area, hosted by iron-formation units in the structurally complex, narrow zone between the granite plutons east and west of Third Portage lake.

The area is dominated by clastic and chemical sedimentary rocks, with minor occurrences of possible mafic metavolcanic rocks. A large part of the area is underlain by monotonous psammitic greywacke locally with layers of silicate-facies and oxide-facies iron-formation, and abundant minor granitic and pegmatitic intrusions. The area of psammitic greywacke broadly coincides with an elliptical structural dome (about 28 km x 18 km) identified by Henderson et al. (1991) and Henderson and Henderson (1994), and here called the Amarulik dome. The Amarulik dome was defined on the basis of outward-dipping bedding and schistosity.

A large area central to the Amarulik dome, previously mapped as intermediate volcanic and volcaniclastic rocks (Henderson et al., 1991; Henderson and Henderson, 1994), has been reinterpreted as psammitic greywacke, reverting to the earlier interpretation of Donaldson (1966) and Schau (1983). The psammitic greywacke typically contains abundant quartz and feldspar grains and lithic clasts in massive, poorly sorted, thick beds. Where thin beds (centimetre scale) are present, these commonly show preferential development of mineral schistosity and, in some cases, crenulation cleavages (Fig. 3a). In a few locations, younging directions were determined from graded bedding. North of Amarulik Lake, graded bedding dips and youngs northward, whereas south and southeast of Amarulik Lake, dips and younging are toward the south (Fig. 2). Graded bedding consistently indicates younging outward around the structural dome. However, local changes in dips and discontinuities in structural trends suggest that the regional significance of the younging determinations may be more complex (*see* 'Structure and metamorphism'). Near Tehek Lake, greywacke generally is more pelitic, containing abundant biotite. Pelitic greywacke contains a strong schistosity, which is apparently a composite fabric partly defined by transposed quartz veinlets and lenticules that outline tight to isoclinal folds. Original bedding features are only rarely recognizable.

Greywacke is interbedded with silicate-facies, garnet-amphibole iron-formation and banded, chert-magnetite iron-formation, commonly with rusty-weathering, sulphidic zones. The iron-formation forms semicontinuous or discontinuous layers, centimetres to metres in width, and single layers cannot generally be traced along strike. However, greywacke with iron-formation interbeds may prove to be a distinctive macroscopic marker unit. Iron-formation-bearing zones are associated with strong aeromagnetic trends (Geological Survey of Canada, 1990) which outline complex patterns of folding and, in some cases, triple-point junctions.

The greywacke contains zones of amphibole-bearing rock in which layering or bedding is variably overgrown by randomly to weakly oriented, medium- to coarse-grained poikiloblasts of green amphibole, occasionally with garnet. The amphibole-bearing rocks are variable in character and association, showing gradational contacts to greywacke, and transitions to silicate-facies iron-formation, as well as to rocks that resemble weakly to moderately foliated, coarse-grained amphibolite or metagabbro. They are commonly interlayered with banded, oxide-facies iron-formation. The amphibole-bearing rocks form a distinctive map unit, to which we apply the descriptive field term 'amphibole hornfels'. Amphibole hornfels is interpreted as metamorphosed sedimentary rock with both chemical and clastic components, with the gradational types representing transitional facies both laterally and vertically through the sedimentary section. Southeast of Third Portage lake, a large unit of amphibole hornfels and associated iron-formation extends to the north toward the Meadowbank gold deposits where similar rocks have been intersected in drill holes.

A distinctive unit of white to buff metacarbonate is present along the northeastern contact of the greywacke, and as septa within granite to the east. A sliver of metacarbonate also

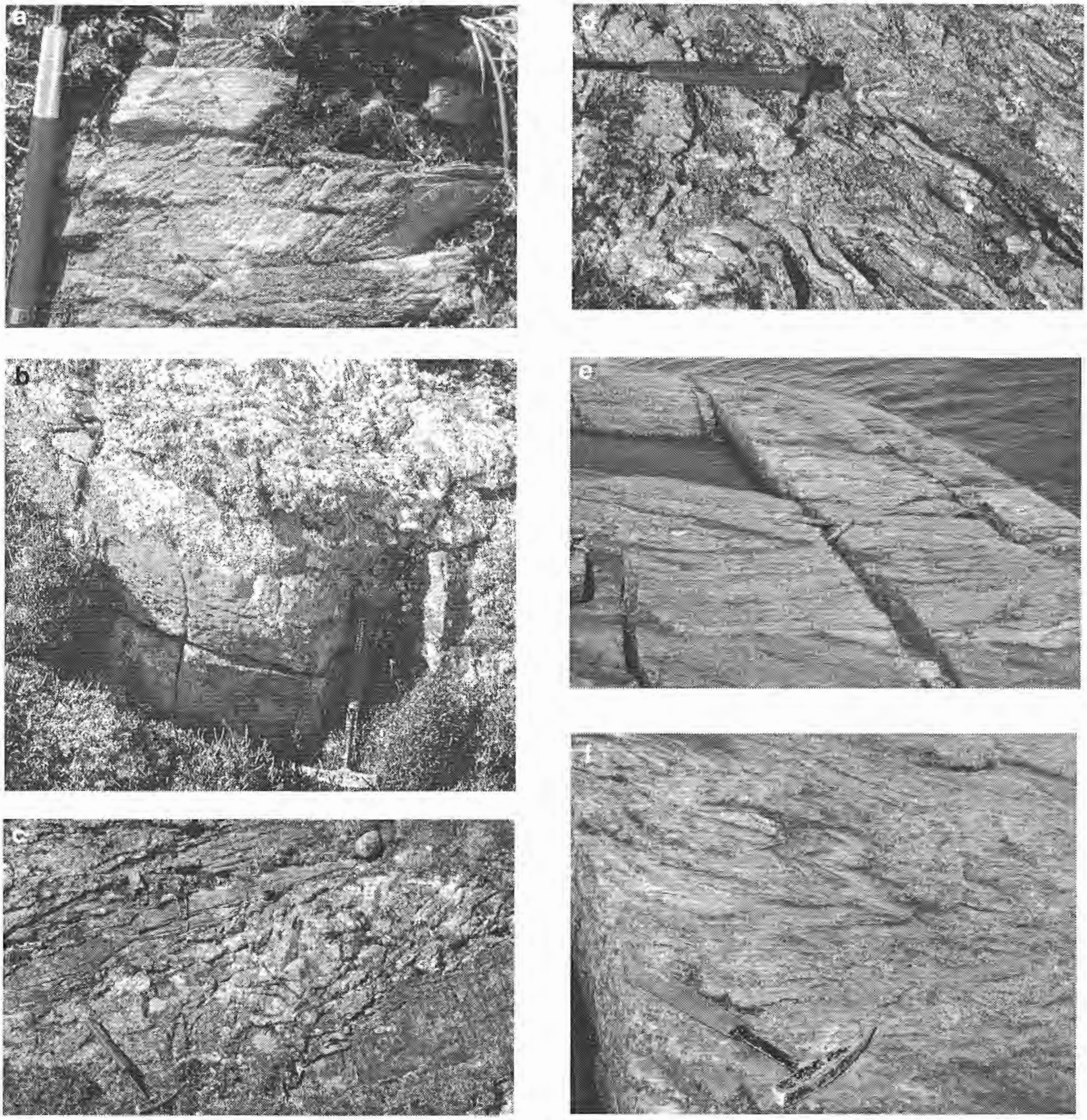

***Figure 3.*** ***a****) Bedding in quartzofeldspathic greywacke defined by relatively coarse-grained, massive or weakly foliated beds and fine-grained beds with a strong foliation. The lower bed is graded, fining upward in the direction indicated by the pencil. The oblique foliation is a crenulation cleavage of an earlier schistosity.* ***b****) Bedded metacarbonate with a medium-grained granular dolomite bed below, overlain by a bed with very coarse dolomite sheaves.* ***c****) Bedded metacarbonate with interlayered granular dolomite beds and very contorted quartz-rich beds with minor carbonate.* ***d****) Detail of folded layering in contorted quartz-carbonate bed.* ***e****) Recumbent isoclinal folds of layering in iron-formation near the contact between supracrustal rocks and foliated granite on Tehek Lake. The hammer handle points west parallel to fold axes.* ***f****) Detail of the folds in e).*

extends toward Third Portage lake, flanked by quartzite and amphibole hornfels. The metacarbonate is characterized by compositional layering (Fig. 3b, c), 0.2–1 m in width, of the following three main types: 1) quartz with minor dolomite and calc-silicate minerals, 2) randomly oriented, very coarse dolomite sheaves (up to 20–30 cm in length), and 3) medium-grained, granular dolomite and minor calcite with fine sprays of tremolite. In quartz-rich layers, second-order layering (1–10 cm thick) is tightly contorted and folded (Fig. 3d). The metacarbonate is associated with banded iron-formation, amphibole hornfels, and massive quartz rocks that may be recrystallized chert or quartzite. The lithological associations and the compositional layering, interpreted as bedding, suggest a chemical sedimentary origin for the metacarbonate.

Orthoquartzite is present in a discontinuous zone along the outer perimeter of the greywacke in the Amarulik dome. Orthoquartzite on both sides of the greywacke on Third Portage lake is partly flanked by iron-formation and ultramafic schist characterized by talc, tremolite, iron-carbonate, and magnetite (Fig. 2). The quartzite is massive or has micaceous interbeds (up to 10 cm thick). Fuchsite is present in bright green flakes or finely disseminated giving a greenish colour to the rock. South of Tehek Lake, bedding is typically marked by pronounced jointing. The orthoquartzite is interleaved with conformable or nearly conformable sheets of massive to weakly foliated granite which can represent 50% of the outcrop area. In some areas, contacts are transitional, marked by the presence of possibly hybrid rocks of white-pink, quartz-rich pegmatite and granite. Near the southernmost shore of Tehek Lake, quartzite contains metamorphic sillimanite, and metagreywacke contains (?)sillimanite-garnet-biotite assemblages.

Southwest of Tehek Lake, amphibole-plagioclase gneiss and quartzite define a complex map pattern due to a combination of folding, shallow dips, and topographic relief. The gneissic layering is defined by variations in the abundance of amphibole, epidote, magnetite, and minor biotite, and schistosity is parallel to layering. Contacts with metagreywacke are either abrupt or transitional, and locally the amphibole-plagioclase gneiss is sulphidic and contains layers of banded iron-formation. These relationships and the dominance of calc-silicate minerals in the gneiss suggest that it may be equivalent to amphibole hornfels, but underwent synkinematic recrystallization at higher metamorphic grade. Correlation of amphibole-plagioclase gneiss with amphibole hornfels would suggest similarity between the lithological sequences in the Tehek Lake area and the area southeast of Third Portage lake. In both areas, there is a general eastward progression from greywacke and iron-formation to amphibole hornfels (with iron-formation) and quartzite.

## STRUCTURE AND METAMORPHISM

The geometry of the Amarulik–Tehek lakes area is partly determined by a series of upright folds defined by the attitudes of bedding and schistosity. The Amarulik structural dome is the largest of these (Fig. 2). Younging directions based on graded bedding consistently suggest younging away from the centre of the dome (Fig. 2). Poles to bedding and schistosity over the dome are quite dispersed, defining a weak girdle about an axis of 276°/11° (Fig. 4a). The axis is approximately parallel to the elongation direction of the dome, interpreted by Henderson and Henderson (1994) as an upright, east-trending, $F_2$ fold. However, the structural pattern is complicated by several dip reversals internal to the dome, some of which define concentric or crescentic domains. For example, in the centre of the dome around Amarulik Lake, dip directions are inward (Fig. 2, locality A). Fabrics and contacts along the northeastern margin of the dome near Tehek Lake also dip inward, placing granite, metacarbonate, and quartzite structurally beneath greywacke. Along the granite contact, isoclinal overturned folds are developed in iron-formation and metacarbonate (Fig. 3e, f), and the axial surfaces of the folds dip toward the dome.

The Amarulik structural dome encompasses several smaller scale, 'triple-point junctions' and discontinuities defined by aeromagnetic trends (Geological Survey of Canada, 1990), and partly reflected by topographic trends and the shapes of lakes. Preliminary interpretation suggests that these correspond with straight-layered domains adjacent to folded domains, and that the domains may represent limb and hinge areas of folds, and/or zones of relatively high and low strain. Until these structural complications and the timing and nature of the dome itself are better understood, regional interpretation of the outward younging indicators should be made with caution.

In the eastern part of the dome, foliations in greywacke trend easterly and have steep dips (Fig. 2, north of locality D). The greywacke and the structural trends are truncated by a steep, north-trending fault which juxtaposes greywacke and mylonitic granite. Lineations in the mylonitic granite plunge steeply suggesting a strong dip-slip component of movement. To the southeast, near the southern contact between granite and quartzite, the attitudes of interleaved granite-quartzite sheets and of schistosity define northerly trending upright folds, consisting of a granite-cored antiform and a synform dominated by quartzite and amphibole-plagioclase gneiss (Fig. 2, localities B, C). The girdles defined by poles to foliations around the antiform and synform have rotational axes of 341°/14° and 332°/28°, respectively (Fig. 4b, c). Lineations, defined by strongly aligned amphibole prisms in the amphibole-plagioclase gneiss, are slightly oblique to the rotational axes, but not obviously folded.

Southeast of Amarulik Lake, bedding and schistosity in greywackes define a southwesterly trending synform (Fig. 2, locality D). The synform was interpreted as an $F_3$ fold based on relationships near Whitehills Lake south of our map area, where the synform deforms an $F_2$ fold of interlayered quartzite and volcanic rocks (Henderson and Henderson, 1994). Poles to bedding and schistosity define a girdle about an axis of 251°/31° (Fig. 4d). Crenulation cleavages are strongly developed in fine-grained beds in greywacke (Fig. 3a), and suggest that the axial plane dips moderately toward the northwest.

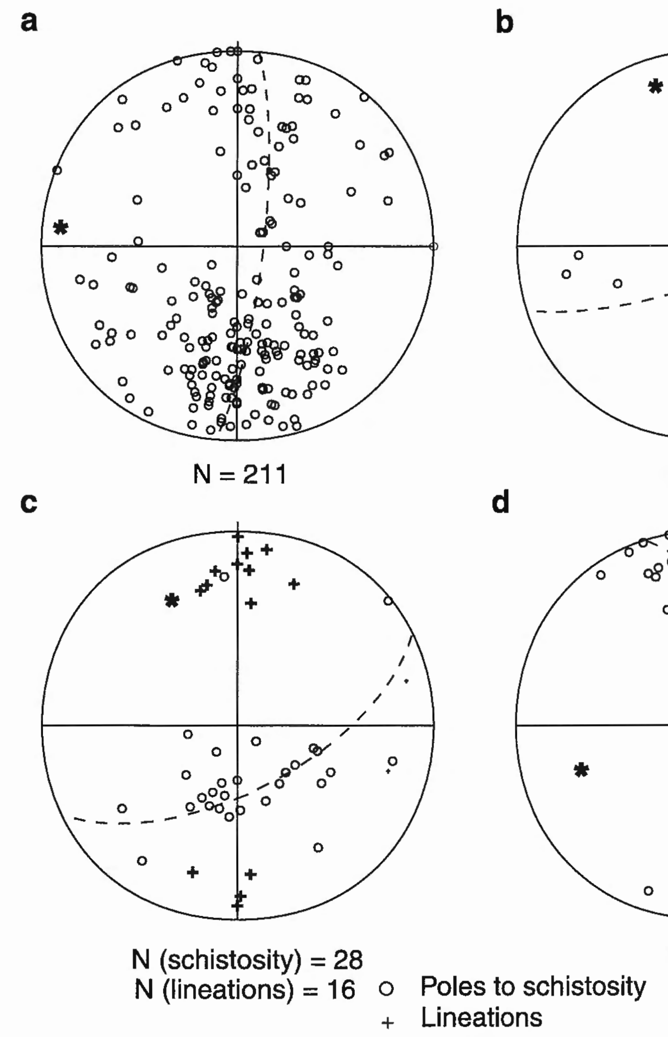


*Figure 4.*

*Equal-area stereographic projections. In each case, the asterisk marks the axis of the girdle defined by schistosities. **a**) Poles to bedding and schistosity in the broad area of the structural dome centred on Amarulik Lake (Fig. 2). The poles are quite dispersed, weakly defining a girdle about a rotational axis of 276°/11°. **b**) Poles to schistosity in the area of the granite-cored antiform southwest of Tehek Lake (Fig. 2, locality B) define a girdle with an axis of 341°/14°. **c**) Poles to bedding and schistosity in the area of the synform involving quartzite and amphibole-plagioclase gneiss (Fig. 2, locality C). The poles define a girdle with an axis of 332°/28°. Mineral lineations in the area cluster about a maximum at 000°/12°. **d**) Poles to bedding and schistosity in greywacke around the synform southeast of Amarulik Lake (Fig. 2, locality D) define a girdle about an axis of 251°/31°.*

The amphibole-garnet-biotite assemblages observed throughout much of the area are typical of amphibolite-facies metamorphic grade. Staurolite was observed in mica schist in one location south of Third Portage lake, but its pale colour suggests it is a zincian staurolite, unreliable as a metamorphic index mineral. Sillimanite in quartzite, and garnet-biotite-(?)sillimanite in metagreywacke, were observed in the southeastern part of the map area on Tehek Lake, consistent with an increase in grade to upper amphibolite facies as noted by Schau (1983). South of Amarulik Lake, the contact between greywacke and mafic volcanic rocks is an easterly trending, schistose, high-strain zone, continuous with a fault across which map units show up to 1500 m of apparent sinistral offset (Fig. 2, between localities B and D). The mafic rocks appear to have assemblages typical of greenschist facies, suggesting an abrupt change in metamorphic grade across the fault.

In a large part of the area, including the Amarulik structural dome, amphibole and garnet porphyroblasts tend to be randomly or weakly oriented, and to overgrow layering and foliation. In the southeast, amphibole in amphibole-plagioclase gneiss and sillimanite in quartzite define schistosity and strong linear fabrics.

## DISCUSSION

We interpret the supracrustal rocks in the Amarulik Lake area as quartzofeldspathic greywacke, rather than intermediate volcanic and volcaniclastic rocks (Henderson and Henderson, 1994). Our field evaluation of the significance of volcanogenic components in the greywacke suggests that these represent reworked transported material that is mixed with material from other sources. The recognition of 'amphibole hornfels' associated with iron-formation and metacarbonate suggests that amphibole-bearing rocks intercalated with greywacke largely reflect input from chemical sedimentary sources, rather than the presence of volcanic rocks. The identification of amphibole hornfels may help to resolve other lithological problems in the Woodburn Lake group. For example, some rocks previously identified as metagabbro and leucogabbro (Zaleski et al., 1997b) may, in fact, be amphibole hornfels. The amphibole hornfels extending from Tehek Lake to Third Portage lake, previously grouped with intermediate volcanic and volcaniclastic rocks (Henderson and Henderson, 1994), continues north to the Meadowbank gold deposits, suggesting that these rocks of mixed chemical and clastic sedimentary parentage may be important constituents in the immediate setting of iron-formation-hosted gold mineralization. The petrogenesis of amphibole hornfels and associated chemical sedimentary rocks are the subject of continuing investigation (R. L'Heureux, M.Sc. in progress).

The predominance of greywacke in the area is critical to the stratigraphic interpretation of the Woodburn Lake group. Our new mapping shows that the ca. 2.8 Ga volcanic rock dated by Roddick et al. (1992) is in fact a clastic sedimentary rock. Roddick et al. (1992) dated two samples from adjacent outcrops (southwest of locality D, Fig. 2), one described as massive dacite quartz-porphyry, and the other as psammitic tuffaceous metagreywacke overlying the dacite. Our mapping and resampling of the sites shows that both samples are greywacke, and that zircons separated from them should be treated as detrital grains. Thus, the published U-Pb zircon geochronology does not determine the depositional age of the sequence.

The distribution of lithological units and the orientations of foliations, including those in the Amarulik structural dome, suggest macroscopic fold interference patterns. Ongoing work directed at understanding these will be critical to resolving regional correlations and relationships between the Pipedream–Third Portage lakes area and the Whitehills Lake area, and the sequence of deformation. Mineral assemblages between Amarulik Lake and Third Portage lake are typical of amphibolite-facies metamorphic grade, whereas north of the Third Portage lake, chloritoid-bearing, greenschist-facies assemblages are prevalent (Ashton, 1988; Zaleski et al., 1997a). This observation suggests that the Meadowbank gold deposits may lie near the greenschist-amphibolite transition.

## ACKNOWLEDGMENTS

The Woodburn Project was initiated by Jack and Mariette Henderson. Collaborators in the broader mapping and research program include John Kerswill and Bruce Kjarsgaard, Mineral Resources Division, and George Jenner, Memorial University. Warner Miles, Geophysical Data Centre, provided various aeromagnetic maps and is involved in their ongoing interpretation. The field program operated out of the Meadowbank camp of Cumberland Resources Ltd., and Brian Alexander, Roger March, and Ewald Gossner of Cumberland are gratefully acknowledged for their co-operation and logistical help during the field season. Rob Rainbird and Simon Hanmer are thanked for reviewing the manuscript.

## REFERENCES

**Annesley, I.R.**
1989: Petrochemistry of the Woodburn Lake Group komatiite suite, Amer Lake, N.W.T., Canada; Ph.D. thesis, University of Ottawa, Ottawa, Ontario, 406 p.

**Armitage, A.E., James, R.S., and Goff, S.P.**
1996: Gold mineralization in Archean banded iron formation, Third Portage Lake area, Northwest Territories, Canada; Exploration Mining Geology, v. 5, p. 1–15.

**Ashton, K.E.**
1988: Precambrian geology of the southeastern Amer Lake area (66H/1), near Baker Lake, N.W.T.; Ph.D. thesis, Queen's University, Kingston, Ontario, 335 p.

**Davis, W.J. and Zaleski, E.**
in press: Geochronological investigations of the Woodburn Lake group, Western Churchill Province: preliminary results; *in* Radiogenic Age and Isotopic Studies: Report 11; Geological Survey of Canada, Paper 98-2.

**Donaldson, J.A.**
1966: Geology, Schultz Lake, District of Keewatin; Geological Survey of Canada, Preliminary Map 7-1966, scale 1:253 440.

**Fraser, J.A.**
1988: Geology of the Woodburn Lake map area, District of Keewatin; Geological Survey of Canada, Paper 87-11, 12 p.

**Gall, Q., Peterson, T.D., and Donaldson, J.A.**
1992: A proposed revision of Early Proterozoic stratigraphy of the Thelon and Baker Lake basins, Northwest Territories; *in* Current Research, Part C; Geological Survey of Canada, Paper 92-1C, p. 129–137.

**Geological Survey of Canada**
1990: Advance release of high resolution 1:20 000 aeromagnetic vertical gradient, total field and VLF-EM survey, Whitehills Lake area, Northwest Territories / Diffusion preliminaire de leves aeromagnetiques du champ total, gradient vertical et d'un leve EM de type TBF, region du Lac Whitehills; Geological Survey of Canada, Open File 2205, scale 1:20 000.

**Henderson, J.R. and Henderson, M.N.**
1994: Geology of the Whitehills-Tehek Lakes area, District of Keewatin, Northwest Territories (parts of 56D, 56E, 66A, and 66H); Geological Survey of Canada, Open File 2923, scale 1:100 000.

**Henderson, J.R., Henderson, M.N., Pryer, L.L., and Cresswell, R.G.**
1991: Geology of the Whitehills-Tehek Lakes area, District of Keewatin: an Archean supracrustal belt with iron-formation-hosted gold mineralization in the central Churchill Province; *in* Current Research, Part C; Geological Survey of Canada, Paper 91-1C, p. 149–156.

**Heywood, W.W. and Schau, M.**
1981: Geology of the Baker Lake region, District of Keewatin; *in* Current Research, Part A; Geological Survey of Canada, Paper 81-1A, p. 259–264.

**Hoffman, P.F.**
1988: United plates of America, the birth of a craton: early Proterozoic assembly and growth of Laurentia; Annual Reviews of Earth and Planetary Sciences, v. 16, p. 543–603.

**Kerswill, J.A., Goff, S.P., Wilkinson, L., Jenner, G.A., Kjarsgaard, B.A., Bretzlaff, R., and Samaris, C.**
1998: An update on the metallogeny of the Woodburn Lake group, western Churchill Province, Northwest Territories; *in* Current Research 1998-C; Geological Survey of Canada, p. 29–41.

**Kjarsgaard, B.A., Kerswill, J.A., and Jenner, G.A.**
1997: Lithostratigraphy and metallogenic implications of komatiite-banded iron-formation - felsic volcanic rocks of the Archean Woodburn Lake group, Pipedream lake, central Churchill Province, Northwest Territories; *in* Current Research 1997-C; Geological Survey of Canada, p. 101–110.

**LeCheminant, A.N., Jackson, M.J., Galley, A.G., Smith, S.L., and Donaldson, J.A.**
1984: Early Proterozoic Amer group, Beverly Lake map area, District of Keewatin; *in* Current Research, Part B; Geological Survey of Canada, Paper 84-1B, p. 159–172.

**Patterson, J.G.**
1986: The Amer belt: remnant of an Aphebian foreland fold and thrust belt; Canadian Journal of Earth Sciences, v. 23, p. 2012–2023.

**Roddick, J.C., Henderson, J.R., and Chapman, H.J.**
1992: U-Pb ages from the Archean Whitehills-Tehek lakes supracrustal belt, Churchill Province, District of Keewatin, Northwest Territories; *in* Radiogenic Age and Isotopic Studies: Report 6; Geological Survey of Canada, Paper 92-2, p. 31–40.

**Sanborn-Barrie, M.**
1994: Structural investigation of high-grade rocks of the Kramanituar complex, Baker Lake area, Northwest Territories; *in* Current Research 1994-C; Geological Survey of Canada, p. 121–133.

**Sanborn-Barrie, M., Carr, S., and Theriault, R.**
1997: 1.9 Ga metamorphism, magmatism and deformation in the Western Churchill Province: U-Pb geochronology from the Kramanituar complex, NWT; Abstract volume, Geological Association of Canada–Mineralogical Association of Canada Annual Meeting, Ottawa '97, p. A131.

**Schau, M.**
1983: Baker Lake map sheet (56D); Geological Survey of Canada, Open File 883, scale 1:125 000.

**Schau, M., Tremblay, F., and Christopher, A.**
1982: Geology of Baker Lake map area, District of Keewatin: a progress report; *in* Current Research, Part A; Geological Survey of Canada, Paper 82-1A, p. 143–150.

**Taylor, F.C.**
1985: Precambrian geology of the Half Way Hills area, District of Keewatin; Geological Survey of Canada, Memoir 415, 19 p.

**Tella, S.**
1994: Geology, Amer Lake (66H), Deep Rose Lake (66G), and parts of Pelly Lake (66F), District of Keewatin, Northwest Territories; Geological Survey of Canada, Open File 2969, scale 1:250 000.

**Tella, S., Heywood, W.W., and Loveridge, W.D.**
1985: A U-Pb age on zircon from a dacite porphyry, Amer Lake map area, District of Keewatin, NWT; *in* Current Research, Part B; Geological Survey of Canada, Paper 85-1B, 371–374.

**Zaleski, E., Corrigan, D., Kjarsgaard, B.A., Jenner, G.A., Kerswill, J.A., and Henderson, J.R.**
1997a: Preliminary results of mapping and structural interpretation from the Woodburn project, western Churchill Province, Northwest Territories; *in* Current Research 1997-C; Geological Survey of Canada, p. 91–100.

**Zaleski, E., Corrigan, D., Kjarsgaard, B.A., Kerswill, J.A., Jenner, G.A., and Henderson, J.R.**
1997b: Geology, Woodburn Lake group, Meadowbank River to Tehek Lake (66H/1, 56E/4), District of Keewatin (Nunavut), Northwest Territories; Geological Survey of Canada, Open File 3461, scale 1:50 000.

**Zaleski, E., L'Heureux, R., Duke, N., Wilkinson, L., and Davis, W.J.**
1999: Komatiitic and felsic volcanic rocks overlain by quartzite, Woodburn Lake group, Meadowbank River area, western Churchill Province, Northwest Territories (Nunavut); *in* Current Research 1999-C; Geological Survey of Canada.

---

Geological Survey of Canada Project 970006

# Metallogeny and geology of the Half Way Hills area, central Churchill Province, Northwest Territories (Nunavut)[1]

J.A. Kerswill, B.A. Kjarsgaard, R. Bretzlaff[2], G.A. Jenner[3], and C. Samaras[3]

Mineral Resources Division, Ottawa

*Kerswill, J.A., Kjarsgaard, B.A., Bretzlaff, R., Jenner, G.A., and Samaras, C., 1999: Metallogeny and geology of the Half Way Hills area, central Churchill Province, Northwest Territories (Nunavut);* in *Current Research 1999-C; Geological Survey of Canada, p. 29–41.*

**Abstract:** The Half Way Hills supracrustal domain contains a complex 'assemblage' including extensive pillowed tholeiitic basalt, minor komatiitic basalt, minor felsic volcanic rocks as well as greywacke, quartzite, conglomerate, and extensive pyritic iron-formation. Two distinct volcanic belts have been tentatively identified.

The northern volcanic belt contains a diverse metal endowment hosted largely by deformed quartz-carbonate veins variably enriched in gold, silver, and base metals. Gold, polymetallic, and Cu-Pb-Zn occurrences are spatially associated with elliptical granitoid plutons, typically possess high Ag/Au ratios, and locally contain anomalous concentrations of one or more of Mo, W, Bi, Sb, and As. Anomalous concentrations of gold have also been identified in carbonate-bearing iron-formation and in extensive carbonate-rich alteration zones in ultramafic-mafic rocks.

Evidence to date suggests that significant metals were concentrated by synvolcanic processes, possibly linked to intrusion of the granitoid plutons.

**Résumé :** Le domaine supracrustal de Half Way Hills contient une «succession» complexe comportant de vastes étendues de basalte tholéiitique en coussins, des quantités mineures de basalte komatiitique et de roches volcaniques felsiques, ainsi que du grauwacke, du quartzite, du conglomérat et de la formation de fer pyritique répandue. Deux ceintures volcaniques distinctes y ont été reconnues provisoirement.

La ceinture volcanique septentrionale contient une gamme de métaux qui sont en grande partie encaissés dans des filons déformés de quartz-carbonate ayant des concentrations variées d'or, d'argent et de métaux communs. Des indices aurifères, des indices polymétalliques et des indices de Cu-Pb-Zn sont associés dans l'espace à des plutons granitoïdes elliptiques; ces indices ont typiquement des rapports Ag/Au élevés et, par endroits, des concentrations anomales d'un ou plusieurs des éléments suivants : Mo, W, Bi, Sb et As. Des concentrations anomales d'or ont également été relevées dans une formation de fer à carbonates et dans de vastes zones d'altération riches en carbonates dans des roches ultramafiques-mafiques.

Les données recueillies à ce jour semblent indiquer que des processus synvolcaniques, possiblement liées à l'intrusion des plutons granitoïdes, auraient contribué à la concentration des métaux.

[1] Contribution to the Western Churchill NATMAP Project
[2] formerly Mineral Resources Division, Ottawa
[3] Department of Earth Sciences, Memorial University, St. John's, Newfoundland

## INTRODUCTION

Metallogenic studies and mapping of rocks in the Half Way Hills supracrustal belt (the central portion of NTS 66 A/9) were initiated in the area adjacent to, and immediately north of, Whitehills Lake (Fig. 1). This paper is a contribution to the mineral deposits/metallogenic component of the Western Churchill NATMAP Project. Our work in the Half Way Hills area included reconnaissance lithogeochemical sampling in 1996 and 1997, detailed examination of mineral showings in 1997 and 1998, and additional mapping and sampling in 1998.

Previous work in the Half Way Hills area included bedrock mapping at 1:250 000 scale (Donaldson, 1966; Schau, 1983), 1:50 000 scale (Taylor, 1985), and 1:100 000 scale (Henderson and Henderson, 1994). P.J. Laporte visited the area in 1985 to examine the potential for economic mineralization and reported several lithogeochemical anomalies (Laporte, 1985). A number of exploration companies have searched for uranium, gold and base metals within the Half Way Hills map area since the early 1970s. Innuit prospectors from the nearby community of Baker Lake are currently active in the area.

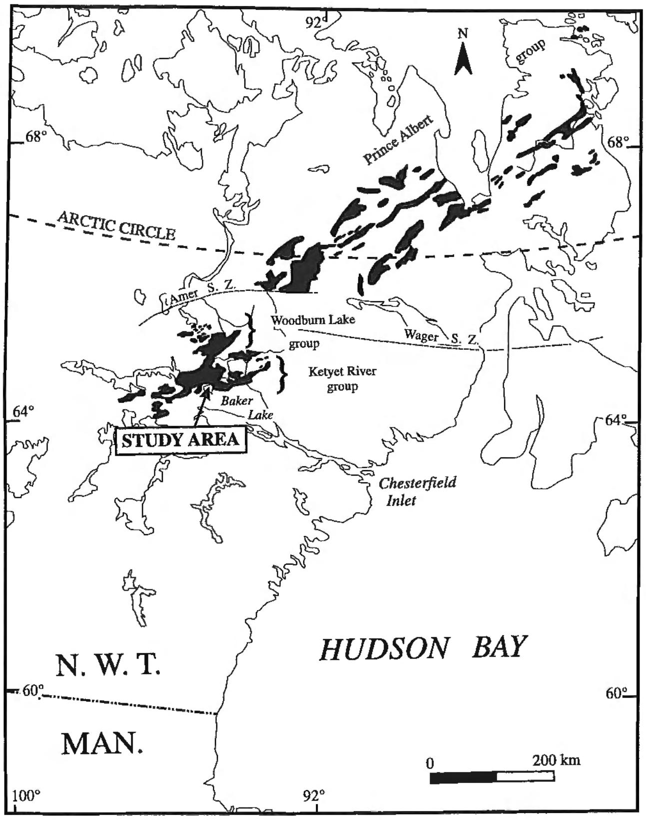


*Figure 1. Location map showing the study area in relation to the general distribution of supracrustal rocks of the Prince Albert group, Woodburn Lake group and Ketyet group in the central Churchill Province. S.Z. = shear zone.*

The overall objectives of this work are to a) develop a better understanding of the distribution and character of the supracrustal rocks, granitoid intrusive rocks, and mineralized localities; b) to identify metallogenic domains most favourable for discovery of economic deposits; c) to develop better empirical exploration guidelines for a variety of potential exploration targets; and, d) to compare the geology and mineral occurrences of this domain to the Third Portage–Pipedream lakes domain to the north, within the Archean Woodburn Lake group.

## GEOLOGY

A simplified geological map of the Half Way Hills volcanic-dominated Archean supracrustal rocks is provided in Figure 2. Field investigations and preliminary lithogeochemical work indicate that the supracrustal rocks to the north of the quartzite may belong to a different sequence/package than those within the quartzite. These sequences are designated the northern and southern volcanic belts on Figure 2. The reader is referred to Taylor (1985) and Henderson et al. (1991) for additional details of the regional geology.

### *Northern volcanic belt*

Previous mapping described the northern volcanic belt as being dominated by pillow basalt, with minor komatiite, felsic volcanic rocks, and greywacke (Taylor, 1985; Henderson et al., 1992). New mapping, however, indicates much greater internal complexity in the basic volcanic rocks. At the northeastern margin of the northern volcanic belt, komatiite (*sl*) outcrops over a true width of 10–35 m. These rocks are quite variable in appearance, e.g. orange-brown, spinifex-textured flows (Fig. 3a); grey, fine-grained, massive flows; and grey-black, polyhedral, jointed flows. Flow morphology and textural characteristics (terminology of Arndt et al., 1977) observed include komatiite with flow-top breccia ($A_1$) zones and spinifex-textured ($A_2$) zones. These textural observations were utilized to determine a primary, south younging-facing direction, consistent with previous work (Taylor, 1985). To the south of the komatiites are brown-green, fine-grained pillow basalt units (Fig. 3b); these rocks are suggested to be stratigraphically above the komatiites, although this may not be the case as these two rock types are separated by a zone of ultramafic schist.

Further south in the belt are dark green, coarse-grained (sub-ophitic texture), pillow basalt units in addition to brown-weathering basaltic to andesitic flows which are variably plagioclase-phyric. The latter are generally observed only in the southern half of the volcanic belt. Structural complexity within the belt precludes understanding stratigraphic relationships between these different volcanic rock types at present. In the northern volcanic belt, both north and south primary facing directions are observed in pillow basalt units. This observation, coupled with recognition of fold closures in the intraflow sediments indicates preservation of $F_1$ isoclinal folds, and suggests that the map width of the supracrustal

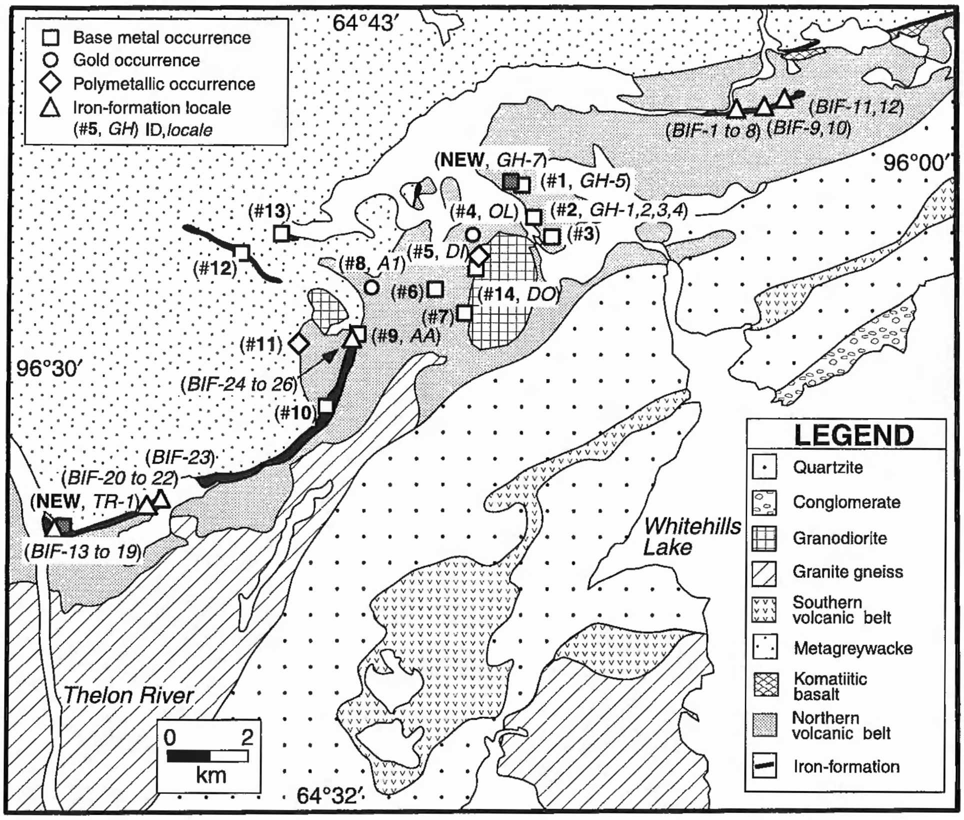


*Figure 2. Generalized geology in the vicinity of Whitehills Lake, adapted from Henderson et al. (1992) and Taylor (1985) with revisions from the results of this study. Mineral occurrences and iron-formation localities described in text are also shown on the map.*

rocks in the northern volcanic belt is greater than the true stratigraphic thickness. In addition, within the northern volcanic belt there are at least three strongly deformed (sheared and/or faulted) east-west-trending zones with associated carbonate alteration.

### Southern volcanic belt

One traverse through the volcanic rocks within the large expanse of quartzite led to recognition of a potentially distinct volcanic belt. These greenstones have a significantly different appearance from those in the northern belt; pillow basalt and komatiite are absent.

### Iron-formation

The laterally extensive iron-formation that outcrops intermittently across the study area was examined and sampled at 26 sites in three main areas, all within the northern volcanic belt. Twelve sites were from an area west of the eastern edge of the study area (BIF-1 through 12); eleven sites were from an area just east of the Thelon River (BIF-13 through 23) and three sites were from the central area in the vicinity of Occurrence #9 (BIF-24 through 26).

Three varieties of iron-formation were identified in all three areas: 1) sulphide-poor, well laminated, cherty oxide to mixed oxide-carbonate, 2) pyritic, well laminated, cherty oxide to mixed oxide-carbonate (Fig. 3c), and 3) pyrite-rich, black carbonaceous mudstone-iron-formation (Fig. 3d). Pyrite occurs most commonly as disseminated cubic grains replacing magnetite or Fe-carbonate in non-cherty layers, or as disseminated grains in cherty layers, but locally constitutes individual sulphide-rich bands/layers. There is no obvious control on the distribution of pyrite by late veins or shear zones.

Much of the iron-formation has a chaotic or breccia-like appearance, probably a combination of early synsedimentary/diagenetic slumping and later tectonic overprint (Fig. 3e). Some pyrite-rich layers appear to be tightly folded. It is often difficult to distinguish between tightly folded cherty and/or carbonate layers and deformed bedding-parallel quartz and/or carbonate veins.

Pyrrhotite and arsenopyrite were not identified during field investigations nor in examination of any cut slabs in the laboratory. Chalcopyrite was rarely observed.

## *Granodiorite-granite intrusions*

Two elliptical granodiorite-granite stocks intrude and cross-cut the rocks of the northern volcanic belt. A well developed foliation (biotite) is observed in these intrusions (Fig. 3f) and a primary magmatic fabric is well developed at their margins. Associated with these granitoid stocks are smaller intrusive bodies of quartz diorite to diorite, which were previously mapped as gabbros.

## *Preliminary lithogeochemistry*

Preliminary results from our new lithochemical studies suggest a variety of basic volcanic rock types in the northern volcanic belt. These data (Table 1, Fig. 4, 5) indicate the belt consists of komatiitic basalt, high-Mg tholeiite, high-Ti, Fe tholeiite and basaltic andesite through andesite volcanic rocks with 'arc-like' geochemical signatures. In particular, the komatiite (Taylor, 1985) is reclassified as komatiitic

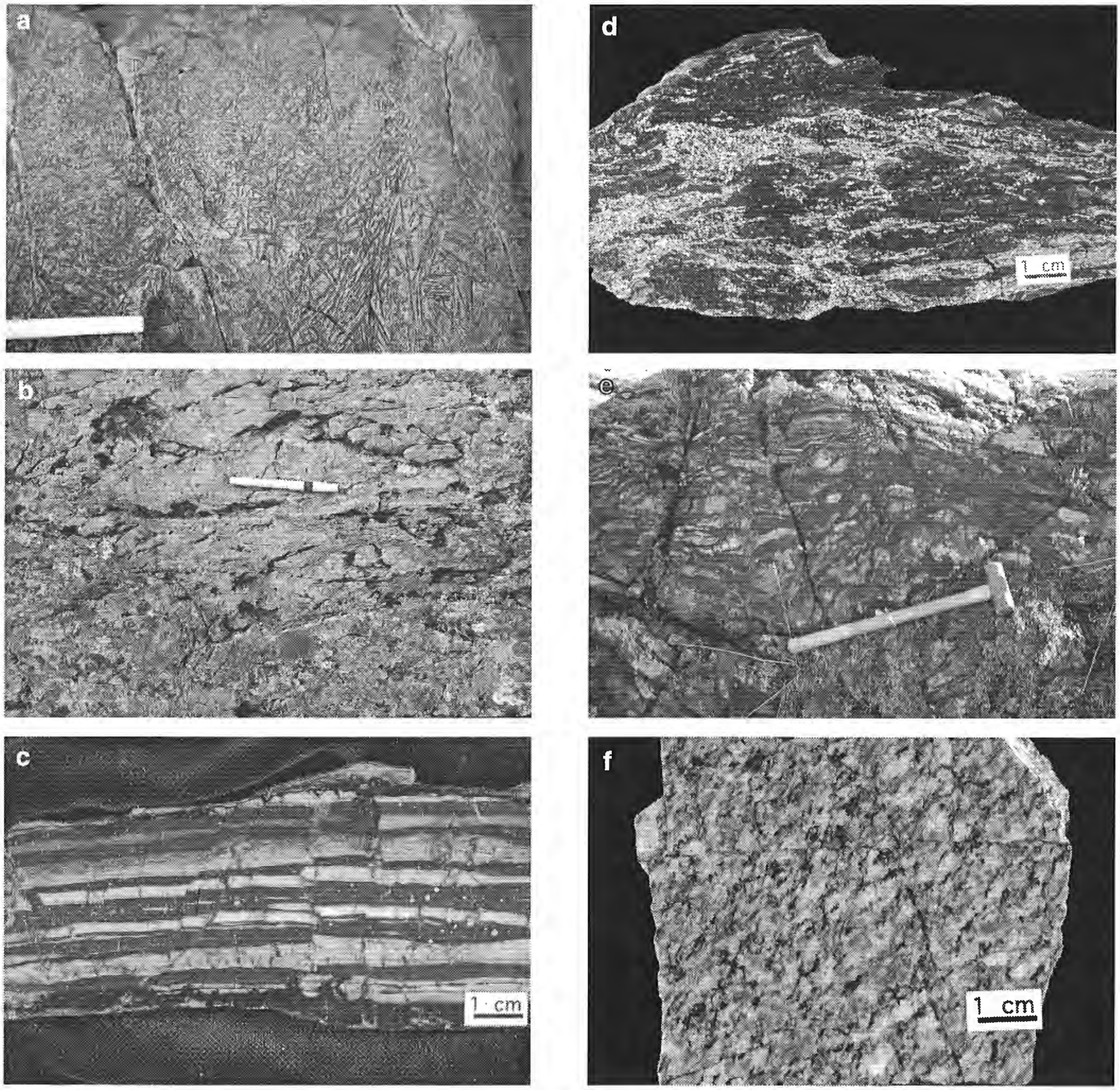


***Figure 3. a)*** *'Bird's foot' spinifex in komatiite. White scale bar 8 cm long.* ***b)*** *Pillow basalt from just south of the komatiites north of BIF-11 locality. Pen for scale bar 13.5 cm long.* ***c)*** *Pyritic cherty oxide-carbonate iron-formation from sample locale BIF-4-1.* ***d)*** *Pyritic sulphide iron-formation-mudstone from sample locale BIF-9-1.* ***e)*** *Iron-formation displaying chaotic layering from sample locale BIF-18.* ***f)*** *Foliated granite from the margin of the larger elliptical pluton in the center of the northern volcanic belt (sample locale DO-X-1).*

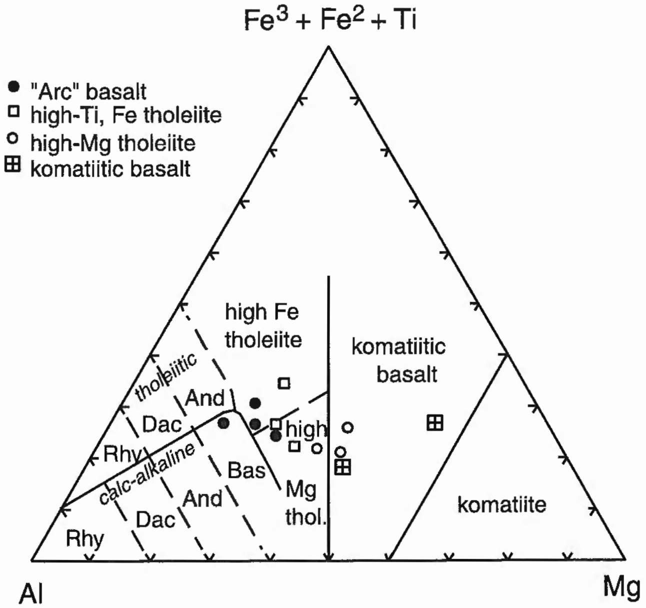


*Figure 4. Representative analyses of volcanic rocks from the Half Way Hills northern volcanic belt plotted on the Jensen cation plot (Jensen, 1976).*

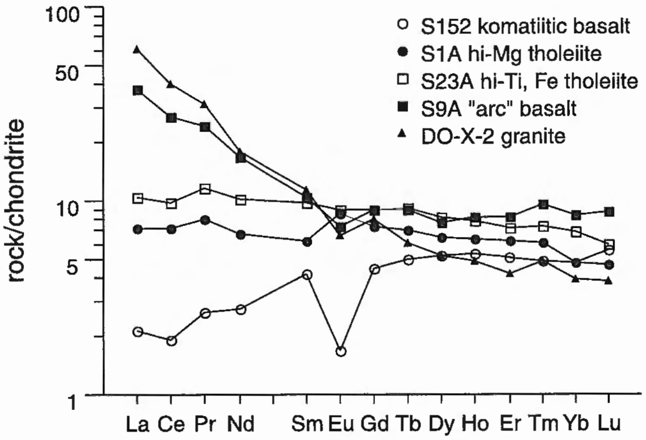


*Figure 5. Rare earth element (REE) distribution patterns for representative volcanic rocks from the Halfway Hills northern volcanic belt. Note light-REE-depleted komatiitic basalt, the flat REE profile for the two tholeiite samples and the light-REE-enriched pattern for the 'arc-like' basalt. The REE distribution pattern for a sample from the marginal phase of the larger elliptical granitoid pluton is also shown. REE normalization values from Nakamura (1974).*

**Table 1.** Preliminary geochemistry on samples from the northern volcanic belt. Major element analyses by XRF fused disc, and volatile analyses by wet chemical methods (both performed at GSC Ottawa). Trace-element analyses by XRF pressed pellet and ICP-MS at Memorial University, Newfoundland.

| Sample# Lithology | S152 Komatiitic basalt | S1A Hi-Mg tholeiite | S23A Hi-Ti,Fe tholeiite | S9A 'Arc' basalt | DO-X-2 Granite |
|---|---|---|---|---|---|
| $SiO_2$ | 43.90 | 51.50 | 47.6 | 48.60 | 74.00 |
| $TiO_2$ | 0.23 | 0.59 | 0.94 | 0.57 | 0.16 |
| $Al_2O_3$ | 6.90 | 12.70 | 14.20 | 13.10 | 13.00 |
| $Fe_2O_3$ | 1.70 | 1.60 | 2.00 | 1.10 | 0.80 |
| FeO | 12.10 | 7.20 | 7.6 | 8.40 | 1.20 |
| MnO | 0.20 | 0.18 | 0.16 | 0.14 | 0.03 |
| MgO | 15.57 | 10.69 | 8.25 | 6.54 | 0.64 |
| CaO | 15.00 | 9.35 | 8.85 | 8.06 | 2.30 |
| $Na_2O$ | 0.00 | 2.60 | 1.80 | 2.50 | 3.30 |
| $K_2O$ | 0.01 | 0.59 | 0.03 | 1.04 | 2.27 |
| $P_2O_5$ | 0.01 | 0.05 | 0.08 | 0.06 | 0.05 |
| $CO_2$ | 0.20 | 0.40 | 4.10 | 6.00 | 0.70 |
| $H_2O$ | 4.40 | 2.90 | 4.90 | 4.40 | 1.10 |
| St | 0.08 | 0.00 | 0.00 | 0.00 | 0.00 |
| TOTAL | 100.30 | 100.40 | 100.50 | 100.50 | 99.60 |
| Li | 21 | 19.03 | 40.71 | 31.48 | 4.45 |
| Rb | 1.04 | 16.60 | 0.55 | 27.16 | 79.46 |
| Cs | 0.28 | 0.20 | 0.04 | 0.95 | 1.28 |
| Sr | 6.7 | 107.7 | 318.9 | 100.25 | 95.47 |
| Ba | 34 | 262 | 13 | 422 | 626 |
| Nb | 0.68 | 2.1 | 2.5 | 3.4 | 7.87 |
| Zr | 13.8 | 33.2 | 38.8 | 67.5 | 102.9 |
| Hf | 0.65 | 0.92 | 1.17 | 2.02 | 3.18 |
| Th | 0.06 | 0.23 | 0.35 | 2.91 | 11.32 |
| U | 0.01 | 0.05 | 0.07 | 0.8 | 2.36 |
| Pb | 0 | 0.72 | 4.91 | 17.3 | 12.89 |
| Ni | 2086 | 214 | 119 | 80 | 0 |
| Cr | 3351 | 618 | 1463 | 24 | 0 |
| V | 140 | 243 | 258 | 243 | 19 |
| Zn | 62 | 22 | 73 | 89 | 0 |
| Cu | 25 | 70 | 34 | 67 | 26 |
| Sc | 18 | 50 | 51 | 30 | 0 |
| La | 0.71 | 2.39 | 3.47 | 12.38 | 20.17 |
| Ce | 1.67 | 6.18 | 8.45 | 23.5 | 34.73 |
| Pr | 0.31 | 0.94 | 1.34 | 2.85 | 3.7 |
| Nd | 1.74 | 4.3 | 6.37 | 10.52 | 11.22 |
| Sm | 0.86 | 1.27 | 1.99 | 2.12 | 2.3 |
| Eu | 0.13 | 0.66 | 0.69 | 0.57 | 0.51 |
| Gd | 1.24 | 2.03 | 2.46 | 2.5 | 2.23 |
| Tb | 0.24 | 0.34 | 0.44 | 0.43 | 0.29 |
| Dy | 1.8 | 2.21 | 2.84 | 2.66 | 1.77 |
| Ho | 0.38 | 0.45 | 0.56 | 0.58 | 0.35 |
| Er | 1.17 | 1.39 | 1.63 | 1.86 | 0.94 |
| Tm | 0.15 | 0.19 | 0.23 | 0.3 | 0.15 |
| Yb | 1.05 | 1.04 | 1.51 | 1.83 | 0.86 |
| Lu | 0.19 | 0.16 | 0.2 | 0.3 | 0.13 |
| Y | 11.27 | 14.37 | 17.28 | 19.37 | 11.15 |
| Ga | 7 | 10 | 11 | 16 | 15 |
| Mo | 0.27 | 0.69 | 0.2 | 0.12 | 0.44 |

Values of major elements in wt. %, values of trace elements in ppm.

basalt, and the basalt is subdivided into three groups on the basis of their major- and trace-element geochemistry. Geochemistry on sample DO-X-2 from the margin of the central elliptical intrusion (Table 1, Fig. 5) suggests a potential affinity with the 'arc-like' basaltic andesite to andesitic volcanic rocks.

## MINERAL OCCURRENCES

Fourteen mineral occurrences were identified in NTS 66 A/9 during a recent compilation of public-domain information (assessment reports filed by exploration companies and published maps, reports, and open files by government agencies). These occurrences have been subdivided into three classes based on metal endowment: 1) gold occurrences containing reported visible gold and/or 2 ppm or more gold, but lacking anomalous concentrations of base metals, 2) base-metal occurrences containing visible base-metal sulphide minerals and/or about 1000 ppm or more Cu, and/or Zn, and/or Pb, and/or Ni, but lacking gold, and, 3) polymetallic occurrences containing significant Au, Pb, and/or Zn. Three of the base-metal occurrences (#9, #10 and #12) are defined on the basis of anomalous Cr and Ni. Information pertinent to the metal endowment of the occurrences as compiled from previous work is presented in Table 2. The mineral occurrences are plotted on Figure 2.

The seven Cu-Pb-Zn occurrences, two polymetallic occurrences, and two gold occurrences all appear to be spatially associated (within 2 km) with the elliptical granitoid intrusions near the centre of the northern volcanic belt. Six of the occurrences lie less than 1 km from the contact of the larger of the two intrusions. The #5 and #14 occurrences are along the western contact of the larger intrusion.

### *Highlights of field and petrographic investigations linked to mineral occurrences*

Visits were made to nine of the occurrences listed in Table 2. All of the occurrences that were examined in the field contain quartz-rich veins, many of which are carbonate bearing. Several generations of veins appear to be present in some occurrences. Sulphide minerals typically occur in the veins, but may occur as disseminated grains within the wall rocks. Veins are typically narrow (<20 cm) and many do not persist for more than a few metres along strike. Most veins appear to be folded and overprinted by penetrative fabrics (Fig. 6a, b).

Most of the mineral occurrences are hosted by mafic volcanic rocks and show carbonatization in the immediate vicinity of the veins. However, base-metal occurrences #1 and #9 are developed within extensive brown-weathering, strongly foliated, carbonate-rich zones containing complex quartz-carbonate vein stockworks and localized concentrations of green mica (Fig. 6c). These zones were described in the field as possibly altered ultramafic-mafic rocks, largely because of the greenish tinge caused by the mica. The assessment reports

**Table 2.** Information on mineral occurrences in NTS 66 A/9. Sources of information are Department of Indian Affairs and Northern Development assessment reports 060660 (#11, #13), 081438 (#1, #2, #3, #9, #10, #11), 081938 (#4, #5, #6, #7), 082136 (#5, #8) and Economic Geology Report 1985-11 (Laporte, 1985) for #12.

| ID | Type | Commodities | Minerals | Name | New Sample ID | Comment | Previously Reported High Assays |
|---|---|---|---|---|---|---|---|
| 1 | Base metal | Pb-Zn-Ag | sph-gal | E of Greyhound Lk -1 | GH-5 | qtz carb veins in fuschite schist/"BIF" | Zn: 8020 ppm; Pb: 7530 ppm; Ag: 35 ppm; Au: 21 ppb |
| 2 | Base metal | Pb-Ti | ilmenite-po-py | E of Greyhound Lk -2 | GH-1 to 4 | qtz carb veins in fuschite schist/"BIF" | Pb: 902 ppm; Ag: 1.5 ppm; Au: 520 ppb; Zn: 143 ppm |
| 3 | Base metal | Pb-Zn | sph-gal | E of Greyhound Lk -3 | | vein in metaseds (float of local source) | |
| 4 | Gold | Au-Ag | cpy | Olivia | OL-1, 2 | quartz veins in basalt | Au: 3300 ppb; Ag: 178 ppm |
| 5 | Polymetallic | Au-Ag-Cu-Pb (Bi) | py, minor cpy, gal | Dingo | DI-1 to 4 | qtz veins along margin of intrusion | Au up to 126 ppm; Ag up to 36 ppm |
| 6 | Base metal | Ag-Cu | cpy | Southwest of Dingo | | quartz vein stockwork in basalt | Ag: 7.2 ppm; Au: 84 ppb |
| 7 | Base metal | Pb-Cu-Ag | tr. gal-cpy | South of Dingo | | qtz vein along granite-basalt contact | Ag: 3.6 ppm; Au:34 ppb |
| 8 | Gold | Au-Ag | ? | Allen 1 | Al-1 | "BIF" ?? | Au: 6.46 ppm; Ag: 66 ppm |
| 9 | Base metal | Cr-Ni | ? | S 28 | AA-1, 2 | qtz carb veins in fuschite schist | Cr: 1920 ppm; Ni: 650 ppm; Pd: 100 ppb |
| 10 | Base metal | Cr-Ni | ? | S 20 | | qtz carb veins in fuschite schist/"BIF" | Cr: 2800 ppm; Ni: 540 ppm; Pd: 100 ppb |
| 11 | Polymetallic | Pb-Zn-Cu-Au | gal-sph-cpy | South of Dagger Lake | | volcanic rocks ?? | Pb: 60000 ppm; Zn: 19000 ppm; Cu: 900 ppm; Au: 4.11 ppm |
| 12 | Base metal | Ni | ? | N end Dagger Lake | | BIF | Ni: 1270 ppm; Zn: 106 ppm; Ag: 0.4 ppm; Au: < 5 ppb |
| 13 | Base metal | Ag-Pb-Ni | py-po?? | W end Greyhound Lk | | BIF | Ag: 17.1 ppm; Pb: 800 ppm; Ni: 1000 ppm |
| 14 | Base metal | Pb | gal | Donaldson vein | DO-1, 2 | qtz carb vein system near intrusion | |
| NEW | Base metal | Pb-Zn-Ag-Cu | gal-sph-cpy | GH-7 locale | GH-7 | qtz carb veins in volcanic rocks | Pb: 77250 ppm; Zn: 9700 ppm, Ag: 57.1 ppm; Cu: 3160 ppm |
| NEW | Base metal | Ni-Cr | py | TR-1 locale | TR-1 | qtz carb vein stock-work in fuschite schist | Ni: 1780 ppm; Cr: 1720 ppm |

Abbreviations: sph – sphalerite, gal – galena, po – pyrrhotite, py – pyrite, cpy – chalcopyrite, BIF – iron-formation for occurrences #1, #2 and #10 refer to such rocks as calc-silicate fuchsite schist with carbonate iron-formation (Table 2). However, our field investigations did not confirm the presence of true chemical sedimentary rocks (carbonate iron-formation) at occurrences #1 and #2.

A carbonate-rich alteration zone remarkably similar to that at occurrence #1 was found at the TR-1 locale just northeast of the carbonate iron-formation near the Thelon River.

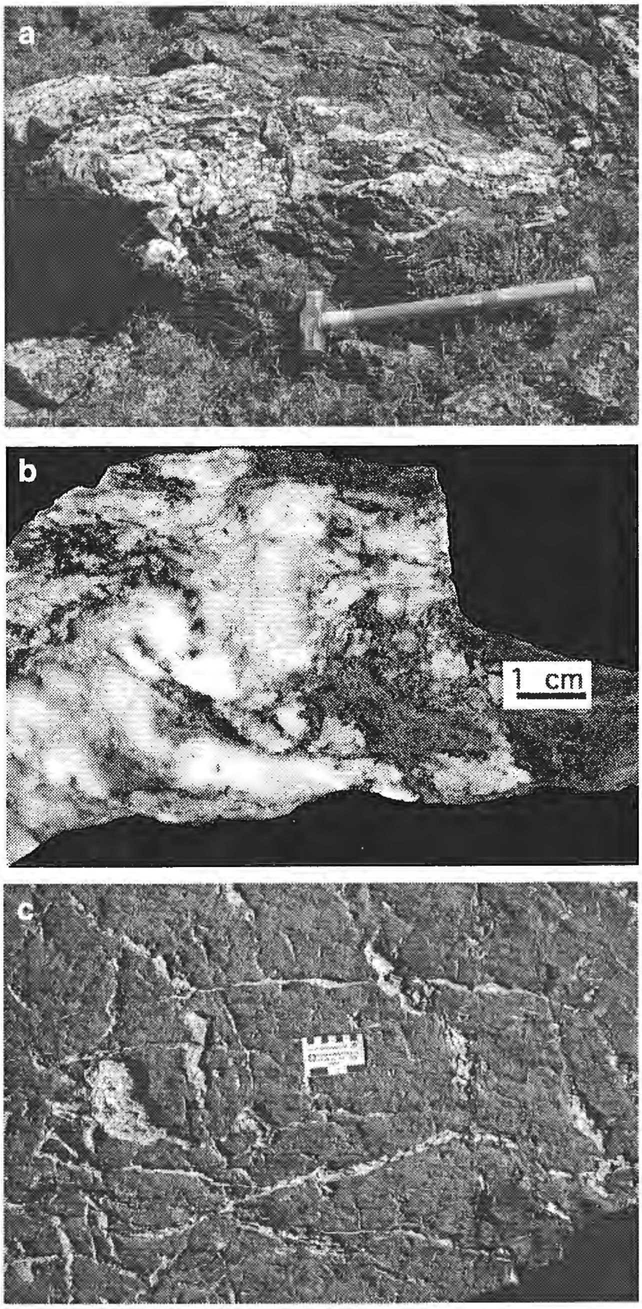


*Figure 6.* ***a)*** *Deformed quartz-carbonate vein system from Occurrence #14 (DO-2 locale).* ***b)*** *Deformed quartz-rich vein from Occurrence #5 (DI-1 locale).* ***c)*** *Carbonate-rich alteration zone with deformed vein stockwork at Occurrence #1 (GH-5 locale).*

### *Lithogeochemical investigations pertinent to mineral occurrences*

Forty-five of the 167 samples that were submitted for lithogeochemical analysis returned anomalous concentrations of one or more elements. Selected data on these samples are presented in Table 3. Some highlights are presented in the following text.

The greatest gold assays were from the vein-bearing carbonate-rich alteration zone developed in ultramafic-mafic rocks at Occurrence #9 (612 ppb from locale AA-1; Fig. 7a) and from a carbonate-rich iron-formation at locale BIF-13 (414 ppb from KZ-97-BIF-13-2; Fig. 7b). Gold values greater than 100 ppb were obtained on 10 more samples from three additional locales (occurrences #4 and #2 and the GH-7 locale).

All five vein samples collected from the GH-7 locale indicate anomalous concentrations of Pb, Zn, Ag, Cu, Sb, and Se. This data indicate that the GH-7 locale qualifies as a new base-metal occurrence.

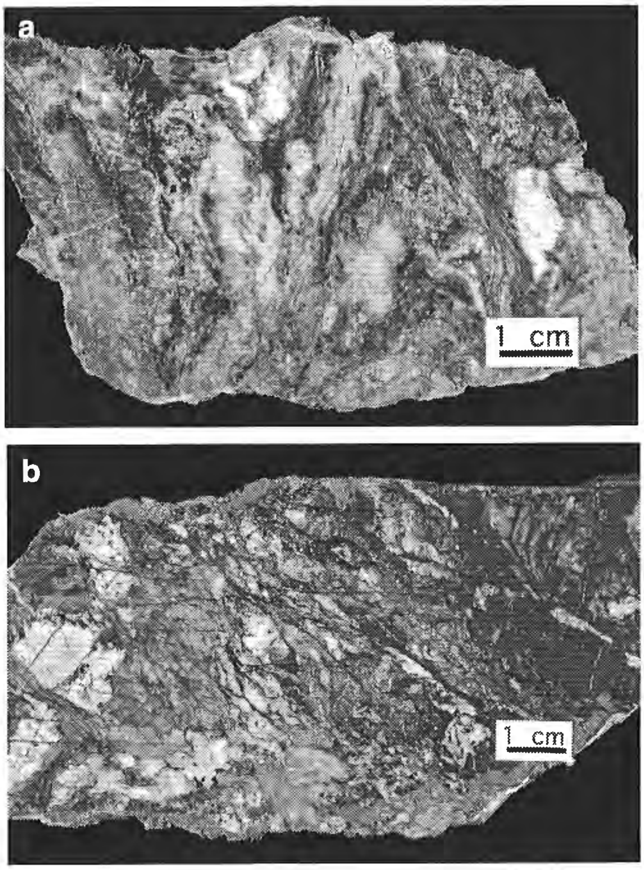


*Figure 7.* ***a)*** *Sample of vein-bearing carbonate-rich alteration zone in mafic-ultramafic volcanic rocks with anomalous gold (Occurrence #9, AA locale).* ***b)*** *Sample of pyrite-bearing carbonate-oxide iron-formation (BIF-13-2) that returned assay of 414 ppb Au.*

Anomalous values for W were obtained in samples from two occurrences (#5 and #2: up to 4770 and 2670 ppm, respectively). Anomalous Mo was also detected in these occurrences (#5: 24 ppm; #2: up to 81 ppm).

Arsenic values of greater than 600 ppm were detected in samples from one Cu-Pb-Zn occurrence and two Ni-Cr occurrences. The anomalous arsenic in the former is accompanied by anomalous W and Mo (*see* above). All samples of variably pyritic oxide-carbonate iron-formation returned values less than 100 ppm As with most less than 20 ppm. However, samples of pyritic iron-formation-mudstone contained up to 322 ppm with many values greater than 40 ppm.

Most samples from the occurrences that were identified in the field as being hosted by probable altered ultramafic-mafic rocks returned assays that were high in Ni, Cr, and Mn as well as in Mg and Ca. It is noteworthy that the TR-1 locale appears to qualify as a new base-metal occurrence because of its high Ni and Cr contents (Ni and Cr greater than 1000 ppm in four samples).

Manganese appears to be a good indicator of the presence of iron-rich carbonate. Samples of mixed oxide-carbonate iron-formation with recessively weathered brownish carbonate layers commonly contain greater than 3000 ppm Mn. Samples of carbonate-rich alteration zones developed in ultramafic-mafic rocks also generally possess greater than 3000 ppm Mn. Samples without visible carbonate typically contain less than 1000 ppm Mn. Other elements that are consistently enriched in samples with iron carbonate are Ca and Mg. This strongly suggests that the iron-bearing carbonate is ankeritic.

Although not apparent in Table 3, samples of the pyritic iron-formation-mudstone contain, as expected, significantly more Al, Ti, and Zr than either the sulphide-poor or sulphide-rich oxide-carbonate iron-formation.

Bivariate plots have been utilized to help characterize the metal endowment of the different types of occurrences (polymetallic, gold, base metal) and iron-formation. A plot of Au vs. Ag (Fig. 8a) indicates that despite a wide range in both gold and silver contents, most samples from the study area possess high Ag/Au ratios. There is a strong direct relationship between Au and Ag for samples from gold occurrences (circles) and Cu-Pb-Zn occurrences (squares). Samples from Ni-Cr occurrences (pentagons) are relatively low in Ag, possess greatly variable Ag/Au ratios, and tend to plot in the same compositional field as iron-formation samples.

Moderate to strong correlations between Au and S are apparent in Figure 8b for samples from Cu-Pb-Zn, gold, and polymetallic occurrences, but not for iron-formation. The lack of direct relationship between Au and S is most apparent in samples of pyritic sulphide iron-formation-mudstone; those samples with the greatest S contain less than 1 ppb Au.

A plot of Au vs. Mn (Fig. 8c) helps compare different styles of mineralization and further illustrates the relationship between gold and Mn-rich iron-carbonate (*see* above). There is significant overlap in the compositional fields for samples from Ni-Cr occurrences and samples of oxide-carbonate iron-formation. Many plot in a field defined by high Mn and enhanced Au. Most samples from gold and Cu-Pb-Zn occurrences plot in a field defined by elevated Au but low Mn. Although the two samples with the greatest gold contents contain high Mn, numerous samples of both carbonate-rich iron-formation and carbonatized ultramafic-mafic rock are low in Au. Furthermore, seven of the samples with greater than 100 ppb Au are poor in Mn.

A plot of Cu vs. Zn (Fig. 8d) indicates that a significant number of samples from gold and Cu-Pb-Zn occurrences contain enhanced concentrations of Cu and Zn. Samples from the new occurrence at the GH-7 locale contain the greatest Zn. Although numerous samples from occurrence #14 possess less than 10 ppm Cu, two samples from this occurrence returned values greater than 150 ppm Cu. Contents of Cu and Zn are below about 100 ppm for all iron-formation samples, but the pyritic iron-formation-mudstone samples consistently contain more Cu and Zn than the oxide-carbonate samples.

## METALLOGENIC IMPLICATIONS

### *Half Way Hills*

The close spatial association between the distribution of all Cu-Pb-Zn, gold, and polymetallic mineral occurrences and the two elliptical granitoid intrusions suggests a genetic link between plutonism and metal deposition. The anomalous concentrations of Ag, Cu, Pb, Zn, and Au in many of these occurrences match the metal endowment characteristic of veins commonly associated with synvolcanic porphyry-epithermal deposits (Kirkham and Sinclair, 1996; Poulsen, 1996). This suggested genetic association is also strongly supported by the anomalous concentrations of both W and Mo that were obtained in samples collected from Occurrences #2 and #5. The deformed character of the veins at numerous locales is also consistent with a possibly synvolcanic rather than late tectonic genesis for much of the mineralization in the study area.

The presence of carbonate that is apparently enriched in Ca, Mn, and Fe in not only the carbonate iron-formation samples from the western area, but also the carbonate-rich zones developed in ultramafic-mafic rocks (Occurrences #1, #9, and the newly recognized TR-1 locale) suggests a possible genetic link between the two styles of carbonate distribution. The overlap of compositional fields for samples of iron-formation and the Ni-Cr occurrences on the Au vs. Ag and Au vs. Mn plots is also consistent with this hypothesis. This implies that the extensive carbonate-rich alteration zones were developed contemporaneously with chemical sedimentation, possibly on or near the sea-floor. Although Occurrence #1 is not spatially associated with obvious carbonate iron-formation (*see* above), the TR-locale is immediately adjacent to carbonate iron-formation in the western area. Occurrence #9 is also located near pyritic oxide iron-formation in the central area, but the iron-formation samples collected at this locale appear to be carbonate poor and are not characterized by visible carbonate or by anomalous Mn, Ca,

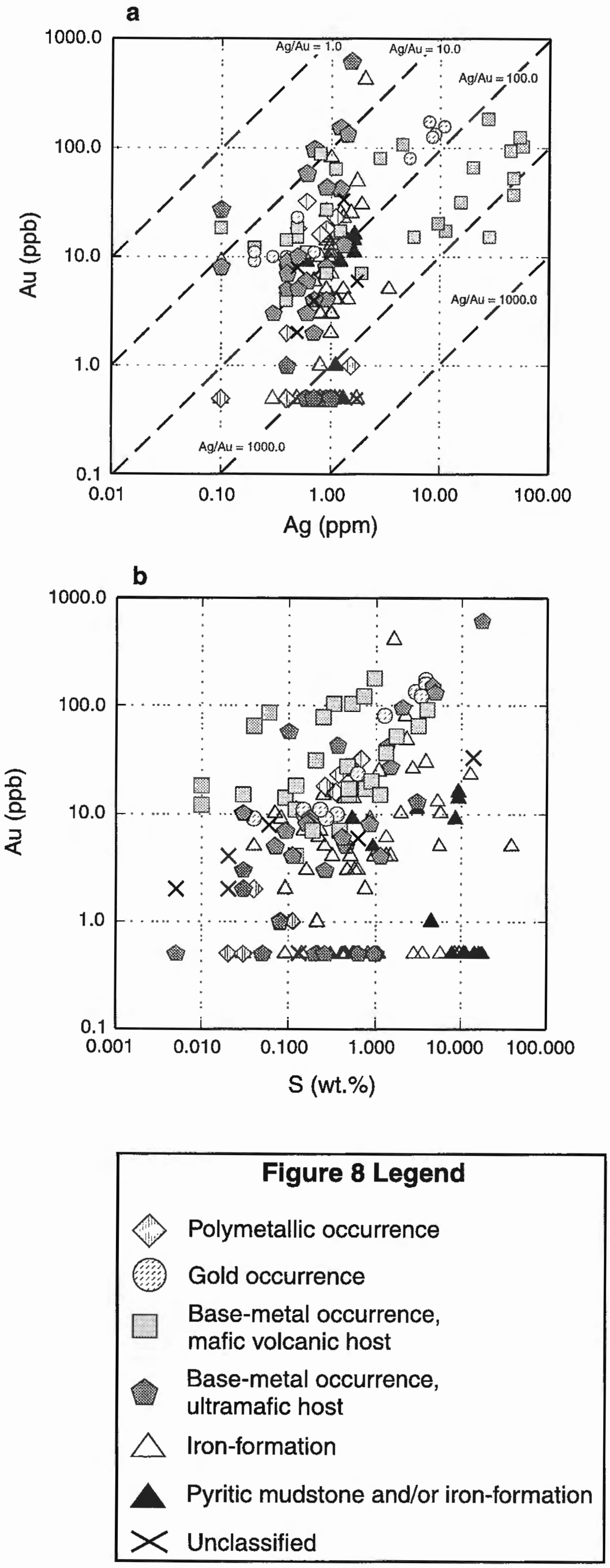


***Figure 8.***

*Bivariate plots for all samples (n=167) collected during this investigation:* ***a)*** *Au vs. Ag,* ***b)*** *Au vs. S,* ***c)*** *Au vs. Mn, and* ***d)*** *Cu vs. Zn.*

**Table 3.** Significant assays from mineral occurrences and iron-formation locales sampled during this investigation.

| Sample ID | Occurrence ID | Type | Host | S wt.% | Au ppb | Ag ppm | Cu ppm | Zn ppm | Cd ppm | Pb ppm | Co ppm |
|---|---|---|---|---|---|---|---|---|---|---|---|
| **Veins in mafic volcanic rocks** | | | | | | | | | | | |
| KZ-97-OL-1-1 | 4 | Gold | 1 | 2.98 | 133.0 | 9.0 | 8170.0 | 195.0 | 2.0 | 27 | 176.0 |
| KZ-97-OL-1-2 | 4 | Gold | 1 | 1.26 | 80.0 | 5.3 | 5810.0 | 168.0 | 2.0 | 7 | 90.0 |
| KZ-97-OL-1-3 | 4 | Gold | 1 | 3.83 | 173.0 | 7.9 | 6970.0 | 201.0 | 2.0 | 23 | 258.0 |
| KZ-97-OL-1-4 | 4 | Gold | 1 | 3.87 | 157.0 | 11.0 | 10070.0 | 217.0 | 4.0 | 20 | 202.0 |
| KZ-97-OL-1-5 | 4 | Gold | 1 | 3.42 | 123.0 | 8.5 | 8570.0 | 160.0 | 2.0 | 21 | 189.0 |
| KZ-97-A1-1-4 | 8 | Gold | 1 | 0.27 | 9.0 | 0.4 | 86.1 | 129.0 | 2.0 | 1 | 80.0 |
| KZ-97-A1-1-5 | 8 | Gold | 1 | 0.15 | 11.0 | 0.2 | 67.4 | 120.0 | 2.0 | 1 | 69.0 |
| KZ-97-GH-1-1 | 2 | Base metal | 1 | 0.33 | 104.0 | 4.4 | 3060.0 | 117.0 | 0.5 | 45 | 37.0 |
| KZ-97-GH-1-2 | 2 | Base metal | 1 | 0.96 | 181.0 | 27.6 | 7430.0 | 153.0 | 2.0 | 88 | 45.0 |
| KZ-97-GH-2-1 | 2 | Base metal | 1 | 0.25 | 79.0 | 2.8 | 2840.0 | 241.0 | 2.0 | 22 | 46.0 |
| KZ-97-GH-4-2 | 2 | Base metal | 1 | 4.08 | 93.0 | 45.1 | 44300.0 | 3480.0 | 68.0 | 268 | 36.0 |
| KZ-97-GH-4-3 | 2 | Base metal | 1 | 3.18 | 65.0 | 20.3 | 32300.0 | 3580.0 | 68.0 | 129 | 89.0 |
| KZ-97-GH-4-4 | 2 | Base metal | 1 | 0.89 | 20.0 | 9.5 | 7510.0 | 703.0 | 9.0 | 72 | 21.0 |
| KZ-97-DO-1-7 | 14 | Base metal | 1 | 0.48 | 15.0 | 5.7 | 171.0 | 22.9 | 0.5 | 612 | 30.0 |
| KZ-97-DO-1-8 | 14 | Base metal | 1 | 0.49 | 17.0 | 11.3 | 173.0 | 10.2 | 0.5 | 1260 | 17.0 |
| KZ-97-GH-7-1 | NEW | Base metal | 1 | 1.72 | 52.0 | 47.5 | 3160.0 | 8190.0 | 124.0 | 69170 | 5.0 |
| KZ-97-GH-7-2 | NEW | Base metal | 1 | 0.52 | 103.0 | 57.1 | 2110.0 | 9700.0 | 217.0 | 12420 | 7.0 |
| KZ-97-GH-7-3 | NEW | Base metal | 1 | 1.35 | 37.0 | 46.7 | 1590.0 | 3680.0 | 64.0 | 77250 | 6.0 |
| KZ-97-GH-7-4 | NEW | Base metal | 1 | 1.12 | 15.0 | 28.6 | 864.0 | 6980.0 | 108.0 | 58290 | 4.0 |
| KZ-97-GH-7-5 | NEW | Base metal | 1 | 0.73 | 124.0 | 54.4 | 2530.0 | 9610.0 | 161.0 | 19910 | 6.0 |
| KZ-97-DI-1-1 | 5 | Polymetallic | 1 | 0.04 | 2.0 | 0.4 | 299.0 | 44.9 | 0.5 | 1 | 29.0 |
| KZ-97-DI-1-2 | 5 | Polymetallic | 1 | 0.11 | 1.0 | 1.5 | 830.0 | 70.5 | 0.5 | 6 | 39.0 |
| KZ-97-DI-1-3 | 5 | Polymetallic | 1 | 0.02 | 0.5 | 0.1 | 162.0 | 53.0 | 0.5 | 1 | 28.0 |
| KZ-97-DI-3-1 | 5 | Polymetallic | 1 | 0.37 | 23.0 | 1.1 | 216.0 | 113.0 | 1.0 | 2 | 53.0 |
| KZ-97-DI-3-2 | 5 | Polymetallic | 1 | 0.67 | 32.0 | 0.6 | 339.0 | 104.0 | 0.5 | 1 | 53.0 |
| **Vein networks in carbonate-rich ultramafic/mafic volcanic rocks** | | | | | | | | | | | |
| KZ-97-GH-5-2 | 1 | Base metal | 2 | 0.01 | 0.5 | 0.7 | 52.6 | 58.1 | 2.0 | 10 | 7.0 |
| KZ-97-GH-5-3 | 1 | Base metal | 2 | 0.03 | 10.0 | 0.5 | 35.9 | 51.2 | 1.0 | 7 | 12.0 |
| KZ-97-GH-5-10 | 1 | Base metal | 2 | 0.36 | 43.0 | 0.9 | 23.6 | 130.0 | 0.5 | 6 | 9.0 |
| KZ-97-AA-1-3 | 9 | Base metal | 2 | 4.62 | 153.0 | 1.2 | 1560.0 | 36.3 | 0.5 | 14 | 67.0 |
| KZ-97-AA-1-4 | 9 | Base metal | 2 | 17.50 | 612.0 | 1.5 | 1120.0 | 30.2 | 1.0 | 19 | 86.0 |
| KZ-97-AA-1-5 | 9 | Base metal | 2 | 4.97 | 133.0 | 1.4 | 1730.0 | 37.0 | 0.5 | 6 | 70.0 |
| KZ-97-AA-2-1 | 9 | Base metal | 2 | 1.00 | 0.5 | 0.7 | 115.0 | 122.0 | 0.5 | 6 | 129.0 |
| KZ-97-AA-2-2 | 9 | Base metal | 2 | 0.97 | 0.5 | 0.9 | 112.0 | 113.0 | 0.5 | 4 | 138.0 |
| KZ-97-AA-2-3 | 9 | Base metal | 2 | 0.63 | 0.5 | 0.6 | 97.1 | 130.0 | 0.5 | 5 | 114.0 |
| KZ-97-AA-2-4 | 9 | Base metal | 2 | 0.20 | 0.5 | 0.6 | 53.0 | 70.1 | 0.5 | 1 | 137.0 |
| KZ-97-AA-2-5 | 9 | Base metal | 2 | 0.26 | 0.5 | 0.8 | 49.9 | 53.3 | 0.5 | 3 | 117.0 |
| KZ-97-TR-1-3 | NEW | . | 2 | 0.84 | 8.0 | 0.1 | 51.3 | 31.0 | 0.5 | 6 | 97.0 |
| KZ-97-TR-1-5 | NEW | . | 2 | 0.41 | 6.0 | 0.6 | 487.0 | 48.0 | 0.5 | 4 | 98.0 |
| KZ-97-TR-1-6 | NEW | . | 2 | 0.45 | 5.0 | 0.5 | 44.1 | 50.0 | 0.5 | 6 | 130.0 |
| KZ-97-TR-1-8 | NEW | . | 2 | 0.16 | 8.0 | 0.9 | 24.7 | 34.4 | 0.5 | 6 | 109.0 |
| **Sulphide-bearing iron-formation** | | | | | | | | | | | |
| KZ-97-BIF-X-1 | NEW | . | 3 | 39.50 | 5.0 | 3.3 | 32.6 | 31.8 | 16.0 | 136 | 6.0 |
| KZ-97-BIF-X-2 | NEW | . | 3 | 1.03 | 0.5 | 0.5 | 20.4 | 8.6 | 0.5 | 7 | 3.0 |
| KZ-97-BIF-13-1 | NEW | . | 3 | 3.92 | 30.0 | 1.9 | 22.9 | 53.7 | 6.0 | 19 | 28.0 |
| KZ-97-BIF-13-2 | NEW | . | 3 | 1.59 | 414.0 | 2.0 | 13.0 | 53.3 | 12.0 | 29 | 11.0 |
| KZ-97-BIF-19-2 | NEW | . | 3 | 2.21 | 81.0 | 1.0 | 5.0 | 43.0 | 5.0 | 22 | 9.0 |

Analyses performed at XRAL, Toronto; most elements by ICP-MS; Au by lead fire assay; S by Leco;
As, Sb, Bi, Te and Se by AAH70. Values of 5 ppm for Sn and W represent half the detection limit for these elements of 10 ppm. Values of 0.5 ppm for Cd and Mo represent half the detection limit for these elements of 1.0 ppm.

| Ni ppm | Cr ppm | V ppm | Mo ppm | Sn ppm | W ppm | As ppm | Se ppm | Sb ppm | Te ppm | Bi ppm | Al wt.% | Ca wt.% | Mg wt.% | Fe wt.% | Mn ppm |
|---|---|---|---|---|---|---|---|---|---|---|---|---|---|---|---|
| | | | | | | | | | | | | | | | |
| 187.0 | 84.0 | 201.0 | 0.5 | 5 | 5 | 360.0 | 7.1 | 4.3 | 0.7 | 4.6 | 8.11 | 8.33 | 1.24 | 9.06 | 779 |
| 109.0 | 79.0 | 136.0 | 0.5 | 5 | 5 | 132.0 | 3.2 | 2.4 | 0.4 | 3.2 | 6.47 | 6.29 | 1.42 | 6.21 | 725 |
| 288.0 | 91.0 | 132.0 | 0.5 | 5 | 5 | 529.0 | 10.2 | 3.9 | 0.6 | 6.1 | 6.36 | 3.74 | 2.03 | 9.80 | 840 |
| 207.0 | 119.0 | 197.0 | 0.5 | 5 | 5 | 383.0 | 9.6 | 4.4 | 0.5 | 6.6 | 7.63 | 7.47 | 1.26 | 9.54 | 755 |
| 215.0 | 73.0 | 148.0 | 0.5 | 5 | 5 | 445.0 | 5.7 | 4.1 | 0.6 | 6.1 | 6.18 | 7.04 | 1.03 | 8.13 | 654 |
| 49.0 | 7.0 | 1080.0 | 0.5 | 5 | 5 | 31.8 | 1.4 | 3.3 | 0.1 | 0.1 | 6.80 | 6.54 | 3.96 | 13.80 | 2100 |
| 45.0 | 9.0 | 1060.0 | 0.5 | 5 | 5 | 32.0 | 0.6 | 3.6 | 0.1 | 0.1 | 6.33 | 6.66 | 3.78 | 13.10 | 2050 |
| 207.0 | 77.0 | 62.0 | 2.0 | 5 | 1370 | 13.6 | 1.2 | 1.7 | 0.2 | 6.7 | 4.67 | 4.69 | 2.37 | 4.29 | 833 |
| 208.0 | 60.0 | 51.0 | 1.0 | 10 | 2670 | 74.4 | 3.4 | 2.0 | 0.4 | 47.5 | 3.81 | 3.00 | 1.76 | 4.88 | 703 |
| 67.0 | 87.0 | 203.0 | 0.5 | 14 | 5 | 32.1 | 1.6 | 1.8 | 0.1 | 5.8 | 7.99 | 3.22 | 2.86 | 9.60 | 1460 |
| 173.0 | 15.0 | 34.0 | 18.0 | 5 | 60 | 264.0 | 3.0 | 4.8 | 0.1 | 1.2 | 1.09 | 1.52 | 1.09 | 6.98 | 356 |
| 256.0 | 57.0 | 41.0 | 81.0 | 5 | 58 | 2690.0 | 2.6 | 11.9 | 0.1 | 16.3 | 1.05 | 0.98 | 1.12 | 6.40 | 333 |
| 39.0 | 24.0 | 27.0 | 9.0 | 5 | 30 | 123.0 | 1.5 | 1.4 | 0.2 | 14.6 | 0.70 | 1.73 | 0.61 | 3.47 | 308 |
| 100.0 | 73.0 | 34.0 | 0.5 | 5 | 5 | 7.4 | 1.5 | 0.1 | 0.6 | 11.7 | 1.61 | 5.35 | 2.55 | 2.44 | 835 |
| 39.0 | 14.0 | 10.0 | 5.0 | 5 | 5 | 6.4 | 2.2 | 0.1 | 1.1 | 26.6 | 0.57 | 1.57 | 0.65 | 1.10 | 265 |
| 5.0 | 5.0 | 13.0 | 0.5 | 5 | 5 | 21.3 | 108.0 | 93.6 | 1.9 | 2.1 | 0.20 | 3.56 | 1.05 | 2.24 | 724 |
| 10.0 | 9.0 | 31.0 | 0.5 | 5 | 5 | 20.0 | 22.8 | 174.0 | 0.3 | 0.5 | 0.61 | 5.57 | 1.69 | 3.33 | 1070 |
| 9.0 | 8.0 | 35.0 | 0.5 | 5 | 5 | 10.9 | 140.0 | 91.3 | 2.5 | 4.5 | 0.62 | 2.44 | 0.91 | 2.14 | 513 |
| 6.0 | 9.0 | 17.0 | 0.5 | 5 | 5 | 5.8 | 33.1 | 47.8 | 0.9 | 0.5 | 0.26 | 1.72 | 0.55 | 1.18 | 334 |
| 11.0 | 9.0 | 29.0 | 0.5 | 5 | 5 | 13.3 | 60.9 | 143.0 | 1.7 | 1.1 | 0.56 | 5.24 | 1.56 | 2.96 | 967 |
| 69.0 | 71.0 | 128.0 | 0.5 | 5 | 4770 | 7.8 | 0.1 | 0.4 | 0.1 | 0.8 | 5.91 | 6.08 | 2.49 | 3.92 | 741 |
| 95.0 | 65.0 | 169.0 | 0.5 | 5 | 23 | 11.8 | 0.3 | 0.8 | 0.1 | 0.3 | 7.41 | 7.43 | 3.53 | 5.34 | 971 |
| 80.0 | 62.0 | 149.0 | 0.5 | 5 | 1900 | 7.6 | 0.1 | 0.4 | 0.1 | 1.0 | 6.77 | 6.55 | 2.73 | 4.39 | 809 |
| 66.0 | 59.0 | 375.0 | 0.5 | 5 | 5 | 23.1 | 0.8 | 1.1 | 0.1 | 0.5 | 6.28 | 6.30 | 3.99 | 10.40 | 2090 |
| 63.0 | 42.0 | 355.0 | 24.0 | 5 | 5 | 29.4 | 1.4 | 1.1 | 0.1 | 2.7 | 8.01 | 5.86 | 3.47 | 10.40 | 1590 |
| | | | | | | | | | | | | | | | |
| 18.0 | 21.0 | 141.0 | 0.5 | 5 | 5 | 8.7 | 0.1 | 0.2 | 0.1 | 0.2 | 0.94 | 19.90 | 6.43 | 10.20 | 2780 |
| 28.0 | 15.0 | 156.0 | 0.5 | 5 | 5 | 19.5 | 0.1 | 1.0 | 0.1 | 0.3 | 1.55 | 18.90 | 6.15 | 9.79 | 2500 |
| 21.0 | 13.0 | 88.0 | 0.5 | 5 | 5 | 4610.0 | 0.2 | 4.8 | 0.2 | 0.9 | 1.36 | 10.70 | 3.29 | 8.24 | 2060 |
| 686.0 | 484.0 | 59.0 | 0.5 | 5 | 5 | 580.0 | 1.3 | 38.3 | 0.2 | 0.2 | 1.44 | 17.70 | 6.45 | 11.80 | 4950 |
| 656.0 | 223.0 | 49.0 | 0.5 | 5 | 5 | 1510.0 | 4.3 | 57.3 | 0.8 | 0.4 | 0.90 | 12.40 | 4.37 | 19.50 | 3550 |
| 698.0 | 1070.0 | 83.0 | 0.5 | 5 | 5 | 646.0 | 1.2 | 44.8 | 0.3 | 0.2 | 2.21 | 16.60 | 5.85 | 12.00 | 4620 |
| 1510.0 | 1390.0 | 114.0 | 0.5 | 5 | 5 | 131.0 | 0.9 | 2.8 | 0.1 | 0.3 | 2.92 | 9.43 | 8.30 | 7.87 | 1690 |
| 1490.0 | 1090.0 | 108.0 | 0.5 | 5 | 5 | 132.0 | 1.2 | 2.2 | 0.1 | 0.2 | 2.72 | 10.20 | 8.21 | 7.76 | 1690 |
| 1600.0 | 1600.0 | 127.0 | 0.5 | 5 | 5 | 126.0 | 1.0 | 2.4 | 0.3 | 0.3 | 3.21 | 8.15 | 8.16 | 7.68 | 1550 |
| 1950.0 | 2900.0 | 143.0 | 0.5 | 5 | 5 | 826.0 | 0.1 | 120.0 | 0.1 | 0.3 | 3.47 | 14.00 | 8.27 | 6.46 | 2210 |
| 1480.0 | 1400.0 | 130.0 | 0.5 | 5 | 5 | 654.0 | 0.1 | 87.7 | 0.1 | 0.2 | 3.08 | 13.80 | 7.72 | 5.55 | 1930 |
| 1460.0 | 1630.0 | 47.0 | 0.5 | 5 | 5 | 82.4 | 0.4 | 1.9 | 0.2 | 0.1 | 1.22 | 14.00 | 9.16 | 4.50 | 1390 |
| 1610.0 | 1720.0 | 48.0 | 0.5 | 5 | 5 | 8.9 | 0.5 | 0.5 | 0.1 | 0.1 | 1.24 | 17.10 | 10.30 | 5.05 | 3620 |
| 1780.0 | 1450.0 | 74.0 | 0.5 | 5 | 5 | 155.0 | 0.3 | 3.5 | 0.1 | 0.1 | 1.91 | 16.40 | 7.03 | 5.86 | 3270 |
| 1360.0 | 1380.0 | 79.0 | 0.5 | 5 | 5 | 159.0 | 0.2 | 3.1 | 0.2 | 0.1 | 2.23 | 16.00 | 7.58 | 5.46 | 3730 |
| | | | | | | | | | | | | | | | |
| 53.0 | 17.0 | 45.0 | 27.0 | 5 | 5 | 10.3 | 2.5 | 0.4 | 0.2 | 0.7 | 0.70 | 0.01 | 0.39 | 32.80 | 631 |
| 16.0 | 109.0 | 11.0 | 2.0 | 5 | 5 | 14.4 | 0.3 | 0.1 | 0.1 | 0.1 | 0.47 | 0.03 | 0.17 | 2.61 | 43 |
| 28.0 | 19.0 | 38.0 | 0.5 | 5 | 5 | 56.6 | 0.8 | 0.6 | 0.2 | 0.6 | 1.31 | 11.10 | 6.12 | 19.10 | 3840 |
| 14.0 | 21.0 | 43.0 | 0.5 | 5 | 5 | 21.3 | 0.8 | 0.9 | 0.1 | 0.1 | 0.97 | 6.24 | 4.11 | 28.20 | 3120 |
| 24.0 | 19.0 | 34.0 | 0.5 | 5 | 5 | 8.8 | 0.3 | 0.6 | 0.1 | 0.1 | 1.28 | 12.30 | 6.17 | 19.40 | 6210 |
| | | | | | | | | | | | | | | | |

or Au. The presence of anomalous Au in the carbonate iron-formation from the eastern area as well as at Occurrence #9 is consistent with a possible genetic link between Fe-Ca-Mn carbonate and Au. However, as previously noted, many Mn-rich samples are poor in Au.

Although it is possible to suggest that synsedimentary/synvolcanic processes contributed to metal concentration in both the metal-rich veins proximal to granitoid intrusions and the carbonate-rich iron-formation/alteration zones in ultramafic/mafic rocks, there is little evidence to indicate that the metal-rich veins were deposited at the same time as the carbonate-rich iron-formation/alteration zones. Reliable geochronological data from the granitoid plutons and the 'arc-like' felsic volcanic rocks within the northern volcanic belt would help test this possibility.

### *Regional comparisons*

Some similarities exist in metal endowment between the Half Way Hills area and the Pipedream lake–Meadowbank gold camp region (Kerswill et al., 1998), suggesting possible metallogenic linkages. A spectrum of gold, base-metal, and polymetallic occurrences are present in both areas. Sulphide-rich iron-formation is abundant in both domains. However, massive-sulphide accumulations have only been recognized in the Pipedream lake area and there are fundamental differences in the range of volcanic rock types in the two areas. True komatiite units (i.e. peridotitic komatiite with >18 wt% MgO) are only known from the Pipedream lake/Meadowbank area, were they are intimately associated with rhyolite (Kjarsgaard et al., 1997). Most other volcaniclastic rocks in the Pipedream lake–Meadowbank area are of dacite-rhyodacite-rhyolite composition; basalt and andesite volcanic rocks are not common. This contrasts sharply with the extrusive rocks in the Half Way Hills, which comprise dominantly pillow basalt and basaltic andesite, andesite with minor komatiitic basalt and rhyodacite, and rhyolite.

It is difficult to compare the iron-formation of the Half Way Hills area with that in the Pipedream lake and Meadowbank areas to the north. The general character and variable gold content of the sulphide-bearing oxide-carbonate iron-formation in the study area resemble that of pyrite-rich oxide iron-formation to the north (Kerswill et al., 1998). The metal endowment of the pyritic iron-formation-mudstone in the study area resembles that of gold-poor but base-metal-bearing, pyrrhotite-rich iron-formation and massive sulphide accumulations to the north (Kerswill et al., 1998). However, the latter are typically Mn rich, whereas the former are Mn poor. The apparent absence of pyrrhotite and arsenopyrite in iron-formation of the Half Way Hills area suggests major differences between the gold-bearing iron-formation of the study area and the gold-rich iron-formation at Meadowbank.

At the broader scale, it is possible to state that the iron-formation-hosted auriferous zones examined to date in the study area appear more similar to hybrid rather than non-stratiform or stratiform iron-formation-hosted gold deposits as described by Kerswill (1993, 1996, 1998). Work is in progress to better define the critical features of gold-bearing iron-formation.

## EXPLORATION GUIDELINES

Silver appears be a useful guide to mineralization of all types. It may be the principal metal enriched in the Half Way Hills area and is directly correlated with gold. Previous work indicated that anomalous silver was present in 7 of 14 occurrences. The lithogeochemical work undertaken in this study indicates that Ag is a component in most occurrences, including the newly reported occurrence to the east of Greyhound Lake (GH-7).

There appear to be at least three possible exploration targets for gold, including carbonate–iron-formation-hosted gold, vein-related gold hosted by carbonate-rich alteration zones developed in ultramafic-mafic rocks, and vein-related gold in mafic volcanic sequences.

As all gold, Cu-Pb-Zn and polymetallic occurrences known to date are spatially associated with the granitoid plutons in the northern volcanic belt, additional exploration concentrated in areas adjacent to these or similar plutons may prove fruitful.

Although Mn-rich carbonate is present in several samples with the greatest gold contents, Mn does not appear to be a reliable guide to gold. Work is in progress to better define those elements that may be useful pathfinders to gold.

## CONCLUSIONS

New mapping and preliminary results from lithogeochemical studies indicate much more internal complexity to the northern volcanic belt than was previously suggested. Our new data indicate the belt consists of komatiitic basalt; high-Mg tholeiite; high-Ti, Fe tholeiite; basaltic andesite through andesite volcanic rocks with 'arc-like' geochemical signatures; felsic volcanic rocks, and interflow sediments of quite variable grain size. In particular, the komatiite (Taylor, 1985) are re-defined as komatiitic basalt, and the basalt are subdivided into three groups on the basis of their major- and trace-element geochemistry.

Exploration targets include polymetallic veins, base-metal-bearing veins, gold-bearing veins, and gold in iron-formation. Silver appears to be the best exploration guide for mineral occurrences in the Half Way Hills. The spatial association of the gold, polymetallic, and Cu-Pb-Zn occurrences with the granitoid plutons, the metal endowment of these occurrences (consistently high Ag/Au ratios, locally high W, Mo, and As), as well as evidence that the veins have been deformed, are consistent with concentration of metals by processes linked to synplutonic, probably synvolcanic processes.

Two new vein-hosted base-metal occurrences were identified as a direct result of our field and lithogeochemical studies. These are the GH-7 and TR-1 locales.

Much work remains to be done to better constrain the timing of the different types of mineral occurrences in the Half Way Hills and elsewhere in western Churchill Province.

## ACKNOWLEDGMENTS

The authors thank Cumberland Resources and McChip Resources for providing access to their helicopters for this work. We also acknowledge useful discussions with Golden Hart Exploration and several Innuit prospectors. XRAL Laboratories provided timely analytical data. Richard Lancaster took the excellent photographs of rock slabs. Ian Jonasson and Charlie Jefferson provided constructive comments that helped improve the manuscript.

## REFERENCES

**Arndt, N.T., Naldrett, A.J., and Pyke, D.R.**
1977: Komatiitic and iron-rich tholeiitic lavas of Munro Township, northeast Ontario; Journal of Petrology, v. 18, p. 319–369.

**Donaldson, J.A.**
1966: Schultz Lake, District of Keewatin, Northwest Territories; Geological Survey of Canada, Map 7-1966, 1:100 000.

**Henderson, J.R. and Henderson, M.N.**
1994: Geology of the Whitehills–Tehek Lakes Area, District of Keewatin, Northwest Territories; Geological Survey of Canada, Open File 2923, scale 1:100 000.

**Henderson, J.R., Henderson, M.N., Pryer, L.L., and Cresswell, R.G.**
1991: Geology of the Whitehills–Tehek area, District of Keewatin: an Archean supracrustal belt with iron-formation-hosted gold mineralization in the central Churchill Province; *in* Current Research, Part C, Geological Survey of Canada, Paper 91-1C, p. 149–156.

**Jensen, L.S.**
1976: A new cation plot for classifying subalkalic volcanic rocks; Ontario Division of Mines, Miscellaneous Paper 66, 22 p.

**Kerswill, J.A.**
1993: Models for iron-formation-hosted gold deposits; *in* Mineral Deposit Modeling, (ed.) R.V. Kirkham, W.D. Sinclair, R.I. Thorpe, and J.M. Duke; Geological Association of Canada, Special Paper 40, p. 171–179.

**Kerswill, J.A.** (cont.)
1996: Iron-formation-hosted stratabound gold; *in* Geology of Canadian Mineral Deposit Types, (ed.) O.R. Eckstrand, W.D. Sinclair, and R.I. Thorpe; Geological Survey of Canada, Geology of Canada, no. 8, p. 367–382 (*also* Geological Society of America, The Geology of North America, v. F-1, p. 367–382).
1998: Exploration guides for iron-formation-hosted Au deposits; Extended Abstracts Volume, (ed.) G. Walton and J. Jambor, British Columbia and Yukon Chamber of Mines–Society of Economic Geologists, Pathways 98, Vancouver, p. 184–186.

**Kerswill, J.A., Goff, S.P., Wilkinson, L., Jenner, G.A., Kjarsgaard, B.A., Bretzlaff, R, and Samaras, C.**
1998: An update on the metallogeny of the Woodburn Lake Group, western Churchill Province, Northwest Territories; *in* Current Research 1998-C, Geological Survey of Canada, p. 29–41.

**Kirkham, R.V and Sinclair, W.D.**
1996: Porphyry copper, gold, molybdenum, tungsten, tin, silver; *in* Geology of Canadian Mineral Deposit Types, (ed.) O.R. Eckstrand, W.D. Sinclair, and R.I. Thorpe; Geological Survey of Canada, Geology of Canada, no. 8, p. 421–446 (*also* Geological Society of America, The Geology of North America, v. F-1, p. 421–446).

**Kjarsgaard, B.A., Kerswill, J.A., and Jenner, G.A.**
1997: Lithostratigraphy and metallogenic implications of komatiite-BIF-felsic volcanic rocks of the Archean Woodburn Lake Group, Pipedream lake, central Churchill Province, Northwest Territories; *in* Current Research 1997-C, Geological Survey of Canada, p. 101–110.

**Laporte, P.J.**
1985: Gold potential of the Ketyet River and Woodburn Lake Groups, Tehek Lake area, NWT; Department of Indian Affairs and Northern Development, Economic Geology Series 1985-11, 24 p.

**Nakamura, N.**
1974: Determination of REE, Ba, Fe, Mg, Na and K in carbonaceous and ordinary chondrites; Geochemica et Cosmochemica Acta, 38, p. 757–775.

**Poulsen, K.H.**
1996: Lode gold; *in* Geology of Canadian Mineral Deposit Types, (ed.) O.R. Eckstrand, W.D. Sinclair, and R.I. Thorpe, Geological Survey of Canada, Geology of Canada, no. 8, p. 323–328 (*also* Geological Society of America, The Geology of North America, v. F-1, p. 323–328).

**Schau, M.**
1983: A preliminary map of Baker Lake, District of Keewatin; Geological Survey of Canada, Open File 883, scale 1:50 000.

**Taylor, F.C.**
1985: Geology, Half Way Hills area, District of Keewatin; Geological Survey of Canada, Map 1602A, scale 1:50 000.

Geological Survey of Canada Project 840003WC

# Stratigraphy and paleogeography of the Paleoproterozoic Baker Lake Group in the eastern Baker Lake basin, Northwest Territories (Nunavut)[1]

R.H. Rainbird, T. Hadlari[2], and J.A. Donaldson[2]
Continental Geoscience Division, Ottawa

*Rainbird, R.H., Hadlari, T., and Donaldson, J.A., 1999: Stratigraphy and paleogeography of the Paleoproterozoic Baker Lake Group in the eastern Baker Lake basin, Northwest Territories (Nunavut);* in *Current Research 1999-C; Geological Survey of Canada, p. 43–53.*

**Abstract:** In this paper we subdivide the Paleoproterozoic South Channel and Kazan formations of eastern Baker Lake basin into four lithofacies assemblages that define a gradational continuum between coarse, proximal, alluvial fan deposits and distal, floodplain playa deposits. Facies distribution, sedimentology, and paleocurrents indicate that alluvium was derived from highlands to the east; coarse conglomerates came mainly from adjacent granulite and anorthosite of the Kramanituar complex; finer grained strata were derived from a granitic source farther to the east. Soft-sediment deformation and sedimentary breccia in the Kazan Formation and irregular contact relationships with subaerial alkalic volcanic rocks of the overlying Christopher Island Formation suggest that explosive volcanism interrupted alluvial sedimentation in eastern Baker Lake basin. Sedimentation style, asymmetric distribution of facies, possible basin margin growth faults, and association with volcanism collectively suggest that Baker Lake basin formed in a transtensional or continental rift setting.

**Résumé :** Dans la partie est du bassin de Baker Lake, les formations paléoprotérozoïques de South Channel et de Kazan sont subdivisées en quatre assemblages de lithofaciès qui définissent un continuum progressif entre des dépôts proximaux à grain grossier de cônes alluvionnaires et des dépôts distaux de playa de plaine d'inondation. La répartition des faciès, la sédimentologie et les paléocourants indiquent que les alluvions proviennent des hautes terres à l'est, que les conglomérats à grain grossier sont principalement issus de granulites et d'anorthosites adjacentes du Complexe de Kramanituar, et que les strates à grain fin dérivent d'une source granitique située plus loin à l'est. La déformation de sédiments tendres et les brèches sédimentaires dans la Formation de Kazan et le contact irrégulier avec les roches volcaniques alcalines subaériennes de la formation sus-jacente de Christopher Island laissent supposer qu'un volcanisme explosif a interrompu la sédimentation alluvionnaire dans la partie est du bassin de Baker Lake. Le style de la sédimentation, la répartition asymétrique des faciès, la présence possible de failles synsédimentaires à la marge du bassin et l'association avec le volcanisme indiqueraient que le bassin de Baker Lake s'est formé dans un milieu de transtension ou de rift continental.

[1] Contribution to the Western Churchill NATMAP Project
[2] Ottawa-Carleton Geoscience Centre, Department of Earth Sciences, Carleton University, Ottawa, Ontario K1S 5B6

## INTRODUCTION

This report is a preliminary interpretation of detailed stratigraphy and sedimentology of the Baker Lake Group observed in eastern Baker Lake basin during the summer of 1998. Work was confined mainly to outcrops of the archipelago and shores of eastern Baker Lake. The principal aim of our study was to establish the stratigraphy of the Baker Lake Group in relation to basin paleogeography, depositional setting, and provenance as a basis for documenting the tectonic evolution of Baker Lake basin. Our efforts are a contribution to the Western Churchill NATMAP Project and represent the first phase of investigation of the tectonosedimentary aspects of Paleoproterozoic (< 1.84 Ga) basins in the western Churchill geological province.

This region was originally mapped by Wright (1955) with subsequent studies of the Dubawnt Group by Donaldson (1965; 1967), detailed sedimentology of the South Channel Formation by Macey (1973), and detailed physical volcanology of the Christopher Island Formation by Blake (1980). Studies of the uranium potential of the central and eastern Baker Lake basin (e.g. Miller, 1980) include sedimentological facies descriptions of the South Channel, Kazan, and Christopher Island formations.

### *Regional geology*

The Baker Lake Group is the lowermost subdivision of the Dubawnt Supergroup (Gall, et al., 1992) and includes the South Channel, Kazan, Christopher Island, and Kunwak formations (Donaldson, 1965; LeCheminant et al., 1979). It outcrops in a series of subbasins aligned along a corridor which extends northeast from Angikuni Lake to Baker Lake (Fig. 1). Our study focuses on the South Channel and Kazan formations, a conformable succession of coarse- to fine-grained, continental redbeds, exposed primarily in the eastern part of Baker Lake basin, at the northeastern end of the corridor (Fig. 1). The South Channel and Kazan formations are unconformably to conformably overlain by the Christopher Island Formation (Donaldson, 1965), a sequence of alkalic volcanic flows and intercalated volcaniclastic rocks. Coarse, alluvial redbeds of the Kunwak Formation conformably overlie the Chistopher Island Formation mainly in the central and southeastern parts of the corridor. The Baker Lake Group is overlain by the Wharton Group, which in turn is overlain by the Barrensland Group (Gall et al., 1992; Fig. 1). The Baker Lake Group unconformably overlies variably deformed Archean and Paleoproterozoic crystalline rocks (*see* legend of Fig. 1). On the south side of Baker Lake basin it locally overlies metavolcanic rocks of the Gibson–MacQuoid greenstone belt (Tella et al., 1997).

### *Local geology*

In the main study area, at the east end of Baker Lake (Fig. 2), the Baker Lake Group unconformably overlies mylonitic granite, gabbro, and associated anorthosite of the Paleoproterozoic Kramanituar complex (Schau and Ashton, 1979; Sanborn-Barrie, 1994). At its northern boundary, along a deep creek gully, the contact has been modified by postdepositional faulting. The South Channel and Kazan formations strike roughly parallel to the margin of Baker Lake, dipping 10–15° inward. The South Channel Formation is best exposed along a northeast-trending strip parallel to the western shoreline of the Bowell Islands (Fig. 2). It also is sparsely exposed on the mainland to the north. The southwestward continuation of this strip outcrops about 25 km to the west; having been separated by approximately 7 km of right lateral strike-slip along a northeast-striking fault, prominent through the central part of Christopher Island (large island at east end of Baker Lake, Fig. 1; *see* Blake, 1980). The Kazan Formation is conformable with the South Channel Formation and is exposed in the archipelago, basinward from the unconformity (Fig. 2). The Christopher Island Formation disconformably overlies the Kazan Formation and, in contrast, displays irregular bedding attitudes with dips locally exceeding 50°. It forms most of the high hills in the archipelago, some of which are inferred to be remnant volcanoes.

## BAKER LAKE GROUP

### *Basal unconformity and regolith*

An erosional unconformity at the base of the South Channel Formation is well exposed on the western Bowell Islands (Fig. 2), where it truncates variably deformed granite and amphibolite. The unconformity surface defines a paleotopography similar to that which exists there today and can be traced intermittently for about 8 km. The unconformity is characterized by red, hematitic alteration, which mantles the paleosurface and infills a network of fractures that penetrate several metres into the basement rocks. This alteration can be seen on lakeshore exposures farther north, where the unconformity can be traced westward for several tens of kilometres from the northeast corner of the lake. Based on the inferred position of the unconformity, the present north and east shorelines of Baker Lake closely conform to the former outline of the basin. Hematitization and chemical weathering is most pronounced on iron-rich and chemically labile protoliths such as amphibolite and gabbroic anorthosite.

Where the South Channel Formation overlies paleotopographic highs it is a coarse, moderately well sorted, clast-supported conglomerate composed of locally derived clast types. In paleotopographic lows the basal conglomerate is composed of angular blocks of underlying basement rocks along with irregular fragments of carbonate, supported by a matrix of red, gritty siltstone (Fig. 3). The carbonate clasts and matrix are derived from a massive to weakly stratified unit that overlies altered basement rocks, beneath the matrix-rich conglomerate. This unit, interpreted to be a paleosol, has a well developed vertical profile best seen in an oblique lakeshore exposure on the western Bowell Islands (approx. 64°03′N; 94°14′W; “r” on Fig. 2). The profile begins with slightly rotated blocks of altered granite or amphibolite (Fig. 3). The unconformity surface and fractures in the underlying basement rock are infilled with hematite and coarse, drusy calcite cement. The disrupted zone passes upward into a zone of more disrupted basement fragments surrounded by red, cherty siltstone and pink chert. The cherty siltstone appears to be replaced by fine, pink and white carbonate, which increases in abundance upsection. The uppermost part of the paleosol is essentially a carbonate-rich zone with irregular patches of cherty, hematitic siltstone and a few small altered fragments of bedrock. Clasts of the carbonate-rich zone material have been incorporated into the basal conglomerate, supporting the idea that it is a calcrete or caliche, formed before deposition of the overlying South Channel Formation conglomerate. The weathering profile reaches a maximum thickness of about 3 m.

### *South Channel and Kazan formations*

For the purposes of our study, the South Channel and Kazan formations are considered to be facies equivalents because the field relationships described herein reflect an almost complete proximal to distal continuum related to grain size (and inferred depositional energy) between lithofacies which have been described as either South Channel or Kazan formations. For descriptive and interpretive purposes we subdivide these strata into four facies assemblages.

### Facies assemblage 1

Facies assemblage 1 equates to strata described elsewhere as South Channel Formation and comprises clast-supported, disorganized conglomerate (Gcd), clast-supported, organized conglomerate (Gco), trough-filling conglomerate (Gt), and trough cross-stratified sandstone (St).

In section T98-1 (Fig. 4), 3–8 m fining-upward cycles are common, beginning with thick, erosive-based, disorganized, cobble conglomerate (Gcd), overlain by horizontally

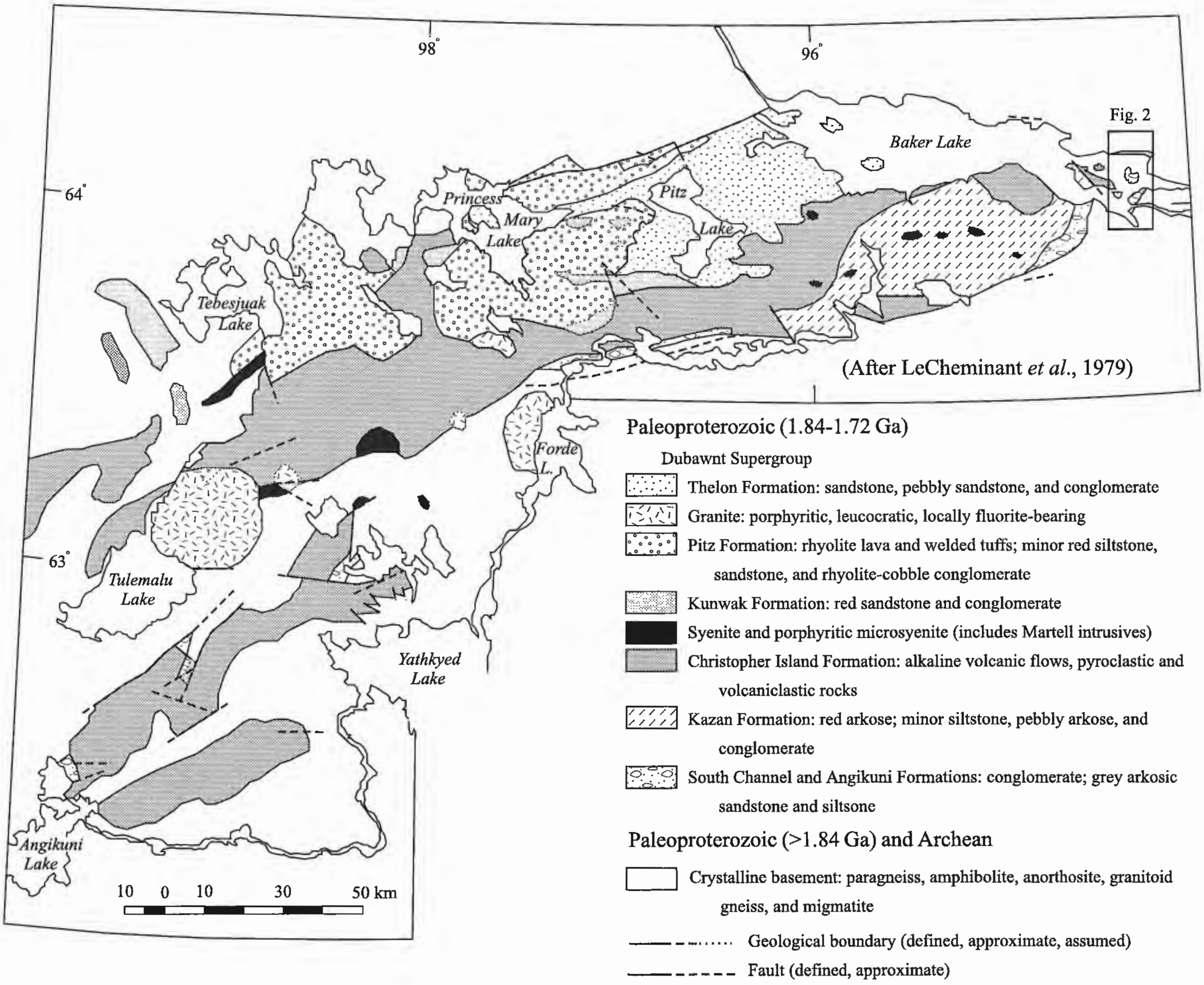


***Figure 1.** Distribution of Baker Lake Group rocks in the Baker Lake basin and smaller subbasins between Angikuni Lake and Yathkyed Lake (after LeCheminant et al., 1979). Box indicates outline of map in Figure 2.*

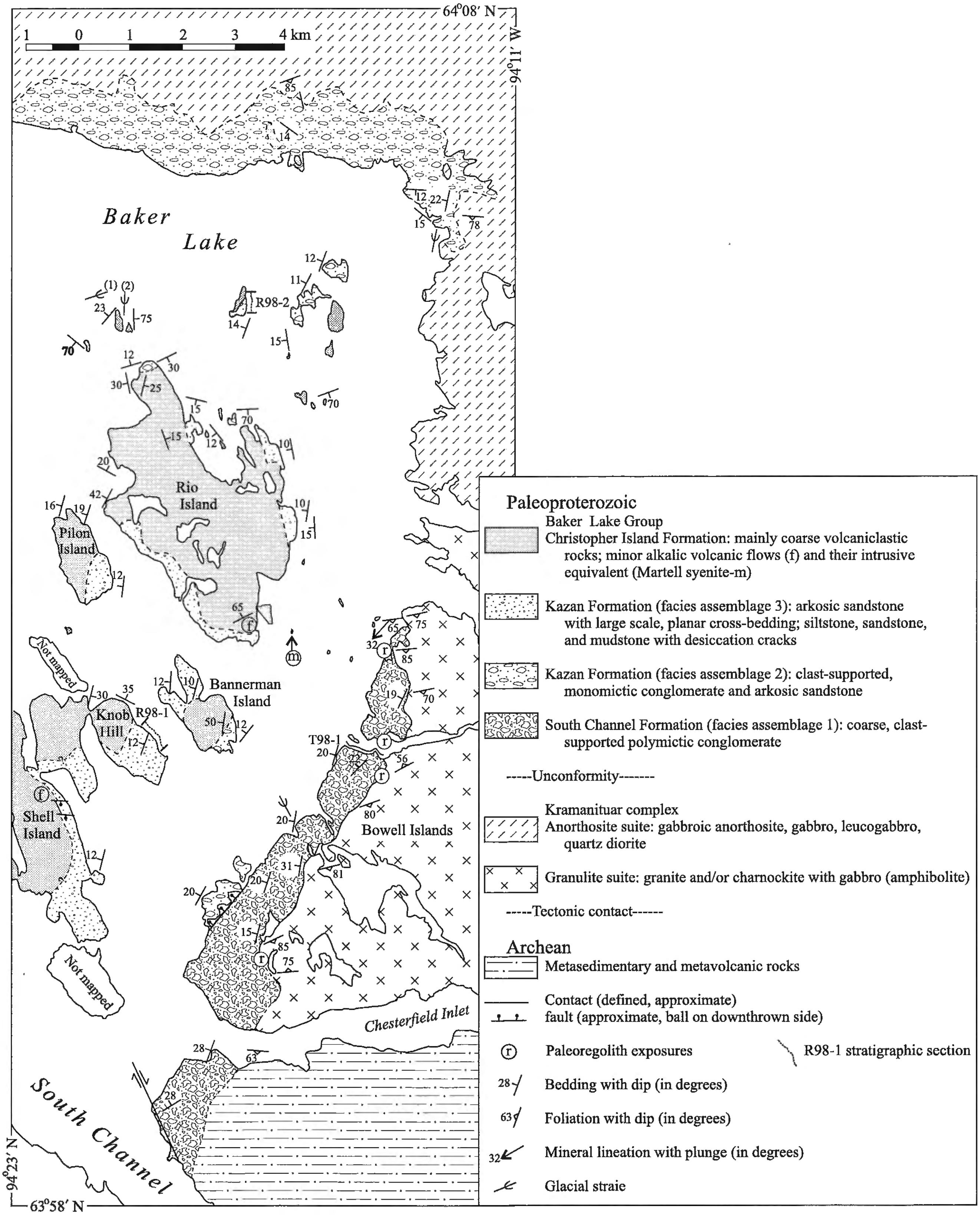


***Figure 2.*** *Geology and facies distribution of the Baker Lake Group in the eastern Baker Lake archipelago, Baker Lake basin.*

stratified, cobble conglomerate (Gco; Fig. 5). Toward the top, clast size decreases, giving way to trough-filling, cobble to pebble conglomerate (Gt). The top of a cycle usually is marked by 10–70 cm thick, trough cross-stratified sandstone (St). Although the sandstone beds are lenticular with erosive upper contacts, the stratal boundary between cycles is laterally continuous. Imbrication is rare, even in the trough-filling conglomerate (Gt) and it is absent in the basal disorganized conglomerate (Gcd). Clasts are predominantly subangular to subrounded; lithologies can be traced to the underlying Kramanituar complex and include (decreasing order of abundance) amphibolite, anorthosite, garnet-bearing granite, and tonalite. The matrix generally is red and consists of coarse, pebbly sand and fine sand to silt.

### Facies assemblage 2

Facies assemblage 2 is the most diverse and comprises trough crossbedded sandstone (St), horizontally stratified sandstone (Sh), massive to horizontally stratified, pebbly sandstone with or without mudstone rip-ups (Sm), clast-supported, organized conglomerate (Gco), ripple crosslaminated siltstone-fine sandstone (Fr), and parallel-laminated siltstone and mudstone, usually with desiccation cracks (Fl). Strata range from light pink for coarse sandstone to darker pink for fine sandstone to blood red for siltstone. Spotting due to oxidation-reduction reactions is common. Detailed petrography of the Kazan Formation indicates that it is arkose±litharenite (Macey 1973).

Together, the facies listed above define fining-upward cycles 0.15–2.0 m thick (Fig. 6). The thickest cycles consist of horizontally stratified, cobble conglomerate (Gco) interbedded with broadly lenticular bodies of massive to faintly stratified, pebbly to cobbly coarse sandstone (Sm). The cycles differ from those of facies assemblage 1 in that they are composed mainly of organized beds; conglomerate clasts are very well rounded, imbricated, and are chiefly of granitoid composition. Most common are cycles beginning with 10–20 cm of conglomerate (Gco), overlain by 10–50 cm of sandstone (Sm and/or St), and capped by a 5–10 cm thick layer of fine-grained sandstone (Sh). Where lateral exposure permits, the upper half of the cycles may be discontinuous, forming broad troughs up to 15 m wide. The most common type of fining-upward cycle begins with medium- to coarse-grained sandstone (Sm), typically with mud chips, overlain by sandstone (St), which is, in turn, overlain by very fine-grained sandstone and siltstone (Fr) and rarely mudstone (Fl) (Fig. 6). Most of the cycles range in thickness from 30 to

*Figure 3. Regolith-breccia of basal Baker Lake Group developed on foliated granite of Kramanituar complex. Note carbonate (white) coatings around angular granite blocks and infill of fractures. Tops toward top of photograph. Pocket knife, for scale, is about 10 cm long.*

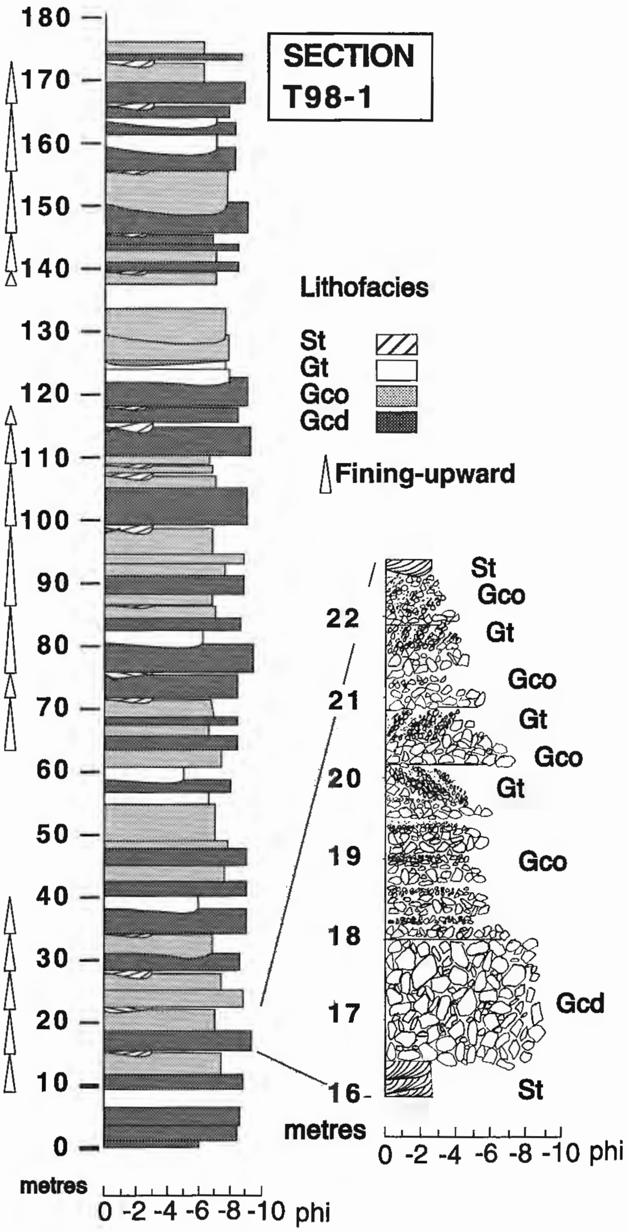


*Figure 4. Graphic log (section T98-1) to illustrate typical stratigraphy and lithology of South Channel and Kazan formations facies assemblage 1. Section located on Figure 2. Scale at base of sections indicates maximum clast size in phi units (-10 = 1024 mm; -4 = 16 mm).*

70 cm. The St layer commonly is a compound bedset or coset of several tabular-trough crossbeds (Fig. 6). Less common are thin 15–30 cm thick cycles of trough crossbedded to ripple crosslaminated siltstone (St or Fr) overlain by a relatively thick layer of desiccation-cracked mudstone (Fl).

**Facies assemblage 3**

Facies assemblage 3 comprises two subfacies associations. The first and most characteristic is similar to the smallest scale cycles of facies assemblage 2. It comprises 10–60 cm thick layers of medium-grained sandstone (Sm, St, or Sr) overlain by siltstone and mudstone (Fl). The cycles of facies assemblage 3 are distinguished by their higher percentage of mudrock; some cycles have just a faint, thin, basal sandstone layer. The most striking feature of this subfacies is ubiquitous desiccation cracks (Fm), which are multigenerational and developed at several different scales (Fig. 7). Generally, the cracks penetrate downward through two-thirds to three-quarters of the layer but in many instances they penetrate the entire layer such that the mudstone layer is broken into blocks set in a matrix of red, silty sandstone. This unit is more than



*Figure 5. **a)** Coarse disorganized, clast-supported conglomerate (Gcd) of facies assemblage 1, from section T98-1. **b)** Top of fining-upward cycle in facies assemblage 1, from section T98-1. Hammer is about 30 cm long.*

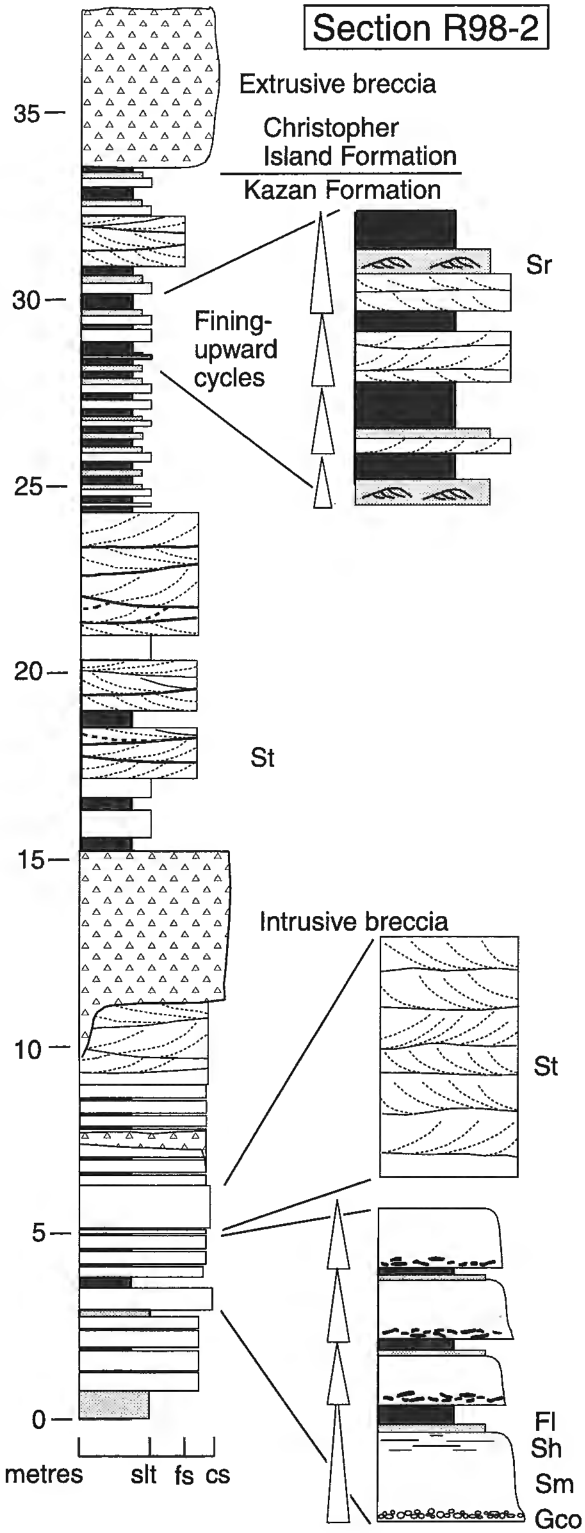


*Figure 6. Graphic log (section R98-2) to illustrate typical stratigraphy and lithology of South Channel and Kazan formations facies assemblage 2. Section located on Figure 2. slt = silt; fs = fine sand; cs = coarse sand.*

50 m thick at section R98-1 (Fig. 8), where it is closely associated with another subfacies composed of large-scale, wedge-planar crossbeds (Sp) separated by about 10 cm interbeds of ripple-laminated sandstone (Sr). This subfacies is characterized by an almost complete lack of fines. The crossbedded facies is composed of texturally mature, medium- to very coarse-grained sandstone. Foreset laminae are mostly normal-graded, although rare reverse graded laminae were noted (Fig. 9). Crossbeds vary in thickness from 1 to 5 m with foreset dips varying from 28°–32°. The sandstone (Sr) interbeds consistently form the bottomset of the large crossbeds. Plan views indicate that straight-crested, symmetrical ripples (l=5 cm h=1 cm) are the dominant type but low amplitude current ripples (l=8 cm h=0.5 cm) also were observed in association with structures we interpret as rain-drop imprints. The large, crossbedded subfacies has an overall thickness of about 30 m in section R98-1 (Fig. 8).

### Facies assemblage 4

Facies assemblage 4 includes a variety of soft-sediment deformation structures including ball-and-pillow structures, slump folds, flame structures, and overturned crossbeds. The most common type is penecontemporaneous sedimentary breccia occurring as dykes, sills, and large irregular intrusions. It is most extensive and best developed in the large crossbedded subfacies of facies assemblage 3 on the northern end of Bannerman Island (Fig. 2), where it consists of angular clasts of red siltstone and fine sandstone in a matrix of medium- to coarse-grained, massive sandstone (Fig. 10). Margins of the intrusion appear to be subvertical and irregular; large blocks of tilted but otherwise undeformed sandstone occur within it. Elsewhere, such as at section R98-2 (Fig. 6), the breccia is confined to a less than 1 m thick sill which gently climbs upsection. Where the sill parallels bedding it is indistinguishable from the sandstone (Sm) facies at the bases of fining-upward cycles in facies assemblage 2. This sill is itself is intruded by a thinner sill composed of lamprophyre, similar in composition to nearby volcanic rocks, suggesting a possible genetic relationship between the two intrusions.

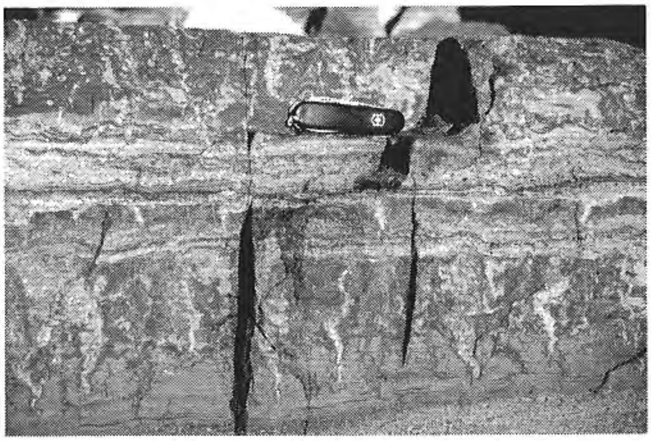

***Figure 7.*** *Dessication cracks in facies assemblage 3.*

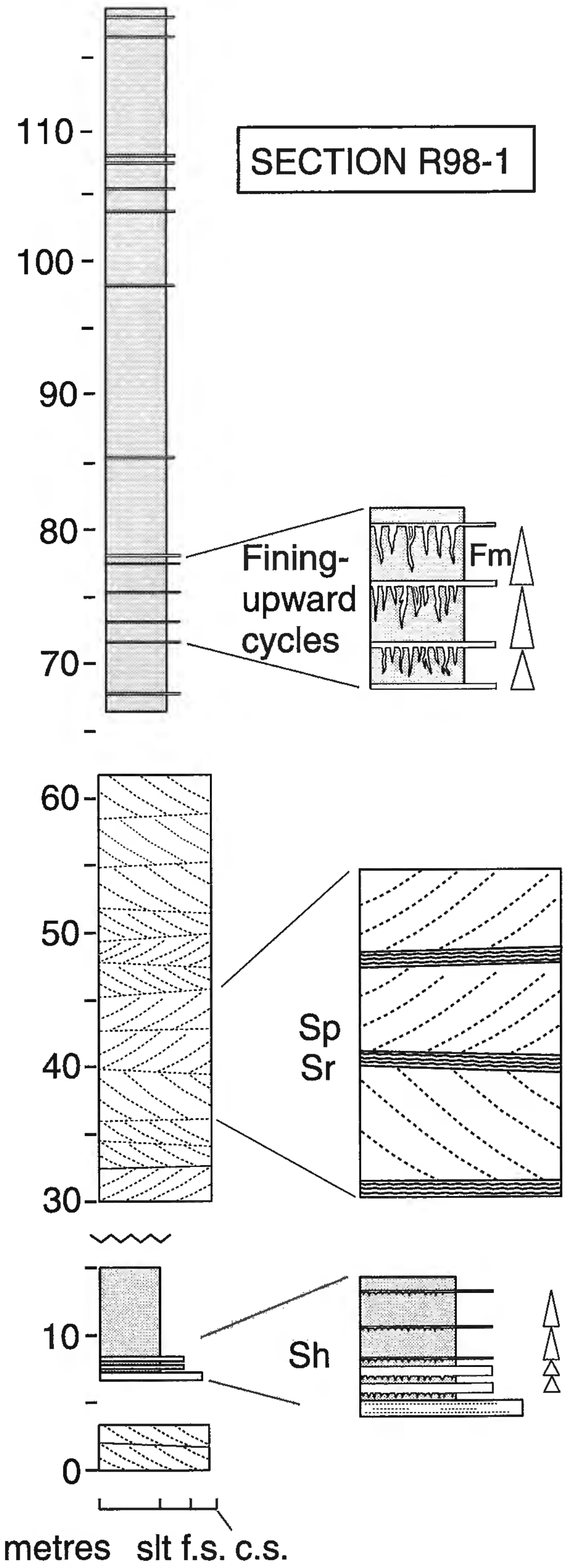


***Figure 8.*** *Graphic log (section R98-1) to illustrate stratigraphy and lithology of South Channel–Kazan formations facies assemblage 3. Section located on Figure 2. slt = silt; f.s. = fine sand; c.s. = coarse sand.*

*Figure 9. Pinstripe lamination in large crossbed foresets of facies assemblage 3 at section R98-1. Coin is 2 cm wide.*

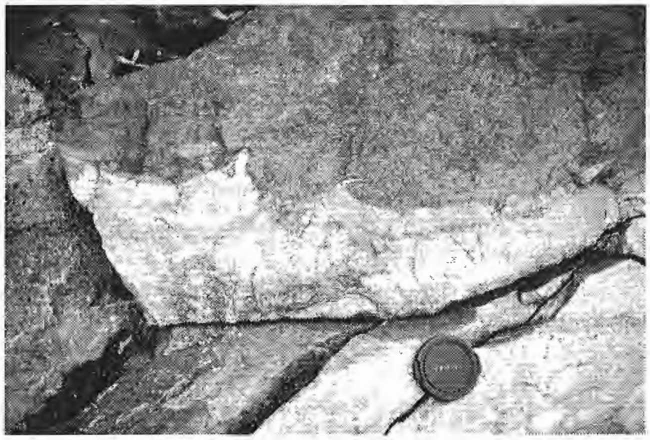

*Figure 11. Sandstone flames indicate soft-sediment injection upward into lava flow.*

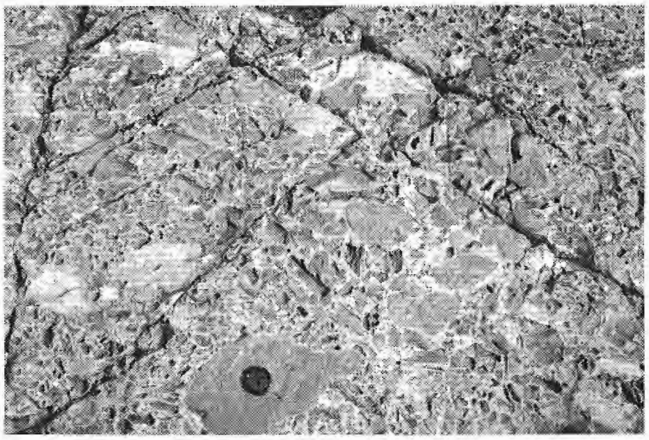

*Figure 10. Intrusive sedimentary breccia composed of angular siltstone blocks in matrix of medium- to coarse-grained sandstone. Lens cap is about 5 cm wide.*

## *Christopher Island Formation*

### Contact with the Kazan Formation

The depositional relationship between the Kazan Formation and the Christopher Island Formation, a point of contention from previous studies (Donaldson, 1965; Blake, 1980), is well exposed in the study area. In eastern Baker Lake basin, the Christopher Island Formation overlies the Kazan Formation with conformity to pronounced angular unconformity; however, numerous features indicate that the Kazan Formation was unlithified at the time of deposition of the Christopher Island Formation. These include very irregular, diffuse boundaries at the margin of lamprophyre intrusions that presumably fed overlying minette lava flows; clasts of very well rounded granite in Christopher Island Formation breccias, presumably liberated from mixing of Kazan Formation conglomerate with cognate volcanic detritus and; flame structures in sandstone directly underlying a minette flow (Fig. 11). Other features, such as extensive intraformational breccia intrusions (Fig. 10), suggest that the Kazan Formation was unlithified and liquefied during earth tremors that accompanied volcanism. Although we did not see interfingering, as has been reported by Blake (1980), it seems unlikely that there was a significant hiatus between deposition of the Kazan and Christopher Island formations.

An important depositional relationship is revealed by viewing the contact from a distance. Invariably the Kazan Formation occupies topographically lower areas with strata gently inclined westward, toward the centre of the basin. Christopher Island Formation strata occupy topographically higher areas, forming rounded hills, 100–200 m high (e.g. Knob Hill on Christopher Island; Fig. 2); constituent flow units display dips up to 50°. A view of Knob Hill from the north shows steeply opposed strata on its flanks; because Kazan Formation strata are almost flat lying, steep dips in the Christopher Island Formation must approximate primary depositional slopes, suggesting that Knob Hill and other prominent hills in eastern Baker Lake are remnant volcanoes.

### Volcaniclastic rocks

Volcaniclastic rocks are the predominant component of the Christopher Island Formation in this area and form deposits more than 1 km thick. They range from thick sections of massive breccia to thinner units of very well stratified, volcanic siltstone and fine-grained sandstone. Breccia units typically are composed of a mixture of cognate and accessory clasts set in a matrix of gritty, reddish-brown siltstone and fine-grained sandstone. Macroscopic examination reveals that the cognate detritus is mainly angular to subrounded, mafic to intermediate, minette volcanic rocks and accessory clasts are mainly subrounded to very well rounded granitoid rocks and quartzite or vein quartz, similar to clasts in the conglomerate of the underlying Kazan Formation. Coarser breccia units generally are poorly sorted and massive. They are well exposed at section R98-2 (Fig. 6), where we observed a sill climbing at low angle through the uppermost Kazan Formation into a very thick (>50 m) section of breccia, which forms the base of the Christopher Island Formation. Finer grained breccia units are better sorted and generally exhibit parallel bedding or low-angle cross-stratification. Pinch-and-swell type low-angle crossbedding, similar to that described in pyroclastic surge deposits (Cas and Wright, 1987), was observed at several localities. Volcanic sandstones and siltstones commonly are interbedded with the breccia units and exhibit an array of fine tractional sedimentary structures such as normal and reverse grading (Fig. 12), climbing ripples, and low-angle crossbedding. Soft-sediment faulting and convolute bedding are common, attesting to syndepositional seismicity. A striking feature of the well bedded breccia facies is the presence of numerous lonestones associated with laminae that appear to have been punctured and dragged downward (Fig. 13). In the context of a volcanic environment, these are interpreted as ballistic ejecta.

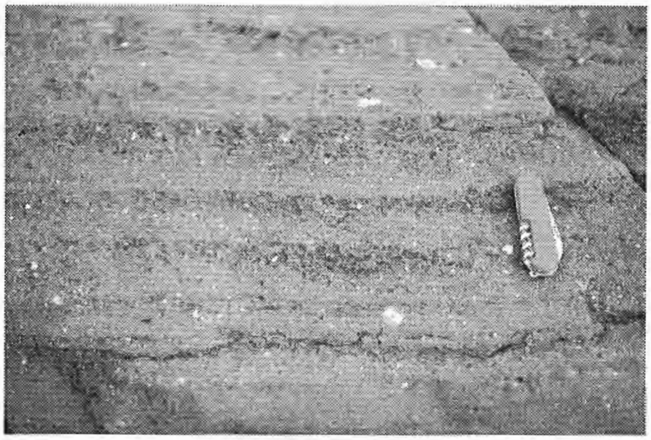

*Figure 12. Reverse-graded laminae in volcaniclastic sandstone of the Christopher Island Formation.*

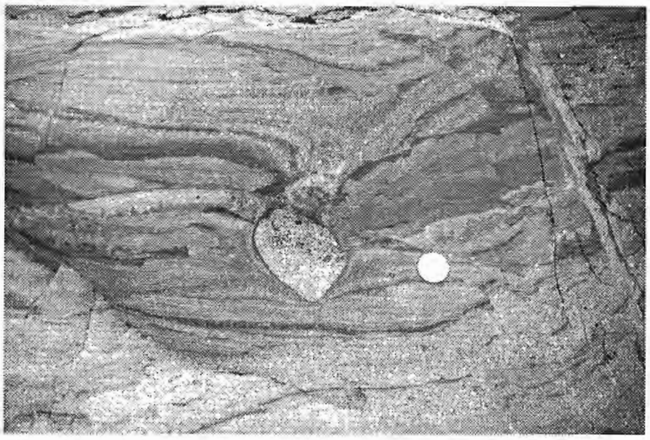

*Figure 13. Lonestone interpreted as basal penetration sag in coarse volcaniclastic sandstone of the Christopher Island Formation.*

**Lava flows**

Lava flows of the Christopher Island Formation are silica undersaturated, potassic to ultrapotassic rocks of the lamproite-minette suite (LeCheminant, et al., 1987; Peterson, 1994). Only two such flows were noted in our reconnaissance of the Christopher Island Formation. An approximately 20 m thick flow at the south end of Rio Island conformably overlies sandstone units of South Channel–Kazan formations facies assemblage 3 (Fig. 11). The flow is of intermediate to mafic composition, being composed of phlogopite and rare clinopyroxene phenocrysts set in a fine-grained, chocolate-brown groundmass containing carbonate amygdules. A second, felsic-intermediate flow, outcropping atop a ridge at the south end of Christopher Island, contains phlogopite, K-feldspar, and rarer clinopyroxene phenocrysts set in a fine grained, pink-weathering, orange-brown groundmass. This flow is at least 10 m thick and conformably overlies red volcaniclastic sandstones which, in turn, conformably overlie interbedded siltstone and fine-grained sandstone of South Channel–Kazan formations facies assemblage 2.

### *Basin-margin faulting*

A prominent northeast- to north-trending, arcuate lineament, corresponding to the easternmost shoreline of Baker Lake, marks an abrupt change from coarse heterolithic conglomerate units of facies assemblage 1 to the monomictic conglomerate and sandstone units of facies assemblage 2 (Fig. 2). The lineament is interpreted as a west-side-down normal fault, possibly a growth fault, which developed in response to crustal extension during initial stages of basin development. On the north side of the basin, an east-striking, south-dipping normal fault juxtaposes steeply dipping facies assemblage 2 strata against gabbroic anorthosite of the Kramanituar complex (Fig. 2). This also may have been a basin margin growth fault, which subsequently was reactivated.

## DEPOSITIONAL ENVIRONMENTS AND PALEOGEOGRAPHY

### *South Channel–Kazan formations*

Coarse conglomerate units of facies assemblage 1 are interpreted to have been deposited on alluvial aprons of a bajada which prograded westerly from the eastern margin of the basin. Clast types in the conglomerate indicate an important contribution of detritus from the immediately adjacent Kramanituar complex, a conclusion also supported by limited paleocurrent information. Deposition was mainly by proximal, high-energy stream floods. Individual flood episodes are manifest as crude fining-upward cycles. Broadly lenticular, finer grained, organized layers at the tops of cycles are interpreted as waning stage, channel fill deposits. Carbonate-cemented horizons within the conglomerate are interpreted as caliche, suggesting a semiarid to arid climate.

Facies assemblage 2 is interpreted as the deposit of braided streams which formed on the medial to distal reaches of alluvial aprons during flash floods. Organized conglomerate units likely were deposited as longitudinal bars or as gravel sheets with massive to plane-bedded sandstone units infilling during waning-stage flow (cf. Boothroyd and Ashley, 1975). The lenticular form of some of the sand bodies is attributed to infilling of channels between longitudinal bars. Sandstone-based, fining-upward cycles are interpreted as the product of low-energy flood events. These and finer grained strata are more common toward the centre of the basin, suggesting deposition on more distal reaches of the apron. Fining-upward cycles are typical of migrating channels and bars in braided fluvial systems (Miall, 1977). Rare cosets of trough crossbedding indicate deposition by three-dimensional channel forms; the lack of internal bounding surfaces suggests deposition by floods with rapidly decreasing flow velocity (cf. Karcz, 1972). Thinner sandstone-based, fining-upward cycles with siltstone to desiccated mudstone tops are considered to be floodplain deposits.

South Channel–Kazan formations facies assemblage 3 is interpreted to represent deposition in ephemeral playa lakes, which formed after each flood event. Sandy layers at the base of some beds are distal bed-load deposits; fine-grained caps to the graded beds are interpreted as suspended load deposits. Each graded bed in the fine-grained facies probably represents an individual flood and likely correlates with the large-scale, fining-upward cycles in more proximal facies of assemblages 1 and 2. In an arid climate, fine-grained sediments in lakes would desiccate quickly, thereby explaining the abundance of shrinkage cracks in these rocks. Wind was the probable agent for transportation of mixed silt and sand, which infill most of the cracks (*see* below).

The large-scale crossbedded sandstones, closely associated with these fine-grained facies, exhibit features consistent with deposition by eolian dunes. These include high textural maturity, the relatively large scale of crossbedding, high angle of repose, and lack of fines. A convincing argument for a windblown origin is the presence of pinstripe lamination, which includes reverse graded foresets, a feature of low angle-of-climb wind ripples (Hunter, 1977). Thin, ripple-bedded bottomsets to the crossbeds are common in eolian environments, where they are interpreted as shallow-water interdune deposits (Kocurek, 1981).

Soft-sediment deformation features of facies assemblage 4 are ascribed to earth tremors preceding and accompanying Christopher Island Formation volcanism. Sedimentary intrusive breccia units are high-energy examples, which in one instance appear to have been a precursor to associated igneous intrusion.

### *Christopher Island Formation*

Several key observations suggest that the eastern Baker Lake basin was an area of active explosive volcanism, which interrupted alluvial braidplain sedimentation, as exhibited by the facies assemblages of the South Channel–Kazan formations. Initially, thin lava flows were extruded onto the unlithified braidplain surface. Soft-sediment deformation features of facies assemblage 4 of the South Channel–Kazan formations indicate that eruption was preceded and accompanied by significant seismicity and localized doming and tilting of the strata. Lava flows were quickly buried by an array of subaerially erupted, volcano-sedimentary rocks. Some of the features we observed, such as ballistic ejecta, pinch-and-swell structure, and reverse-graded laminae, point to deposition by air-fall, pyroclastic surge, and pyroclastic flow. The great thickness and attitudes of the volcaniclastic strata suggest eruption of tephra from numerous volcanic centres. The resulting volcanic edifices, possibly tuff-cones (Cas and Wright, 1987), likely formed rapidly, with little time for subsidence and reworking by water. Remnants of the volcanoes are still preserved today as prominent hills and islands of the eastern Baker Lake archipelago and are additional to the volcanic centres proposed by Blake (1980).

## CONCLUSIONS

In this paper we have subdivided the South Channel and Kazan formations of the eastern Baker Lake basin into four lithofacies assemblages that define a gradational continuum from coarse, proximal, alluvial fan deposits, through medial braided stream facies, into distal flood-plain playa deposits. Although, for mapping purposes, this sequence was broken into separate formations, they should be treated as facies and time-stratigraphic equivalents. Facies distribution, sedimentology, and paleocurrents indicate that alluvium was derived from highlands to the east; clasts in facies assemblage 1 conglomerates came mainly from the immediately adjacent granulite units of the Kramanituar complex; clasts in facies assemblage 2 are from an as yet unrecognized granitic source.

Along the basal unconformity, abundant sediment-filled fractures in the basement, angularity of the basement surface and derived fragments, sporadic calcrete coatings (some of which have been broken and incorporated into the paleosol), and widespread hematitization of the paleosol indicate that both mechanical and chemical weathering played important roles in providing detritus for infilling of Baker Lake basin. A desert setting in which frequent temperature fluctuations accommodated both freeze-thaw cycles and recurring to arid conditions is inferred.

Soft-sediment deformation, sedimentary breccia units in the Kazan Formation, and an irregular contact between it and the overlying Christopher Island Formation indicate that alkalic volcanism interrupted alluvial sedimentation. Sedimentation style, asymmetric distribution of facies, recognition of possible basin margin growth faults and association with volcanism suggests that Baker Lake basin formed in a transtensional or continental rift setting.

## ACKNOWLEDGMENTS

We thank Skyward Aviation, Huisson Aviation, and GSC 'Broken Drum' campers for logistical support. Thanks also to Katherine Venance for drafting Figures 1 and 2 and to Larry Aspler for reviewing the manuscript.

## REFERENCES

**Blake, D.H.**
1980: Volcanic rocks of the Paleohelikian Dubawnt Group in the Baker Lake-Angikuni Lake Area, District of Keewatin, N.W.T.; Geological Survey of Canada, Bulletin 309, 39 p.

**Boothroyd, J.C. and Ashley, G.M.**
1975: Process, bar morphology and sedimentary structures on braided outwash fans, northeastern Gulf of Alaska; *in* Glaciofluvial and Glaciomarine Sedimentation, (ed.) A.V. Jopling and B.C. McDonald; Society of Economic Paleontologists and Mineralogist, Special Publication No. 23, p. 193–222.

**Cas, R.A.F. and Wright, J.V.**
1987: Volcanic Successions: Modern and Ancient; Allen and Unwin, London, United Kingdom, 528 p.

**Donaldson, J.A.**
1965: The Dubawnt Group, District of Keewatin and Mackenzie; Geological Survey of Canada, Paper 64-20, 11 p.
1967: Study of the Dubawnt Group; *in* Report of Activities, Part A; Geological Survey of Canada, Paper 67-1A, p. 23–25.

**Gall, Q., Peterson, T.D., and Donaldson, J.A.**
1992: A proposed revision of early Proterozoic stratigraphy of the Thelon and Baker Lake basins, Northwest Territories; *in* Current Research, Part C; Geological Survey of Canada, Paper 92-1C, p. 129–137.

**Hunter, R.E.**
1977: Terminology of cross-stratified sedimentary layers and climbing-ripple structures; Journal of Sedimentary Petrology, v. 47, p. 697–706.

**Karcz, I.**
1972: Sedimentary structures formed by flash floods in southern Israel; Sedimentary Geology, v. 7, p. 161–182.

**Kocurek, G.**
1981: Significance of interdune deposits and bounding surfaces in eolian dune sands; Sedimentology, v. 28, p. 753–780.

**LeCheminant, A.N., Leatherbarrow, R.W., and Miller, A.R.**
1979: Thirtymile Lake Map Area, District of Keewatin, *in* Current Research, Part B; Geological Survey of Canada, Paper 79-1B, p. 319–327.

**LeCheminant, A.N., Miller, A.R., and LeCheminant, G.M.**
1987: Early Proterozoic alkaline igneous rocks, District of Keewatin, Canada: petrogenesis and mineralization; *in* Geochemistry and Mineralization of Proterozoic Volcanic Suites, (ed.) T.C. Pharaoah, R.D. Beckinsale, and D. Rickard; Geological Society, Special Publication No. 33, p. 219–240.

**Macey, G.**
1973: A sedimentological comparison of two Proterozoic red-bed successions (the South Channel and Kazan formations of Baker Lake, N.W.T., and the Martin Formation at Uranium City, Saskatchewan); MSc. thesis, Carleton University, Ottawa, Ontario, 175 p.

**Miall, A.D.**
1977: A review of the braided river depositional environment; Earth Science Reviews, v. 13, p. 1–62.

**Miller, A.R.**
1980: Uranium geology of the eastern Baker Lake basin, District of Keewatin, Northwest Territories; Geological Survey of Canada, Bulletin 330, 63 p.

**Peterson, T.D.**
1994: Early Proterozoic ultrapotassic volcanism of the Keewatin hinterland, Canada.; *in* 5th International Kimberlite Conference: Kimberlites, Related Rocks and Mantle Xenoliths, (ed.) H.O.A. Meyer and O.H. Leonardos; Companhia de Pesquisa de Recursos Minerais, Brasilia, p. 221–235.

**Sanborn-Barrie, M.**
1994: Structural investigation of high-grade rocks of the Kramanituar complex, Baker Lake area, Northwest Territories; *in* Current Research 1994-C; Geological Survey of Canada, p. 121–133.

**Schau, M. and Ashton, K.E.**
1979: Granulites and plutonic complexes, northeast of Baker Lake, District of Keewatin, *in* Current Research, Part A; Geological Survey of Canada, Paper 79-1A, p. 311–316.

**Tella, S., LeCheminant, A.N., Sanborn-Barrie, M., and Venance, K.E.**
1997: Geology and structure of parts of MacQuoid Lake map area, District of Keewatin, Northwest Territories; *in* Current Research 1997-C; Geological Survey of Canada, p. 123–132.

**Wright, G.M.**
1955: Geological notes on the central district of Keewatin, Northwest Territories, Geological Survey of Canada, Paper 55-17.

Geological Survey of Canada Project 970006

# Proterozoic reworking in western Churchill Province, Gibson Lake–Cross Bay area, Northwest Territories (Kivalliq region, Nunavut). Part 1: general geology[1]

S. Hanmer, S. Tella, H.A. Sandeman, J.J. Ryan, T. Hadlari[2], and A. Mills[2]
Continental Geoscience Division, Ottawa

*Hanmer, S., Tella, S., Sandeman, H.A., Ryan., J.J., Hadlari, T., and Mills, A.,1999: Proterozoic reworking in Western Churchill Province, Gibson Lake–Cross Bay area, Northwest Territories (Kivalliq region, Nunavut). Part I: general geology;* in *Current Research 1999-C; Geological Survey of Canada, p. 55–64.*

**Abstract:** The northeastern part of the Neoarchean MacQuoid supracrustal belt comprises the Gibson–MacQuoid homoclinal belt of homogeneous metasedimentary rocks, tonalitic orthogneiss units and plutons, structurally overlain to the north by a belt of mafic to intermediate volcanic flows and volcaniclastic rocks, intruded by tonalitic to granodiorite plutons. The Cross Bay plutonic complex is separated from the supracrustal belt by the Big lake shear zone. Metamorphosed, ca. 2.19 Ga, mafic dykes are involved in Paleoproterozoic regional deformation in both the plutonic complex and the shear zone.

**Résumé :** La partie nord-est de la ceinture supracrustale néoarchéenne de MacQuoid englobe la ceinture homoclinale de Gibson–MacQuoid composée de roches métasédimentaires homogènes, d'orthogneiss tonalitiques et de plutons, que recouvre structuralement au nord une zone de coulées volcaniques mafiques à intermédiaires et de roches volcanoclastiques recoupée par des plutons tonalitiques à granodioritiques. Le complexe plutonique de Cross Bay est séparé de la ceinture supracrustale par la zone de cisaillement de Big Lake. Des dykes mafiques métamorphisés, qui remontent à vers 2,19 Ga, ont subi une déformation paléoprotérozoïque d'importance régionale tant dans le complexe plutonique que dans la zone de cisaillement.

---

[1] Contribution to the Western Churchill NATMAP Project
[2] Department of Earth Sciences, Carleton University, Ottawa, Ontario K1S 5B6

## INTRODUCTION

The Western Churchill NATMAP Project involves the Geological Survey of Canada (GSC), the Government of the Northwest Territories (GNWT), and Indian and Northern Affairs Canada (INAC). In 1998, the second phase of the GSC's three year field program, an investigation of the geology of parts of the MacQuoid Lake (NTS 55 M) and Gibson Lake (NTS 55 N) map areas (Fig. 1) was undertaken between Gibson Lake and Chesterfield Inlet. Particular emphasis was placed on establishing the nature and extent of Paleoproterozoic tectonothermal reworking of older, Archean rocks. Bedrock mapping was undertaken at 1:50 000 scale (Fig. 1), building on the previous work of Tella et al. (1997b, c; LeCheminant et al., 1997). Previous bedrock mapping in the area was mostly at 1:250 000 scale, or smaller (Wright, 1967; Reinhardt and Chandler, 1973; Reinhardt et al., 1980; Tella and Schau, 1994), as well as local detailed work (Sanborn-Barrie, 1994). The map area contains the Sandhill Zn-Cu-Pb-Ag prospect (Armitage et al., 1994, 1995), the Suluk Ni-Cu-Co occurrence (Armitage et al., 1997), and the Akluilâk diamondiferous lamprophyre dyke (MacRae et al., 1996). In this report, we present a systematic overview of the lithological characteristics of the map area (Fig. 1). Structural observations are presented elsewhere (Hanmer et al., 1999b; Ryan et al., 1999).

### *Geological overview*

The map area (Fig. 1) includes the eastern part of the Archean MacQuoid supracrustal belt (Miller and Tella, 1995; Tella et al., 1997a, b, c) and the Cross Bay plutonic complex. The MacQuoid supracrustal belt is divided into a southern, predominantly metasedimentary homocline with panels of gneissic tonalite, flanked to the north by a predominantly volcanic belt intruded by tonalite-granodiorite plutons. The oval Cross Bay plutonic complex is principally composed of tonalitic and dioritic gneiss units and granite intrusions. Along its southern margin, the plutonic complex is separated from the supracrustal belt by an approximately east-trending, strike-slip, mylonitic shear zone. Folding and boudinage of east-trending, mafic dykes (ca. 2.19 Ga, Tella et al., 1997a, c) indicates that significant Paleoproterozoic deformation occurred in the Cross Bay complex.

## GIBSON–MACQUOID HOMOCLINE

The southern part of the map area is underlain by the moderately (average 40–50°) north-northwest-dipping Gibson–MacQuoid homocline, composed of panels of clastic metasedimentary rocks with subordinate mafic volcanic rocks, gneissic tonalite, and tonalite plutons (Fig. 1, 2). The metasedimentary rocks are predominantly uniform biotite±garnet semipelitic rocks, with abundant biotite psammitic rocks. With few exceptions, the metasedimentary rocks show little evidence of primary compositional layering. However, the semipelitic rocks are locally layered on an approximately 10 cm scale (Fig. 3). Laminated, quartz-magnetite iron-formation occurs in layers, 5 cm to 30 m thick, set in laterally discontinuous, 100–500 m thick, aluminous garnet±sillimanite pelite horizons. Relatively minor volumes of mafic rocks are interlayered with the metasedimentary rocks. In general, they are fine-grained, homogeneous amphibolite, with locally well developed, compositional banding on the 2–5 cm scale, and rarely preserved pillow structures. They probably represent original mafic flows and associated volcaniclastic sediments.

Tonalitic rocks represent approximately 50% of the homocline (Fig. 1, 2), but also constitute a significant proportion of the map area as a whole. Accordingly, representative descriptions of the range of tonalitic lithologies are given here, and variations will be noted as appropriate for other parts of the map area. We recognize three textural end-members (agmatitic gneiss, 'vein gneiss', and plutonic tonalite), with mutual gradations, which may vary from tonalite to diorite. Although hornblende is generally the primary mafic mineral, it may be extensively replaced by biotite.

Agmatitic gneiss is derived from tonalite with abundant mafic inclusions. The inclusions are generally fine-grained and homogeneous amphibolite, and tend to be close packed within the tonalite host, resembling an inflated agmatite. Locally, long (10–50 m), narrow screens of amphibolite separated by thin slivers of tonalite suggest intrusion of tonalite veins into a large amphibolite mass. The planar deformation fabric superposed on this magmatic structure imparts a gneissic layering to the rock at the outcrop scale. Local variation in the continuity of the layering may reflect relatively low strain; in other places it is due to disruption (boudinage) of layering with further deformation. In general, the gneiss contains few inclusions of the adjacent metasedimentary panels, its contacts tend to be abrupt, and its relationship to the wall rocks is commonly equivocal.

Tonalitic 'vein gneiss' derives its appearance from the presence of long, narrow (5–10 cm), pink granitic veins, subconcordantly emplaced along the regional foliation in the host tonalite (Fig. 4). The 'gneissic' aspect is derived from a synkinematic igneous fabric, which is further accentuated by deformation. This tonalite contains far fewer mafic inclusions than the agmatitic gneiss. Nevertheless, fine-grained, homogeneous amphibolite inclusions are present, generally as large, widely dispersed, elliptical bodies measuring up to 500 m by 100 m along their principal horizontal axes. Metasedimentary inclusions do occur near the contacts, and the adjacent semipelitic wall rock may take on a paragneissic appearance due to the development of abundant plagioclase porphyroblasts and tonalite stringers. These features point to intrusive emplacement of the tonalite.

The plutonic variety of tonalite does not exhibit a gneissic banding, and contains few inclusions except adjacent to its margins. It is foliated, but locally preserves an igneous texture. The tonalite tends to be leucocratic, and is commonly gradational to biotite granodiorite. In contrast to the gneissic varieties which are everywhere concordant to the supracrustal rocks of the Gibson–MacQuoid homocline, the tonalite plutons may exhibit ovoid shapes characteristic of stocks or plugs (Fig. 1).

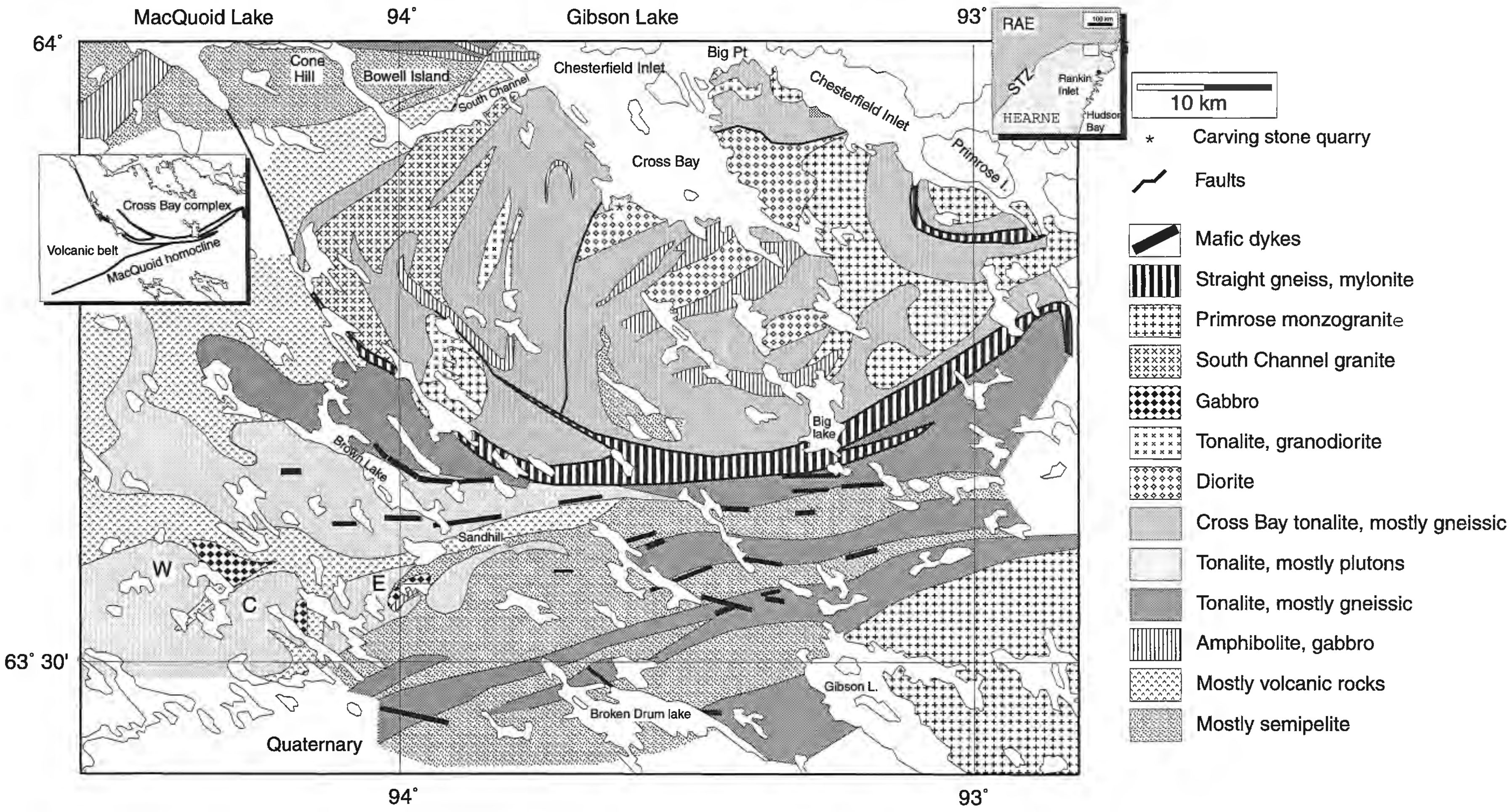


***Figure 1.*** *Generalized geology of the Gibson Lake–Cross Bay area. The letters W, C, and E are western, central, and eastern plutons, respectively. STZ=Snowbird tectonic zone.*

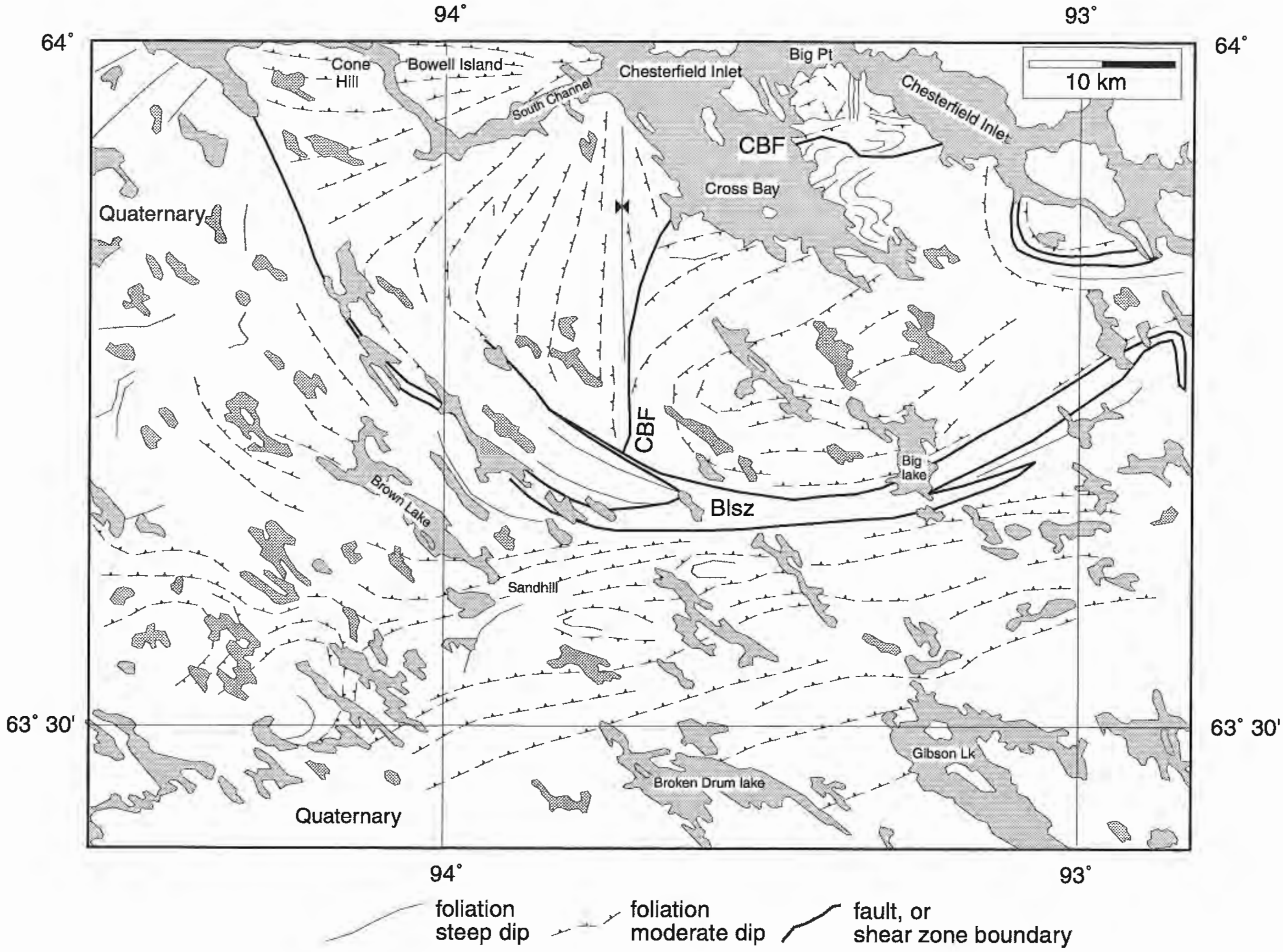


*Figure 2. Structural elements of the Gibson Lake–Cross Bay area. Blsz=Big lake shear zone. CBF=Cross Bay fault.*

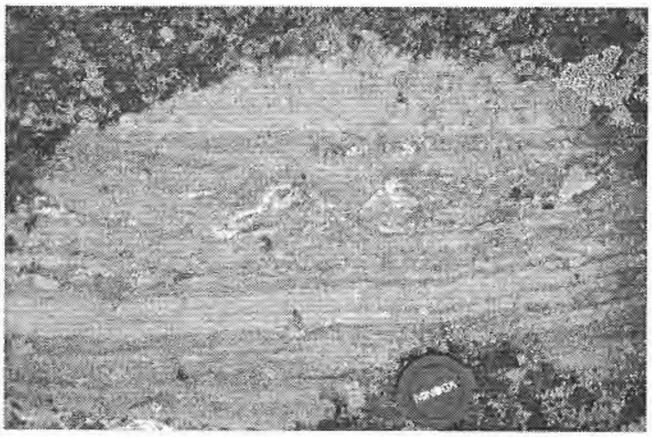

*Figure 3. Rare layering in semipelite, Gibson–MacQuoid homocline.*

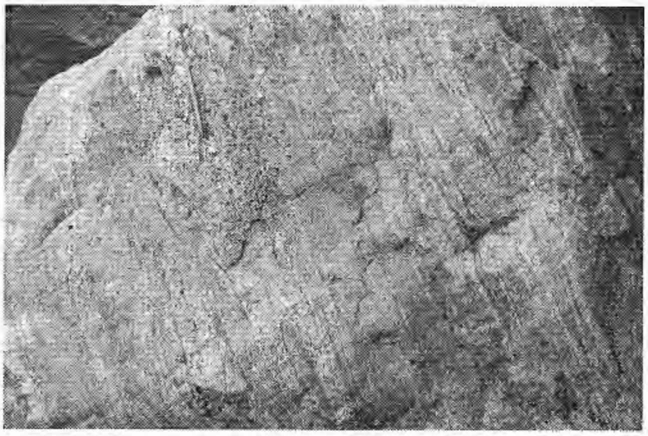

*Figure 4. Tonalitic 'vein gneiss', Cross Bay plutonic complex.*

## VOLCANIC BELT

The western part of the map area is underlain by volcanic and tonalitic rocks, with subordinate metasedimentary rocks, and is divisible into a southern domain and a poorly exposed northern domain (Fig. 1). The southern domain can be traced with continuity into the volcanic rocks of the western segment of the MacQuoid supracrustal belt (Tella et al., 1997c). To the east, it structurally overlies the Gibson–MacQuoid homocline, whereas to the west it forms the northern envelope to three tonalite-granodiorite plutons (Fig. 1, 2). The northern domain is poorly exposed, except along South Channel, Chesterfield Inlet, and the observed northerly to northeasterly strike trends have been juxtaposed by faulting (Hanmer et al., 1999b).

### *Volcanic rocks (southern domain)*

The southern domain is a moderately (average 30–40°) north-dipping homoclinal panel (Fig. 1, 2). As noted to the west (Tella et al., 1997c), the volcanic rocks are grossly mafic in the south and intermediate in the north. The mafic rocks are generally fine-grained, massive to compositionally layered amphibolite units. In the latter case, variation in amphibole/plagioclase ratio occurs on a 1–5 cm scale (Fig. 5). Locally, small (25 cm long), relict pillow structures are preserved, with metamorphosed hornblende-garnet selvages about 1 cm thick (Fig. 6). Although some of the more thinly layered amphibolite units may be derived by the deformation of pillowed flows, the thickness of most of the layering suggests that it is probably derived from primary bedding in volcaniclastic sediments. Alternatively, it could represent highly deformed, thin, subaqueous sheet flows, although no supporting primary evidence has been identified.

Volcanic rocks of intermediate composition are generally fine grained, homogeneous, and light grey. Locally, 2–3 mm, angular to elliptical feldspar grains or light coloured rock fragments up to 5 mm long are preserved, distributed through the rock at the hand specimen scale (Fig. 7). Such rocks are interpreted as crystal and lapilli tuffs, respectively. Rare felsic volcanic rocks occur to the northwest and the southeast of the central tonalite-granodiorite pluton (Fig. 1). They are light coloured, fine grained, locally contain quartz eyes and angular fragments up to 5 cm long of the same composition as the matrix, and are interpreted as tuff and lithic tuff units.

### *Volcanic rocks (northern domain)*

Volcanic rocks of the northern domain occur in two areas, separated by extensive Quaternary cover. Northwest of Brown Lake (Fig. 1), mafic volcanic rocks are generally fine-grained amphibolite units, interpreted as predominantly mafic volcanic rocks, similar to those described to the south. They also include subordinate intermediate to felsic volcanic rocks. However, on the southwest side of the northerly to northwesterly trending package, primary volcanic features such as pillows (Fig. 8) and volcaniclastic textures are unusually well preserved, and the prograde metamorphic

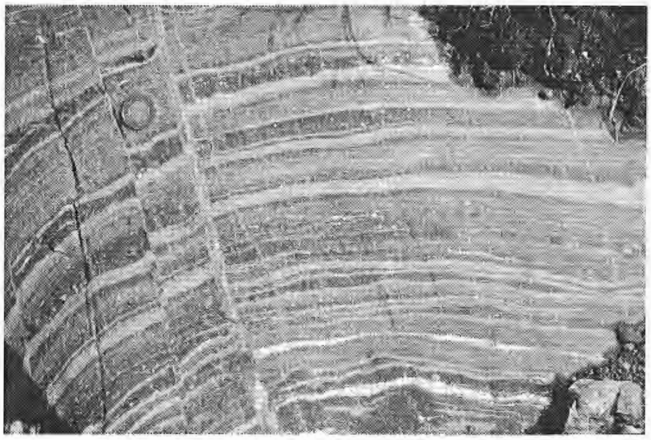

***Figure 5.*** *Layering in deformed mafic rocks, southern domain, volcanic belt.*

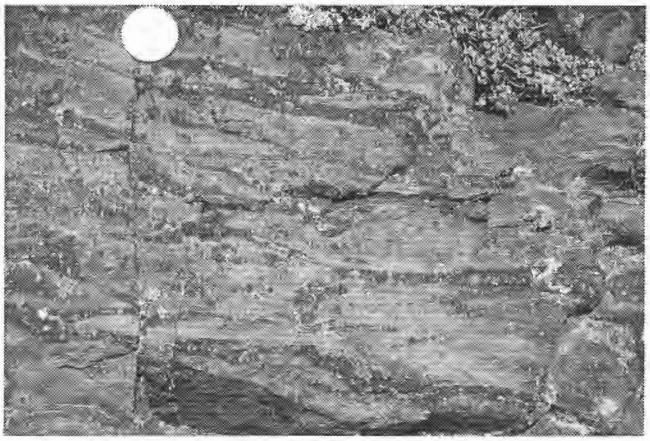

***Figure 6.*** *Relict pillows, southern domain, volcanic belt.*

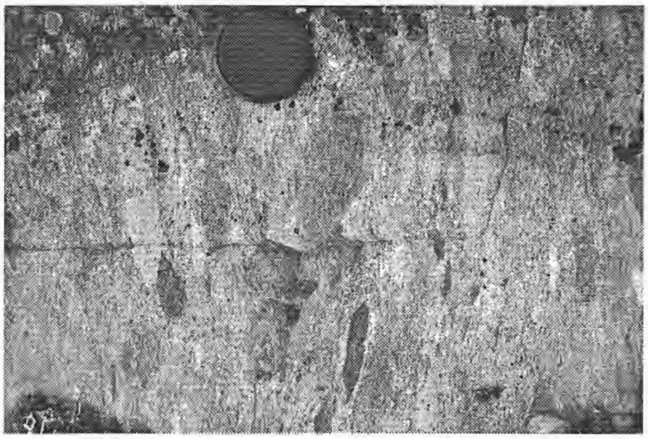

***Figure 7.*** *Volcanic fragments in intermediate composition matrix, southern domain, volcanic belt.*

assemblage is dominated by chlorite. Otherwise, the mafic volcanic rocks are hornblende-garnet bearing, commonly with decussate hornblende needles.

Along South Channel (Fig. 1), southwest-trending, intermediate and subordinate mafic volcanic rocks contain a high proportion of fragmental lithologies. In some cases, angular fragments up to 5 cm long are of similar composition to the matrix; these rocks are interpreted as lithic tuffs. In other cases, abundant fragments of tonalite with smooth outlines, 25 cm long in the deformed state, dominate the clast population in polymictic volcanic conglomerate units, which may represent debris flows. This implies that nonfoliated, tonalitic plutonic rocks were present at the time of volcanism.

Lateral continuity between the predominantly mafic and intermediate volcanic packages is questionable. The intervening ground between the two areas of volcanic rocks is occupied by poorly exposed granodiorite whose northerly structural trends appear discordant to those of the southwest-trending, intermediate volcanic rocks. Where the two packages most closely approach each other, their structural trends are mutually perpendicular. The two volcanic packages appear to be tectonically juxtaposed (Hanmer et al., 1999b), and it is possible that they are stratigraphically independent.

*Figure 8. Well preserved pillows, northern domain, volcanic belt.*

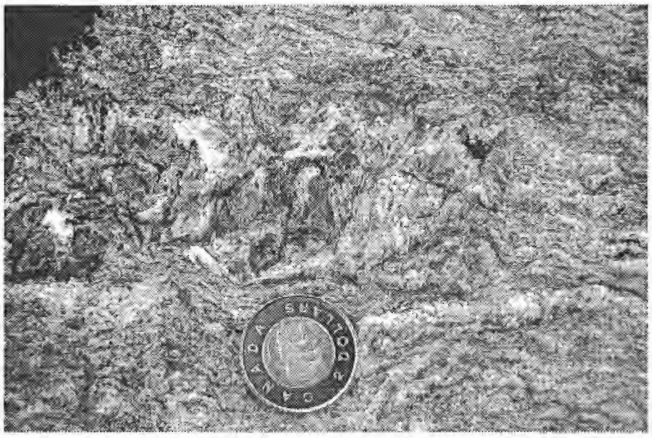

*Figure 9. Staurolite (dark) and (?)sillimanite (light) in aluminous psammite, southern domain, volcanic belt.*

### *Metasedimentary rocks*

In the southern domain of the volcanic belt (Fig. 1), map-scale panels of somewhat aluminous semipelite, quartz-rich biotite-muscovite psammite, and muscovitic quartzite occur between panels of volcanic rocks, east of the central tonalite-granodiorite pluton. Staurolite-garnet-andalusite-sillimanite-kyanite semipelite predominates to the west of the Sandhill prospect, whereas the psammitic rocks are more voluminous to the east. South of the Sandhill prospect, the quartz-rich psammitic rocks are also staurolite-andalusite-(?)sillimanite bearing (Fig. 9). As in the Gibson–MacQuoid homocline, the metasedimentary rocks tend to be uniform. Bedding is usually highlighted by loose concentrations of staurolite in the semipelite units, and by local 5 cm thick, quartzite layers in the psammite units. A single lens of quartzite, up to 10 m thick by 100 m long, occurs on the south side of the Sandhill prospect. No primary features are preserved in any of these rocks.

In the northern domain of the volcanic belt, metasedimentary rocks are less abundant than to the south. The metasedimentary rocks intercalated with the mafic volcanic rocks north of Brown Lake (Fig. 1) are very similar to those just described. Garnet-sillimanite-kyanite semipelite and biotite psammite are the dominant lithologies. At one extensive outcrop, they are interlayered with a 25 m thick quartz pebble conglomerate (Fig. 10) and a 1 m by 25 m lens of quartzite. Development of this quartzite-conglomerate lens within an

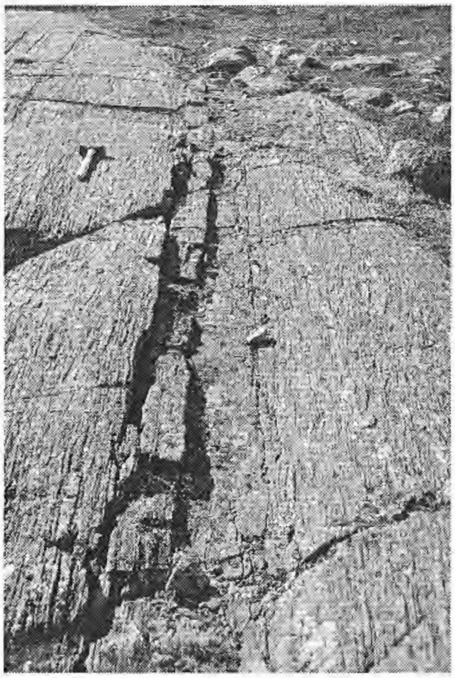

*Figure 10. Quartz pebble conglomerate with arenite bed (recessive), northern domain, volcanic belt.*

otherwise immature section suggests derivation by sediment-gravity flow processes (i.e. channel flow) from nearshore sources external to the immediate depositional basin.

Intermediate volcanic rocks around South Channel (Fig. 1) are locally interlayered with uniform garnet-biotite semipelitic rocks that, at least locally, carry incipient quartzofeldspathic segregations. However, fine-grained, thinly layered (2–10 cm), turbiditic rocks (Fig. 11), possibly composed of volcanogenic debris, outcrop along the south shore of Bowell Island. To the north, the intermediate volcanic rocks are flanked by an east-trending panel of uniform semipelitic rocks, with widespread, abundant garnet-sillimanite-kyanite and pervasive quartzofeldspathic segregations (Fig. 12). The latter contain several concordant, map-scale panels of gabbro. These metasedimentary rocks do not appear to link laterally with similar lithologies to the south, and may represent an independent package, intercalated with the intermediate volcanic rocks of South Channel. At the northern limit of the map area (Fig. 1), subordinate, interlayered mafic volcanic rocks contain relatively undeformed, garnetiferous pillowed flows. These supracrustal rocks are in abrupt, possibly faulted contact with strongly foliated tonalite-quartz diorite and mylonitic rocks of the Kramanituar complex (Sanborn-Barrie, 1994).

### *Tonalitic rocks*

Three map-scale occurrences of tonalitic rocks are associated with the volcanic belt (Fig. 1). North of Brown Lake, a northwest-trending panel of gneissic tonalite (agmatitic and vein types) is very similar to that described from the Gibson–MacQuoid homocline. A second panel of tonalite-diorite trends eastward through Brown Lake, turning progressively northwards as one approaches the western limit of the map area. The tonalite-diorite is laterally variable in composition, but cannot be divided into individual plutons at the scale of our mapping. It is relatively free of inclusions and, although pervasively foliated, preserves interlocking igneous textures. East of Brown Lake it is concordant to the supracrustal wall rocks, but to the west it is interdigitated with the volcanic rocks. It is here that primary features are well preserved in the latter (*see* above). The overall impression is that the tonalite-diorite panel is a foliated, semiconcordant, plutonic body that has not registered the same intensity of deformation as most of the rocks in the map area.

The southwestern corner of the map area is underlain by three plutons of tonalite-granodiorite (Fig. 1). As in the tonalite-diorite panel described above, they have the textural appearance of foliated plutons. Their northern margins have a deeply scalloped geometry, concordant to the wall rock structure, such that they are separated by vertical, synformal keels occupied by the mafic volcanic and sedimentary rocks. Local crosscutting relationships at the contacts, and abundant misoriented angular xenoliths of country rock in the margins, demonstrate that the tonalite-granodiorite was intruded into the volcanic belt. The central pluton has been dated at ca. 2.68 Ga (Tella et al., 1997a). From these observations, the tonalite-granodiorite is interpreted to have been emplaced late synkinematically with respect to Neoarchean regional deformation (*see also* Hanmer et al., 1999b).

### *Gabbro*

Three gabbro bodies occur in the southwestern corner of the map area (Fig. 1). The first occupies a triangular area between the central and eastern tonalite-granodiorite plutons. It is variably foliated, and carries xenolithic rafts of strongly deformed mafic volcanic rocks. The second occurs on the east side of the central tonalite-granodiorite pluton. It varies from isotropic, medium-grained gabbro to fine-grained amphibolite, is locally foliated, and contains xenolithic rafts of strongly deformed tonalite. Both of these gabbro units were apparently emplaced during the regional deformation history. The third, the Suluk gabbro, lies east of the eastern tonalite-granodiorite pluton. It has been described in detail by Armitage et al. (1997), who considered it to have been emplaced during the Paleoproterozoic, and to be potentially related to the MacQuoid dykes (*see* below). It is an isotropic pluton, with considerable grain size and compositional variation, that cuts its foliated wall rocks.

***Figure 11.*** *Finely layered turbiditic rocks, northern domain, volcanic belt.*

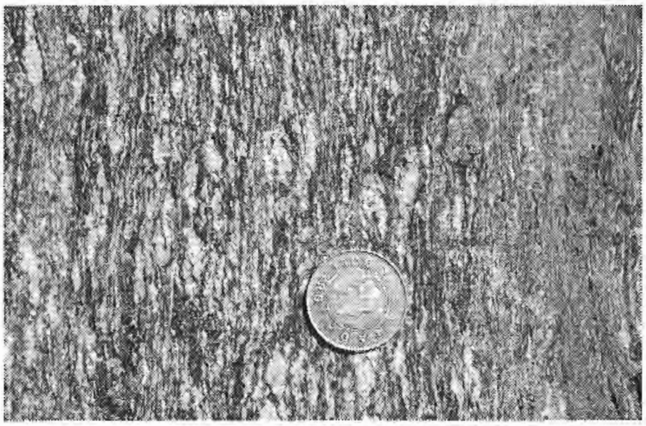

***Figure 12.*** *Garnet-sillimanite semipelite with pervasive quartzofeldspathic segregations, Bowell Island.*

## CROSS BAY PLUTONIC COMPLEX

An oval area underlain by orthogneiss units and plutonic rocks straddles Cross Bay to the north and east of the supracrustal rocks. It comprises a central tonalite to gabbro domain, intruded to the east and west by granitic plutons. The tonalite units are principally agmatitic to 'vein gneiss', commonly intruded by pervasive, semiconcordant sheets of biotite monzogranite-granodiorite, and narrow, feathery, diabase dykes. The granitoid sheets, 5 cm to 50 m thick, range from equigranular and medium to fine grained, to pegmatitic, to K-feldspar augen 'granite', and show a wide range of deformation states. South of Cross Bay, the tonalite intrudes large, map-scale panels of diorite, gabbro, and undifferentiated amphibolite. All of the rocks in this tonalite-diorite-gabbro association are well foliated and/or lineated (Fig. 13), with the exception of some of the gabbro occurrences. Primary hornblende in the tonalite and diorite units is totally replaced by biotite. Most of the map-scale panels of diorite and gabbro lie south and east of Cross Bay, and are separated from more uniformly tonalite compositions by the Cross Bay fault, identified on the basis of structural discordance (Fig. 1, 2; Hanmer et al, 1999b).

The western side of the Cross Bay complex contains a large, arcuate pluton of coarse (3–4 cm), commonly K-feldspar phyric, biotite granite-granodiorite, referred to here as the South Channel granite (*sensu lato*; Fig. 1). It is variably foliated parallel to its curved margins, ranging from isotropic, to augen granite, to very locally mylonitic. At the map scale it interdigitates semiconcordantly with the tonalite gneiss, but is locally discordant to the wall-rock foliation. At the outcrop scale, moderately foliated granite locally contains strongly foliated, concordant rafts of tonalite. To the northwest, moderately to well foliated granite is in sheeted contact with well foliated intermediate volcanic and metasedimentary rocks. These observations suggest that the granite was emplaced and deformed after the principal deformation of its wall rocks.

***Figure 13.*** *Diorite (dark) cut by tonalite (medium grey) cut by thin granitic sheets (light), all strongly foliated, Cross Bay plutonic complex.*

The eastern side of the Cross Bay complex includes an irregular-shaped mass of leucocratic, biotite monzogranite, referred to here as the Primrose monzogranite bodies (Fig. 1). Variation in colour, texture, and deformation state suggests the presence of several discrete plutons, which we cannot delimit at the scale of our mapping. In general, they are pink to cream, fine to medium grained, equigranular, and moderately foliated to isotropic, with well preserved igneous textures. Fluorite is common in leucocratic, isotropic varieties, which may be correlative with granite dated at ca. 1.83 Ga (Tella and Schau, 1994). Foliations tend to be marked by biotite alignment, rather than by strong, quartzofeldspathic shape fabrics. Locally, the monzogranite units include well foliated xenoliths of tonalite gneiss, and veins of nonfoliated monzogranite crosscut foliation in the tonalite and diorite wall rocks. Clearly, much of the Primrose monzogranite mass was emplaced after the principal deformation of its host rock. However, the range of deformation states, and the local presence of well foliated monzonite, suggest that some of these granitic rocks may have witnessed significant deformation. Monzogranite and granodiorite plutons and sheets, of similar aspect, also occur outboard of the Primrose monzogranite bodies, north of the Cross Bay fault on Big Point peninsula (Fig. 1).

The Primrose monzogranite bodies include a map-scale arcuate raft of generally agmatitic tonalite gneiss (Fig. 1). Monzogranite veining is so pervasive that parts of the raft are essentially monzogranite charged with assimilated inclusions of tonalite gneiss. Accordingly, the raft is a large inclusion in the younger monzogranite. However, within the raft, a discrete, arcuate band of tonalite straight gneiss (Hanmer, 1988) is heavily intruded by concordant monzogranite sheets that participate in the straight gneiss fabric. Both the tonalitic and monzogranitic components of the straight gneiss are thoroughly recrystallized (annealed), such that all shape fabrics have been destroyed. The contrast in settings and structural aspect indicates that this monzogranite is older than those which host the tonalite raft.

## BIG LAKE SHEAR ZONE

The southern margin of the Cross Bay plutonic complex is marked by a steeply dipping belt of straight gneiss and ribbon mylonite, up to 2 km thick (Fig. 1). Foliation in the straight gneiss and mylonite units is steeply dipping, and carries a generally east-trending, subhorizontal lineation. At the map scale, the shear zone appears to be laterally restricted. East of Big lake and north of Brown Lake it splays into several branches that appear to terminate within the map area. The western segment of the shear zone is stitched by a circular pluton of isotropic monzogranite and associated monzonite (Fig. 1), which clearly cuts and straddles the shear zone.

## DYKES

At least two major dyke sets occur in the map area. The MacQuoid dykes are the eastward extension of the ca. 2.19 Ga Tulemalu mafic dyke swarm (Tella et al, 1997a, c). In the present map area they occur as thick (up to 500 m), steeply dipping sheets, outcropping as elevated ridges up to 5 km long, and discontinuously traceable for tens of kilometres (Fig. 1). They are coarse grained, locally plagioclase-phyric, and commonly have preserved chilled margins. The dykes are predominantly composed of hornblende and plagioclase. However, they contain local anhydrous patches of variable size that preserve coronitic garnet with clinopyroxene and plagioclase. In the southern part of the map area, the internally isotropic dykes generally trend 070°–120°. They crosscut the regional foliation and compositional layering in both the Gibson–MacQuoid homocline and the tonalitic rocks associated with the volcanic belt (Fig. 1). Even where they are clearly postkinematic to the deformation in their wall rocks, and preserve right-angled jogs and bayonet structures in their contacts, the dyke walls are commonly undulose on the scale of 10–50 m. The dykes are also seen to branch, locally perpendicularly, and to turn back into the main trend at some distance (50–100 m) from the main dyke.

In several places within the Big lake shear zone, the fabric of the annealed straight gneiss wraps around a 90° bend in the margin of a MacQuoid dyke. In the Cross Bay complex, at least six mafic dykes, each conforming to the field characteristics of the MacQuoid dykes to the south, were folded, foliated, and/or lineated during deformation involving the enclosing tonalitic wall rocks. Accordingly, we conclude that the Big lake shear zone and the Cross Bay complex have witnessed regionally extensive Paleoproterozoic deformation and metamorphism after ca. 2.19 Ga.

Narrow (25 cm to 2 m) lamprophyre dykes, dated at ca. 1.83 Ga (MacRae et al., 1996), are very common throughout the map area. They are variable in orientation, but the majority trend approximately northwest. For the most part, they are not deformed, although it is not uncommon for dykes, crosscutting at a high angle to wall rock foliation, to contain a wall-parallel or oblique internal fabric. Both foliated and isotropic lamprophyre dykes occur in the discovery outcrop of the diamondiferous Akluilâk dyke, near the Sandhill prospect (Fig. 1). Similar dykes within the isotropic Primrose and stitching monzogranite plutons also carry internal foliations. Such fabrics are related to the local conditions of dyke emplacement and cooling, and do not necessarily reflect a regional tectonometamorphic event. Fine-grained, potassic dykes of hornblende syenite share the same field relations as the lamprophyre dykes, and are spatially associated with them locally.

## CARVING STONE

Carving stone is currently quarried in a small-scale operation on the northwest side of Cross Bay (Fig. 1). The material appears to be predominantly chlorite-tremolite-talc rock. Several new sites of similar material have been identified, where it appears to be derived from metamorphosed mafic to ultramafic dykes. They are described in detail elsewhere (Hanmer et al., 1999a). However, we note here that several of the occurrences lie within the Big lake shear zone (Fig. 1), and may therefore be Paleoproterozoic.

## SUMMARY

The northeastern MacQuoid supracrustal belt comprises the Gibson–MacQuoid homoclinal belt of homogeneous metasedimentary rocks, tonalitic orthogneiss units, and plutons, structurally overlain to the north by a belt of mafic to intermediate volcanic flows and volcaniclastic rocks, intruded by tonalitic to granodiorite plutons. A second metasedimentary belt lies on the north side of the volcanic rocks. To the north and east of the supracrustal belt, the Cross Bay plutonic complex is composed of tonalitic to gabbroic gneiss units, intruded by a variety of late synkinematic, granitic plutons. The plutonic complex is separated from the supracrustal belt by the steeply dipping, mylonitic, Big lake shear zone, up to 2 km thick. Metamorphosed, ca. 2.19 Ga, MacQuoid dykes crosscut the supracrustal rocks and their deformation fabrics, but are involved in regional deformation in both the plutonic complex and the shear zone. Accordingly, a widespread thermal event affected the entire map area after ca. 2.19 Ga, but pervasive regional deformation was confined to the northern half.

## ACKNOWLEDGMENTS

We are grateful to Erika Greiner, Nancy MacDonald, Mark Quigley, and Gillian Royle for their outstanding, enthusiastic assistance in the field, and to Laura Adams, our wonderful cook. This work could not have been undertaken without the generous support of the Polar Continental Shelf Project. Our Huisson Aviation helicopter crew, pilot Terry Halton and engineer Matt Weeks, provided unsurpassed service throughout the summer, especially in the teeth of adversity. Expediting was by M&T Enterprises. We benefited from visits (long and short term) by our colleagues Rob Berman, Bill Davis, Penny Henderson, John Kerswill, Carolyn Relf, and Rob Rainbird, and geophysical assistants Greg Clark, M.J. Mancini, and Thor Bochonko. We thank Larry Aspler for critically reading the manuscript.

## REFERENCES

**Armitage, A.E., Miller, A.R., and MacRae, N.D.**

1994: Geology of the Sandhill Zn-Cu showing in the Gibson Lake area, District of Keewatin, Northwest Territories; *in* Current Research 1994-C; Geological Survey of Canada, p. 147–155.

1995: Geological setting of the Sandhill Zn-Cu-Pb-Ag prospect in the Gibson-MacQuoid lake area, District of Keewatin, Northwest Territories; *in* Current Research 1995-C; Geological Survey of Canada, p. 213–224.

1997: Paleoproterozoic Ni-Cu-Co sulphide mineralization, Suluk occurrence, Gibson-MacQuoid Lake area, western Churchill Province, Northwest Territories; *in* Current Research 1997-C; Geological Survey of Canada, p. 61–70.

**Hanmer, S.**

1988: Ductile thrusting at mid-crustal level, southwestern Grenville Province; Canadian Journal of Earth Sciences, v. 25, p. 1049–1059.

**Hanmer, S., Sandeman, H.A., Tella, S., Ryan, J. J., Hadlari, T. and Mills, A.**

1999a: Preliminary petrography of current and potential carving stone, Gibson Lake–Cross Bay area, Northwest Territories (Kivalliq region, Nunavut); *in* Current Research 1999-C; Geological Survey of Canada.

**Hanmer, S., Tella, S., Sandeman, H.A., Ryan, J.J., Hadlari, T., and Mills, A.**
1999b: Proterozoic reworking in Western Churchill Province, Gibson Lake–Cross Bay area, Northwest Territories (Kivalliq region, Nunavut). Part II: regional structural geology; *in* Current Research 1999-C; Geological Survey of Canada.

**LeCheminant, A.N., Tella, S., Sanborn-Barrie, M., and Venance, K.E.**
1997: Geology, Parker Lake South, District of Keewatin, Northwest Territories; Geological Survey of Canada, Open File 3405, scale 1:50 000.

**MacRae, N.D., Armitage, A.E., Miller, A.R., Roddick, J.C., Jones, A.L., and Mudry, M.P.**
1996: The diamondiferous Akluilâk lamprophyre dyke, Gibson Lake area, NWT; *in* Searching for Diamonds in Canada, (ed.) A.N. LeCheminant, D.G. Richardson, R.N.W. DiLabio, and K.A. Richardson; Geological Survey of Canada, Open File 3228, p. 101–107.

**Miller, A.R. and Tella, S.**
1995: Stratigraphic setting of semiconformable alteration in the Spi Lake area, Kaminak greenstone belt, Churchill Province, Northwest Territories; *in* Current Research 1995-C; Geological Survey of Canada, p. 175–186.

**Reinhardt, E.W. and Chandler, F.W.**
1973: Gibson-MacQuoid Lake map area, District of Keewatin; *in* Report of Activities, Part A; Geological Survey of Canada, Paper 73-1A, p. 162–165.

**Reinhardt, E.W., Chandler, F.W., and Skippen, G.B.**
1980: Geological map of the MacQuoid Lake (NTS 55M, E1/2) and Gibson Lake (NTS 55N, W1/2) map areas, District of Keewatin; Geological Survey of Canada, Open File 703, scale 1:250 000.

**Ryan, J.J., Hanmer, S., Tella, S., and Sandeman, H.A.**
1999: Detailed structural studies, Gibson Lake–Cross Bay–MacQuoid Lake area, Northwest Territories (Kivalliq region, Nunavut); *in* Current Research 1999-C; Geological Survey of Canada.

**Sanborn-Barrie, M.**
1994: Structural investigation of high-grade rocks of the Kramanituar complex, Baker Lake area, Northwest Territories; *in* Current Research 1994-C; Geological Survey of Canada, p. 121–133.

**Tella, S. and Schau, M.**
1994: Geology, Gibson Lake (east-half), District of Keewatin, Northwest Territories; Geological Survey of Canada, Open File 2737, scale 1:50 000.

**Tella, S., Davis, W., Berman, R.G., Stern, R., and LeCheminant, A.N.**
1997a: Tectonothermal history of the MacQuoid Lake supracrustal belt, District of Keewatin, Northwest Territories, Canada; Geological Society of America, Abstracts with Programs, v. 29, p. 277–278.

**Tella, S., LeCheminant, A.N., Sanborn-Barrie, M., and Venance, K.E.**
1997b: Geology, parts of MacQuoid Lake, District of Keewatin, Northwest Territories; Geological Survey of Canada, Open File 3404, scale 1:50 000.
1997c: Geology and structure of parts of the MacQuoid Lake area, District of Keewatin, Northwest Territories; *in* Current Research 1997-C; Geological Survey of Canada, p. 123–132.

**Wright, G.M.**
1967: Geology of the southeastern Barren Grounds, parts of the Districts of Mackenzie and Keewatin (Operations Keewatin, Baker, Thelon); Geological Survey of Canada, Memoir 350, p. 91.

---

Geological Survey of Canada Project 970006

# Proterozoic reworking in western Churchill Province, Gibson Lake–Cross Bay area, Northwest Territories (Kivalliq region, Nunavut). Part 2: regional structural geology[1]

S. Hanmer, S. Tella, H.A. Sandeman, J.J. Ryan, T. Hadlari[2], and A. Mills[2]
Continental Geoscience Division, Ottawa

*Hanmer, S., Tella, S., Sandeman, H.A., Ryan, J.J., Hadlari, T., and Mills, A., 1999: Proterozoic reworking in western Churchill Province, Gibson Lake–Cross Bay area, Northwest Territories (Kivalliq region, Nunavut). Part 2: regional structural geology;* in *Current Research 1999-C; Geological Survey of Canada, p. 65–75.*

**Abstract:** The principal structural elements in the Gibson Lake–Cross Bay map area are, the Gibson–MacQuoid $D_2$ homocline, overlain with possible structural discordance by a volcanic belt, intruded by Neoarchean, syn-$D_2$ plutons; and the Cross Bay plutonic complex, wherein $S_2$ is deformed about south-plunging, $F_3$ folds, associated with a coaxial $L_3$ extension lineation, and east-northeast-trending, $F_4$ folds. The plutonic complex is bounded to the south by the pre-, syn-, and post-$D_4$, dextral, strike-slip Big lake shear zone. Metamorphosed, ca. 2.19 Ga, MacQuoid dykes everywhere postdate $S_2$, but within the Cross Bay complex and the Big lake shear zone they were deformed during $D_3$-$D_4$. Therefore, $D_3$ and $D_4$ are regional Paleoproterozoic events. Granitic plutons within the plutonic complex were intruded after $D_2$ and before $D_4$ fabrics, respectively, and represent Paleoproterozoic magmatic events.

**Résumé :** Les principales composantes structurales présentes dans la région cartographique du lac Gibson et de la baie Cross sont les suivantes : l'homoclinal $D_2$ de Gibson–MacQuoid que surmonte vraisemblablement en discordance structurale une zone volcanique recoupée par des plutons néoarchéens contemporains de la phase $D_2$; et le complexe plutonique de Cross Bay, dans lequel la schistosité $S_2$ est déformée autour de plis $F_3$ à plongement sud, associés à une linéation d'étirement $L_3$ coaxial et à des plis $F_4$ à orientation est-nord-est. Le complexe plutonique est limité au sud par la zone de cisaillement de Big Lake à rejet horizontal dextre qui est à la fois antérieur et postérieur à la phase $D_4$ et contemporain de cette phase. Les dykes métamorphisés de MacQuoid d'environ 2,19 Ga sont partout postérieurs à la schistosité $S_2$, mais dans le complexe de Cross Bay et la zone de cisaillement de Big Lake, ils ont été déformés au cours des phases $D_3$ et $D_4$. Par conséquent, les phases $D_3$ et $D_4$ constituent des événements régionaux du Paléoprotérozoïque. Les plutons granitiques dans le complexe plutonique ont été mis en place après la phase $D_2$ et avant la phase $D_4$, respectivement; ils représentent donc des événements magmatiques paléoprotérozoïques.

[1] Contribution to the Western Churchill NATMAP Project
[2] Department of Earth Sciences, Carleton University, Ottawa, Ontario K1S 5B6

## INTRODUCTION

The Western Churchill NATMAP Project involves the Geological Survey of Canada (GSC), the Government of the Northwest Territories (GNWT), and Indian and Northern Affairs Canada (INAC). In 1998, the second phase of the GSC's three year field program, an investigation of the geology of parts of the MacQuoid Lake (NTS 55 M) and Gibson Lake (NTS 55 N) map areas (Fig. 1) was undertaken between Gibson Lake and Chesterfield Inlet. Particular emphasis was placed on establishing the nature and extent of Paleoproterozoic tectonothermal reworking of older, Archean rocks. Bedrock mapping was undertaken at 1:50 000 scale, building on earlier work by Tella et al. (1997b, c). In this report, we examine the regional structural geology of the map area (Fig. 1). An overview of the lithological characteristics is presented in a companion paper (Hanmer et al., 1999), to which the reader is referred. Frequent reference will be made here to lithologies and lithological relationships that have been described therein. More detailed, targeted, structural observations are presented elsewhere (Ryan et al., 1999; Mills et al., 1999).

### *Geological overview*

The map area includes the eastern part of the Archean MacQuoid supracrustal belt (Tella et al., 1997a, b, c) and the Cross Bay plutonic complex (Fig. 1). The MacQuoid supracrustal belt is divided into the Gibson–MacQuoid homocline, a predominantly metasedimentary belt with panels of gneissic tonalite, flanked to the north by a predominantly volcanic belt intruded by tonalite-granodiorite plutons. The oval Cross Bay plutonic complex is principally composed of tonalitic gneiss units, crosscut by the Primrose and South Channel granitic plutons. Along its southern margin, the plutonic complex is separated from the supracrustal belt by the approximately east-trending, strike-slip, Big lake shear zone. Regionally extensive Paleoproterozoic deformation occurred in the Cross Bay complex. Unless otherwise indicated, 'the foliation' refers to the dominant, layer-parallel foliation developed in a given outcrop or area.

## FABRICS AND FOLDS

### *Gibson–MacQuoid homocline and volcanic belt*

The spatial distribution of foliation and lineation orientations in the map area is complex (Fig. 2). The Gibson–MacQuoid homocline comprises moderately (40–50°) northwestward-dipping, concordant panels of semipelitic, psammitic, and pelitic metasedimentary rocks, with subordinate mafic volcanic and volcaniclastic rocks; and tonalitic agmatitic and 'vein gneiss'. A single, penetratively developed, L/S shape fabric is composed of a foliation and a sporadically developed, moderately to steeply pitching, north- to northeast-plunging, extension lineation. In the southern domain of the volcanic belt, layering, where present, is similarly moderately northward- to north-northeast-dipping (Fig. 3). It is ubiquitously parallel to an L/S shape fabric, in which a strong extension lineation is widely developed and typically oriented down the dip. Isolated isoclinal folds of layering and foliation occur in both the homocline and the volcanic belt (Fig. 4). Their axes are generally lineation-parallel, and they do not appear to form systematic fold trains. The foliation in the volcanic belt wraps concordantly around the ca. 2.68 Ga (Tella et al., 1997a) western, central, and eastern tonalite-granodiorite plutons (W, C, and E in Fig. 1, *see also* Fig. 2), which intrude the strongly foliated volcanic rocks and include them as misoriented xenoliths. Within the two synformal keels separating the plutons, the foliation and layering are essentially vertical, and carry a particularly strong extension lineation, pitching very steeply to the north and northeast. The concordant foliation within the plutons dips outward, and steepens toward the intrusive contacts. It carries a northeast-plunging, extension lineation, parallel to that in the shallowly dipping, volcanic rocks on the north side of the plutons. These observations indicate that the plutons were intruded and deformed after Neoarchean deformation in their wall rocks had initiated.

Within the tonalite and volcanic rocks north and west of Brown Lake, the foliation switches abruptly, from northeast dipping to southwest dipping and concordant to the boundary of the Cross Bay complex (locality A, Fig. 2), while the general azimuth of the extension lineation switches from north to northwest. Although it is conceivable that the change in dip is due to a hitherto undetected splay of the Big lake shear zone, we cannot eliminate the possibility of a dislocated, regional-scale, synformal fold. In the vicinity of South Channel, the foliation in the northern domain of the volcanic belt remains concordant to the Cross Bay complex, but dips moderately (about 50°) to the northwest (locality B, Fig. 2). It passes progressively across strike into the metasedimentary rocks on Bowell Island and Cone Hill peninsula, where it dips steeply (about 75°) to the north. In both of these areas, the foliation carries a moderately (about 25°) westward-plunging, extension lineation.

### *Cross Bay plutonic complex*

The Cross Bay plutonic complex comprises a central tonalitic gneiss domain, intruded to the east and west by younger granitic plutons (Fig. 1). The tonalitic gneiss domain can be further subdivided into predominantly tonalite units to the west, and a tonalite-diorite-gabbro association to the east.

#### South-plunging folds

Foliation and layering in the gneiss are locally deformed about small-scale, isolated, isoclinal folds. On a larger scale, they are also deformed by shallowly (about 20°) plunging, open to tight, upright folds, which control the map pattern (Fig. 1; locality C, Fig. 2). In the northern part of Big Point peninsula, these folds are broad, open warps outlined by gneissic layering and foliation, and by voluminous veins, sheets, and map-scale ridges of generally very weakly foliated monzogranite, pervasively injected along the gneissic layering of the tonalite host rock. West of Cross Bay, similarly oriented structures range from outcrop- to map-scale, open to tight folds, the largest of which is a very tight

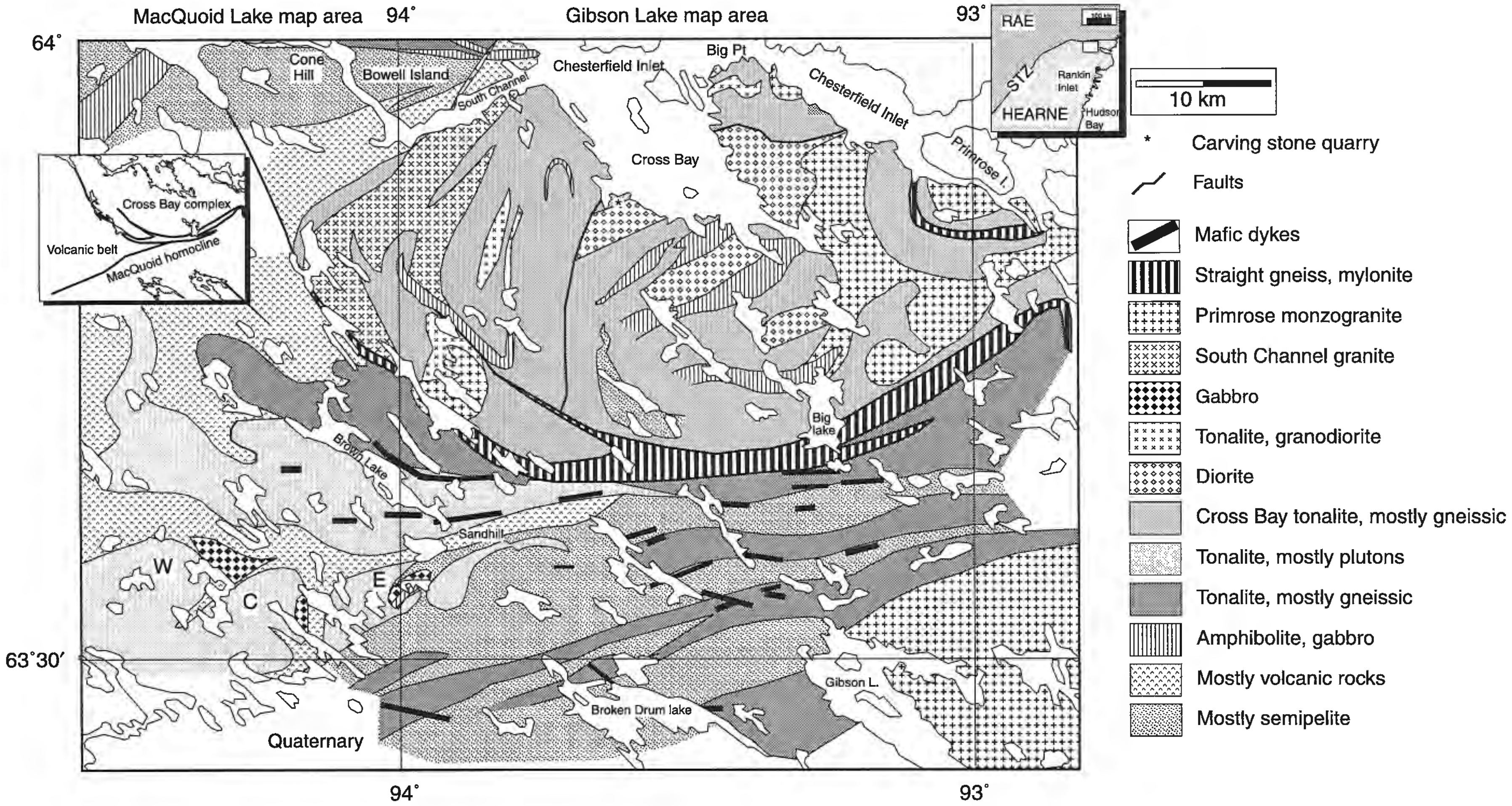


***Figure 1.*** *Generalized geology of the Gibson Lake–Cross Bay area. The letters W, C, and E are western, central, and eastern plutons, respectively; STZ=Snowbird tectonic zone.*

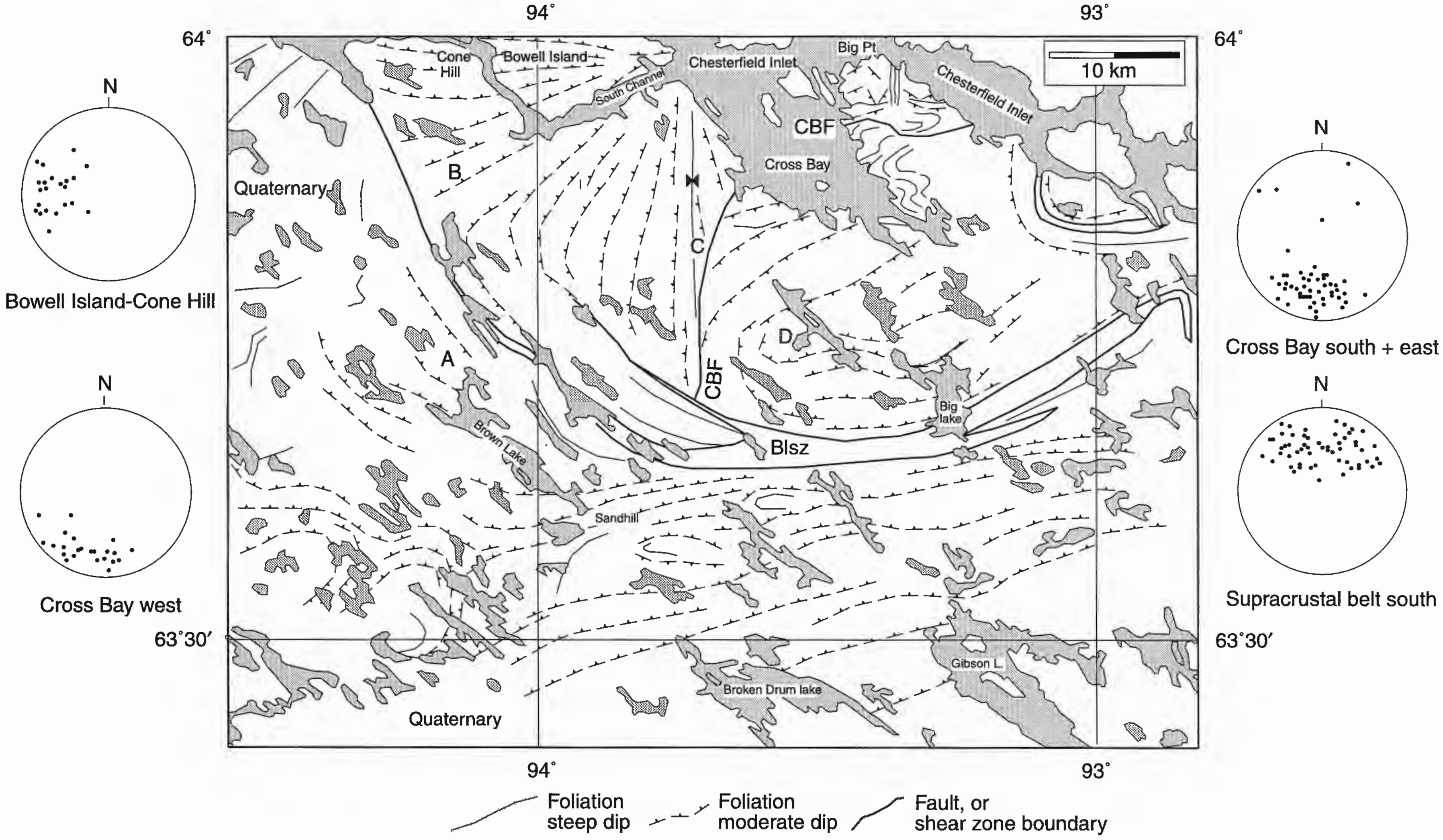


***Figure 2.*** *Structural elements of the Gibson Lake–Cross Bay area, with selected extension lineation plots. The letters A, B, C, and D are localities discussed in the text; Blsz=Big lake shear zone; CBF=Cross Bay fault.*

synform, whose limbs both dip moderately to steeply to the west (locality C, Fig. 2). At the outcrop scale, folds show similar relationships to granitic veins and sheets as those just described. A strong, pervasive, extension lineation is regionally developed in both the tonalitic gneiss units and the granitic rocks, parallel to the fold axes. In the gneiss units it forms part of an L/S tectonite in combination with the folded foliation, whereas in the granitic rocks it generally forms a new L fabric. Although the development of the extension lineation does not require the local presence of the folds, it is certainly enhanced in the axial zones of outcrop-scale closures. This latter relationship is also present at the map scale. These observations suggest that the extension lineation is related in time to the folding event, and superimposed on the older foliation in the tonalitic gneiss units. However, the lack of a direct spatial correlation between the presence of folds and the extension lineation suggests that the latter is ultimately related to the far-field boundary conditions of the deformation that generated the folds, as opposed to resulting from the folding process *per se*.

### East-northeast-trending folds

South and east of Cross Bay, the map pattern is dominated by moderately (about 40°) east-northeast plunging, map-scale, upright folds of layering and foliation in the tonalite-diorite-gabbro association (Fig. 1; locality D, Fig. 2). Smaller, map-scale folds in the southern part of Big Point peninsula also appear to deflect the western boundary of the Primrose monzogranite (Fig. 1). Furthermore, the arcuate form of the map-scale tonalite raft within the monzogranite appears to reflect the same fold pattern, except that it plunges to the west-southwest (Fig. 1, 2), possibly as a result of rotation within the magmatic host. In the northern part of Big Point peninsula, a single, very open, shallowly west-plunging member of this fold set refolds outcrop-scale examples of the south-plunging, lineation-parallel folds (Fig. 2). South of Cross Bay, open, south-plunging, map-scale warps of foliation and layering occur in the axial zone of the major east-northeast-plunging fold (locality D, Fig. 2), and a pervasive, south-plunging extension lineation is well developed throughout the northern limb of the fold. Taken together, these observations indicate that the south-plunging folds and coaxial extension lineation predate the east-northeast-trending folds. In general, no new fabric elements accompany the younger fold set. However, northeast of Big lake (Fig. 1), a moderately plunging, porpoising extension lineation occurs in association with, and coaxial to, east-northeast-trending folds, such that L tectonite units are present in the fold hinges, and L/S fabrics in the fold limbs.

At the western end of the Cross Bay complex, the internal foliation and the external contacts of the coarse-grained, variably deformed, South Channel granite (*sensu lato*) pluton dip moderately to steeply (40–70°) to the west and describe an arc, concave to the east (Fig. 1, 2). The central and northern segments of the granite carry a very weakly developed, west- to northwest-plunging, dip-parallel extension lineation. Continuity of the arcuate foliation pattern around the western end of the Cross Bay complex is only demonstrable within the granite. Northwest and northeast structural trends in the wall rocks appear to be tectonically juxtaposed (*see* below), and the map-scale panels of wall rock within the granite are discontinuous. The granite was intruded after the principal deformation of its wall rocks (Hanmer et al., 1999), and it carries an internal, discordant extension lineation. Therefore, we suggest that its shape and deformation fabric may be related to the local conditions of its emplacement.

### *Big lake shear zone*

A steeply dipping belt of S>L porphyroclastic straight gneiss and ribbon mylonite units, up to 2 km thick, marks the southern margin of the Cross Bay complex and separates it from the supracrustal rocks to the south and west (Fig. 1, 2, 5, 6). The participation of garnet hornblende in the fabrics of mafic rocks, and the crystal-plastic behaviour of most feldspars in all lithologies, is indicative of deformation at amphibolite-facies conditions. Foliation in the straight gneiss and mylonite units is generally steeply dipping, and carries an east-trending, subhorizontal lineation. Locally, a variety of shear-sense criteria (delta porphyroclasts, pressure shadows,

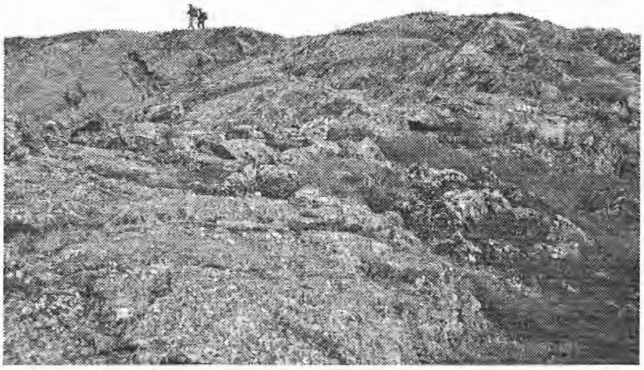

***Figure 3.*** *Northward-dipping $S_2$, southern domain, volcanic belt.*

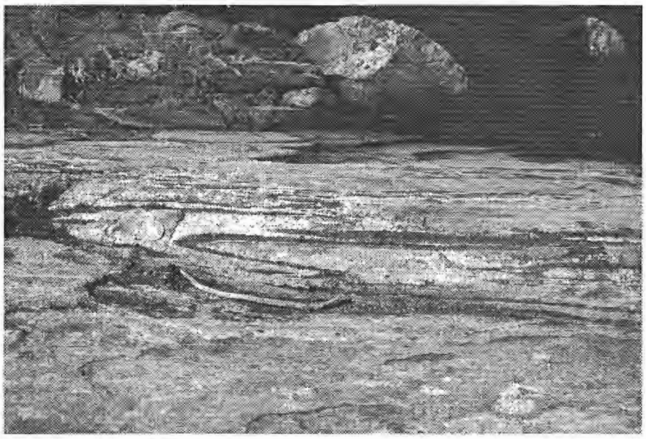

***Figure 4.*** *Isolated isoclinal folds of $S_2$, Gibson–MacQuoid homocline.*

rotated fold axial planes, asymmetrical shear bands, C/S fabrics, foliation fish) indicates the shear zone is a dextral, strike-slip structure (Fig. 7, 8). At the map scale, the shear zone appears to be laterally restricted. East of Big lake and north of Brown Lake it branches into several mylonitic splays that appear to terminate within the map area (Fig. 1).

The central and eastern segments of the shear zone are principally composed of recrystallized (annealed) straight gneiss (Fig. 9). The outcrop-scale aspect of the straight gneiss units combines the characteristics of two end members, 1) a uniformly straight layered, tonalite-amphibolite gneiss, with a remarkably constant, fine grain size, generally lacking a shape fabric, and 2) a fine- to medium-grained, homogeneous, clean tonalite with K-feldspar porphyroclasts derived by the mechanical breakdown of granitic pegmatite. In many cases, abundant transposed pegmatitic veins lend a general streaky aspect to the straight gneiss units. Excellent ribbon fabrics are commonly preserved in monzogranitic veins, where present.

The western segment of the shear zone differs from the central and eastern parts. It dips steeply to the southwest, concordant to the boundary of the Cross Bay complex, and carries an oblique, moderately northwest-plunging, extension lineation. It is predominantly composed of spectacular, garnet-bearing ribbon and laminated mylonite units (Fig. 10, 11) derived from garnet amphibolite and anorthositic protoliths, plus tonalite and granitic veins. These mylonite units were cut by voluminous sheets of monzogranite, which were subsequently converted to ribbon mylonite, up to 100 m thick. The protoliths to the mylonite units appear to represent a lithological association that has not yet been identified south of Chesterfield Inlet, but are similar to the protoliths of mylonite units of the Kramanituar and Uvauk complexes

*Figure 5. Amphibolite and tonalite layers in straight gneiss, Big lake shear zone.*

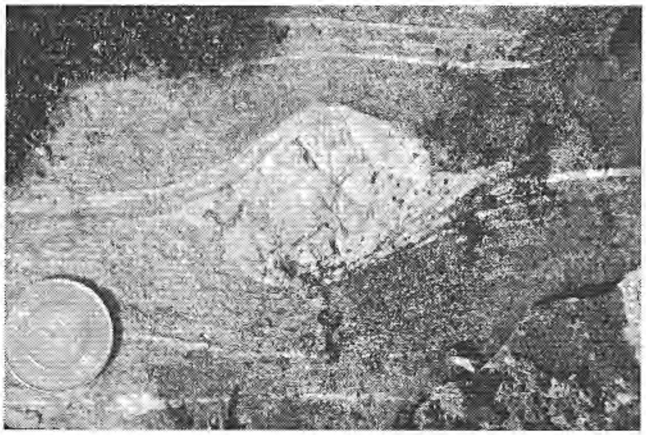

*Figure 7. Dextral delta porphyroclast in annealed straight gneiss, Big lake shear zone.*

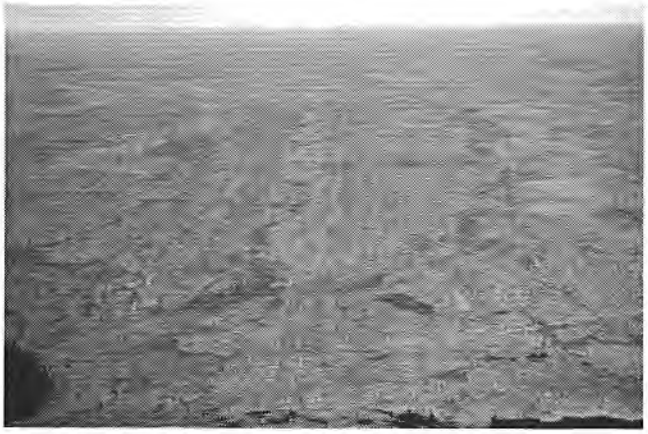

*Figure 6. Aerial view of Big lake shear zone, near Big lake.*

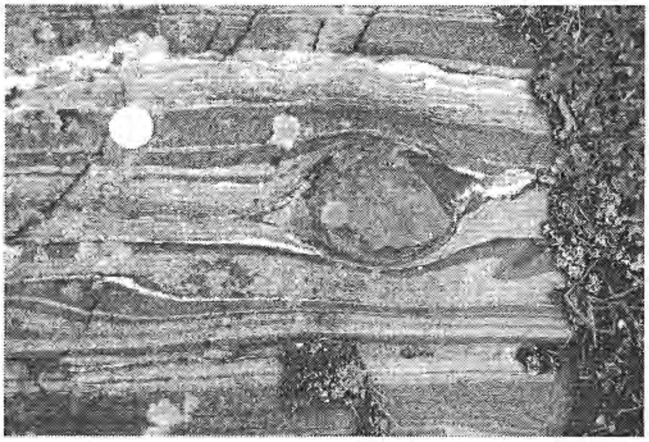

*Figure 8. Z-folded layering in annealed straight gneiss, with dextral hornblende pressure shadows on clinopyroxenite inclusion, Big lake shear zone.*

exposed along its north shore (Tella et al., 1993; Sanborn-Barrie, 1994; Mills et al., 1999). Further details of the shear zone are given elsewhere (Ryan et al., 1999).

### Terminations and extensions

To the west, the shear zone divides into two splays (Fig. 1). The northern splay truncates the axial traces of the shallowly south-plunging folds and the associated coaxial extension lineation. On the north side of the splay, the north-striking, gneissic fabric is deformed into moderately to steeply plunging, map-scale, Z-folds within a zone a few kilometres wide. This appears to be a ductile process zone associated with dextral slip on the narrow splay as it attenuates to the northwest.

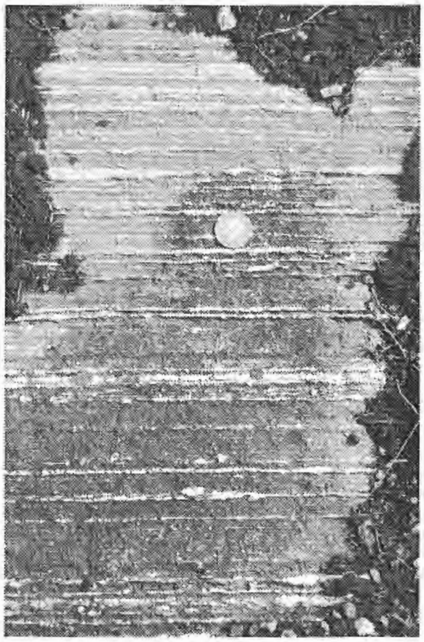

***Figure 9.*** *Porphyroclastic annealed straight gneiss, Big lake shear zone.*

The southern splay can be traced in outcrop to a point due north of Brown Lake, whence it is obscured by Quaternary deposits (Fig. 1). However, aeromagnetic data (Geological Survey of Canada, 1987) indicate a discrete linear feature with a potential dextral separation of about 20 km projecting through the northwest corner of the map area. We suggest that this is either the northwest continuation of the southern splay, or a late fault which cuts out the western end of the shear zone. In either case, it appears to account for the structural discordances across its trace.

### *Cross Bay fault*

A map-scale discordance in the three-dimensional foliation pattern within the Cross Bay complex requires the presence of a discrete structural break, the Cross Bay fault (Fig. 1, 2). The fault has no geological expression on the ground, and its trace is drawn according to cartographic evidence. Southwest of Cross Bay, the fault trace is interpolated where it abruptly separates north-trending, moderately to steeply (40–60°) west-dipping foliation from similarly inclined foliation dipping to the southeast. It also separates tonalite gneiss to the west, and the tonalite-diorite-gabbro association to the east. On Big Point peninsula, it is drawn between 1) folded tonalite gneiss, pervasively injected by monzogranite veins and sheets to the north, abruptly juxtaposed with 2) planar, foliated diorite cut by occasional pegmatite veins to the south. The high ground underlain by the diorite at the contact suggests that this segment of the fault may dip to the south.

## RELATIVE AND ABSOLUTE AGE CONSTRAINTS

In contrast to the multiple planar fabrics identified in the western segment of the MacQuoid supracrustal belt (Tella et al., 1997b), rocks in the present map area only carry a single, layer-parallel foliation, with very few exceptions. Reexamination of selected areas at the boundary between the two map areas indicates that the foliation we have mapped in the Gibson–MacQuoid homocline and the southern domain

***Figure 10.*** *Granitoid ribbon mylonite, Big lake shear zone.*

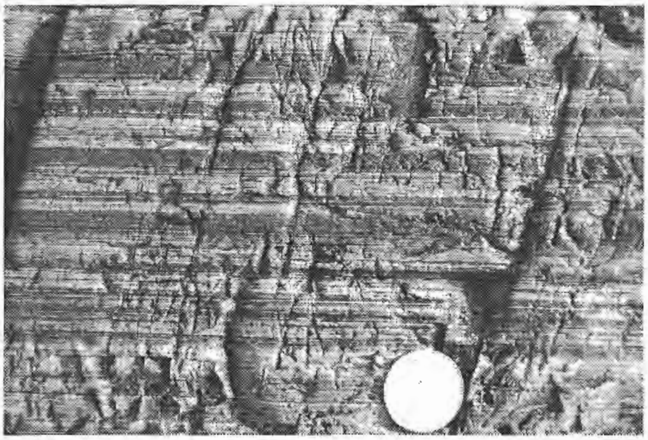

***Figure 11.*** *Mafic ribbon mylonite, with garnet amphibolite and tonalitic layers, Big lake shear zone.*

of the volcanic belt is $S_2$, derived by the transposition of an older $S_0/S_1$ fabric during the Neoarchean (Ryan et al., 1999). In the absence of evidence for later, pervasive reworking of $S_2$, we interpret the associated extension lineation as $L_2$. Metamorphosed, ca. 2.19 Ga, MacQuoid dykes (Tella et al., 1997a) cut $S_2/L_2$, thereby placing a minimum age on the deformation fabrics, and a maximum age on the metamorphism that affected the dykes. The synkinematic, tonalite-granodiorite plutons in the southwest corner of the map area (Fig. 1) constrain the age of $D_2$ at ca. 2.68 Ga (Tella et al., 1997a).

Similar MacQuoid dykes are folded and boudined within the tonalite gneiss units of the Cross Bay complex (Fig. 12; *see also* Hanmer et al., 1999). In some cases, the initial cross-cutting relationship between the dyke and the host rock foliation is preserved. All of the folded examples are deformed about approximately north-south axial planes associated with the shallowly south-plunging folds developed in the tonalite gneiss. Therefore, these folds, as well as the contemporaneous, coaxial extension lineation, are the product of regional Paleoproterozoic deformation superposed upon a foliation and gneissic layering predating dyke formation. If, by analogy with the fabrics outside of the Cross Bay complex, the fabric predating dyke formation is $S_2$, then the south-plunging folds and extension lineation are $F_3/L_3$. These structures have so far only been identified within the Cross Bay complex. However, outcrop-scale, open to moderate, upright, symmetrical folds, with north-south axial planes, are locally developed in well layered parts of the southern domain of the volcanic belt, and in the Big lake shear zone (Fig. 13). They are not associated with any new fabric elements, and their northerly plunge is determined by the initial orientation of the fabrics being folded. Nonetheless, they may be equivalent to the north-south folds developed in the Cross Bay complex, and therefore Paleoproterozoic. In the volcanic belt, such folds would be similarly designated $F_3$ because they fold $S_2$ fabrics. The map-scale, east-northeast-trending folds in the Cross Bay plutonic complex deform $F_3$ folds, and are therefore designated $F_4$.

South of Big lake (Fig. 1), the recrystallized, straight gneiss fabric espouses several 90° bends as it wraps around a deep embayment in the margin of a MacQuoid dyke (*see* Fig. 14). The dyke is internally undeformed, except for some minor shear zones, and preserves a chilled margin. It is likely that the embayment is primary, similar to jogs and bends observed in postkinematic MacQuoid dykes in the Gibson–MacQuoid homocline (Hanmer et al., 1999). The key observation is that the mylonitic fabric of the straight gneiss developed, or was reworked, after emplacement of the MacQuoid dyke, and subsequently recrystallized (annealed). Therefore, a significant part of the mylonitic history of the shear zone is Paleoproterozoic.

The Paleoproterozoic history of the Big lake shear zone is probably polyphase in nature. Timing of the initiation of the shear zone remains unconstrained, and could conceivably predate the MacQuoid dykes. As noted above, the western part of the shear zone truncates the axial traces of the shallowly south-plunging folds of the Cross Bay complex, and therefore postdates $F_3/L_3$. To the east, strain gradients have been locally identified on either side of the shear zone. For example, within the Gibson–MacQuoid homocline, trains of shallowly north-northeast- to east-plunging folds of foliation and layering are locally developed within a few kilometres of the shear zone. These folds carry a well developed extension lineation in their hinge zones, parallel to that in the shear zone, and are transposed into the now annealed straight gneiss units within 100 m of the shear zone boundary. A similar coaxial relationship was noted above between shallowly plunging, east-northeast-trending folds and a locally developed extension lineation to the northeast of Big lake. We suggest that it is possible that some of the east-northeast-trending folds in the Cross Bay complex may have formed as a result of activity on the shear zone. These folds are geometrically comparable with the map-scale, $F_4$ folds in the Cross Bay complex. However, the shear zone truncates the Cross Bay

***Figure 12.*** *Folded MacQuoid dyke, Cross Bay plutonic complex.*

***Figure 13.*** *$F_3$ folding of layered mylonite, Big lake shear zone.*

fault (Fig. 1), which itself cuts $F_4$ folds in Big Point peninsula (Fig. 2). We suggest the Big lake shear zone was active before, during, and after $D_4$.

Granitic rocks in the Cross Bay complex may also help constrain the timing of folding and shear zone activity in the map area. The 'stitching' monzogranite pluton northeast of Brown Lake is texturally similar to some of the Primrose monzogranite bodies affected by $F_4$ folding (Fig. 1). Similar monzogranite bodies were emplaced into the mylonite and straight gneiss units of the Big lake shear zone, and subsequently mylonitized. Dating the granitic rocks will constrain the time window during which the $F_4$ folds, the Cross Bay fault, and the shear zone were active. Furthermore, lamprophyre dykes (ca. 1.83 Ga; MacRae et al., 1996), which cut the Primrose and the stitching monzogranite bodies, also intrude the shear zone. In the western segment, they cut ribbon mylonite units, but develop internal, dextral, C/S fabrics and were subsequently folded, thereby demonstrating that the shear zone was still active at that time. The Primrose monzogranite bodies could also provide a minimum age for the straight gneiss units within the tonalite raft (Fig. 1), and allow comparison with similar tectonite units in the Big lake shear zone.

## METAMORPHISM

In the volcanic belt, aluminous metasedimentary rocks contain prekinematic to synkinematic andalusite enclosed by the $S_2$ foliation and partially replaced by (?)sillimanite. Late synkinematic staurolite-(?)kyanite overgrow $S_2$, which is also deflected about the ends of the crystals. Mafic volcanic rocks commonly contain 2–3 mm garnets, enclosed by $S_2$ developed in a fine-grained hornblende-plagioclase matrix. Plagioclase rims commonly preserve the garnet shape, suggestive of postkinematic decompression. Intermediate volcanic rocks commonly carry needle-like to elongate hornblende porphyroblasts, randomly oriented (decussate) within the regional foliation plane (Fig. 15). Spectacular examples also occur in pillow lavas just west of the map area, where Tella et al. (1997b) interpreted this phenomenon as a contact effect adjacent to late, postkinematic plutons. However, the porphyroblastesis is areally extensive and appears to represent a postkinematic, regional metamorphic event of unknown age.

## SPECULATIVE BOUNDARY CONDITIONS

It is premature to define boundary conditions for the structural history of the map area. Nevertheless, certain relationships raise specific questions that should be highlighted. The amphibolite-facies, layer-parallel, $S_2$ transposition foliation in the Gibson–MacQuoid homocline has a uniformly moderate northward dip, with a locally steeply pitching $L_2$. Similar orientations, albeit somewhat steeper in the vicinity of the syn-$D_2$, tonalite-granodiorite plutons, are recorded in the southern domain of the volcanic belt, associated with a dip-parallel $L_2$. When combined with data for the western segment of the MacQuoid supracrustal belt (Tella et al., 1997b), this geometry has been documented for a crustal-scale panel, 150 km long by 30 km wide. Taken together with the local presence of relatively weakly strained, greenschist-facies rocks in the volcanic belt (Hanmer et al., 1999), these observations raise the possibility that the $D_2$ fabrics may be the product of tangential shearing on moderately dipping surfaces, i.e. thrusting. However, no direct corroboration has been found on the ground (e.g. sheared contacts, structural asymmetry, metamorphic inversion, repeated stratigraphy, etc.). Nonetheless, we note that southeast-verging, late Archean thrust tectonics have been identified in the Yathkyed greenstone belt, 150 km along strike to the southwest (Relf et al., 1998).

Although there is no direct evidence for thrusting within the Gibson–MacQuoid homocline and the volcanic belt, their external boundaries may represent map-scale faults. There is an overall geometrical discordance between the uniform orientation of the homocline, and the scalloped form of the immediately overlying volcanic belt. Whereas the latter is a function of the emplacement of the dome-like, tonalite-granodiorite plutons, they are nevertheless absent from the homocline. The distribution of lithologies within the volcanic belt east of 94°W is compatible with the form of a map-scale, isoclinal, neutral fold, with the Sandhill prospect located in the northern limb (Fig. 16). Seen in this light, the northern

*Figure 14. Annealed, porphyroclastic straight gneiss fabric wraps around 90° bend in contact of MacQuoid dyke, Big lake shear zone.*

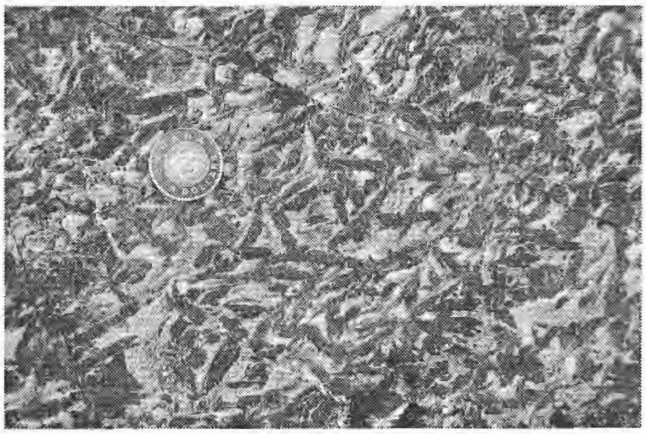

*Figure 15. Decussate hornblende crystals in intermediate volcanic rock, southern domain, volcanic belt.*

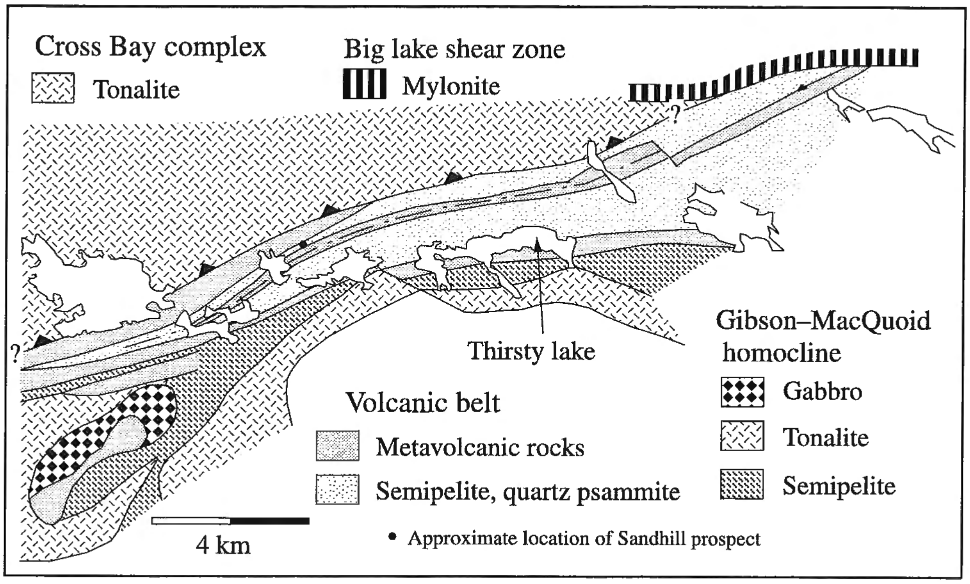


***Figure 16.*** *Sketch map of the eastern part of the volcanic belt, southern domain in the vicinity of the Sandhill prospect. Dot-dash line is the axial trace of a possible isoclinal, neutral fold.*

contact with the tonalitic gneiss cuts obliquely across the fold, progressively eliminating the northern limb as one passes eastward. We speculate that the upper and lower boundaries of the southern domain of the volcanic belt may be faults, and that those faults may be thrusts.

The $L_3$ extension lineation is developed in the northern part of the Cross Bay complex, adjacent to Chesterfield Inlet. Granulite-facies rocks on the north side of the inlet (Sanborn-Barrie, 1994; Mills et al., 1999) were rapidly unroofed at ca. 1.9 Ga (Sanborn-Barrie et al., 1997). We speculate that if the exhumation were tectonically driven, the granulite rocks would be located in the footwall of a south-dipping extensional fault. A south-plunging extension lineation in the adjacent hanging wall is potentially compatible with such speculation. A preliminary test would be to date the lineation.

## SUMMARY


The principal structural elements in the map area are fourfold. 1) The northeastern part of the 150 km long, Gibson–MacQuoid $D_2$ homocline is overlain with possible structural discordance by 2) a volcanic belt, intruded by Neoarchean, syn-$D_2$ plutons. 3) The Cross Bay plutonic complex comprises two structural domains, separated by the cryptic, post-$F_4$, Cross Bay fault. In the western domain, $S_2$ is deformed about south-plunging, $F_3$ folds, associated with a coaxial, $L_3$ extension lineation. $L_3$ is also present on the north limb of an $F_4$ fold that deforms the entire eastern domain. The plutonic complex is bounded to the south by 4) the pre-, syn- and post-$D_4$, dextral, strike-slip Big lake shear zone, up to 2 km thick, composed of annealed porphyroclastic straight gneiss and ribbon mylonite units.

Metamorphosed, ca. 2.19 Ga, MacQuoid dykes everywhere postdate $S_2$, but within the Cross Bay complex and the Big lake shear zone they were deformed during $D_3$-$D_4$; accordingly $D_3$ and $D_4$ are regional Paleoproterozoic events. The South Channel and Primrose granitic plutons were intruded after $D_2$ and before $D_4$ fabrics, respectively.


## ACKNOWLEDGMENTS


We are grateful to Erika Greiner, Nancy MacDonald, Mark Quigley, and Gillian Royle for their outstanding, enthusiastic assistance in the field, and to Laura Adams, our wonderful cook. This work could not have been undertaken without the generous support of the Polar Continental Shelf Project. Our Huisson Aviation helicopter crew, pilot Terry Halton and engineer Matt Weeks, provided unsurpassed service throughout the summer, especially in the teeth of adversity. We thank Larry Aspler for critically reading the manuscript.


## REFERENCES


**Geological Survey of Canada**
1987: Magnetic Anomaly Map of Canada; Geological Survey of Canada, Map 1255A, scale 1:5 000 000.

**Hanmer, S., Tella, S., Sandeman, H.A., Ryan, J.J., Hadlari, T., and Mills, A.**
1999: Proterozoic reworking in western Churchill Province, Gibson Lake–Cross Bay area, Northwest Territories (Kivalliq region, Nunavut). Part I: general geology; *in* Current Research 1999-C; Geological Survey of Canada.

**MacRae, N.D., Armitage, A.E., Miller, A.R., Roddick, J.C., Jones, A.L., and Mudry, M.P.**
1996: The diamondiferous Akluilâk lamprophyre dyke, Gibson Lake area, N.W.T.; *in* Searching for Diamonds in Canada, (ed.) A.N. LeCheminant, D.G. Richardson, R.N.W. DiLabio, and K.A. Richardson; Geological Survey of Canada, Open File 3228, p. 101–107.

**Mills, A., Berman, R., and Hanmer, S.**
1999: Geology of the Uvuak complex, Northwest Territories (Kivalliq region, Nunavut); *in* Current Research, Geological Survey of Canada.

**Relf, C., Irwin, D., MacLachlan, K., and Mills, A.**
1998: New insights into the geology of the Yathkyed Lake greenstone belt, western Churchill Province, Northwest Territories; *in* Current Research 1998-C; Geological Survey of Canada, p. 67–75.

**Ryan, J.J., Hanmer, S., Tella, S., and Sandeman, H.A.**
1999: Detailed structural studies, Gibson Lake–Cross Bay–MacQuoid Lake area, Northwest Territoies (Kivalliq region, Nunavut); *in* Current Research 1999-C; Geological Survey of Canada.

**Sanborn-Barrie, M.**
1994: Structural investigation of high-grade rocks of the Kramanituar complex, Baker Lake area, Northwest Territories; *in* Current Research 1994-C; Geological Survey of Canada, p. 121–133.

**Sanborn-Barrie, M., Carr, S., Hanmer, S., Berman, R., and Thériault, R.**
1997: 1.9 Ga metamorphism, magmatism and deformation of the Kramanituar Complex, NWT: tectonic implications for the western Churchill Province and the Snowbird tectonic zone; Geological Association of Canada–Mineralogical Association of Canada, Program with Abstracts, p. 130–131.

**Tella, S., LeCheminant, A.N., Sanborn-Barrie, M., and Venance, K.E.**
1997b: Geology and structure of parts of the MacQuoid Lake area, District of Keewatin, Northwest Territories; *in* Current Research 1997-C; Geological Survey of Canada, p. 123–132.

**Tella, S., LeCheminant, A.N., Sanborn-Barrie, M., and Venance, K.E.**
1997c: Geology, parts of MacQuoid Lake, District of Keewatin, Northwest Territories; Geological Survey of Canada, Open File 3404, scale 1:50 000.

**Tella, S., Davis, W., Berman, R.G., Stern, R., and LeCheminant, A.N.**
1997a: Tectonothermal history of the MacQuoid Lake supracrustal belt, District of Keewatin, Northwest Territories, Canada; Geological Society of America, Abstracts with Programs, v. 29, p. 277–278.

**Tella, S., Schau, M., Armitage, A.E., and Loney, B.C.**
1993: Precambrian geology and economic potential of the northeastern parts of Gibson Lake map area, District of Keewatin, Northwest Territories; *in* Current Research, Part C; Geological Survey of Canada, Paper 93-1C, p. 197–208.

---

Geological Survey of Canada Project 970006

# Preliminary petrography of current and potential carving stone, Gibson Lake–Cross Bay area, Northwest Territories (Kivalliq region, Nunavut)[1]

S. Hanmer, H.A. Sandeman, S. Tella, J.J. Ryan, T. Hadlari[2], and A. Mills[2]
Continental Geoscience Division, Ottawa

*Hanmer, S., Sandeman, H.A., Tella, S., Ryan, J.J., Hadlari, T., and Mills, A., 1999: Preliminary petrography of current and potential carving stone, Gibson Lake–Cross Bay area, Northwest Territories (Kivalliq region, Nunavut);* in *Current Research 1999-C; Geological Survey of Canada, p. 77–86.*

**Abstract:** Carving stone, used by artisans in the local hamlets of Rankin Inlet and Baker Lake, is quarried in a small-scale operation on the south side of Cross Bay, Chesterfield Inlet. This report presents a preliminary petrographic description and comparison of the currently quarried carving stone, and of similar materials from other sites identified in the course of regional bedrock mapping during the 1998 field season in the Gibson Lake–Cross Bay area.

**Résumé :** La pierre à sculpter utilisée par les artisans dans les hameaux de Rankin Inlet et de Baker Lake est extraite artisanalement sur la rive sud de la baie Cross dans l'inlet Chesterfield. Le présent rapport donne une description préliminaire des caractéristiques pétrographiques de cette pierre et fait une comparaison entre la pierre à sculpter en cours d'extraction et des matériaux similaires provenant d'autres sites identifiés lors de travaux de cartographie régionale du substratum rocheux réalisés pendant la campagne de terrain de 1998 dans la région du lac Gibson et de la baie Cross.

[1] Contribution to the Western Churchill NATMAP Project
[2] Department of Earth Sciences, Carleton University, Ottawa, Ontario K1S 5B6

## INTRODUCTION

The Western Churchill NATMAP Project involves the Geological Survey of Canada (GSC), the Government of the Northwest Territories (GNWT), and Indian and Northern Affairs Canada (INAC). In 1998, the second phase of the GSC's three year field program, an investigation of the geology of parts of the MacQuoid Lake (NTS 55 M) and Gibson Lake (NTS 55 N) map areas (Fig. 1) was undertaken between Gibson Lake and Chesterfield Inlet. Particular emphasis was placed on establishing the nature and extent of Paleoproterozoic tectonothermal reworking of older, Archean rocks. Bedrock mapping was undertaken at 1:50 000 scale (Fig. 1), building on the earlier work of Tella et al. (1997a, b; LeCheminant et al., 1997). Previous bedrock mapping in the area was mostly at 1:250 000 scale, or smaller (Wright, 1967; Reinhardt and Chandler, 1973; Reinhardt et al., 1980; Tella and Schau, 1994), as well as local detailed work (Sanborn-Barrie, 1994). The map area contains the Sandhill Zn-Cu-Pb-Ag prospect (Armitage et al., 1994, 1995), the Suluk Ni-Cu-Co occurrence (Armitage et al., 1997), and the Akluilâk diamondiferous lamprophyre dyke (MacRae et al., 1996). Carving stone (*see also* Bell, 1990), used by artisans in the local hamlets of Rankin Inlet and Baker Lake, is quarried in a small-scale operation on the south side of Cross Bay (Fig. 1). In this report, we present a preliminary petrographic description and comparison of the currently quarried carving stone, and of similar materials from other sites identified in the course of our regional bedrock mapping during the 1998 field season. X-ray diffraction analysis was used to identify talc. Regional geological and structural observations pertaining to the map area are presented elsewhere (Hanmer et al., 1999a, b; Ryan et al., 1999; Mills et al., 1999). Global Positioning System (GPS) locations for the sites are given in Universal Transverse Mercator (UTM) co-ordinates.

### *Geological overview*

The following is a summary of the field-based descriptions and preliminary interpretations presented elsewhere by Hanmer et al. (1999a, b), to which the interested reader is referred. The map area (Fig. 1) includes the eastern part of the Archean MacQuoid supracrustal belt (Tella et al., 1997a, b), and the Cross Bay plutonic complex. The MacQuoid supracrustal belt is divided into 1) the predominantly metasedimentary, Gibson–MacQuoid, $D_2$ homocline, with panels of gneissic tonalite, overlain to the north, with possible structural discordance, by 2) a predominantly volcanic belt intruded by Neoarchean, syn-$D_2$, tonalite-granodiorite plutons. 3) The oval Cross Bay plutonic complex is principally composed of tonalitic gneiss units and the Primrose and South Channel granitic plutons. The complex comprises two structural domains, separated by the cryptic, post-$F_4$ Cross Bay fault. In the western domain, $S_2$ is deformed about south-plunging $F_3$ folds, associated with a coaxial $L_3$ extension lineation. $L_3$ is also present on the north limb of an $F_4$ fold that deforms the entire eastern domain. The plutonic complex is bounded to the south by 4) the pre-, syn-, and post-$D_4$, dextral, strike-slip Big lake shear zone, up to 2 km thick, composed of annealed porphyroclastic straight gneiss and ribbon mylonite units.

Metamorphosed, ca. 2.19 Ga (Tella et al., 1997a, b), MacQuoid dykes everywhere postdate $S_2$, but within the Cross Bay complex and the Big lake shear zone they were folded and boudined during $D_3$-$D_4$; accordingly $D_3$ and $D_4$ are regional Paleoproterozoic events. The South Channel and Primrose granitic plutons were intruded after $D_2$ and before $D_4$ fabrics, respectively.

## ACTIVE QUARRY PITS

Carving stone is currently extracted in a small-scale operation, approximately 1 km from the southern shore of Cross Bay, Chesterfield Inlet (Fig. 1). Two shallow open pits, each measuring approximately 10 m by 10 m, have been worked using hand tools. The carving stone is light to medium grey, and uniformly fine grained. It contains few macroscopic veins and large fracture-free blocks can be readily obtained. It is very soft and easily scratched with any metal instrument. In places, it has a distinctly silky feel, suggesting a significant proportion of talc. With a hand lens, it appears to be composed of randomly oriented, millimetre-scale laths and needles of light grey amphibole. The quarry pits appear to be located within large inclusions of ultramafic material within a gneissic tonalite host.

Two specimens of carving stone were examined with a petrographic microscope. In specimen 98TXS1000A, blocky, 2–3 mm, chlorite pseudomorphs, and round, 1 mm carbonate grains, are set in a matrix composed of carbonate, and intimately mixed chlorite and talc (Fig. 2). The chlorite and talc are slightly elongate (3:2) and up to 50 μm long. The trace of a relict foliation is marked by thin carbonate seams, smaller, elongate chlorite clots, and a patchy shape fabric in the chlorite-talc component of the matrix. This relict foliation is parallel to the trace of axial planes of local microcrenulations which deform a relict, earlier foliation in chlorite-talc lithons. Equant or irregularly shaped carbonate grains, up to 1 mm, scattered through the chlorite-sericite matrix, do not participate in either of the shape fabrics. Elongate (up to 10:1) laths of colourless tremolite, up to 20 μm thick, grow across all matrix shape fabrics. Irregularly shaped grains of opaque minerals, up to 500 μm long, are randomly scattered without relation to the matrix microstructure, or to the distribution of other mineral phases. They constitute about 2–3% of the rock by volume. Overall, the microstructure is homogeneous at the scale of the low-power field of view, i.e. approximately 7 mm.

The talc and chlorite components of the matrix are interpreted to be the products of hydration and breakdown of mafic phases such as pyroxene. The carbonate component of the aggregate seems to be introduced as it is not accompanied by Ca-silicate minerals, such as epidote, which form when calcium is released during the breakdown of precursor minerals such as plagioclase. It would appear that the carving stone is derived from an ultramafic protolith, most likely a pyroxenite.

In specimen 98TXS1000B, blocky, polycrystalline chlorite mats, up to 5 mm across, are set in a matrix of 50 μm chlorite-talc and coarser talc laths (Fig. 3). The chlorite is

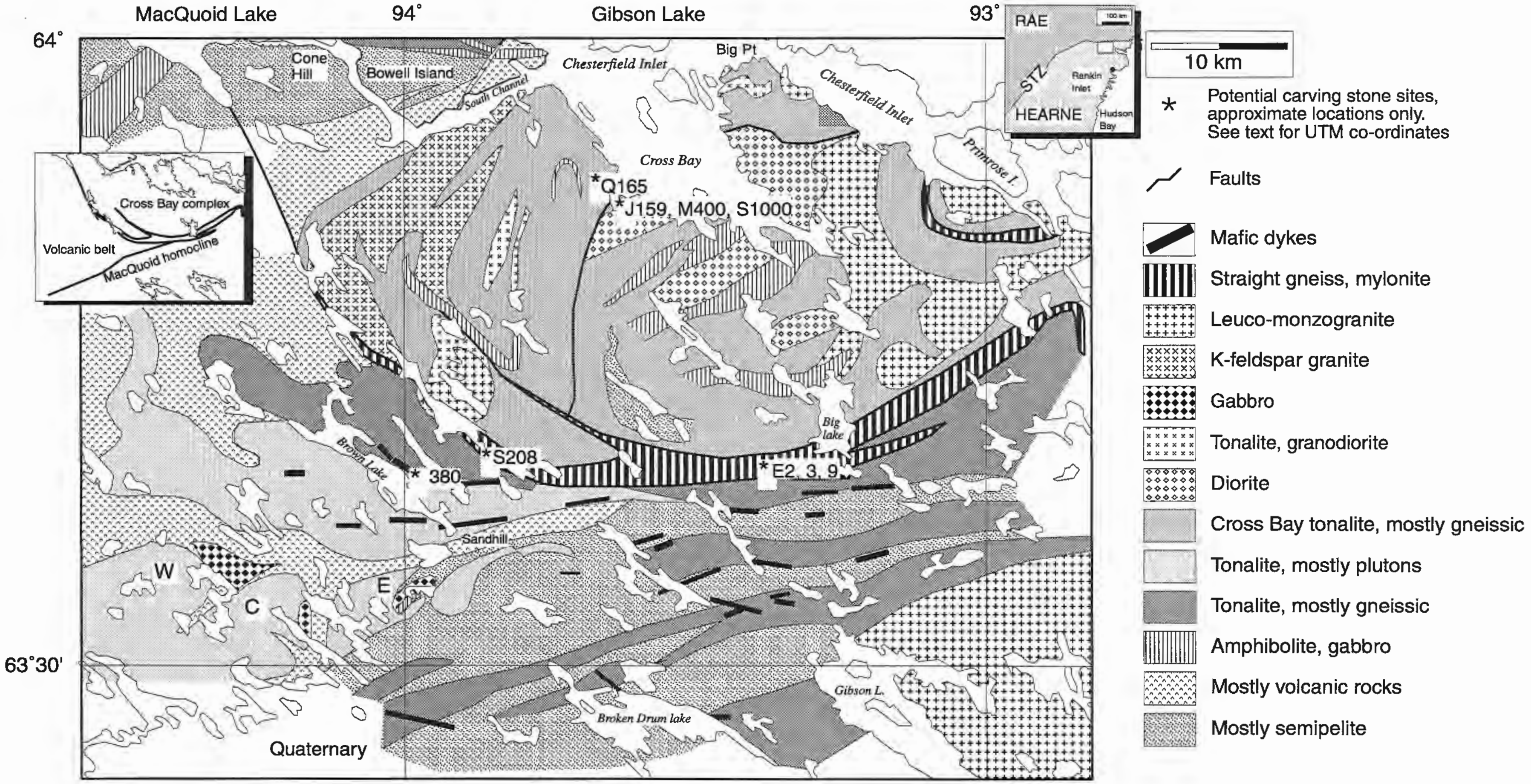


***Figure 1.*** *Generalized geology of the Gibson Lake–Cross Bay area. The letters W, C, and E are western, central, and eastern plutons, respectively; STZ=Snowbird tectonic zone.*

faintly straw yellow-green pleochroic, and exhibits grey to anomalous brown birefringence colours. Rare relics of clinopyroxene are preserved within the pseudomorphs. The matrix phyllosilicate minerals tend to be aligned and mark a relict foliation. Talc comprises over 50% by volume of the rock. Larger talc plates show no regard for the shape fabric, and elongate (5:1) tremolite-actinolite grains, 500 μm long, are commonly aligned along or across it. Blocky opaque grains, generally up to 100 μm, but locally up to 1 mm, are evenly dispersed throughout the aggregate, and account for approximately 10% of the rock volume. Overall, the microstructure is homogeneous at the scale of the width of the thin section, i.e. approximately 2 cm. Although this carving stone is apparently derived from a similar pyroxenite protolith to that of 98TXS1000A, the greater talc content suggests a greater degree of alteration. It is therefore somewhat surprising that specimen 98TX1000A has the silkier feel in hand specimen.

In specimen 98TXM400, large (3 mm) clotty pseudomorphs of polycrystalline chlorite after (?)pyroxene are set in a polycrystalline matrix of 500 μm tremolite, talc, and colourless chlorite (Fig. 4). Discrete flakes of talc have developed by grain growth in the ultrafine-grained, matrix component. Smaller tremolite and chlorite grains in the matrix locally define an earlier penetrative foliation, whereas larger tremolite grains appear to be aligned in a relict, spaced crenulation cleavage at a high angle to the foliation. Blocky, opaque grains, mostly in the size range 100–200 μm, but up 600 μm, account for approximately 10% of the rock by volume. Overall, the microstructure is homogeneous at the scale of the low-power field of view, i.e. approximately 7 mm. This carving stone appears to have been derived by the hydrothermal alteration of a pyroxenite.

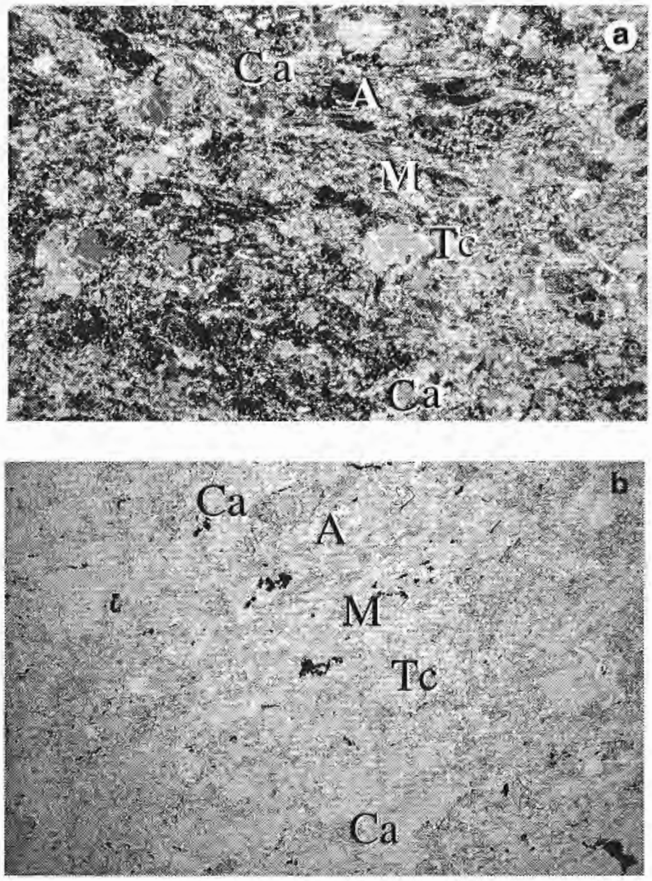


*Figure 2. Specimen 98TXS1000A, under a) crossed nicols and b) in plane-polarized light. Chlorite-talc shows the trace of a relict, microcrenulated foliation. Equant carbonate and elongate tremolite grains grow across all matrix shape fabrics. Opaque minerals are disseminated throughout the aggregate. A, amphibole; Ca, carbonate; M, matrix; Tc, talc. Long side of photograph is 7.5 mm.*

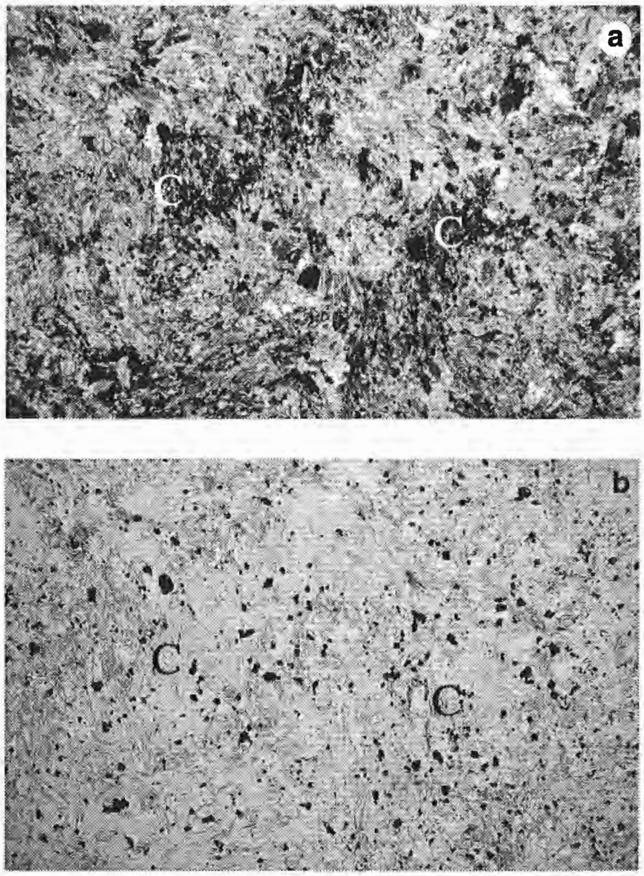


*Figure 3. Specimen 98TXS1000B, under a) crossed nicols and b) in plane-polarized light. Polycrystalline chlorite pseudomorphs in matrix of chlorite-talc with a relict foliation. Talc comprises over 50% of the rock. Talc flakes and elongate tremolite-actinolite grains overgrow the foliation. Dispersed opaque grains form 10% of the aggregate. C, chlorite. Long side of photograph is 7.5 mm.*

## NEW OCCURRENCES

### *Southwest Cross Bay shore*

Just north of the currently active quarry pits, a prominent ridge is formed by a homogeneous, brown-weathering, ultramafic rock with occasional veins, 2–4 cm thick, of fibrous amphibole or serpentine (UTM 469940, 7081850). The rock is a lens in the tonalite gneiss, measuring 500 m long by up to 100 m thick. The hardness of the rock is variable, but in general it is readily scratched with a steel hammer head. With a hand lens, on the fresh surface, it appears to composed of randomly oriented, millimetre-scale laths of grey to green amphibole. Locally, it has a soapy to silky feel. Overall, the fresh rock shows significant colour variation ranging from grey to dark green.

Two specimens were optically examined in thin section. Specimen 98TXJ159A is an isotropic rock composed of 0.5–1 mm elongate grains with no matrix (Fig. 5). A few relict, blocky grains of tremolite (or possibly cummingtonite), 1 mm across, appear to be pseudomorphs after pyroxene, the grain shape of which they still preserve. Other tremolite grains are elongate and up to 5 mm in length. Although they are isolated from one another, they show a distinct alignment. Grains of tremolite-actinolite are smaller (500 µm) and blade-like, though stubby in shape. They tend to be aligned with the larger elongate tremolite grains, marking a relict foliation. Actinolite forms small cores within the more elongate tremolite laths, and are dusted with opaque inclusions. Minor talc and chlorite are either intergrown with the amphibole, or present as equant plates. Rare, relict clinopyroxene is locally preserved. Scattered, blocky opaque grains, up to 200 µm, constitute approximately 5% of the aggregate. Overall, because of the long tremolite grains, the microstructure is homogeneous at the scale of the width of the thin section, i.e. approximately 2 cm.

Specimen 98TXJ159B (Fig. 6) is texturally similar to specimen 98TXJ159A. Blocky, 1 mm pseudomorphs of cummingtonite, locally replaced by faintly green, pleochroic

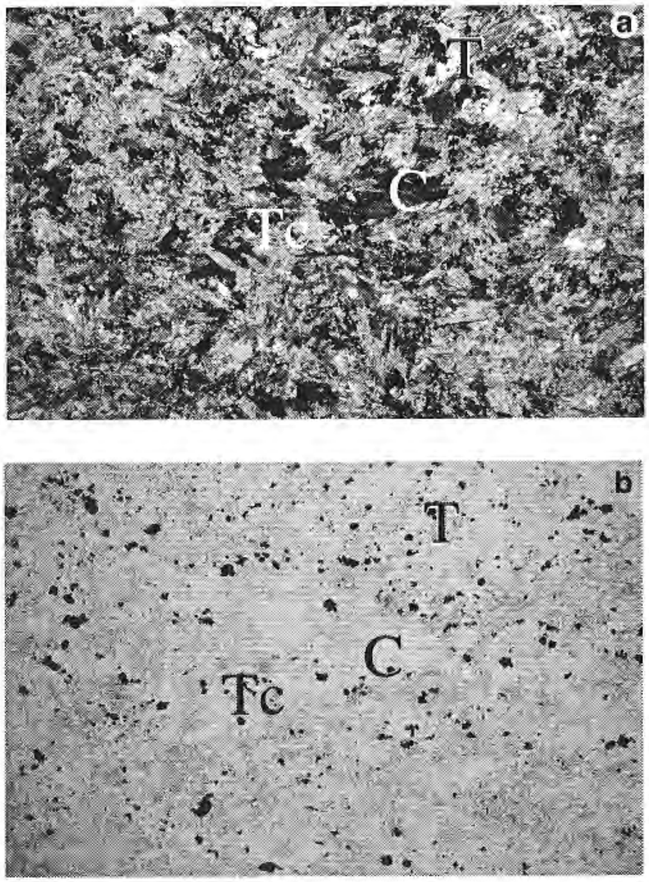


*Figure 4. Specimen 98TXM400, under **a**) crossed nicols and **b**) in plane-polarized light. Chlorite pseudomorphs in a tremolite-talc-chlorite matrix. Larger tremolite grains are aligned in a relict, spaced crenulation cleavage. Opaque grains form 10% of the aggregate. C, chlorite; T, tremolite; Tc, talc. Long side of photograph is 7.5 mm.*

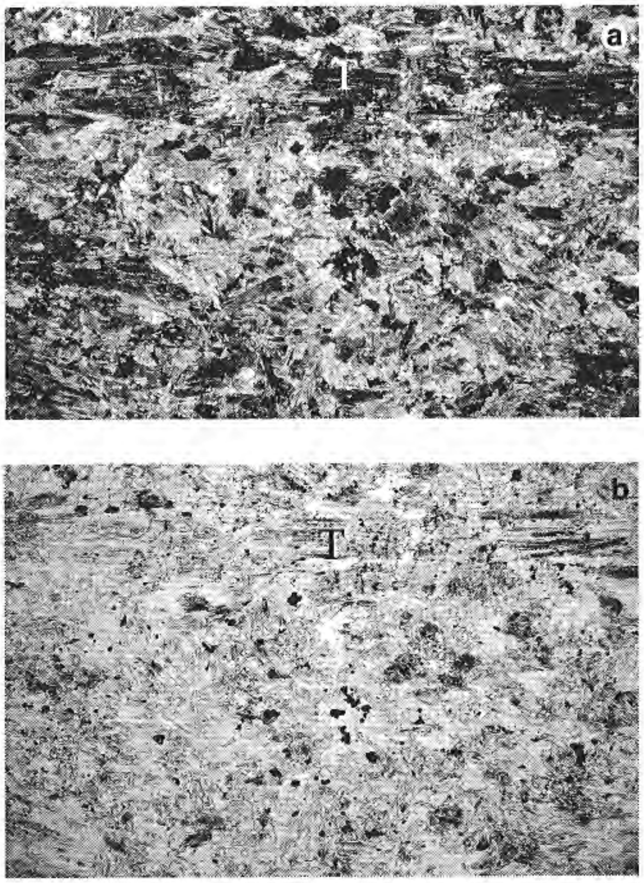


*Figure 5. Specimen 98TXJ159A, under **a**) crossed nicols and **b**) in plane-polarized light. Aggregate of elongate tremolite grains with relict tremolite pseudomorphs after pyroxene. Smaller grains mark a relict foliation, parallel to an alignment of isolated, larger laths. Scattered, opaque grains form 5% of the aggregate. T, tremolite. Long side of photograph is 7.5 mm.*

chlorite, are intergrown with green, pleochroic amphibole (possibly hornblende) and yellow, pleochroic phlogopite. They also contain corroded relics of colourless clinopyroxene. The cummingtonite pseudomorphs appear to be replacing blocky hornblende grains, and show good polysynthetic lamellar twinning. Other hornblende grains tend to be somewhat smaller (500 μm), blocky, and coarsely polycrystalline. Late, acicular, colourless tremolite grains grow across the other phases. Talc is indicated by X-ray diffraction analysis, but is difficult to detect optically. Overall, the microstructure is homogeneous at the scale of the low-power field of view, i.e. approximately 7 mm. It appears that both of these rocks are derived from plagioclase-free protoliths, such as a pyroxenite.

A few kilometres to the northwest, strongly lineated, heterogeneously folded, tonalite gneiss contains large (5 m) xenoliths of an ultramafic rock (UTM 469010, 7081355). Specimen 98TXQ165 was optically examined in thin section. Large (5 mm), blocky grains of slightly pleochroic, green amphibole are dusted with opaque inclusions (Fig. 7). They are set in a coarse (500 μm) matrix of polycrystalline, faintly pleochroic chlorite, talc, and tremolite, with scattered, equant, 500 μm carbonate±clinozoisite±apatite grains. The chlorite forms polycrystalline patches and stringers, apparently representing pseudomorphs and veins. Fragments of colourless pyroxene are either present as grains in the matrix, or as corroded relics within amphibole and chlorite pseudomorphs. Abundant, blocky, opaque grains (200 μm) are patchily dispersed though the rock. Locally, the cores of the large, blocky, amphibole grains are entirely replaced by dense concentrations of opaque grains. The grains are also concentrated at the boundaries between lobate volumes of inclusion-free material within the large, dusty, amphibole grains. Overall, the microstructure is somewhat heterogeneous, even at the thin-section scale. The presence of clinozoisite is suggestive of a minor plagioclase component in a pyroxene-rich protolith.

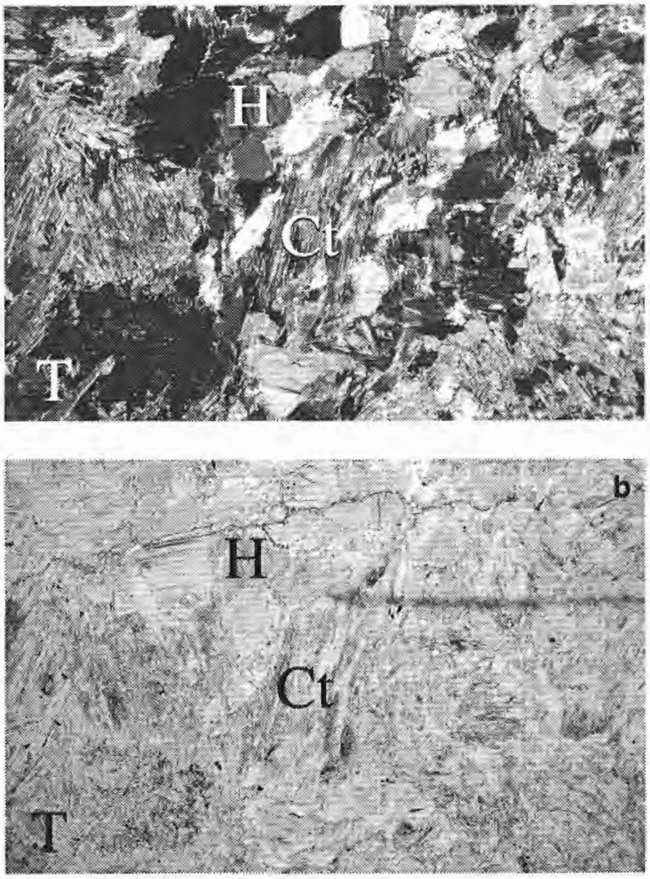


***Figure 6.*** *Specimen 98TXJ159B, under **a**) crossed nicols and **b**) in plane-polarized light. Blocky cummingtonite pseudomorphs and coarsely polycrystalline amphibole (possibly hornblende). Acicular tremolite grains cut the other phases. Ct, cummingtonite; H, (?)hornblende; T, tremolite. Long side of photograph is 7.5 mm.*

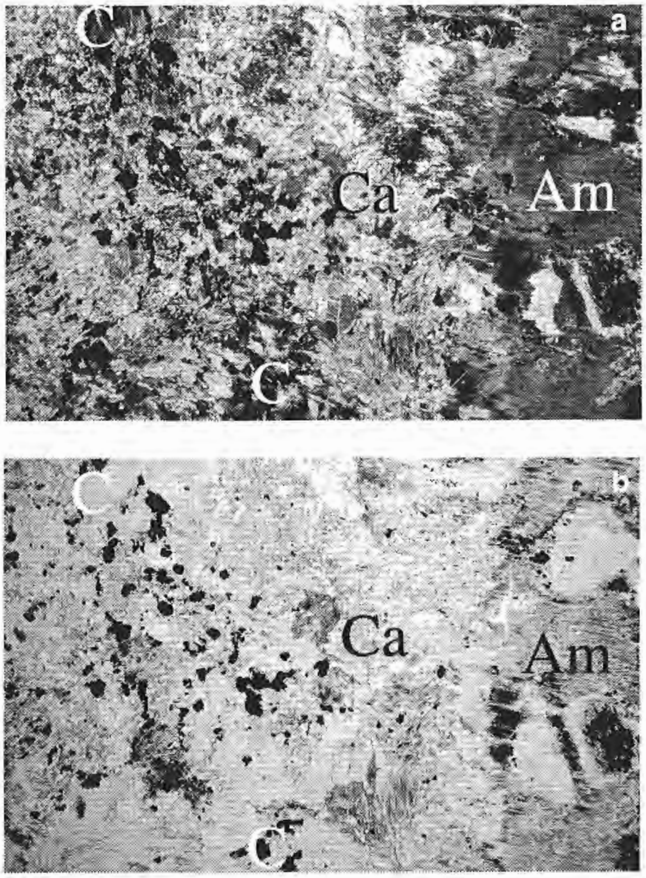


***Figure 7.*** *Specimen 98TXQ165, under **a**) crossed nicols and **b**) in plane-polarized light. Large amphibole grains, dusted with opaque inclusions, set in a coarse matrix of chlorite, talc, and tremolite. Chlorite forms polycrystalline patches and stringers. Abundant, blocky, opaque grains are patchily dispersed throughout the aggregate. Am, amphibole; C, chlorite; Ca, carbonate. Long side of photograph is 7.5 mm.*

### *Southwest of Cross Bay*

Approximately 25 km southwest of Cross Bay, quartzofeldspathic mylonite of the Big lake shear zone forms a prominent ridge where the shear zone swings from an east trend to a northwest trend (UTM 449607, 7067941). On the ridge top is a sheet of dark grey to green rock, 5 m wide, at least 50 m long, with parallel sides that are concordant to the mylonite fabric. In hand specimen it is composed of randomly oriented, acicular amphibole grains. The absence of boudinage, fracture, or folding suggests that this is a sill, emplaced relatively late with respect to the shear zone activity. Specimen 98TXS208 is composed of blocky, 3 mm, pleochroic, green hornblende grains in a matrix of equant, lighter green hornblende (Fig. 8). Other rock-forming minerals include yellow-brown, pleochroic phlogopite, up to 1 mm, plus interstitial talc, small chlorite grains, and occasional, small talc laths. The talc also occurs as discrete amorphous masses. The aggregate contains no opaque grains, and exhibits a very weak shape fabric. Overall, the microstructure is homogeneous at the scale of the width of the thin section, i.e. approximately 2 cm. The rock was probably derived by the hydration and alteration of a pyroxenite sill.

Approximately 5 km west of the previous station, an anomalously thick (up to 500 m) MacQuoid dyke with gabbroic texture shows field evidence of hydrothermal alteration (UTM 451490, 7059836). Under the hand lens, the rock appears to be composed of randomly oriented, elongate amphibole laths, and locally has a silky feel. Specimen 98TX380A (Fig. 9) is composed of blocky, green, pleochroic chlorite pseudomorphs after pyroxene, with local development of a fine-scale graphic intergrowth with a high-relief granular phase, possibly titanite. Some pseudomorphs preserve simple twins. Radial spherulitic sprays, 500 μm across, of fine-grained actinolite are locally preserved. Interstitial, cloudy plagioclase grains are euhedral, stubby, 1 mm long laths with polysynthetic albite and pericline twins. Minor talc is indicated by X-ray diffraction analysis, but is difficult to detect optically. Overall, the microstructure is homogeneous at the scale of the width of the thin section, i.e. approximately 2 cm. The protolith was clearly a gabbro.

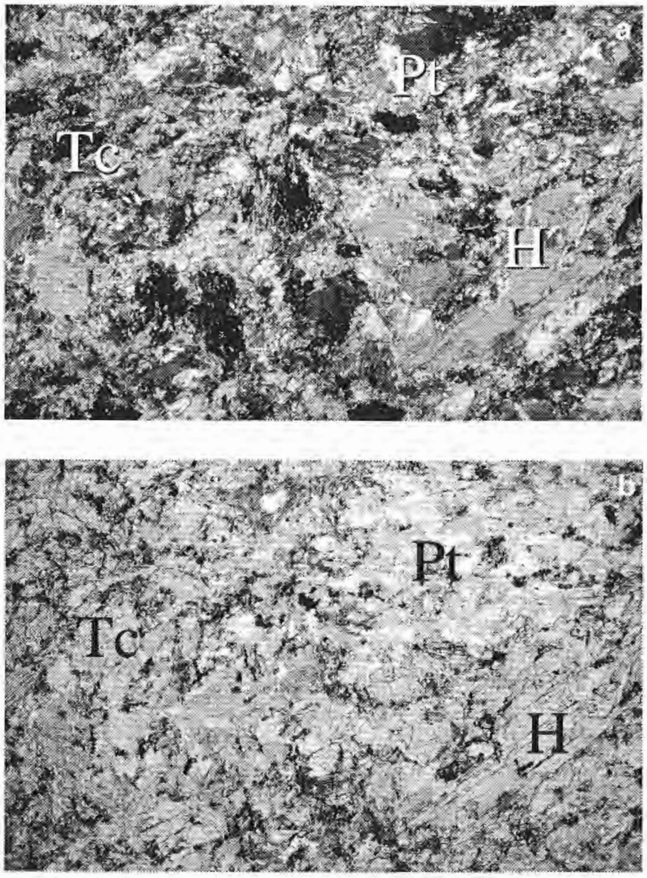


***Figure 8.*** *Specimen 98TXS208,under **a**) crossed nicols and **b**) in plane-polarized light. Blocky hornblende in an isotropic hornblende matrix, with local phlogopite and interstitial talc. The talc also occurs as discrete amorphous masses. H, hornblende; Pt, phlogopite; Tc, talc. Long side of photograph is 7.5 mm.*

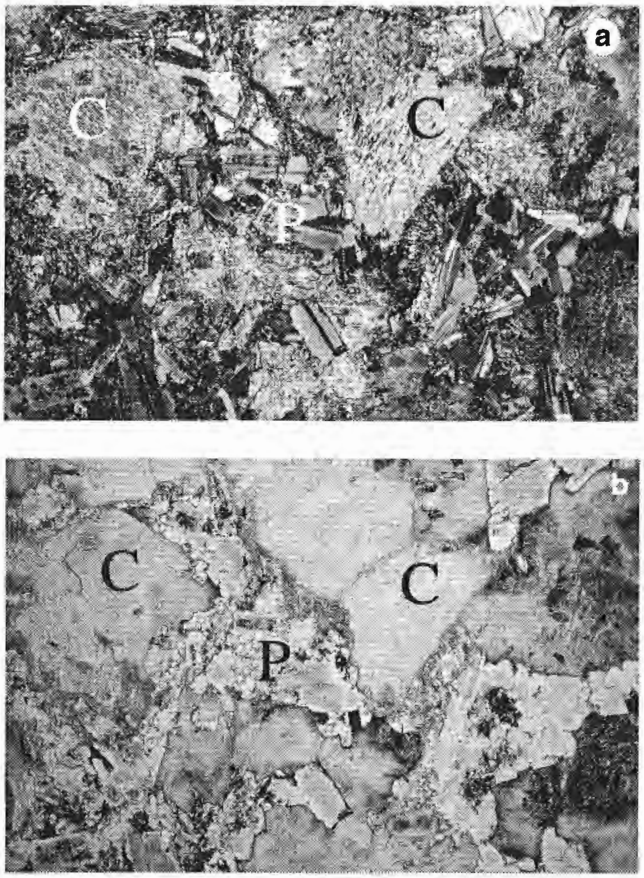


***Figure 9.*** *Specimen 98TX380A,under **a**) crossed nicols and **b**) in plane-polarized light. Chlorite (C) pseudomorphs after pyroxene, and interstitial, cloudy plagioclase grains (P).Long side of photograph is 7.5 mm.*

### *South of Cross Bay*

Twenty kilometres south of Cross Bay, the Big lake shear zone runs east-west through the southern part of what we have informally named Big lake (Fig. 1). Tonalitic mylonite units of the Big lake shear zone contain several lenses of fine-grained, dark material of uncertain parentage. In the field, this material appears to be made of randomly oriented, needle-like amphibole grains, and locally has a softness and silky feel very similar to that of the currently exploited carving stone. Three specimens from just west of Big lake were examined in thin section. Specimen 98TXE002 (UTM 483491, 7060019) and 98TXE003 (UTM 484299, 7060110) are from tectonic inclusions, 5 m by 1.5 m, in mylonitic tonalite gneiss with moderate quartz ribbon development. Specimen 98TXE009B comes from a 20 m by 10 m outcrop, entirely composed of the sample material (UTM 482510, 7059941). Its boundaries with the tonalite gneiss are not exposed. Metre-scale clots and veins of coarse biotite aggregates are developed throughout the outcrop.

Specimen 98TXE002 is composed of a coarse aggregate of randomly oriented tremolite, almost free of opaque phases (Fig. 10). The colourless tremolite varies from blocky grains (1.5–2 mm) to elongate, sheaf-like needles, over 2 mm long. Abundant, coarse (1.5–2 mm), talc plates form a diffuse band within the tremolite matrix, as well as occurring as isolated plates scattered throughout the tremolite aggregate. Chlorite occurs as polycrystalline patches. Because of the presence of the talc-rich band, the rock is heterogeneous at the thin-section scale. Its origins are equivocal. It is a calc-silicate rock, but because it is quartz free, it may not be derived from a sedimentary protolith. It could be the product of hydrothermal alteration of a Ca-Mg-rich clinopyroxenite.

Specimen 98TXE003 is essentially composed of 500 μm dolomite grains with scattered, randomly oriented, elongate grains and needles of tremolite-actinolite, polycrystalline chlorite, and talc (Fig. 11). The chlorite occurs as isolated, equant patches (possibly pseudomorphs). Talc forms plates up to 1 mm across, scattered throughout the rock. Opaque grains form elongate clumps, up to 5 mm long,

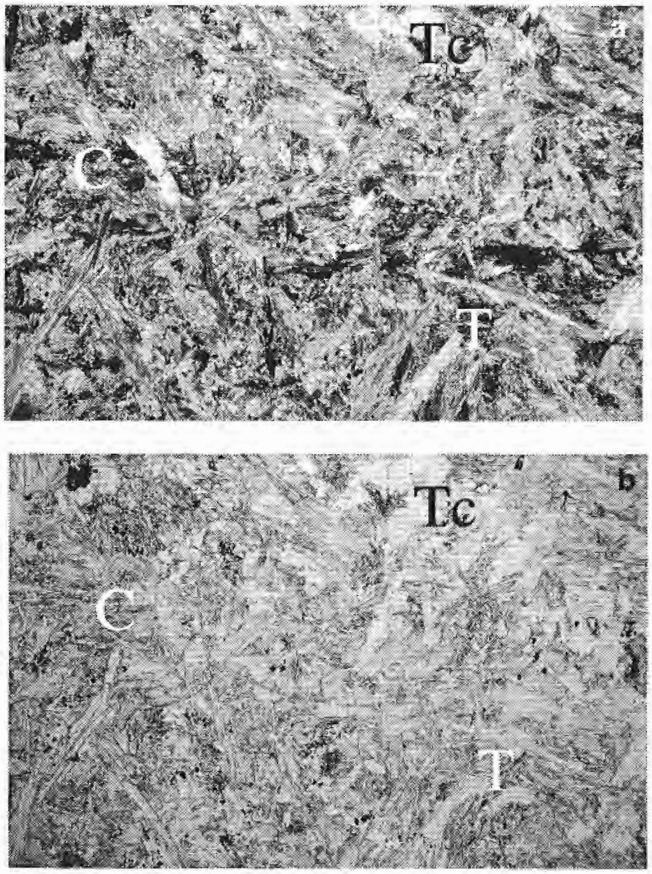


*__Figure 10.__ Specimen 98TXE002, under __a__) crossed nicols and __b__) in plane-polarized light. Coarse aggregate of randomly oriented tremolite, almost free of opaque phases, with isolated talc plates. C, chlorite; T, tremolite; Tc, talc. Long side of photograph is 7.5 mm.*

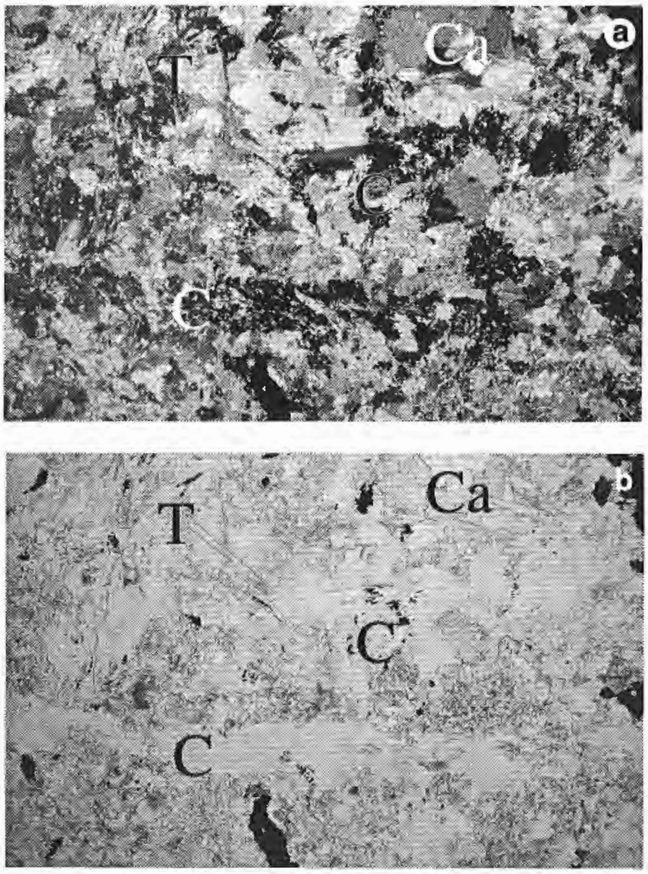


*__Figure 11.__ Specimen 98TXE003,under __a__) crossed nicols and __b__) in plane-polarized light. Carbonate matrix with randomly oriented tremolite-actinolite, polycrystalline chlorite patches, and scattered talc plates. Chlorite also forms discrete veins. Opaque grains form elongate clumps. C, chlorite; Ca, carbonate; T, tremolite. Long side of photograph is 7.5 mm.*

inhomogeneously distributed through the aggregate. They are all elongate in the same direction, possibly marking a relict foliation. Titanite is a minor accessory phase. This specimen contains a 1 cm thick, fibrous dolomite-chlorite-talc vein, wherein the fibres lie at a high angle to the vein wall. Even away from the main vein, smaller chlorite veins render the rock locally heterogeneous. Overall, the microstructure is homogeneous at the scale of the width of the thin section, i.e. approximately 2 cm. Although the rock contains enough dolomite to be a marble of sedimentary derivation, the possibility that the overall composition is the result of wholesale replacement during metasomatic alteration cannot be excluded.

Specimen 98TXE009B is a crystalline aggregate of pleochroic actinolite that exhibits three habits (Fig. 12). Large, prismatic crystals, up to 3 mm by 1 mm, occur with smaller (250–1000 μm) interstitial grains of actinolite. These are all cut by elongate, acicular grains, 3 mm by 0.25 mm, which constitute the predominant component of the aggregate. The acicular grains mark a weak, relict fabric, as well as a second population of elongate grains that cut the foliation, and appear to be randomly oriented. Yellowish chlorite is a local interstitial phase, as are rare plagioclase (possibly albite) grains charged with amphibole inclusions. Talc is indicated by X-ray diffraction analysis, but is difficult to detect optically. Opaque phases are absent. Overall, because of the long, acicular grains, the microstructure is homogeneous at the scale of the width of the thin section, i.e. approximately 2 cm. The rock was probably derived by the hydration and alteration of a pyroxenite.

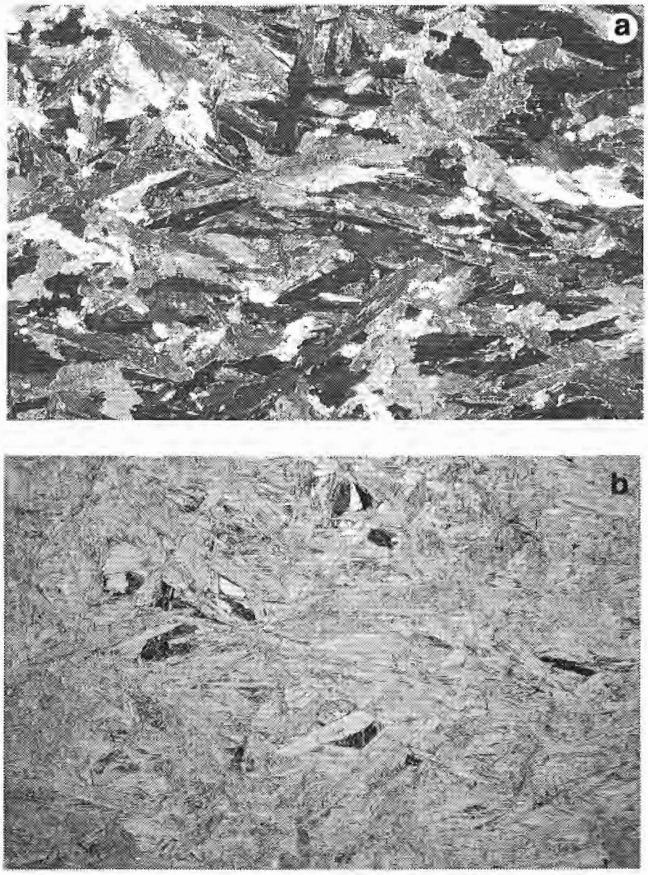


***Figure 12.*** *Specimen 98TXE009B, under* ***a)*** *crossed nicols and* ***b)*** *in plane-polarized light. Large, prismatic actinolite, with smaller interstitial grains, all cut by elongate actinolite laths aligned in a relict foliation. Opaque phases are absent. Long side of photograph is 7.5 mm.*

## SUMMARY

From the field and petrographic observations presented above, it appears that the currently quarried carving stone, as well as similar materials from other sites, is derived from pyroxenitic protoliths that have experienced intensive hydrothermal alteration, locally associated with the introduction of carbonate. In the case of specimen 98TX380A, the protolith is a Paleoproterozoic gabbroic dyke. Specimen 98TXS208 is a pyroxenite sill emplaced late to postkinematically into the Paleoproterozoic Big lake shear zone. Field relations allow that the material from the central segment of the shear zone (specimens 98TXE002, 98TXE003, and 98TXE009B) could represent highly deformed equivalents of either the gabbro and/or the pyroxenite intrusions. Specimens 98TXJ159A and 98TXJ159B may represent an intrusive sheet within the tonalite gneiss, but definitive evidence is lacking. Specimens 98TXS1000A, 98TXS1000B, and 98TXQ165 are inclusions within tonalite gneiss, but it is unclear whether they are magmatic or tectonic inclusions.

Most of the materials from the new-found sites are harder than the currently quarried carving stone. However, they are still soft enough to be readily scratched with a steel hammer head. Should they prove suitable for carving, the materials represented by specimens 98TXJ159A, 98TXJ159B, and 98TXS208 are the most voluminous. The near-coastal specimen 98TXJ159 site is easily accessible from Chesterfield Inlet, either by boat or snowmobile. The ridge of the specimen 98TXS208 site should be free of snow in the spring, while snowmobile travel is still feasible.

## ACKNOWLEDGMENTS

We are grateful to Erika Greiner, Nancy MacDonald, Mark Quigley, and Gillian Royle for their outstanding, enthusiastic assistance in the field, and to Laura Adams, our wonderful cook. This work could not have been undertaken without the generous support of the Polar Continental Shelf Project. Our Huisson Aviation helicopter crew, pilot Terry Halton and engineer Matt Weeks, provided unsurpassed service throughout the summer, especially in the teeth of adversity. We thank Jeanne Percival (GSC) for the X-ray diffraction analyses.

# REFERENCES

**Armitage, A.E., Miller, A.R., and MacRae, N.D.**
1994: Geology of the Sandhill Zn-Cu showing in the Gibson Lake area, District of Keewatin, Northwest Territories; *in* Current Research 1994-C; Geological Survey of Canada, p. 147–155.
1995: Geological setting of the Sandhill Zn-Cu-Pb-Ag prospect in the Gibson-MacQuoid lake area, District of Keewatin, Northwest Territories; *in* Current Research 1995-C; Geological Survey of Canada, p. 213–224.
1997: Paleoproterozoic Ni-Cu-Co sulphide mineralization, Suluk occurrence, Gibson-MacQuoid Lake area, western Churchill Province, Northwest Territories; *in* Current Research 1997-C; Geological Survey of Canada, p. 61–70.

**Bell, R T.**
1990: A new source of carvingstone (soapstone) near Baker Lake, N.W.T.; *in* Current Research, Part C; Geological Survey of Canada, Paper 90-1C, p. 279–280.

**Hanmer, S., Tella, S., Sandeman, H.A., Ryan, J.J., Hadlari, T., and Mills, A.**
1999a: Proterozoic reworking in western Churchill Province, Gibson Lake–Cross Bay area, Northwest Territories (Kivalliq region, Nunavut). Part I: general geology; *in* Current Research 1999-C; Geological Survey of Canada.
1999b: Proterozoic reworking in western Churchill Province, Gibson Lake–Cross Bay area, Northwest Territories (Kivalliq region, Nunavut). Part II: regional structural geology; *in* Current Research 1999-C; Geological Survey of Canada.

**LeCheminant, A.N., Tella, S., Sanborn-Barrie, M., and Venance, K.E.**
1997: Geology, Parker Lake South, District of Keewatin, Northwest Territories; Geological Survey of Canada, Open File 3405, Geological Survey of Canada, scale 1:50 000.

**MacRae, N.D., Armitage, A.E., Miller, A.R., Roddick, J.C., Jones, A.L., and Mudry, M.P.**
1996: The diamondiferous Akluilâk lamprophyre dyke, Gibson Lake area, N.W.T.; *in* Searching for Diamonds in Canada, (ed.) A.N. LeCheminant, D.G. Richardson, R.N.W. DiLabio, and K.A. Richardson; Geological Survey of Canada, Open File 3228, p. 101–107.

**Mills, A., Berman, R., and Hanmer, S.**
1999: Geology of the Uvauk complex, Northwest Territories (Kivalliq region, Nunavut); *in* Current Research 1999-C; Geological Survey of Canada.

**Reinhardt, E.W. and Chandler, F.W.**
1973: Gibson-MacQuoid Lake map area, District of Keewatin; *in* Report of Activities, Part A; Geological Survey of Canada, Paper 73-1A, p. 162–165.

**Reinhardt, E.W., Chandler, F.W., and Skippen, G.B.**
1980: Geological map of the MacQuoid Lake (NTS 55M, E1/2) and Gibson Lake (NTS 55N, W1/2) map areas, District of Keewatin; Geological Survey of Canada, Open File 703, scale 1:250 000.

**Ryan, J.J., Hanmer, S., Tella, S., and Sandeman, H.A.**
1999: Detailed structural studies, Gibson Lake–Cross Bay–MacQuoid Lake area, Northwest Territories (Kivalliq region, Nunavut); *in* Current Research 1999-C; Geological Survey of Canada.

**Sanborn-Barrie, M.**
1994: Structural investigation of high-grade rocks of the Kramanituar complex, Baker Lake area, Northwest Territories; *in* Current Research 1994-C; Geological Survey of Canada, p. 121–133.

**Tella, S. and Schau, M.**
1994: Geology, Gibson Lake (east-half), District of Keewatin, Northwest Territories; Geological Survey of Canada, Open File 2737, scale 1:50 000.

**Tella, S., LeCheminant, A.N., Sanborn-Barrie, M., and Venance, K.E.**
1997a: Geology and structure of parts of the MacQuoid Lake area, District of Keewatin, Northwest Territories; *in* Current Research 1997-C; Geological Survey of Canada, p. 123–132.
1997b: Geology, parts of MacQuoid Lake, District of Keewatin, Northwest Territories; Geological Survey of Canada, Open File 3404, scale 1:50 000.

**Wright, G.M.**
1967: Geology of the southeastern Barren Grounds, parts of the Districts of Mackenzie and Keewatin (Operations Keewatin, Baker, Thelon); Geological Survey of Canada, Memoir 350, p. 91.

Geological Survey of Canada Project 970006

# Detailed structural studies, Gibson Lake–Cross Bay–MacQuoid Lake area, Northwest Territories (Kivalliq region, Nunavut)[1]

J.J. Ryan, S. Hanmer, S. Tella, and H.A. Sandeman
Continental Geoscience Division, Ottawa

*Ryan, J.J., Hanmer, S., Tella, S., and Sandeman, H.A., 1999: Detailed structural studies, Gibson Lake–Cross Bay–MacQuoid Lake area, Northwest Territories (Kivalliq region, Nunavut);* in *Current Research 1999-C; Geological Survey of Canada, p. 87–96.*

---

**Abstract:** The Gibson Lake–Cross Bay–MacQuoid Lake area comprises a multiply deformed Archean terrane, tectonothermally reworked in the Paleoproterozoic. Multiple foliations in the western volcanic belt illustrate that the regional foliation is a second generation feature ($S_2$), formed by transposition of layering and a layer-parallel foliation ($S_1$). The $S_2$ appears to have developed at ca. 2.68 Ga. Two subsequent generations of folds modified the $S_2$ during the Paleoproterozoic. South-plunging $F_3$ folds are restricted to the Cross Bay complex, whereas east-northeast-trending, $F_4$ folds control much of the map pattern in the volcanic belt and southeastern part of the Cross Bay complex. The complex is bounded to the south by the Big lake shear zone, a 50 km long, dextral, strike-slip structure. The main phase of deformation and metamorphism in the shear zone is Paleoproterozoic, and its western segment is stitched by a late-stage (possibly ca. 1.83 Ga) granite.

**Résumé :** La région du lac Gibson, de la baie Cross et du lac MacQuoid comporte un terrane archéen qui a subi des déformations multiples et, au Paléoprotérozoïque, un remaniement par voies tectonique et thermique. Des schistosités multiples dans la ceinture volcanique occidentale démontrent que la schistosité régionale est une caractéristique de deuxième génération ($S_2$) formée par transposition d'une stratification et d'une schistosité parallèle à la stratification ($S_1$). La schistosité $S_2$ s'est vraisemblablement formée vers 2,68 Ga. Deux générations ultérieures de plis ont modifié la schistosité $S_2$ au cours du Paléoprotérozoïque. Des plis $F_3$ à plongement vers le sud ne sont présents que dans le complexe de Cross Bay, alors que des plis $F_4$ de direction est-nord-est contrôlent en bonne partie la configuration cartographique de la ceinture volcanique et de la partie sud-est du complexe. Celui-ci est limité au sud par la zone de cisaillement de Big lake, une structure de cisaillement dextre de 50 km de longueur. La phase principale de déformation et de métamorphisme dans la zone de cisaillement remonte au Paléoprotérozoïque; le segment occidental de la zone est soudé par un granite tardif qui remonterait possiblement à environ 1,83 Ga.

---

[1] Contribution to the Western Churchill NATMAP Project

## INTRODUCTION

This study is part of the Western Churchill NATMAP Project, a collaborative effort between the Geological Survey of Canada (GSC), the Government of the Northwest Territories (GNWT), Indian and Northern Affairs Canada (INAC), and industry. During the 1998 field season, the second phase of the GSC's three year field program, an investigation of the geology of parts of the MacQuoid Lake (NTS 55 M) and Gibson Lake (NTS 55 N) map areas (Fig. 1) was undertaken between MacQuoid Lake, Gibson Lake, and Chesterfield Inlet.

The Gibson Lake–Cross Bay–MacQuoid Lake area (Fig. 1) comprises a multiply deformed Archean terrane that was tectonothermally reworked in the Paleoproterozoic (Hanmer et al., 1999a, b). The lithotectonic division of the area (Fig. 1) is fourfold, 1) a southern panel of northwest-dipping metasedimentary rocks and gneissic tonalite sheets termed the Gibson–MacQuoid homocline; 2) an overlying metavolcanic belt to the north and west, hosting several tonalite-granodiorite plutons; 3) the Cross Bay plutonic complex in the northeast, comprising gneissic tonalite and biotite-altered, diorite-gabbro host rocks, and younger granite bodies; and 4) a zone of annealed straight gneiss and ribbon mylonite units which comprise the 'Big lake shear zone'. Rock types, lithological associations, and regional structural geology of the map area are described elsewhere (Tella et al., 1997a, b; Hanmer et al., 1999a, b). This report focuses on two aspects of the structural geology from the 1998 field mapping, the character, origin, and deformational history of the 'regional foliation'; and the character, geometry, and shear history of the 'Big lake shear zone'.

Volcanic and sedimentary rocks of the Neoarchean MacQuoid supracrustal belt were intruded by ca. 2.68 Ga tonalite units that are synkinematic with respect to development of the Neoarchean 'regional foliation' (Tella et al., 1997a, b; Hanmer et al., 1999a, b). Paleoproterozoic intrusive rocks that help unravel the tectonothermal history in the area include the ca. 2.19 Ga MacQuoid dyke swarm (Tella et al., 1997a, b), ca. 1.83 Ga lamprophyre dykes (MacRae et al., 1996), and ca. 1.83 Ga isotropic granite (Tella et al. 1997a). MacQuoid dykes crosscut the Neoarchean foliation throughout the map area and are themselves affected by two episodes of Paleoproterozoic deformation, and an associated amphibolite-facies metamorphism, in the Cross Bay complex (Hanmer et al., 1999a, b). The MacQuoid dykes influenced flow in the Big lake shear zone, indicating that the shear zone is largely a Paleoproterozoic structure.

We address three questions regarding the regional foliation. 1) Is the regional foliation a first or second generation feature? 2) Is the regional foliation the same generation of fabric across the map area? 3) Are the east-northeast-trending, map-scale folds in the western volcanic belt and southeastern part of the Cross Bay complex the same generation? With regards to the Big lake shear zone, we address six questions. 1) How are the strain gradients and boundaries of the shear zone manifest? 2) Why does the foliation vary in character across strike? 3) Under what metamorphic conditions was the shear zone active? 4) What is its age? 5) What is its sense of shear? 6) Is the emplacement of particular igneous rocks in the western segment related to the shear zone?

## STRUCTURES NEAR MUSKOX LAKE

Our regional mapping in the Gibson Lake–Cross Bay–MacQuoid Lake area has shown that the regional foliation throughout the Cross Bay complex and the Gibson–MacQuoid homocline is characterized by a dominant, layer-parallel foliation (Hanmer et al., 1999b). The trace of the foliation and layering ($S_0$) outlines subsequent regional folds in the Cross Bay complex and in the volcanic belt, whereas the orientation of the foliation in the Gibson–MacQuoid homocline has a monotonous 40–50° dip to the north-northwest. A single main foliation in the north and east parts of the map is inconsistent with the observation by Tella et al. (1997b) of polyphase foliation development in the supracrustal rocks around MacQuoid Lake to the southwest. There, Tella et al. (1997b) described southeast-verging, shallow to recumbent, $F_1$ folds of layering, and an associated, regionally pervasive, layer-parallel, $S_1$ foliation. They described northeast-plunging, $F_2$ folds overprinting the $S_0/S_1$ layering, and northeast- to east-northeast-trending, upright, $S_2$ foliation. The apparent discrepancy in the record of regional foliation between areas could not be resolved during our mapping in the northeast, therefore a detailed mapping project was undertaken in the Muskox lake area of the western volcanic belt (Fig. 2). This area is ideal for evaluation of foliation development because it records multiple foliations and strain distribution is heterogeneous enough for the local preservation of primary features in the supracrustal rocks (e.g. pillows, bedded conglomerate units). Based on observations at Muskox lake, and through regional form surface mapping (Hanmer et al., 1999b), we extrapolate the history of fabric development there across the Gibson Lake–Chesterfield Inlet area to the northeast.

Our mapping at Muskox lake (Fig. 2) shows that the pervasive main foliation as described by Tella et al. (1997b) is in fact not a single foliation, but is a composite foliation ($S_1/S_2$) developed by the transposition of layering and a layer-parallel foliation ($S_1$). Furthermore, the northeast-trending upright $F_2/S_2$ structures of Tella et al. (1997b) are third generation features at the scale of the Muskox lake area, and are fourth generation structures when reconciled with the Gibson Lake–Cross Bay–MacQuoid Lake area as a whole (Hanmer et al., 1999b).

### *The $S_1/S_2$ transposition foliation*

$S_1$ is difficult to characterize in the Muskox lake area (Fig. 2) because it is strongly overprinted by $F_2$ structures. $S_1$ is best preserved in the northwest part of the Muskox lake area within open, minor $F_2$ folds, and is manifest as a compositional banding (Fig. 3), or as a strong grain-scale cleavage or pervasive shape fabric parallel to strongly flattened primary features (e.g. clasts, pillows). In the northwest part of the

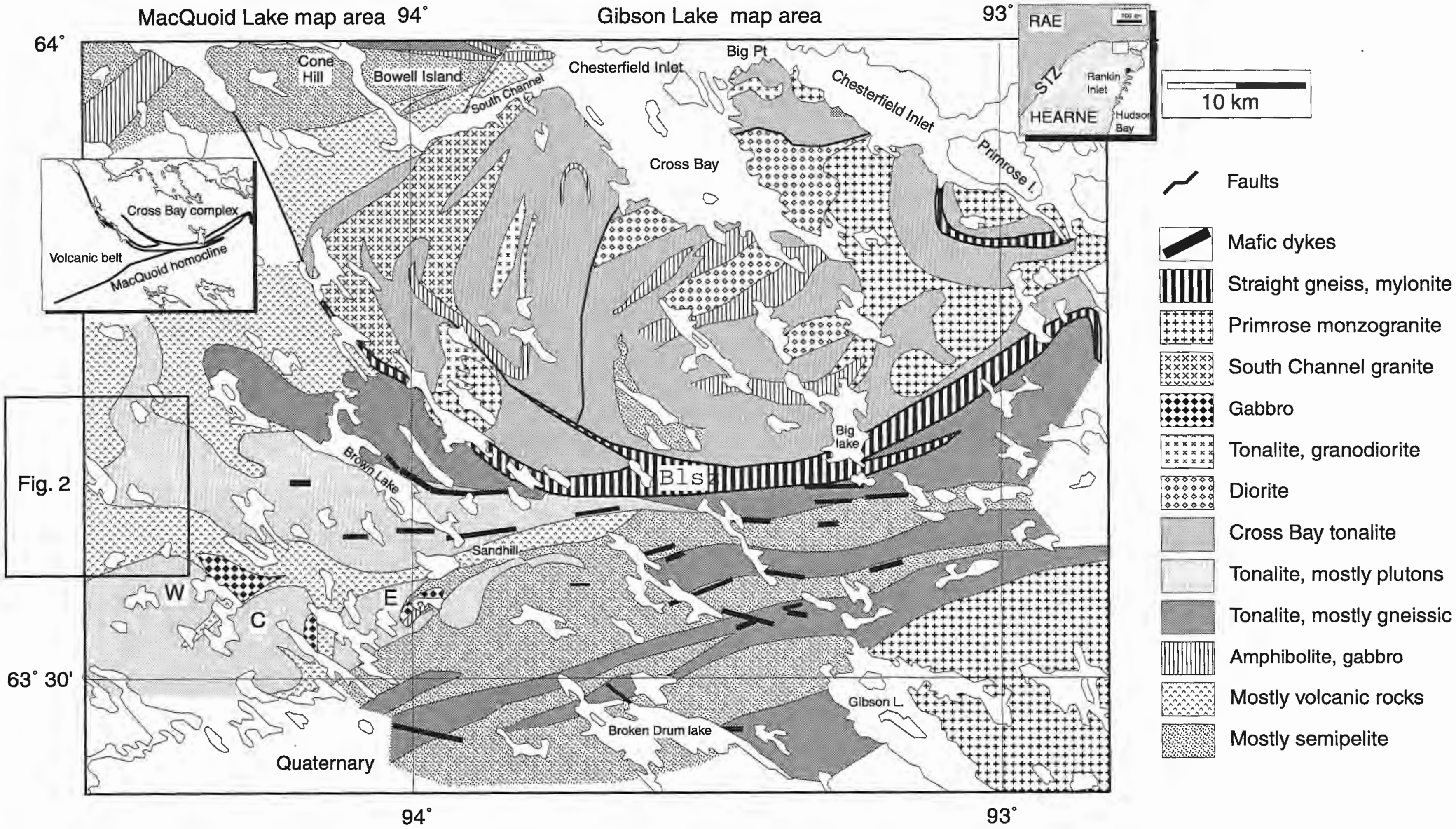


***Figure 1.*** *Overview map of the Gibson Lake–Cross Bay–MacQuoid Lake area (from Hanmer et al., 1999b). The fourfold division of the area is shown as an inset map. The Big lake shear zone (Blsz) and Figure 2 are highlighted. STZ=Snowbird tectonic zone; W, C, and E are western, central, and eastern plutons, respectively.*

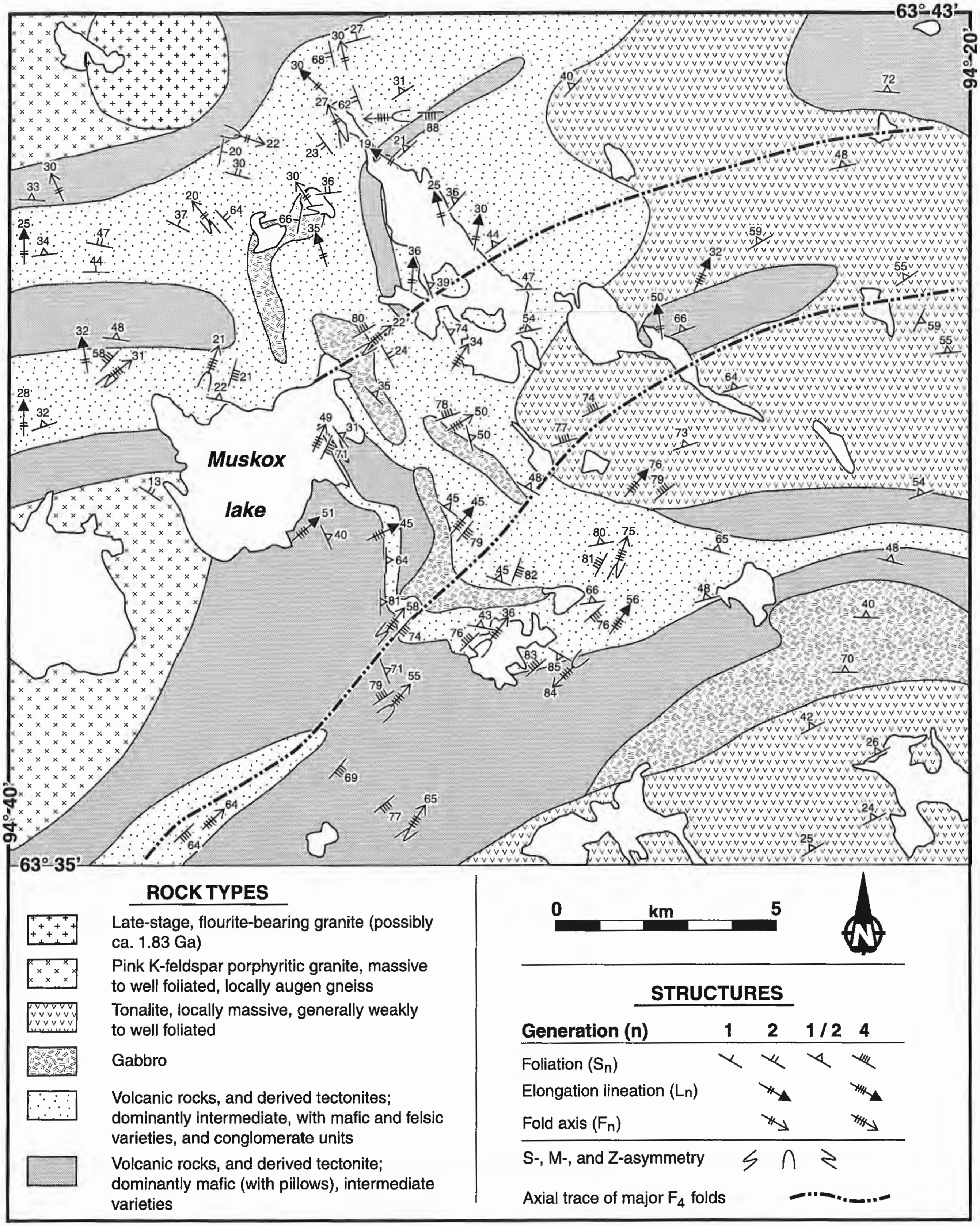


*Figure 2. Detailed structural map of the Muskox lake area, in the western part of the volcanic belt. The traces of map-scale, $F_4$ folds are drawn for clarity. Lithological contacts in the western half of the area are adapted from Tella et al. (1997b).*

Muskox lake area, $S_1$ tends to be parallel to layering, and dips shallowly to moderately north or northwest. In the southeast, $S_1$ is generally obliterated by intense $F_2$ deformation.

Kilometre-scale, $F_2$ folds in the northwest part of the map area exhibit variable stages of axial-planar, $S_2$ development. These folds are better defined by the geometry of $S_1$ and minor $F_2$ folds at the outcrop scale than by the map-scale trace of rock units (Fig. 2). $F_2$ folds generally trend northwest, verge southwest, and have a shallowly northeast-dipping axial surface. In the hinge region of $F_2$ folds, the expression of $S_2$ within a given outcrop can vary from open crenulations of the $S_1$, without a pervasive $S_2$ (Fig. 3), to well developed $S_2$ crenulation cleavage where there is almost complete transposition of $S_1$. On the limbs of the kilometre-scale, $F_2$ folds, $S_1$ and $S_2$ have a small obliquity, and field distinction of the two fabrics is difficult. Figure 4 illustrates an example from a volcanic breccia in which a grain-scale, $S_1$ cleavage, parallel to flattened clasts, is overprinted by an oblique, $S_2$ differentiated crenulation cleavage.


***Figure 3.** $S_1$ preserved as compositional banding in shallowly north-northwest-plunging, $F_2$ folds (parallel to pencil). This location is within the hinge region of a kilometre-scale, $F_2$ closure.*

The distinction between $S_1$ and $S_2$ becomes more difficult in the eastern and southern parts of the Muskox lake area, where layering, $S_1$, and $S_2$ are parallel. Immediately east of Muskox lake (Fig. 2), there is almost no record of $S_1$ except for within discontinuous to rootless, intrafolial isoclinal $F_2$ folds of $S_1$ (Fig. 5) and layering, and $S_2$ forms an axial-planar fabric to the $F_2$ folds. Even where there is no new axial-planar foliation associated with the $F_2$ folds, the isoclinal nature of the $F_2$ folding has transposed the $S_1$ foliation and layering into the $S_2$ orientation. Where $F_2$ folds are lacking, it is rarely possible to distinguish $S_1$ from $S_2$, and the regional foliation is therein generalized as an $S_1/S_2$ composite foliation (Fig. 2). The local preservation of $S_1$ within the kilometre-scale, $F_2$ folds of $S_1$ and layering, as well as the progressive tightening of $F_2$ folds and obliteration of $S_1$ foliation to the south and east that lead us to interpret $S_2$ as having formed by transposition of an $S_1$ foliation and layering.

Grain-scale fabrics defining both $S_1$ and $S_2$ in the Muskox lake area are overprinted by porphyroblasts (garnet and hornblende in mafic to intermediate volcanic rocks) associated with regional metamorphism. Therefore, the age of fabric development relative to mineral growth does not help to distinguish $S_1$ and $S_2$.

The orientation of $F_2$ folds varies widely across the Muskox lake area, however, they generally plunge shallowly to moderately north to northwest. Evidence for extension parallel to the $F_2$ fold axes is locally demonstrated by rodded primary features (e.g. phenocrysts, clasts) with aspect ratios of 10:1:1, probably indicating that the $F_2$ transposition deformation had a large component of north-northwest extension. The enveloping surface of $S_2$ across subsequent folds locally records a shallowly north-dipping attitude, and probably represents the orientation in which the foliation developed. In the absence of constraints on the boundary conditions of this deformation, it is not possible to constrain the kinematic framework in terms of possible contractional or extensional tectonics.

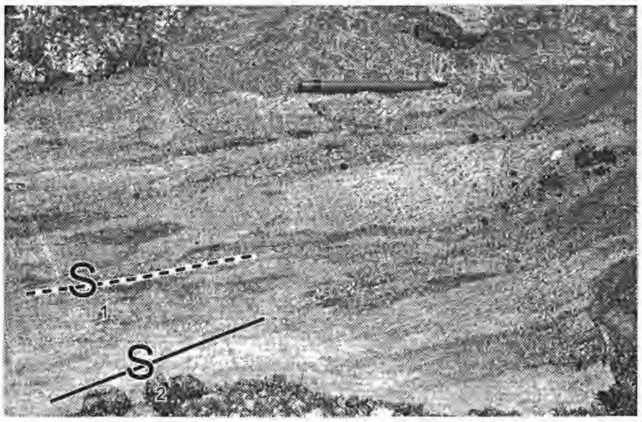


***Figure 4.** $S_2$ differentiated crenulation cleavage overprinting $S_1$, which is parallel to flattened clasts in a volcanic breccia.*


***Figure 5.** Shallowly north-plunging, intrafolial isoclinal $F_2$ fold associated with the transposition of the $S_1$ foliation. The $F_2$ axial surface (parallel to the pencil) dips shallowly north. Photograph is of a steeply dipping surface.*

A form surface map of the 'main foliation' across the Gibson Lake–Cross Bay–MacQuoid Lake area (*see* Fig. 2, Hanmer et al., 1999b) indicates that it is the same generation as the $S_1/S_2$ transposition foliation at Muskox lake. We attribute the general lack of $S_1$ preservation in the Gibson–MacQuoid homocline and in the Cross Bay complex to more complete $D_2$ transposition of $S_1$ and layering as compared to that near Muskox lake.

### *Map-scale, east- to northeast-trending folds*

The map pattern of the Muskox lake area is strongly influenced by east-northeast-trending, map-scale folds of $S_1/S_2$ and layering (Fig. 2). These folds were designated $F_2$ structures by Tella et al. (1997b). However, because they affect the northwest-trending, $F_2$ folds described above, and fold $S_2$, they are $F_3$ structures at the scale of the Muskox lake area. We designate these folds $F_4$ regionally because we correlate them

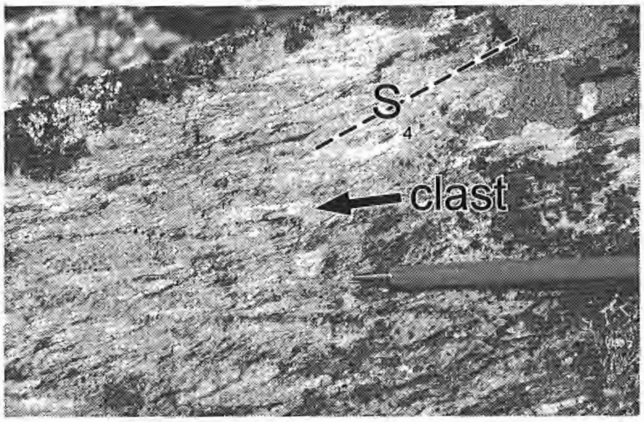


***Figure 6.*** *Penetrative $S_4$ cleavage crosscutting a strong composite $S_1/S_2$ fabric (parallel to pencil), defined by flattened clasts in a felsic volcanic breccia. In this case, there is no crenulation associated with the $F_4$ deformation.*

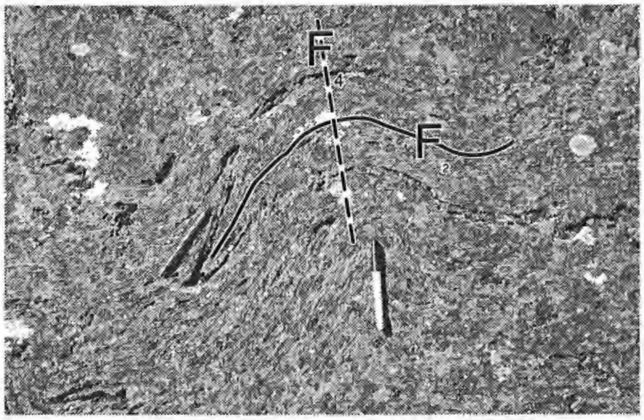


***Figure 7.*** *$S_1$ folded about tight $F_2$ folds (parallel to pencil), refolded by the northeast-trending, $F_4$ folds (axial trend is parallel to the marker pen), without the development of an $S_4$ fabric.*

with comparable Paleoproterozoic structures found throughout the southeastern part of the Cross Bay complex to the east (Fig. 1; *see also* Hanmer et al., 1999b). South-plunging, map- to outcrop-scale, $F_3$ folds of $S_2$ are localized in the northern part of the Cross Bay complex (Hanmer et al., 1999b), and are not recorded in the Muskox lake area.

The $F_4$ folds in the Muskox lake area (Fig. 2) have steeply dipping, north-northeast-trending axial surfaces. Fold axes plunge shallowly to steeply north-northeast, varying with the dip of $S_2$ and layering on which they are developed. Stretched porphyroblasts generally define a weak to strong elongation lineation ($L_4$) parallel to the $F_4$ axes. Outcrop-scale, $F_4$ folds of $S_1/S_2$ are parasitic to the map-scale folds, and like map-scale, $F_4$ folds, they form open structures. Unlike $F_4$ folds southeast of Cross Bay (Hanmer et al., 1999b), those in the volcanic belt locally have well developed axial-planar fabrics ($S_4$). $S_4$ fabrics trend between east-northeast to north-northeast, and are consistently steeply dipping (Fig. 2). The $S_4$ foliation varies in character from weak crenulation of $S_2$, to pervasive new cleavage with no crenulation development (Fig. 6). Even where pervasively developed, $S_4$ is readily distinguished from $S_2$ because it overprints peak-metamorphic minerals. Rare examples of overprinting between $S_1$, $F_2$, and $F_4$ are seen in the same outcrop (Fig. 7), and are consistent with the map pattern (Fig. 2). The intensity of $S_4$ development is strongly controlled by the relative competence of the rock type, grain size, and the intensity of pre-existing fabrics.

## THE BIG LAKE SHEAR ZONE

The Paleoproterozoic Big lake shear zone (*see* below) is an east-striking, steeply dipping zone of intensely sheared rocks that marks the southern boundary of the Cross Bay complex (Fig. 1; Hanmer et al., 1999a, b). The shear zone, which is as wide as 2 km, is described in segments in this report, due to lithological and structural differences along strike.

### *The central and eastern segments*

The central and eastern segments of the Big lake shear zone comprise mylonitic rocks of variable character. The northern and southern margins of the shear zone consist of belts of porphyroclastic, relatively coarse-grained, annealed straight gneiss, whereas the internal part is composed of fine-grained ribbon mylonite. We use the term straight gneiss to describe those mylonite units whose grain size has been significantly coarsened during postmylonitization, secondary grain growth. The gneissosity is defined by straight, continuous compositional layers, 1 mm to more than 30 mm thick, derived by mechanical degradation of previous layering, dykes, and phenocrysts. We use the term ribbon mylonite to describe those rocks that have a finer grained (generally <1 mm), more fissile layering that has not undergone significant postmylonitization, secondary grain growth. The ribbon mylonite is derived predominantly from pink to red, monzogranite veins, and other quartz-rich rocks. The ribbon fabric is defined chiefly by quartz layers that have a strong grain-scale shape fabric. The variation in character of the mylonites across the shear zone is largely a function of differences in the age of the fabric relative to the Paleoproterozoic metamorphism. Chlorite locally helps define the fabric in the fissile ribbon mylonite, whereas hornblende is a common constituent of the straight gneiss. We interpret the annealed straight gneiss as representing the older part of the deformation history, which experienced amphibolite-grade metamorphism during and after shear deformation. We interpret the ribbon mylonite as representing deformation during the later, lower grade portion of the metamorphic cycle.

The annealed straight gneiss foliation in the central and eastern segments is locally difficult to distinguish from the $S_2$ foliation in orthogneiss and paragneiss wall rocks. Unlike the foliation in the wall rocks, however, the straight gneiss units are consistently steeply dipping, contain spectacular porphyroclastic panels (Fig. 8), and have a well developed, subhorizontal, east- or west-plunging extension lineation.

Porphyroclasts in the mylonite are composed primarily of quartz and feldspar, derived from dismembered pegmatite. Porphyroclasts of garnet, hornblende, and possibly clinopyroxene are also locally abundant. Although the majority of winged porphyroclasts in the central and eastern segments are symmetrical, the asymmetrical variety are dominated by delta geometry and dextral asymmetry (Fig. 8; *see* Fig. 7, Hanmer et al., 1999b), indicative of dextral shear along the Big lake shear zone. Other dextral, shear-sense indicators include asymmetric, shear drag Z-folds, asymmetrically pulled-apart boudins of amphibolite layers (Fig. 9), oblique shape fabrics, and shear bands. Fabric elements and shear-sense indicators in the central and eastern segments prescribe a dextral, strike-slip shear zone of monoclinic symmetry.

The strain gradient on the southern margin of the shear zone tends to be more abrupt than that of the north margin, however, both vary between abrupt to gradational along strike. Recognition of the southern boundary is more straightforward where the shallowly to moderately dipping regional foliation abruptly assumes a vertical dip. This transition is seen locally over a width of 3–10 m. On the north margin, the transition between the shear zone foliation and the $S_2$ regional foliation occurs over a width of tens of metres to hundreds of metres, and is manifest as a change in the tightness of upright folds of the gneissosity. Away from the shear zone, open folds of gneissosity are developed, whereas isoclinal folds occur nearer the shear zone. Hanmer et al. (1999b) concluded that because these folds have comparable style and orientation to $F_4$ folds, this portion of the deformation history of the shear zone is probably synchronous with $F_4$ deformation.

### *The western segment*

The western segment of the Big lake shear zone is distinct from the central and eastern segments because it encompasses a wider variety of rock types, has a strong topographical expression, and is 'stitched' by a late isotropic granite (Fig. 1). Rocks in the western segment include paragneiss, orthogneiss, homogeneous tonalite, monzogranite, diabase, lamprophyre, anorthosite, and garnet-plagioclase amphibolite. The strong topographical expression (Fig. 10) is

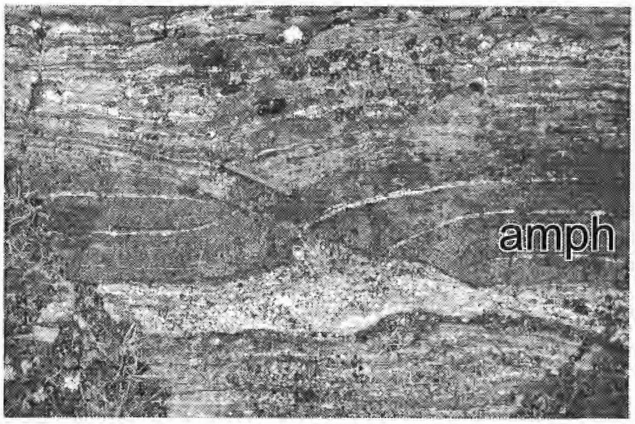


***Figure 9.*** *Asymmetrically pulled-apart amphibolite (amph) layer within the central portion of the Big lake shear zone.*

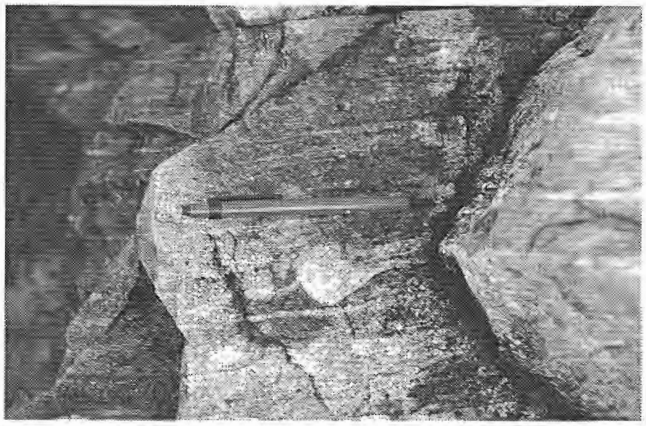

***Figure 8.*** *Dextrally rotated, winged delta porphyroclast of potassium feldspar (derived from dismembered pegmatite). This is a horizontal surface and the rock has a shallow extension lineation.*

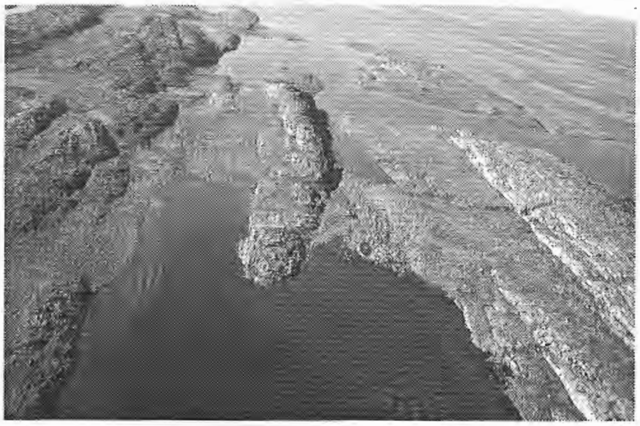

***Figure 10.*** *Aerial photograph of the western segment of the Big lake shear zone, looking northwest. Ridges are generally defined by the less deformed, coarser grained rocks, whereas the low ground comprises the more fissile ribbon mylonite.*

controlled chiefly by grain size, whereby fine-grained, fissile mylonite forms lowlands, and coarse-grained, lesser deformed rocks (including the wall rocks) form ridges. The western segment contains mylonite units which have the finest grain size of any in the map area. This character appears to be independent of rock type, because examples of aphanitic mylonite derived from monzogranite, anorthosite, diabase, and mafic rocks of uncertain protolith occur together.

The anorthositic mylonite units represent one of the more interesting, though volumetrically minor (<10%), rock types in the western segment. They contain more than 95% plagioclase and thin (1–8 mm) mafic layers (Fig. 11). The mafic layers are probably derived from the mechanical break down and transposition of primary pyroxene in the original gabbroic anorthosite, and are now composed of tiny (<1 mm) randomly oriented, acicular, actinolitic hornblende. The random orientation of these amphibole crystals indicates that they grew after deformation. In contrast, plagioclase layers have remained remarkably fine grained (<50–100 μm), probably demonstrating a different response by the two mineral groups to the prevailing metamorphic conditions at that time. Rare occurrences of weakly foliated to massive gabbroic anorthosites were observed east and west of the western segment, and may represent the protolith of the anorthositic mylonite. Coarse-grained, garnet-plagioclase-hornblende amphibolite gneiss units occur with the anorthositic mylonite units, and probably have a mafic igneous protolith. Foliation intensity in these rocks varies from massive with weak layering, to fissile mylonite (*see* Fig. 11, Hanmer et al., 1999b).

Small-scale observations in the in the western segment provide evidence for synkinematic localization of magma in the shear zone. A localized suite of northwest-trending, 1–2 m thick, diabase dykes of unknown age (not to be confused with the MacQuoid dykes) occur within and adjacent to the southwestern extremity of the shear zone, and are subparallel to the shear foliation. Internal foliation in the dykes varies in intensity from weak to mylonitic with proximity to the shear zone. The mylonitized dykes are aphanitic and poorly

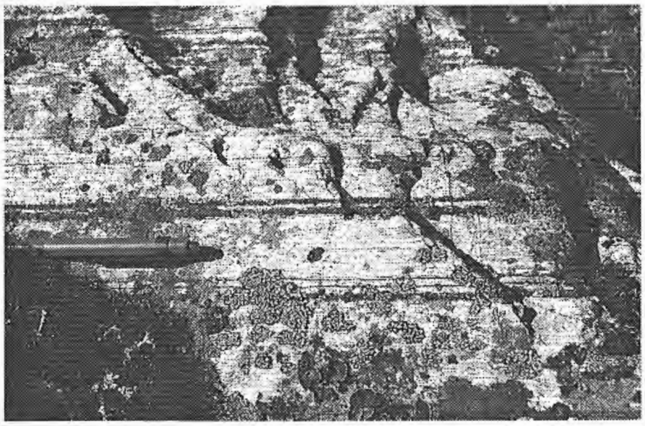

***Figure 11.*** *Anorthositic mylonite in the western segment of the Big lake shear zone. The thin (1–8 mm) mafic layers are now defined by randomly oriented tiny (<1 mm), actinolitic hornblende needles.*

***Figure 12.*** *Folded wisps of mylonitized tonalite within an internally mylonitized, 1 m wide, vertical diabase dyke in the Big lake shear zone. Fold axes plunge shallowly to the right, parallel to an intense extension lineation.*

cleaved, and some have spectacularly folded internal foliations (Fig. 12), defined in part by wisps of mylonitized tonalite inclusions. These folds are coaxial with the shallow extension lineation. Although internally mylonitized, the dykes locally preserve a slight discordance with the shear fabric, indicating that the dykes postdate a portion of the shear history, and are possibly synkinematic. The high degree of internal strain in some dykes might suggest that they deformed at elevated temperature. These dykes have been observed only in the western segment, where they appear to be localized (*see* 'Discussion')

The steeply to moderately dipping foliation in the western segment of the shear zone trends broadly northwest, and its dip varies from southwest to northeast locally along strike. This represents a marked difference between the western segment and the central and eastern segments, where the foliation is more consistently steeply dipping. The associated extension lineation also differs by plunging shallowly to the northwest, and locally steepening to more than 45° where the foliation makes local east-west bends. In further contrast to the eastern and central segments, sinistral shear-sense indicators are more abundant than the dextral variety, although both types are rare relative to farther east along the shear zone. The reason for the difference in the lineation-foliation geometry and apparent shear sense is not clear, although it probably indicates that flow was accommodated differently in the western versus the eastern and central segments (*see* 'Discussion').

Garnet-plagioclase-hornblende assemblages were in apparent thermal stability during shear zone activity, indicating that deformation occurred under middle amphibolite-facies conditions. Large porphyroclasts of intergrown garnet and clinopyroxene in these rocks suggest that higher grade rocks also were affected by this deformation. Garnet porphyroclasts in some strands of ribbon mylonite were completely pseudomorphed by chlorite. Chlorite pseudomorphs, and the presence of fine, randomly oriented actinolitic-hornblende in mafic layers in the anorthositic mylonite, probably indicate that a hydration event occurred after the thermal peak of metamorphism, and after cessation of shear in those rocks.

Hanmer et al. (1999a, b) described a diabase dyke correlated with the 2.19 Ga MacQuoid swarm (Tella et al., 1997a) that influenced flow in the Big lake shear zone, and thus interpreted shear activity along the zone as being largely Paleoproterozoic. We interpret the amphibolite-facies metamorphism recorded in both the shear zone and in the MacQuoid dykes as the same Paleoproterozoic metamorphic event. A series of 10–100 m thick sheets of pink monzogranite crosscuts the foliation on the northeast side of the western segment, and they therein demonstrably form a large proportion of the ribbon mylonite. The age of the monzogranites is presently unknown, but is probably Paleoproterozoic. The isotropic stitching granite in the western segment is similar in appearance to a ca. 1.83 Ga, flourite-bearing granite (Tella et al., 1997a) from the adjoining area to the west. If the correlation of the two granite bodies is correct, the significant movement along the shear zone must have occurred prior to ca. 1.83 Ga. Lamprophyre dykes, interpreted on the basis of commingling textures as being comagmatic with the stitching granite, also crosscut the mylonite. The diamondiferous Akluilâk lamprophyre dyke, located 12 km to the south, has been dated at ca. 1.83 Ga (MacRae et al., 1996). The lamprophyre dykes generally preserve pristine phlogopite, and some exhibit mild chlorite alteration. These rocks thus did not experience thermal conditions greater than greenschist facies after ca. 1.83 Ga. Rare examples of folded and cleaved lamprophyres, one of which records dextral C-S fabrics, were noted in the shear zone. These observations indicate that minor movements probably occurred along the zone after emplacement of the stitching pluton and associated lamprophyre dykes.

## DISCUSSION

The Gibson Lake–Cross Bay–MacQuoid Lake area has a characteristic, regionally pervasive, single foliation, parallel to most lithological layering. Detailed mapping in the Muskox lake area in the western part of the volcanic belt illustrated that the regional foliation is derived by the transposition of layering and a layer-parallel tectonic foliation ($S_1$). For this reason, the regional foliation across the map area is designated $S_2$, even where transposition is too advanced for preservation of $S_1$. Hanmer et al. (1999b) described tonalite plutons, one of which yielded a U-Pb zircon age of ca. 2.68 Ga (Tella et al., 1997a), as being synkinematic with respect to $D_2$ deformation, suggesting that $S_2$ was largely developed by that time, and is thus a Neoarchean fabric.

The Paleoproterozoic (postdating ca. 2.19 Ga) east- to northeast-trending, $F_4$ folds are best developed in the western volcanic belt, and within the southeastern part of the Cross Bay complex. In the volcanic belt, most $F_4$ folds plunge steeply to moderately east-northeast, with a strong associated extension lineation parallel to the fold axes and a locally well developed $S_4$ axial-planar foliation. $F_4$/$L_4$ relationships are similar in the Cross Bay complex (Hanmer et al., 1999b), however, $S_4$ is generally not observed outside of the volcanic belt. In fact, development of penetrative foliations occurred only during $D_1$ and $D_2$ deformation.

The Big lake shear zone was active under amphibolite-facies conditions during the Paleoproterozoic (after 2.19 Ga), and localized greenschist facies strands suggest that deformation continued during the retrograde part of the metamorphic cycle. We presently cannot constrain the timing at which the Big lake shear zone initiated, and it is conceivable that initial movement on the zone occurred in the Neoarchean. The growth of retrograde mineral assemblages after the cessation of the main mylonitization event indicates that the shear zone underwent a late-stage fluid flux, without significant coarsening of grain size of the mylonite (particularly plagioclase in anorthosite).

The anorthosite and garnet-plagioclase amphibolite units in the western segment of the shear zone bear a striking resemblance to rocks in the Kramanituar and Uvauk complexes exposed to the north of Chesterfield Inlet (Tella et al., 1993; Sanborn-Barrie, 1994; Mills et al., 1999). We speculate that the emplacement of the anorthosite units and mafic igneous protolith of the garnet-plagioclase amphibolite may be related to deformation along the western segment of the shear zone. This interpretation is consistent with the apparently synkinematic diabase dykes concentrated there, and the broadly synkinematic, pink monzogranite that forms much of the ribbon mylonite. The more complicated relationship between foliations, lineations, and shear-sense indicators in the western segment is consistent with a deformation path that is distinct from that along the eastern extent of the zone. If the northwest trend of the western segment is the initial trajectory of the shear zone at that location, the western segment was probably in an extensional regime during bulk dextral shear along the central and eastern segments. An extensional jog within the shear zone would have been an ideal setting for the synkinematic localization of magma, consistent with the various igneous rocks observed in the western segment.

## ACKNOWLEDGMENTS

Discussions in the field with Rob Berman and Bill Davies contributed to the ideas presented herein. Our understanding of the Big lake shear zone has particularly benefited from mapping by Mark Quigley for a B.Sc. dissertation at the University of Toronto. A more complete list of acknowledgments is given in Hanmer et al. (1999b). Sally Pehrsson is thanked for a very constructive review of the manuscript.

## REFERENCES

**Hanmer, S., Tella, S., Sandeman, H.A., Ryan, J.J., Hadlari, T., and Mills, A.**

1999a: Proterozoic reworking in western Churchill Province, Gibson Lake–Cross Bay area, Northwest Territories (Kivalliq region, Nunavut). Part 1: general geology; in Current Research 1999-C; Geological Survey of Canada.

1999b: Proterozoic reworking in Western Churchill Province, Gibson Lake–Cross Bay area, Northwest Territories (Kivalliq region, Nunavut). Part 2: regional structural geology; *in* Current Research 1999-C; Geological Survey of Canada.

**MacRae, N.D., Armitage, A.E., Miller, A.R., Roddick, J.C., Jones, A.L., and Mudry, M.P.**
1996: The diamondiferous Akluilâk lamprophyre dyke, Gibson Lake area, N.W.T.; *in* Searching for Diamonds in Canada, (ed.) A.N. LeCheminant, D.G. Richardson, R.N.W. DiLabio, and K.A. Richardson; Geological Survey of Canada, Open File 3228, p. 101–107.

**Mills, A., Berman, R., Hanmer, S., and Tella, S.**
1999: Geology of the Uvuak complex, Northwest Territories (Kivalliq region, Nunavut); *in* Current Research 1999-C; Geological Survey of Canada.

**Sanborn-Barrie, M.**
1994: Structural investigation of high-grade rocks of the Kramanituar complex, Baker Lake area, Northwest Territories; *in* Current Research 1994-C; Geological Survey of Canada, p. 121–133.

**Tella, S., Davis, W., Berman, R.G., Stern, R., and LeCheminant, A.N.**
1997a: Tectonothermal history of the MacQuoid Lake supracrustal belt, District of Keewatin, Northwest Territories, Canada; Geological Society of America, Abstracts with Programs, v. 29, p. 277–278.

**Tella, S., LeCheminant, A.N., Sanborn-Barrie, M., and Venance, K.E.**
1997b: Geology and structure of parts of the MacQuoid Lake area, District of Keewatin, Northwest Territories; *in* Current Research 1997-C; Geological Survey of Canada, p. 123–132.

---

Geological Survey of Canada Project 970006

# Geology of the Uvauk complex, Northwest Territories (Kivalliq region, Nunavut)[1]

A. Mills[2], R. Berman, and S. Hanmer
Continental Geoscience Division, Ontario

*Mills, A., Berman, R., and Hanmer, S., 1999: Geology of the Uvauk complex, Northwest Territories (Kivalliq region, Nunavut);* in *Current Research 1999-C; Geological Survey of Canada, p. 97–106.*

**Abstract:** The Uvauk complex comprises anorthosite, gabbroic anorthosite, diorite, gabbro, and quartzofeldspathic gneiss that have been strongly deformed and metamorphosed at granulite grade, with a subsequent, pervasive, amphibolite-grade overprint. Detailed mapping of the western portion of the complex suggests that the anorthosite represents a synkinematic intrusion into diorite and quartzofeldspathic gneiss wall rocks. Field relations do not unequivocally indicate whether wall rocks had undergone an earlier, Archean, granulite-facies, mylonitization event, or whether all deformation and metamorphism is related to one progressive event.

Sinistral shear-sense indicators to the north and dextral shear-sense indicators to the south of the anorthosite indicate eastward transport of the anorthosite body with respect to its wall rocks. The shallow, east-plunging lineation and limited metamorphic contrast across the wall rocks suggest minimal vertical displacement.

**Résumé :** Le complexe d'Uvauk comprend de l'anorthosite, de l'anorthosite gabbroïque, de la diorite, du gabbro et du gneiss quartzofeldspathique qui ont été intensément déformés et métamorphisés au faciès des granulites, avec une surimpression pénétrative ultérieure au faciès des amphibolites. La cartographie détaillée de la portion occidentale du complexe donne à penser que l'anorthosite représente une intrusion syncinématique dans de la diorite et du gneiss quartzofeldspathique encaissants. Les données de terrain n'indiquent pas sans aucun doute si les roches encaissantes ont subi une mylonitisation archéenne plus ancienne au faciès des granulites ou si toute la déformation et le métamorphisme est liée à un épisode progressif unique.

La présence d'indicateurs directionnels de cisaillement senestre au nord et de cisaillement dextre au sud de l'anorthosite montre qu'il y a eu transport vers l'est du massif anorthositique par rapport aux roches encaissantes. La présence d'une linéation peu profonde à plongement vers l'est et d'un contraste métamorphique atténué dans l'ensemble des roches encaissantes est indicatrice d'un déplacement vertical minimal.

[1] Contribution to Western Churchill NATMAP Project
[2] Department of Earth Sciences, Carleton University, Ottawa, Ontario K1S 5B6

## INTRODUCTION

The Uvauk complex comprises an anorthositic suite and lithologically diverse wall rocks that have been intensely deformed together at granulite facies (Tella et al., 1993, 1994a, b; Tella and Schau, 1994). The Kramanituar (Sanborn-Barrie, 1993, 1994), Hanbury Island (Tella and Annesley, 1988), and Daly Bay (Gordon, 1988; Gordon and Lawton, 1995) complexes show lithological and tectonic similarities to the Uvauk complex (Tella et al., 1993), and together form part of the geophysically defined Snowbird tectonic zone (Hoffman, 1988; Fig. 1). Preliminary U-Pb geochronology yielded ca. 2.56 Ga zircon and ca. 2.59 Ga monazite from wall rock several hundred metres south of the anorthosite, ca. 1.94 Ga zircon from the western part of the anorthosite, and a ca. 2.77 Ga $T_{DM}$ age from anorthosite east of the present study area (Tella et al., 1994a). These data were interpreted to indicate that granulite-facies mylonite units, formed at ca. 2.59 Ga and about 12 kbar and ca. 1.94 Ga at about 10 kbar (Tella and Schau, 1994), were juxtaposed along a cryptic fault.

The work reported here forms part of the first author's M.Sc. thesis, aimed at re-examining previous interpretations based on reconnaissance work, and evaluating the tectonometamorphic history of this segment of the Snowbird tectonic zone. This paper presents a detailed bedrock geology of a critical portion of the Uvauk complex (Fig. 2), documents variations in structural fabrics and metamorphic assemblages, and provides a context for subsequent detailed geochronological and petrological study.

### *General geology*

The Uvauk complex comprises anorthosite and gabbroic anorthosite interpreted here to be intrusive into lithologically diverse wall rocks. Rocks in the complex generally are spectacular, east-trending, granulite-facies, ribbon mylonite, although lower strain domains occur both in the core of the anorthosite and along the southern margin. The anorthosite forms a sheet which is shallowly west-dipping to the east (Tella et al., 1993). The northern and southern margins converge to the west near Uvauk Inlet where the mylonite fabric dips steeply to the south (Tella et al., 1993). Wall rocks to the south consist of quartzofeldspathic gneiss, diorite, and gabbroic rocks that have all been intensely deformed to produce an approximately 1 km thick sequence of straight gneiss. Layered mafic to intermediate volcanogenic rocks and tonalite to the north of the anorthosite sheet exhibit lower strain fabrics.

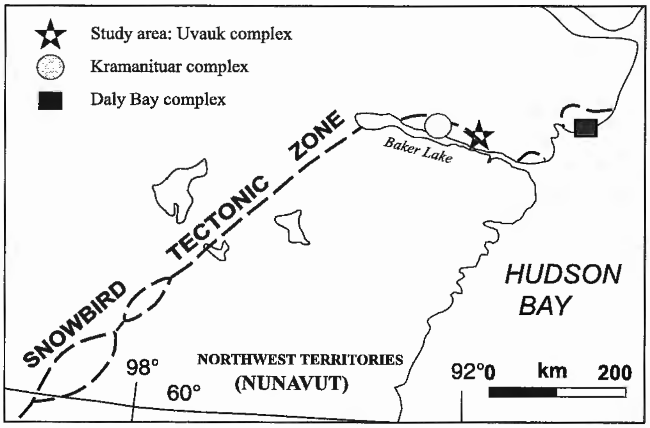


*Figure 1. Location map showing the Snowbird tectonic zone which separates the Rae and the Hearne subprovinces of the Western Churchill Province; the authors' study area, the Uvauk complex; and the lithologically and metamorphically similar complexes, Kramanituar and Daly Bay.*

## LITHOLOGICAL DESCRIPTIONS

### *Anorthosite suite*

The anorthosite of the Uvauk complex is dominantly white weathering where there is very little mafic material (<5%), but commonly contains horizons of gabbroic anorthosite and

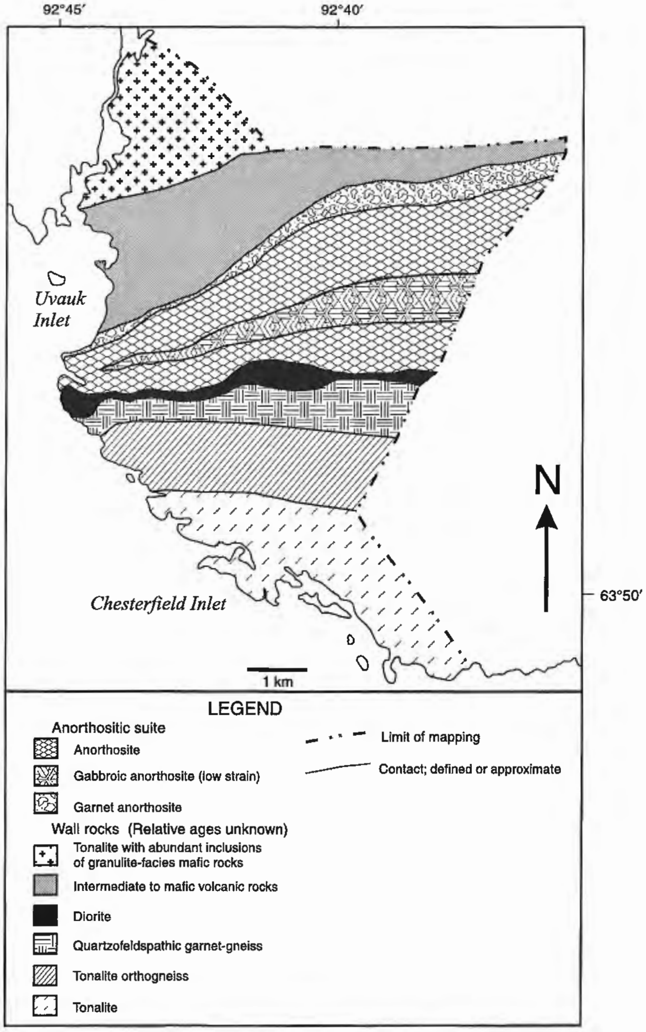


*Figure 2. Simplified geology of the westernmost portion of the Uvauk complex.*

rare anorthositic gabbro. The mafic component is dominantly clinopyroxene, but hornblende, biotite, and rare orthopyroxene are locally present. The entire sheet of anorthosite is mylonitic, with mafic crystals exhibiting aspect ratios of greater than 10:1. Locally, compositional layering is discernable, but no unequivocal top indicators were observed.

The anorthosite is variable in composition and deformation state, and thickens from about 1 km in the west to about 3.5 km to the east of the study area. Marked differences characterize the north and south margins. The northern margin consists of highly strained, garnetiferous anorthosite that may be related to a slightly different primary composition. This is supported by rare, garnet-bearing, anorthosite layers that are intercalated with garnet-free anorthosite. In contrast, extremely coarse-grained, gabbroic anorthosite of lower strain outcrops toward the southern margin. Both margins are marked by a well banded phase, with bands ranging in composition from pyroxenite to anorthosite and primary igneous layering locally preserved. This marginal phase is garnet rich to the north, with garnets ranging up to several centimetre in size at Uvauk Inlet to the west. Rare millimetre-scale garnets were observed locally in the marginal phase to the south.

The core of the sheet is characterized by lower strain gabbroic anorthosite that, in places, exhibits excellent flaser texture defined by augen-shaped pyroxene crystals. Within this panel, clinopyroxene crystals average 5 cm and are rimmed by hornblende (Fig. 3). Extremely heterogeneous deformation patterns are displayed in 1–10 m wide bands of gabbroic anorthosite (colour index about 40) associated with this central panel of less deformed, flaser anorthosite. The width of this lens ranges from about1 km in the east and thins to the west to its termination.

Field observations indicate that the anorthosite was intruded into wall rocks. South of the anorthosite sheet, narrow (tens of centimetres) lenses of anorthosite are conformable with the mylonitic wall rock. One 10–20 cm wide anorthosite lens exhibits flaser texture with clinopyroxene up to 3 cm in length. The unstrained contact and low-strain state of the anorthosite relative to the surrounding ultramylonite suggests that the anorthosite represents a dyke or sill that was emplaced late with respect to deformation. At one locality along the southern contact, an approximately 5 m wide anorthosite body crosscuts the straight gneiss wall rocks, although the contact is not exposed.

*__Figure 3.__ Gabbroic anorthosite showing good flaser texture. Note the attenuation of the mafic bands, consisting of clinopyroxene rimmed by hornblende.*

### *Mafic dykes*

The anorthosite suite is intruded by fine-grained, black, mafic dykes that are typically 1–5 m thick, and are thickest in the southern and central parts of the anorthosite where they may be up to 40–50 m thick. The northern part of the anorthosite is characterized by thinner (5–30 cm) dykes that are interpreted to be highly attenuated (Fig. 4).

The dykes are highly strained and have been metamorphosed under granulite facies. They exhibit a strong fabric parallel to their contacts and to the host rock fabric. The granulite-facies assemblage garnet-clinopyroxene is preserved in most dykes, with local evidence for late garnet growth with respect to deformation. Retrograde development of hornblende-plagioclase is pervasive, with common plagioclase moats around garnet, especially toward the west and in the north. Locally, millimetre-scale tonalite veins are present within the dykes to the north and in the west.

## SOUTHERN WALL ROCKS

### *Diorite*

A homogeneous green-grey- to buff-weathering, clinopyroxene-plagioclase rock, interpreted to be derived from diorite, occurs immediately south of the anorthosite. Although the diorite is dominantly straight layered and ultramylonitic, a small proportion is somewhat less deformed. Locally, igneous textures are preserved in low-strain pods.

*__Figure 4.__ Narrow (centimetre- to tens of centimetre-scale), mafic dykes cutting the anorthosite toward the northern part of the anorthosite complex. These dykes are interpreted to have been highly attenuated along with the anorthosite, whereas wider dykes to the south appear to be less deformed.*

The diorite is intercalated with sheets of quartzofeldspathic, garnet-bearing gneiss, amphibolite, and a noritic rock which may be related to the anorthosite. The thickness of the diorite is highly variable, ranging from tens of metres to hundreds of metres in thickness, possibly due to a map-scale boudinage.

## *Quartzofeldspathic garnet-gneiss*

A cream- to buff-weathering, garnet-bearing, quartzofeldspathic gneiss comprises a relatively thick (about 500 m) sequence south of the diorite. This unit is characterized by a pockmarked surface caused by garnets that have weathered out of the rock. The gneiss exhibits considerable variation in composition and is locally garnet free. While most layers contain biotite after garnet, others retain 4–5 mm, pink to lavender, unaltered garnets. Most of the unit is ultramylonitic but a decreasing strain gradient can be tracked towards its southern margin.

This unit is intercalated with a variety of lithologies. Mafic rocks within this unit range from tens of centimetres up to several metres in width, and typically contain the granulite assemblage clinopyroxene-garnet with subordinate plagioclase. Although most are very fine grained, some coarser grained, more plagioclase-rich pockets within laterally continuous horizons contain coronitic garnets around the clinopyroxene. These rocks commonly exhibit a strong fabric parallel to their margins and are conformable with the surrounding quartzofeldspathic gneiss.

Leuconorite with variable grain size also occurs within the gneiss. The more leucocratic varieties contain larger (up to 1.5 cm), flaser-textured orthopyroxene crystals, and about 65–70% plagioclase. Finer grained varieties typically contain a higher proportion of smaller orthopyroxene crystals (up to 5 mm), and about 40–45% plagioclase. Although the relationship between the norite and the quartzofeldspathic gneiss is generally not clear, at one locality where deformation is less intense, the norite crosscuts the quartzofeldspathic gneiss. Petrological work will investigate whether this intrusive, plagioclase-rich rock is related to the main anorthosite body.

## *Tonalite orthogneiss*

The tonalite orthogneiss is well banded and clinopyroxene bearing with abundant concordant and locally crosscutting pyroxenite dykes (Fig. 5). The banding is on the scale of tens of centimetres and reflects variation in proportion of clinopyroxene as well as the transposition of dykes. Pyroxenite layers are generally laterally continuous and 10–30 cm in thickness, but are locally boudined. Pyroxenite boudins are locally altered to amphibole and possibly talc. This map unit is characterized by abundant inclusions of supracrustal rocks and common east-trending, clinopyroxene-garnet gabbroic dykes which are locally boudinaged.

The northern portion of this unit contains inclusions of a garnet-bearing, quartzofeldspathic rock which locally contains tourmaline. These inclusions, interpreted as xenoliths, are similar in appearance to the garnet-bearing, quartzofeldspathic gneiss and provide evidence for an intrusive contact between the tonalite and the quartzofeldspathic unit to the north. The presence of tourmaline suggests a derivation of the quartzofeldspathic unit from a sedimentary protolith.

***Figure 5.** A relatively late pyroxenite dyke that crosscuts folding in granulite-facies tonalite orthogneiss.*

Within the tonalite orthogneiss, a range of sedimentary lithologies comprise a 10–30 m thick sequence which was observed at three different locations across strike. These include a brown-to beige-weathering, layered, tremolite- and magnetite-bearing carbonate iron-formation (about 5 m), a plagioclase-rich, tremolite calc-silicate with minor magnetite, quartzite (5–10 cm), and a dark brown to grey, tourmaline-bearing garnet-biotite-pelite. Lenses of leuconorite (up to metre-scale), amphibolite, and 1–3 m wide pyroxenite dykes, locally altered to amphibolite, are also present.

## *Tonalite*

A foliated, medium-grained, biotite-tonalite with abundant inclusions of amphibolite and semipelite lies immediately south of the tonalite orthogneiss. In contrast to the tonalite orthogneiss, this tonalite appears significantly less strained, does not include the same supracrustal assemblage, and is not cut by east-trending, garnet-clinopyroxene, mafic dykes. This is a biotite-bearing, medium-grained, grey to white tonalite with amphibolite rafts that range up to 50–100 m in thickness. A 100 m thick sequence of plagioclase porphyroblastic, garnet-biotite semipelite occurs at the northern margin of the unit. Some metre-scale rafts of similar material are present farther south, but become less abundant as amphibolite rafts become more voluminous. Rafts of amphibolite are common throughout this map unit but become thinner and less voluminous farther south along the shore of the inlet.

The southernmost part of the tonalite is essentially devoid of inclusions, with the exception of thin wisps of amphibolite. It is cut by veins of monzogranite with potassium feldspar porphyroblasts that are locally completely separated from the veins within which they were injected. The tonalite is cut by a white, coarse-grained tonalite. The late tonalite is coarse grained, white, and locally contains hornblende xenocrysts which may have been mechanically assimilated from amphibolite inclusions.

Gabbro dykes, sills, and pods intrude the tonalite in the southern part of the map unit but were not seen in the tonalitic orthogneiss or any other rock unit. The dykes trend 240–245°, range from 10 to 30 m in thickness, and the foliation in the surrounding tonalite appears to deflect around them. They are coarse grained, consist of clinopyroxene and plagioclase, and locally contain coronitic garnets.

## NORTHERN WALL ROCKS

### *Intermediate to mafic volcanic rocks*

A sequence of grey-weathering, intermediate arenite and amphibolite lies immediately north of the anorthosite. The intermediate rocks are well layered and consist predominantly of plagioclase-biotite-hornblende and epidote. They are characterized by subhedral plagioclase crystals up to 5 mm in diameter and a fine-grained matrix of hornblende-plagioclase with abundant, randomly oriented, euhedral plagioclase laths. These are interpreted to be of volcanic origin based on their composition, centimetre-scale layering, and local plagioclase porphyritic horizons. The mafic rocks within this map unit include banded and locally biotitized amphibolite that is intercalated with the intermediate rocks. Peak metamorphic grade within these rocks is difficult to assess in the field due to the pervasive formation of retrograde biotite.

Injection of medium- to coarse-grained, white tonalite veins is ubiquitous in this map unit. The volume of tonalite increases to the north and grades into the adjacent map unit. Monzogranite is present in veins and commonly displays a protomylonitic fabric. A 10–15 m thick panel of quartzofeldspathic, garnet-bearing gneiss, comparable to the quartzofeldspathic garnet-gneiss south of the anorthosite, is also present north of the anorthosite, but was only observed at one locality. A 20–40 m thick sheet of well-banded intermediate gneiss is also included in this unit. A low-strain pod displaying compositional layering between plagioclase-rich and clinopyroxene-rich layers (*see* Fig. 11) facilitated identification of this rock as diorite, but elsewhere, it is mylonitic and resembles the diorite found south of the anorthosite.

### *Mafic granulite-grade rocks and tonalite*

Towards the northern limit of the intermediate to mafic volcanic unit (Fig. 2), tonalite-granodiorite intrusions are more abundant while the volcanic component decreases and forms rafts of supracrustal rocks within the granitoid rocks. The mapped contact marks the position where the proportion of granitoid rocks exceeds that of the supracrustal rocks. No intermediate volcanic rocks were observed north of the contact with the granitoid rocks and the mafic component is a highly biotitized amphibolite. These screens become less common farther north (<20%) where fine- to medium-grained, green-weathering, mafic granulite rocks are included within, injected by, and locally brecciated by the granitoid rocks (Fig. 6).

The granitoid body ranges from granodiorite to tonalite in composition. In the north, tonalite contains large (tens of metres to 200 m) inclusions of granulite-grade, mafic rocks which are locally intruded by an orthopyroxene-bearing diorite or leuconorite that contains sparse coronitic garnet. Biotitized amphibolite rafts are present only locally in this northern domain where mafic granulite inclusions are prevalent. To the south, granodiorite is biotite bearing and contains coarse (1–2 cm) alkali feldspar phenocrysts and randomly oriented biotitized amphibolite inclusions which range from several metres to 2–3 cm in width.

The granulite-grade mafic rocks are green weathering and exist in two main varieties, a fine-grained clinopyroxene-garnet±plagioclase gabbro and a medium-grained pyroxenite. Compositional banding, at 2–3 cm scale, defined by variable plagioclase content, is present locally. Pyroxenite plugs (up to 25 m wide) may represent boudinaged dykes, or may be small stocks. The association of homogeneous, fine-grained mafic rocks with subordinate, layered, mafic rocks resembles a mafic volcanic sequence with the pyroxenite representing dykes or sills.

The granulite-grade mafic rocks in the northern part of the map area are likely xenoliths within the surrounding tonalite, although they may be genetically related to a large mafic granulite region to the northwest (Tella et al., 1993). They have a fabric that is discordant between adjacent blocks and with the surrounding tonalite. The foliation in the tonalite wraps around the large (50–100 m thick), rigid xenoliths, whereas smaller amphibolite inclusions have deformed within the tonalite. A strong L-tectonite fabric is exhibited by coarse-grained, granitic injections that brecciate the mafic rocks. The granite veins are locally foliated at their margins. An L>S fabric is also exhibited by the tonalite away from the mafic xenoliths. A well developed, down-dip lineation is ubiquitous in these rocks.

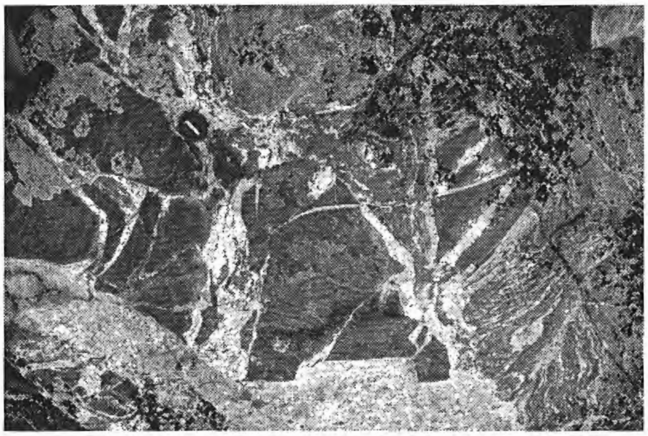

***Figure 6.** Agmatite consisting of coarse- to medium-grained granite with foliated margins injected into and brecciating fine-grained, mafic, granulite-grade rocks.*

## STRUCTURAL OBSERVATIONS

### *Planar and linear fabrics*

Fabrics exhibited by rocks within the Uvauk complex are defined by well developed ribbons as most of the rocks are mylonitic to ultramylonitic. Plagioclase ribbons are discernable in the anorthosite where ribbons of mafic minerals are also present but the cleaner, more plagioclase-pure anorthosite is commonly sugary and no clear foliation can be measured. The straight layering of the diorite and quartzofelspathic gneiss reflects the reduction in grain size that produced these ultramylonitic rocks. Quartz ribbons are common within the quartzofeldspathic garnet-gneiss and rare, minute quartz ribbons are present locally within the diorite.

The foliation within the anorthosite is east-striking and dips steeply to moderately to the south (Fig. 7a). Towards the north and east, foliations in the anorthosite and northern wall rocks strike east-northeast. In the southern wall rocks, foliations range from east-striking to more east-southeast to the east and southeast-trending towards the north shore of Chesterfield Inlet.

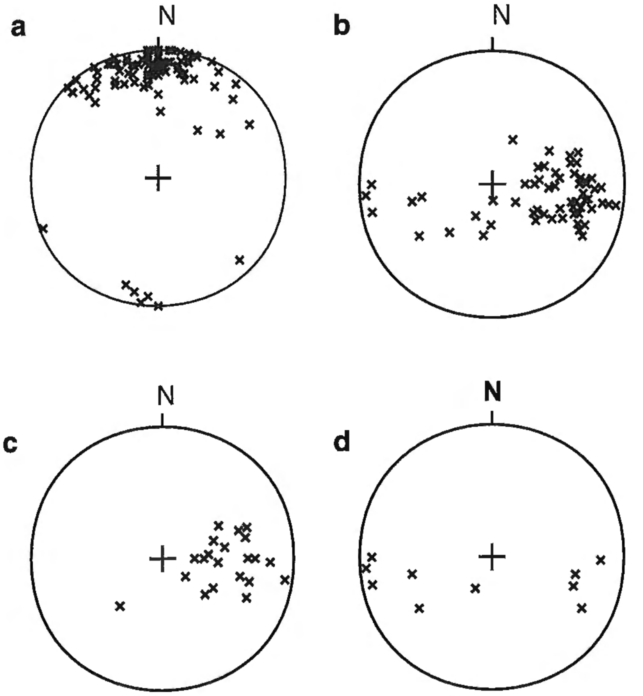


*Figure 7. Stereoplots illustrating various structural elements within the study area: **a**) poles to planes showing an overall steeply south-dipping foliation for the entire map area; **b**) lineations within the study area showing variation from shallow to moderately steep easterly plunge and a smaller number of west-plunging lineations; **c**) lineations taken within the anorthosite show a good cluster plunging moderately to the east; **d**) Variation from shallow, east-plunging to shallow, west-plunging lineations within the diorite unit, south of the anorthosite (see text for discussion).*

Extension lineations are well developed throughout the Uvauk complex and most commonly plunge east between 20°–40° (Fig. 7b, 8). Lineations within the anorthosite show a relatively tight, east-plunging cluster (Fig. 7c). Variation from this pattern is seen primarily along the southern margin of the anorthosite and the wall rocks to the south. In particular, shallowly west-plunging lineations are localized along a narrow belt, within the diorite, immediately south of the anorthosite. The diorite shows both shallow, east- and west-plunging lineations (Fig. 7d), possibly related to map-scale boudinage of this lithology (*see* Fig. 2). Alternatively, the diorite may have been exposed to a more protracted history of deformation with variations in flow through time, possibly related to polyphase deformation.

### *Shear-sense indicators*

Shear-sense indicators found south of the anorthosite include rotated feldspar (Fig. 9) and garnet porphyroblasts (Fig. 10), as well as boudins of amphibolite within tonalite orthogneiss, and composite shape fabrics in pelitic inclusions. A vast majority of all shear-sense indicators south of the anorthosite were delta porphyroblasts that indicate dextral sense of shear. Asymmetrical extensional shear bands occur in one locality in coarse-grained, monzogranitic intrusions within the tonalite near the shore to the south. Consistent dextral shear sense coupled with a shallow, east-plunging lineation suggests lateral displacement with a small component of north-side-down movement.

Although few shear-sense indicators were observed north of the anorthosite, all but one suggest sinistral shear along the northern margin. Shear-sense indicators within the

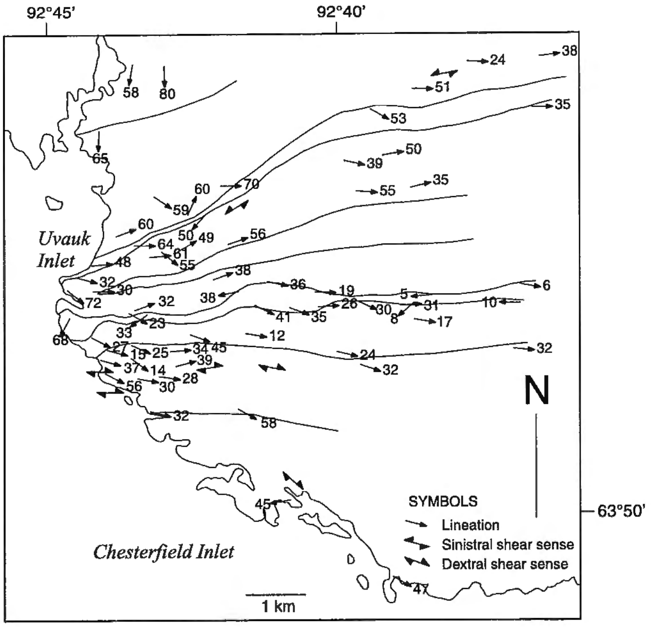


*Figure 8. Distribution of lineation measurements and shear-sense indicators within the study area (refer to Fig. 2 for lithological details).*

anorthosite and toward its northern margin include a sinistrally rotated, mafic dyke boudin, and an S-fold within the anorthosite. Sinistral shear sense related to the fold can be inferred here because the fold axis lies at a high angle to the mineral lineation. One dextrally rotated delta porphyroblast was noted at the northern margin of the western portion of the anorthosite where deformation is highly complex. However, much of the deformation in this part of the complex appears to be related to local rheological heterogeneities.

Sinistral shear sense was also determined in the 20–40 m wide sheet of diorite within the northern wall rocks. Modal layering displayed in a 3 m wide, low-strain pod is perpendicular to the east-northeast-striking, mylonite fabric displayed by the surrounding material (Fig. 11a). However, rotation of this fabric into the flow plane is interpreted to be a consequence of transposition of the mylonite fabric. The sigmoidal form of the banding in the low-strain pod appears to be due to rotation and attenuation of the enclosing foliation, reflecting anticlockwise rotation of the fabric into the flow plane (Fig. 11b).

### *Mafic dykes associated with anorthosite*

Deformation of the dykes is highly variable, and the differences in deformation style have been interpreted to reflect the extent of deformation, rather than rheological differences. Nearly all exhibit a penetrative fabric that is parallel to that in the anorthosite and parallel to the dyke margins. Many dykes display a strong mylonitic fabric and may be isoclinally folded with the anorthosite (Fig. 12a), and others are boudinaged. Despite the abundance of these features indicating early dyke emplacement relative to deformation, late emplacement of some dykes is indicated by preservation of bayonets on dyke margins (Fig. 12b) and rare examples of dykes truncating the mylonite fabric in the anorthosite at a low angle (Fig. 12c). One late dyke was observed to crosscut strongly deformed dykes within the anorthosite (Fig. 12d).

***Figure 9.*** *A rotated, delta-type, feldspar porphyroblast showing dextral shear sense within the southernmost part of the tonalite unit.*

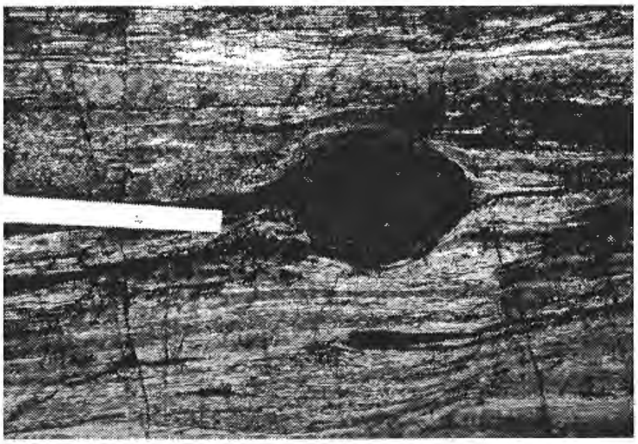

***Figure 10.*** *A large, rotated, delta-type, garnet porphyroblast showing dextral shear sense within the tonalite orthogneiss.*

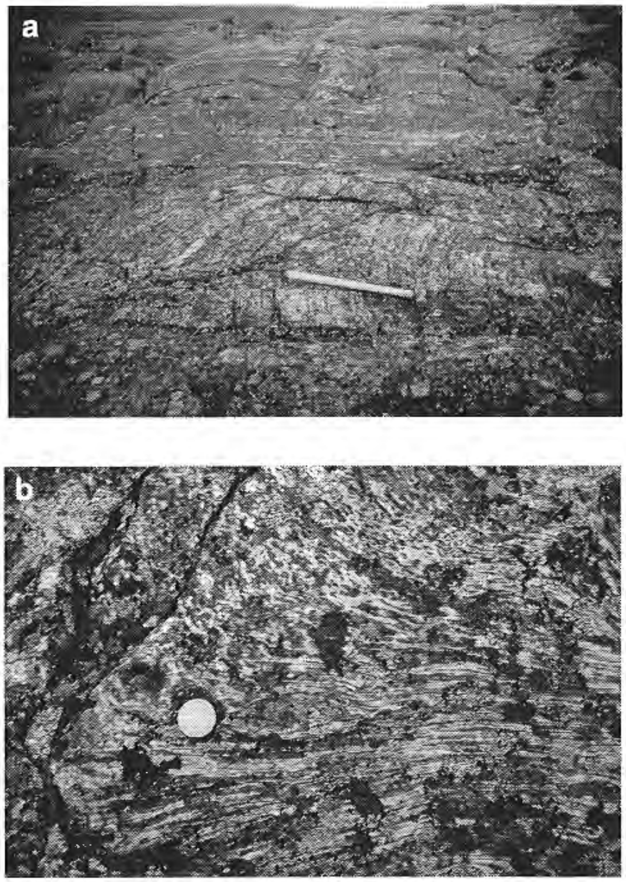


***Figure 11.*** *Sinistral shear sense inferred from low-strain, diorite pod north of anorthosite:* ***a****) modal layering in diorite pod (foreground) is perpendicular to surrounding mylonite fabric (parallel to hammer);* ***b****) primary modal layering of low-strain pod (upper part of photograph) is transposed into the flow plane (lower part of photograph) by progressive rotation and attenuation of its extremities.*

The variation in dyke deformation is, therefore, inferred to indicate synkinematic emplacement with respect to deformation.

## METAMORPHISM

Metamorphic grade within the Uvauk complex is dominantly granulite facies, but an amphibolite-facies overprint is pervasive within both the anorthosite and most of the wall rocks (Fig. 13). The diorite south of the anorthosite contains the granulite-facies assemblage garnet+clinopyroxene. Assessment of peak metamorphic grade of the quartzofeldspathic gneiss and tonalitic orthogneiss is difficult due to the lack of diagnostic metamorphic mineral assemblages and the presence of a retrograde metamorphic overprint. Granulite conditions may be indicated, however, by mafic horizons within the quartzofeldspathic gneiss that contain clinopyroxene+garnet, locally retrogressed to garnet-amphibolite or amphibolite.

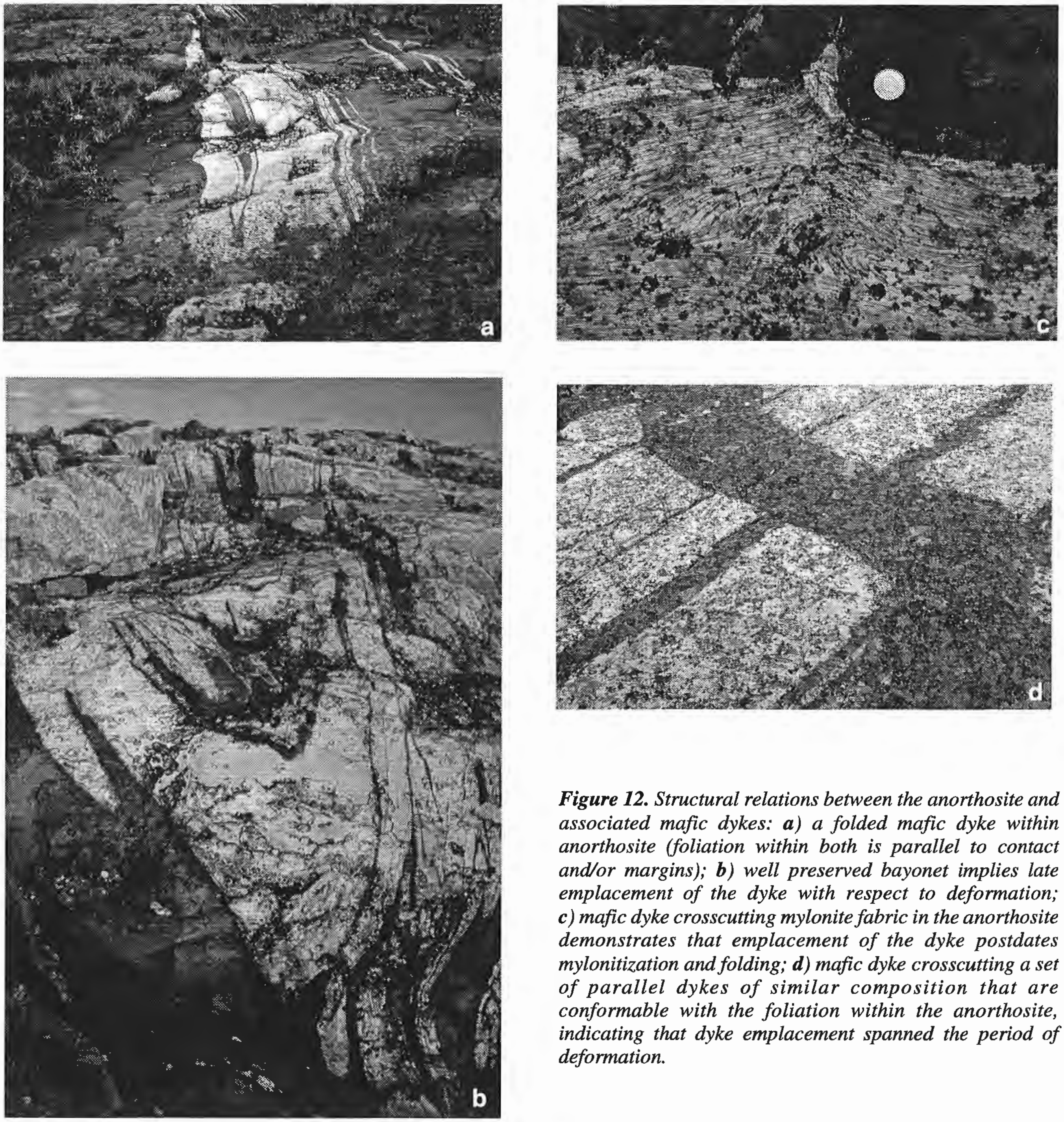

*Figure 12. Structural relations between the anorthosite and associated mafic dykes: **a**) a folded mafic dyke within anorthosite (foliation within both is parallel to contact and/or margins); **b**) well preserved bayonet implies late emplacement of the dyke with respect to deformation; **c**) mafic dyke crosscutting mylonite fabric in the anorthosite demonstrates that emplacement of the dyke postdates mylonitization and folding; **d**) mafic dyke crosscutting a set of parallel dykes of similar composition that are conformable with the foliation within the anorthosite, indicating that dyke emplacement spanned the period of deformation.*

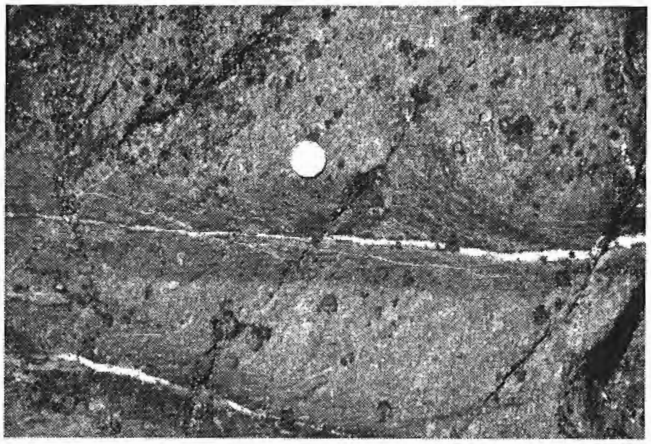

*Figure 13. Granulite to amphibolite retrogression indicated by amphibolite-grade assemblage proximal to a late quartzofeldspathic vein, with granulite-grade (clinopyroxene+ garnet) assemblage preserved farther from the vein.*

The wall rocks immediately north of the anorthosite are dominantly amphibolite grade, although, in the eastern part of the map area, garnet amphibolite appears to contain relict clinopyroxene that may indicate that granulite-facies conditions were attained. Farther north, granulite-grade, gabbroic rocks are common, and were mapped by Tella et al. (1993) as part of a much larger area of mafic granulite rocks within the Uvauk complex to the northwest.

## DISCUSSION

Detailed mapping of the west side of the Uvauk complex indicates that the anorthosite intrudes adjacent wall rocks, although subsequent deformation is evident. The progressive southward decrease in strain exhibited by the quartzofeldspathic garnet-gneiss provides evidence supporting an autochthonous origin for the mylonitized Uvauk complex. The current study has also revealed that the mafic layers within the anorthosite are dykes, and their spatial restriction within the anorthosite suggests that they may be genetically related to the anorthosite. Evidence from field relations suggests that the mafic dykes are synkinematic with respect to mylonitization and, if a petrogenetic link is established, then the anorthosite must also be synkinematic. Therefore, it is possible that mylonitization and metamorphism within the Uvauk complex are related to late synkinematic emplacement of the anorthosite and subsequent progressive deformation. In this scenario, the Archean age obtained by Tella et al. (1994a) would represent an older protolith for the wall rocks relative to the younger anorthosite.

Alternatively, the mylonitized wall rocks south of the anorthosite may represent an Archean shear zone that was reactivated during the Proterozoic. Differences in deformation state and metamorphic textures between the anorthosite and surrounding wall rocks suggest this possibility. The coarse-grained, gabbroic anorthosite along the southern margin of the anorthosite sheet exhibits the lowest strain fabrics of the entire suite. Juxtaposition of this lower strain intrusive material with ultramylonitic gneiss suggests that either the anorthosite was rheologically stiff relative to the wall rocks, or that this volume of anorthosite was emplaced late with respect to deformation, or that the wall rocks had undergone previous deformation. The last is consistent with Tella et al.'s (1994a) interpretation of the geochronological data. However, progressive deformation, beginning prior to anorthosite intrusion and continuing through dyke emplacement, is another possibility that cannot yet be ruled out.

The geometry of the anorthosite resembles a fold closure to the west. However, the most compelling evidence for folding comes from the presence of the marginal phase on both the north and south sides of the anorthosite sheet. The low-strain, gabbroic anorthosite in the core of the intrusion tapers and disappears to the west (Fig. 1), consistent with a fold geometry. Although, many isoclinal folds are displayed at the potential fold nose in the west, much of the deformation there is related to local heterogeneities within the deforming material and no fold closure is traced on the ground. Despite limited evidence for a regional-scale fold closure, it is clear that the rocks to the west have undergone the most intense deformation. Opposing shear sense north and south of the anorthosite implies that the anorthosite body has moved east relative to the wall rocks. The shallow lineation and limited metamorphic contrast across the wall rocks suggest minimal vertical displacement. The overall geometry of the anorthosite, kinematic indicators, and the increased intensity of strain displayed in the west are compatible with regional-scale boudinage of the anorthosite, with the most highly deformed rocks in the west representing the boudin neck.

## ACKNOWLEDGMENTS

The authors would like to thank Nancy MacDonald who consistently provided excellent assistance in the field; Sharon Carr and Subhas Tella for their help, advice, and constructive reviews of this manuscript; Gillian Royle for her cheerful and helpful assistance; and Hamish Sandeman for his suggestions, criticisms, and support.

## REFERENCES

**Gordon, T.M.**
1988: Precambrian geology of the Daly Bay area, District of Keewatin; Geological Survey of Canada, Memoir 422, 21 p.
**Gordon, T.M. and Lawton, D.C.**
1995: Geometry of the allochthonous Daly Bay Complex, Northwest Territories: a model constrained by geology and a three-dimensional gravity interpretation; Canadian Journal of Earth Sciences, v. 32, p. 1292–1302.

**Hoffman, P.F.**
1988: United plates of America, the birth of a craton: Early Proterozoic assembly and growth of Laurentia; Annual Review of Earth and Planetary Sciences, v. 16, p. 543–603.

**Sanborn-Barrie, M.**
1993: Structural investigation of high-grade rocks of the Kramanituar complex, Baker Lake area, Northwest Territories; *in* Current Research, Part C; Geological Survey of Canada, Paper 93-1C, p. 137–146.
1994: Structural investigation of high-grade rocks of the Kramanituar complex, Baker Lake area, Northwest Territories; *in* Current Research, 1994-C; Geological Survey of Canada, p. 121–133.

**Tella, S. and Annesley, I.R.**
1988: Hanbury Island Shear Zone, a deformed remnant of a ductile thrust, District of Keewatin, N.W.T.; *in* Current Research, Part C; Geological Survey of Canada, Paper 88-1C, p. 283–289.

**Tella, S. and Schau, M.**
1994: Geology, Gibson Lake east-half, District of Keewatin, Northwest Territories; Geological Survey of Canada, Open File 2737, scale 1:250 000.

**Tella, S., Roddick, J.C., and Schau, M.**
1994a: Geochronological constraints on the tectono-metamorphic history of the allochthonous Uvauk gabbro-anorthosite-granulite complexes, central Churchill Province, District of Keewatin, NWT, Canada, Geological Association of Canada-Mineralogical Association of Canada 1994, Programs with Abstracts, p. 111.

**Tella, S., Schau, M., Armitage, A.E., and Loney, B.C.**
1993: Precambrian geology and economic potential of the northeastern parts of Gibson Lake map area, District of Keewatin, Northwest Territories; *in* Current Research, Part C; Geological Survey of Canada, Paper 93-1C, p. 197–208.

**Tella, S., Schau, M., and Roddick, J.C.**
1994b: Significance of juxtaposed mid-crustal mylonite zones of contrasting ages, Uvauk complex, central Churchill Province, District of Keewatin, NWT, Canada; Abstracts and Programs, GSA Annual Meeting, Seattle Geological Society of America, v. 26, p. A-135.

---

Geological Survey of Canada Project 880014

# Precambrian geology, northern Angikuni Lake, and a transect across the Snowbird tectonic zone, western Angikuni Lake, Northwest Territories (Nunavut)[1]

Lawrence B. Aspler[2], Jeffrey R. Chiarenzelli[3], Brian L. Cousens[4] and David Valentino[5]

Continental Geoscience Division, Ottawa

*Aspler, L.B., Chiarenzelli, J.R., Cousens, B.L. and Valentino, D., 1999: Precambrian geology, northern Angikuni Lake, and a transect across the Snowbird tectonic zone, western Angikuni Lake, Northwest Territories (Nunavut);* in *Current Research 1999-C; Geological Survey of Canada, p. 107–118.*

**Abstract:** Greenschist-grade remnants of 2.68 Ga volcanic, siliciclastic, and carbonate sequences were deposited in shallow water on transitional or continental crust. Tholeiitic major-element trends, MORB-like trace-element patterns with signatures of crustal contamination, and mostly positive $\varepsilon_{nd}t$ values suggest back-arc basin or continental-rift deposition. Granitic to gabbroic gneiss complexes disrupt supracrustal domains. Geochemical and isotopic data suggest upper-mantle derivation of the gabbro, and granite production by crustal melting, presumably during 2.61 Ga intracontinental lithospheric shearing. Amphibolite-grade mylonitic rocks and younger greenschist-grade cataclasites, distributed throughout western Angikuni Lake, continue across the geophysically defined Snowbird tectonic zone. High- and low-grade tectonism, and changes in structural level between Archean domains occurred before Christopher Island volcanism (ca. 1.83 Ga). The Angikuni Formation (conglomerate, arkose, semipelite) reflects continental sedimentation in an isolated fault-bounded trough tilted before the onset of Christopher Island volcanism. It is probably tectonostratigraphically equivalent to the South Channel and Kazan formations in southern Baker Lake Basin.

**Résumé :** Des restes métamorphisées au faciès des schistes verts de successions volcaniques, silicoclastiques et carbonatées de 2,68 Ga ont été déposés en eau peu profonde sur une croûte continentale ou de transition. Les tendances des éléments majeurs tholéiitiques, la configuration des éléments traces qui rappelle le basalte de dorsale médio-océanique et présente des signatures de contamination crustale, et les valeurs $\varepsilon_{nd}t$ presque toutes positives suggèrent une accumulation dans un bassin d'arrière-arc ou un rift continental. Des complexes de gneiss granitiques à gabbroïques recoupent les domaines supracrustaux. Les données géochimiques et isotopiques indiqueraient que les gabbros proviennent du manteau supérieur et que les granites se sont formés par fusion de la croûte, vraisemblablement au cours du cisaillement lithospérique intracontinental de 2,61 Ga. Des roches mylonitiques du faciès des amphibolites et des roches cataclastiques plus jeunes du faciès des schistes sont réparties dans toute la partie occidentale du lac Angikun et se prolongent dans l'ensemble la zone tectonique de Snowbird, qui a été définie géophysiquement. Des événements tectoniques de haute et de basse intensité et des modifications dans le niveau structural entre les domaines de l'Archéen ont eu lieu avant le volcanisme dont a été l'objet l'île Christopher (vers 1,83 Ga). La Formation d'Angikuni (conglomérat, arkose, semipélite) traduit une sédimentation continentale dans une dépression isolée, limitée par des failles, qui a été basculée avant que ne commence le volcanisme dans l'île Christopher. Elle est probablement le pendant tectonostratigraphique des formations de South Channel et de Kazan dans la partie sud du bassin de Baker Lake.

---

[1] Contribution to the Western Churchill NATMAP Project

[2] 23 Newton Street, Ottawa, Ontario K1S 2S6
[3] Environmental Research Center, State University of New York at Oswego, Oswego, New York, U.S.A. 13126
[4] Department of Earth Sciences, Carleton University, Ottawa, Ontario K1S 5B6
[5] Department of Earth Sciences, State University of New York at Oswego, Oswego, New York, U.S.A. 13126

## INTRODUCTION

A contribution to the Western Churchill NATMAP Project, this report summarizes results of studies in the Angikuni Lake area, near the western flank of the Hearne Province (Fig. 1). These studies build on reconnaissance work (Blake, 1980; Tella and Eade, 1985; Eade, 1986) and address 1) the depositional environments and tectonic settings of Neoarchean supracrustal rocks; 2) the record of Neoarchean and Paleoproterozoic plutonic, metamorphic, and structural events; 3) the significance of the boundary between the Hearne and Rae provinces (Snowbird tectonic zone); and 4) the stratigraphy and sedimentology of the lower Baker Lake Group (Paleoproterozoic).

Fieldwork in 1998 was focused in two areas. In northern Angikuni Lake (65 J/5), Neoarchean lithostructural domains I–IV are unconformably overlain by extensive Paleoproterozoic exposures that constitute the lower part of the Baker Lake Group (Angikuni and Christopher Island formations; Fig. 2). In western Angikuni Lake, amphibolite-grade mylonitic rocks, previously mapped to the south and east, continue across the geophysically defined Snowbird tectonic zone, but are cut by younger zones of greenschist-facies cataclasite (Fig. 3). Geochemical and Sm/Nd isotopic studies were centered on domains I–III in southern and northern Angikuni Lake (Fig. 4; Cousens, 1998).

## NORTHERN ANGIKUNI LAKE: NEOARCHEAN LITHOSTRUCTURAL DOMAINS

Neoarchean structural domains I–V, defined and described in more detail elsewhere (Aspler et al., 1998a) extend into the northern Angikuni Lake area (Fig. 2). Domain I consists of predominantly greenschist- to amphibolite-grade mafic volcanic rocks, including amygdaloidal subaqueous sheet flows, pillow lava, and tuff. Within the volcanic rocks is a thin lens consisting of three shallow-water components: cross-stratified, carbonate-cemented arkose; polymictic, framework-intact conglomerate (with mafic volcanic, felsic volcanic, and sparse granitic clasts); and microbial laminated dolostone.

The boundary between domains I and II is an approximately 0.5 km wide, near-vertical, upper-amphibolite-grade, mylonitic shear zone. Mineral and stretching lineations plunge shallowly (5–15°) and shear-sense indicators are consistently dextral. A suite of syntectonic intrusive bodies, ranging in composition from gabbro to granite, contain the mylonitic fabric and are transposed along the shear zone, but are also locally discordant. Domain II is a complex of upper-amphibolite- to granulite-grade (Eade, 1986) granite, gabbro, orthogneiss, and paragneiss. Supracrustal gneiss bodies, the oldest components of domain II, range in size from mappable

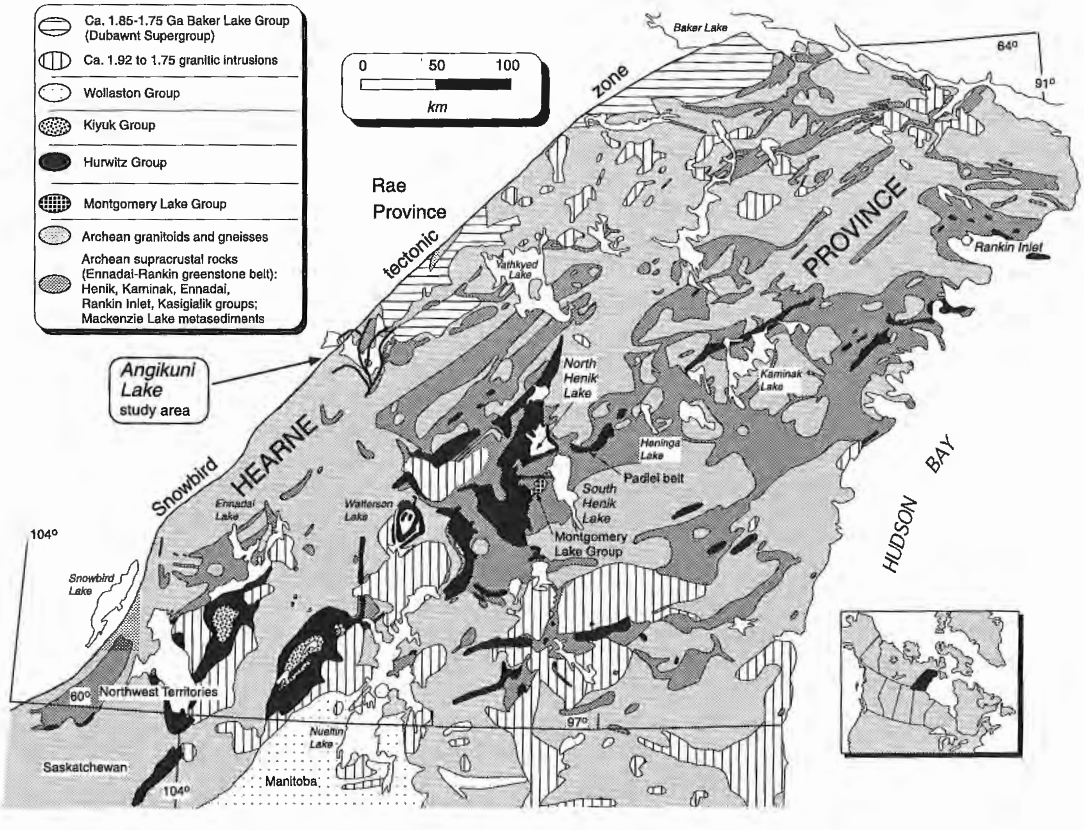


*__Figure 1.__ Location of study area, generalized geology of the Hearne Province, Northwest Territories (simplified after Aspler and Chiarenzelli, 1996).*

screens, to metre-scale layers, to partially assimilated xenoliths. Granitic orthogneiss outcrops throughout this domain, and coarse-grained granite forms map-scale lozenges that are enveloped by anastomosing zones of gneiss. The granites crosscut gneiss, but also contain mylonitic and protomylonitic fabrics and hence are syntectonic. One such granite, sampled close to the shear zone between domains I and II, has yielded a preliminary U-Pb zircon age of ca. 2.61 Ga (W. Davis, unpub. data, 1997). Most outcrops of domain II are cut by variably deformed, metamorphosed, and oriented gabbroic dykes. Although the gabbros cut layering in host gneiss and granite, they commonly contain an internal fabric, and are locally transposed into the gneissic layering. In addition, they are cut by leucosomal pods injected from the host gneiss, and mylonitized equivalents occur within the shear zone that separates domains I and II. Thus, the gabbros are considered syntectonic.

In contrast to the straight mylonite zone separating domains I and II, the boundary between domain II and domain III is marked by short fault segments with north, northwest, and northeast trends. Some of these faults define near-vertical zones of greenschist-facies, granitic cataclasite. Similar zones are also found within both domains. Two unconformity-bounded(?) sequences are exposed in domain III. The lower sequence consists of three subunits: 1) mafic to felsic volcanic rocks; 2) interbedded microbial laminates (locally stromatolitic), pelitic rocks and intermediate to felsic tuff units; and 3) mafic volcanic rocks. Interfingering of component rock types indicates that these subunits are conformable, but their stratigraphic order remains uncertain. Top indicators in the middle carbonate-pelite unit suggest that it overlies the mixed mafic-felsic volcanic unit and underlies the mafic volcanic unit. Loveridge et al. (1988) reported U-Pb zircon ages, from what we presume to be the lowest unit, of 2680 +29/-25 Ma (containing ca. 3.04 Ga xenocrystic zircon; Eade, 1986).

The upper sequence is exposed in the southwest corner of 65 J/5 and in the western and central parts of northern Angikuni Lake (Fig. 2). At the base of the upper sequence is a subunit of interlayered subarkose and framework-intact quartz-pebble conglomerate. Metre-scale mudstone interbeds are common. In view of the paucity of mudrocks in prevegetative continental deposits, mixing of mature arenites and conglomerates with mudstones suggests shallow-subaqueous, rather than subaerial, deposition. On a large island in the west-central part of northern Angikuni Lake, is a unique interval of iron-formation in which magnetite is concentrated at the top of centimetre- to decimetre-scale sandstone to pelite fining-upward sequences. Occurring within a sequence of relatively mature sandstone and conglomerate, this iron-formation was probably deposited in a shallow shelf (but below wave base) setting (*see* Eriksson et al., 1994, for other examples). A second unique interval, exposed on the southeast corner of the lake (Fig. 2), contains fine-grained sandstone, siltstone, and mudstone. Small-scale wave ripples (wavelength = 5 cm; height = 0.7 cm) and mudcracks signify shoaling to shallow-water and emergent conditions.

The conglomerate contains clasts reworked from older quartz-rich sandstones. Basal beds are pyritic and yield high nickel, chromium and vanadium, and detectable platinum and palladium values signifying erosion of an ultramafic source. This combination suggests derivation from quartz arenite–ultramafic sequences in the Rae Province such as the Prince Albert Group (e.g. Schau, 1997) or the Woodburn Group (e.g. Zaleski et al., 1997). In addition, Sm-Nd isotopic study of a mudrock interbed yielded an initial $\varepsilon_{Nd}t$ value of -2.0 ± 0.8 (assuming a depleted mantle $\varepsilon_{Nd}t$ value of +3 at 2680 Ma), suggesting that it includes detritus derived from significantly older (hundreds of Ma) crust. Tentatively, we interpret the lower contact of this subunit to be an unconformity because 1) the abrupt appearance of quartz-pebble conglomerate above mafic and felsic volcanic rocks requires a period of intense weathering; 2) the unit appears to cut out lower sequence stratigraphy; and 3) the unit appears to be distributed as outliers (Fig. 2; paleoflow infills(?)).

Domain IV consists of units of granite, granodiorite, and granitic gneiss containing rare enclaves of mafic volcanic rock. Domains IV and III are separated by a northeast-trending faulted/intrusive contact similar to the zones of granitic breccia that separate domains II and III. This contact is offset by northwest-trending cross faults which also contain zones of cataclastite. Both lithologies and northwest-trending fabrics in domain IV continue across the geophysical trace of the Snowbird tectonic zone. Along the southwest margin of 65 J/5, rocks of both domain III and domain IV are cut by a north-trending zone of cataclasite (Figs. 2, 3). This zone forms the eastern boundary to down-dip lineated gneiss units that constitute domain VI in western Angikuni Lake (*see* below).

## GEOCHEMISTRY OF DOMAINS I–III

Figure 4 summarizes geochemical and isotopic data from domains I–III (please refer to Cousens, 1998). Volcanic rocks from domains I and III range in composition from basalt to dacite. Together with gabbro from domain II, they plot within the tholeiitic field (Fig 4a). All three follow a tholeiitic fractionation trend in major-element chemistry (Fig. 4b).

Trace-element patterns (normalized to Primitive Mantle) for domain I mafic volcanic rocks (Fig. 4c), domain II gabbro (Fig. 4d) and domain III mafic volcanic rocks (Fig. 4e) are MORB-like (mid-ocean ridge basalt), but generally display greater abundances of Ba, Rb, and K (possibly due to post-eruptive metasomatism). Samples with light-REE-enriched patterns have the highest $SiO_2$ contents, and the magnitude of negative Nb anomalies increases as the patterns become more light-REE enriched. This suggests that evolution of the more felsic magmas was accompanied by increasing assimilation of granitic basement. In contrast to domain II gabbro, domain II granitic rocks exhibit strong enrichment in the light REEs and Th, strong depletion in the heavy REEs, and extremely large negative Nb/Ta anomalies (Fig. 4d), characteristic of crustal melts.

The $\varepsilon_{nd}t$ values range from +3.0 to -1.7 in domain I volcanic rocks, +3.8 to -2.6 in domain III volcanic rocks, and +3.8 to +1.0 in domain II gabbro (Fig. 4f). In lavas from domains I and III, $\varepsilon_{nd}t$ decreases with increasing $SiO_2$, indicating that isotopic variability is most likely due to contamination by older, unexposed continental crust. In domain II gabbro, $\varepsilon_{nd}t$ and $SiO_2$ are not strongly correlated, suggesting depleted mantle sources that may have been isotopically variable.

## WESTERN ANGIKUNI LAKE: A TRANSECT ACROSS THE SNOWBIRD TECTONIC ZONE

As defined by previous mapping in southern Angikuni Lake (Aspler et al., 1998a, b), domain V consists of well foliated magnetite-bearing granite, local granitic gneiss, and rare slivers of mafic volcanic rock (Fig. 3). The northern margin of domain V is a northwest-trending curvilinear shear zone which consists of interleaved, upper-amphibolite-grade, porphyroclastic gneiss, mylonitic granodiorite and gabbro, granodiorite gneiss, and foliated magnetite-bearing granite. In addition, discontinuous strips of greenschist-grade cataclasite occur along its length. The cataclasite is typically nonfoliated and consists of granitic and mylonitic fragments cut and separated by variably oriented, narrow (millimetre-scale and less), chloritic veinlets and irregular zones of pseudotachylite. The shear zone displays shallow to moderate northeast dips (15–60°) and a down-dip stretching direction defined by isoclinal fold hinges and mineral lineations. The primary goal of the 1998 transect was to trace this shear zone north and west, and to establish possible relationships to the Snowbird tectonic zone.

In western Angikuni Lake, the shear zone expands to a broad area of gneissic, mylonitic, and cataclastic rocks, herein specified as domain VI (Fig. 3). Domain VI forms the rim to a large north-plunging antiform that is cored by domain V and has an apparent down-plunge extent of at least 20 km (Fig. 3). The western limb of this antiform extends across the geophysically defined trace of the Snowbird tectonic zone. The predominant rock type in domain VI is granodioritic gneiss, and subunits generally lack adequate continuity to permit separation at a scale of 1:50 000. Subunits continuous from southern Angikuni Lake include porphyroclastic gneiss (Fig. 5), mylonitic granodiorite (Fig. 6), mylonitic gabbro, foliated magnetite-bearing granite, and cataclasite (Fig. 7). Mylonite, porphyroclastic gneiss, and cataclasite are dispersed as bands throughout domain VI and together constitute about 30% of the domain. Domain VI also contains garnet-hornblende mafic gneiss lenses, lamprophyric sills, migmatitic lenses, megacrystic granodiorite, and variably deformed bodies of granite, aplite, and pegmatite.

The antiform defined by domains V and VI is asymmetric. On the eastern flank and in the hinge region, extension lineations are down-dip. Shear-sense indicators are inconsistent and imply both north-side-up and north-side-down motion. At the outcrop and hand-specimen scales, congugate shear bands signify a component of progressive coaxial deformation. However, at the map scale, sigma and delta porphyroclasts

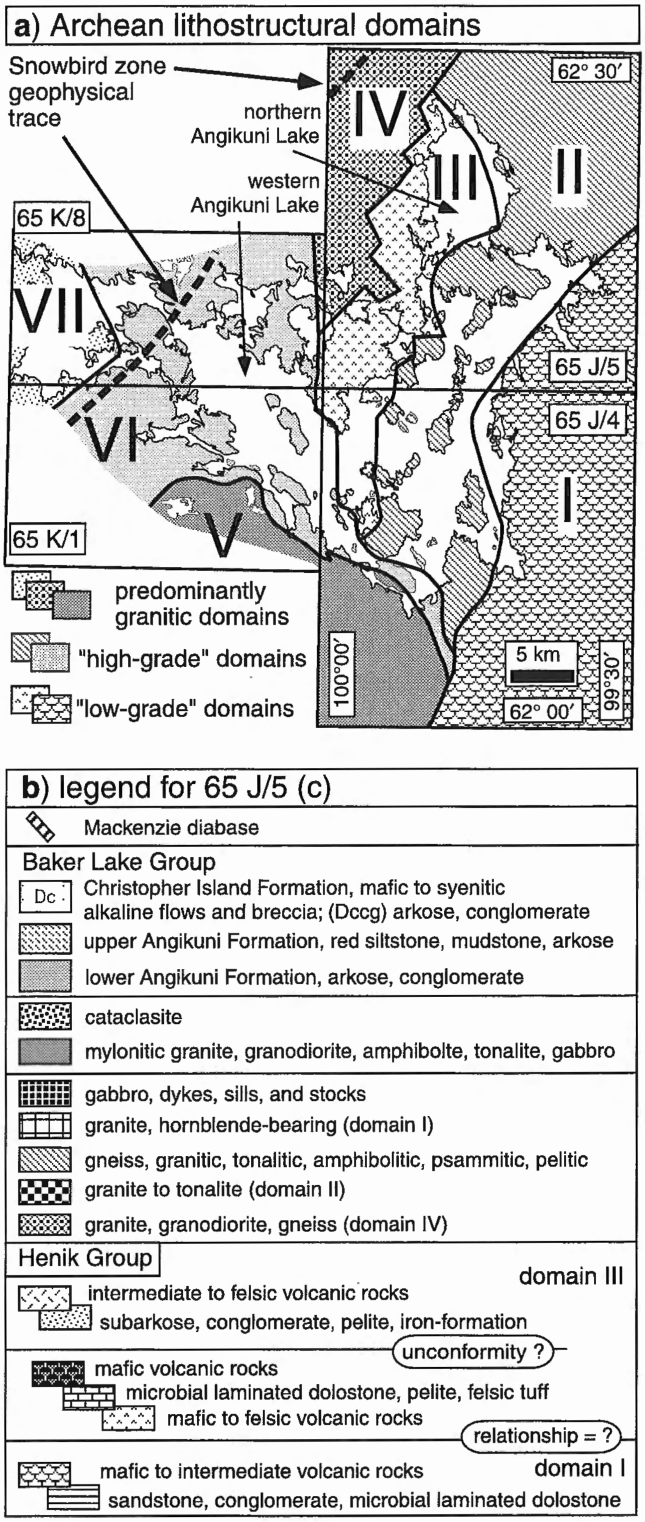


***Figure 2. a)** Neoarchean lithostructural domains, Angikuni Lake area. **b)** and **c)** Simplified geological map, northern Angikuni Lake area (65 J/5). Domain III geochronology from Loveridge et al. (1988); Domain II geochronology from W. Davis, (unpub. data, 1997).*

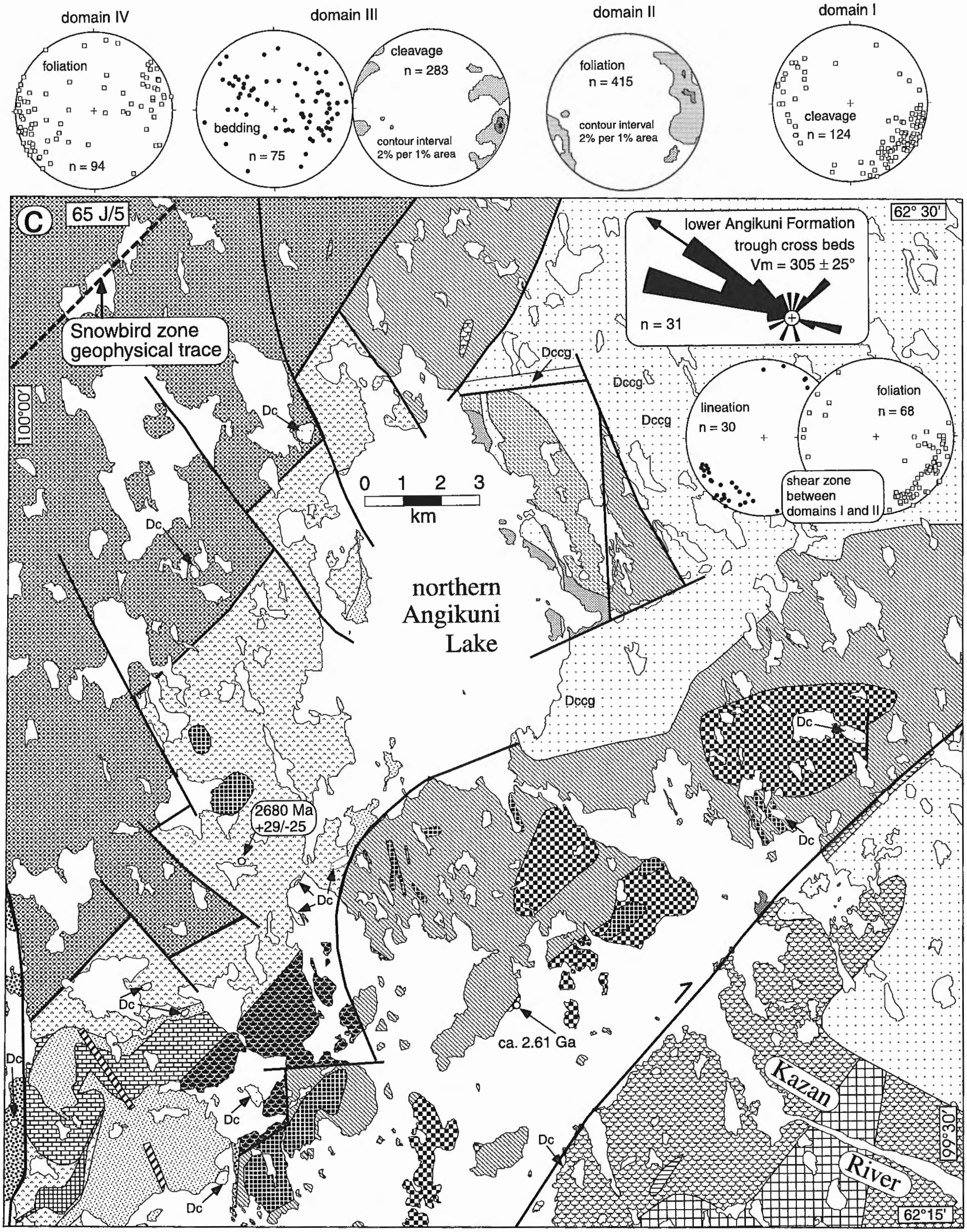
domain IV
foliation
n = 94
domain III
bedding
n = 75
cleavage
n = 283
contour interval
2% per 1% area
domain II
foliation
n = 415
contour interval
2% per 1% area
domain I
cleavage
n = 124
C
65 J/5
62° 30'
lower Angikuni Formation
trough cross beds
Vm = 305 ± 25°
n = 31
Snowbird zone
geophysical trace
100°00'
Dccg
lineation
n = 30
foliation
n = 68
shear zone
between
domains I and II
0 1 2 3
km
northern
Angikuni
Lake
Dc
2680 Ma
+29/-25
ca. 2.61 Ga
Kazan
River
99°30'
62°15'

*Figure 2c.*

and C-S fabrics also conflict (Fig. 3b) indicating strong flow partitioning. On the western flank of the antiform, extension lineations are strike-parallel. Again, shear-sense indicators conflict at the local (shear bands) and map scale (sigma and delta porphyroclasts, C-S fabrics), yielding both dextral-oblique and sinistral-oblique movement. The central part of the apical region contains small (1–3 km), late-syntectonic, granite plutons. Shallowly north-plunging L-tectonites occur on the western side of the apical zone. The western flank of the antiform is transected by a northeast-trending zone of greenschist-facies cataclasite up to 1 km wide. Strike-lineated amphibolite-grade mylonite and porphyroclastic gneiss continue west of this cataclasitic zone and contain opposing shear-sense indicators (sigma and delta porphyroclasts, C-S fabrics, shear bands, and asymmetric pull-aparts).

West of the cataclasitic zone, domain VI gneiss bodies are intruded by a body of megacrystic syenite to quartz syenite which contains potassium feldspar phenocrysts up to 10 cm. This body extends for about 8 km to the western shore of Angikuni Lake, and is defined herein as domain VII. Commonly massive or weakly foliated, the syenite also contains decimetre-scale zones with remarkably abrupt strain gradients that display transitions from weakly foliated rock to greenschist-grade, strike-lineated ultramylonite (Fig. 8). Again, at the map scale, sigma and delta porphyroclasts and C-S fabrics show both dextral and sinistral motion (Fig. 3b). Domain VII also contains lenses of strike-parallel (northeast-trending) and discordant (northwest-trending) cataclasite. The northern part of the domain VI–domain VII contact is marked by a wedge containing lenses of

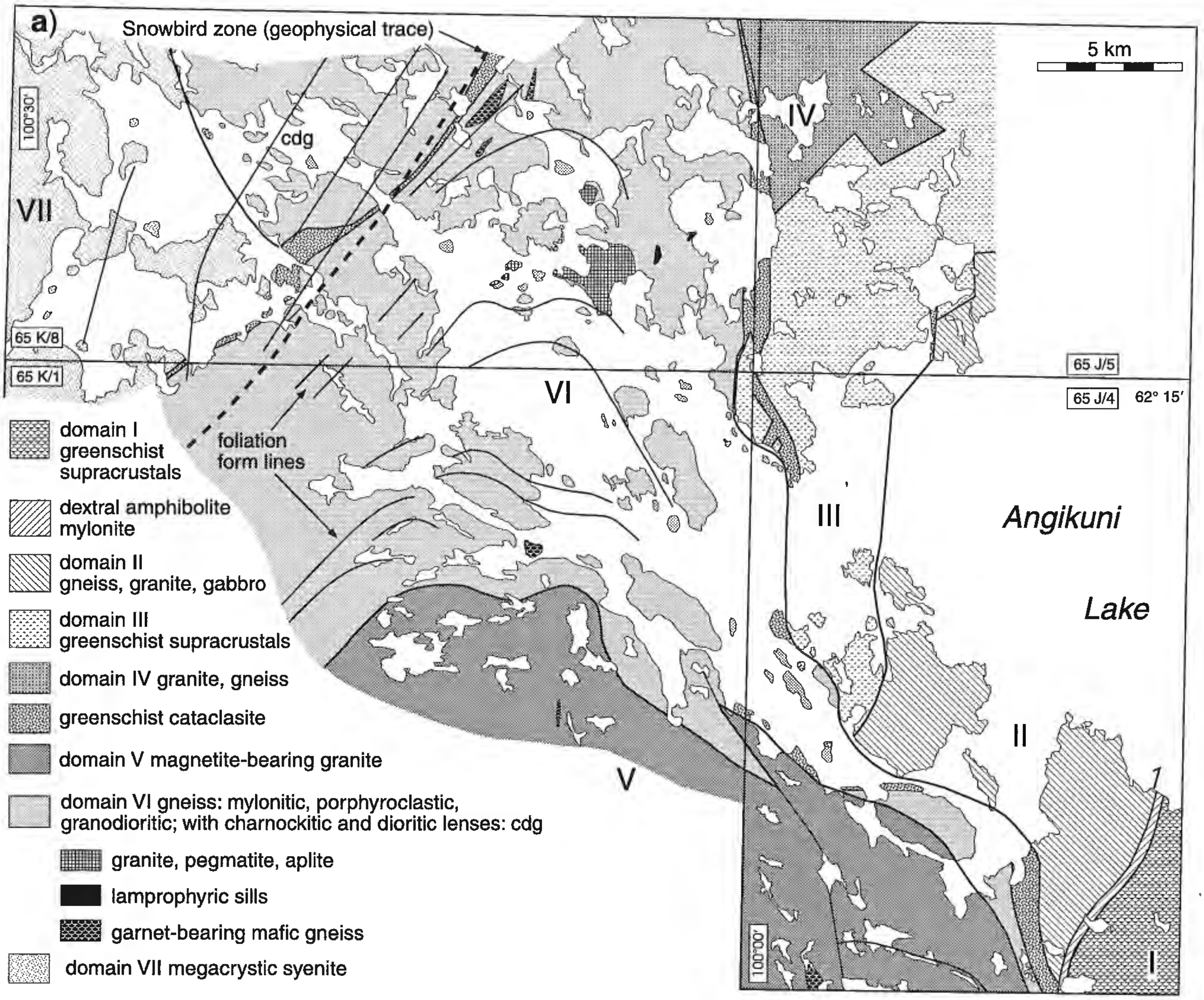


***Figure 3.** Simplified lithologic **a)** and structure **b)** maps, western Angikuni Lake.*

charnockitic and dioritic gneiss (cdg, Fig. 3a). Retaining igneous textures, these lenses likely represent border phases of the syenitic pluton.

If the Snowbird tectonic zone can be defined as a discrete geological entity at the latitude of Angikuni Lake, the kilometre-scale cataclasite belt would be an appropriate marker. However, because high-grade tectonite underlies much of western Angikuni Lake, low-grade cataclasite forms narrow strips throughout the area, and domain VI rocks extend across the geophysical trace of the Snowbird zone, we suggest that Snowbird-related strain is distributed heterogeneously to at least the eastern shores of Angikuni Lake. To explain interdomain geometric relationships and apparent differences in structural level, we tentatively suggest the following: 1) north-side-up movement of domain II relative to domains I and V, and north-side-up movement of domain VI relative to domain V (under upper amphibolite conditions); 2) dextral strike-slip between domains I and II (also under upper amphibolite conditions); and 3) down-dropping of domain III relative to domains II and IV, and partial reactivation of the high-grade tectonites along zones of cataclasite. The relative timing of greenschist-facies cataclasites and amphibolite-facies ductile mylonites is clear: the cataclasites consistently crosscut the higher grade tectonites. However, a major point of uncertainty is the absolute time interval separating the high- and low-grade 'events'. Do the cataclasites represent changes in strain rate and/or temperature during a single Archean event, or do they reflect significantly younger (Paleoproterozoic) rejuvenation? Rocks of the Baker Lake Group provide the only available constraint. All tectonites are

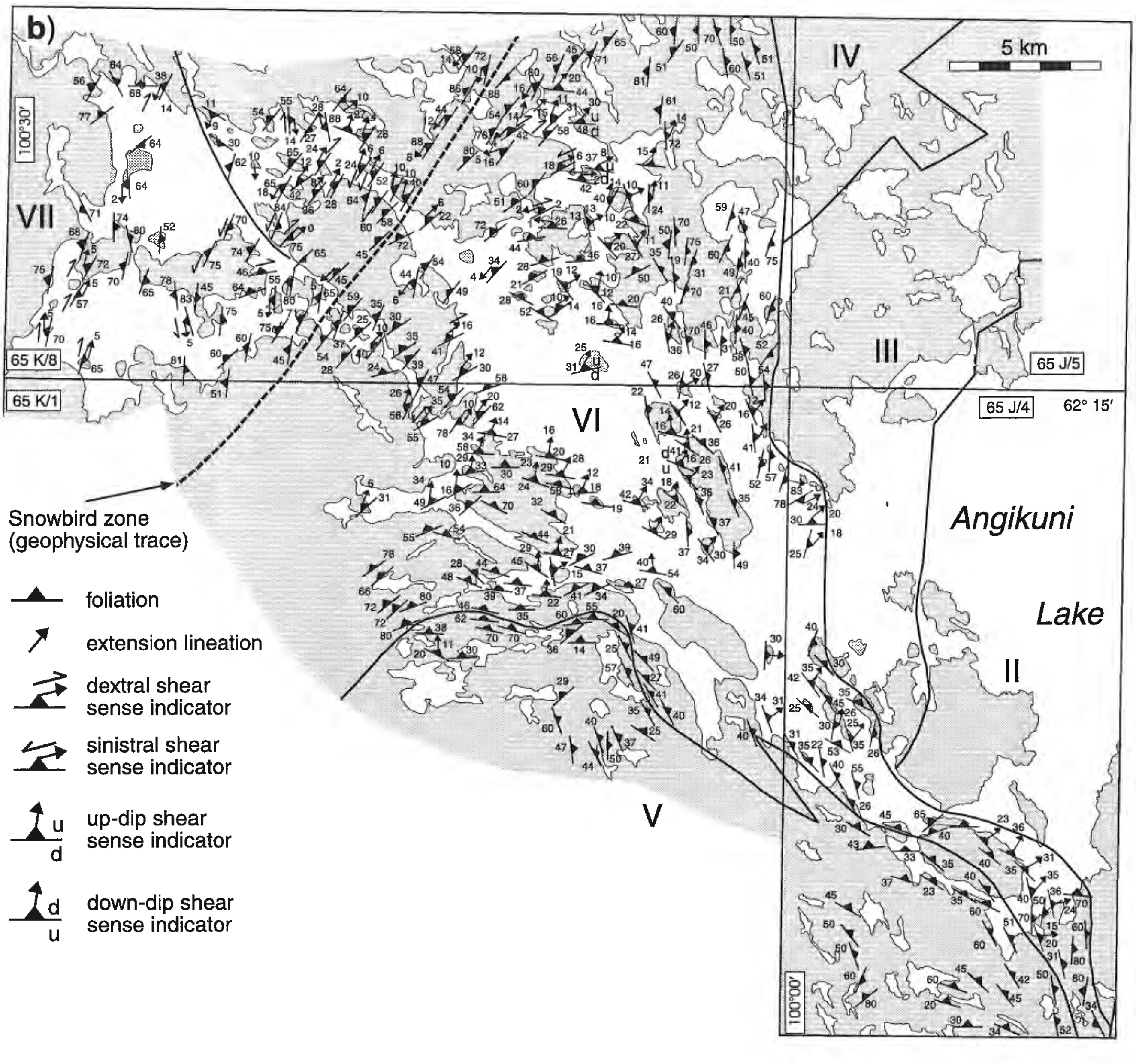


*Figure 3b.*

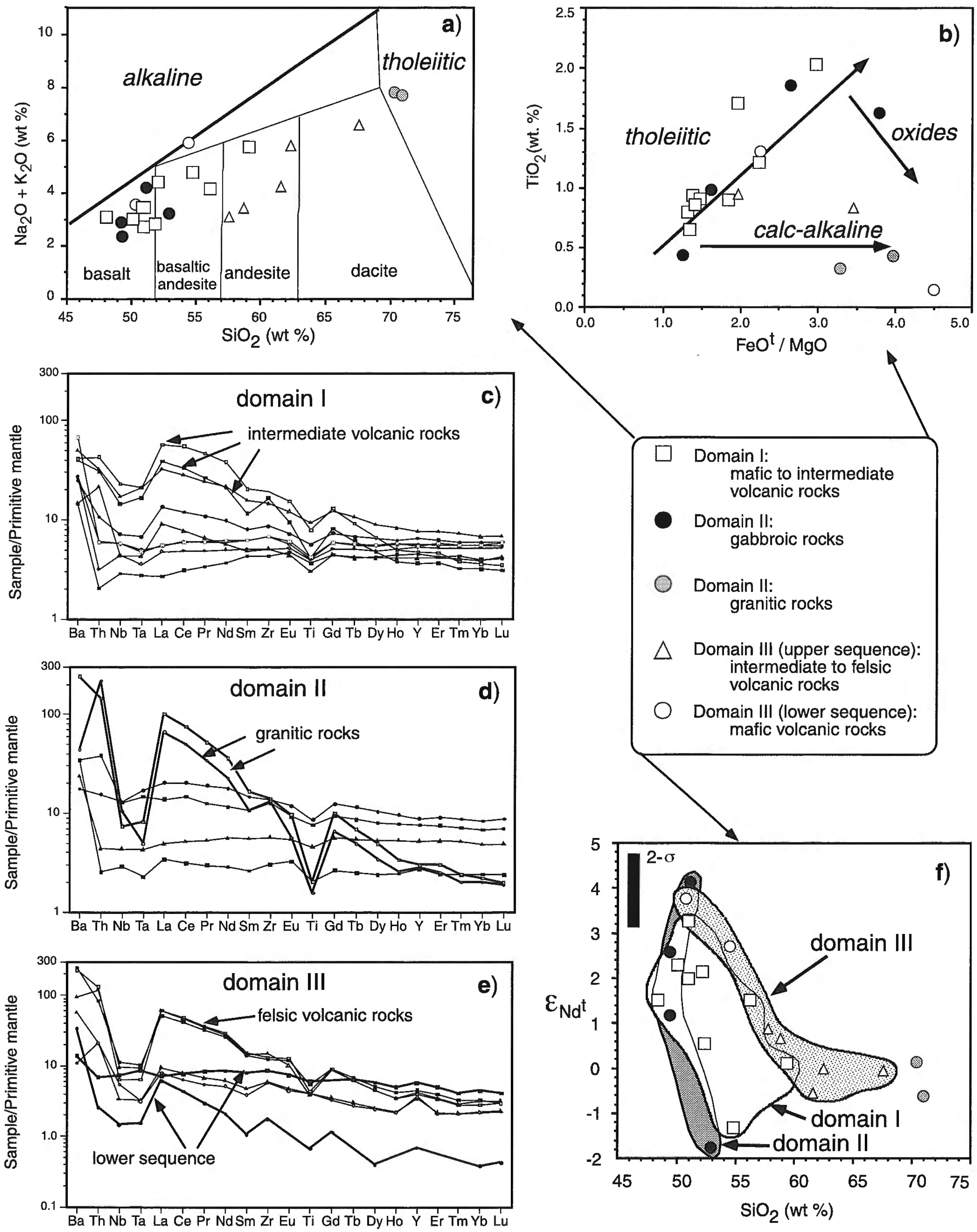

a)
alkaline
tholeiitic
basalt
basaltic andesite
andesite
dacite
$Na_2O + K_2O$ (wt %)
$SiO_2$ (wt %)
b)
tholeiitic
oxides
calc-alkaline
$TiO_2$ (wt. %)
$FeO^t$ / MgO
c)
domain I
intermediate volcanic rocks
Sample/Primitive mantle
Ba Th Nb Ta La Ce Pr Nd Sm Zr Eu Ti Gd Tb Dy Ho Y Er Tm Yb Lu
d)
domain II
granitic rocks
Sample/Primitive mantle
Ba Th Nb Ta La Ce Pr Nd Sm Zr Eu Ti Gd Tb Dy Ho Y Er Tm Yb Lu
e)
domain III
felsic volcanic rocks
lower sequence
Sample/Primitive mantle
Ba Th Nb Ta La Ce Pr Nd Sm Zr Eu Ti Gd Tb Dy Ho Y Er Tm Yb Lu
Domain I: mafic to intermediate volcanic rocks
Domain II: gabbroic rocks
Domain II: granitic rocks
Domain III (upper sequence): intermediate to felsic volcanic rocks
Domain III (lower sequence): mafic volcanic rocks
f)
2-σ
domain III
domain I
domain II
$\varepsilon_{Nd}t$
$SiO_2$ (wt %)

***Figure 4.*** *Geochemical and isotopic plots, domains I-III (please refer to Cousens, 1998).* ***a)*** *Classification of volcanic rocks in domains I and III using total alkalis vs. silica content (le Bas et al., 1986). The bold line distinguishes Hawaiian alkaline from tholeiitic lavas (Macdonald and Katsura, 1964).* ***b)*** *$TiO_2$ vs. FeO/MgO: domain I and III volcanic rocks and domain II gabbros follow the tholeiitic trend of $TiO_2$ enrichment as the magmas evolve, followed by late-stage depletion as titanomagnetite becomes a fractionating phase.* ***c), d),*** *and* ***e)*** *Abundances of incompatible elements normalized to primitive mantle (Sun and McDonough, 1989) for domains I, II, and III, respectively.* ***f)*** *$\varepsilon_{Nd}t$ vs. silica summary plot, where t = 2680 Ma for domains I and III (Loveridge et al., 1988) and T = 2610 Ma for domain II (W. Davis, unpub. data, 1997).*

***Figure 5.*** *Domain VI, porphyroclastic gneiss. Isoclinally folded leucocratic dykes are dismembered in a tonalitic host. Note hinge thickening and limb-thinning below pen.*

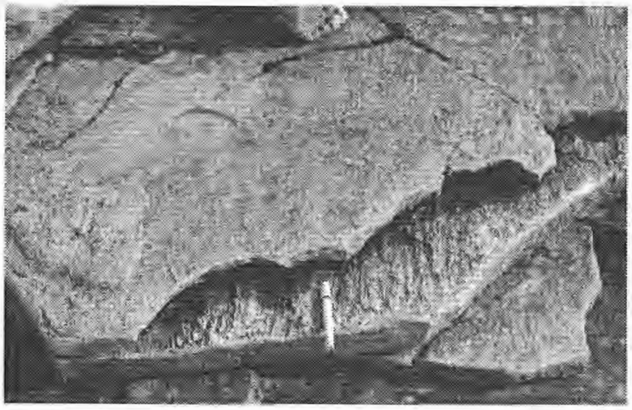

***Figure 6.*** *Domain VI, shallowly dipping granodioritic gneiss with down-dip stretching lineation.*

***Figure 7.*** *Domain VI, Granitic cataclasite. Crossed polarizers; width of photo is 5.5 mm.*

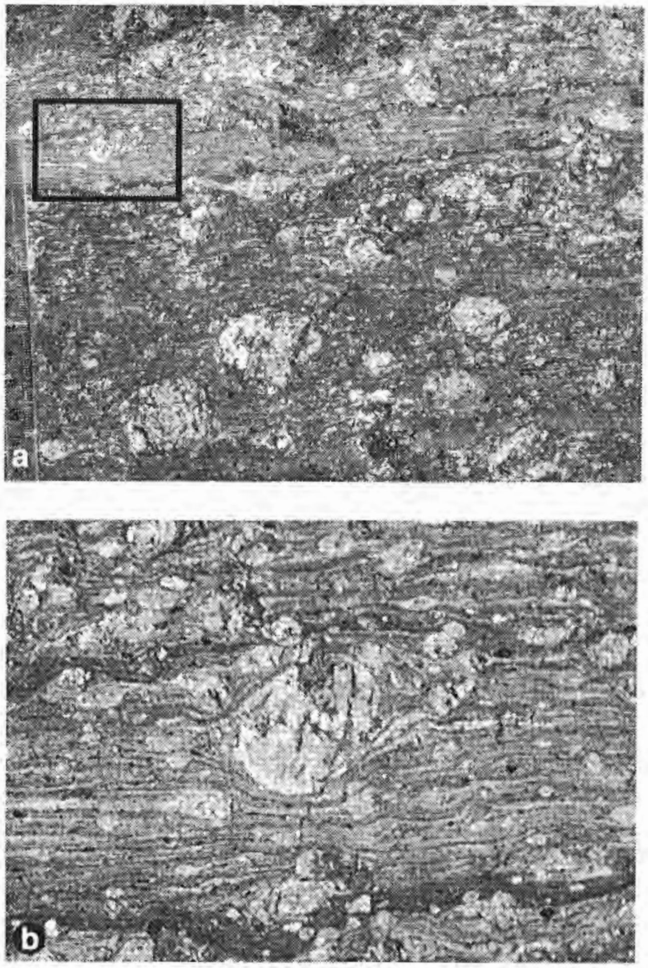

***Figure 8.*** ***a)*** *Domain VII, mylonitic shear zone in megacrystic quartz syenite.* ***b)*** *Close-up of ultramylonite in a) with delta porphyroclast indicating dextral shear.*

unconformably overlain by volcanic rocks of the Christopher Island Formation and are cut by related lamprophyric dykes. Hence, ductile deformation, cataclastic deformation, and changes in structural level between structural domains occurred before Christopher Island Formation magmatism. However current age estimates for Christopher Island Formation magmatism are imprecise: 1850 +30/-10 (U-Pb zircon, Tella et al. 1985); 1825 ± 12 Ma ($^{40}Ar/^{39}Ar$ hornblende, Roddick and Miller, 1994) and 1832 ± 28 Ma (Pb-Pb isochron, apatite, MacRae et al., 1996).

## BAKER LAKE GROUP

Continental siliciclastic and volcanogenic rocks of the Baker Lake Group (Dubawnt Supergroup, Gall et al., 1992) define two northeast-trending sub-basins in the northern Angikuni Lake area and form small outliers across the region (Fig. 2). In the central part of the northern sub-basin, a wedge of Angikuni Formation (Blake, 1980) outcrops unconformably between Archean basement and the Christopher Island Formation. The lower part of the Angikuni Formation consists of tan-coloured, carbonate-cemented, parallel and cross-stratified arkose with metre-scale interbeds of conglomerate and pebbly sandstone. Decimetre-scale trough crossbeds in arkose indicate northwest paleocurrents (Fig. 2).The conglomerate is clast supported and contains angular to subrounded gneissic and granitic clasts in a coarse-grained sand to granule matrix. The upper part of the Angikuni Formation consists of red siltstone, mudstone, and parallel-stratified, fine-grained sandstone, and contains abundant mudcracks, mudchip breccia layers, and wave ripple marks. These rocks were probably deposited in fluvial (lower part) and sand flat/playa (upper part) environments. An angular discordance between the Angikuni and Christopher Island formations is well exposed near the eastern shores of northern Angikuni Lake (Fig. 2). Shallowly (~10°) east-dipping Christopher Island mafic and felsic minette flows lie above steeply (~ 45°) east-dipping Angikuni strata, forming a tongue that cuts the lower-upper Angikuni Formation contact. The Angikuni Formation wedge at northern Angikuni Lake probably represents an isolated fault-bounded trough tilted before Christopher Island Formation flood volcanism.

Blake (1980) considered the Angikuni Formation to lie unconformably beneath the South Channel Formation, a thick, locally developed, basal fanglomerate unit defined from the eastern Baker Lake region (Donaldson, 1965; Rainbird et al., 1999). Immediately north of, and in fault-contact with, the Angikuni Formation is a strip of non-carbonate-cemented, framework-intact, polymictic conglomerate, granulestone, pebbly sandstone, and arkose that is conformably overlain by Christopher Island Formation flows and breccia (Dccg Fig. 2). Blake (1980) assigned this strip, as well as open-framework, polymictic cobble-conglomerate and cross-stratified red arkose to the south and east, to the South Channel Formation. However, because the latter are interlayered with volcanic flows on scales of 5–10 m, they are more appropriately interpreted as an integral part of the Christopher Island Formation, and we now consider that the strip of conglomerate is a basal Christopher Island lens (cf. Aspler et al., 1998a).

Blake (1980) also considered the Angikuni Formation to be restricted to its type area. However, the section at Angikuni Lake is remarkably similar to mudcracked and ripple-marked siltstone, mudstone, and fine-grained sandstone that outcrop beneath the Christopher Island Formation north of 'Rack Lake', approximately 25 km to the east (at about 62°27'N /99°00'W). Furthermore, Gall et al. (1992), emphasized the lithological similarities between the Angikuni Formation and the Kazan Formation (Donaldson, 1965), which outcrops beneath the Christopher Island Formation south of Baker Lake, and suggested abandoning the term 'Angikuni Formation'. We contend that the term is useful and should be retained as a local designator, but suggest that the Angikuni, South Channel, and Kazan formations are tectonostratigraphically equivalent. Together, these units represent variants of continental sedimentation in local fault-bounded depocentres before blanketing by the Christopher Island Formation.

Elsewhere in the northern sub-basin, and in the southern sub-basin, the Christopher Island Formation directly overlies basement. It consists of massive to layered phlogopite-bearing mafic and felsic minette flows, and volcanic breccia units containing intraformational volcanic clasts (with irregular margins and alteration rinds), local vesicular bombs and foliated basement pebbles, and rare accretionary lapilli interbeds. Minette dykes, likely feeders to the flows, occur throughout the region and display strong northeast trends. Local vent facies comprise beds containing up to 70% angular basement clasts (to 50 cm) interlayered with volcanic flows. Interbeds of cross-stratified red arkose and open-framework polymictic conglomerate (Dccg, Fig. 2) indicate fluvial sedimentation coeval with volcanism.

Beyond the limits of the two sub-basins, the Christopher Island Formation is exposed as scattered outliers, most of which are too small to represent on Figure 2. Volcanic flows coat the basement surface in these outliers, defining an exhumed paleotopography with a minimum relief of 25 m (*see also* Donaldson, 1965). With the exception of local sedimentary infilling of paleojoints, a paleoregolith is absent. The outliers are significant because they demonstrate that changes in structural level of Archean basement took place before Christopher Island Formation volcanism (*see* above) and that volcanic rocks once blanketed the entire region.

## SUMMARY AND DISCUSSION

Neoarchean supracrustal rocks in the Angikuni area were deposited in relatively shallow water, and provenance data indicate subaerial exposure of a continental hinterland at the time of sedimentation. Shallow-water rocks derived from a continental hinterland imply deposition on, or close to, continental crust. This is in contrast to the Henik Lakes region, in the central part of the Ennadai–Rankin greenstone belt, where shallow-water deposits are restricted to aprons surrounding felsic volcanic edifices in an ensimatic setting (e.g. Aspler et al., 1999). Furthermore, ca. 3.04 Ga xenocrystic zircon from a 2.68 Ga volcanic sample in domain III (Eade, 1986; Loveridge et al., 1988) suggests subjacent Mesoarchean basement at the time of extrusion.

The combination of shallow-water deposits associated with continental crust, tholeiitic major-element geochemistry, trace-element geochemistry with MORB-like and crustal contamination signatures, and mainly positive $\varepsilon_{nd}t$ values (indicating depleted mantle derivation) implies that supracrustal rocks in domains I and III most likely formed in a back-arc basin or in a continental rift unrelated to subduction.

Supracrustal remnants in gneissic/plutonic rocks of domains II, IV, V, and VI were likely derived from structural and plutonic disruption of volcano-sedimentary units of domains I and III. Domain II gabbro was probably derived from depleted upper mantle that was isotopically variable (positive $\varepsilon_{nd}t$ values not correlated to $SiO_2$), but domain II granitic rocks display geochemical characteristics of crustal melts. We tentatively suggest that intracontinental lithospheric shearing at ca. 2.61 Ga released gabbroic melts from the upper mantle and that crustal melting during shearing (possibly aided by heat related to release of these gabbroic melts) produced granitic magmas.

Amphibolite-grade tectonites and greenschist-grade cataclasites are distributed throughout the Angikuni Lake region and rocks from domain VI can be followed across the geophysical trace of the Snowbird tectonic zone. At this latitude, Snowbird-related deformation appears to be distributed heterogeneously across a broad area. The absolute time interval between low- and high-grade tectonism remains uncertain. A geochronological study (K. MacLachlan; GSC, GNWT) will test if the greenschist-facies cataclasites are related to the high-grade tectonites, or if they reflect a significantly younger (Paleoproterozoic) deformation history. Any changes in structural level related to the two 'events' occurred before Christopher Island volcanism, dated at some time between ca. 1.88 Ga and 1.81 Ga.

Thick sections of fanglomerate and volcanogenic rocks in the Baker Lake Group require active Paleoproterozoic faulting. Fluvial and playa redbeds (conglomerate, arkose, and semipelitic rock) of the Angikuni Formation were likely deposited in a local fault-bounded trough that experienced tilting prior to Christopher Island Formation volcanism. These rocks are probable tectonostratigraphic equivalents to the South Channel and Kazan formations exposed in Baker Lake Basin. Direct field evidence of syndepositional faulting in the Christopher Island Formation along the present margins of sub-basins in the Angikuni Lake area is lacking. Such faults likely remain buried, and the present extent of the sub-basins, as well as scattered outliers throughout the region, probably signifies thermal subsidence beyond the limits of active faulting.

## ACKNOWLEDGMENTS

This project is funded by the Northwest Territories Geology Division, Indian Affairs and Northern Development Canada (Yellowknife), with support from the Geological Survey of Canada. Gary, Lois, and Shawn Gurke (Treeline Lodge, Nueltin Lake) provided efficient logistics and pilot Gord Clark (Jackson Air Services) flew safe camp moves. We thank Al Donaldson, Rob Rainbird, and Thomas Hadlari for discussions regarding their continuing work in Baker Lake Basin, and Rachelle Lacroix for digital imaging. Field visits by Simon Hanmer, Al Donaldson, and Rex Brommecker (WMC International Ltd.) in 1997, and by Kate MacLachlan in 1998, helped our mapping. Constructive critical comments by J.A. Donaldson, S. Hanmer, K. MacLachlan, and R. Rainbird substantially improved the paper.

## REFERENCES

**Aspler, L.B. and Chiarenzelli, J.R.**
1996: Stratigraphy, sedimentology and physical volcanology of the Henik Group, central Ennadai–Rankin greenstone belt, Northwest Territories, Canada: Late Archean paleogeography of the Hearne Province and tectonic implications; Precambrian Research, v. 77, p. 59–89.

**Aspler, L.B., Barham, B.A., and Chiarenzelli, J.R.**
1999: Results of integrated geolgical and aeromagnetic mapping, and recent exploration, Henik and Hurwitz groups, Noomut River, Northwest Territories (Nunavut); *in* Current Research 1999-C, Geological Survey of Canada.

**Aspler, L.B., Chiarenzelli, J. R., Powis, K., and Cousens, B.L.**
1998a: Progress report: Precambrian geology of the Angikuni Lake area, District of Keewatin, Northwest Territories; *in* Current Research 1998-C, Geological Survey of Canada, p. 55–66.
1998 b: Geology of southern Angikuni Lake area, District of Keewatin, Northwest Territories; Geological Survey of Canada, Open File 3608, scale 1:50,000.

**Blake, D.H.**
1980: Volcanic rocks of the Paleohelikian Dubawnt Group in the Baker Lake–Angikuni Lake area, District of Keewatin, Northwest Territories; Geological Survey of Canada Bulletin 309, 39 p.

**Cousens, B.L.**
1998: Geochemistry and neodymium systematics of Archean and Proterozoic igneous rocks from the Angikuni and Yathkyed lakes areas, western Churchill Province, Northwest Territories; Indian Affairs and Northern Development Canada, Open File EGS 1998-6, 41 p.

**Donaldson, J.A.**
1965: The Dubawnt Group, districts of Keewatin and Mackenzie; Geological Survey of Canada, Paper 64-20, 11 p.

**Eade, K.E.**
1986: Precambrian geology of the Tulemalu Lake–Yathkyed Lake area, District of Keewatin. Geological Survey of Canada Paper 84-11, 31 p.

**Eriksson, K.A., Krapez, B., and Fralick, P.W.**
1994: Sedimentology of Archean greenstone belts: signatures of tectonic evolution; Earth-Science Reviews, v. 37, p. 1–88.

**Gall, Q., Peterson, T.D., and Donaldson, J.A.**
1992: A proposed revision of the Early Proterozoic stratigraphy of the Thelon and Baker Lake basins, Northwest Territories; *in* Current Research, Part C; Geological Survey of Canada, Paper 92-1C, p. 129–137.

**le Bas, M.J., le Maitre, R.W., Streckeisen, A., and Zanettin, B.**
1986: A chemical classification of volcanic rocks based on the total alkali-silica diagram; Journal of Petrology, v. 27, p. 745–750.

**Loveridge, W.D., Eade, K.E., and Sullivan, R.W.**
1988: Geochronological studies from Precambrian rocks from the southern District of Keewatin; Geological Survey of Canada, Paper 88-18, 36 p.

**MacDonald, G.A. and Katsura, T.**
1964: Chemical composition of Hawaiian lavas; Journal of Petrology, v. 5, p. 82–135.

**MacRae, N.N., Armitage, A.E., Miller, A.R., Roddick, J.C., Jones, A.L., and Mudry, M.P.**
1996: The diamondiferous Akluilâk lamprophyre dyke, Gibson Lake area, N.W.T., *in* Searching for Diamonds in Canada, (ed.) A.N. LeCheminant, D.G. Richardson, R.N.W. DiLabio, and K.A. Richardson; Geological Survey of Canada Open File 3228, p. 101–107.

**Rainbird, R.H., Hadlari, T., and Donaldson, J.A.**
1999: Stratigraphy and paleogeography of the Paleoproterozoic Baker Lake Group in the eastern Baker Lake Basin, Northwest Territories (Nunavut); *in* Current Research 1999-C, Geological Survey of Canada.

**Roddick, J.C. and Miller, A.R.**
1994: An $^{40}Ar$-$^{39}Ar$ age from the REE-enriched Enekatcha ultrapotassic intrusive suite and implications for timing of ultrapotassic magmatism in the central Churchill Province, Northwest Territories. *in* Geological Survey of Canada, Current Research 1994-F, p. 69-74.

**Schau, M.**
1997: Geology of the Archean Prince Albert Group in the Richards Bay area, northeastern Melville Peninsula, District of Franklin, Northwest Territories; Geological Survey of Canada, Bulletin 385, 44 p.

**Sun, S.S. and McDonough, W.F.**
1989: Chemical and isotopic systematics of oceanic basalts; implications for mantle composition and Processes; *in* Magmatism in the Ocean Basins, (ed.) A.D. Saunders and M.J. Norry; Geological Society of London, Special Publication 42, p. 313–345.

**Tella, S. and Eade, K.E.**
1985: Geology, Kamilukuak Lake, District of Keewatin, Northwest Territories; Geological Survey of Canada, Map 1629A, scale 1:250 000.

**Tella, S., Heywood, W.W., and Loveridge, W.D.**
1985: A U-Pb age from a quartz syenite intrusion, Amer Lake, District of Keewatin; a part of the Churchill structural province; *in* Current Research, Part B; Geological Survey of Canada, Paper 85-1B, p. 367–370.

**Zaleski, E., Corrigan, D., Kjarsgaard, B.A., Jenner, G.A., Kerswill, J.A., and Henderson, J.R.**
1997: Preliminary results of mapping and structural interpretation from the Woodburn project, western Churchill Province, Northwest Territories; *in* Current Research 1997-C, Geological Survey of Canada, p. 91–100.

# Review and progress report of Proterozoic granitoid rocks of the western Churchill Province, Northwest Territories (Nunavut)[1]

T.D. Peterson and O. van Breemen
Continental Geoscience Division, Ottawa

*Peterson, T.D. and van Breemen, O., 1999: Review and progress report of Proterozoic granitoid rocks of the western Churchill Province, Northwest Territories (Nunavut);* in *Current Research 1999-C; Geological Survey of Canada, p. 119–127.*

**Abstract:** Proterozoic granitoid rocks in the western Churchill Province comprise two age groups: a ca. 1.83 Ga group (Hudson granitoid rocks), mainly present in a region extending northeast from west of Hudson Bay to Melville Peninsula, and a ca. 1.76 Ga group (Nueltin suite) restricted to the southwest. The older intrusions are typically equigranular, calc-alkaline, sodic granitic to granodioritic rocks with partly concordant contacts. They were approximately coeval with minette dykes of the Dubawnt Supergroup. The younger plutons are typically rapakivi granite with chilled discordant contacts. They are enriched in LREEs, Zr, and Th, and mafic-felsic mingling textures are common. The boundary between the petrogenetic domains partly corresponds to major Proterozoic faults. The Nueltin-bearing Dubawnt domain featured subsidence and terrigenous basin formation at 1.85–1.7 Ga.

**Résumé :** Des granitoïdes protérozoïques de la partie occidentale de la Province de Churchill comprennent des roches appartenant à deux groupes d'âges, un d'environ 1,83 Ga (roches granitoïdes hudsoniennes) qui se rencontre essentiellement dans une région s'étendant vers le nord-est à partir de l'ouest de la baie d'Hudson jusqu'à la presqu'île Melville, et un autre d'environ 1,76 Ga (suite de Nueltin) qui se trouve uniquement au sud-ouest. Les intrusions les plus anciennes comportent typiquement des roches granodioritiques à granitiques sodiques, calco-alcalines, équigranulaires, aux contacts en partie concordants. Elles sont à peu près contemporaines des dykes de minette du Supergroupe de Dubawnt. Les plutons plus récents sont typiquement des granites rapakiviques aux contacts discordants figés. Ils sont enrichis en éléments de terres rares légers, en zirconium et en thorium et ont souvent des textures de mélange de composantes mafiques et felsiques. La limite entre les domaines pétrogénétiques correspond en partie à des failles majeures du Protérozoïque. Dans le domaine de Dubawnt qui renferme la suite de Nueltin, il y a eu affaissement et formation de bassins terrigènes à 1,85–1,7 Ga.

[1] Contribution to the Western Churchill NATMAP Project

## INTRODUCTION

Between about 2.0 Ga and 1.70 Ga, the Churchill Province served as the principal hinterland for the assembly of Laurentia (Hoffman, 1988), and it featured degrees and types of deformation, metamorphism, and magmatism not seen in the large foreland provinces (Slave and Superior). However, the same style of magmatic activity is recorded in some other portions of Laurentia, such as the Svecofennian Orogen (1.90–1.77 Ga) and Transscandinavian granite-porphyry belt (1.83–1.65 Ga) of Baltica (Lindh and Persson, 1990). In both regions, there is a close association between minette dykes and anorogenic calc-alkaline granite plutons near 1830 Ma, followed about 100 million years later by more alkaline rapakivi granite intrusions (LeCheminant et al., 1987a; Branigan, 1989). There are also more modern examples of postorogenic granite-minette associations, e.g. the Caledonian (Siluro-Devonian) Southern Uplands of Scotland (Rock et al., 1986).

This report presents the initial results of a project to characterize the ages and petrology of the Proterozoic granitoid intrusions of the western Churchill Province (Fig. 1). One goal is to provide means of subdividing the western Churchill Province on the basis of magmatic and inherited U-Pb zircon ages, and perhaps model Nd ages and geochemistry. The project draws heavily on data generated by active and older projects, as well as map and sample archives. We particularly note use of the material of Davidson (1969), Eade (1970, 1972), Reinhardt and Chandler (1973), LeCheminant (LeCheminant et al., 1979, 1981, 1983, 1987a), and Tella (1993, 1994; Tella et al., 1985). Many of the U-Pb ages were obtained by C. Roddick (Loveridge et al., 1987; LeCheminant et al., 1987b, and others cited above). Unless otherwise noted, all U-Pb ages in this report were obtained from magmatic zircons.

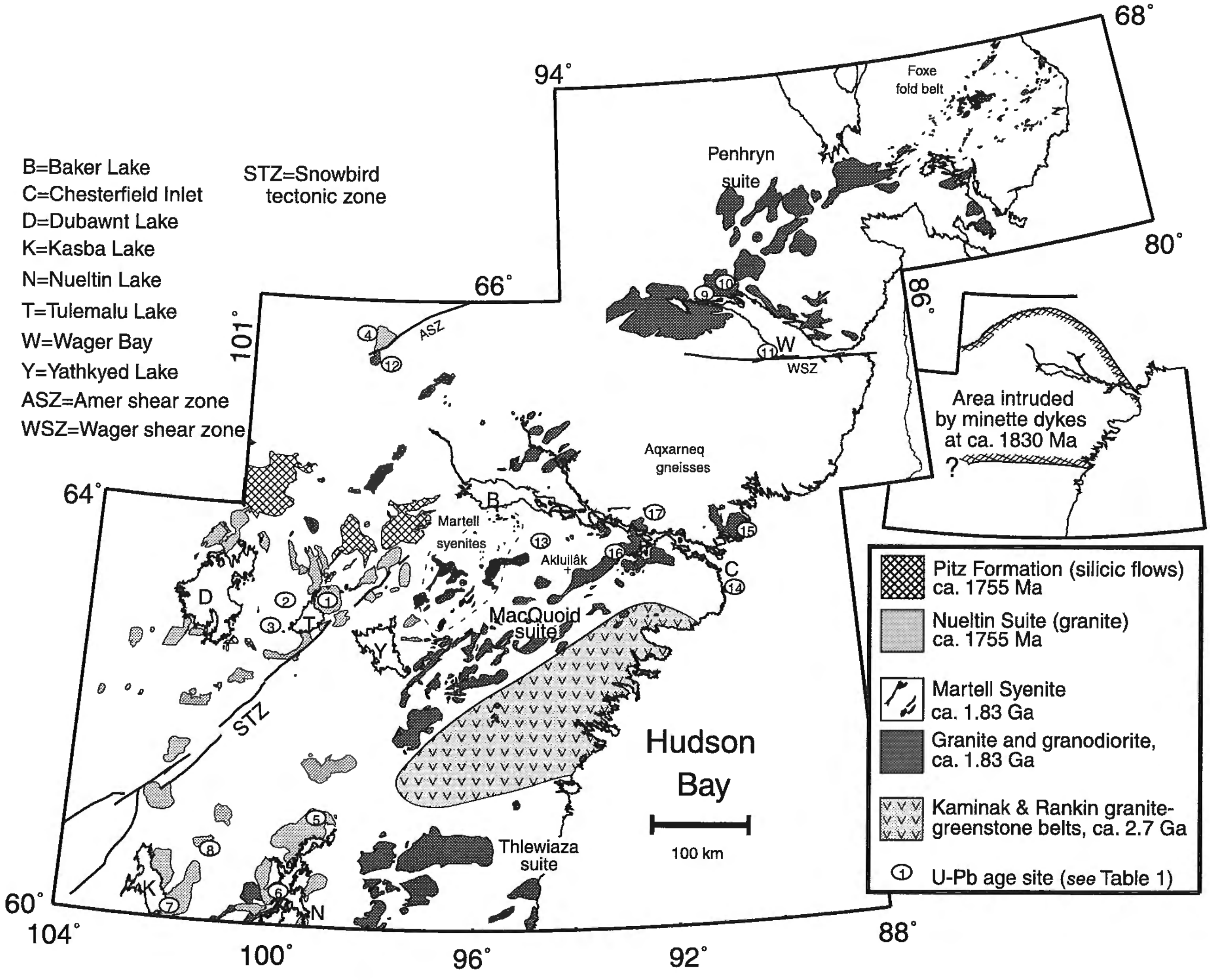


***Figure 1.** Locations of known and interpreted early Proterozoic granitoid intrusions in the western Churchill Province. Based on digital compilations of maps by Peterson (1994), Tella (1997), and Patterson and LeCheminant (1985).*

## U-Pb AGES AND DISTRIBUTION

There are 17 U-Pb zircon magmatic ages of Proterozoic granitoid rocks in the area of Figure 1, six of which were recently obtained by ion probe analysis (SHRIMP: Stern, 1997) of zircon rims, and cores of homogeneous zircons (O. van Breemen and T.D. Peterson, unpub. manuscript, 1998) (Table 1). Two age groups are present (Fig. 2). One ranges from 1840 to 1808 Ma (n=9), and the other from 1764 to 1752 Ma (n=8). We will refer to the older granitoid rocks, which cluster along the northwestern shore of Hudson Bay, as the Hudson granitoid group. The younger group is termed the Nueltin suite (for Nueltin Lake, where a prominent plutonic complex is present).

### *Hudson granitoid and minette intrusions*

The dated Hudson granitoid rocks encompass a region trending northeast from the north edge of the Kaminak greenstone belt west of Hudson Bay, across Chesterfield Inlet to north of Wager Bay. Mapping and outcrop descriptions by Eade (1970) indicate that Proterozoic granite intrusions south of the Kaminak belt, near the Thlewiaza River, are probably the same type and age. This latter granite field is bounded to the south by the Chipewyan batholith of the Trans-Hudson orogen, emplaced at about 1850 Ma (Lewry, 1981). Calc-alkaline outliers of this batholith to the north and northwest have been dated at 1840–1810 Ma (Annesley et al., 1997).

Undated plutons were assigned to the Hudson granitoid group on the basis of descriptions from mapping reports (reviewed in the following section), and examination of sample archives. To aid discussion, they have been divided into three geographically separated suites termed the Penrhyn, MacQuoid, and Thlewiaza suites (Fig. 1). Individual plutons and pluton clusters of the MacQuoid and Penrhyn suites are strongly oriented northeast-southwest, whereas the Thlewiaza suite has a less well developed, east-west orientation. The orientations reflect the regional structural trends, with most deformation preceding granite emplacement.

No zircons from granite intrusions emplaced within the metasedimentary rocks of the Penrhyn Group (Foxe fold belt, extreme northeast corner of Fig. 1) have been dated. These granitic rocks were considered by Henderson (1983) to be synmetamorphic or formed shortly after peak metamorphism, with the age of metamorphism constrained by Rb-Sr

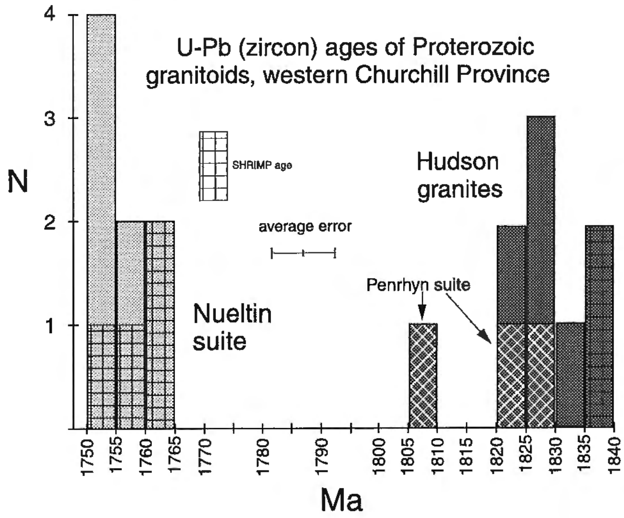


*Figure 2. Histogram of Proterozoic granitoid U-Pb (zircon) ages within the area of Figure 1. Based on conventional U-Pb ages (cited in text), and ion probe ages (van Breemen and Peterson, unpub. manuscript, 1998). Precise SHRIMP ages, as currently calculated, were used in this figure.*

**Table 1.** U-Pb ages of Proterozoic granitoids, western Churchill Province.

| Sample | Age (Ma) | Locale & age reference | |
|---|---|---|---|
| 1. 78LAAT-209 | 1756 ± 11 | Pamiutuq pluton | A. LeCheminant (unpub. data, 1987) |
| 2. 82LAAT-305 | 1752 ± 2 | Tulemalu Lake | A. LeCheminant (unpub. data, 1987) |
| 3. WN-615-79 | 1753 +3/-2 | SW Tulemalu | Loveridge et al., 1987 |
| 4. 82TX-S188 | 1751 +5/-3 | Amer shear zone (north) | Tella, 1994 |
| 5. 93-57-25 | ca. 1.76 Ga | Watterson Lake | this study |
| 6. CZ-12-85 | ca. 1.75 Ga | Nueltin Lake | this study |
| 7. EA-107-68 | ca. 1.76 Ga | Kasba Lake | this study |
| 8. EA-100-68 | ca. 1.76 Ga | Ennedai lake | this study |
| 9. 85LAA-315 | 1823 ± 3 | Wager Bay | LeCheminant et al., 1987b |
| 10. 85LAA-168 | 1826 +4/-3 | Wager Bay | LeCheminant et al., 1987b |
| 11. 5-HSA-94-2 | 1808 ± 2 | Wager Bay | Henderson and Roddick, 1990 |
| 12. 82TX-S48 | 1833 +11/-8 | Amer shear zone (south) | Tella et al., 1998 |
| 13. 96TX-026 | 1827 ± 3 | MacQuoid Lake | Tella et al., 1997 |
| 14. 86TX-107 | 1826 ± 3 | SE Chesterfield Inlet | Tella, 1993 |
| 15. 92RAL-8 | ca. 1.84 Ga | Gibson Lake | this study |
| 16. 87TXA-138 | ca. 1.84 Ga | NE Chesterfield Inlet | this study |

*Errors quoted are 2σ. See Figures 1 and 5 for locations.

cooling ages of 1804±16 Ma. The belt northwest of Wager Bay, with three ages, was informally termed the Ford Lake suite by LeCheminant et al. (1987b), but these plutons contain numerous inclusions of Penrhyn Group lithologies (Henderson et al., 1986), so we incorporate them into the Penrhyn suite.

Scattered plutons north and west of Baker Lake, some cut by minette dykes, have the same petrography and field relations as the MacQuoid suite (LeCheminant et al., 1981, 1983). An aphanitic rhyolite dome informally termed Sugarloaf, which erupted through sandstones predating minette units (Kazan Formation) in the Baker Lake basin, 30 km north of Kazan Falls (Blake, 1980) is the only volcanic centre known that might be equivalent to the MacQuoid suite.

The limit of the minette dyke swarm, depicted in the inset to Figure 1, was obtained from LeCheminant et al. (1987b), and is only approximately known. At least one minette dyke sample has been collected southwest of the boundary as shown, west of Kasba Lake (Hanmer, 1997). Ages for these zircon-poor dykes and the equivalent intrusive stocks (Martell syenite) are few and of poor quality. A U-Pb (monazite+apatite) age of 1832±28 Ma was obtained for the diamondiferous Akluilâk dyke (MacRae et al., 1996; *see* Fig. 1). Hornblende from an ultrapotassic stock south of Dubawnt Lake yielded a $^{40}Ar/^{39}Ar$ age of 1825±12 Ma (Roddick and Miller, 1994). A quartz syenite associated with minette dykes from near Amer Lake yielded a zircon age of 1850+30/-10 Ma (Tella et al., 1985). In the Gibson Lake area, Tella et al. (1993) observed two ages and strike directions for minette dykes; one predated and the other postdated Hudson granite. Thus, the available data indicate that the Hudson granitoids and the minette dyke swarm were coeval over a period of about 20–30 million years.

### *Nueltin suite*

Except for a single example north of the Amer shear zone (Tella, 1994), the Nueltin suite is restricted to the southwest part of the study area. According to Eade (1970), some Proterozoic, granitic rocks predating Nueltin suite rocks are present west of Nueltin Lake, but elsewhere the geographic separation between the two age groups is sharp. Rhyolite to dacite extrusive equivalents of the Nueltin granite (Pitz Formation, middle Dubawnt Supergroup) are widespread southwest of Baker Lake, along the eastern edge of the Thelon basin, and southeast of Dubawnt Lake.

## FIELD RELATIONS AND PETROGRAPHY

The Hudson granitoid rocks, as described by numerous authors, are remarkably uniform in their field relations and petrography (Fig. 3). Within the plutons, the granite units are typically nonfoliated, equigranular, and medium grained, with sparse biotite. Plagioclase and alkali feldspar are nonidiomorphic and present in approximately equal abundance, and myrmekite replacing alkali feldspar is commonly present. Magnetite is ubiquitous and titanite is common. Zircons from Hudson granitoid rocks in this study are complexly

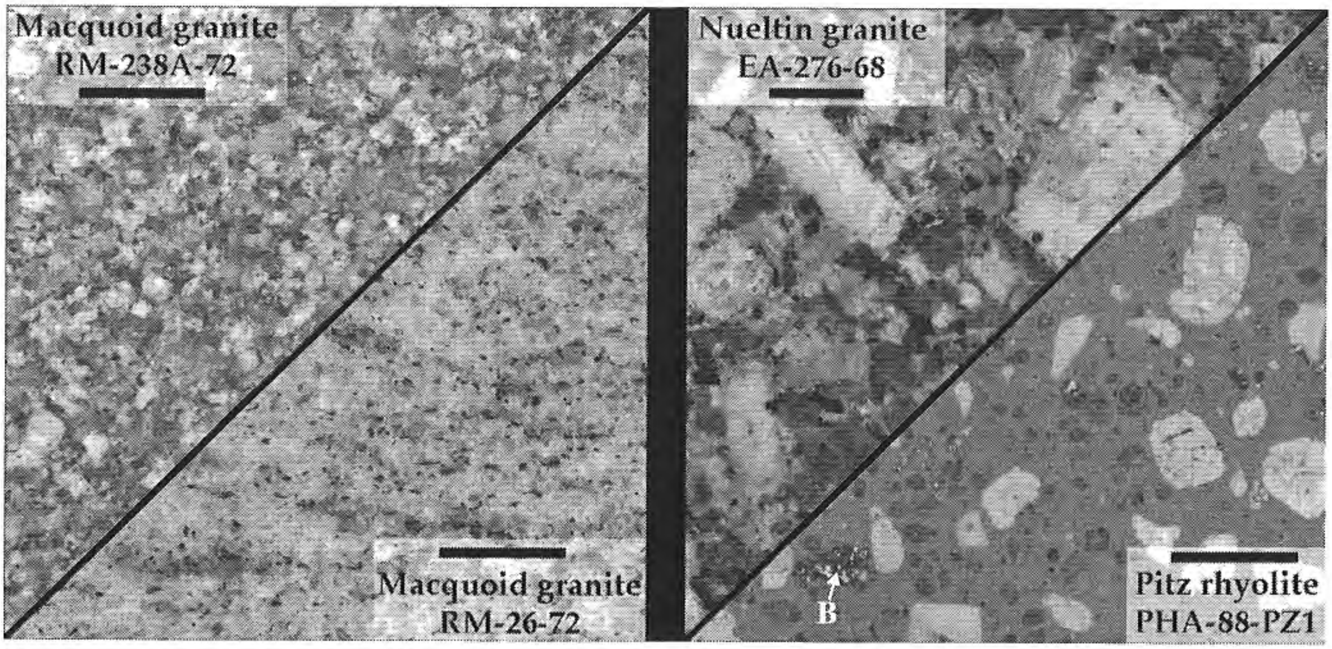


*Figure 3. Polished slabs of typical samples from the MacQuoid suite (MacQuoid Lake area), the Nueltin suite (Nueltin Lake area), and the Pitz Formation (Dubawnt Lake). Note the equigranular texture of the MacQuoid granite units (white=plagioclase, dark grey=quartz, light grey=alkali feldspar), and the faint foliation in the lower sample. Large white crystals in the Nueltin granite are K-feldspar phenocrysts. Basaltic blebs (B) are common in the Pitz Formation rhyolite, which contains both alkali feldspar and quartz phenocrysts (rounded bodies are air bubbles). Scale bars are 1 cm.*

zoned, with large rounded cores in about 50% of the grains. The only significant exceptions to this description are some plutons of the Penrhyn suite near Wager Bay, which consist of megacrystic granite units through monzodiorite units, plus minor gabbro (LeCheminant et al., 1987b). This group is also geochemically anomalous (Fig. 4, and below).

At their margins, most Hudson granitoid plutons are contaminated by partly resorbed xenoliths, contain an undulating relict foliation defined by aligned biotite, and may have a sill-like geometry (e.g. LeCheminant et al., 1981). Some plutons north of the Kaminak greenstone belt appear to have been emplaced in a comagmatic (possibly injection) migmatite (Davidson, 1969); those in the MacQuoid Lake area commonly have gradational contacts with country rocks (Reinhardt and Chandler, 1973; Tella et al., 1993), or may be discordant. Plutons in the Foxe fold belt are mostly discordant (Henderson, 1983). No cases of chilled contacts have been recorded; however, some contact zones are weakly porphyritic (e.g. LeCheminant et al., 1983). Mafic inclusions are invariably coarsely recrystallized (mainly to hornblende) and may be locally mixed to produce heterogeneous monzodiorite.

In contrast, granite bodies of the Nueltin suite are always discordant, strongly porphyritic (quartz and alkali feldspar, Fig. 3), and chilled at their margins. Pluton centres, particularly those of the southern belt between Kasba Lake and

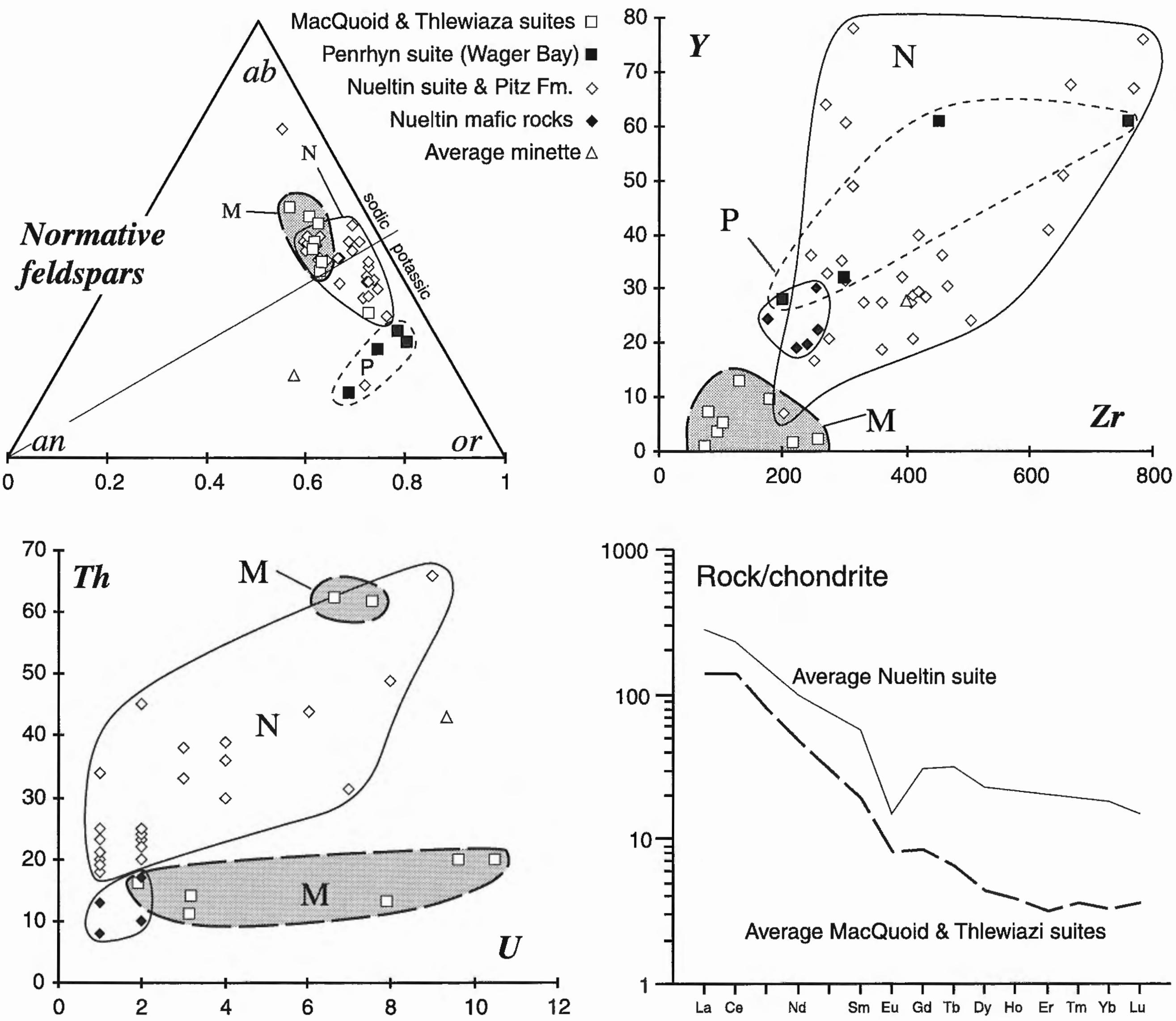


***Figure 4.*** *Plots of normative feldspars, Y-Zr, Th-U, and REEs. Single outliers have been omitted from circumscribed fields. M=MacQuoid and Thlewiaza suites, N=Nueltin suite, P=Penrhyn suite (Wager Bay only). Data from Booth (1983), LeCheminant et al. (1987b), Peterson et al. (1994), H. Sandeman (pers. comm., 1998), and this study.*

Nueltin Lake, are typically very coarse, with biotite books up to 1 cm in diameter (e.g. Charbonneau and Swettenham, 1986). Zircons from the southern belt utilized in this study display fine, delicate zoning and cores are very rarely present. The chilled margins resemble rhyolite units of the Pitz Formation (middle Dubawnt Supergroup), which locally are intruded by Nueltin granite (e.g. the Pamiutuq pluton, Booth, 1983). These field relations, plus the common presence of miarolitic cavities, indicate that the Nueltin granite was emplaced at shallow levels (LeCheminant et al., 1981). Numerous examples of rapakivi texture have been observed in the Nueltin suite, though it is not everywhere present.

Nueltin granite intrusions can be associated with aphanitic or plagioclase-phyric mafic to intermediate dykes and gabbroic bodies, and may display mingling with mafic melts which produced varieties of monzodiorite (e.g. Booth, 1983). In particular, the south end of the McCrae Lake dyke (*see* Fig. 5) is well mingled with a pluton near Tebesjuak Lake (LeCheminant et al., 1981). Centimetre-scale mafic blebs in granite bodies may have chilled borders (LeCheminant et al., 1987a). The aphanitic dykes consist of interlocking, acicular clinopyroxene and feldspar with microphenocrysts of magnetite, and are rich in quartz xenocrysts. Mingling with small volumes of mafic melt is also observed in some samples of the Pitz Formation (Fig. 3). An identical mafic-felsic association occurs in the rapakivi granite field of the Svecofennian orogen (Rämö and Haapala, 1990).

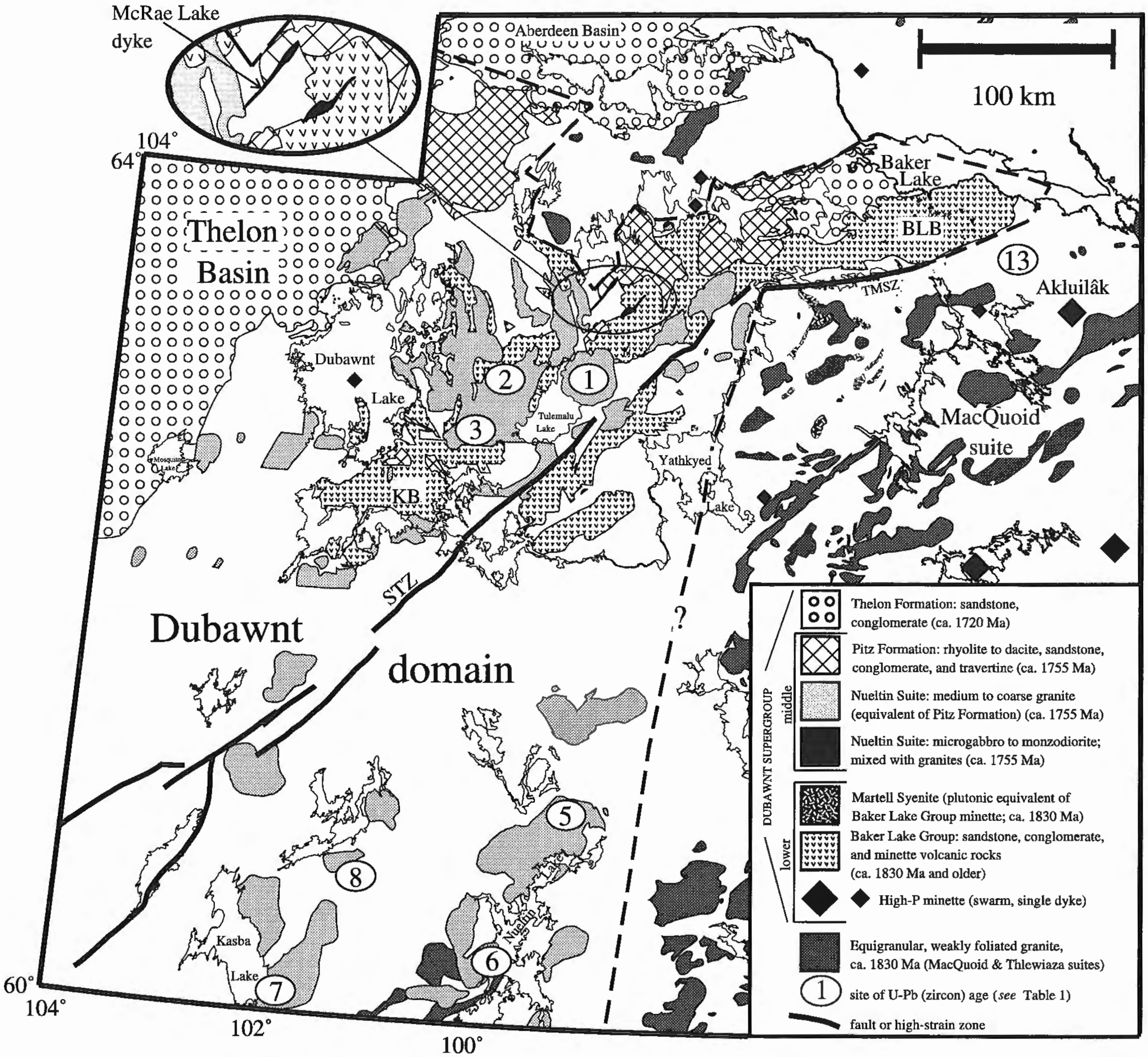


***Figure 5.*** *Proterozoic (ca. 1.85–1.7 Ga) geology of the Dubawnt domain. TMSZ=Thirty Mile high-strain zone, STZ=Snowbird tectonic zone, KB=Kamilukuak basin, BLB=Baker Lake basin (Baker Lake Group).*

## GEOCHEMISTRY

### *Hudson granitoid and minette units*

The MacQuoid and Thlewiaza granitoid rocks are characterized by relatively high normative An contents (and correspondingly high Ca and Al), and K/Na<1 (Fig. 4). In many respects they resemble the Archean postvolcanic granitoid rocks of the local greenstone belts (e.g. the Gill Lake granite stocks of the Kaminak belt: Park and Ralser, 1992), and are broadly calc-alkaline in nature. Rare-earth elements can be strongly fractionated (Ce/Yb=20–220), and most samples exhibit small positive or negative Eu anomalies.

The megacrystic plutons of the Penrhyn suite near Wager Bay more closely resemble the Nueltin suite (below, and Fig. 4) than other Hudson granite intrusions. The analyses published by LeCheminant et al. (1987b) are of three strongly potassic granite samples with pronounced negative Eu anomalies, and one monzodiorite sample with a small anomaly, all LREE-enriched.

Details of the geochemistry of the minette dykes have been presented elswhere (Peterson et al., 1994). Statistical analysis of 104 minette analyses, including those of Beaudoin (1998) and Digel (1986) has led to the recognition of two distinct groups. Outside the area encompassed by the Nueltin suite, most minette dykes are relatively enriched in Ba, Ti, Zr, Mg, Ni, Cr, and especially P; this group includes the diamondiferous Akluilâk dykes. We will refer to these as high-P minette dykes. Included in the high-P group are some samples showing only modest enrichments, but bearing phlogopite phenocrysts with xenocrystic, high-Ti cores (LeCheminant et al., 1987a). Only one high-P minette sample is within the Nueltin granite field, sample PHA-89-K/8 from Dubawnt Lake (*see also* MacRae et al., 1996).

### *Nueltin granite and associated mafic rocks*

The Nueltin plutons and Pitz Formation volcanic rocks span a compositional range of dacite to rhyolite, and mainly have K/Na>1. They are substantially enriched in Y, Zr, Th, and REE relative to most Hudson granitoid rocks, and have less fractionated REE compositions (average Ce/Yb=60). Most samples display strong negative Eu anomalies.

Analyses of mafic rocks associated with the Nueltin granitic rocks are suspect because of possible mixing with granite; however, four of five analyses (Booth 1983; this study) are of transitional alkali basalt-sodic trachyte (=benmoreite), with trace element patterns similar to, though less extreme than, the minette samples. In geochemical plots the benmoreite samples cluster at the less enriched end of the Nueltin silicic rock field. It is tentatively concluded that these rocks have an alkali basalt parent.

### *Neodymium isotopes*

The available Nd isotope data (Dudás et al., 1991; Peterson et al., 1994) indicate that the two granite age groups cannot be distinguished on this basis. The Nueltin suite spans a range of $\varepsilon_{Nd,1750\,Ma}$ of -8.6 to -10.5 (at 1830 Ma, $\varepsilon_{Nd}$=-7 to -9.4). MacQuoid suite samples are in the range $\varepsilon_{Nd,1830\,Ma}$ = -8.9 to -9.7; a single value from the Penrhyn suite is $\varepsilon_{Nd,1830\,Ma}$=-10.25. All of these are within, but on the low side of, the range of the minette dykes and flows ($\varepsilon_{Nd,1830\,Ma}$=-5 to -11). Depleted mantle model ages for all of these rocks are in the range 2.9–2.5 Ga.

## INTERPRETATIONS

### *Sources*

The Nd isotopic data unequivocally point to a predominantly crustal origin for all Proterozoic granite bodies in the western Churchill Province. The model Nd ages are similar to those of most analyzed Archean rocks from the western Churchill Province (Dudás et al., 1991; Theriault et al., 1994), and indicate that the presently exposed Archean rocks could have been sources for the Proterozoic plutons.

The Hudson granitoid rocks are nowhere associated with regional anatexis, but the absence of chilled borders, local association with possible injection migmatite (Davidson, 1969), and small degrees of partial melt in associated metasediments in the Foxe fold belt (Henderson, 1983), indicate they were mostly emplaced at midcrustal levels. Their even grain size indicates a small temperature interval of crystallization, which inhibited the formation of phenocryst populations. Hence, the melts were probably multiply saturated (quartz+two feldspars) at the site of emplacement. Multiple saturation, and enthalpic losses leading to rapid crystallization, may have been promoted by the digestion of xenoliths.

In contrast, the strongly porphyritic textures of the Nueltin granite suite imply a wide temperature interval of crystallization, and their chilled borders indicate relatively cool wall rocks. Given the common presence of mingled mafic melts, the Nueltin granite melts were probably generated by injection of basaltic magma into brittly faulted crust (Booth, 1983). Three factors indicate that their source region was mainly higher in the crust than was that for the Hudson granite units, 1) the well preserved mingling textures, including chilled borders in some basaltic blebs, are consistent with density-stratified magma chambers only slightly below the current level of exposure; 2) some Pitz–Nueltin centres (Booth, 1983), and also the very similar rapakivi granite units of Fennoscandia (Rämö and Haapala, 1990), have been interpreted as exhumed collapsed calderas, implying subvolcanic magma chambers; and 3) under $H_2O$-saturated conditions, higher K/Na ratios, a feature of the Nueltin suite, are favoured by lower pressure.

### *Petrogenetic domains*

The contrasts of the emplacement style and level of the two suites are so dramatic that we propose to recognize the southwestern portion of the Churchill Province as a distinct petrogenetic domain (Fig. 5), which we will refer to as the Dubawnt domain. Its boundary is defined as the line separating ca. 1840–1810 Ma plutons (granitoid and Martell syenite) from Nueltin granite units and the Pitz Formation of the middle Dubawnt Supergroup; this line can also be drawn to exclude high-P minette rocks. As such, the Dubawnt domain is a diachronous igneous province; however, its northern half contains all of the fault-bounded basins of the Baker Lake Group, and so it apparently also corresponds to a crustal block exposed at higher average levels than crust immediately outside the domain. Uplift northeast of this region at about 1830–1720 Ma was previously deduced from the shedding of clastic debris from the Aqxarneq granulite gneiss massif into the early Baker Lake basin, as well as westerly paleocurrents and westerly decreasing clast size in the Thelon Formation (Donaldson, 1965).

Along its northern and northeastern edge, the petrogenetic boundary corresponds closely to major faults and shear zones, such as the Thirty Mile high-strain zone (LeCheminant et al., 1979; Fig. 5), and the extensive fault system forming the northern edge of the Baker Lake Group (e.g. LeCheminant et al., 1981). Its continuation to the northwest is obscured by the younger Thelon Formation. South of Yathkyed Lake, the nature and precise position of the domain boundary are not constrained.

The Snowbird tectonic zone may be a significant internal boundary within the Dubawnt domain. Southeast of the Snowbird tectonic zone there are no exposures of the Pitz Formation and relatively few of the Baker Lake Group, and according to Eade (1972), to the south there are some small plutons of the Hudson group, intruded by exceptionally coarse-grained Nueltin granite bodies. These features are all consistent with a slightly lower exposure level than that northeast of the Snowbird tectonic zone. We suggest that the Dubawnt domain consists of one or a pair of subsided crustal wedges which dropped mainly at their northeastern apices. This style of subsidence, previously documented in the structure and sedimentology of the wedge-shaped Kamilukuak basin southeast of Dubawnt Lake (Peterson and Rainbird, 1990), is consistent with easterly indentation of the Slave Province near 1840 Ma (Hoffman, 1988).

Granite units and mafic dykes near 1.76 Ga are rare outside the Dubawnt domain, but K-Ar ages (biotite and hornblende) near 1.76 Ga are widespread in the western Churchill Province (e.g. Loveridge et al., 1987). The selective distribution of rapakivi granite units in the western Churchill Province may reflect a relative abundance of deep brittle faults in the Dubawnt domain, which provided easy ascent paths for mafic melts that were unable to penetrate to crustal levels elsewhere.

## ACKNOWLEDGMENTS

We thank Richard Stern for his assistance with SHRIMP analyses. Lori Wilkinson extracted portions of digital maps north of 64°N for Figure 1. Tony LeCheminant kindly allowed the use of unpublished ages. Reviews by and discussions with Tony LeCheminant, Subhas Tella, and Larry Aspler were very valuable. A review by Bill Davis greatly improved the manuscript.

## REFERENCES

**Annesley, I.R., Madore, C., Rupan, S., and Krogh, T.E.**
1997: U-Pb geochronology of thermotectonic events in the Wollaston Lake area, Wollaston Domain: a summary of 1994-1996 results; *in* Summary of Investigations 1997; Saskatchewan Geological Survey, Miscellaneous Report 97-4, p. 162–173.

**Beaudoin, Y.**
1998: Petrology, geochemistry and Sr/Nd isotopic analysis of lamprophyre dykes: Kaminak Lake area, central Churchill Province, Northwest Territories, Canada; B.Sc. thesis, The University of Ottawa, Ottawa, Ontario, 90 p.

**Blake, D.H.**
1980: Volcanic rocks of the Paleohelikian Dubawnt Group in the Baker Lake - Angikuni Lake area, District of Keewatin, N.W.T.; Geological Survey of Canada, Bulletin 309, 39 p.

**Booth, G.W.**
1983: The petrology and geochemistry of the Pamiutuq Lake batholith, Northwest Territories; M.Sc. thesis, University of Toronto, Toronto, Ontario, 176 p.

**Branigan, N.P.**
1989: Hybridisation in Middle Proterozoic high-level ring complexes, Åland, SW Finland. Precambrian Research v. 45, p. 83–96.

**Charbonneau, B.W. and Swettenham, S.S.**
1986: Gold occurrence in radioactive calc-silicate float at Sandybeach Lake, Nueltin Lake area, District of Keewatin; *in* Current Research, Part A; Geological Survey of Canada, Paper 86-1A, p. 803–808.

**Davidson, A.**
1969: Precambrian geology, Kaminak Lake map-area, District of Keewatin; Geological Survey of Canada, Paper 69-51, 27 p.

**Digel, S.G.**
1986: A petrographic and geochemical study of a lamprophyre dyke swarm in the Churchill Province, Rankin Inlet area, District of Keewatin, N.W.T.; B.Sc. thesis, Queen's University, Kingston, Ontario, 44 p.

**Donaldson, J.A.**
1965: The Dubawnt Group, Districts of Keewatin and Mackenzie; Geological Survey of Canada, Paper 64-20, p. 23–25.

**Dudás, F.Ö., LeCheminant, A.N., and Sullivan, R.W.**
1991: Reconnaisance Nd isotopic study of granitoid rocks from the Baker Lake region, District of Keewatin, N.W.T., and observations on analytical procedures; *in* Radiogenic and Isotopic Studies: Report 4; Geological Survey of Canada, Paper 90-2, p. 101–112.

**Eade, K.E.**
1970: Geology of Ennedai Lake map-area (65C), District of Keewatin; Geological Survey of Canada, Paper 70-45, 19 p.
1972: Geology of Nueltin Lake and Edehon Lake (west half) map-areas, District of Keewatin; Geological Survey of Canada, Paper 72-21, 72 p.

**Hanmer, S.**
1997: Geology of the Striding-Athabasca mylonite zone, northern Saskatchewan and southeastern District of Mackenzie, Northwest Territories; Geological Survey of Canada, Bulletin 324, 92 p.

**Henderson, J.R.**
1983: Structure and metamorphism of the Aphebian Penrhyn Group and its Archean basement complex in the Lyon Inlet area, Melville Peninsula, District of Keewatin. Geological Survey of Canada Bulletin 324, 50 p.

**Henderson, J.R., and Roddick, J.C.**
1990: U-Pb age constraint on the Wager shear zone, District of Keewatin, N.W.T.; *in* Radiogenic Age and Isotopic Studies: Report 3; Geological Survey of Canada, Paper 89-2, p. 149–152

**Henderson, J.R., LeCheminant, A.N., Jefferson, C.W., Coe, K., and Henderson, M.N.**
1986: Preliminary account of the geology around Wager Bay, District of Keewatin; *in* Current Research, Part A; Geological Survey of Canada, Paper 86-1A, p. 159–176.

**Hoffman, P.F.**
1988: United Plates of America, the birth of a craton: early Proterozoic assembly and growth of North America; Annual Reviews Earth Science Letters, v. 16, p. 543–603.

**LeCheminant, A.N., Ashton, K.E., Chiarenzelli, J., Donaldson, J.A., Best, M.A., Tella, S., and Thompson, D.L.**
1983: Geology of Aberdeen Lake map area, District of Keewatin: Preliminary Report; *in* Current Research, Part A; Geological Survey of Canada, Paper 83-1A, p. 437–448

**LeCheminant, A.N., Ianelli, T.R., Zaitlan, B., and Miller, A.R.**
1981: Geology of Tebesjuak Lake map area, District of Keewatin: A Progress Report; *in* Current Research, Part B; Geological Survey of Canada, Paper 81-1B, p. 113–128.

**LeCheminant, A.N., Leatherbarrow, R.W., and Miller, A.R.**
1979: Thirty Mile Lake map area, District of Keewatin; *in* Current Research, Part B; Geological Survey of Canada, Paper 79-1B, p. 319–327

**LeCheminant, A.N., Miller, A.R., LeCheminant, G.M.**
1987a: Early Proterozoic alkaline igneous rocks, District of Keewatin, Canada: petrogenesis and mineralization; *in* Geochemistry and Mineralization of Proterozoic Volcanic Suites, (ed.) T.C. Pharaoh, R.D. Beckinsdale, and D. Rickard; Geological Society, Special Publication 33, p. 219–240.

**LeCheminant, A.N., Roddick, J.C., Tessier, A.C., and Bethune, K.M.**
1987b: Geology and U-Pb ages of early Proterozoic calc-alkaline plutons northwest of Wager Bay, District of Keewatin; *in* Current Research, Part A; Geological Survey of Canada, Paper 87-1A, p. 773–782

**Lewry, J.F.**
1981: Lower Proterozoic arc-microcontinent collisional tectonics in the western Churchill Province; Nature, v. 294, p. 69–72

**Lindh, A., and Persson, P.-O.**
1990: Proterozoic granitoid rocks of the Baltic Shield - trends of development; *in* Mid-Proterozoic Laurentia-Baltica, (ed.) C.F. Gower, T. Rivers, and B. Ryan; Geological Association of Canada, Special Paper 38, p. 23–40.

**Loveridge, W.D., Eade, K.E., and Roddick, J.C.**
1987: A U-Pb age on zircon from a granite pluton, Kamilukuak Lake area, District of Keewatin, establishes an upper limit for the age of the Christopher Island Formation, Dubawnt Group; *in* Radiogenic and Isotopic Studies: Report 1; Geological Survey of Canada, Paper 87-2, p. 67–71.

**MacRae, N.D., Armitage, A.E., Miller, A.R., Roddick, J.C., Jones, A.L., and Mudry, M.P.**
1996: The diamondiferous Akluilâk dyke, Gibson Lake area, N.W.T.; *in* Searching for Diamonds in Canada, (ed.) A.N. LeCheminant, D.G. Richardson, R.N.W. DiLabio, and K.E. Richardson, Open File 3228, p. 101–107.

**Park, A.F. and Ralser, S.**
1992: Precambrian geology of the southwestern part of the Tavani map area, District of Keewatin, Northwest Territories; Geological Survey of Canada, Bulletin 416, 81 p.

**Patterson, J.G. and LeCheminant, A.N.**
1985: A preliminary geological map of the northeastern Barren Grounds, parts of the District of Keewatin and Franklin; Geological Survey of Canada, Open File 1138, scale 1:1 000 000.

**Peterson, T.D.**
1994: Geology, Dubawnt River, N.W.T.; Geological Survey of Canada, Open File 2922, scale 1:500 000.

**Peterson, T.D. and Rainbird, R.H.**
1990: Tectonic and petrological significance of regional lamproite-minette volcanism in the Thelon and Trans-Hudson hinterlands, Northwest Territories; *in* Current Research, Part C; Geological Survey of Canada, Paper 90-1C, p. 69–79.

**Peterson, T.D., Esperança, S., and LeCheminant, A.N.**
1994: Geochemistry and origin of the Proterozoic ultrapotassic rocks of the Churchill Province, Canada; Mineralogy and Petrology, v. 51, p. 251–276.

**Rämö, O.T, and and Haapala, I.**
1990: The rapakivi granites of eastern Fennoscandia: a review with insights into their origin in the light of new Sm-Nd isotopic data; *in* Mid-Proterozoic Laurentia-Baltica, (ed.) C.F. Gower, T. Rivers, and B. Ryan; Geological Association of Canada, Special Paper 38, p. 401–415.

**Reinhardt, E.W. and Chandler, F.W.**
1973: Gibson-MacQuoid Lake map area, District of Keewatin; *in* Report of Activities, Part A; Geological Survey of Canada, Paper 73-1A, p. 162–165.

**Rock, N.M.S., Gaskarth, J.W., and Rundle, C.C.**
1986: Late Caledonian dyke-swarms in southern Scotland: a regional zone of primitive K-rich lamprophyres and associated vents; Journal of Geology, v. 94, p. 505–522.

**Roddick, J.C. and Miller, A.R.**
1994: An $^{40}Ar$-$^{39}Ar$ age from the REE-enriched Enekatcha ultrapotassic intrusive suite and implications for timing of ultrapotassic magmatism in the central Churchill Structural Province, N.W.T.; *in* Radiogenic Age and Isotope Studies: Report 8; Geological Survey of Canada, Current Research 1997-F, p. 1–31.

**Stern, R.A.**
1997: The GSC sensitive high resolution ion microprobe (SHRIMP): analytical techniques of zircon U-Th-Pb age determinations and performance evaluation; *in* Radiogenic Age and Isotope Studies: Report 10; Geological Survey of Canada, Current Research 1994-F, p. 69–74.

**Tella, S.**
1993: Geology, Chesterfield Inlet, District of Keewatin, Northwest Territories; Geological Survey of Canada, Open File 2756, scale 1:250 000.
1994: Geology, Amer Lake (66H), Deep Rose Lake (66G), and parts of Pelly Lake (66F), District of Keewatin, Northwest Territories; Geological Survey of Canada, Open File 2969, scale 1:250 000.
1997: Geology, Maguse River, N.W.T.; Geological Survey of Canada, Open File 3546, scale 1:1 000 000.

**Tella, S., Davis, W., Berman, R.G., Stern, R., and LeCheminant, A.N.**
1997: Tectonothermal history of the MacQuoid Lake supracrustal belt, District of Keewatin, Northwest Territories, Canada; Geological Society of America, Abstracts with Program, v. 29, p. A-277.

**Tella, S., Heywood, W.W., and Loveridge, W.D.**
1985: A U-Pb age on zircon from a quartz syenite intrusion, Amer Lake map area, District of Keewatin; *in* Current Research, Part B; Geological Survey of Canada, Paper 85-1B, p. 367–370.

**Tella, S., Roddick, J.C., and Davis, W.**
in press: Geochronological constraints on the multiple displacement history of the Amer mylonite zone, Churchill structural province, District of Keewatin, Northwest Territories, Canada; Geological Society of America, Abstracts with Program.

**Tella, S., Schau, M., Armitage, A.E., and Loney, B.C.**
1993: Precambrian geology and economic potential of the northeastern parts of Gibson Lake map area, District of Keewatin, Northwest Territories; *in* Current Research, Part C; Geological Survey of Canada, Paper 93-1C, p. 197–208.

**Thériault, R. J., Henderson, J. B., and Roscoe, S. M.,**
1994: Nd isotopic evidence for early to mid-Archean crust from high grade gneisses in the Queen Maud Block and south of the McDonald Fault, western Churchill Province, Northwest Territories; *in* Radiogenic Age and Isotopic Studies: Report 8; Current Research 1994-F, p. 37–42.

# A relative ice-flow chronology for the Keewatin Sector of the Laurentide Ice Sheet, Northwest Territories (Kivalliq region, Nunavut)[1]

I. McMartin and P.J. Henderson
Terrain Sciences Division, Ottawa

*McMartin, I. and Henderson, P.J., 1999: A relative ice-flow chronology for the Keewatin Sector of the Laurentide Ice Sheet, Northwest Territories (Kivalliq region, Nunavut);* in *Current Research 1999-C; Geological Survey of Canada, p. 129–138.*

**Abstract:** Systematic, ice-flow-indicator mapping in the Kivalliq region, Northwest Territories (Nunavut), suggests the following sequence of ice movements within the Keewatin Sector of the Laurentide Ice Sheet: 1) to the southwest, from a centre of ice flow located northeast of the study area, 2) to the south, from an undetermined position, 3) to the east-southeast, and 4) to the southeast, from a divide located northwest of the Keewatin Ice Divide. Ice flow from the Keewatin Ice Divide ranged from eastward to southward and observations suggest that the divide axis may lie slightly further to the northwest than originally thought. An old northward flow was also recognized around Yathkyed Lake, indicating that an ancestral ice divide existed southeast of the lake, prior to the southward flow. The ice-flow record reflects shifting ice-flow centres and the migration of an ice divide within the Laurentide Ice Sheet in Keewatin.

**Résumé :** La cartographie systématique des marques d'écoulement glaciaire dans la région de Kivalliq, Territoires du Nord-Ouest (Nunavut), révèle la succession suivante des mouvements glaciaires dans le secteur Keewatin de l'Inlandsis laurentidien: (1) mouvement vers le sud-ouest, depuis un centre d'écoulement situé au nord-est de la région d'étude; (2) mouvement vers le sud, depuis une localité indéterminée; (3) mouvement vers l'est-sud-est; et (4) mouvement vers le sud-est depuis une ligne de partage située au nord-ouest de la ligne de partage des glaces du Keewatin. La direction de l'écoulement glaciaire depuis la ligne de partage des glaces du Keewatin a varié d'est à sud. Les observations portent à croire que l'axe de la ligne de partage pourrait se situer un peu plus vers le nord-ouest que ce que l'on croyait à l'origine. Un ancien mouvement glaciaire vers le nord a été reconnu aux environs du lac Yathkyed et indique qu'une ancienne ligne de partage des glaces existait au sud-est du lac avant que ne se produise l'écoulement vers le sud. Ces mouvements glaciaires reflètent le déplacement de centres d'écoulement glaciaire et la migration d'une ligne de partage des glaces dans le secteur Keewatin de l'Inlandsis laurentidien.

[1] Contribution to the Western Churchill NATMAP Project

## INTRODUCTION

Ice-flow-indicator mapping has been undertaken in the Kivalliq region, Northwest Territories (Nunavut), by the Geological Survey of Canada as part of the Western Churchill NATMAP Project (Fig. 1). This work was initiated to provide ice-flow-indicator maps (10 sheets, 1:250 000), based on systematic mapping of glacial striae and other ice-inscribed, small-scale features on outcrops, and to build on the existing 1:125 000 scale GSC surficial geology maps. The objectives are 1) to improve our understanding of the glacial history in an area of complex ice flow and thick drift, 2) to test existing models on the inception, growth, and disintegration of the Keewatin Sector of the Laurentide Ice Sheet (Shilts, 1980; Andrews, 1982; Dyke et al., 1982; Boulton et al., 1985; Dyke and Prest, 1987; Boulton and Clark, 1990a, b), and 3) to assist mineral exploration. This paper reports preliminary data and interpretations, based on fieldwork undertaken in 1997 and 1998 in the MacQuoid, Gibson, Ferguson, and Kaminak Lakes areas (Fig. 1).

## PREVIOUS WORK

From observations gathered along the major waterways of the 'Barrens' in 1893 and 1894, Tyrrell (1897) was the first to report on the existence of a 'Keewatin Glacier' centered in the Keewatin District of the Northwest Territories. He proposed three stages in the growth and decline of the ice sheet from centres of outflow moving progressively to the southeast: 1) a centre north of Dubawnt Lake, 180 km northwest of the study area, from which the ice flowed southward as far south as the Manitoba–Northwest Territories boundary during ice buildup, 2) a centre northwest of Yathkyed Lake, immediately north of Tulemalu Lake, during full glacial maximum, and 3) several small centres of outflow during deglaciation as the ice sheet diminished in size, including one located "on the hills southeast of Yathkyed Lake, while another seems to have been located north of Baker Lake" (Tyrrell, 1897, p. 179F).

It was not until the early 1950s that new geological fieldwork provided a more detailed record of ice-flow indicators in Keewatin. With the advent of topographic maps, airphotos, and aircraft support, the Geological Survey of Canada launched three major field programs in the 'barren grounds': Operations Keewatin, Baker, and Thelon in 1952, 1954, and 1955, respectively (Wright, 1967). Regional mapping of 'surficial features' was included in all three programs and several maps and reports showing the orientation of streamlined landforms, eskers, and striae were published during the following years (Lord, 1953; Wright, 1955, 1957; Lee, 1959; Craig and Fyles, 1960). As a result of this work, Lee et al. (1957) defined the Keewatin Ice Divide as the zone occupied by the last glacial remnants of the Laurentide Ice Sheet west

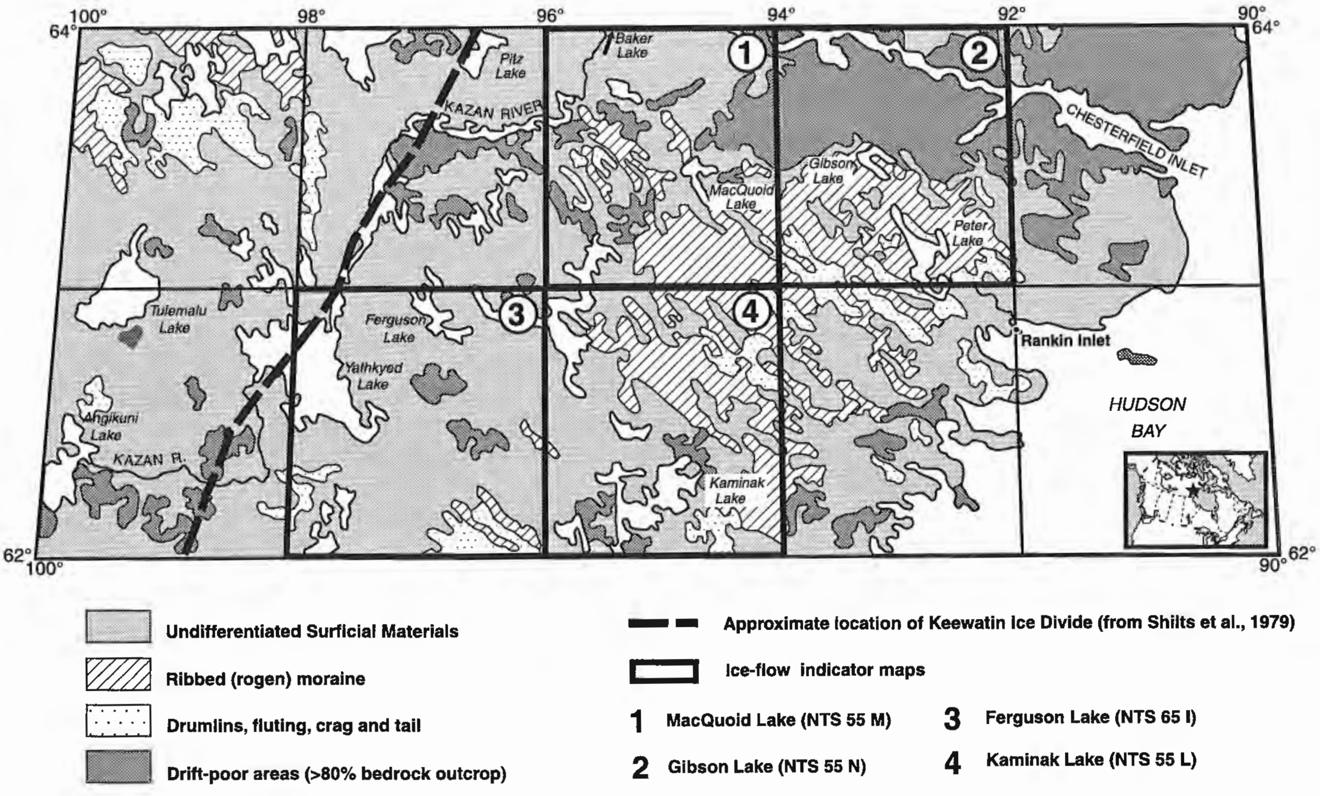


*Figure 1. Location map of study area within the Western Churchill NATMAP Project area showing the axis of the Keewatin Ice Divide. Background shows generalized surficial geology (modified from Aylsworth and Shilts, 1989).*

of Hudson Bay. During the same period, several university geologists collected striae data in selected areas of Keewatin (Bird, 1953; Neil and Putnam, 1955; Taylor, 1956) or compiled streamlined landforms based on airphoto interpretation (Dean, 1953; Downie et al., 1953). Conflicting observations on the sense of ice flow east of Baker and Yathkyed Lakes arose between the Geological Survey of Canada field geologists and most university workers. Nonetheless, most authors, with the exception of J.B. Tyrrell, E.M. Neil, and D.F. Putnam, accepted the model of a single dome centred over Hudson Bay during glacial maximum (Flint, 1943). Prest et al. (1968) summarized the work of Lee and others on the glacial map of Canada, showing crosscutting striae with undetermined relative ages. Andrews (1973) postulated a splitting of the dome into two late-glacial centres of outflow east and west of the bay.

In the early 1970s, the Geological Survey of Canada started a major field program in Keewatin based primarily on till sampling to assist mineral exploration. Ice-flow indicators suggesting pervasive glacial flow towards Hudson Bay and glacial dispersal trains of distinctive Dubawnt Supergroup lithologies extending southeast from Baker Lake to the coast provided new evidence supporting J.B. Tyrrell's concept of the 'Keewatin Ice Sheet' and redefined the Keewatin Ice Divide as a long-lived feature of the Laurentide Ice Sheet (Shilts and Boydell, 1974; Cunningham and Shilts, 1977; Kaszycki and Shilts, 1979; Shilts et al., 1979; Shilts, 1980, 1982). Aylsworth and Shilts (1989, p. 3) reported that "although the dispersal center had migrated eastward and southward...it probably migrated no more than 100 km". Whereas most of this work failed to recognized the significance of the relative ice-flow chronology identified earlier by Tyrrell (1897) and others in the 1950s, it showed convincing evidence against a long-term centre of an ice sheet over Hudson Bay.

In 1978, field work by Nadeau and Schau (1979), east of Baker Lake along Chesterfield Inlet, provided evidence for eastward transport of Dubawnt Group rocks and the existence of an ice-flow centre west of Baker Lake. As part of a detailed till-sampling and geochemical program in areas of gold mineralization zones in central Keewatin, Coker et al. (1992) determined the sequence of ice-flow directions and a possible old northward flow south of Yathkyed Lake. Based on field data accumulated in the 1970s, Klassen (1995) recognized the predominance of a southeastward flow in the Baker Lake area, from a divide located north and west of the last position of the Keewatin Ice Divide.

## ICE-FLOW CHRONOLOGY

Systematic ice-flow-indicator mapping was carried out in the Kaminak (NTS 55 L), Ferguson (NTS 65-I), MacQuoid (NTS 55 M), and Gibson (NTS 55 N) lakes areas during the summers of 1997 and 1998. Special attention was given to multidirectional faceted outcrops. This region is entirely located east of the Keewatin Ice Divide as defined by Shilts et al. (1979) (Fig. 1). The glacial erosional record is based on the measurement of the orientation of striae, grooves, rat tails, crescentic gouges, chattermarks, and roches moutonnées. Measurements were commonly taken on clean shoreline outcrops and on subhorizontal surfaces to avoid influence by local topography. The sense of movement was derived from rat tails, crescentic gouges, chattermarks, and roches moutonnées where present, or from stoss and lee topography. Relative ages of striated facets were interpreted based on the following criteria, summarized by Lundqvist (1990, p. 62): "a set located in a lee-side position relative to another, is usually older, a set just touching the top parts of the outcrop will have been formed by the youngest movement, and a set preserved only in depressions and other low positions may be interpreted as being older". We may add that a deeper set (groove) is usually older than a finer set (microstriae). However, along actively eroding shoreline, Veillette and Roy (1995) have shown that this is not always the case. A 'vanished protector' can be responsible for older striated surfaces appearing younger than they really are. The ice-flow-indicator maps presented here were compiled digitally (Fig. 2–5), based on new field observations, and glacial landforms (drumlins, eskers, ribbed moraines) obtained from existing surficial maps (Arsenault et al., 1981; Aylsworth et al., 1981a, b, 1984).

### *1) Southwestward flow*

One of the oldest ice flows in the study area was to the southwest, as recorded by isolated deep striae and grooves trending 209 to 235° (Fig. 2, 3, 5). In Chesterfield Inlet, and at one site along Kaminak Lake, this event appears to precede the regional southeastward event and all preceding events. Striae trending in a similar direction were reported at a few sites by Tyrrell (1897) in Chesterfield Inlet and south of the Thelon River along the Dubawnt River. Along the Ferguson River, he attributed them to a northeast flow. Taylor (1956) reported that the oldest record of ice flow in the Back River area north of the study area was to the southwest.

### *2a) Southward flow*

The second-oldest event is more pervasive throughout the four map areas, although it was not observed in the Yathkyed, Ferguson, and Parker Lakes areas. Ice flow during this event was southward and south-southeastward, as recorded by striae trending 151 to 181° preserved on protected sides of the striated surfaces formed by late southeastward flows (Fig. 2–5). This early southerly flow has been recorded sporadically by Tyrrell (1897), Lord (1953), and Lee (1959), and appears occasionally on the 1:125 000 scale GSC surficial geology maps. Evidence for southward glacial transport of erratics has been reported by Cunningham and Shilts (1977) in the Pitz Lake area, and by Shilts et al. (1979) based on the occurrence of Dubawnt erratics in till as far south as the Manitoba border (at least). Geochemical composition of till collected in drill core south of Pitz Lake indicates an early southward flow (Klassen, 1995).

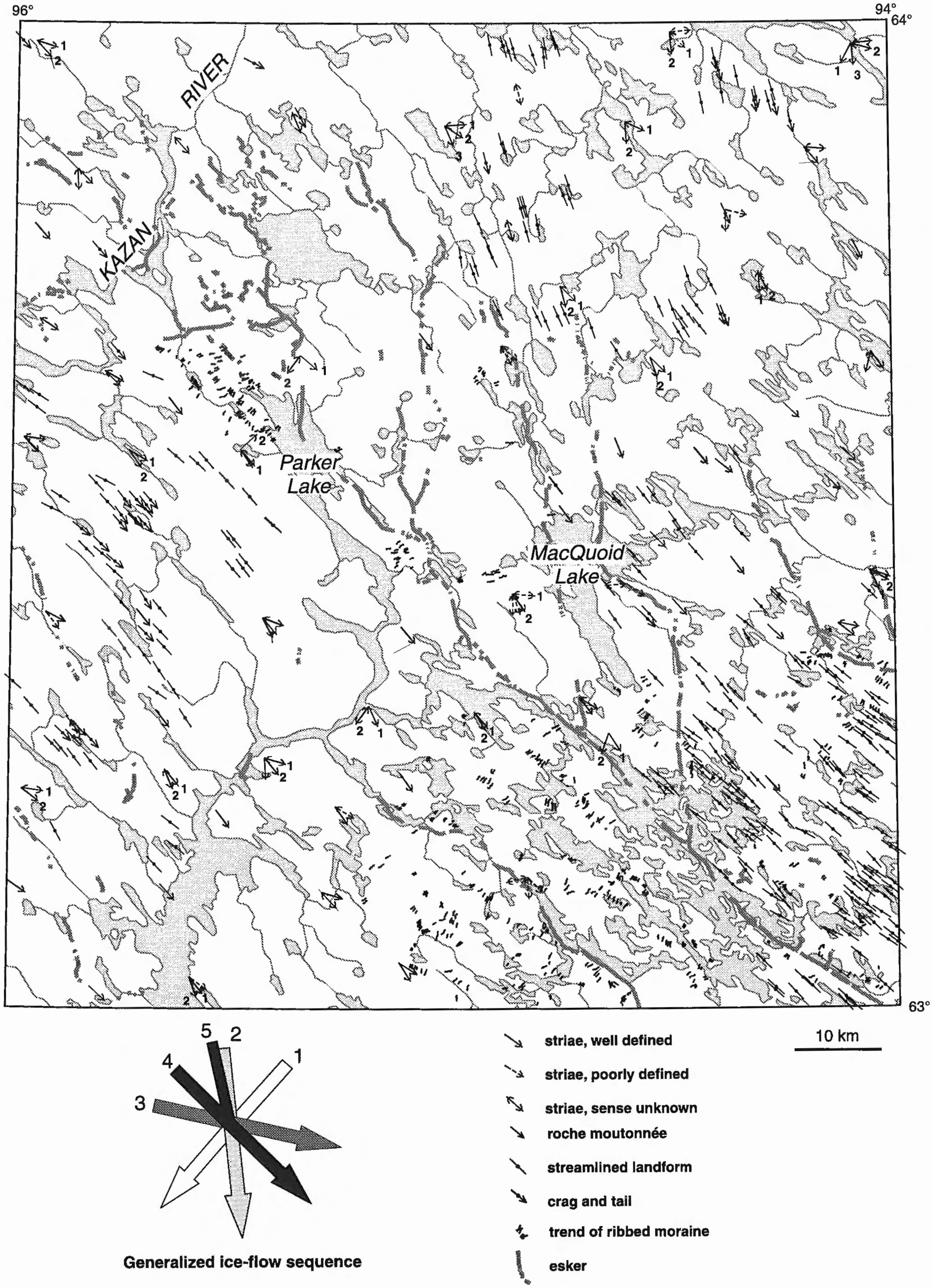


***Figure 2.*** *Ice-flow-indicator map of MacQuoid Lake area (NTS 55 M) compiled from glacial erosional record (1 = oldest). Glacial landforms (streamlined landforms, crag and tail, ribbed moraines, esker) were obtained from Aylsworth et al. (1981a).*

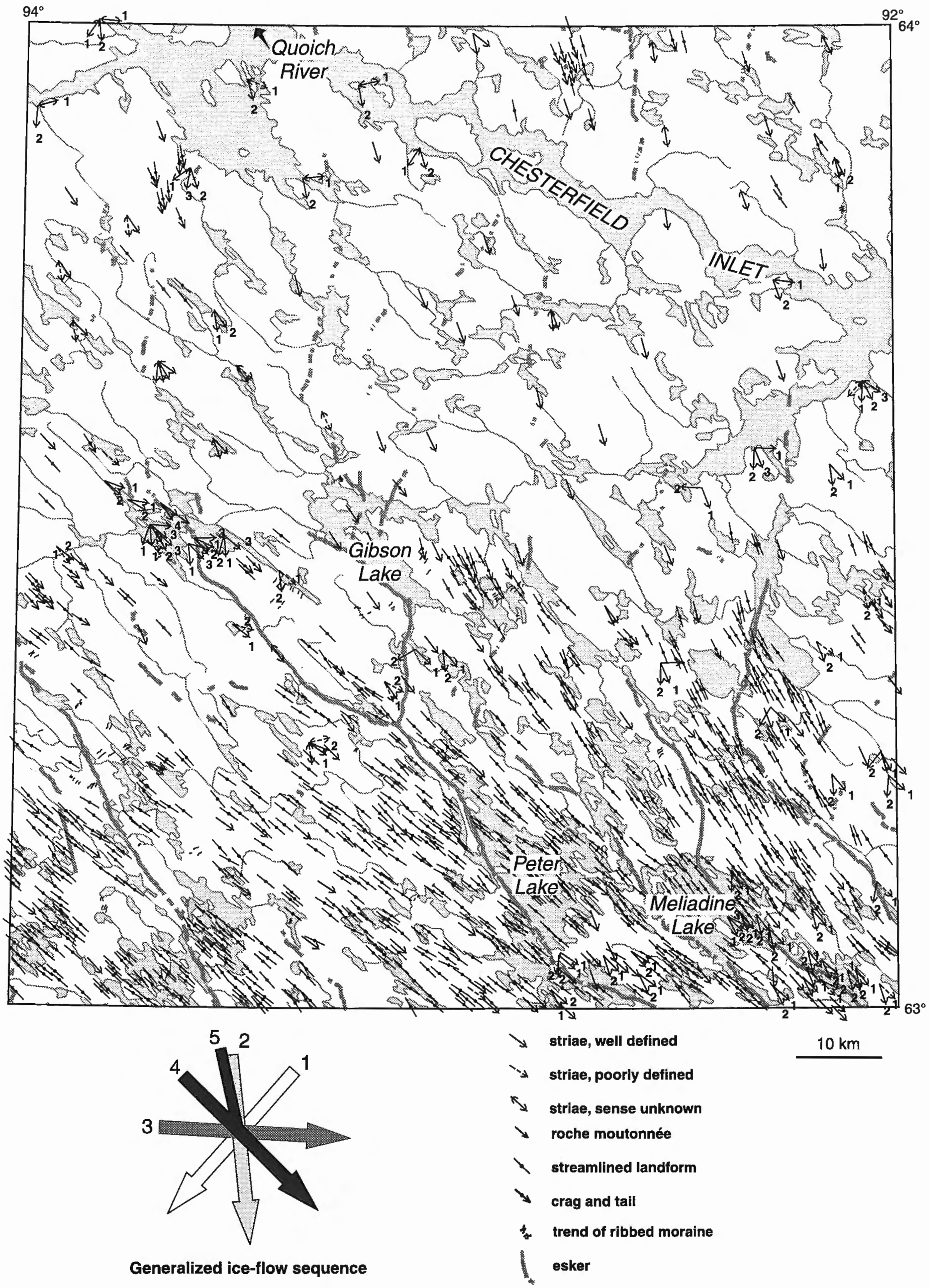


***Figure 3.*** *Ice-flow-indicator map of Gibson Lake area (NTS 55 N) compiled from glacial erosional record (1 = oldest). Glacial landforms (streamlined landforms, crag and tail, ribbed moraines, esker) were obtained from Aylsworth et al. (1984).*

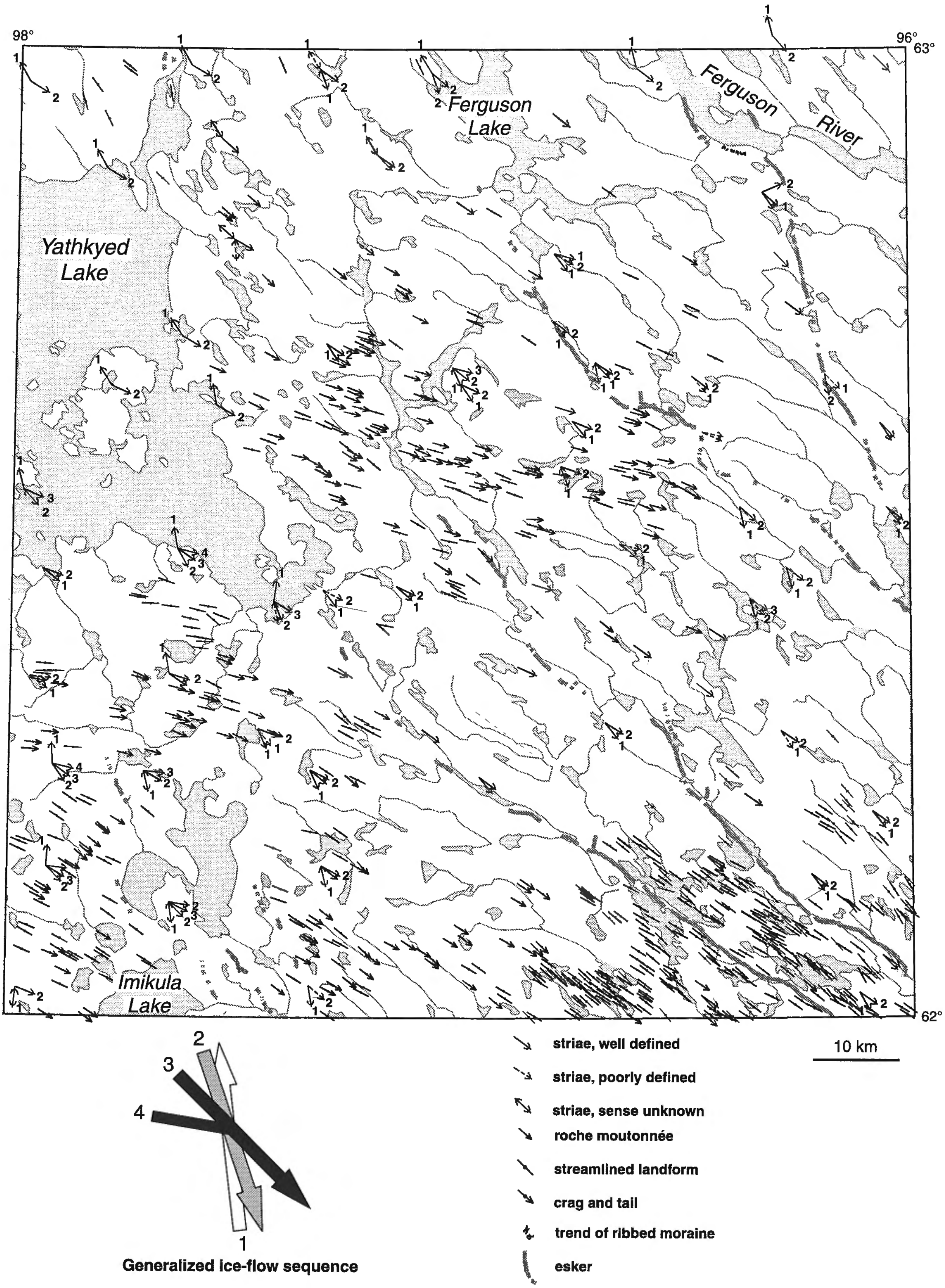


***Figure 4.*** *Ice-flow-indicator map of Ferguson Lake area (NTS 65-I) compiled from glacial erosional record (1 = oldest). Glacial landforms (streamlined landforms, crag and tail, ribbed moraines, esker) were obtained from Aylsworth et al. (1981b).*

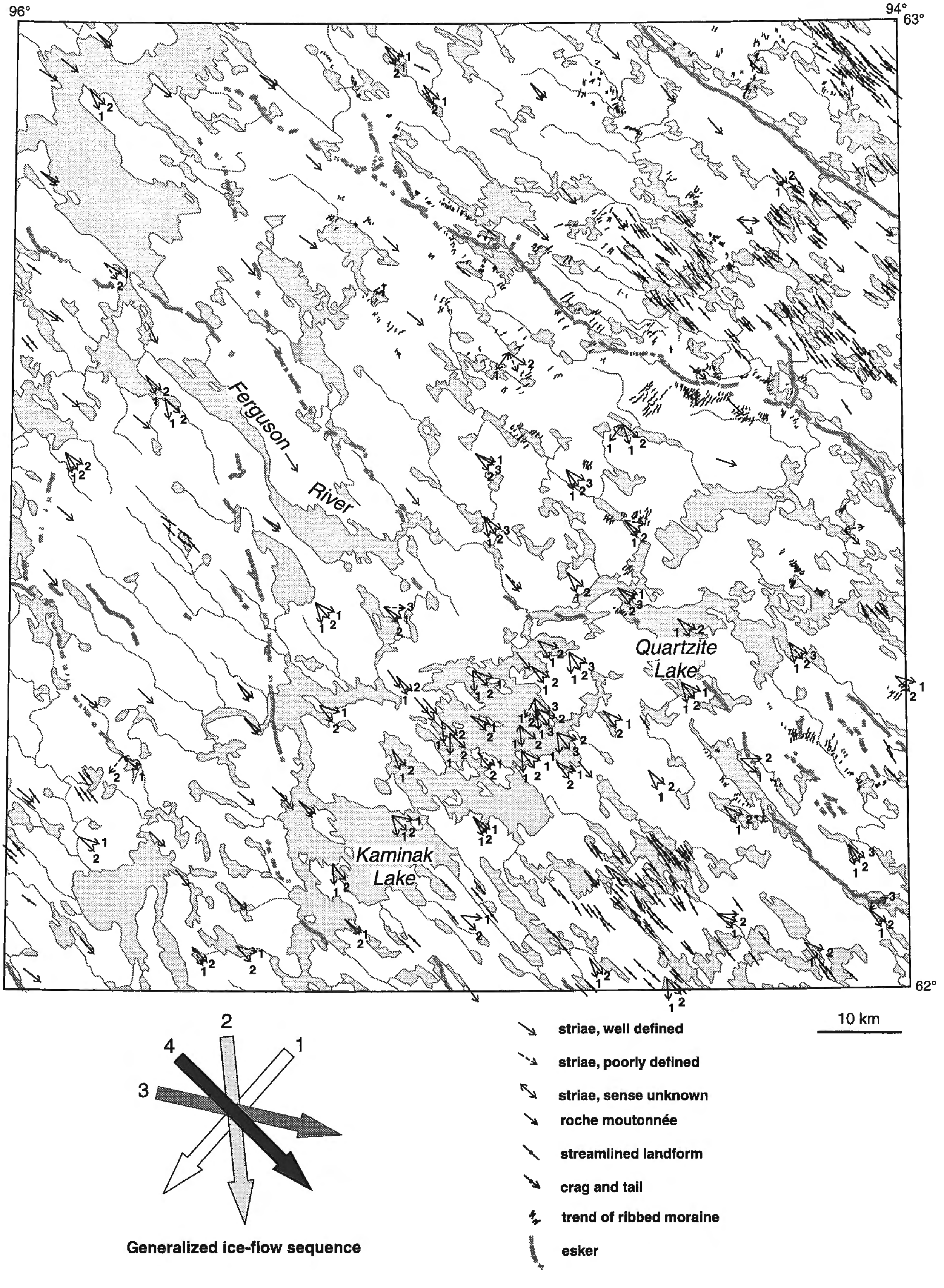


*Figure 5. Ice-flow-indicator map of Kaminak Lake area (NTS 55 L) compiled from glacial erosional record (1 = oldest). Glacial landforms (streamlined landforms, crag and tail, ribbed moraines, esker) were obtained from Arsenault et al. (1981).*

### *2b) Northward flow in the Yathkyed Lake area*

Northwest of a southwest-northeast-trending line which lies in between Imikula Lake and Ferguson River (Fig. 4), the sequence of ice-flow events preceding the predominant southeastward flow differs from the rest of the study area. The oldest ice-flow event in this area was towards the north and the northwest (324 to 006°). Numerous outcrops are moulded in two opposite directions, sometimes three, forming small trigonal pyramids, where each surface is generally well preserved and striated. This area is characterized by landforms with both southeast and north-northwest orientations adjacent to each other, low hummocky moraines, and the absence of eskers (Fig. 4). Erratic boulders of Proterozoic dolomite are found in the Yathkyed Lake greenstone belt and are interpreted to indicate northward transport from outcrops of Hurwitz Group rocks at Imikula Lake. The northward flow appears to be postdated by the southward flow. Based on northward-flowing indicators measured along the northern shore of Yathkyed Lake, Tyrrell (1897) defined the presence of a late centre of outflow southeast of Yathkyed Lake during deglaciation. However, along Ferguson Lake, Tyrrell (1897) found a similar set of striae which he thought was older than the main southeast event. The lack of outcrop has prevented confirmation of Tyrrell's younger northward flow on the northern shore of Yathkyed Lake. Where age relationships were defined, the northward flow was always found to predate the southeastward event. Lord (1953) also reported an old northward flow west of Imikula Lake. Over the fine-grained mafic volcanic rocks of the Yathkyed Lake greenstone belt, Coker et al. (1992) reported an early set of striae, indicating a probable northerly ice-flow direction.

### *3) Eastward flow*

The third-oldest regional event was basically eastward, and evidence is found mainly in the Kaminak Lake (99 to 124°) and MacQuoid Lake (88 to 110°) map areas (Fig. 2, 5), and in the northern Gibson Lake map area (75 to 114°) (Fig. 3). Age relationships interpreted at a few sites suggest that it postdated the southward flow and occurred immediately before the main regional southeastward flow. North of Chesterfield Inlet, Nadeau and Schau (1979) have observed roches moutonnées indicating a pervasive eastward flow preceding the last and main south-southeastward flow in that region, and eastward transport of red erratics as far east as the Quoich River. In sections along the Kazan River south of Baker Lake, Klassen (1995) reported that the lower till was deposited by ice flowing eastward prior to the southeastward ice flow. Along the coast east of Rankin Inlet, the recently emerged bedrock outcrops show well preserved surfaces striated at 114 to 122° (McMartin, 1998).

### *4) Main regional southeastward flow*

In the four map areas, dominant striae and roches moutonnées trend 95 to 177° (Fig. 2–5), indicating a regional ice-flow event to the southeast, as recorded earlier by Tyrrell (1897), Lord (1953), Neil and Putnam (1955), Wright (1955), Lee (1959), Shilts and Boydell (1974), Shilts et al. (1979), and Coker et al. (1992). Drumlinoid landforms and eskers follow this regional trend. In the Yathkyed Lake area, ice-flow indicators record a shift from an early southeastward to an eastward direction. At several sites, two or three sets of striae indicate this counterclockwise shift (Fig. 4). This sequence is reversed in the Chesterfield Inlet area and north of MacQuoid Lake (Fig. 2, 3), where the striation record indicates a clockwise shift from southeastward to a more southerly direction. These late shifts are related to ice flowing from the Keewatin Ice Divide. The regional southeastward flow is the predominant direction of glacial transport within the study area (Shilts, 1973; Ridler and Shilts, 1974; DiLabio, 1979; Coker et al., 1992; Klassen, 1995) and explains the strong southeastward glacial dispersal train of Dubawnt Supergroup rocks which extends to the coast of Hudson Bay and beyond (Kaszycki and Shilts, 1979; Shilts et al., 1979; Shilts, 1980).

### *5) Late convergence of flow towards eskers*

In the vicinity of large continuous eskers which traverse the area, ice-flow indicators younger than the main southeast regional set are found at right angles or oblique to the esker direction (Fig. 2–5), suggesting lateral movements of ice towards the esker ridge (Repo, 1954; Kaszycki and DiLabio, 1986; Veillette, 1986). Within these corridors (<3–4 km), the regional southeast-trending striae and drumlins are generally preserved. In some areas however, for example, along parts of the eskers in the Peter Lake and Meliadine Lake area (Fig. 3), the late convergence of flow dominates the landscape such that DeGeer moraines, and more rarely ribbed moraines, are reoriented obliquely to the southeast-trending drumlins (McMartin, 1998).

## DISCUSSION

Observations of glacial erosional features collected in 1997–1998 between Yathkyed Lake and Chesterfield Inlet suggest that there have been at least four distinct regional ice movements within the Keewatin Sector of the Laurentide Ice Sheet in Keewatin. 1) The earliest advance was to the southwest, from an outflow centre located northeast of the study area. 2) The southwestward flow was succeeded by a regional southward flow originating from an undetermined position north of the study area. 3) A regional east-southeastward flow preceded the main southeast event. 4) Finally, the predominant southeastward event occurred throughout the study area, from a divide located north and west of the study area, and northwest of the axis of the Keewatin Ice Divide. An old northward flow found in the Yathkyed Lake area suggests that an ancestral ice divide existed southeast of the lake, prior to the southward flow.

Ice flow from the Keewatin Ice Divide ranged from eastward to southward within the four map areas under study. This flow reflects the arcuate configuration of the divide in Keewatin. On the northwestern side of the divide, in the Baker Lake area, Klassen (1995) has shown that the final northwestward ice flow had minimal effect on drift composition. North of Yathkyed Lake, age relationships between north-northwestward and southeastward ice-flow indicators were not clearly defined, although they tend to suggest that the current position of the axis of the Keewatin Ice Divide, as shown by Shilts et al. (1979), may lie slightly further to the northwest.

The sequence of ice flows presented here shows that a zone of outflow within the Laurentide Ice Sheet existed in Keewatin, possibly through much of its Wisconsinan history, as proposed by Shilts (1980). On the other hand, the numerous multifaceted outcrops in the study area indicate shifting ice-flow centres, where relatively slight shifts in either the configuration or location of the zone of outflow, or both, produced large changes in ice-flow directions (Boulton and Clark, 1990a, b). Based on the compilation of glacial lineations from satellite images, Boulton and Clark (1990a, b) suggested that the Laurentide Ice Sheet had a dynamic behaviour, with shifts in the location of centres of mass up to 1000–2000 km, and that erratic dispersal patterns, such as the Dubawnt train, could reflect changing, rather than stable, patterns of flow.

Since the 1970s, little has been published on ice-flow indicators in Keewatin. However, several workers have continued to propose models on the history of the Laurentide Ice Sheet and the Keewatin Ice Divide. Models that suggest a long-term centre of an ice sheet over Hudson Bay during the Late Wisconsinan Maximum (Flint, 1943; Denton and Hughes, 1981) are not supported by the striation record presented in this paper. However, some of the existing models are in part compatible with our observations. Andrews (1973) delimited six possible centres of outflow on the basis of the intersections of strandline tilt directions, including one near Chesterfield Inlet and one at the eastern end of Great Slave Lake, which is in agreement with either the southward or the eastward striations recorded in the study area. Dyke and Prest (1987) and Dyke and Dredge (1989) postulated an eastward migration of up to 500 km for a dome centred in central Keewatin (from 18 to 9 ka), with associated east-southeastward ice-flow lines. Boulton and Clark (1990b) suggested an early outflow position of early Wisconsinan age in northeast Keewatin (Flow stage A, p. 338), agreeing with the old southwestward flow presented here. These authors also positioned an early centre of outflow approximately 250 km north of the study area (Flow Stage B, p. 338), compatible with the old southward striations, and identified a southeastern shift in an ice divide centred in Keewatin during the growth, maximum extent, and decay of the Laurentide Ice Sheet. The results presented in this paper will further constrain these models.

Ice-flow-indicator mapping and stratigraphic studies to the north and west of Yathkyed Lake will provide additional information to establish regional ice-flow events in the area of the Keewatin Ice Divide. Detailed surficial mapping and till-provenance studies have been initiated in the Rankin Inlet and MacQuoid Lake areas to support mineral exploration over poorly exposed greenstone belts.

## ACKNOWLEDGMENTS

Special thanks to S. Khan, W. Carter, and C. St-Pierre for assistance in the field. We are grateful to C. Relf (Indian and Northern Affairs Canada) and D. Irwin (Government of the Northwest Territories) for providing logistical support in the Yathkyed Lake area in 1997. We would also like to thank S. Hanmer and the GSC bedrock-mapping group at Kaminak Lake and Gibson Lake camps for sharing logistics, mapping expertise, and field assistance. J.J. Veillette provided a thoughtful review. This study was funded by the Western Churchill NATMAP Project. Polar Continental Shelf Project provided helicopter support.

## REFERENCES

**Andrews, J.T.**
1973: The Wisconsin Laurentide Ice Sheet: dispersal centers, problems of retreat, and climatic implications; Arctic and Alpine Research, v. 5, p. 185–199.
1982: On the reconstruction of Pleistocene ice sheets: a review; Quaternary Science Reviews, v. 1, p. 1–30.

**Arsenault, L., Aylsworth, J.M., Kettles, I.M., and Shilts, W.W.**
1981: Surficial geology, Kaminak Lake, District of Keewatin; Geological Survey of Canada, Map 7-1979, scale 1:125 000.

**Aylsworth, J.M. and Shilts, W.W.**
1989: Glacial features around the Keewatin Ice Divide: districts of MacKenzie and Keewatin; Geological Survey of Canada, Paper 88-24, 21 p.

**Aylsworth, J.M., Boydell, A.N., Cunningham, C.M., and Shilts, W.W.**
1981a: Surficial geology, MacQuoid Lake, District of Keewatin; Geological Survey of Canada, Map 11-1980, scale 1:125 000.

**Aylsworth, J.M., Boydell, A.N., and Shilts, W.W.**
1984: Surficial geology, Gibson Lake, District of Keewatin; Geological Survey of Canada, Map 1-1984, scale 1:125 000.

**Aylsworth, J.M., Cunningham, C.M., and Shilts, W.W.**
1981b: Surficial geology, Ferguson Lake, District of Keewatin; Geological Survey of Canada, Map 2-1979, scale 1:125 000.

**Bird, J.B.**
1953: The glaciation of Central Keewatin, Northwest Territories, Canada; American Journal of Science, v. 251, p. 215–230.

**Boulton, G.S. and Clark, C.D.**
1990a: A highly mobile Laurentide ice sheet revealed by satellite images of glacial lineations; Nature, v. 346, p. 813–817.
1990b: The Laurentide ice sheet through the last glacial cycle: the topology of drift lineations as a key to the dynamic behaviour of former ice sheets; Transactions of the Royal Society of Edinburgh, v. 81, p. 327–347.

**Boulton, G.S., Smith, G.D., Jones, A.S., and Newsome, J.**
1985: Glacial geology and glaciology of the last mid-latitude ice sheets; Journal of the Geological Society of London; v. 142, p. 447–474.

**Coker, W.B., Spirito, W.A., DiLabio, R.N.W., and Hart, B.R.**
1992: Geochemistry (till, gossan and lake sediment - Au and PGE) and surficial geology of the Ferguson, Yathkyed and Contwoyto Lakes areas, NWT; *in* Geological Survey of Canada, Open File 2484, p. 93–97.

**Craig, B.G. and Fyles, J.G.**
1960: Pleistocene geology of Arctic Canada; Geological Survey of Canada, Paper 60-10, 21 p.

**Cunningham, C.M. and Shilts, W.W.**
1977: Surficial geology of the Baker Lake area, District of Keewatin; *in* Report of Activities, Part B, Geological Survey of Canada, Paper 77-1B, p. 311–314.

**Dean, W.G.**
1953: The drumlinoid landforms of the "Barren Grounds", N.W.T.; The Canadian Geographer, no. 3, p. 19–30.

**Denton, G.H. and Hughes, T.J. (Ed.)**
1981: The last great ice sheets; John Wiley and Sons, New York, 484 p.

**DiLabio, R.N.W.**
1979: Drift prospecting in uranium and base-metal mineralization sites, District of Keewatin, Northwest Territories, Canada; *in* Prospecting in areas of glaciated terrain, Institute of Mining and Metallurgy, London, p. 91–100.

**Downie, M.J., Evans, A.G., and Wilson, J.T.**
1953: Glacial features between the Mackenzie River and Hudson Bay plotted from air photographs; Geological Society of America Bulletin, v. 64, p. 1413–1414.

**Dyke, A.S. and Dredge, L.A.**
1989: Quaternary geology of the northwestern Canadian Shield; *in* Chapter 3 of Quaternary Geology of Canada and Greenland, (ed.) R.J. Fulton; Geological Survey of Canada, Geology of Canada, no. 1, p. 189–214 (*also* Geological Society of America, The Geology of North America, v. K-1, p. 189–214).

**Dyke, A.S. and Prest, V.K.**
1987: Late Wisconsinan and Holocene history of the Laurentide Ice Sheet; Géographie physique et Quaternaire, v. 41, no. 2, p. 237–263.

**Dyke, A.S., Dredge, L.A., and Vincent, J.-S.**
1982: Configuration and dynamics of the Laurentide Ice Sheet during the Late Wisconsin Maximum; Géographie physique et Quaternaire, v. 36, no. 1–2, p. 5–14.

**Flint, R.F.**
1943: Growth of the North American ice sheet during the Wisconsin age; Geological Society of America Bulletin, v. 54, p. 325–362.

**Kaszycki, C.A. and DiLabio, R.N.W.**
1986: Surficial geology and till geochemistry, Lynn Lake–Leaf Rapids region, Manitoba; *in* Current Research, Part B, Geological Survey of Canada, Paper 1986-1B, p. 245–256.

**Kaszycki, C.A. and Shilts, W.W.**
1979: Average depth of glacial erosion, Canadian Shield; *in* Current Research, Part B, Geological Survey of Canada, Paper 1979-1B, p. 395–396.

**Klassen, R.A.**
1995: Drift composition and glacial dispersal trains, Baker Lake area, District of Keewatin, Northwest Territories; Geological Survey of Canada, Bulletin 485, 68 p.

**Lee, H.A.**
1959: Surficial geology of southern District of Keewatin and the Keewatin Ice Divide, Northwest Territories; Geological Survey of Canada, Bulletin 51, 42 p.

**Lee, H.A., Craig, B.G., and Fyles, J.G.**
1957: Keewatin Ice Divide; Geological Society of America Bulletin, v. 68, no. 12, pt. 2, p. 1760–1761.

**Lord, C.S.**
1953: Geological notes on the southern District of Keewatin; Geological Survey of Canada, Paper 53-22, 11 p.

**Lundqvist, J.**
1990: Glacial morphology as an indicator of the direction of glacial transport; *in* Glacial Indicator Tracing, (ed.) R. Kujansuu and M. Saarnisto; Balkema, Rotterdam, Netherlands, p. 61–70.

**McMartin, I.**
1998: Surficial mapping and till provenance studies in the Meliadine Trend, Rankin Inlet area: a progress report; *in* Program and Abstracts of Talks and Posters, 1998 Geoscience Forum, Yellowknife, NWT Chamber of Mines, p. 78–80.

**Nadeau, L. and Schau, M.**
1979: Surficial geology near the mouth of the Quoich River, District of Keewatin; *in* Current Research, Part A, Geological Survey of Canada, Paper 79-1A, p. 389–390.

**Neil, E.M. and Putnam, D.F.**
1955: Observations concerning the Keewatin Centre of Glaciation; The Canadian Geographer, no. 5, p. 29–32.

**Prest, V.K., Grant, D.R., and Rampton, V.N.**
1968: Glacial map of Canada, Geological Survey of Canada, Map 1253A, scale 1:5 000 000.

**Repo, R.**
1954: Om forhallandet mellan rafflor och asar (in Finnish) (On the relationship between eskers and striae); Geologi, v. 6, no. 5, p. 45.

**Ridler, R.H. and Shilts, W.W.**
1974: Exploration for Archean polymetallic sulphide deposits in permafrost terrains: an integrated geological/geochemical technique; Kaminak Lake area, District of Keewatin; Geological Survey of Canada, Paper 73-34, 33 p.

**Shilts, W.W.**
1973: Drift prospecting; geochemistry of eskers and till in permanently frozen terrain: District of Keewatin; Northwest Territories; Geological Survey of Canada, Paper 72-45, 34 p.
1980: Flow patterns in the central North American ice sheet; Nature, v. 286, no. 5770, p. 213–218.
1982: Quaternary evolution of the Hudson/James Bay region; Naturaliste canadien, v. 109, p. 309–332.

**Shilts, W.W. and Boydell, A.N.**
1974: Terrain mapping in the Churchill–Chesterfield Inlet corridor, District of Keewatin; *in* Current Research, Part A, Geological Survey of Canada, Paper 74-1A, p. 253–256.

**Shilts, W.W., Cunningham, C.M., and Kaszycki, C.A.**
1979: Keewatin Ice Sheet — re-evaluation of the traditional concept of the Laurentide Ice Sheet; Geology, v. 7, p. 537–541.

**Taylor, R.S.**
1956: Glacial geology of north-central Keewatin, Northwest Territories, Canada; Bulletin of the Geological Society of America, v. 67, p. 943–956.

**Tyrrell, J.B.**
1897: Report on the Doobaunt, Kazan and Ferguson rivers and the north-west coast of Hudson Bay; Geological Survey of Canada, Annual Report, no. 618, p. 1F–218F.

**Veillette, J.J.**
1986: Former southwesterly ice flows in the Abitibi–Timiskaming region: implications for the configuration of the late Wisconsinan ice sheet; Canadian Journal of Earth Sciences, v. 23, p. 1724–1741.

**Veillette, J.J. and Roy, M.**
1995: The spectacular cross-striated outcrops of James Bay, Quebec; *in* Current Research 1995-C, Geological Survey of Canada, p. 243–248.

**Wright, G.M.**
1955: Geological notes on Central District of Keewatin, Northwest Territories; Geological Survey of Canada, Paper 55-17, 17 p.
1957: Geological notes on Eastern District of Keewatin, Northwest Territories; Geological Survey of Canada, Paper 56-10, 23 p.
1967: Geology of the southeastern barren grounds, parts of the Districts of Mackenzie and Keewatin; Geological Survey of Canada, Memoir 350, 91 p.

Geological Survey of Canada Project 960007

# Tectonic assembly and Proterozoic reworking of the northern Yathkyed greenstone belt, Northwest Territories (Nunavut)[1]

C. Relf[2], K. MacLachlan,[3] and D. Irwin[3]
Continental Geoscience Division, Ottawa

*Relf, C., MacLachlan, K., and Irwin, D., 1999: Tectonic assembly and Proterozoic reworking of the northern Yathkyed greenstone belt, Northwest Territories (Nunavut);* in *Current Research 1999-C; Geological Survey of Canada, p. 139–146.*

**Abstract:** Regional mapping in the Yathkyed greenstone belt has revealed two distinct tectonostratigraphic units in the hanging wall of the Tyrrell shear zone. The geometrically lower tectonostratigraphic unit comprises mainly amphibolite and monzogranite, whereas the structurally higher unit consists of a package of mixed flows and associated volcaniclastic and clastic sedimentary rocks intruded by foliation-parallel sheets of tonalite. A shear zone of unknown displacement sense separates the two tectonostratigraphic units. The Tyrrell shear zone at the base of the greenstone belt records early (possibly Archean) reverse displacement, followed by Paleoproterozoic dextral-normal movement.

Foliation-parallel gossans with strike lengths up to 3 km and alteration assemblages containing sericite±chlorite±carbonate were documented in volcanic rocks of the upper tectonostratigraphic unit. The timing of formation of these mineralized zones is unclear, although evidence for a Proterozoic thermal overprint suggests late remobilization of metals may have contributed to the mineral potential of the area.

**Résumé :** La cartographie régionale de la ceinture de roches vertes de Yathkyed a mis en évidence deux unités tectonostratigraphiques distinctes dans le toit de la zone de cisaillement de Tyrrell. L'unité tectonostratigraphique géométriquement inférieure est composée essentiellement d'amphibolite et de monzogranite, alors que l'unité structuralement plus élevée est constituée d'un assemblage de coulées mélangées et de roches volcanoclastiques et sédimentoclastiques associées que recoupent des feuillets de tonalite parallèles à la foliation. Une zone de cisaillement dont le sens de déplacement est inconnu sépare les deux unités tectonostratigraphiques. La zone de cisaillement de Tyrrell située à la base de la ceinture de roches vertes témoigne d'un déplacement inverse précoce (possiblement Archéen), suivi d'un mouvement dextre normal au Paléoprotérozoïque.

Des chapeaux de fer parallèles à la foliation, d'une longueur de jusqu'à 3 km parallèlement à la direction, et des assemblages d'altération contenant de la séricite±chlorite±fuchsite ont été observés dans des roches volcaniques de l'unité tectonostratigraphique supérieure. La chronologie de la formation de ces zones minéralisées est mal connue, mais des indices d'une surimpression thermique au Protérozoïque donnent à penser qu'une remobilisation tardive des métaux a peut-être contribué au potentiel minéral de la région.

[1] A contribution to the Western Churchill NATMAP
[2] Geology Division, Department of Indian Affairs and Northern Development, P.O. Box 1500, Yellowknife, Northwest Territories X1A 2R3
[3] Resources, Wildlife and Economic Development, Government of the Northwest Territories, P.O. Box 1320, Yellowknife, Northwest Territores X1A 2L9

## INTRODUCTION

This paper reports results from the third and final summer of bedrock mapping in the Yathkyed Lake area, western Churchill Province. The project was funded jointly by the Department of Resources, Wildlife and Economic Development, Government of the Northwest Territories, and the Northwest Territories Geology Division, Department of Indian Affairs and Northern Development Canada. The project provided support for the field components of an M.Sc. and a B.Sc. thesis study. Collaborative geochemical, geochronological, and thermobarometric studies are being carried out by the Geological Survey of Canada under the auspices of the Western Churchill NATMAP Project. Results of these concurrent studies will be reported elsewhere.

Previous geological work in the Yathkyed Lake area (Eade, 1985, 1986; assessment reports; Geological Survey of Canada, 1981) provided evidence for a possible tectonic break along the southeastern margin of the Yathkyed greenstone belt, and highlighted gaps in the internal stratigraphy of the belt. Mapping during the first two years of the current project (Relf, 1996; Irwin et al., 1998) revealed that 1) the greenstone belt may comprise two lithologically distinct packages of volcanic and associated sedimentary rocks; 2) the belt may be an overturned panel that was thrust southeastward (present co-ordinates) along the Tyrrell shear zone during the late Archean; and 3) the Paleoproterozoic tectonothermal overprint was significant in this part of the Churchill Province, and included an episode of north-south crustal extension (Relf et al., 1997; 1998; MacLachlan et al., 1998). Mapping during 1998 focused on further delineating map units and unravelling their deformation histories; tracing the Tyrrell shear zone northeastward from 1997 mapping; and distinguishing Proterozoic from Archean structural elements.

## REGIONAL GEOLOGICAL SETTING

The study area (Fig. 1) is located about 300 km west-southwest of Rankin Inlet, Northwest Territories (Kivalliq region of Nunavut), and is underlain by Archean metavolcanic and metasedimentary rocks, intruded by syn- to post-tectonic granitoid rocks. Paleoproterozoic sedimentary rocks unconformably overlie the greenstone belt, and are locally crosscut by granitoid veins and east-trending, diabase dykes tentatively correlated with the ca. 2.19 Ga Tulemalu swarm (LeCheminant et al., 1997).

Rocks of the greenstone belt were interpreted to define a regionally overturned, northwest-dipping panel that is bound along its southeastern margin (structural base) by the Tyrrell shear zone (Relf et al., 1998). Early displacement along the Tyrrell shear zone involved oblique (sinistral) reverse displacement and was followed by dextral movement accompanied by north-south extension. The early displacement is interpreted to have occurred at ca. 2.62 Ga based on a syntectonic granitoid dyke (K. MacLachlan, unpub. data, 1998), and may represent a regional shortening event during which the greenstone belt was thrust southeastward (present co-ordinates) above a package of mixed granitoid and orthogneiss units. These rocks locally contain abundant amphibolite-grade supracrustal screens which may be related to the Kaminak greenstone belt. Subsequent dextral shearing, after ca. 1.82 Ga (K. MacLachlan, unpub. data, 1998) may have coincided with uplift of the proposed metamorphic core complex at Nowyak Lake, 60 km to the southwest in the 1996 map area (Relf et al., 1997; *see* Fig. 1).

## MAP UNITS

Archean rocks in the study area can be subdivided into three broad units based on their tectonostratigraphic position (*see* Fig. 2). Two of these units sit above the Tyrrell shear zone,

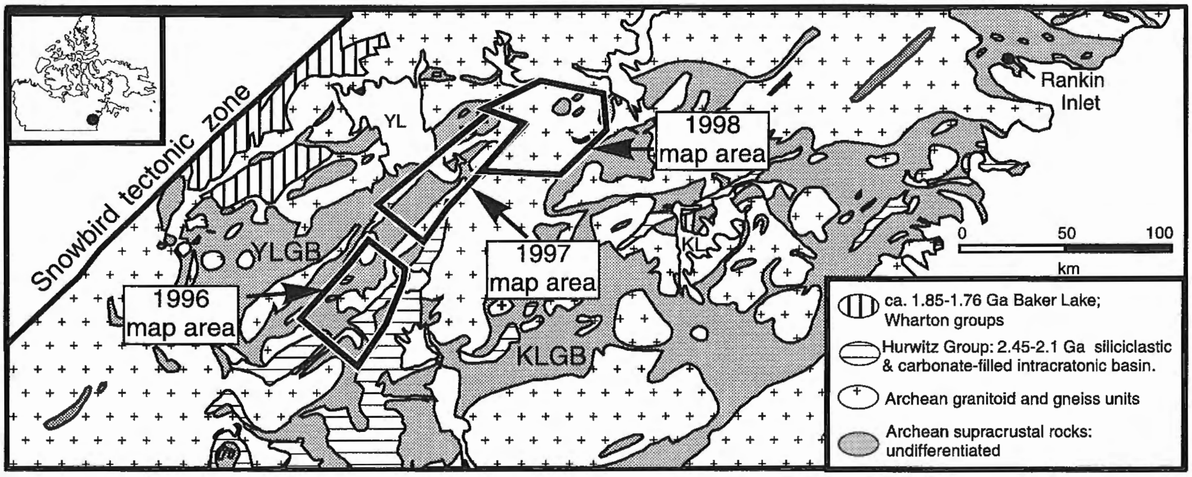


***Figure 1.*** *Simplified geology of part of the western Churchill Province, showing location of study area. YLGB, Yathkyed Lake greenstone belt; KLGB, Kaminak Lake greenstone belt; YL, Yathkyed Lake; KL, Kaminak Lake. Modified after Aspler and Chairenzelli (1996).*

and are referred to in the following sections as the structurally higher and lower tectonostratigraphic units. The third unit includes all rocks in the footwall of the Tyrrell shear zone. The relationships between the three units and the shear zones that bound them are discussed further in a later section (*see* 'Tectonostratigraphic relations').

### *Higher tectonostratigraphic unit*

Supracrustal rocks of the higher tectonostratigraphic unit include a package of mixed volcanic and associated volcaniclastic rocks and psammitic to pelitic sedimentary rocks. The contact between the sedimentary rocks and mixed volcanic package is transitional, and is marked by interlayered psammite units and volcaniclastic rocks. The supracrustal sequence is intruded by sheets of foliation-parallel biotite tonalite.

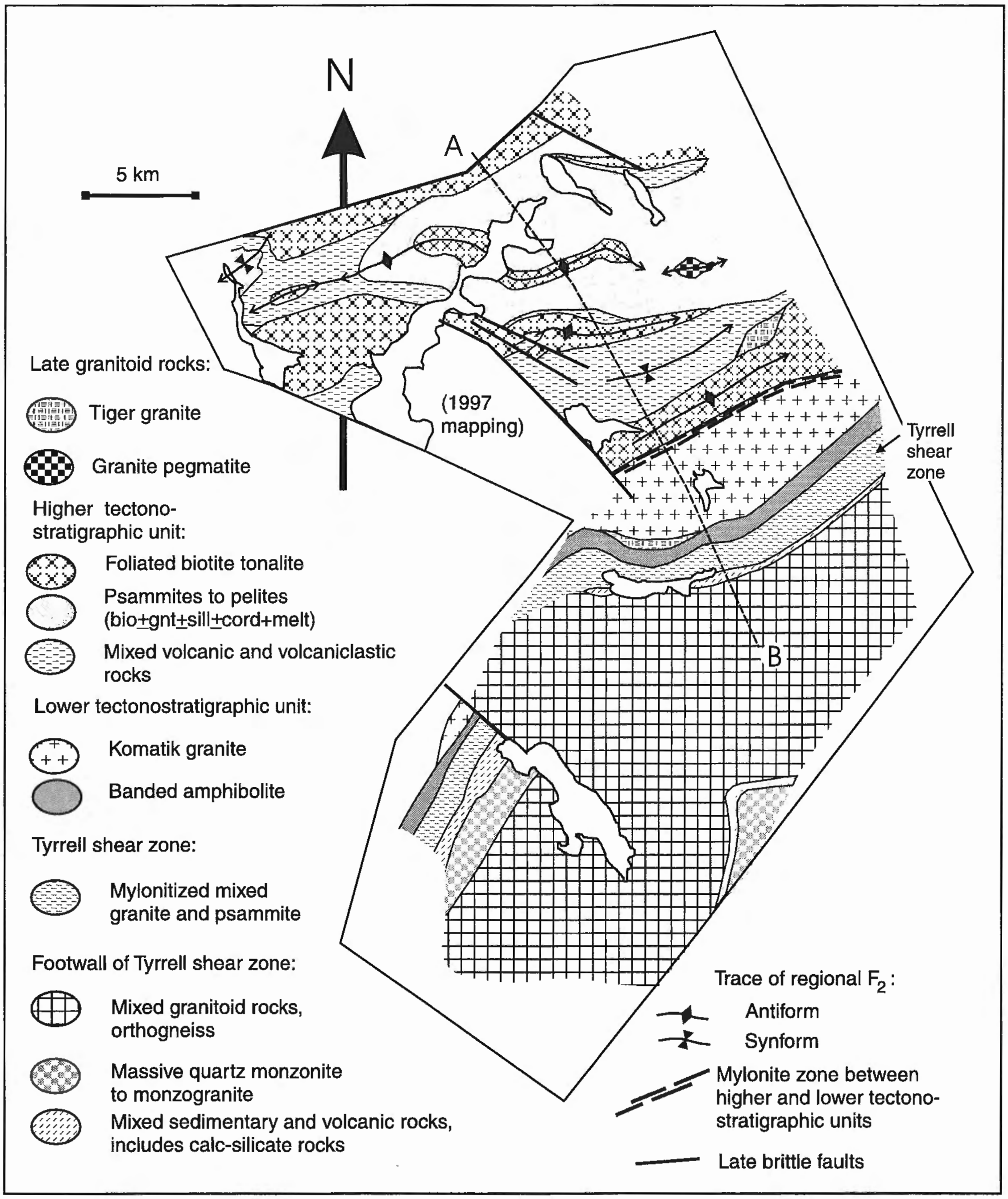


***Figure 2.*** *Simplified geology of the northern Yathkyed greenstone belt. Line shows surface trace of cross-section in Figure 5; bio=biotite, gnt=garnet, sill=sillimanite, cord=cordierite.*

The mixed volcanic package consists predominantly of mafic, locally pillowed flows, with an increasing proportion of intermediate to felsic material towards the northwest. Siliceous zones within the mafic-dominated part of the package are interpreted as silicified basalt, as they appear to be gradational with the surrounding mafic rocks. Rock types in the more mixed part of the package include thinly bedded tuffs and volcaniclastic sedimentary rocks, iron-formation (silicate, sulphide, and carbonate facies), and intermediate plagioclase-porphyritic and felsic rocks. All of these rocks are strongly foliated and preserve amphibolite-facies mineral assemblages, making it difficult to tell if they are volcanic or intrusive in origin. In addition to its compositional heterogeneity, the mixed volcanic package is characterized by the presence of numerous foliation-parallel gossans, some of which have strike lengths of several kilometres. These are described below (*see* 'Mineral potential').

Metasedimentary rocks consisting of psammite, semipelite, and pelite lie to the north and northwest of the main unit of mixed volcanic rocks. Mineral assemblages in pelite units include biotite-sillimanite-garnet, biotite-sillimanite-cordierite-garnet, and biotite-muscovite-sillimanite-garnet. Foliation-parallel lenses and blebs of granitic material are abundant in pelitic beds. They commonly contain accessory garnet, and are interpreted as locally derived, anatectic melt.

The contact between the mixed volcanic package and the clastic sedimentary rocks is characterized by a mixed zone up to 1 km wide in which beds of pelitic to psammitic composition are interlayered with plagioclase+hornblende-rich layers. Irregular, wispy compositional layering within hornblende-bearing layers and the presence, locally, of subhedral to euhedral plagioclase crystals within biotite-rich beds suggest a mixed sediment source.

Foliation-parallel sheets of moderately foliated to gneissic biotite tonalite to granodiorite occur within the sedimentary and mixed volcanic units. Where contacts between the tonalite and its host rock are exposed, the tonalite locally crosscuts the foliation at a low angle. However, tonalite sheets are typically foliation parallel and strongly foliated, and are therefore interpreted to have been emplaced relatively early in the tectonic history of the area. The tonalite unit appears to be restricted to the higher tectonostratigraphic unit.

### *Lower tectonostratigraphic unit*

The lower tectonostratigraphic unit consists of amphibolite and foliated biotite monzogranite (Fig. 2). The amphibolite occupies the immediate hanging wall of the Tyrrell shear zone, and define the structural base of the Yathkyed greenstone belt in this area.

The amphibolite units define a high ridge characterized by strongly foliated, locally banded amphibolite-facies mafic rocks. Metamorphic assemblages include plagioclase-hornblende, plagioclase-hornblende-garnet, plagioclase-hornblende-epidote, and plagioclase-hornblende-actinolite. Late chlorite locally overgrows the amphibolite along the foliation. Rusty, pyrite-rich layers, locally rich in garnet, occur within the amphibolite, and are interpreted as metamorphosed iron-formation. Local rusty layers lacking garnet have an unknown origin. Although primary volcanic features are absent within the present map area, the amphibolite unit can be traced southwestward into a unit of pillowed flows mapped in 1997 (Irwin et al., 1998), and is therefore interpreted to be high-grade metavolcanic rocks.

A unit of weakly foliated, pink-weathering biotite monzogranite, informally named the Komatik granite by Relf et al. (1998), structurally overlies and intrudes the amphibolite (Fig. 2). Inclusions of strongly foliated to gneissic granite to tonalite of unknown origin occur within the Komatik granite. The northwestern margin of the granite is marked by a mylonite zone up to 30 m wide (*see* 'Structural elements', below) which separates it from tonalite of the higher tectonostratigraphic package. Although it is sheared, abundant tonalite screens within the Komatik granite in this area suggest that the contact is, at least in part, intrusive.

### *Tyrrell shear zone*

A thin (about 500 m) unit consisting of mixed sedimentary and granitic rocks structurally underlies the amphibolite to the southeast. The unit comprises psammitic to semipelitic rocks injected along their foliation by up to 60% (by volume) monzogranite to syenogranite and hornblende diorite to tonalite, all of which are sheared together in the appproximately 2 km wide Tyrrell shear zone. The Tyrrell shear zone is further described below (*see* 'Structural elements').

### *Tyrrell shear zone footwall*

Footwall rocks of the Tyrrell shear zone in the present study area include mixed granitoid rocks, granitic gneiss units, and a package of distinctive supracrustal rocks. The last include thinly bedded, quartz-rich arenite, calc-silicate rocks comprising tremolite-carbonate-biotite-quartz, quartz-actinolite- plagioclase, and quartz-hornblende-plagioclase±carbonate, psammite, and banded mafic to felsic rocks interpreted to be volcanic in origin. The arenite and calc-silicate rocks share similarities with subarkose and calc-silicate schist units of the Tavani Formation (Hurwitz Group) mapped to the southwest by Irwin et al. (1998), and with sedimentary rocks of the enigmatic Montgomery Lake Group which sits stratigraphically between the Proterozoic Hurwitz Group and the Archean Henik Group south of the study area (Aspler et al., 1992).

The intrusive component of the footwall unit includes a range of variably foliated granitoid rocks, including biotite monzogranite, muscovite+garnet-bearing leucocratic syenogranite, massive quartz monzonite, and granitic to tonalitic gneiss. Only the monzonite is represented as a separate unit in Figure 2.

### *Late (?)Archean granitoid rocks*

A distinctive K-feldspar megacrystic syenogranite to syenite, informally named the Tiger granite, occurs along the northern edge of the amphibolite ridge (Fig. 2). The Tiger granite comprises K-feldspar megacrysts up to 10 cm long in a fine- to medium-grained groundmass of dark green amphibole, quartz, K-feldspar, and plagioclase, and ranges from massive to mylonitic. Mylonite zones within the unit are generally small (<50 cm wide) with sharp strain gradients. Locally the Tiger granite is strongly foliated, and the flattened K-feldspar crystals impart an irregular, striped texture. Numerous granitic dykes, interpreted to be related to the Komatik granite, intrude the Tiger granite, indicating a relative chronology for the two units. A second amphibole-bearing monzogranite to syenogranite occurs at the structural base of the mixed volcanic unit (Fig. 2), and is tentatively correlated with the Tiger granite. This unit contains partially digested amphibolite blocks suggesting assimilation of wall rock and/or inclusion of source rock xenoliths.

Massive to weakly foliated, biotite±muscovite monzogranite to syenogranite and associated pegmatite intrude all units described above. These granitoids are locally characterized by accessory garnet, and are interpreted as products of partial melting of crustal material.

### *Proterozoic rocks*

Variably deformed, diabase dykes crosscut Archean map units in the study area, and appear to be restricted to the hanging wall of the Tyrrell shear zone. Where least deformed, the dykes strike roughly east, and preserve diabasic textures. Elsewhere, they are overprinted by amphibolite-facies mineral assemblages (hornblende-plagioclase), have a moderate to strong foliation, and are variably folded and boudined. Based on field relations and correlation with similar dykes in the MacQuoid Lake area (Tella et al., 1997), the dykes are tentatively interpreted to be part of the ca. 2.19 Ga Tulemalu swarm (Le Cheminant et al., 1997).

In the south-central part of the map area, a swarm of these dykes intrudes the Komatik granite, and defines what appears to be a truncated Z-fold with spectacular north-striking crenulations (Fig. 3). The deformation history of these dykes comprises part of a B.Sc. thesis study at Carleton University.

Minette dykes occur locally throughout the study area. They are typically less than 1 m in width, and are characterized by their grey-brown weathered surface and the presence of biotite phenocrysts. These dykes crosscut the regional foliation, are relatively undeformed and unmetamorphosed and thus, are interpreted to be related to rocks of the ca. 1.83 Ga (MacRae et al. 1995) Christopher Island Formation (Peterson and Rainbird, 1990). Rare examples of deformed and metamorphosed lamprophyres also occur and may be Archean.

## STRUCTURAL ELEMENTS

Structural elements in the greenstone belt are similar to those described for the area immediately to the west by Relf et al. (1998). The predominant foliation in the area, designated $S_{main}$, is defined by alignment of phyllosilicate minerals and amphibole, and is generally parallel to compositional

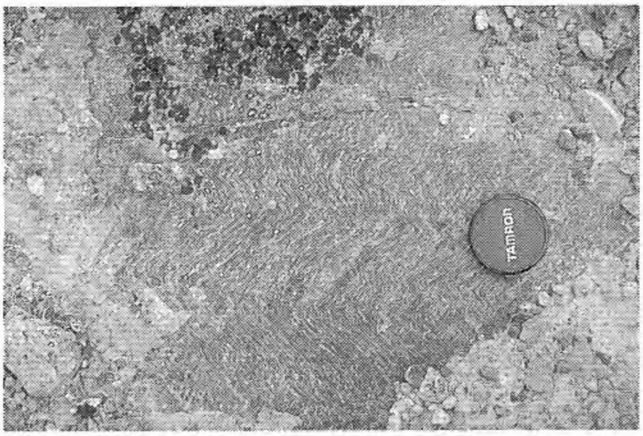

***Figure 3.*** *Crenulated amphibolite-facies diabase dyke (Tulemalu dyke) in hanging wall of Tyrrell shear zone.*

layering (possibly bedding). Across the map area, $S_{main}$ ranges from southwest-striking in the western part of the area where it adjoins 1997 mapping, to west-striking in the east (Fig. 2). Two sets of folds deform $S_{main}$ (Fig. 2). The first set, designated $F_2$, consists of upright to steeply overturned, east- to northeast-striking folds which are doubly plunging as a result of north- to northeast-striking crossfolds ($F_3$). $F_3$ folds define Z-asymmetric folds of $S_{main}$ with wavelengths of several kilometres.

The Tyrrell shear zone, recognized in 1997 (*see* Relf et al., 1998; Irwin et al., 1998), sits below the amphibolite at the structural base of the greenstone belt (Fig. 2). It occurs within a unit of mixed granitoid and metasedimentary rocks, and parallels $S_{main}$ in the greenstone belt. Within the map area, the dip of the shear zone is generally less than 40° to the north and/or northwest, although on the short limbs of Z-folds it is commonly somewhat steeper. Based on 1997 mapping, the movement history along the Tyrrell shear zone was interpreted to have involved early reverse displacement with a minor sinistral component followed by oblique normal-dextral displacement. Uranium-lead zircon and monazite analyses from four granitoid dykes suggest early movement occurred sometime after ca. 2.62 Ga, and late extension occurred after ca. 1.82 Ga (K. MacLachlan, unpub. data, 1998). Within the present map area, a strong, gently north-plunging extension lineation is present along much of the shear zone, and shear-sense indicators (shear bands, σ-type porphyroclasts) record primarily dextral shearing. Evidence for early reverse displacement is rare, and is limited to subhorizontal, asymmetric, open S-folds of mylonitic fabric.

Locally the Tyrrell shear zone has juxtaposed amphibolites in the hanging wall against mixed sediments that preserve biotite-grade assemblages in the footwall. It is not clear which shearing event (early thrusting or late dextral-normal movement) caused this metamorphic juxtaposition. Despite the possibility of postkinematic re-equilibration, thermobarometric studies of assemblages on both sides of the fault may be able to provide at least a minimum estimate of the amount of relative uplift.

East of Yathkyed Lake, the Tyrrell shear zone is folded about subhorizontal northeast-trending, open folds (*see* Irwin et al., 1998; Relf et al., 1998). Folding followed late dextral displacement (the extension lineation is folded; Irwin et al., 1998), and therefore postdated ca. 1.82 Ga. Although the age of the $F_3$ crossfolds in the upper tectonostratigraphic unit of the present study area is unknown, their parallelism with the Proterozoic folds that deform the Tyrrell shear zone suggests they may postdate ca. 1.82 Ga as well.

A second shallowly northwest-dipping shear zone, parallel to the Tyrrell shear zone, was identified within the Yathkyed greenstone belt during 1998 mapping. It occurs along the upper contact of the Komatik granite, and separates the granite in the footwall from the mixed volcanic package in the hanging wall. The shear zone is defined by a zone up to 30 m wide of mylonitized granite with an associated mineral stretching lineation which pitches moderately (approximately 30-60°) northeast. Although no unequivocal shear-sense indicators were found along this shear zone, the lineation has a similar orientation to that associated with late dextral-normal displacement in the Tyrrell shear zone, suggesting that both shear zones may record Proterozoic dextral movement. Evidence for early (Archean) thrust displacement across the shear zone was not found.

In the northernmost part of the map area, an enigmatic mylonite zone about 15 m wide dips steeply towards 210°. Shear-sense indicators are sparse along the shear zone, but a few shear bands recording reverse displacement were identified. The timing of this shear zone is uncertain, although it deforms and is spatially associated with several approximately east-trending, diabase dykes, tentatively interpreted as ca. 2.2 Ga Tulemalu dykes. The regional significance of this shear zone is unknown, but its apparent timing suggests that it could be related to Proterozoic dextral movement on the Tyrrell shear zone. Several other small, roughly east-northeast-striking mylonite zones occur within the belt and could also be related to Proterozoic deformation.

## METAMORPHISM

Metamorphic assemblages throughout most of the map area record amphibolite-facies metamorphic conditions. Locally, the pelitic rocks preserve evidence for two metamorphic events (Fig. 4). Relict, pale pink garnets are preserved in the cores of retrograded porphyroblasts within the assemblage biotite-sillimanite-garnet-melt. Within the matrix, poikiloblastic, dark red garnets are present in the same rock. Biotite, which defines $S_{main}$, generally wraps around these garnets, but locally is truncated by them, suggesting their growth accompanied, but outlasted, the shortening event that produced $S_{main}$.

In the Tyrrell shear zone some biotite-muscovite schist units contain small (5 mm) poikiloblastic cordierites. These cordierites locally overgrow a dextral C-S fabric which is believed to be Proterozoic (ca. 1.82 Ga; K. MacLachlan, unpub. data, 1998), and thus the metamorphism is also assumed to be Proterozoic. Elsewhere, randomly oriented muscovite overgrows Proterozoic mylonite and provides further evidence that Proterozoic heating was significant and that, at least locally, it outlasted deformation. Although there are no constraints on the timing of the latest fabric development in the biotite-sillimanite-cordierite-bearing pelite mentioned above, the second growth of garnet is interpreted to be related to the Proterozoic event recognized within the Tyrrell shear zone. The timing of earlier metamorphism is uncertain, but is assumed to be Archean and could have occurred during early thrust movement along the Tyrrell shear zone.

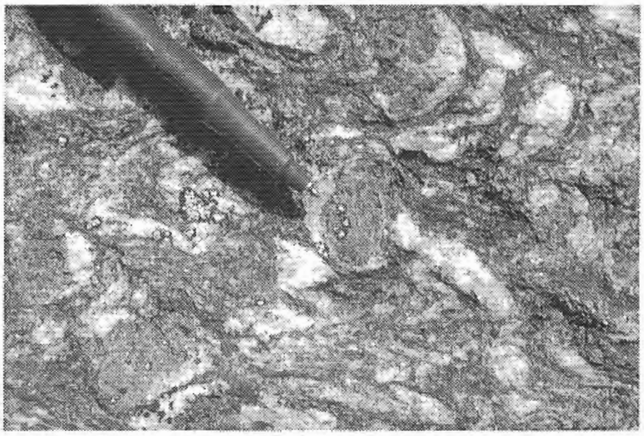

***Figure 4.*** *Amphibolite-facies pelite showing early garnet inclusions in cordierite, sillimanite, biotite, granitic melt, and late garnet in the matrix. Foliation wraps around and is locally overgrown by later garnets.*

## TECTONOSTRATIGRAPHIC RELATIONS

Figure 5 is a schematic cross-section through the map area, and highlights tectonostratigraphic relationships within this part of the Yathkyed greenstone belt. The lower tectonostratigraphic unit, described above, sits in the hanging wall of the Tyrrell shear zone, and consists of mixed amphibolite units overlain by a sheet, up to 4 km thick, of Komatik granite. Although no younging indicators are preserved in the lower tectonostratigraphic unit within the present map area, the amphibolite can be traced westward into southeast-younging, greenschist-facies, pillowed volcanic rocks (Irwin et al., 1998). Based on this correlation, it is suggested here that the amphibolite units are part of an overturned, fault-bounded panel.

The higher tectonostratigraphic unit includes the mixed volcanic package, the psammite-pelite unit, and associated tonalite sheets that intrude both (Fig. 5). This unit is in fault contact with the lower tectonostratigraphic unit. Lithological contacts and $S_{main}$ within the upper tectonostratigraphic unit define a broad antiform-synform pair in the hanging wall of the bounding fault. Regional younging direction is unknown, so it is unclear whether the unit is a downward-facing panel like its lower counterpart.

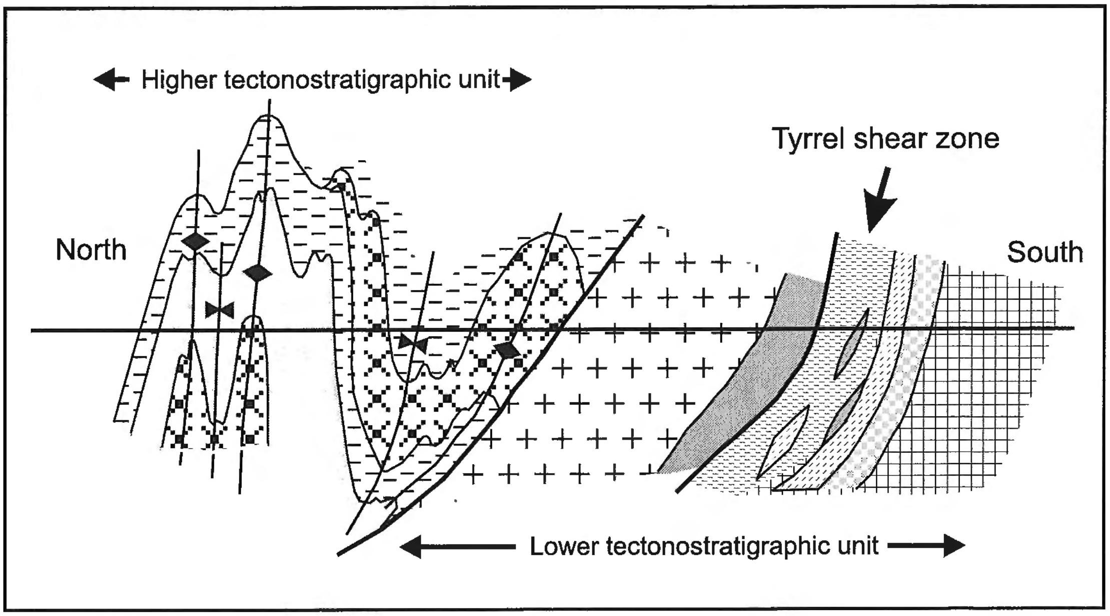


*Figure 5. Schematic cross-section through the northern Yathkyed greenstone belt, showing tectonostratigraphic units. Some data projected onto line. For lithological symbols see Figure 2.*

It is interesting to note that the complex folding pattern preserved in the upper tectonostratigraphic unit appears to be absent from the lower unit; perhaps this reflects different early (prefaulting) tectonic histories for the two units.

The magnitudes of displacement along the Tyrrell shear zone and the shear zone separating the upper and lower tectonostratigraphic units are unknown. Although the presence of tonalite screens in the Komatik granite in the footwall of the western shear zone suggests the contact may be primarily intrusive, the apparent contrast in deformation histories across it suggests displacement may have been regionally significant. Similarly, while no marker units have been identified to quantify the amount of movement along the Tyrrell shear zone, several observations suggest it might have been significant; firstly, there are local contrasts in metamorphic grade between lithologically different lozenges within the shear zone; secondly, the shear zone juxtaposes distinct supracrustal sequences, which may have significantly different ages; and finally, the Tulamulu dykes abruptly disappear across the shear zone.

## MINERAL POTENTIAL

Rocks of the mixed volcanic package host numerous foliation-parallel (possibly stratabound) gossans that can be traced discontinuously along strike for up to 3 km. These gossans are associated with a variety of alteration assemblages, including quartz-sericite, chlorite-sericite, and sericite-fuchsite, and locally contain up to 75% sulphides (pyrite±chalcopyrite±pyrrhotite). Gossanous layers within the mixed volcanic package also include silicate-, carbonate-, and sulphide-facies iron-formation units which are commonly distinguished by the presence of magnetite and/or garnet. One iron-formation was traced for nearly 4 km along the contact between the volcanic package and the psammite-pelite unit. Locally, this iron-formation displays garnet+pyrite growth along vuggy quartz veins. Assay analyses of grab samples from selected gossans yielded up to 900 ppm Cu, 500 ppm Zn. Gold assay data are presently unavailable.

## SUMMARY

The Yathkyed greenstone belt sits structurally above a (likely late Archean) thrust fault (the Tyrrell shear zone) that was reactivated in the early Proterozoic. The belt can be subdivided into two tectonostratigraphic units, separated by a shear zone of uncertain displacement sense and regional significance. The higher tectonostratigraphic unit consists of mixed volcanic rocks which grade into psammitic to pelitic rocks, folded into a steeply overturned antiform-synform pair. The lower tectonostratigraphic unit comprises a ridge of amphibolite (interpreted to be high-grade, mafic volcanic rocks) overlain by a 4 km thick panel of granite. Structurally below the amphibolite is a sheared, mixed unit of sedimentary rocks and granite, which defines the Tyrrell shear zone. The recognition of these tectonostratigraphic units raises interesting questions about the relationship between the upper and lower parts of the greenstone belt — do the lower amphibolite and upper mixed volcanic units share a common origin, or were they formed in different tectonic settings; and if so, are their mineral potentials distinctly different? Geochemical and geochronological studies are underway to address these questions.

Based on the limited geochronological data available to date from the map area, it is clear that the Paleoproterozoic tectonothermal overprint was more pronounced here than in some parts of the Churchill Province. For example, the Paloeproterozoic (ca. 1.82 Ga.) dextral shear fabric along the Tyrrell shear zone is locally overgrown by cordierite and muscovite. The impact of this thermal overprint on the mineral potential of the area could be significant, as metamorphic conditions were sufficient to allow mobility of metals. Thermobarometric studies, coupled with geochronological data, will help to determine the degree of Proterozoic reworking and evaluate its impact on the distribution of metals within the belt.

## ACKNOWLEDGMENTS

The authors would like to thank Perry Hancock and Hamish Tatty of M&T Enterprises in Rankin Inlet for providing expediting services during the field season. Helicopter support was provided by Custom Helicopters, Helimax, and Polar Continental Shelf through Huissan Aviation. Terry Halton and Matt Weeks in particular are thanked for their excellent service. Brad Harvey, Lara Lewis, Chris Studdnicki-Gizbert, and Mariska ter Meer provided extremely capable and entertaining field assistance, and their contribution to the project is gratefully acknowledged.

Critical reviews of the manuscript were provided by Simon Hanmer and Tony Peterson, and helped to clarify the expression of our ideas.

## REFERENCES

**Aspler, L.B. and Chairenzelli, J.R.**
1996: Geological compilation of the Hearne Province, south-central District of Keewatin; Northwest Territories Geology Division, Department of Indian Affairs and Northern Development, Yellowknife, EGS Open File 1996-02, scale 1:50 000.

**Aspler, L.B., Bursey, T.L., and LeCheminant, A.N.**
1992: Geology of the Henik, Montgomery Lake, and Hurwitz groups in the Bray-Montgomery-Ameto lakes area, southern District of Keewatin, Northwest Territories; *in* Current Research, Part C; Geological Survey of Canada, Paper 92-1C, p. 157–170.

**Eade, K.E.**
1985: Geology, Tulemalu Lake-Yathkyed Lake, District of Keewatin, Northwest Territories; Geological Survey of Canada, Map 1064A, scale 1:250 000.
1986: Precamrian geology of the Tulemalu Lake-Yathkyed Lake area, District of Keewatin; Geological Survey of Canada, Paper 84-11, 31 p.

**Geological Survey of Canada**
1981: Magnetic anomaly map of the Dubwant River area; Map 1567A, scale 1:1 000 000.

**Irwin, D., Relf, C., and MacLachlan, K.**
1998: Geology and mineral potential of the southeastern Yathkyed Lake area (parts of 65I/3, 4, 5, 6 10 & 11), western Churchill Province; Department of Indian Affairs and Northern Development, Yellowknife, Northwest Territories, EGS Open File 1998-07, scale 1:50 000.

**LeCheminant, A.N., Buchan, K.L., van Breemen, O., and Heaman, L.H.**
1997: Paleoproterozoic continental break-up and reassembly: Evidence from 2.19 Ga diabase dykes swarms in the Slave and western Churchill Provinces, Canada; Geological Association of Canada–Mineralogical Association of Canada Annual Meeting, Program with Abstracts, p. A86.

**MacLachlan, K., Relf, C., and Irwin, I.**
1998: Geochronological studies of a greenstone belt-bounding shear zone, western Churchill Province, NWT; Geological Association of Canada, Abstracts, v. 23, p. A-115.

**MacRae, N.D., Armitage, A.E., Jones, A.L., and Miller, A.R.**
1995: A diamondiferous lamprophyre dike, Gibson Lake area, Northwest Territories; International Geology Review, v. 37, p. 212–229.

**Peterson, T.D. and Rainbird, R.J.**
1990: Preliminary report on the geology of northwestern Dubwant Lake area, Distraict of Keewatin; *in* Current Research, Part C; Geological Survey of Canada, Paper 90-1C, p. 69–79.

**Relf, C.**
1996: Geology of the Nowyak Lake area, parts of NTS 65 G/9, 15, 16; 65 H/13; 65 I/4; and 65 J/1. NWT Geology Division, DIAND, EGS Open File 1996-19.

**Relf, C., Irwin, D., MacLachlan, K., and Mills, A.**
1998: New insights into the geology of the Yathkyed Lake greenstone belt, western Churchill Province, Northwest Territories; *in* Current Research 1998-C; Geological Survey of Canada, p. 67–75.

**Tella, S., LeCheminant, A.N., Sanborn-Barrie, M., and Venance, K.E.**
1997: Geology and structure of parts of the MacQuoid Lake area, District of Keewatin, Northwest Territories; *in* Current Research 1997-C; Geological Survey of Canada, p. 123–132.

Geological Survey of Canada Project 970006

# Preliminary investigation of significant mineral occurrences in the central Rankin–Ennadai supracrustal belt, Kaminak Lake area, Northwest Territories (Nunavut)[1]

S.P. Goff[2] and J.A. Kerswill
Mineral Resources Division, Ottawa

*Goff, S.P. and Kerswill, J.A., 1999: Preliminary investigation of significant mineral occurrences in the central Rankin–Ennadai supracrustal belt, Kaminak Lake area, Northwest Territories (Nunavut);* in *Current Research 1999-C; Geological Survey of Canada, p. 147–156.*

---

**Abstract:** The central portion of the Rankin–Ennadai supracrustal belt contains a large number of mineral occurrences, including several major vein gold, polymetallic vein, and volcanic-associated massive sulphide deposits.

Work to date indicates that most significant gold occurrences contain complex multistage, carbonate-bearing vein systems in which at least some gold-rich veins clearly predate regional deformation and metamorphism. Deformed, pyritic, quartz-sericite schists of similar character to alteration zones in massive sulphide deposits are present in some gold occurrences.

Polymetallic vein occurrences contain high Au, Ag, Cu, and Zn, high Ag/Au ratios, locally anomalous Bi, Se, Te, As, and Mo, and pyritic quartz-sericite schist. Both the veins and schistose alteration zones are deformed and metamorphosed.

The critical features of polymetallic vein and some vein gold occurrences are similar to those of many porphyry and/or epithermal deposits and suggest a major contribution to metal concentration by synvolcanic processes.

**Résumé :** La partie centrale de la ceinture supracrustale de Rankin–Ennadai contient de nombreux indices de minéralisation, notamment plusieurs grands gisements dont des gisements d'or filonien, des gisements polymétalliques filoniens et des gisements de sulfures massifs associés à des roches volcaniques.

Les travaux réalisés à ce jour indiquent que les plus importants indices aurifères contiennent des réseaux filoniens complexes à plusieurs phases qui renferment des carbonates et dans lesquels au moins certains des filons aurifères sont nettement antérieurs à la déformation régionale et au métamorphisme. Des schistes quartzo-sériciteux pyritiques déformés, qui ressemblent à des zones d'altération dans des gisements de sulfures massifs, se rencontrent dans certains indices aurifères.

Les indices polymétalliques filoniens sont riches en Au, Ag, Cu et Zn. Leurs rapports Ag/Au sont élevés et ils contiennent des concentrations localement anomales de Bi, Se, Te, As et Mo ainsi que du schiste quartzo-séricíteux. Les filons et les zones d'altération schisteuses sont déformés et métamorphisés.

Les caractéristiques essentielles des indices polymétalliques filoniens et de certains indices aurifères ressemblent à celles de bon nombre de gisements porphyriques ou de gisements épithermaux et portent à croire que des processus synvolcaniques auraient joué un rôle majeur dans la concentration des métaux.

---

[1] Western Churchill NATMAP Project
[2] NWT Geology Division, DIAND, P.O. Box 1500, Yellowknife, Northwest Territories X1A 2R3

## INTRODUCTION

The Archean Rankin-Ennadai greenstone belt of the western Churchill Province has significant exploration potential for gold and base-metal deposits. References to previous geological mapping are provided on recent maps by Hanmer et al. (1998b), Irwin and Relf (1998), and Irwin et al. (1998). A digital compilation of information of more than 200 mineral occurrences has been recently published (Goff and Mills, 1998).

This paper is a contribution to the mineral deposits and metallogenic component of the Western Churchill NATMAP Project and is largely based on our work in the Kaminak belt in 1997 and previous investigations by the first author. It presents highlights of the recent compilation of mineral occurrences, field visits to a number of mineral occurrences, and lithogeochemical investigations of selected samples from the mineral occurrences. The overall objectives of this work are to help identify metallogenic domains most favourable for discovery of economic deposits, develop better empirical exploration guidelines, develop better genetic models for different deposit types, and compare the geology and mineral occurrences of this area to other greenstone belts covered by the Western Churchill NATMAP Project.

## GEOLOGICAL FRAMEWORK

The Kaminak Lake to Heninga Lake area represents one of the best exposed areas in the central part of the Archean Rankin–Ennadai supracrustal sequence.

In the Kaminak Lake area, an assemblage of mafic to felsic volcanic and volcaniclastic rocks, plus siliciclastic sedimentary rocks with iron-formation, was defined as the Kaminak Group (Davidson, 1970). Several discontinuous packages of volcanic and volcaniclastic rocks were mapped by Hanmer et al. (1998a). Previous workers have proposed one (Davidson, 1970) to four (Ridler and Shilts, 1974) cycles of mafic to felsic volcanism, whereas recent U-Pb zircon ages by Davis et al. (1998) yield two clusters of ages for felsic volcanism (2706-2695 Ma and 2687-2681 Ma), consistent with at least two felsic cycles.

Regional deformation and metamorphism is late Archean and is influenced by tonalite to granodiorite plutonism at about 2679 Ma (Davis et al., 1998) and subsequent post-tectonic granite plutonism. A north- to northeast-trending diabase dyke swarm, the Kaminak dykes at 2.45 Ga (Heaman, 1994), is affected by a Proterozoic metamorphic event, the grade of which increases from greenschist at Kaminak Lake to amphibolite further north (Davidson, 1970). Quartz pebble conglomerate and orthoquartzite of the Proterozoic Hurwitz Group are preserved in a prominent east-northeast-trending graben along the north shore of Kaminak Lake. A gabbro which intruded these rocks gave a U-Pb baddeleyite age of 2111 ± 1 Ma (Heaman and LeCheminant, 1993), providing further evidence for Proterozoic magmatism in the area.

## MINERAL OCCURRENCES

Over 160 of the more significant metallic mineral occurrences as compiled by Goff and Mills (1998) were subdivided empirically into three principal classes based on metal endowment. Gold occurrences are defined as those that contain visible gold and/or greater than 2 ppm Au; base-metal occurrences are those with one or more visible base-metal sulphides (chalcopyrite, galena, and sphalerite) and/or greater than 1000 ppm Cu, Pb, or Zn; polymetallic occurrences are those with visible gold and/or greater than 2 ppm Au in addition to visible base-metal sulphides and/or greater than 1000 ppm Zn or Pb. Where sufficient field information is available, occurrences have been designated as either vein-related or volcanic-associated massive sulphide. The latter type includes mineralization judged to be largely conformable massive sulphide accumulations and/or generally discordant stringer mineralization that is commonly associated with the conformable massive sulphide accumulations. Where little is known about the geometry of the mineralization, the occurrences are designated as unclassified. In some cases it is difficult to distinguish between stringer zones and more typical veins. The occurrences are plotted on Figure 1 according to metal endowment (gold, base metal, and polymetallic) and deposit type (massive sulphide affinity versus vein). Three molybdenum occurrences and five uranium occurrences are also included in Figure 1.

### *Vein gold occurrences*

Gold occurrences are linked to quartz-carbonate veins in a variety of host rocks. The more significant occurrences commonly involve several stages of pyrite-iron carbonate-quartz veining associated with generally east- to northeast-trending, layer-parallel shear zones in mafic to felsic volcanic and volcaniclastic rocks. Three deposits are highlighted in the following text.

The Cache deposit has reserves estimated at 0.364 Mt grading 9.26 g/t Au (Ali et al., 1989). Drilling by Cyprus Canada Inc. and Noble Peak Resources Ltd. in 1994 suggests that the 250 m long mineralized zone plunges to the west to a depth of 300 m. The deposit is hosted by subaqueous felsic breccia, tuff, and epiclastic conglomerate associated with subvolcanic rhyodacitic domes. The east-trending mineralized zone is strike parallel and comprises at least three generations of quartz-iron carbonate veining. Prominent east-trending, vertically dipping veins, up to 30 cm thick contain accessory pyrite and display alteration haloes with pervasive iron carbonate developed within the host volcaniclastic rocks. These first generation veins are boudinaged by an east-trending, anastomosing penetrative cleavage ($S_1$) which variably deformed the carbonate alteration zones and left a network of thin sericite-rich layers. Chlorite, quartz, and sericite pressure shadows on pyrite porphyroblasts in the wall rock suggest that sulphidation and metamorphism preceded $S_1$. A set of thinner, relatively undeformed veins (second generation), dipping less than 35° north and west, contain steeply dipping fibres of quartz and carbonate, indicating near-vertical extension. A north-trending, steeply dipping set of

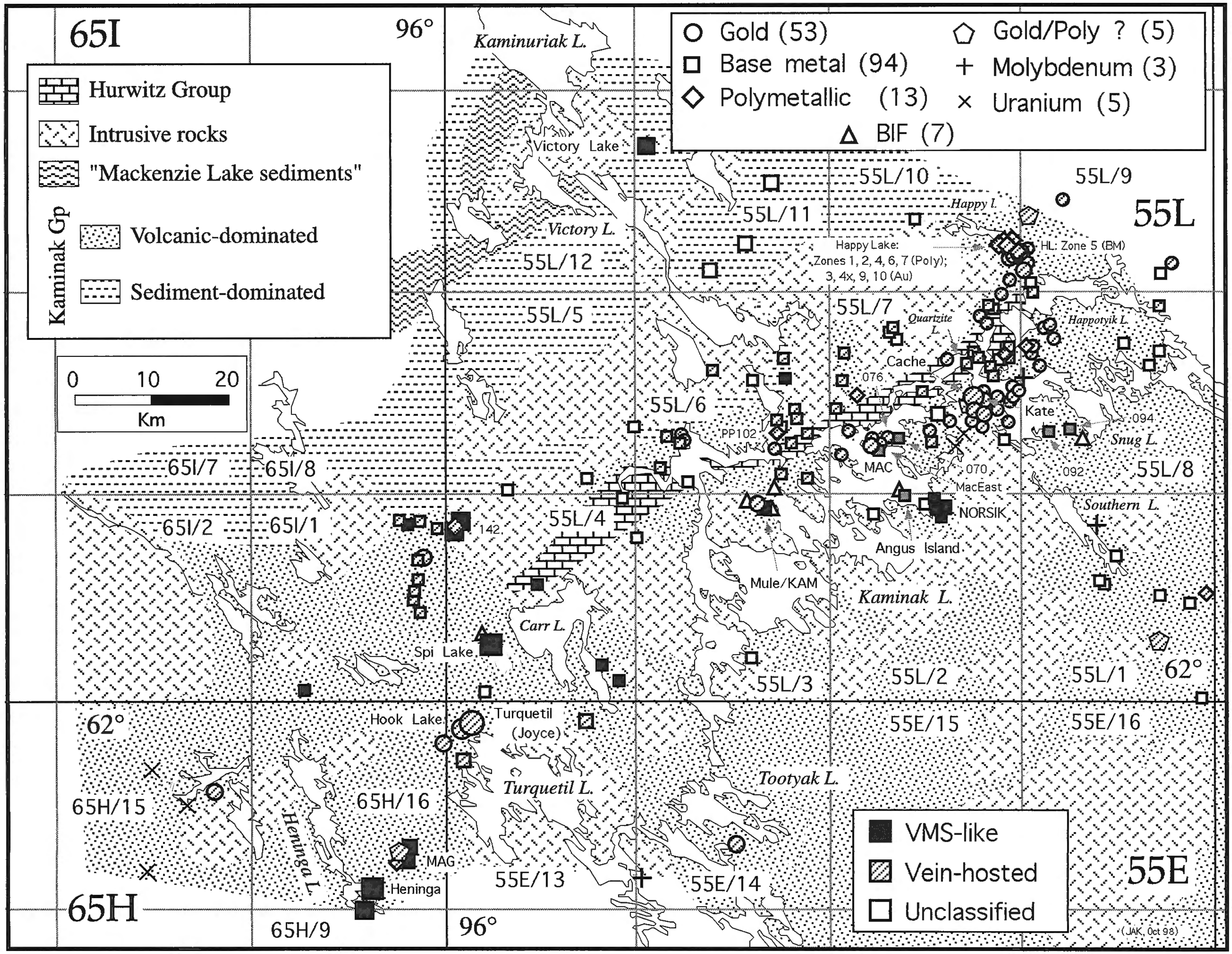


***Figure 1.*** *Simplified geological map of the central part of the Rankin–Ennadai supracrustal belt adapted from Hanmer et al. (1998a). Mineral occurrences are shown on the map according to class (metal endowment) and deposit type. BIF=banded iron-formation; VMS=volcanic-associated massive sulphide.*

quartz veins (third generation) cuts the adjacent rhyodacite dome. Gold is associated with disseminated pyrite in each of the different vein sets suggesting multiple periods of gold and sulphide deposition and/or remobilization. Rare sphalerite and galena have also been observed in each vein set. Figure 2 displays the deformed character of the early gold-rich, east-trending veins.

Notable gold mineralization is associated with the Turquetil Lake 'shear' zone — a deformed carbonate alteration zone, over 10 km in length, within an east-northeast-striking package of mafic flows and felsic volcaniclastic rocks. It is one of the rare alteration zones which contains arsenopyrite and tetrahedrite. The two best exposed occurrences are at Turquetil Lake and Hook Lake. The Turquetil deposit, on the JOYCE claim northeast of Turquetil Lake, has been estimated to contain 3.5 Mt grading 2.4 g/t gold, including a higher grade zone of 0.5 Mt averaging 6.31 g/t of gold (Jones, 1997). Drilling in 1996 by Midasco Gold Corp. extended the known depth extent of the deposit to over 300 m (Goff, 1997). The alteration of the host rocks varies in intensity. Miller (1992) noted that intense alteration of mafic volcanic rocks and associated gabbro, along one drill fence, produced an assemblage of iron dolomite, ankerite, paragonite, and quartz, with associated pyrite, chalcopyrite, arsenopyrite, and gold. The deposit is composed of a series of northwest-dipping, en echelon quartz carbonate veins, some showing vuggy quartz, and containing pyrite plus disseminations and lenticular aggregates of arsenopyrite. High gold assays are associated with arsenopyrite. These veins are deformed and boudinaged by an anastomosing, penetrative cleavage, represented by a web of thin sericite zones which postdates the carbonate alteration. Deformation postdates sulphide growth and has produced

*Figure 2. Deformed gold-bearing, east-trending quartz-carbonate veins from the Cache gold occurrence.*

*Figure 3. Deformed gold-bearing, en echelon, quartz-carbonate veins from the Turquetil gold occurrence (Hook Lake locale).*

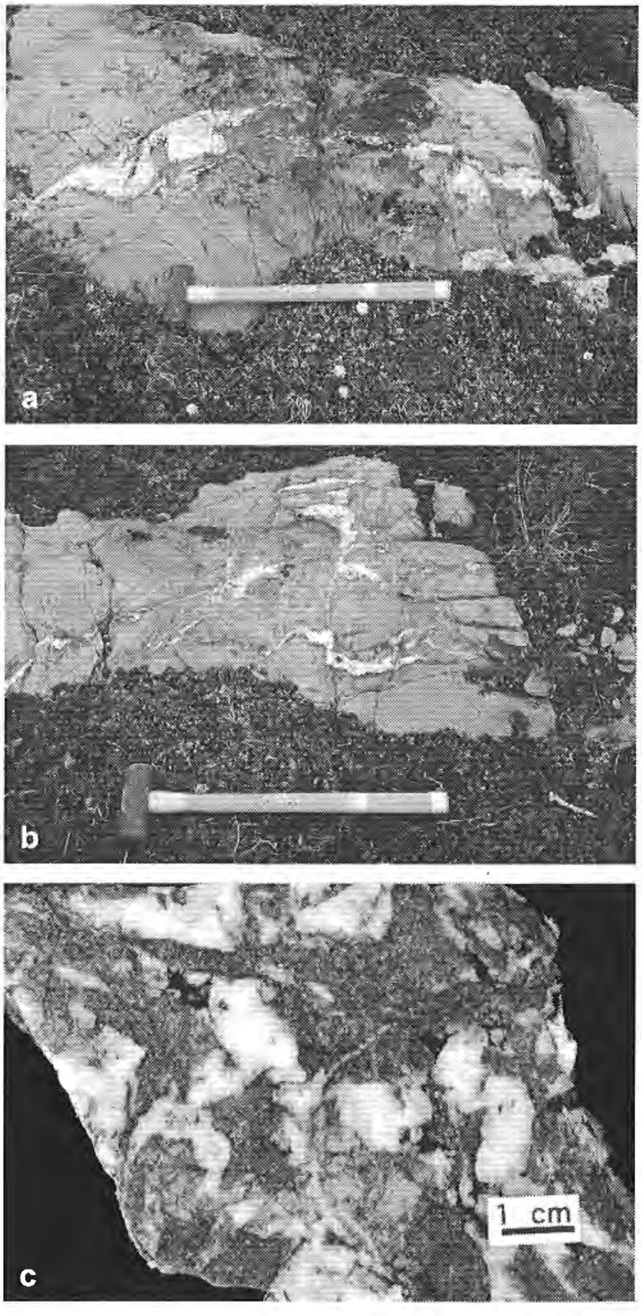


*Figure 4. Deformed gold-bearing, quartz-carbonate veins from the Mac gold occurrence.*

cataclasis of arsenopyrite aggregates and overgrowths of fibrous quartz, chlorite, and sericite in pressure shadows on arsenopyrite. A later set of thin, subhorizontal, extensional quartz carbonate veins with fibrous quartz overprint the gold-rich veins. Figure 3 depicts the deformed character of the gold-rich, en echelon, quartz-carbonate veins.

The Mac zone outcrops on a small island in massive mafic flows which show typical greenschist-facies (epidote-chlorite-actinolite) metamorphism. In places these rocks are intensely altered by carbonate and have localized zones of epidote alteration and silicification. Gold-bearing quartz veins form stockworks and horse-tails, notably at the margins of a prominent gabbro plug; some veins are crack-seal type. The host metabasalt displays an apparent lack of penetrative deformation; however, many of the gold-bearing veins are folded, attenuated, and boudinaged and have clearly undergone ductile deformation. Disseminated pyrite is associated with gold and occurs in both veins and altered wall rocks where it forms up to 30 modal per cent. Drilling at Mac (Troup et al., 1989) revealed several pyritic zones containing pervasive carbonate and quartz veining, with, in places, K-feldspar. The main zone of gold mineralization, up to 15 m wide, straddles a sheared contact between massive, mafic volcanic rocks and albite-quartz-sericite schist. This schistose zone, probably a deformed tuff, extends below the alteration zone and overlies felsic volcaniclastic rocks. Figure 4 shows good examples of deformed veins at Mac.

### *Polymetallic vein occurrences*

Polymetallic occurrences, mostly linked to quartz-carbonate veins are widely distributed, but are most abundant in a cluster at Happy Lake, where eleven separate auriferous zones have been drilled in an area of 2 km by 1 km (Knowles et al., 1988). Most of the zones are of the polymetallic class and display a north-south structural trend; however, three of the most southeasterly zones (zones 4X, 9, and 10) show an east-west structural trend and contain high Cu and Au concentrations, but no significant Zn or Pb.

The polymetallic veins at Happy Lake are hosted by intermediate to felsic tuff units altered to sericite, chlorite, biotite, and K-feldspar, plus interlayered argillitic to cherty beds, within a package of sheared mafic to felsic volcanic and volcaniclastic rocks. Some mineralization is associated with the margins of rhyodacite sills. A layer-parallel cleavage is most intensely developed in the altered interflow tuff units and sedimentary rocks, commonly producing a sericite schist. Lenticular aggregates of pyrite, sphalerite, and chalcopyrite occur within or marginal to veins of quartz and quartz-carbonate, up to 30 cm wide, and are boudinaged by the main cleavage. A southwest-plunging crenulation of the main cleavage has deformed a phase of thin, essentially barren quartz veins. Strand (1988) suggested an early stage of chalcopyrite-sphalerite with minor pyrrhotite overprinted by later pyrite-arsenopyrite and minor gold in Zone 1. Figure 5 clearly shows that both the metal-rich veins and the minerals developed within the schistose alteration zones are folded and overprinted by the main regional cleavage as well as a crenulation cleavage.

### *Base-metal occurrences of massive sulphide affinity*

Volcanic-associated massive sulphide occurrences are mainly in the thick felsic to intermediate breccia and lapilli-tuff packages at the southwest end of the study area, the most notable being the Heninga Lake deposit and the Spi and Mag occurrences. However, the recent discovery of the Victory Lake massive sulphide in NTS 55 L/11 (Armitage, 1997), indicates that potential for discovery of volcanic-associated massive sulphide deposits is not restricted to the southwest portion of the Kaminak greenstone belt.

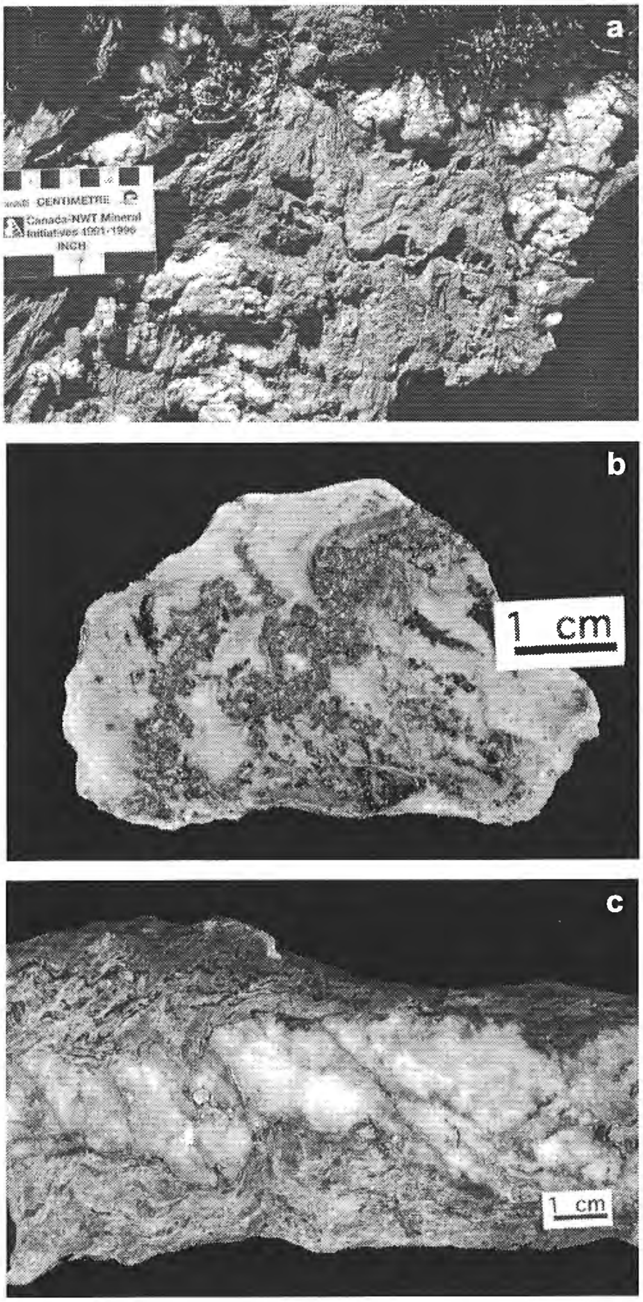


***Figure 5.*** *Deformed sulphide-bearing quartz-rich veins and sericitic alteration zones from the polymetallic Happy Lake occurrences;* ***a****) outcrop;* ***b****),* ***c****) hand sample.*

The Heninga Lake deposit is composed of three separate, steeply dipping, east-trending zones of semimassive to massive (>50%) sulphide. A reserve of 5.0 Mt with 8.5% Zn, 0.2% Cu, 110.0 g/t Ag, and 1.0 g/t Au was determined for the West zone by Inco Co. Ltd. after drilling in 1996 (Goff, 1997). The West zone is the largest, composed of a single lens measuring 400 m long by 4 m thick. The West and Central zones consist of massive chalcopyrite, pyrite, and minor pyrrhotite capped by layered pyrite-sphalerite, whereas the East zone consists entirely of layered pyrite-sphalerite; these layered zones locally contain minor galena and tetrahedrite. Both the West and Central zones lie above stringer sulphide zones: these discordant veins of interconnected sulphide may represent conduits for fluids which deposited the overlying sulphide masses (Leggett, 1980). Magnetite layers have been observed in drill core intersections of the layered zones. The layered zone forms a sharp contact with overlying tuffs. An alteration envelope of quartz, chlorite, sericite, carbonate, and disseminated pyrite surrounds the deposit.

The Mag Lake zone is 7 km northeast of, and appears to be along strike from the Heninga Lake deposit. A geological reserve of 0.72 Mt of 3.7% Zn, 2.6% Cu, 37.7 g/t Ag, and 0.37 g/t Au was calculated after drilling in 1996 by Inco Co. Ltd. (Goff, 1997). The deposit consists of layered sphalerite-pyrite, similar to the Heninga Lake East zone, and may represent a distal lens of the Heninga Lake hydrothermal system.

The Spi Lake occurrence lies within a prominent southeast-striking, 5 km wide belt of felsic volcaniclastic rocks, just west of Carr Lake. The occurrence consists of two sheared, concordant, podiform sulphide bodies, the Northern and Southern zones, which are 365 m apart, and are 180 m and 215 m in length, respectively (Laporte, 1976). Massive to layered pods with associated stringer zones show the same compositional variation as at Heninga Lake; however, exhalative chert beds less than 1 m thick are present at Spi Lake and contain both disseminated pyrite and thin, lenticular, bedding-parallel aggregates of pyrite-sphalerite. An alteration halo of disseminated pyrite was seen in the tuffaceous matrix of the wall rocks. Miller and Tella (1995) described an alteration assemblage of similar composition to that at Heninga Lake and found a zone of silicification 5 km to the southeast and along strike from the Spi Lake deposit.

Massive sulphide deposits are notably absent from the northeast end of Kaminak Lake with the exception of the thin, pyrite-sphalerite stringer zones on the NORSIK claims in NTS 55 L/2. An enigmatic sphalerite-bearing, magnetite-rich carbonate zone exposed on Angus Island (NTS 55 L/7) may represent a possible massive sulphide occurrence. Figure 6 illustrates tightly folded sphalerite-bearing veins from this occurrence.

The West zone of the Victory Lake massive sulphide in NTS 55 L/11 is an overturned layered unit, at least 4 m thick, with an underlying stringer zone. The alteration envelope of pyrite, muscovite, quartz±andalusite, staurolite, and gahnite is unique to this area and represents amphibolite-facies metamorphism of sericitic hydrothermal alteration (Armitage, 1997).

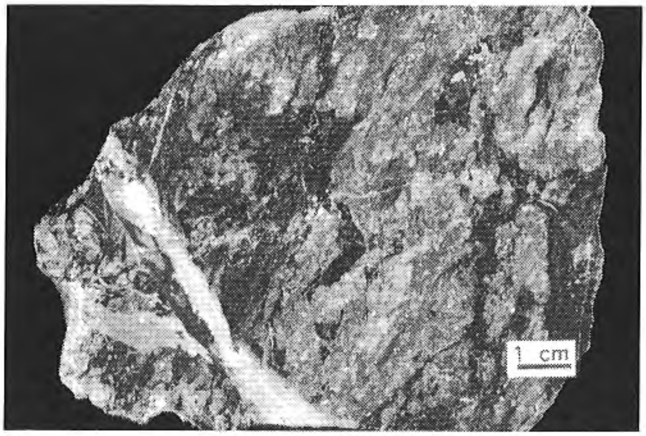


***Figure 6.*** *Deformed sphalerite-bearing quartz-rich veins in slab from the Angus Island base-metal occurrence.*

With rare exceptions, volcanic-associated massive sulphide occurrences have high silver concentrations and less than 2 ppm Au. Vein-related gold and base-metal occurrences are common in the vicinity of some massive sulphide deposits.

### *Vein-hosted base-metal occurrences*

Numerous vein-related base-metal occurrences are distributed throughout the study area (Fig. 1). However, they are most common in the vicinity of gold occurrences near Kaminak Lake and Quartzite Lake. For example, veins carrying base metals, but poor in both carbonate and gold are within the volcanic package which hosts the Cache deposit.

### *Proterozoic veins*

Of the occurrences which clearly postdate Proterozoic Hurwitz Group strata, almost all are chalcopyrite-bearing quartz and quartz-carbonate veins with less than 300 ppb Au and no sphalerite or galena. Similar and more numerous veins which cut Archean volcanic suites may also be Proterozoic.

Pyrite- and chalcopyrite-bearing, late, straight quartz veins, up to 2 m wide, cut the primary foliation that deforms the polymetallic veins at Happy Lake. These veins are probably Proterozoic.

## HIGHLIGHTS OF LITHOGEOCHEMICAL INVESTIGATIONS

Lithogeochemical data on samples collected by us from more than 40 occurrences have been displayed on a variety of bivariate diagrams in an effort to better characterize the metal endowments of the different classes and/or types of mineral occurrences and to identify possible genetic linkages between different classes and/or types.

Examination of the Au versus Ag plot (Fig. 7a) indicates that metal-rich samples from base-metal (massive sulphide) occurrences plot within a compositional field characterized by high Ag/Au ratios that is distinct from the fields defined by metal-rich samples from gold and polymetallic occurrences. Considering those samples with greater than 1 ppm Au and Ag, most from gold occurrences possess Ag/Au ratios close to 0.10 and most from polymetallic occurrences plot closer to a ratio of 1.0; however, there is some overlap between samples from gold and polymetallic occurrences. One sample from the enigmatic Angus Island occurrence plots within the field defined by samples from massive sulphide occurrences.

Examination of the Cu versus Zn plot (Fig. 7b) indicates considerable overlap between polymetallic and base-metal samples and that most samples from gold occurrences are poor in both Cu and Zn. However, two samples from the Mac gold occurrence and one from the 083 locale plot within the field defined by polymetallic and base-metal samples.

Examination of the Au versus Zn plot (Fig. 7c) indicates good separation of the fields for metal-rich samples from the three different classes of occurrences. However, there is overlap between some Zn-poor samples from polymetallic occurrences and those from gold occurrences. On this diagram, four samples from the enigmatic Angus Island occurrence and one sample from the enigmatic 092 locale plot within the field defined by samples from massive sulphide occurrences.

Examination of the Pb versus Zn plot (Fig. 7d) indicates good separation between metal-rich samples from polymetallic and massive sulphide occurrences, largely because Pb is not a major component in any of the polymetallic occurrences that were sampled. Most samples of gold occurrences possess low contents of both Pb and Zn. On this diagram three samples from the enigmatic Angus Island occurrence fall within the massive sulphide field.

Different samples from the same occurrence sometimes plot in different areas of the same diagram suggesting several distinct styles and/or stages of mineralization. This is most obvious for samples from Spi Lake which fall into different clusters in the Cu versus Zn and Pb versus Zn diagrams. Samples from the different zones at Happy Lake also plot in different areas of the Cu versus Zn and Au versus Zn diagrams.

Samples from occurrences of uncertain deposit type commonly plot within the compositional fields of those from known deposit types, suggesting similar styles of mineralization. For example, as noted above, several samples from the enigmatic Angus Island occurrence plot within the massive sulphide field defined by samples from Spi Lake, MAG, and NORSIK. It may be appropriate to reclassify Angus Island as a massive sulphide deposit.

Work to date indicates that the zones of pyritic quartz-sericite schist that were identified at four polymetallic occurrences in the Happy Lake area and at the Cache and Kate gold occurrences are characterized by depletion of sodium, calcium, and strontium with enrichment of aluminum and potassium. Similar alteration was identified in samples from the Spi Lake, MAG, and NORSIK massive sulphide occurrences.

Anomalous concentrations of one or more of As, Sb, Bi, Mo, W, Se, Te, Sn, and Mn were detected in samples collected during this investigation. The metal endowments of nine base-metal, six polymetallic, and four gold occurrences are summarized in Table 1. Information regarding the presence of deformed metal-rich veins and zones of pyritic, quartz-sericite schist is also provided.

Examination of Table 1 indicates that anomalous concentration Te, Se, Bi, As, Mo, and Sb were detected in one or more of the three massive sulphide deposits. Samples from the polymetallic veins at Happy Lake contain anomalous concentrations of Te, Se, Bi, As, and Mo. The polymetallic vein occurrence at PP102 is also enriched in Bi and Mo. The gold occurrences are variably enriched in one or more of Te, Bi, As, Sb, Se, W, and Mo. The Mac and Turquetil gold occurrences each contain anomalous W, Te, and Se. Angus Island and Mule/KAM, the two occurrences associated with iron-formation, are both enriched in Mn.

## METALLOGENIC IMPLICATIONS

Complex vein systems containing multiple generations of quartz-carbonate veins have been identified in the gold occurrences at Cache, Turquetil, and Mac, and in the polymetallic vein occurrences near Happy Lake. In each of these occurrences, at least some metal-rich veins as well as associated hydrothermal alteration zones have been overprinted by deformation and metamorphism. This indicates that significant gold and base metals were deposited prior to development of late shear zones.

Several lines of evidence suggest that metal deposition and alteration in the above-mentioned occurrences were at least partly controlled by synvolcanic processes. The presence of zones of pyritic quartz-sericite schist displaying depletion of Na, Ca, and Sr accompanied by enhanced Al and K is particularly important as such zones were identified in all the clearly synvolcanic massive sulphide occurrences that were visited during this investigation. At the global scale, pyritic, quartz-sericite schist is developed at many synvolcanic massive sulphide and porphyry and/or epithermal deposits (Franklin, 1996; Kirkham and Sinclair, 1996; R. Mason, abstract presented at Prospectors and Developers Association of Canada meeting, 1998). Furthermore, the elevated Au, Ag, Cu, and Zn contents, relatively high Ag/Au ratios, and locally anomalous concentrations of Bi, Se, Mo, As, and Te of the polymetallic vein occurrences at Happy Lake and elsewhere are characteristic of many synvolcanic porphyry and epithermal deposits (Kirkham and Sinclair, 1996). The overlap of compositional fields on the bivarite plots between samples from polymetallic vein and massive sulphide occurrences and between samples from polymetallic vein and gold occurrences is also consistent with concentration of gold and base metals in polymetallic occurrences and some gold occurrences by synvolcanic processes.

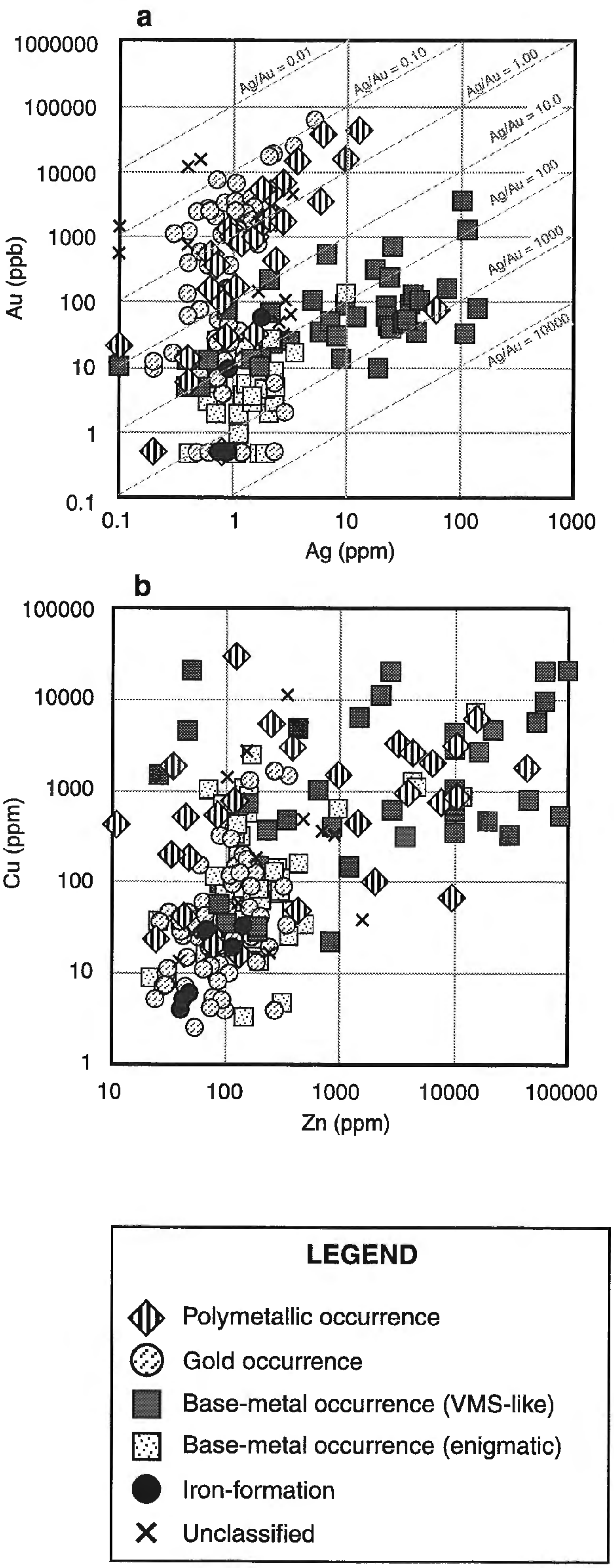


***Figure 7.***

*Scattergrams for **a**) Au versus Ag, **b**) Cu versus Zn, **c**) Au versus Zn, and **d**) Pb versus Zn.*

**Table 1.** Metal endowment and other critical features of selected mineral occurrences that were sampled during this investigation. VMS=volcanic-associated massive sulphide; BIF=banded iron-formation.

| Occurrences | Au | Ag | Cu | Zn | Pb | As | Sb | Bi | Mo | W | Se | Te | Sn | Mn | Deformed stringer zones/veins | Deformed quartz sericite schist | Alteration (low Na, Ca; high Al, K) |
|---|---|---|---|---|---|---|---|---|---|---|---|---|---|---|---|---|---|
| **Base metal** | | | | | | | | | | | | | | | | | |
| Spi Lake (VMS) | ++ | +++ | ++ | ++ | +++ | + | ++ | ++ | - | - | +++ | +++ | - | - | + | ++ | +++ |
| MAG (VMS) | +++ | +++ | ++ | +++ | ++ | ++ | + | ++ | - | - | +++ | +++ | - | - | ? | ++ | ++ |
| NORSIK (VMS) | + | ++ | + | +++ | + | + | + | +++ | + | - | + | ++ | + | - | ? | ++ | ++ |
| Angus Island (??) | + | ++ | ++ | ++ | - | + | - | ++ | - | - | ++ | +++ | - | + | ++ | - | - |
| Mac East (??) | - | - | - | - | - | - | - | - | - | - | - | - | - | - | + | + | + |
| Mule/KAM (VMS/BIF) | - | + | + | - | - | - | - | + | - | - | ++ | +++ | - | + | ? | - | - |
| 070 (??) | - | - | - | - | + | - | + | - | - | - | - | - | - | - | ? | - | - |
| 092 (??) | - | - | + | + | - | - | - | - | - | - | (+) | - | + | - | ? | - | - |
| 094 (??) | - | - | - | - | - | - | - | - | - | - | - | - | - | - | ? | - | - |
| **Polymetallic** | | | | | | | | | | | | | | | | | |
| Happy Lake (all 4 zones) | +++ | + | + | ++ | - | ++ | - | ++ | + | - | ++ | +++ | - | - | ++ | +++ | ++ |
| HL Zone 1 | +++ | + | - | ++ | - | ++ | - | ++ | - | - | + | +++ | - | - | +++ | +++ | +++ |
| HL Zone 2 | +++ | + | + | + | - | - | - | ++ | - | - | ++ | +++ | - | - | + | + | + |
| HL Zone 3 | ++ | + | + | - | - | - | - | ++ | + | - | ++ | +++ | - | - | ++ | ++ | ++ |
| HL Zone 4 | ++++ | ++ | ++ | ++ | - | ++ | - | +++ | - | - | ++ | +++ | - | - | +++ | + | - |
| 142 | - | - | - | + | - | - | - | - | - | - | (-) | + | - | - | ? | ? | ? |
| PP102 | +++ | ++ | ++ | - | - | - | - | ++ | + | - | ++ | ++ | - | - | ? | ++ | ++ |
| **Gold** | | | | | | | | | | | | | | | | | |
| Mac | ++++ | + | + | - | - | + | - | + | + | + | + | +++ | - | - | +++ | ? | ? |
| Turquetil (Joyce) | +++ | - | - | - | - | ++++ | ++ | ++ | - | + | + | +++ | - | - | ++ | ? | ? |
| Cache | +++ | + | - | - | - | + | + | + | - | - | - | ++ | - | - | ++ | ++ | ++ |
| Kate | +++ | + | - | - | - | - | - | ++ | - | - | + | ++ | - | - | + | + | + |

**For metals:** "-" = not anomalous (<10 times crustal abundance); "+" = weakly anomalous (>10 times crustal abundance); "++" = anomalous (>100 times crustal abundance); "+++" = strongly anomalous (>1000 times crustal abundance); "++++" = very strongly anomalous (>10 000 times crustal abundance);
**For last 3 columns:** "-" = not recognized; "+" = present; "++" = well developed; "+++" = intense development; "?" = unknown.

## EXPLORATION GUIDELINES

Recognition that synvolcanic processes may have contributed to deposition of gold and base metals in polymetallic vein occurrences and some gold deposits in the study area, suggests potential for discovery of metal-rich porphyry and/or epithermal deposits in the Rankin–Ennadai supracrustal belt. Areas of known polymetallic occurrences may be particularly favourable for discovery of additional synvolcanic mineralization.

Although enhanced concentrations of Ag, Zn, and Pb may be the best indicators of a contribution by synvolcanic processes to metal concentration, a significant number of our samples from massive sulphide, polymetallic vein, and vein-gold occurrences contain anomalous concentrations of one or more of Mo, Bi, Te, Se, W, Sb, and As. This suggests that these elements may also be useful exploration guides to synvolcanic deposits.

Identification of strongly deformed veins and zones of pyritic, quartz-sericite schist may also indicate the presence of synvolcanic mineralization.

## CONCLUSIONS

The metal endowment, style of alteration, and overprinting of metal-rich veins and alteration zones by deformation and metamorphism in several polymetallic occurrences and some gold occurrences are consistent with concentration of gold and base metals by synvolcanic processes linked to large-scale hydrothermal systems.

Much work remains to be done to better define the timing of metal deposition relative to volcanism, sedimentation, plutonism, deformation, and metamorphism. If synvolcanic processes and early structures did make a significant contribution to metal concentration in occurrences additional to those of volcanic-associated massive sulphide affinity, then the chances of discovering economically significant gold and/or base-metal deposits are greatly enhanced.

## ACKNOWLEDGMENTS

We would like to thank Simon Hanmer and Tony Peterson for providing us with a logistical base at the GSC Kaminak Lake camp. Access to the Polar Continental Shelf Project helicopter enabled us to visit a significant number of mineral occurrences. Stephanie Douma was of great help in getting samples organized for polished thin sections and lithogeochemistry. Richard Lancaster provided excellent photographs of rock slabs. XRAL Laboratories of Don Mills provided timely lithogeochemical analyses.


## REFERENCES


**Ali, A.A., Troup, W.R., and Otton, B.C.**
1989: Report on the 1989 field program of geological mapping, channel sampling, trenching, reconnaissance mapping and sampling of the Quartzite Lake claims; Northwest Territories Geology Division, Indian Affairs and Northern Development, Yellowknife, Assessment report No. 082888, 19 p. and appendices.

**Armitage, A.A.**
1997: The Victory Lake volcanic-associated base metal prospect, Kivalliq Region, Nunavut District, NWT: a project summary; Program and Abstracts of Talks and Posters, NWT Geoscience Forum 25th Anniversary Yellowknife; Northwest Territories Geology Division, Indian Affairs and Northern Development, Yellowknife, p. 10–13.

**Davidson, A.**
1970: Precambrian geology, Kaminak Lake map-area, District of Keewatin (55L); Geological Survey of Canada, Paper 69-51, 27 p.

**Davis, W.J., Hanmer, S., Peterson, T.D., Rainbird, R., Ryan, J., and Sandeman, H.A.I.**
1998: Preliminary U-Pb geochronology of volcanic rocks in the Kaminak belt, Western Churchill Province, Kivalliq Region, Northwest Territories; Program and Abstracts of Talks and Posters, NWT Geoscience Forum Yellowknife; Northwest Territories Geology Division, Indian Affairs and Northern Development, Yellowknife, p. 30–31.

**Franklin, J.M.**
1996: Volcanic-associated massive sulphide base metals; *in* Geology of Canadian Mineral Deposit Types, (ed.) O.R. Eckstrand, W.D. Sinclair, and R.I. Thorpe, Geological Survey of Canada, Geology of Canada, no. 8, p. 158–183 (*also* Geological Society of America, The Geology of North America, v. F-1).

**Goff, S.P.**
1997: Keewatin Region; in Exploration Overview 1996, Northwest Territories, Part 2; Northwest Territories Geology Division, Indian Affairs and Northern Development, Yellowknife, p. 11–14.

**Goff, S.P. and Mills, A.**
1998: Significant mineral occurrences of the central Rankin-Ennadai supracrustal belt: Spi-Kaminak-Quartzite Lakes and Heninga-Kogtok Lakes: (NTS 55 E/13-14, 55 L/1-16, 65 H/15-16 & 65 I/1-2); Northwest Territories Geology Division, Indian Affairs and Northern Development, Yellowknife, EGS 1998-15, spreadsheet with descriptive notes.

**Hanmer, S., Peterson, T.D., Sandeman, H.A.I., Rainbird, R., and Ryan, J.J.**
1998a: Geology of the Kaminak greenstone belt from Padlei to Quartzite Lake, Kivalliq region, Northwest Territories; *in* Current Research 1998-C; Geological Survey of Canada, p. 85–94.

**Hanmer, S., Rainbird, R., Sandeman, H.A.I., Peterson, T.D., and Ryan, J.J.**
1998b: Field contributions to thematic studies related to the Kaminak greenstone belt, Kivalliq region, Northwest Territories; *in* Current Research 1998-C; Geological Survey of Canada, p. 77–84.

**Heaman, L.M.**
1994: 2.45 Ga global mafic magmatism: Earth's oldest auperplume?; *in* Abstracts of the Eighth International conference on geochronology, cosmochronology and isotope geology, (ed.) M.A. Lauphere, G.B. Dalrymple, and B.D. Turrin; United States Geological Survey, Circular 1107, p. 132.

**Heaman, L.M. and LeCheminant, A.N.**
1993: Paragenesis and U-Pb systematics of baddeleyite (ZrO2); Chemical Geology, v. 110, p. 95–126.

**Irwin, D.A. and Relf, C.**
1998: Geological compilation of the Kaminak Lake area (southern half of 55L), western Churchill Province; Northwest Territories Geology Division, Indian Affairs and Northern Development, Yellowknife, EGS 1998-08, scale 1:125 000.

**Irwin, D.A., Hanmer, S., Sandeman, H.A., Rainbird, R.H., Peterson, T.D., Relf, C., Ryan, J.J., Goff, S.P., Mills, A., and Kerswill, J.A.**
1998: Geology of Carr-Kaminak-Quartzite Lakes area, Kivaliq region, Northwest Territories; Geological Survey of Canada, Open File 3649, scale 1:125000.

**Jones, A.**
1997: A guide to mineral deposits of the Northwest Territories; Minerals Oil and Gas Division, Resources Wildlife and Economic Development, Government of the Northwest Territories, 126 p.

**Kirkham, R.V. and Sinclair, W.D.**
1996: Porphyry copper, gold, molybdenum, tungsten, tin, silver; *in* Geology of Canadian Mineral Deposit Types, (ed.) O.R. Eckstrand, W.D. Sinclair, and R.I. Thorpe, Geological Survey of Canada, Geology of Canada, no. 8, p. 421-446 (*also* Geological Society of America, The Geology of North America, v. F-1).

**Knowles, U.M., Knowles, R.J., and Jensen, M.C.**
1988: Geological, geochemical and geophysical Surveys and diamond drill report, Permit No. 1086 - NTS 55L/10 SE; Northwest Territories Geology Division, Indian Affairs and Northern Development, Yellowknife, assessment report No. 082565, 40 p. and appendices.

**Laporte, P.J.**
1976: Keewatin District and Melville Peninsula; in Mineral Industry Report 1973, Northwest Territories; NWT Geology Division, Indian Affairs and Northern Development, Yellowknife, EGS 1976-9, p. 10–33.

**Leggett, S.R.**
1980: The South Heninga Lake Copper-Zinc deposit, District of Keewatin, NWT; M.Sc. thesis, University of Manitoba, Winnipeg, Manitoba, 67 p.

**Miller, A.R.**
1992: Gold Metallogeny, Churchill Structural Province; Project Summaries, Canada-NWT Mineral Development Subsidiary Agreement 1987-1991; Geological Survey of Canada, Open File 2484, p. 157–160.

**Miller, A.R. and Tella, S.**
1995: Stratigraphic setting of semiconformable alteration in the Spi Lake area, Kaminak greenstone belt, Churchill Province, Northwest Territories; *in* Current Research 1995-C; Geological Survey of Canada, p. 185–186.

**Ridler, R.H.and Shilts, W.W.**
1974: Exploration for Archean polymetallic sulphide deposits in permafrost terrains: an integrated geological-geochemical technique, Kaminak Lake area, District of Keewatin; Geological Survey of Canada, Paper 73-34, 33 p.

**Strand, P.**
1988: Noble Peak Resources Ltd., Happy Lake Project, Zone 1: an example of gold mineralization in the Archean Kaminak Group, Rankin Inlet - Ennadai greenstone belt, eastern Northwest Territories; B.Sc. Thesis, University of Toronto, Toronto, Ontario, 114 p.

**Troup, W.R., Ali, A.A., Otton, B.C., and Beales, P.L.**
1989: Report on the 1989 diamond drilling, sampling, mapping and geophysical surveys, Kaminak Lake area, Southwin project; Northwest Territories Geology Division, Indian Affairs and Northern Development, Yellowknife, assessment report No. 082891, 37 p. and appendices.


Geological Survey of Canada Project 840003WC

# Results of integrated geological and aeromagnetic mapping, and recent exploration, Henik and Hurwitz groups, Noomut River, Northwest Territories (Nunavut)[1]

Lawrence B. Aspler[2], Bruce A. Barham[3], Jeffrey R. Chiarenzelli[4]
Continental Geoscience Division, Ottawa

*Aspler, L.B., Barham, B.A., and Chiarenzelli, J.R., 1999: Results of integrated geological and aeromagnetic mapping, and recent exploration, Henik and Hurwitz groups, Noomut River, Northwest Territories (Nunavut);* in *Current Research 1999-C; Geological Survey of Canada, p. 157–168.*

**Abstract:** Henik Group (Neoarchean) supracrustal rocks, including iron-formation marker horizons, were deposited in a deep-water lava plain–slope-basin setting across at least 6000 $km^2$ in central Ennadai–Rankin greenstone belt. Hurwitz Group (2.45–2.11 Ga) rocks record continental to marine intracratonic-basin sedimentation. Archean rocks experienced synplutonic folding, faulting, and metamorphism ($D_1$, probably Archean), east-northeast-trending folding that was followed by dextral faulting ($D_2$; Paleoproterozoic(?)) and cross faulting ($D_3$). At recently discovered prospects in the Henik Group, gold (with disseminated pyrite and pyrrhotite) is concentrated in quartz veins and carbonate-pyrite alteration zones in gabbro ('Esker' prospect); quartz-carbonate-chlorite veins in magnetite iron-formation interbedded with turbiditic semipelite ± felsic tuff ('Ironside' prospect); quartz-carbonate veins in iron carbonate–quartz-albite schist, apparently derived from metasomatism of variolitic pillow lava ('Napartok' prospect); and quartz-carbonate-biotite veins in magnetite iron-formation interbedded with turbiditic semipelite ('River' prospect). All four prospects appear to be related to $D_2$ or later structures.

**Résumé :** Les roches supracrustales du groupe néoarchéen de Henik, notamment des horizons repères de formation de fer, se sont déposées en eau profonde dans un milieu de plaine de laves–bassin de talus sur au moins 6 000 $km^2$ dans la partie centrale de la ceinture de roches vertes d'Ennadai–Rankin. Les roches du Groupe de Hurwitz (2,45–2,11 Ga) témoignent d'une sédimentation continentale à marine dans un bassin intracratonique. Les roches archéennes ont été l'objet de plissement, de fracturation et de métamorphisme synplutoniques ($D_1$, vraisemblablement archéen), de plissement à orientation est-nord-est qui a été suivi par la formation de failles dextres ($D_2$; Paléoprotérozoïque(?)), et de la formation de failles transversales ($D_3$). Dans des zones d'intérêt récemment découvertes dans le Groupe de Henik, l'or (accompagné de pyrite et de pyrrhotite disséminées) est concentré dans des filons de quartz et des zones d'altération de carbonate-pyrite dans du gabbro (zone d'intérêt d'«Esker»); dans des filons de quartz-carbonate-chlorite dans de la formation de fer à magnétite intercalée avec de la semipélite turbiditique ± du tuff felsique (zone d'intérêt d'«Ironside»); dans des filons de quartz-carbonate dans du carbonate de fer–schiste à quartz et albite, apparemment issus du métasomatisme de laves en coussins variolitiques (zone d'intérêt de «Napartok»); et dans des filons de quartz-carbonate-biotite dans de la formation de fer à magnétite intercalée avec de la semipélite turbiditique (zone d'intérêt de «River»). Les quatre zones d'intérêt seraient apparentées à des structures $D_2$ ou à des structures plus récentes.

[1] Contribution to the Western Churchill NATMAP Project
[2] 23 Newton Street, Ottawa, Ontario K1S 2S6
[3] Comaplex Minerals Corp., Suite 901, 1015 Fourth Street S.W., Calgary, Alberta T2R 1J4
[4] Environmental Research Center, State University of New York at Oswego, Oswego, New York, U.S.A. 13126

## INTRODUCTION

One focus of the Western Churchill NATMAP Project is to establish the tectonic significance of supracrustal remnants that define the greater Ennadai–Rankin greenstone belt (Fig. 1). A related question, of long-standing concern in many Archean granite-greenstone *terrains* (e.g. Pettijohn, 1970), concerns the primary extent of the basins in which the supracrustal rocks were deposited. Do the remnants represent a relatively continuous depocentre that was structurally dismembered, or do they reflect multiple depocentres that were tectonically accreted as exotic *terranes*? Although accretionary-type models have gained ascendancy in recent years (e.g. Card, 1990; Taira et al., 1992; Myers, 1995), physical continuity of depositional basins over large areas has been inferred in many granite-greenstone terrains, and field and geochronological data call into question interpretations that structural breaks within some greenstone belts are sutures marking terrane boundaries (Slave Province: Padgham, 1992; Superior Province: Heather et al., 1995; Yilgarn Craton, Australia: Nelson, 1997; Belingwe greenstone belt, Zimbabwe: Blenkinsop et al., 1993).

Part of the uncertainty stems from the limited lateral continuity of stratigraphic units in volcanic terrains, where local subenvironments related to magmatic centres produce a complex array of interfingering facies (e.g. Orton, 1995). Iron-formation horizons may be the best substitute for marker units in Archean greenstone belts lacking a 'layer cake' stratigraphy (Goodwin and Ridler, 1970; Heather et al.,1996). They are distinctive, relatively continuous, and have a marked aeromagnetic expression that permits tracing through areas of poor outcrop. In addition, iron-formation units form in many depositional environments (Fralick and Barrett, 1995) and they constitute mainly chemogenic deposits that accumulate during times of volcanic quiescence. Hence they may represent trans-facies condensed intervals having the potential to define sequence boundaries for the application of Phanerozoic-style sequence stratigraphy to Archean greenstones (*see* Eriksson et al., 1994; Krapez, 1996).

New mapping in the Noomut River area (Fig. 1, 2), aided by high-resolution aeromagnetic data provided by Comaplex Minerals Corp. (Fig. 3), demonstrates that iron-formation units continue from Magnet Bay on South Henik Lake eastward for at least 60 km. These iron-formation units have proven invaluable in documenting the stratigraphy and structure of the Henik Group, the local name for Neoarchean

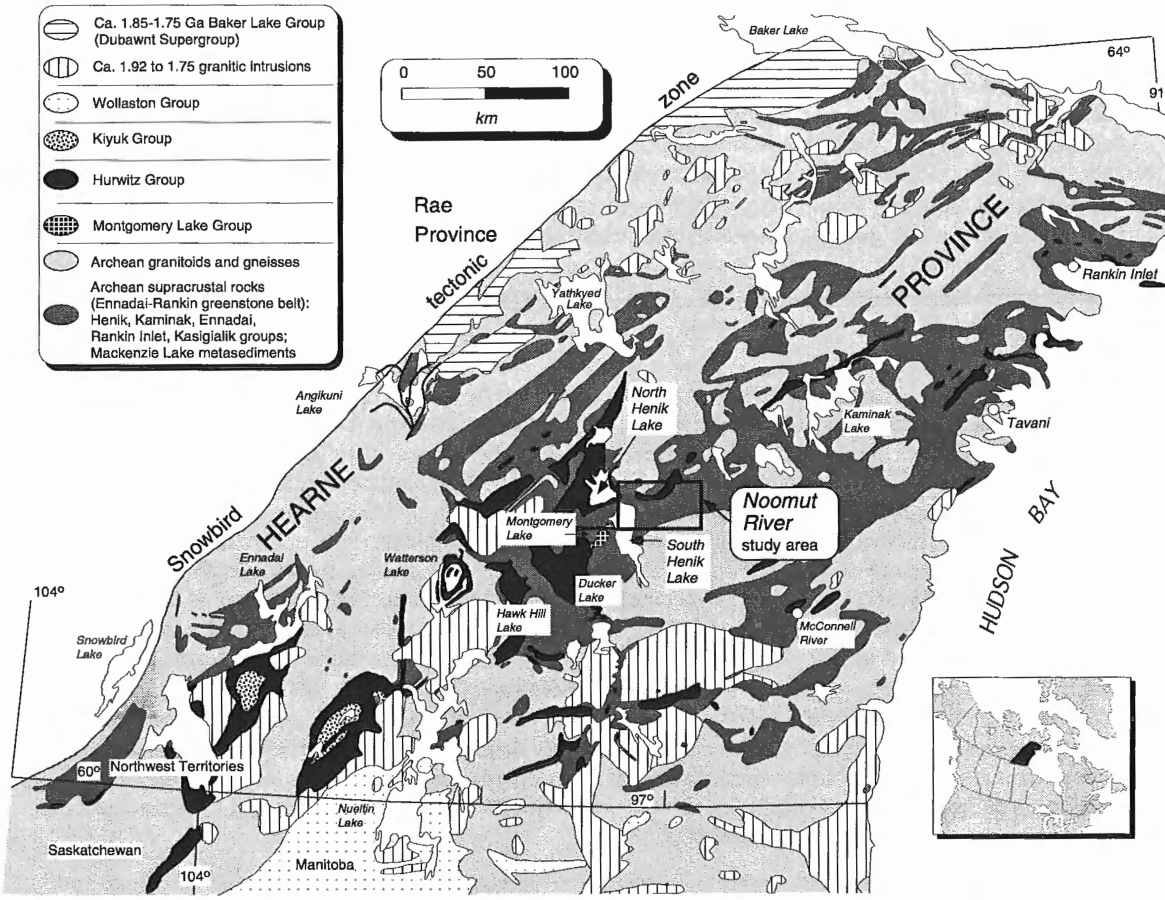


*Figure 1. Location of study area, simplified geology of the Hearne Province, Northwest Territories (after Aspler and Chiarenzelli, 1996a).*

supracrustal rocks in the central part of the Ennadai–Rankin greenstone belt (Eade, 1974). In this paper we outline the stratigraphy, sedimentology, and physical volcanology of the Henik Group in the Noomut River area, emphasizing the use of iron-formation units as marker beds, and consider the implications for the Ennadai–Rankin greenstone belt. We also summarize the geology of the Hurwitz Group (Paleoproterozoic) which is infolded with the Henik Group and evaluate the roles of Archean and Paleoproterozoic deformation. This will set the context for a summary outlining the results of recent gold exploration in the Noomut River area.

## HENIK GROUP

### *Stratigraphic framework*

In the central part of the Ennadai–Rankin greenstone belt, oxide-facies iron-formation units have been mapped from the Ducker Lake area approximately 35 km north to the area west of the Henik lakes (Fig. 1). New mapping confirms that these iron-formation units extend across the Noomut River area to at least Harling Lake (Fig. 2, 3). Figure 4 is a stratigraphic chart which, using the iron-formation units as a datum, illustrates correlations of subunits within the Henik Group.

In Figure 4, informal stratigraphic subdivisions outlined in Aspler and Chiarenzelli (1996a) are retained. However, new data necessitate revision of previous stratigraphic correlations. In the Noomut River area, rocks are considered to be entirely within unit A2, a mixed sedimentary-volcanic assemblage consisting of mafic volcanic rocks (A2mv); felsic to intermediate volcanic rocks (A2f); interfingering turbiditic sandstone-mudstone sets, felsic to intermediate tuff, mafic flows and intraformational conglomerate (A2i); and magnetite-bearing iron-formation (A2tif). Exposures of A2mv in the northwestern part of the Noomut River area are continuous with rocks previously mapped as part of unit A3 in the Magnet Bay area (Aspler and Chiarenzelli, 1997a). New mapping demonstrates that this section underlies iron-formation-bearing unit A2tif and is not part of unit A3 (Fig. 4).

### *Unit Descriptions*

The lowermost subfacies in the Noomut River area is unit A2mv (Fig. 2, 4). It consists predominantly of mafic volcanic flows cut by gabbroic dykes, sills, and stocks. The flows are non-amygdaloidal, thickly bedded, and display massive, pillowed, and sheet-flood morphologies. Pillow breccia and variolitic horizons are common. Rare lenses include sulphide-facies iron-formation (banded and colloform pyrite and chert) and rhyolitic flows. In the northwestern part of the area, A2mv is overlain by a wedge of felsic to intermediate volcanic flows, tuff, breccia and agglomerate units (A2f). The breccia and agglomerate units are monomictic, and form massive beds up to 10 m thick. In the breccia units, angular clasts up to 1 m have sharp clast boundaries and are self-supporting; in the agglomerates, amoeboid clasts display indistinct boundaries and are supported by a crystal-rich matrix.

Elsewhere in the Noomut River area, unit A2mv is overlain by unit A2i (Fig. 2, 4). Turbiditic sandstone-mudstone sets and intermediate to felsic tuff form end-member subfacies within A2i. The turbiditic rocks consist of laterally continuous decimetre-scale sandstone to mudstone fining-upward sequences and centimetre- to millimetre-scale rhythmites. Rarely preserved are vertical profiles arranged in the sequence sharp base – massive or graded arkose –parallel stratification (±ripple drift cross-stratification) – siltstone – mudstone. Sandstone to pelite ratios within single sequences range from 3/7 to 9/1. However, for most of A2i, the sandstone component is predominant, particularly in the eastern Noomut River area where massive sandstone (± pebbly sandstone) forms amalgamated beds several metres thick that are separated by thin mudstone partings. The turbiditic rocks also contain local lenses of conglomerate with intraformational clasts (chert, iron-formation, mafic and felsic volcanic rock) and metre-scale massive or parallel-stratified sandstone interbeds. In low-strain zones, the tuff subfacies consists of decimetre- to metre-scale sheets of coarse, zoned feldspar euhedra and broken euhedra, and trace bipyramidal quartz. Juvenile feldspar-phyric fragments up to 10 cm (some with distorted internal lamination) are locally abundant. Rarely, variation in crystal size or concentration defines layering or graded bedding. More typically, pervasive carbonate-alteration and a penetrative cleavage combine to obliterate primary textures, and the tuffs units outcrop as sericite schist.

Oxide-facies iron-formation is interbedded with unit A2i turbiditic and crystal tuff subfacies, both as thick (~ 300 m) members and as thin (ca. ~ 10 m) isolated layers (unit A2tif). Magnetite-bearing rip-up clasts are common at the base of the mass flow/pyroclastic deposits, and the iron-formation contains abundant soft-sediment folds, faults (including fold-fault gravity-slide pairs), dykes, load casts, and flame structures. Magnetite is concentrated in the pelitic parts of decimetre-scale fining upward sequences and millimetre-scale sandstone-mudstone rhythmites. These concentrations contain internal rhythmites of siltstone, dense black magnetite, and white microquartz. The siltstone consists of angular detrital feldspar and quartz grains in a microquartz cement. Siltstone-magnetite contacts are locally graded, with magnetite content increasing upward, and some magnetite layers contain isolated, angular, detrital silt grains. Microbands of magnetite and microquartz form a continuum, from those with almost pure magnetite (± lenses of microquartz) to those with subequal magnetite and microquartz.

### *Interpretation*

Unit A2 subfacies in the Noomut River area are interpreted within the context of a subaqueous lava plain–slope-basin depositional model developed for the central part of the Ennadi–Rankin greenstone belt (Aspler and Chiarenzelli, 1996a). Water depth was primarily below storm wave-base as indicated by preservation of delicate lamination in pelitic and iron-formation units; absence of features suggestive of subaerial exposure, oscillatory flow, or tidal currents; and lack of interfingering rocks that could represent laterally adjacent shelf, coastal, or continental environments.

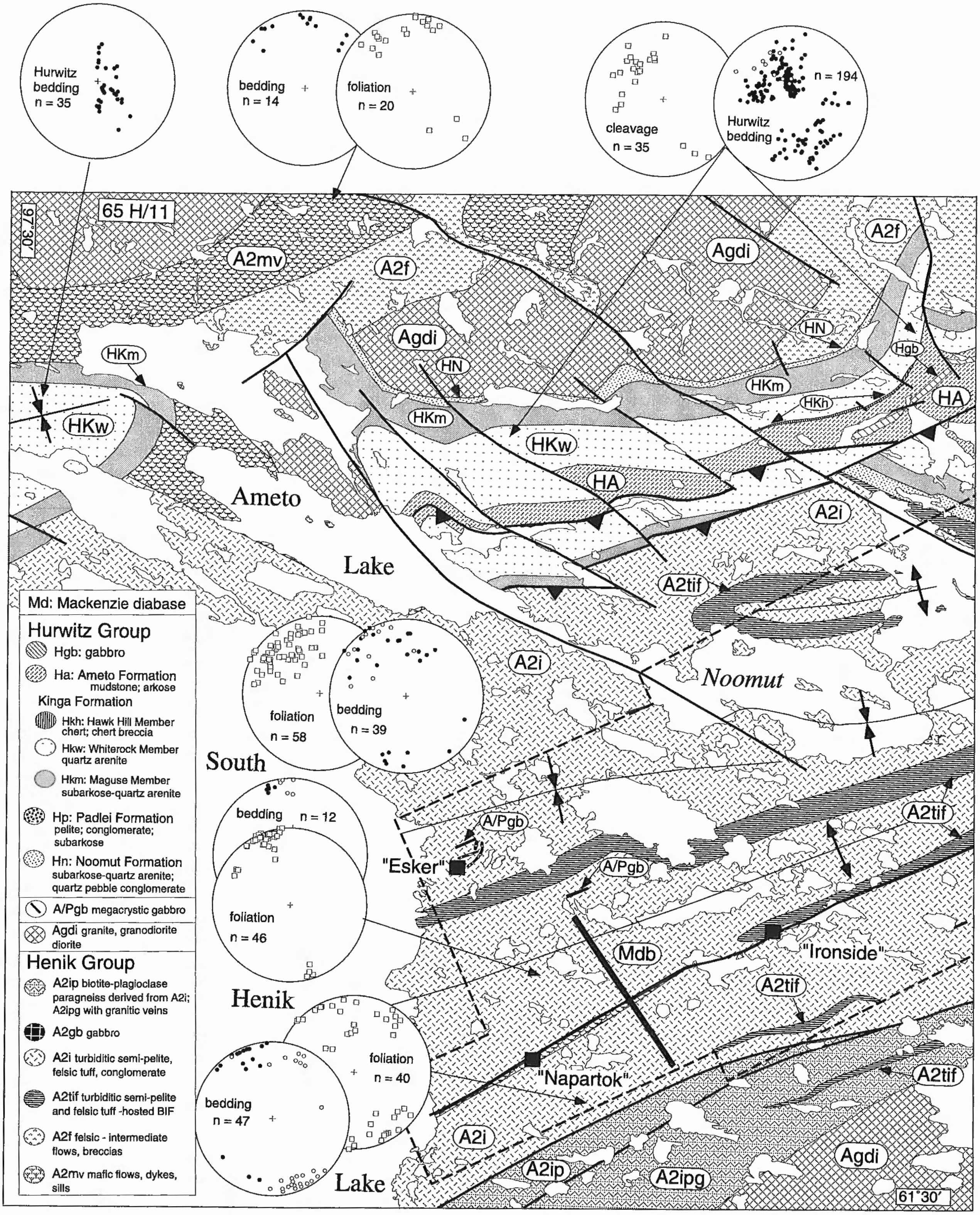


***Figure 2.*** *Simplified geological map, Noomut River area (65 H/10 and 65 H/11) area. Key to stereonets: solid circles = upright bedding, open circles = overturned bedding; open boxes = foliation.*

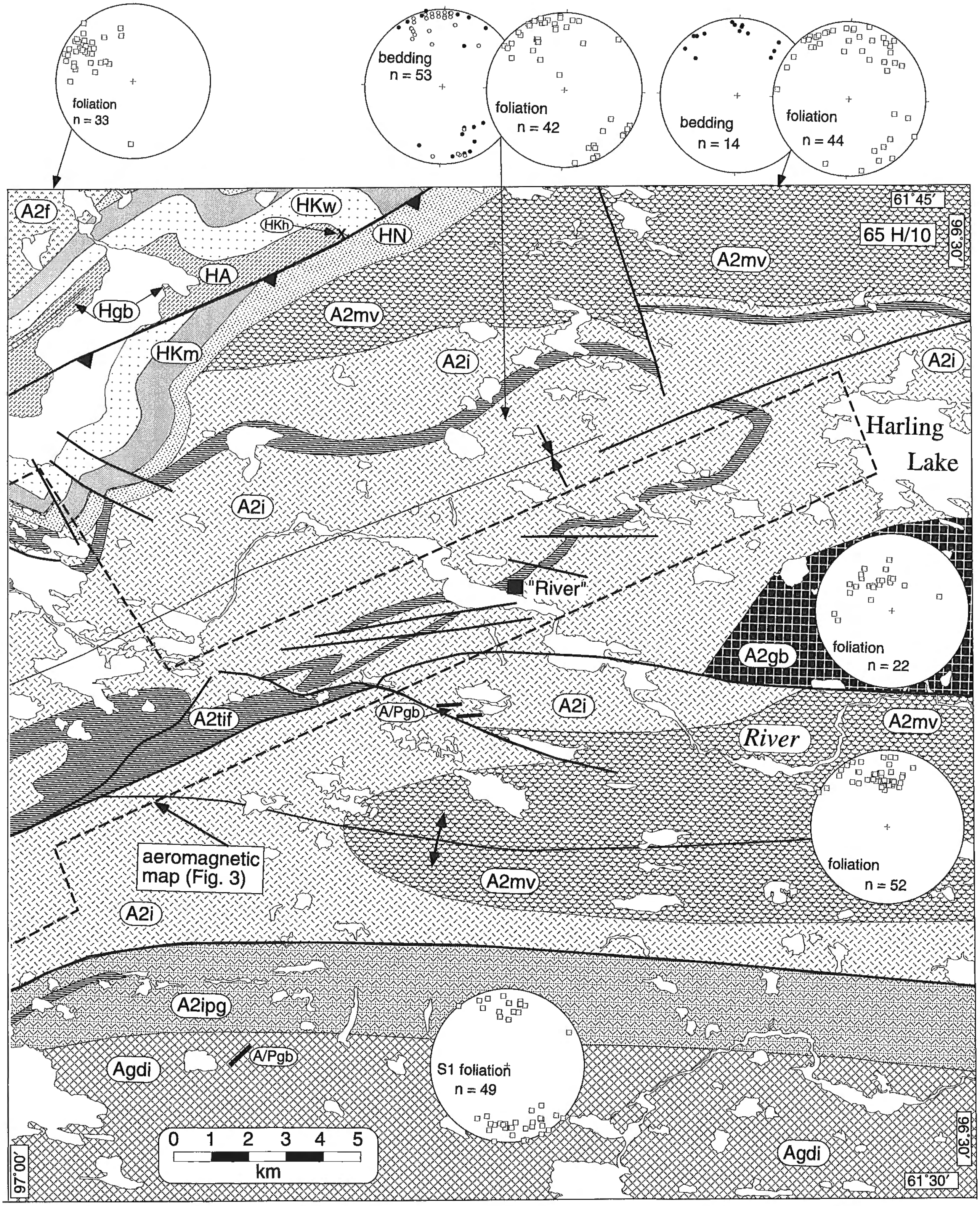


*Figure 2. (cont.)*

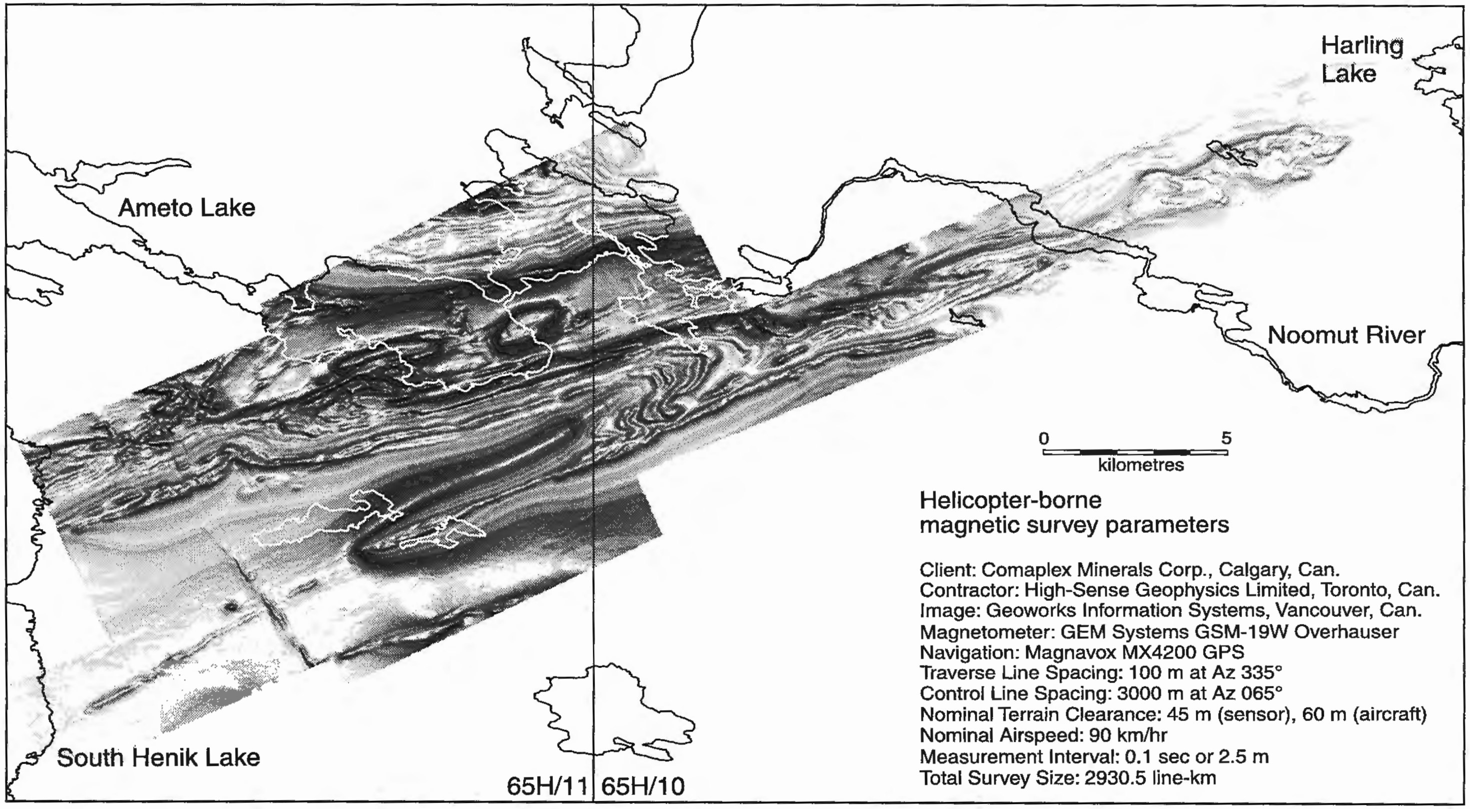


***Figure 3.*** *Aeromagnetic map, central Noomut River area. Courtesy of Comaplex Minerals Corp.*

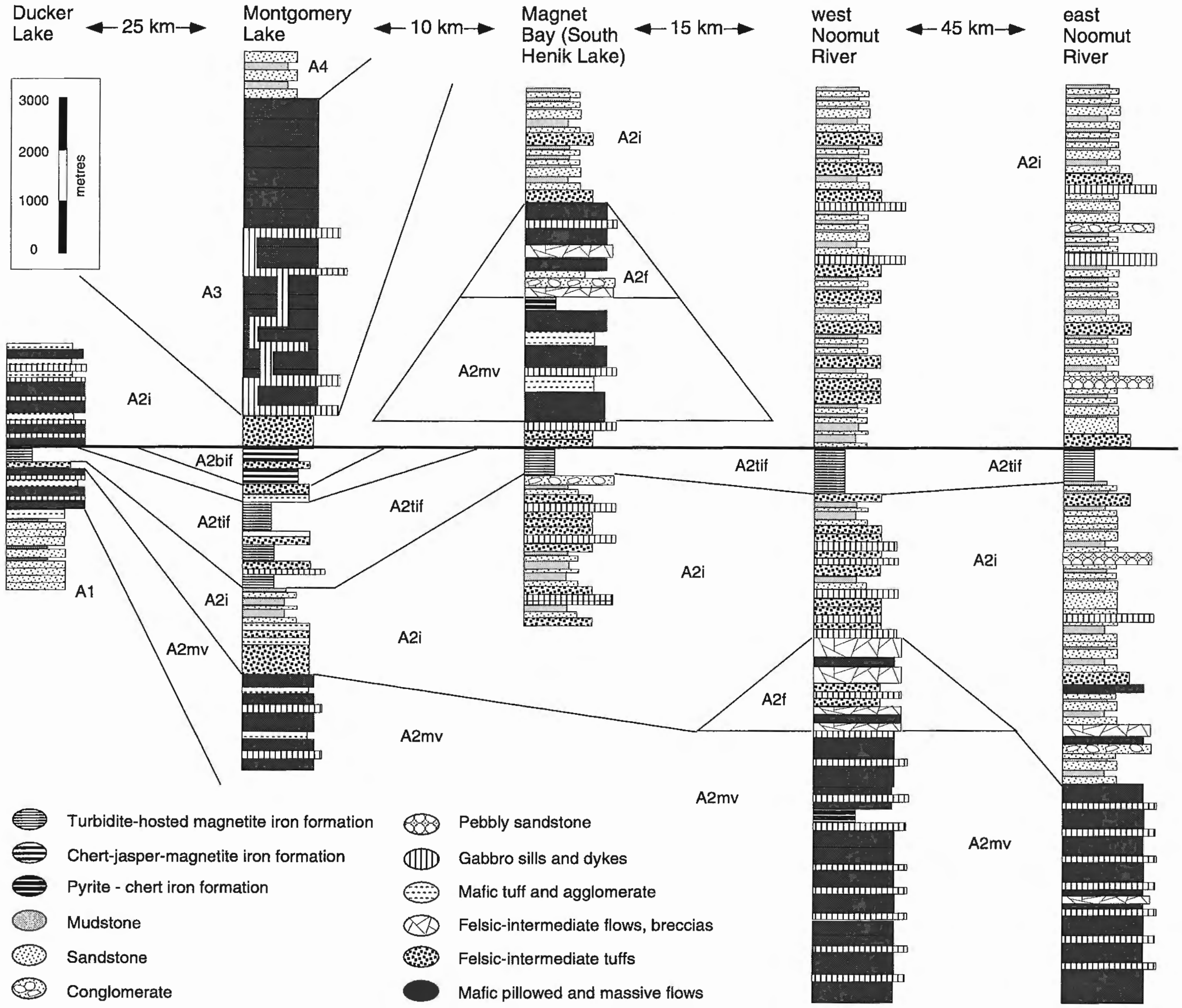


***Figure 4.*** *Stratigraphy of the Henik Group, central Ennadai–Rankin greenstone belt (revised after Aspler and Chiarenzelli, 1996a).*

Mafic rocks of unit A2mv are interpreted to represent a subaqueous lava plain containing local sulphidic pools (pyrite-chert lenses). Volcanism on the plain was primarily effusive, with interlayering of massive, sheet, and pillowed flows and pillow breccia resulting from varying rates of flood-like extrusion (e.g. Gregg and Fink, 1995). The paucity of amygdules and pyroclastic beds is probably a consequence of high confining pressure in relatively deep water (e.g. Sylvester et al., 1997). Wedges of felsic to intermediate breccia, agglomerate, and massive flows (unit A2f) likely signify buildup of stratovolcanic domes during waning stages of mafic volcanism. Both hot (amoeboid clasts with indistinct boundaries) and cold (angular clasts with sharp boundaries) emplacement mechanisms are indicated. Equivalent rocks in the Magnet Bay area (Fig. 4) contain interbeds of framework-intact monomictic conglomerate (with well rounded felsic clasts) and wavy-bedded, carbonate-cemented sandstone, indicating that some of the domes reached emergent to near-emergent levels.

Accompanying waning mafic volcanism, and possibly related to isostatic sinking, sedimentary subunits onlapped the lava plain, forming a transgressive vertical profile. The crystal and pebbly tuff subfacies of unit A2i probably formed by both pyroclastic and epiclastic processes related to felsic to intermediate volcanism. Although diagnostic evidence of primary pyroclastic deposition is rarely preserved (juvenile fragments with distorted laminae), the predominance of angular and broken feldspar euhedra suggests that the tuff units, if not strictly pyroclastic, experienced minimal reworking. Some may have ultimately formed by gravity sliding of unconsolidated pyroclastic debris initially deposited on domal flanks.

In the turbiditic facies of unit A2i, the range in scale and sandstone/mudstone ratio is thought to reflect a continuum of sediment gravity-flow processes, from low-concentration turbidity currents (mud-rich) to debris flows or high-concentration turbidity currents (sand rich ± pebbly beds; *see* Ghibaudo, 1992; Shanmugam, 1997). Lacking paleocurrent data, we cannot rule out the possibility that some of the rhythmites were deposited by contour currents (*see* Stow et al., 1998). Conglomerate-sandstone lenses are interpreted as submarine channel deposits rather than lags that delineate major breaks in sedimentation because they define lenses within the turbiditic rocks, consist of angular intraformational clasts, and individual beds are not traceable beyond about 1 km.

Iron-formation units of unit A2tif are considered volcanogenic hydrothermal deposits formed during times of minimal volcanism, both by chemical sedimentation and by spillover from low-concentration turbidity currents. We infer that the siliciclastic-free, magnetite-microquartz microbands are entirely undiluted, background, chemogenic deposits that accumulated between pyroclastic and sediment gravity-flow pulses. Grading of siltstone to magnetite, and the occurrence of detrital feldspar and quartz silt indicate concurrent physical sedimentation. The abundance of soft-sediment deformation structures, including gravity slides, signifies that some of the iron-formation was deposited on a slope. The graded siltstone to magneite layers likely reflect reworking of chemogenic oozes initially deposited up-slope and ultimately deposited as lutitic detritus.

### *Regional considerations*

Recent mapping indicates that a single basin covered an area of at least 6000 km$^2$ in the central segment of the Ennadi–Rankin greenstone belt. How much farther this basin extended is an open question. Based largely on the distribution of iron-formation, Goodwin (1973) suggested continuity east to McConnell River and north to Tavani (Fig. 1). This concept remains to be tested in its entirety. However, we suggest that, at least between the Henik Lakes and Kaminak Lake areas, the idea of a single depocentre is valid, and that differences between the two areas reflect relative proximity to a major felsic magmatic centre near Kaminak Lake.

Supracrustal rocks continue between the two areas without a significant structural break. In addition, outcrops of iron-formation at Tootyak Lake in the southern Kaminak Lake region (*see* Hanmer et al., 1998) are indistinguishable from those at Noomut River. Furthermore, distinctive felsic to intermediate breccia, conglomerate, and carbonate-cemented cross-stratified sandstone units in the Kaminak area, interpreted to have formed by near-emergent emplacement and reworking of a large volcanic dome (Hanmer et al., 1998), are strikingly similar to unit A2f in the Henik Lake area. However, relative to the Henik area, the Kaminak area appears to be characterized by a greater abundance of: volcanic breccia, conglomerate, and sandstone; texturally mature polymictic conglomerate and sandstone; vesicular and amygdaloidal mafic flows; and mafic pyroclastic tuff (*see* Hanmer et al., 1998). Using zonation of iron-formation facies, Ridler and Shilts (1974) inferred northward shallowing within the Kaminak area. We suggest a regional shallowing northeast from the Henik region toward a major felsic volcanic centre (and physiographic dome) near Kaminak Lake, and that differences between the two areas do not indicate a fundamental difference in tectonic setting.

## GRANODIORITE, GRANITE, DIORITE

Two felsic plutonic bodies are exposed in the Noomut River area (Agdi, Fig. 2). In the south, pervasively foliated biotite-hornblende granodiorite units cut turbiditic rocks, crystal tuff, and iron-formation. Both the pluton and a ca. 2.5 km border zone of biotite-plagioclase-hornblende paragneiss (A2ipg) contain variably oriented and deformed late-plutonic granitic sheets. Commonly crosscutting the host fabric, these sheets also contain a foliation concordant to the host rocks and are folded. Although plutonism may have started before, and continued during deformation (*see* Paterson et al., 1989), late magmatic stages were likely late-syntectonic to post-tectonic. The zone of paragneiss containing abundant granitic sheets passes abruptly northwest to a wedge of paragneiss lacking such sheets (A2ip). This wedge in turn passes abruptly to greenschist-grade protolith (A2i, Fig. 2). The sharp transitions and wedge geometry suggest merging of a fault splay to a master fault. Although outcrop is poor, this master fault is inferred to continue to the eastern limit of the map area (Fig. 2).

In the northern part of the area, units A2mv and A2f are cut by rocks that constitute part of a large composite pluton that extends beyond the limits of the map area. The predominant lithology is locally foliated hornblende-biotite granodiorite, but dioritic to gabbroic phases are also represented. Near the margins of the pluton are supracrustal rafts which contain a pervasive internal fabric. However, both supracrustal and plutonic rocks are cut by late-stage granitic dykes that range from undeformed to well foliated. Hence emplacement of the pluton was likely late syntectonic.

## MEGACRYST-BEARING GABBRO

Distinctive plagioclase-megacryst-bearing northeast-trending gabbro dykes, up to 25 m wide, are sparsely distributed in the Noomut River area (A/Pgb, Fig. 2). Although volumetrically insignificant, the dykes serve as important markers to separate local deformation events and will be valuable for testing regional structural correlations. In the south (Fig. 2), an undeformed dyke cuts cleanly across well foliated granodiorite considered to have been deformed during '$D_1$' (*see* below). Farther north, megacryst-bearing dykes cut Henik Group strata that were previously tilted to near-vertical attitudes during $D_1$. However, these dykes also contain a penetrative fabric (Fig. 5). Thus, geochronological study of the dykes will potentially establish the maximum age of $D_1$ and the minimum age of $D_2$ (*see* below).

## HURWITZ GROUP

North of Noomut River and Ameto Lake, Archean supracrustal and plutonic rocks are unconformably overlain by Paleoproterozoic rocks of the Hurwitz Group. The Hurwitz Group is a ca. 2.45–2.1 Ga (Heaman and LeCheminant, 1993; Heaman, 1994) assemblage of siliciclastic and carbonate rocks thought to have been deposited in an intracratonic basin that occupied the interior of the Hearne Province during the protracted breakup of Kenorland, a speculative Neoarchean–earliest Paleoproterozoic supercontinent (Aspler and Chiarenzelli, 1998). Continental deposits from the lower Hurwitz Group exposed in the area (Fig. 2) include auriferous pyritic quartz-pebble conglomerate and subarkose to quartz arenite (Noomut Formation; fluvial); semipelite (Padlei Formation; glacigenic/cold climate fluvial, lacustrine); subarkose to quartz arenite (Maguse Member; fluvial); supermature quartz arenite (Whiterock Member; lacustrine); and chert and chert breccia (Hawk Hill Member; sinter). These rocks are considered to represent the initial sag stage of basin expansion. This was terminated by abrupt basin-centre deepening and drowning, and deposition of mudstone and arkose (± microbial laminate) of the Ameto Formation (for details *see* Aspler and Chiarenzelli, 1996b; 1997b).

## STRUCTURAL GEOLOGY

A continuing theme of the Western Churchill NATMAP Project is to separate Archean and Proterozoic thermotectonic events. In the Noomut River area, evidence of Paleoproterozoic deformation occurring after ca. 2.1 Ga is provided by Hurwitz Group exposures which define a doubly-plunging, east-northeast-trending syncline, the core of which is imbricated by northwest-vergent thrusts (Fig. 2). The basement-cover contact is folded, one of the thrust faults juxtaposes Henik Group above Hurwitz Group, and numerous northwest-trending cross faults (likely formed late in the folding history as space-accommodating structures) which cut the Hurwitz Group also penetrate basement. These structures demonstrate Paleoproterozoic deformation of Archean rocks. Close to Hurwitz Group exposures, pre-Hurwitz Group deformation of Archean rocks is demonstrated by foliated clasts in basal conglomerates, and structural discordance at the Hurwitz–Henik unconformity, where steeply dipping Henik rocks are overlain by gently dipping Hurwitz strata.

We recognize three structural generations in Archean rocks. The oldest ('$D_1$') is uniquely identifiable only in the southern part of the area, and is manifested by a pervasive foliation in the granodioritic pluton and in the zone of paragneiss (A2ipg and A2ip, Fig. 2) which flanks the pluton. A megacryst-bearing gabbro cuts cleanly across well foliated granodiorite, separating '$D_1$' from '$D_2$' (*see* below). Elsewhere in the map area, we are generally unable to make the distinction between a $D_1$ foliation intensified during $D_2$ and a foliation originating during $D_2$. Hence foliation measurements portrayed in Figure 2 are mainly of unknown generation. Identification of large-scale $D_1$ structures is also uncertain. The splay and master faults inferred on the basis of sharp transitions between A2ipg, A2ip, and A2i (*see* above) are likely candidates.

Between the zone of paragneiss and Hurwitz Group exposures, the Henik Group is deformed by a series of tight to isoclinal east-northeast-trending folds with steeply dipping axial surfaces (Fig. 2). Although younging data demand fold closures, hinge zones are not well exposed and we have relied heavily on aeromagnetic data to interpret their geometry. We infer that these folds are $D_2$ structures because of evidence suggesting a previous episode of tilting: 1) at two localities, megacrystic gabbro dykes cut steeply dipping Henik Group strata and, in contrast to the unfoliated dyke cutting the granodioritic pluton (*see* above) these dykes contain a foliation (Fig. 5); and 2) limbs of individual folds are inconsistently overturned, and fold hinges plunge steeply. However, we cannot rule out the possibility that some of the folds initiated during $D_1$ and were tightened during $D_2$. North of the inferred master fault in the south-central part of 65 H/10, a west-plunging, north-vergent anticline cored by mafic volcanic rocks displays a moderately south-dipping axial surface and is overturned to the north. Because its extrapolated axial trace is cut at a high angle by an east-northeast-trending fault we relate to $D_2$ (*see* below), this fold might be a $D_1$ structure. The rocks in the central part of the map area commonly contain a bedding-parallel cleavage, but because $S_1$-$S_2$ overprinting is only rarely preserved (Fig. 6), we are generally unable to specify which generation of deformation this cleavage belongs to.

An east-northeast-trending fault extends from South Henik Lake to the eastern limit of mapping. Based on the asymmetry of minor folds in iron-formation-bearing unit A2tif in its footwall (well expressed in Fig. 3), we infer that this fault has a dextral component. Because of similarity in trend, we tentatively link this fault to progressive $D_2$ strain and breaching of $D_2$ folds. For two reasons, both tenuous, $D_2$ may be Paleoproterozoic. First, the east-northeast-trending


***Figure 5.** Plagioclase- megacryst-bearing gabbro dyke with well defined foliation in groundmass. This dyke cross cuts steeply dipping strata containing a pre-existing fabric and the foliation is considered $S_2$.*


*Figure 6. Unit A2i sandstone to siltstone fining-upward sequence. The $S_2$ pressure solution cleavage (striping from upper right to lower left in siltstone layer) overprints bedding-parallel $S_1$.*

fault appears to represent the continuation of the Bray Thrust which, north of Montgomery Lake, juxtaposes Archean rocks above the Hurwitz Group (Aspler and Chiarenzelli, 1997b). However, tracing the fault across the approximately 15 km width of South Henik Lake is uncertain. Second, the east-northeast-trending structures in Archean rocks are subparallel to those in the Hurwitz Group, although similarity in trend may be coincidence. Dating of the megacryst-bearing gabbro would possibly establish the maximum age of $D_2$.

Northeast- and northwest-trending cross faults ('$D_3$') cut and deflect $D_2$ structures in Archean rocks. Locally adjacent to these faults, near-vertical bedding and cleavage are folded in a series of box and chevron cascade folds with shallowly dipping axial surfaces. A cleavage related to these folds is only locally developed, but a cleavage-cleavage lineation is common. The cross faults likely formed to accommodate constrictions related to $D_2$ folding, similar to those cutting the Hurwitz Group.

## RECENT EXPLORATION

Basal Hurwitz Group pyritic quartz-pebble-rich conglomerate units (Noomut Formation) have been historical gold targets in the belt extending from Noomut River to Kinga Lake. Previously considered the Montgomery Lake Group

**Table 1.** Recent gold prospects, Comaplex Minerals Corp., Noomut River area.

| Name of Prospect | UTM E/N Zone 14 NAD 27 | Gold Occurrence Type / Host Rocks | Minerals Associated with auriferous rocks | Selected Sampling and Drilling Results |
|---|---|---|---|---|
| **Esker** | 592370<br>6829440 | Quartz–iron carbonate veins in deformed and altered gabbro/diabase, lesser quartz-carbonate veins in quartz-carbonate-sericite schist | Sulphides: pyrite and lesser pyrrhotite in vein margins, minor chalcopyrite, molybdenite<br><br>Other: iron carbonate, muscovite, albite, green mica, tourmaline, titanite | Surface samples to 55.5 g/t Au<br><br>DDH97-13:<br>2.35 g/t Au over 70.95 m with 6.43 g/t Au over 12.9 m;<br>12.22 g/t Au over 2.5 m<br><br>DDH97-15:<br>8.18 g/t Au over 13.27 m<br><br>DDH97-23:<br>7.24 g/t Au over 5.0 m |
| **Ironside** | 600800<br>6827425 | Quartz-chlorite-carbonate veins and chlorite-sulphide replacement zones in oxide iron-formation | Sulphides: pyrite, arsenopyrite, lesser pyrrhotite, chalcopyrite<br><br>Other: iron carbonate, chlorite, biotite, calcite | Surface samples to 116 g/t Au<br><br>DDH96-1:<br>5.75 g/t Au over 3.0 m<br>Surface samples to 3.7 g/t Au |
| **Napartok** | 594830<br>6823870 | Quartz–iron carbonate veins, disseminated sulphides in iron carbonate–sericite-albite schist at mafic volcanic-sediment contact | Sulphides: pyrrhotite, lesser pyrite, arsenopyrite<br><br>Other: iron carbonate, albite, sericite, tourmaline, chlorite, anatase | DDH96-6:<br>18.3 g/t Au over 3.0 m<br><br>DDH96-7:<br>9.2 g/t Au over 2.5 m |
| **River** | 620000<br>6837050 | Quartz-carbonate-biotite veins, disseminated sulphides in chlorite schist, massive pyrite seams in argillaceous chert-poor iron-formation | Sulphides: pyrite, pyrrhotite<br><br>Other: biotite, carbonate | Surface samples to 84 g/t Au |

(*see* Aspler and Chiarenzelli, 1996b), the Noomut Formation has been recognized west to Oftedal Lake, containing up to 4212 ppb Au (Aspler and Chiarenzelli, 1997a). Many pebbles are pyrite-chert composites indistinguishable from Henik Group sulphidic iron-formation, indicating, at least in part, a paleoplacer origin.

Recent exploration in the Henik Group by Comaplex Minerals Corp. has identified several quartz-carbonate-vein-associated gold prospects (Table 1). At the 'Esker' prospect, gabbroic bodies cut, and are folded with, felsic rocks (quartz-sericite-carbonate schists) of both hypabyssal and extrusive origin. Gold occurs in quartz-carbonate veins and zones of carbonate-pyrite alteration, principally in the gabbros near lithological contacts. The veins contain a late, moderately southwest-plunging mineral lineation (fibrous quartz and iron carbonate) that is found only in the Esker area. The best mineralization is in hinge zones of open to tight southwest-plunging folds. Nearby post-$D_1$/pre-$D_2$ megacrystic-bearing gabbro units display pervasive sericitic alteration and a concordant penetrative fabric.

The 'Ironside' and 'Napartok' prospects are along the east-northeast-trending $D_2$ dextral-oblique fault that extends across the center of the area (Fig. 2). At the Ironside prospect, auriferous quartz-carbonate-chlorite veins are hosted by magnetite iron-formation interbedded with turbiditic semipelite (± felsic tuff). Adjacent to well mineralized veins, magnetite is replaced by a chlorite-pyrite-arsenopyrite assemblage. At the Napartok prospect, gold is in a subvertical zone of quartz-veined iron carbonate–quartz-albite-sulphide (pyrrhotite+pyrite+arsenopyrite) schist at the contact between variolitic mafic volcanic rocks and semipelite. Local preservation of variolites suggests derivation of the schist from mafic volcanic rocks. In core samples, pyrrhotite pseudomorphs pyrite, and commonly displays pressure shadow textures. At the 'River' prospect, auriferous quartz-carbonate-biotite veins, associated with pyrrhotite and pyrite, and rare massive pyrite seams, occur in magnetite iron-formation intervals interbedded with turbiditic semipelites. The veins are associated with east-northeast-trending $D_3$ cross faults and shallowly southwest-plunging cascade folds that overprint moderately west-plunging tight to isoclinal $D_2$(?) folds.

Recently discovered gold prospects in the Henik Group are associated with zones of iron carbonate–sulphide alteration and quartz-carbonate-sulphide veins. Concentrations of alteration and veins occur within geochemically favoured competent host rocks, within or adjacent to $D_2$ or later structures. Dating of megacryst-bearing gabbros can potentially test if these prospects are examples of Proterozoic gold in Archean rocks.

## ACKNOWLEDGMENTS

This project constitutes a Western Churchill NATMAP collaboration on the part of the Northwest Territories Geology Division of Indian Affairs and Northern Development Canada (Yellowknife), Comaplex Minerals Corp., and the Geological Survey of Canada. Participation by Comaplex was critical to the project and we thank Phil Mudry and Murray Pyke for their support, and Marcelle Hauseux and Sandor Surmacz for recognizing the gold potential of the area. We appreciate the expertise of pilot James Boles (Custom Helicopters) and cook Sharon Brown, and thank Simon Hanmer for arranging the industry–NATMAP field trip to Kaminak Lake in 1997. Simon Hanmer and Carolyn Relf provided constructive critical reviews.

## REFERENCES

**Aspler, L.B., and Chiarenzelli, J.R.**
1996a: Stratigraphy, sedimentology and physical volcanology of the Henik Group, central Ennadai–Rankin greenstone belt, Northwest Territories, Canada: Late Archean paleogeography of the Hearne Province and tectonic implications; Precambrian Research, v. 77, p. 59–89.
1996b: Relationship between the Montgomery Lake and Hurwitz groups, and stratigraphic revision of the lower Hurwitz Group, District of Keewatin; Canadian Journal of Earth Sciences, v. 33, p. 1243–1255.
1997a: Archean and Proterozoic Geology of the North Henik Lake area, District of Keewatin, Northwest Territories; *in* Current Research 1997-C; Geological Survey of Canada, p. 145–155.
1997b: Initiation of ca. 2.45–2.1 Ga intracratonic basin sedimentation of the Hurwitz Group, Keewatin Hinterland, Northwest Territories, Canada; Precambrian Research, v. 81, p. 265–297.
1998: Two Neoarchean supercontinents?: evidence from the Paleoproterozoic; Sedimentary Geology, v. 120, p. 75–104.

**Blenkinsop, T.G., Fedo, C.M., Bickle, M.J., Eriksson, K.A., Martin, A., Nisbet, E.G., and Wilson, J.F.**
1993: Ensialic origin for the Ngezi Group, Belingwe greenstone belt, Zimbabwe; Geology, v. 21, p. 1135–1138.

**Card, K.D.**
1990: A review of the Superior Province of the Canadian Shield, a product of Archean accretion; Precambrian Research., v.48, p. 99–156.

**Eade, K.E.**
1974: Geology of Kognak River area, District of Keewatin, Northwest Territories; Geological Survey of Canada Memoir 377, 66 p.

**Eriksson, K.A., Krapez, B., and Fralick, P.W.**
1994: Sedimentology of Archean greenstone belts: signatures of tectonic evolution; Earth-Science Reviews, v. 37, p. 1–88.

**Fralick, P., and Barrett, T.J.**
1995: Depositional controls on iron formation associations in Canada; *in* Sedimentary Facies Analysis, (ed.) A.G. Plint; International Association of Sedimentologists Special Publication 22, p. 137–156.

**Ghibaudo, G.**
1992: Subaqueous sediment gravity flow deposits: practical criteria for their field description and classification; Sedimentology, v. 39, p. 423–454.

**Goodwin, A.M.**
1973: Archean iron-formations and tectonic basins of the Canadian Shield; Economic Geology, v. 68, p. 915–933.

**Goodwin, A.M. and Ridler, R.H.**
1970: The Abitibi orogenic belt; *in* Basins and Geosynclines of the Canadian Shield, (ed.) A.J. Baer; Geological Survey of Canada Paper 70-40, p. 1–30.

**Gregg T.K.P., and Fink, J.H.**
1995: Quantification of submarine lava-flow morphology through analog experiments; Geology, v. 23, p. 73–76.

**Hanmer, S., Peterson, T.D., Sandeman, H.A.I., Rainbird, R.H., and Ryan, J.J.**
1998: Geology of the Kaminak greenstone belt from Padlei to Quartzite Lake, Kivalliq Region, Northwest Territories *in* Current Research 1998-C; Geological Survey of Canada, p. 85–94.

**Heaman, L.M.**
1994: 2.45 Ga global mafic magmatism: Earth's oldest superplume?; *in* Abstracts of the Eighth International Conference on Geochronology, Cosmochronology and Isotope Geology, (ed.) M.A. Lauphere, G.B. Dalrymple, B.D. Turrin; United States Geological Survey Circular 1107, p. 132.

**Heaman, L.M. and LeCheminant, A.N.**
1993: Paragenesis and U-Pb systematics of baddeleyite ($ZrO_2$); Chemical Geology, v. 110, p. 95–126.

**Heather, K.B., Shore, G.T., and van Breemen, O.**
1995: The convoluted "layer-cake": an old recipe with new ingredients for the Swayze greenstone belt, southern Superior Province, Ontario; *in* Current Research 1995-C; Geological Survey of Canada, p. 1–10.
1996: Geological investigations in the Swayze greenstone belt, southern Superior Province, Ontario: a final field update; *in* Current Research 1996-C; Geological Survey of Canada, p. 125–136.

**Krapez, B.**
1996: Sequence stratigraphic concepts applied to the identification of basin-filling rhythms in Precambrian successions; Australian Journal of Earth Sciences, v. 43, p. 355–380.

**Myers, J.S.**
1995: The generation and assembly of an Archean supercontinent: evidence from the Yilgarn craton, western Australia; *in* Early - Precambrian Processes, (ed.) M.P. Coward and A.C. Ries; Geological Society of London, Special Publication 95, p. 143–154.

**Nelson, D.R.**
1997: Evolution of the granite-greenstone terranes of the Eastern Goldfields, Western Australia: SHRIMP U-Pb zircon constraints; Precambrian Research, 83, p. 57–81.

**Orton, G.J.**
1995: Facies models in volcanic terranes: time's arrow versus time's cycle; *in* (ed.) A.G. Plint Sedimentary Facies Analysis; International Association of Sedimentologists Special Publication 22, p. 157–193.

**Padgham, W.A.**
1992: Mineral deposits in the Archean Slave Structural Province; lithological and tectonic setting; Precambrian Research, v. 58, p. 1–24.

**Paterson, S.R., Vernon, R.H., and Tobisch, O.T.**
1989: A review of criteria for the identification of magmatic and tectonic foliations in granitoids; Journal of Structural Geology, v. 11, p. 349–363.

**Pettijohn, F.J.**
1970: The Canadian Shield, a status report; *in* Basins and Geosynclines of the Canadian Shield, (ed.) A.J. Baer; Geological Survey of Canada Paper 70-40, p. 239–265.

**Ridler, R.H. and Shilts, W.W.**
1974: Exploration for Archean polymetallic sulphide deposits in permafrost terrains: an integrated geological/geochemical technique; Kaminak Lake area, District of Keewatin; Geological Survey of Canada Paper 73-34, 33 p.

**Shanmugam, G.**
1997: The Bouma sequence and the turbidite mind set; Earth-Science Reviews, v. 42, p. 201–229.

**Stow, D.A., Faugères, J.-C., Viana, A., and Gonthier, E.**
1998: Fossil contourites: a critical review; Sedimentary Geology, v. 115, p. 3–31.

**Sylvester, P.J., Harper, G.D., Byerly, G.R., and Thurston, P.C.**
1997: Volcanic aspects; *in* Greenstone Belts, (ed.) M.J. de Wit and L.D. Ashwal; Clarendon Press, Oxford, United Kingdom, p. 55–90.

**Taira, A., Pickering, K.T., Windley, B.F., and Soh, W.**
1992: Accretion of Japanese island arcs and implications for the origin of Archean greenstone belts; Tectonics, v. 11, p. 1224–1244.

# Lithotectonic framework of the Trans-Hudson Orogen in the northwestern Reindeer Zone, Saskatchewan: an update from recent mapping along the Reindeer Lake transect

D. Corrigan, S.J. Pehrsson, T.G. MacHattie[1], L. Piper[1], D. Wright[2], B. Lassen[3], and J. Chakungal[4]
Continental Geoscience Division, Ottawa

*Corrigan, D., Pehrsson, S.J., MacHattie, T.G., Piper, L., Wright, D., Lassen, B., and Chakungal, J., 1999: Lithotectonic framework of the Trans-Hudson Orogen in the northwestern Reindeer Zone, Saskatchewan: an update from recent mapping along the Reindeer Lake transect;* in *Current Research 1999-C; Geological Survey of Canada, p. 169–178.*

**Abstract:** The northwestern Reindeer Zone along Reindeer Lake, Saskatchewan, consists of a stack of juvenile lithotectonic terranes and sedimentary basins accreted to the Archean Hearne Province during Paleoproterozoic collision, and a younger molasse basin (McLennan (Sickle) Group) deformed with the above during postcollisional convergence. Along the southern shore of Reindeer Lake, the McLennan Group fluvial-littoral sediments are folded and imbricated with older supracrustal rocks tentatively correlated with the Central Metavolcanic Belt, which are themselves thrust onto meta-turbidites of the Burntwood Group. La Ronge Domain lithologies have been mapped as far north as the southern margin of the Wathaman Batholith, calling into question the existence of the Rottenstone Domain. The structural geometry along the transect is dominated by large-scale recumbent folds ($F_1$), orogen-parallel, south-verging reclined to recumbent non-cylindrical folds ($F_2$) contemporaneous with south-directed thrusting, and large-wavelength upright cross folds ($F_3$).

**Résumé :** La partie nord-ouest de la zone de Reindeer, le long du lac Reindeer en Saskatchewan, est constituée d'un empilement de terranes lithotectoniques et de bassins sédimentaires accrétés à la province archéenne de Hearne au cours d'une collision au Paléoprotérozoïque, et d'un bassin molassique plus récent (Groupe de McLennan (Sickle)) qui a été déformé avec l'empilement pendant une convergence postérieure à la collision. Le long de la rive sud du lac Reindeer, les roches sédimentaires fluviales et littorales du Groupe de McLennan sont plissées et imbriquées avec des roches supracrustales plus anciennes mises en corrélation provisoirement avec la ceinture de roches métavolcaniques centrale; ces roches supracustales chevauchent les roches turbiditiques métamorphisées du Groupe de Burntwood. Les roches du domaine de La Ronge ont été cartographiées vers le nord jusqu'à la bordure sud du batholite de Wathaman, ce qui remet en question l'existence du domaine de Rottenstone. La géométrie structurale le long du transect est dominée par la présence de grands plis couchés ($F_1$), de plis non cylindriques reclinés à couchés ($F_2$) de vergence sud qui sont parallèles à l'orogène et contemporains d'un chevauchement dirigé vers le sud, et de plis transversaux droits ($F_3$) de grande longueur d'onde.

[1] Department of Earth Sciences, Memorial University, St. John's, Newfoundland A1B 5X5
[2] Department of Geological Sciences, University of Saskatchewan, 114 Science Place, Saskatoon, Saskatchewan S7N 5E2
[3] Geological Museum, Oster Voldgade 5-7, DK-1350 Copenhagen K, Denmark
[4] Department of Earth Sciences, University of Western Ontario, London, Ontario N6A 5B8

## INTRODUCTION

In 1997, the Geological Survey of Canada (GSC) and the askatchewan Geological Survey joined in a collaborative effort aimed at enhancing our understanding of the 'La Ronge–Lynn Lake Bridge' as well as the lithotectonic framework of the Reindeer Zone of the Trans-Hudson Orogen. The first season of fieldwork resulted in the publication of two contiguous 1:20 000 scale maps (Maxeiner, 1997; Corrigan et al., 1997), as well as the initiation of a more regional coverage at 1:50 000 scale (Corrigan et al., 1998). During this past summer, mapping at 1:50 000 scale was continued both to the southwest and north, to extend coverage to the north flanks of Glennie and Kisseynew domains and into the Wathaman Batholith, respectively. In this report we present new observations on the La Ronge–Kisseynew–Glennie domain boundaries along the southern shore of Reindeer Lake. We also present evidence suggesting that the La Ronge Domain extends north to the Wathaman Batholith, thereby inferring that the La Ronge Domain may have been accreted to the Archean Hearne Province margin prior to emplacement of the batholith at ca. 1865 Ma.

## REGIONAL GEOLOGY

The Trans-Hudson Orogen in northern Saskatchewan (northwestern Reindeer Zone) forms a collage of west-southwest-striking, northerly dipping juvenile belts that were accreted to the Archean Hearne margin during Paleoproterozoic collision (Lewry et al., 1990). From south to north, or from lower to higher structural levels along the Reindeer Lake transect, these belts consist of the Glennie, Kisseynew, La Ronge, and Rottenstone domains (Fig. 1). The ca. 1865–1850 Ma Wathaman Batholith (Ray and Wanless, 1980; Fumerton et al., 1984; Bickford et al., 1986, Meyer et al., 1992) separates the Rottenstone Domain from

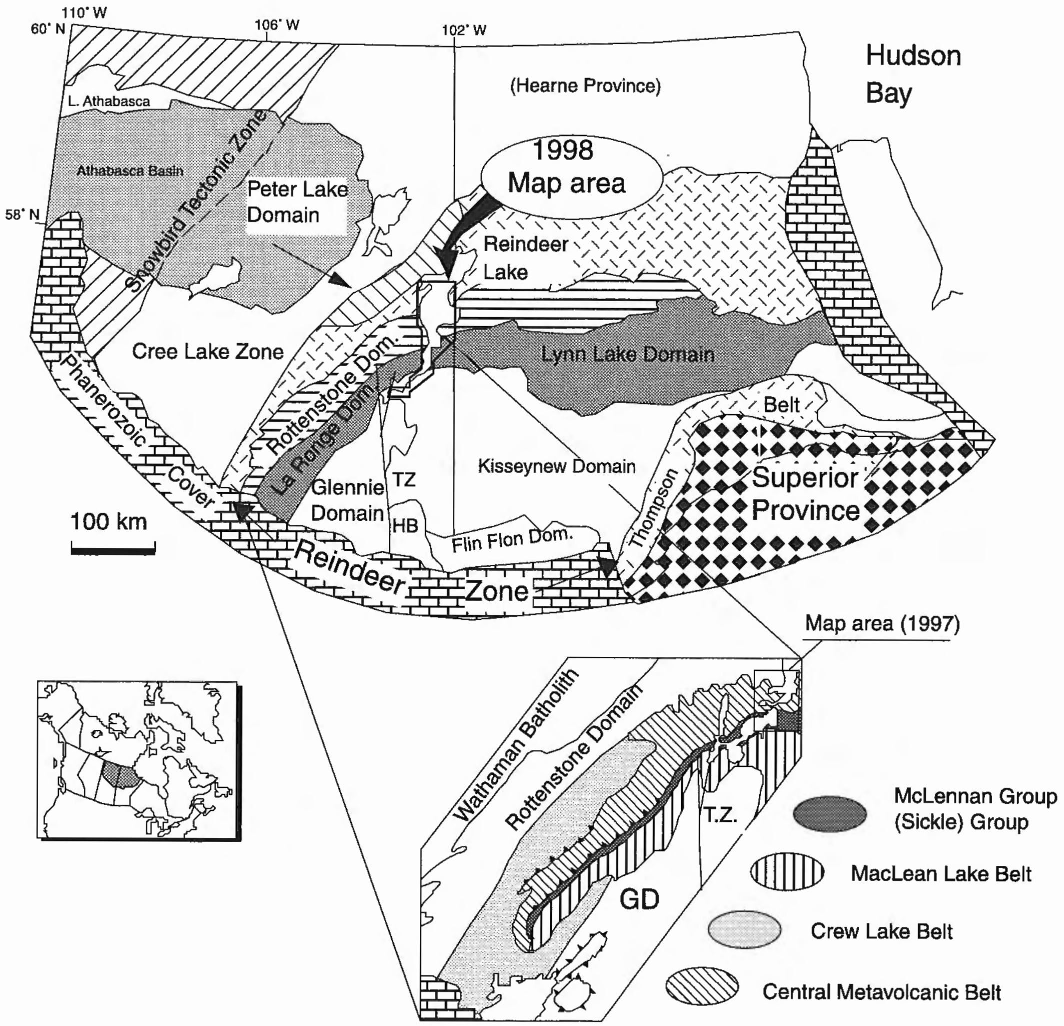


*__Figure 1.__ Generalized map of the Trans-Hudson Orogen along the Reindeer Zone, showing the distribution of the major lithotectonic domains. HB, Hanson Lake Block; TZ, Tabbernor Fault Zone; GD, Glennie Domain; RD, Rottenstone Domain; LRD, La Ronge Domain. Modified after Lewry et al. (1990). Location of the 1997 and 1998 map areas is shown.*

the Archean Peter Lake Domain. It is bounded on its southern flank by the Reilly Lake shear zone, and on its northern flank by the Parker Lake shear zone (Stauffer and Lewry, 1993). A detailed outline of previous mapping in the Reindeer Lake area is listed in Corrigan et al. (1998).

## TECTONOSTRATIGRAPHY

### *Kisseynew Domain/MacLean Lake Belt*

Previously, the Kisseynew Domain between Wapus and Numabin Bay (Fig. 2) had been subdivided into two units, namely arkosic rocks of the McLennan Group and predominantly turbiditic rocks of the Burntwood Group (Stauffer et al., 1979; Gilboy, 1980; Sibbald, 1977; Johnston, 1983). As a result of the last two summers of mapping, we have identified a more complex tectonostratigraphic relationship between predominantly arkosic rocks of the McLennan Group, supracrustal and granitoid rocks of unknown origin tentatively correlated with the La Ronge Domain, and meta-turbiditic rocks of the Burntwood Group. We present the new stratigraphy below.

#### McLennan (Sickle) Group

The McLennan Group (Stauffer et al., 1980; Zwanzig, 1990) (Fig. 2) consists predominantly of magnetite-bearing, pink to grey arkoses that are locally interlayered with 1–30 cm thick diopside-and quartz-rich calc-silicate layers (Fig. 3). Rare biotite-muscovite psammite and minor amounts of polymictic conglomerate are also present, with the conglomerate restricted to the stratigraphic base of the sedimentary succession (Corrigan et al., 1997; Maxeiner, 1997). Sillimanite nodules (faserkiesel) are common in the arkose, where they are deformed into flattened ellipsoids up to 30 cm long. Primary sedimentary structures such as compositional layering, laminated beds, and trough crossbeds are common in low-strain domains. The polymictic conglomerate contains granitoid, fine-grained volcanic, and sedimentary clasts supported in a biotite- and locally amphibole-rich matrix.

#### Levesque Bay supracrustal assemblage

Tectonically interleaved with the McLennan Group arkoses, and separated from them by narrow high-strain zones, is a heterogeneous rock package comprising garnet amphibolite, garnet-biotite±sillimanite psammite and pelite, impure quartzite, calc-silicate gneiss, diopside marble, and minor sillimanite-anthophyllite±cordierite gneiss interpreted as altered volcanogenic rock. In contrast to the less than 1.84 Ga (Ansdell and Yang, 1995) magnetite-bearing lithologies of the McLennan Group, this rock package contains disseminated and nodular sulphides, and is intruded by ca. 1.87 Ga (Corrigan et al., unpub. rept.) tonalitic and leucotonalitic sheets.

Garnet amphibolite (Fig. 4) constitutes up to 100 m thick sheets that are continuous over at least 10 km. It is typically flanked by sulphide-rich calc-silicate gneiss and rusty graphitic semipelite, and is locally interlayered with thin ultramafic bands. Light green calc-silicate pods with the assemblage epidote-diopside-plagioclase-scapolite±calcite form up to 25% of the garnet amphibolite unit. The calc-silicate gneiss contains the assemblage diopside-quartz-calcite-phlogopite, and is commonly interlayered with a laminated quartzite and calc-silicate rock, and with rusty, graphite-bearing semipelite. Grey, migmatitic, garnet-biotite±sillimanite gneiss, likely derived from a turbidite, forms an important component of this package. It locally contains thin calc-silicate and quartzitic bands, and appears to be stratigraphically concordant with the above-mentioned units. The turbidite locally contains abundant graphite that is either disseminated in the matrix, or occurs as coarse flakes in leucosomes. On the south shore of Reindeer Lake, in Fleming Bay, orthopyroxene porphyroblasts have been observed in hornblende gneiss interlayered with the calc-silicate gneiss.

#### Burntwood Group

The Burntwood Group, which is the most abundant component of the Kisseynew Domain, has been interpreted to extend to the southern shore of Reindeer Lake (Johnston and Thomas, 1984). These rocks consist of stromatic migmatite, metatexite (Fig. 5), and diatexite derived from psammitic to pelitic turbidite with rare calc-silicate layers. The migmatite has the assemblage biotite-plagioclase-K-feldspar-quartz±garnet±cordierite±sillimanite±graphite, with feldspar porphyroblasts up to 6 cm in size. On the shore of Deep Bay, the diatexite is massive, suggesting that its formation during peak metamorphism postdated regional deformation. Orthopyroxene-bearing gneiss of mafic to intermediate composition, perhaps derived from gabbroic to tonalitic intrusive sheets or dykes, forms a minor component of the Burntwood Group investigated this summer. Their existence at the interface between the Glennie and Kisseynew domains had been previously reported (Gilboy, 1980), but not their occurrence on the southern shore of Reindeer Lake.

### *Glennie Domain*

Two exposures of the Glennie Domain on Reindeer Lake were investigated. On the southeastern shore of Deep Bay, a sheet of granodioritic orthogneiss, interpreted to form the northern limit of Glennie Domain (Johnston and Thomas, 1984), occurs more or less concordantly with Burntwood Group metatexitic to migmatitic turbidite. However, the turbidite outcropping north and south of the granodiorite is virtually identical in composition and fabric. Furthermore, thin granodioritic sheets also occur in Burntwood turbidite, and more importantly, no strain gradient has been observed between the granodiorite and meta-turbidite. Integrating these observations, we suggest that the proposed Glennie Domain granodiorite sheets are simply intrusive bodies in the Kisseynew (i.e. Burntwood Group) turbidite. Rare but widespread occurrences of metamorphic orthopyroxene in rocks of mafic to intermediate composition, as well as the assemblage cordierite-sillimanite-K-feldspar in rocks of pelitic composition, have been observed in the Burntwood Group.

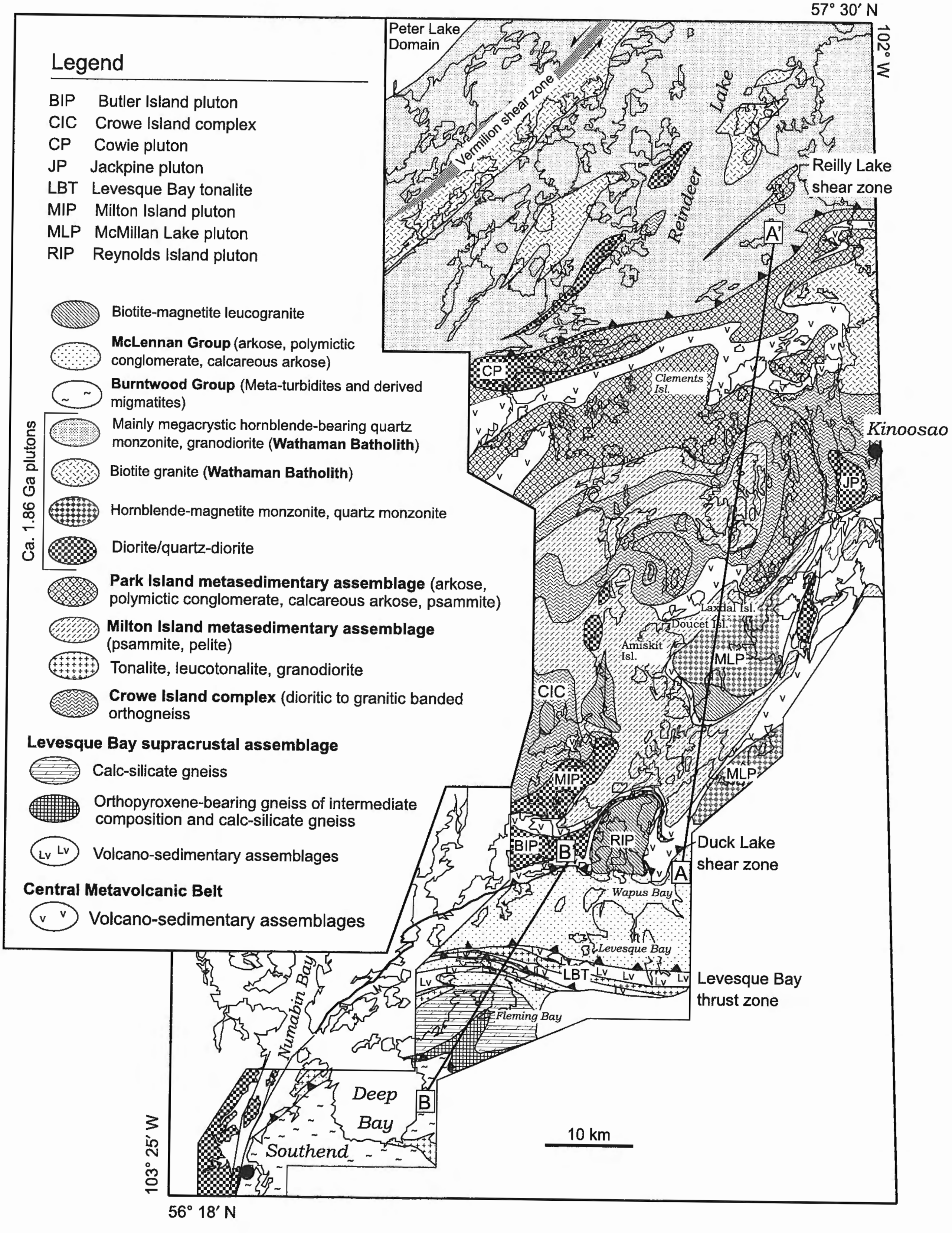


*Figure 2. Generalized geological map of the Reindeer Lake area based on mapping from the past two summers. Lines A–A′ and B–B′ refer to the cross-sections in Figure 11. Geological contacts have been projected onto Reindeer Lake, for clarity.*

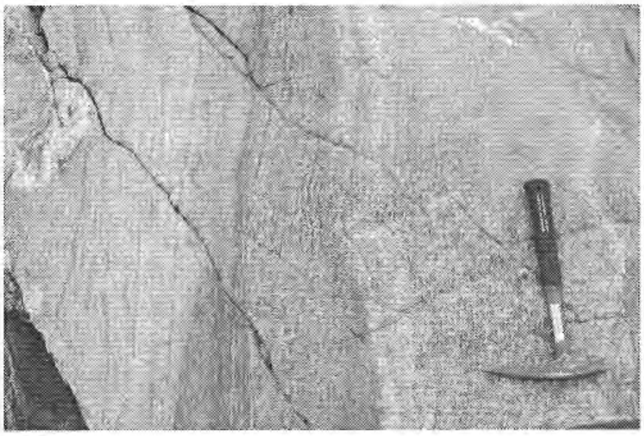

*Figure 3. Calc-silicate bed (darker coloured band in the central part of the outcrop photograph) in pink arkose, on shore of Brenton Island (64 D/10). Hammer for scale.*

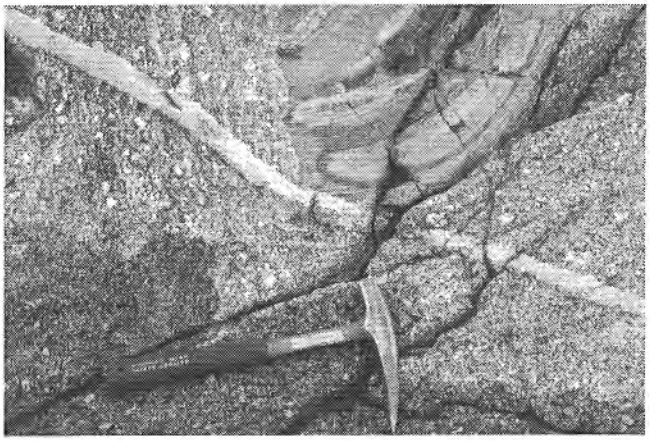

*Figure 5. Block of 'undigested' psammitic gneiss with calc-silicate layers, in massive diatexite. White spots are feldspar porphyroblasts. Eastern shore of Deep Bay (64 D/7), hammer for scale).*

*Figure 4. Banded garnet amphibolite with stretched-out calc-silicate pods (light coloured bands), on island in Levesque Bay (64 D/10). Hammer for scale.*

This suggests that it has attained upper-amphibolite- to granulite-facies metamorphism, which contrasts sharply with the lower- to middle-amphibolite-facies assemblages of the La Ronge Domain.

In the Numabin Bay area, granodiorite, biotite gneiss, and hornblende gneiss mapped by Johnston (1983), had been interpreted by Johnston and Thomas (1984) as Glennie Domain equivalents. We have revisited these outcrops and our observations suggest that the hornblende gneiss is locally orthopyroxene-bearing and appears to be derived from a migmatitic and highly strained granodioritic orthogneiss hosting numerous supracrustal and metaplutonic enclaves. This hornblende±orthopyroxene gneiss also forms large rafts enclosed within a moderately recrystallized diorite to granodiorite pluton similar in texture and composition to the 1858 ± 2 Ma (Corrigan et al., unpub. rept.) Butler Island diorite of the La Ronge Domain (Fig. 2). This suggests that the hornblende gneiss predates ca. 1.86 Ga, but its absolute age is as yet unconstrained.

## *La Ronge Domain–Rottenstone Domain transition*

The 1998 mapping continued northward in an attempt to better understand the nature of Rottenstone Domain and its relationship with the Central Metavolcanic Belt of the La Ronge Domain. Among the most important observations is that supracrustal rocks form a much greater component of the Rottenstone Domain than was previously recognized, and that the volcanic rocks, which extend almost as far north as the Wathaman Batholith, are in many aspects similar to those of the Central Metavolcanic Belt of the La Ronge Domain. For this reason, we will put the name Rottenstone Domain in quotes ("") in the text below, when referring to parts of the map area interpreted as the Rottenstone Domain in Johnston and Thomas (1984). The Milton Island metasedimentary assemblage (also part of the La Ronge Domain) also extends farther north, where it is structurally and stratigraphically overlain by a siliciclastic metasedimentary package comprising polymictic conglomerate, arkose, calcareous arkose, and semipelite (herein named the Park Island metasedimentary assemblage).

### Central Metavolcanic Belt

In 1997, Maxeiner (1997) and Corrigan et al. (1997, 1998) identified two strands of the Central Metavolcanic Belt at the southern margin of the La Ronge Domain, which they named the Lawrence Point and Reed Lake volcanogenic belts. Work in 1998 identified volcanic rocks and their reworked and/or altered equivalents north of these belts, previously interpreted as migmatite and amphibolite of the Rottenstone Domain (Stauffer et al., 1979, 1980). The supracrustal rocks are particularly well preserved at two localities, in the Laxdal Island and Clements Island area, respectively (Fig. 2). In both areas, volcaniclastic rocks predominate, with smaller amounts of mafic volcanic rocks with possible relict pillows and amphibolites containing angular, darker and finer grained fragments interpreted as possible flow-top breccia. Medium grey to black (intermediate to mafic) reworked volcanic rocks containing angular felsic (rhyolitic to dacitic) clasts are also common (Fig. 6) and could either represent felsic volcanic fragments in redeposited mafic to intermediate volcanic tuff, or ripped-up felsic volcanic fragments in intermediate to mafic tuff. Thin flows or tuff horizons of dacitic to rhyolitic composition are less abundant than the mafic protoliths. Thin pelitic and quartzite layers are also present.

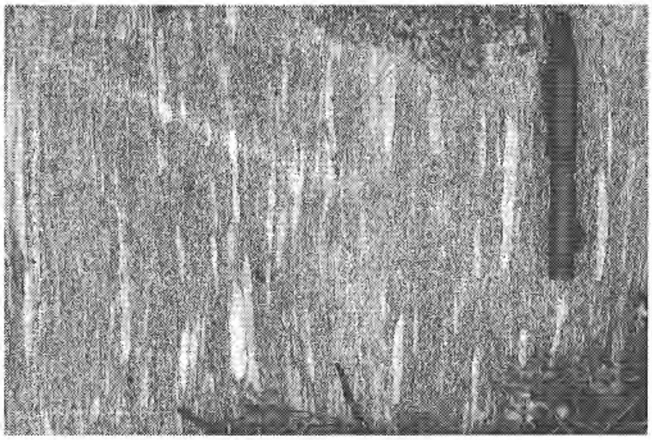

*Figure 6. Deformed, light coloured, angular rhyolitic fragments in andesitic matrix; La Ronge Domain, Doucet Island (64 D/16). Flare projector (10 cm) for scale.*

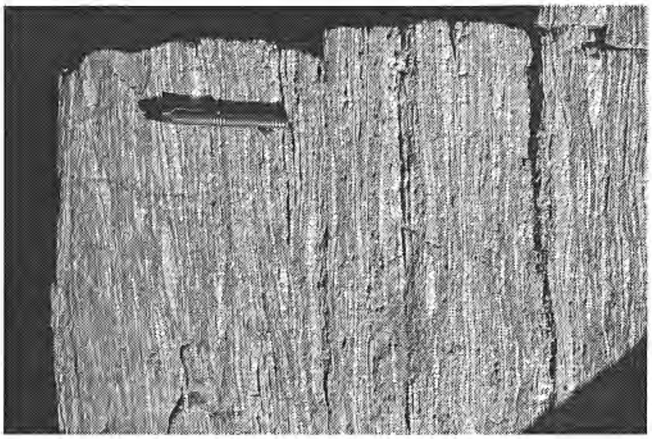

*Figure 7. Oxide-facies banded iron-formation consisting of thin, alternating magnetite (dark) and quartz (light) layers (64 D/16; UTM 658200E, 6310600N). Note the stretched-out and transposed character of the quartzite layers. Flare projector (10 cm) for scale.*

Both oxide- and silicate-facies banded iron-formation occur within the supracrustal rocks of the Central Metavolcanic Belt. Oxide-facies banded iron-formation (Fig. 7) occurs on Doucet Island and coincides with a strong positive magnetic anomaly (Geological Survey of Canada, 1966; GSC map 7152-G). It is at least 15 m thick, but of unknown strike length. Silicate-facies banded iron-formation occurs on the north shore of Laxdal Island, and in thin bands in the Clements Island area (Fig. 2). Outcrops associated with this rock type typically feature recessive grooves exposing more-resistant euhedral garnets up to 2 cm in diameter, and are generally associated with gossans.

A distinctive package of banded orthogneiss of mixed dioritic, tonalitic, granodioritic, and granitic composition occurs throughout the 'Rottenstone Domain' and is spatially associated with the volcanogenic package described above. This unit is compositionally heterogeneous and is characterized by multiple injections of progressively more-felsic melts in mafic to intermediate precursors. Dynamic recrystallization is pervasive, and the degree of partial melting ranges from incipient, to about 40%. The southernmost extent of this orthogneiss suite (named the 'Crowe Island complex' in last year's report) was interpreted as the possible plutonic root of the La Ronge arc (Corrigan et al., 1998). Preliminary U-Pb ages of 1892 ± 2 and 1886 ± 4 Ma (Corrigan et al., unpub. rept.) obtained respectively from a tonalite and a granite from this suite, support this interpretation.

### Milton Island metasedimentary assemblage

The Milton Island metasedimentary assemblage (Corrigan et al., 1998) consists of variably migmatized, finely graded, and thinly layered psammite and semipelite that contain white stromatic migmatitic segregations (leucosome) of pure quartz and/or granitic composition, separated from the paleosome by thin biotite-rich selvages. The sediments are biotite-bearing, with the local occurrence of graphite, muscovite, and fibrolite, and the rare presence of garnet. One of the characteristic features is the local occurrence of green apatite in the leucosome. This unit is remarkably homogeneous over a wide area, although it is locally interlayered with thin (up to a few tens of metres) volcanic or epiclastic rocks, as well as rare calc-silicate bands.

### Park Island metasedimentary assemblage

A distinctive and previously unrecognized package of siliciclastic rocks made up of a basal conglomerate, arkose, calcareous arkose, and psammite, has been identified between

Amiskit Island and the Wathaman Batholith (Fig. 2). Some of its features, such as the presence of large faserkiesel nodules, are similar to those of the McLennan (Sickle) Group, but it is, in detail, quite different. It sits structurally on top of the Central Metavolcanic Belt and the Milton Island assemblage. The polymictic conglomerate contains cobble- to pebble-size clasts (Fig. 8) and occurs at the structural base of the Park Island assemblage. It is clast supported at the structural bottom and grades into matrix supported towards the top, coinciding with a gradual change in matrix composition from mafic to felsic dominated, with both hornblende and biotite present in variable proportions. Clasts are predominantly fine grained and comprise, in order of decreasing abundance, syenite and monzonite, felsic volcanic, intermediate volcanic, calc-silicate and mafic volcanic, quartz pebble, and oxide-facies banded iron-formation.

The arkose is a pink to grey, K-feldspar-dominated rock with local well preserved sedimentary structures such as trough crossbeds (Fig. 9) and upper-flow-regime laminar beds. Thin, greenish, calc-silicate beds with diopside-quartz-calcite mineralogy are locally present. Biotite (with rare hornblende) and magnetite porphyroblasts form the main mafic minerals. Although arkose is the predominant rock type, it locally grades into semipelite, depending on the relative abundance of biotite and K-feldspar. Partial melting has affected this unit to varying degrees, from only minor migmatitic segregation to almost complete remobilization (Fig. 10), with the proportion of leucosome generally increasing towards the Wathaman Batholith. Large enclaves of the arkose are enclosed within the 1865–1850 Ma Wathaman Batholith, constraining its minimum age of deposition.

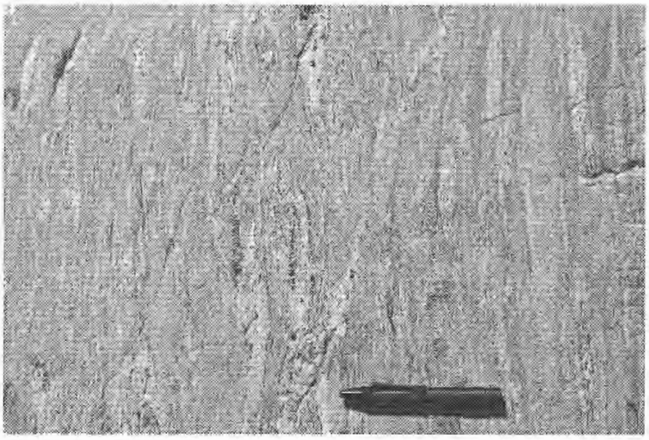

***Figure 8.*** *Polymict conglomerate near the base of the Park Island metasedimentary assemblage. Flare projector (10 cm) for scale.*

***Figure 9.*** *Cross-beds in magnetite and biotite bearing arkose from the Park Island metasedimentary assemblage. Pocket knife for scale.*

***Figure 10.*** *Intensely migmatized arkose from the Park Island metasedimentary assemblage on the north shore of Bray Island, about 1.5 km south of the Wathaman Batholith (64 E/2). Note the arkosic paleosomes (dark grey blocks), biotite schlieren, and abundant granitic neosomes.*

## Plutonic rocks

Numerous plutons up to a few tens of kilometres in size occur in the La Ronge and 'Rottenstone' domains (Fig. 2). They range in composition from ultramafic and gabbroic (small plugs and dykes) to dioritic and quartz dioritic (Butler Island, Milton Island, Walter Island, and Cowie plutons), monzodioritic and granodioritic (Jackpine Bay pluton), monzogranitic (McMillan Lake pluton), to granitic (unnamed pluton north of Kinoosao). In contrast to the banded orthogneiss described above, they are compositionally homogeneous, and generally preserve relict igneous minerals and textures. They also crosscut fabrics and structures in the enclosing supracrustal rocks and orthogneiss and are themselves affected by regional deformation at high metamorphic grade, This suggests that they postdate the first regional tectonometamorphic event ($D_1$-$M_1$; *see* below) but predate $D_2$-$M_2$. A U-Pb age of 1858 ± 2 Ma was obtained on the Butler Island diorite (Corrigan et al., unpub. rept.), suggesting that this 'suite' is contemporaneous with the Wathaman Batholith.

### *Wathaman Batholith*

Most of the Wathaman Batholith in the map area consists of coarse-grained to K-feldspar-megacrystic, hornblende-bearing quartz monzonite to granodiorite, with a smaller amount of coarse-grained to megacrystic granite and minor diorite. The central part of the batholith is generally only mildly recrystallized, with well preserved igneous minerals and crystal zoning. It is bounded to the south by the Reilly Lake shear zone (Stauffer and Lewry, 1993), a ductile shear zone about 100 m thick. Consistent down-dip extension lineations and rare winged feldspar porphyroclasts suggest a reverse, top-to-the-south sense of shear (*see also* Lafrance and Varga, 1996). About 10 km south of the Peter Lake Domain margin, a steep mylonite zone about 1 or 2 km thick (herein named the Vermilion shear zone), carries subhorizontal extension lineations and evidence of sinistral shear. Enclosed within the Wathaman Batholith are a few domains consisting of foliated and thoroughly recrystallized biotite granite, granodiorite, and diorite that may either form the earliest, most deformed phases of the batholith, or rafts of country rock. Since rafts of the Park Island arkose were also found within the batholith, we suggest that the foliated granitoids may also represent fragments of the ca. 1.89 Ga Crowe Island orthogneiss complex.

## STRUCTURAL AND METAMORPHIC FRAMEWORK

Based on geochronological data (Corrigan et al.,unpub. rept.) and tectonostratigraphic relationships (Corrigan et al., 1998; this study), four distinct structural levels can be identified along the Reindeer Lake transect (Fig. 11). The Central Metavolcanic Belt and associated gneiss of the Crowe Island complex are the oldest recognizable protoliths and form 'level 1'. The Milton Island metasedimentary assemblage, which sits stratigraphically on top of the Central Metavolcanic Belt and Crowe Island complex (Corrigan et al., 1998), forms 'level 2'. The Park Island metasedimentary assemblage, which was deposited unconformably on rocks of levels 1 and 2, forms structural 'level 3'. Structural 'level 4' consists of the younger McLennan and Burntwood groups.

Three major episodes of ductile deformation are observed in the area (Sibbald, 1977; Stauffer et al., 1979; Maxeiner, 1997; Corrigan et al., 1998). The earliest recognizable deformation event, as suggested by map patterns observed this past summer between the Duck Lake shear zone and the Wathaman Batholith, consists of large-scale recumbent folds ($F_1$) that involve the Central Metavolcanic Belt and the Milton Island

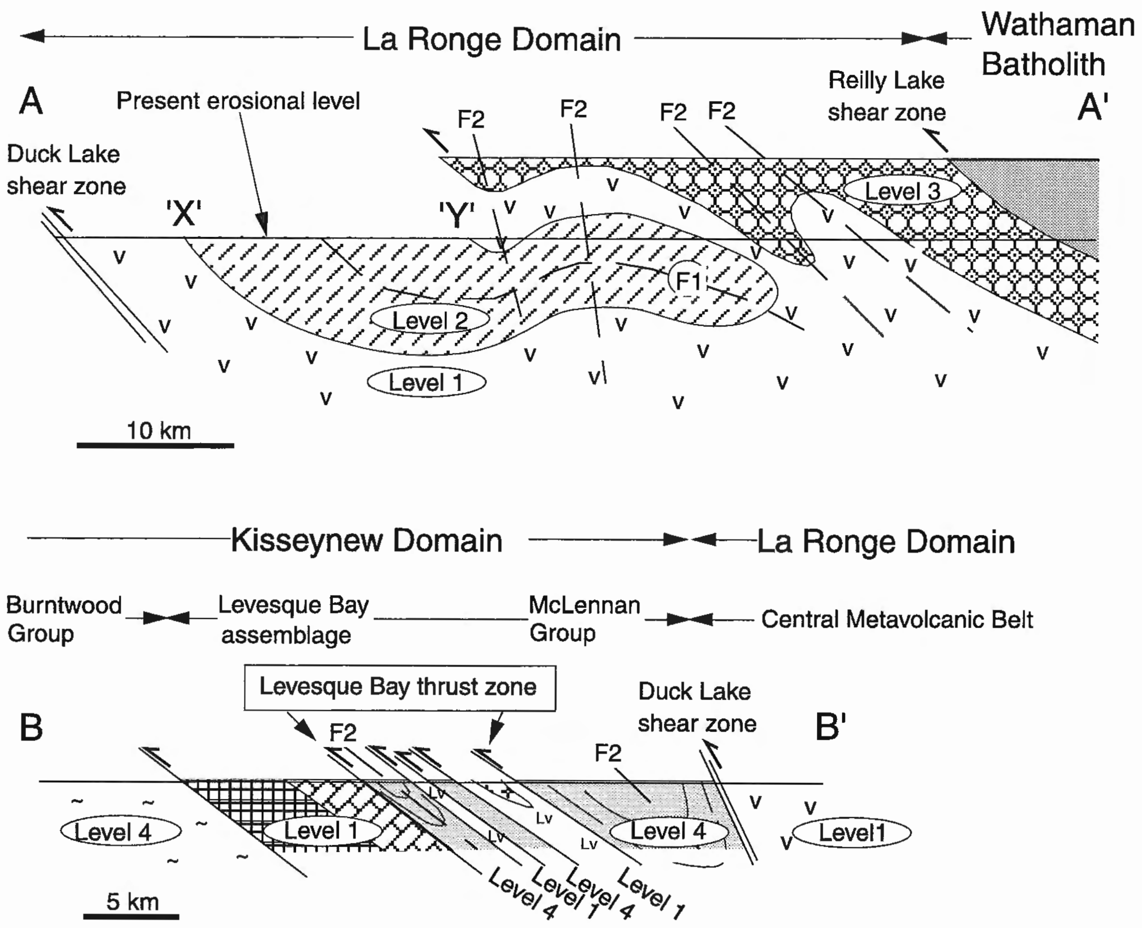


*Figure 11. Schematic cross-sections interpreted from the geological map (Figure 2) and measured foliation attitudes. Vertical scale exaggerated. See text for explanations.*

sedimentary assemblage (Fig. 11). The $M_1$ metamorphism mainly produced phyllosilicates ($S_1$) parallel to bedding planes ($S_0$). Corrigan et al. (1998) presented evidence suggesting that rocks of the Central Metavolcanic Belt (level 1) grade upwards into the Milton Island metasedimentary assemblage (level 2) at location 'X' in Figure 11. The presence of Central Metavolcanic Belt volcanic rocks sitting structurally above the Milton Island assemblage, as shown at locality 'Y' in Figure 11, suggests that $F_1$ is likely a south-verging recumbent syncline. However, younging directions have not been observed in the upper limb of the inferred syncline.

The siliciclastic-dominated Park Island metasedimentary assemblage (structural level 3) contains clasts of both the Central Metavolcanic Belt and the Milton Island metasedimentary assemblage, and is therefore younger. Although it is slightly sheared along its structural and stratigraphic base, it cannot form an allochthonous nappe, since it incorporates detritus interpreted to be derived from the Central Metavolcanic Belt and the Milton Island metasedimentary assemblages. At its northern margin, the Park Island assemblage is intruded by the Wathaman Batholith, constraining its deposition to greater than 1865 Ma. Based on these constraints, we suggest that the Park Island metasediments were deposited unconformably onto the older, previously folded Central Metavolcanic Belt–Milton Island package, and later infolded with them during a second phase of deformation ($D_2$).

The $D_2$ event is the most regionally pervasive and consists of the formation of south-verging reclined and recumbent folds and south-directed ductile thrust zones, coincident with the growth of peak metamorphic assemblages ($M_2$). Mineral and extension lineations ($L_2$) plunge consistently north, and $F_2$ axial traces strike predominantly west to west-southwest. Peak mineral assemblages are contained within $F_2$ axial planes, as well as in $S_2$ mylonitic foliations. Shear zones have localized at three different localities. The Reilly Lake and Duck Lake shear zones (Fig. 11) developed along the structural base of the Wathaman Batholith and La Ronge Domain, respectively, and are associated with down-dip mineral and extension lineations. In contrast, the Levesque Bay thrust zone (Fig. 11), forms an imbricated stack of thin thrust slices of level 1 supracrustal basement (possible La Ronge Domain) and McLennan(Sickle) cover (structural level 4). Map-scale isoclinal to tight fold closures have been observed in McLennan Group metasediments, with the bounding shear zones parallel to the fold limbs. In contrast with the fabrics in the Reilly Lake and Duck Lake shear zones, lineations in the Levesque Bay thrust zone plunge obliquely to the north-northeast, and, in garnet amphibolite, are outlined by the syn-thrusting replacement of garnet by plagioclase, suggesting a reduction in metamorphic pressures during tectonic exhumation. Without further geochronological constraints on the timing of $D_2$ deformation, we consider the Levesque Bay thrust zone to be generally related to (but not necessarily synchronous with) movement along the Reilly Lake and Duck Lake shear zones.

The last major regional deformation event ($D_3$) involved the formation of large-wavelength upright open folds ($F_3$) with axial traces oriented approximately to the north-northeast (Fig. 12). The effect of $F_3$ on $F_1$ and $F_2$ is best observed in the La Ronge Domain between Duck Lake and Reilly Lake shear zones (Fig. 2) where pre-$D_3$ foliations were shallow. The $D_3$ deformation seems to have been associated only locally with the growth of axial-planar chlorite and muscovite, suggesting that it occurred late in the evolution of the orogen, at relatively low metamorphic conditions. Preliminary U-Pb titanite ages of ca. 1.78 Ga, interpreted as cooling of metamorphic temperatures below ca. 600°C (Corrigan et al., unpub. rept.), were obtained from two samples from the La Ronge Domain, providing a maximum age for $D_3$.

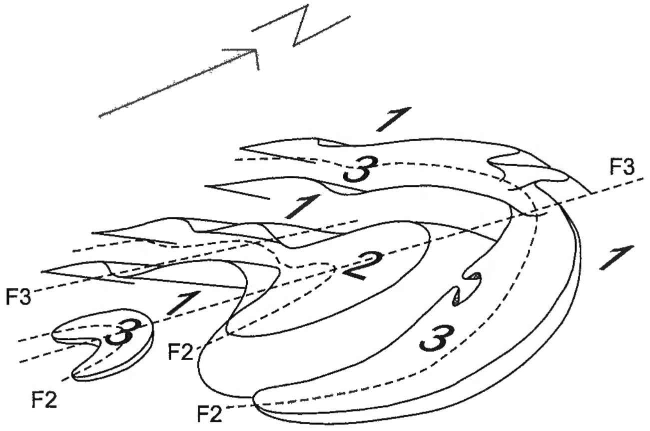


*Figure 12. Schematic 3-D sketch of a part of the map between Amiskit Island and the Wathaman Batholith, showing the attitude of planes bounding levels 1, 2, and 3. Fold shapes and plunges were interpreted from field measurements. Represents an area about 30 km x 30 km.*

## DISCUSSION

The identification of crustal slices predating 1.87 Ga tectonically imbricated with McLennan Group arkoses along the southern shore of Reindeer Lake sheds new light on the nature of the La Ronge–Kisseynew–Glennie transition. Corrigan et al. (1998) speculated that the north-to-south progression of lithofacies from polymictic conglomerate to arkose, to calcareous arkose, to calc-silicate gneiss with amphibolite, and finally to the Burntwood Group metaturbidites, represented a progressive facies change from fluvial-littoral to deep marine deposits in a basin opening towards the south. This model fit U-Pb data that indicate that the McLennan(Sickle) Group and Burntwood Group may have been deposited at about the same time at ca. 1.84 Ga (Ansdell and Yang, 1995). However, the new U-Pb zircon age of ca. 1.87 Ga obtained for a tonalite intruding the Levesque Bay assemblage (Corrigan et al., unpub. rept.), and the observation that the supracrustal rocks are separated from the McLennan Group arkoses by zones of high strain, points to a more complicated lithotectonic architecture than was previously inferred. It suggests instead that the McLennan arkose units (cover) are tectonically imbricated in 'fold-thrust' geometry with an older volcano-sedimentary assemblage (basement), perhaps related to the Central Metavolcanic Belt.

Another important observation derived from this summer's mapping is the expansion of La Ronge Domain lithologies as far north as the Wathaman Batholith, and the identification of a new package of fluvial to littoral sedimentary rocks (Park Island assemblage) that unconformably overlies supracrustal and orthogneissic rocks of the La Ronge Domain. The recognition of La Ronge Domain lithologies north of the domain's present limit poses significant constraints on the exact nature of the Rottenstone Domain, at least along the Reindeer Lake transect. Moreover, the observation that the Wathaman Batholith intrudes the La Ronge Domain implies that the latter had been accreted to the Hearne margin as early as 1865 Ma, as suggested in earlier models (e.g. Lewry et al., 1990). The tectonic environment in which the Park Island metasediments were deposited is yet unconstrained, but the possibility that they formed during $D_1$ in a forearc basin between the accreting La Ronge arc and the Hearne margin is our preferred working hypothesis.

## ECONOMIC POTENTIAL

The recognition of metavolcanic and associated sedimentary rocks along the southern shore of Reindeer Lake and in the northern extension of the La Ronge Domain in an area previously included in the Rottenstone Domain provides new targets for mineral exploration. Specific targets include the oxide- and silicate-facies banded iron-formation and associated gossan zones on Doucet and Laxdal islands (west-central NTS sheet 64 D/16), sulphide mineralization and silicate-facies iron-formation on a small island about 3 km north of Halfway Island (north-central NTS sheet 64 E/01), as well as small sulphide-enriched zones in supracrustal assemblages on Brenton Islands, and in Fleming Bay along the south shore Reindeer Lake (NTS map sheet 64 D/10).

## ACKNOWLEDGMENTS

Otto and Shirley Olson at the Kinoosao CO-OP are thankfully acknowledged for their logistical help. The crews at Osprey Wings and La Ronge Aviation provided excellent air service. Linda Eckhardt and staff of Arctic Lodge are acknowledged for their permission to set up our second camp on their property, for their great hospitality, and their help in repairing one of our outboard motors. Special thanks to Steve Lucas and Marc St-Onge who provided significant insights during a visit in the field, and especially to Marc for his much appreciated assistance during camp demobilization in late August. Reviews by Wouter Bleeker and John Percival greatly improved the manuscript.

## REFERENCES

**Ansdell, K.M. and Yang, H.**
1995: Detrital zircons in the McLennan Group meta-arkoses and MacLean Lake Belt, western Trans-Hudson Orogen; *in* Lithoprobe, Trans-Hudson Orogen Transect, (ed.) Z. Hajnal and J. Lewry; v. 48, p. 190–197.

**Bickford, M.E., Van Schmus, W.R., Macdonald, R., Lewry, J.F., and Pearson, J.G.**
1986: U-Pb zircon geochronology project for the Trans-Hudson: current sampling and recent results; *in* Summary of Investigations 1986, Saskatchewan Geological Survey, Saskatchewan Energy and Mines, Miscellaneous Report 86-4, p. 101–107.

**Corrigan, D., Bashforth, A., and Lucas, S.**
1997: Geology and structural evolution of the La Ronge–Lynn Lake Belt in the Butler Island area (parts of 64D-9 and -10), Reindeer Lake, Saskatchewan; *in* Summary of Investigations 1997, Saskatchewan Geological Survey, Saskatchewan Energy and Mines, Miscellaneous Report 97-4, p. 18–30.

**Corrigan D., Maxeiner, R., Bashforth, A., and Lucas, S.**
1998: Preliminary report on the geology and tectonic history of the Trans-Hudson Orogen in the northwestern Reindeer Zone, Saskatchewan; *in* Current Research, Part C; Geological Survey of Canada, Paper 98-1C, p. 95–106.

**Fumerton, S.L., Stauffer, M.R., and Lewry, J.F.**
1984: The Wathaman Batholith: largest known Precambrian pluton; Canadian Journal of Earth Sciences, v. 21, p. 1082–1097.

**Geological Survey of Canada**
1966: Reindeer Lake south, Saskatchewan–Manitoba; Geological Survey of Canada, Map 7152G, scale 1:253 440

**Gilboy, C.F.**
1980: Geology of the Reindeer Lake south (southeast) area (NTS area 64 D-SE); Saskatchewan Department of Mines, Mineral Resources Report 198, 62 p.

**Johnston, W.G.Q.**
1983: Geology of the Southend area; Saskatchewan Energy and Mines, Open File 82-4, 151 p.

**Johnston, W.G.Q., and Thomas, M.W.**
1984: Compilation bedrock geology series, Reindeer Lake south, NTS area 64 D; Saskatchewan Energy and Mines, Report 230, scale 1:250 000.

**Lafrance, B., and Varga, M.**
1996: Structural studies of the Parker Lake shear zone and the Reilly Lake shear zone, Reindeer Lake; *in* Summary of Investigations 1996, Saskatchewan Geological Survey, Saskatchewan Energy and Mines, Miscellaneous Report 96-4, p. 119–124.

**Lewry, J.F., Thomas, D.J., MacDonald, R., and Chiarenzelli, J.**
1990: Structural relations in accreted terranes of the Trans-Hudson Orogen, Saskatchewan: telescoping in a collisional regime?; *in* The Early Proterozoic Trans-Hudson Orogen of North America, (ed.) J.F. Lewry and M.R. Stauffer; Geological Association of Canada, Special Paper 37, p. 75–94.

**Maxeiner, R.O.**
1997: Geology of the Lawrence Bay (Reindeer Lake) Area, Northeastern La Ronge Domain; *in* Summary of Investigations 1986, Saskatchewan Geological Survey, Saskatchewan Energy and Mines, Miscellaneous Report 86-4, p. 3–17.

**Meyer, M.T., Bickford, M.E., and Lewry, J.F.**
1992: The Wathaman Batholith: an early Proterozoic arc in the Trans-Hudson orogenic belt, Canada; Geological Society of America Bulletin, v. 104, p. 1073–1085.

**Ray, G.E., and Wanless, R.K.**
1980: The age and geological history of the Wollaston, Peter Lake, and Rottenstone domains in northern Saskatchewan; Canadian Journal of Earth Sciences, v. 17, p. 333–347.

**Sibbald, T.I.I.**
1977: The geology of the Milton Island area (west half); Saskatchewan Department of Mineral Resources, Report 153, 38 p.

**Stauffer, M.R., and Lewry, J.**
1993: Regional setting and kinematic features of the Needles Falls Shear Zone, Trans-Hudson Orogen; Canadian Journal of Earth Sciences, v. 30, p. 1338–1354.

**Stauffer, M.R., Langford, F.F., Coleman, L.C., and Mossman, D.J.**
1979: Geology of the area around Amiskit Island, Reindeer Lake (part of NTS area 64 D-N.E.); Saskatchewan Department of Mineral Resources, Report 191, 21 p.
1980: Geology of the Reindeer Lake North (Southeast) Area; Saskatchewan Department of Mineral Resources, Report 200, 21 p.

**Zwanzig, H.V.**
1990: Kisseynew gneiss belt in Manitoba: stratigraphy, structure, and tectonic evolution; *in* The Early Proterozoic Trans-Hudson Orogen of North America, (ed.) J.F. Lewry and M.R. Stauffer; Geological Association of Canada, Special Paper 37, p. 95–120.

Geological Survey of Canada Project 970015

# Geology of the Mesoarchean Wallace Lake greenstone belt, southeastern Manitoba[1]

C. Sasseville[2] and K.Y. Tomlinson
Continental Geoscience Division, Ottawa

*Sasseville, C. and Tomlinson, K.Y., 1999: Geology of the Mesoarchean Wallace Lake greenstone belt, southeastern Manitoba;* in *Current Research 1999-C; Geological Survey of Canada, p. 179–186.*

**Abstract:** The Wallace Lake greenstone belt at the southern margin of the North Caribou terrane contains a basal panel of Mesoarchean platformal sediments, the Conley Formation. The sequence is transgressive and presumably in unconformable contact with a tonalitic basement. Ultramafic volcanic rocks including spinifex-textured komatiite units occur in the upper Conley Formation. It is conformably overlain by a predominantly mafic volcanic succession, the Big Island Formation. On Siderock Lake a volcanogenic polymictic conglomerate occurs at the base of the Siderock Formation which overlies, possibly unconformably, the mafic volcanic rocks of the Big Island Formation. Four folding events are recognized in the Wallace Lake area, only two of which define the map-scale interference geometry. Mineralization and alteration appear to be structurally controlled in the northern Wallace Lake belt. The Wallace Lake stratigraphy may correlate with that in the Steep Rock belt of the Wabigoon Subprovince, forming strong evidence for rifting of a 3 Ga Superior protocraton.

**Résumé :** La ceinture de roches vertes de Wallace Lake, sur la marge sud du terrane de North Caribou, renferme un panneau basal de roches sédimentaires de plate-forme du Mésoarchéen, la Formation de Conley. La succession est transgressive et vraisemblablement en contact discordant avec le socle tonalitique. Des roches volcaniques ultramafiques, y compris des komatiites à texture spinifex, sont présentes dans la partie supérieure de la Formation de Conley, sur laquelle repose en concordance une succession principalement volcano-mafique, la Formation de Big Island. Au lac Siderock, un conglomérat polygénique volcanogénique se rencontre à la base de la Formation de Siderock qui repose, possiblement en discordance, sur les roches volcaniques mafiques de la Formation de Big Island. Dans la région du lac Wallace, on a individualisé quatre phases de plissement, dont deux seulement définissent la géométrie d'interférence à l'échelle de la carte. Dans la partie septentrionale de la ceinture de Wallace Lake, la structure semble avoir contrôlé la minéralisation et l'altération. Une corrélation pourrait exister entre la stratigraphie de la ceinture de Wallace Lake et celle de la ceinture de Steep Rock dans la Sous-province de Wabigoon, ce qui milite fortement en faveur d'une distension d'un protocraton de la Province du lac Supérieur il y a 3 Ga.

[1] Contribution to Western Superior NATMAP Project
[2] Earth and Planetary Sciences, McGill University, 3450 University St., Montreal, Quebec H3A 2A7

## INTRODUCTION

The Western Superior NATMAP (National Mapping Program) focuses on relationships between fragments of old (3.0–2.8 Ga) continental crust that occur sporadically throughout the region, and the predominant 2.75–2.70 Ga supracrustal sequences that in part have oceanic affinities (Thurston and Chivers, 1990). Where well preserved, the old continental blocks comprise ca. 3 Ga tonalite unconformably overlain by thin quartzite and carbonate units, interpreted as platformal cover sequences (Thurston and Chivers, 1990). The sedimentary cover is overlain by komatiitic and tholeiitic volcanic rocks, which have locally been demonstrated to have plume-like geochemical affinities (e.g. Steep Rock; Tomlinson et al., 1996), and may mark the rifting of a 3 Ga Superior protocraton. The Wallace Lake greenstone belt is similar to other Mesoarchean greenstone belts and contains a basal platformal sedimentary sequence overlain by mafic to ultramafic volcanic rocks. The Wallace Lake belt is of key importance because the sedimentary cover is cut by a 2.92 Ga tonalite dyke (D. Davis, unpub. report, 1994) thereby establishing a minimum age of deposition of the platformal sequence. This indicates that rifting of the 3 Ga protocontinent did not immediately precede the 2.75–2.70 Ga assembly event but is more likely to have occurred during the Mesoarchean.

Several aims of the Western Superior NATMAP project are achievable through mapping and associated studies in the Wallace Lake belt. The immediate goals of the project are to address the following specific questions: 1) the nature of the basal contact of the sedimentary sequence with surrounding granitoids is unknown; the contact may be unconformable, tectonic, or the granitoids may be intrusive; 2) the internal stratigraphy of the Wallace Lake belt requires re-examination in the light of regional observations of Mesoarchean sequences. These rocks may represent "...one of the best developed and exposed sections of the Mesoarchean platform assemblage in the Superior Province..." (Poulsen et al., 1996); and 3) of particular importance is the age and relationship of the volcanic rocks (particularly the komatiite) to the sedimentary sequence. Komatiitic rocks in the adjacent Garner Lake area to the south are ca. 2.85 Ga (Brommecker et al., 1993). Are the Wallace Lake komatiitic rocks equivalent to the Garner Lake komatiitic rocks, or part of an older sequence? Are the 2.75–2.70 Ga volcanic and sedimentary rocks of the main Rice Lake belt to the south (Poulsen et al., 1996) also represented in the Wallace Lake belt, and if so, what is the relationship to the older units? 4) Finally, it is important to understand the structural history of the Wallace Lake belt. The three phases of deformation postdating 2.705 Ga documented in the Rice Lake belt should also be recorded at Wallace Lake, but the nature of early deformation (predating 2.92 Ga) (Poulsen et al., 1996) is cryptic. In this paper we present new findings on the stratigraphy and structural geology of the Wallace Lake belt and discuss the regional implications of the results.

## METHODOLOGY

This year fieldwork consisted primarily of shoreline mapping of Wallace and Siderock lakes. Particular attention was given to recognizing the facing directions and the foliation relationships. Due to the numerous foliations present in the area it was not always possible to assign them to specific deformation events. Instead, foliations were commonly distinguished based on their style, intensity, etc. Descriptive terms are based solely on field observations.

## STRATIGRAPHY OF THE WALLACE LAKE BELT

### *Previous work*

The stratigraphy defined by McRitchie (1971) was based on comparisons with, and correlations to, the Rice Lake belt. McRitchie defined the Wallace Lake Subgroup as containing three formations, the Siderock Lake Formation (at the base), the overlying Big Island Formation, and the Conley Formation at the top of the stratigraphy. He described the Siderock Lake Formation as comprising acid-intermediate volcanic wacke and phyllite, minor siliceous limestone and dolomite lenses, acid-intermediate volcanic breccia, thin mafic volcanic breccia (ash flow tuff), and basal phyllitic carbonate-rich volcanic wacke. The Big Island Formation was described as comprising mafic volcanic rocks. The Conley Formation was described in detail as follows: in the western area he found basal tremolite-actinolite schist overlain by quartzite, thick iron-formation, siliceous limestone, thin mafic lavas, ferruginous argillite-mudstone, trondhjemite-bearing conglomerate, and interlayered arkose, grit, quartzite, and greywacke. In the eastern area he reported argillite-mudstone with minor greywacke and basal graphitic slate, thin iron-formation and argillite-mudstone with thin pillow lavas. McRitchie (1971) also recognized a facies change in the Conley Formation, from predominantly argillaceous at Siderock Lake to mainly arenaceous on Wallace Lake. The iron-formation persists throughout this facies change. Due to the general scarcity of way-up criteria and the lack of geochronological controls, there was limited structural analysis. McRitchie (1971) raised the possibility that the stratigraphy might in reality be the opposite way up. That conjecture has been supported by recent studies (Brommecker et al., 1993; Poulsen et al., 1996). Geochronology has shown that the Wallace Lake belt is Mesoarchean and specifically that the Conley Formation was deposited prior to 2920 Ma (the age of a crosscutting tonalite dyke) and later than 2999 Ma (the age of detrital zircons within the basal sediments; D. Davis, unpub. report, 1994). The Wallace Lake belt can therefore no longer be correlated with the 2.73 Ga Rice Lake belt and McRitchie's (1971) stratigraphy requires revision.

### *Conley Formation*

The new mapping shows that the Conley Formation is at the base of the Wallace Lake belt stratigraphy, as suggested in recent studies (Brommecker et al., 1993; Poulsen et al., 1996) and the stratigraphy of McRitchie (1971) is upside down. Numerous way-up criteria, including graded beds, crossbeds (Sasseville et al., in press), and detailed internal stratigraphy (Fig. 2, column A) confirm that the Conley Formation underlies the volcanic rocks of the Big Island Formation. Furthermore, the region in sector A (Fig. 1) may preserve an unconformity between the basal tonalite-bearing conglomerate (trondhjemite conglomerate of McRitchie 1971) and a tonalite basement, mapped as part of the Wanipigow plutonic complex (McRitchie, 1971). Both the tonalite and tonalite clasts in the conglomerate show the same equigranular igneous texture, with hypidiomorphic blue quartz and minor biotite. This relationship will be tested by detailed mapping to define the nature of the contact and by geochronology.

A buff-weathering carbonate appears near the top of the Conley Formation beneath the iron-formation in southern Wallace Lake. Serpentinite and talc-schist lenses are reported at the carbonate-iron-formation interface in drill logs (C. Cameron, unpub. report, 1979) and were mapped on Big Island this summer. This association was also reported further west at the Jeep mine and Johnson gold showing by Theyer (1983) who proposed a continuous carbonate horizon from the Jeep mine to the Conley shaft on Wallace Lake. The upper contact of the Conley Formation is concordant with the Big Island Formation. Above the iron-formation, an interbedded succession (100 m thick) of mafic-derived sediments, arkoses, mafic flows, and pillow lavas is overlain by an ultramafic volcanic-lens horizon, which marks the top of the Conley Formation and the base of the Big Island Formation (sector B, Fig. 1; column B, Fig. 2).

### *Intrusive gabbro*

Ophitic gabbro dykes up to 3 m wide cut the Conley Formation south of Conley Bay. One of these is cut by the quartz porphyry dyke dated at 2.92 Ga (D. Davis, unpub.

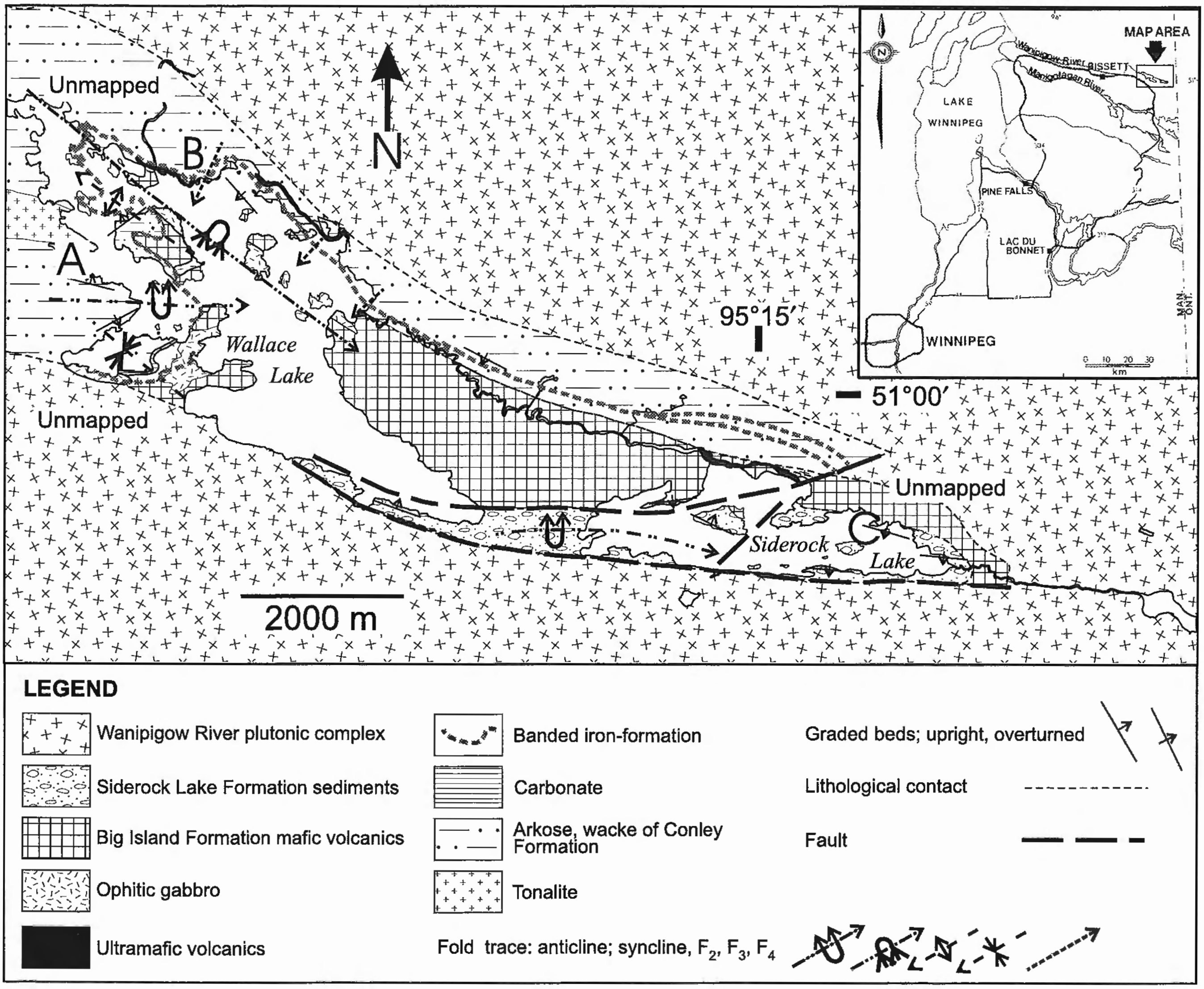


*Figure 1. Sketch map of the Wallace Lake belt, based on 1998 fieldwork; modified after McRitchie (1971).*

report, 1994; Poulsen et al., 1996). These gabbro dykes may be feeders to two large sill-like, ophitic gabbro bodies (Fig. 1) that occur at the interface of the Conley and Big Island formations. These gabbro sills may be synvolcanic intrusions related to the mafic volcanic rocks of the Big Island Formation. This hypothesis will be tested with geochemistry.

### *Big Island Formation*

The Big Island Formation comprises mafic to intermediate volcanic flows. Rare lenses of siltstone, iron-formation, chert, and arkose are widespread as interflow sediments. The mafic flows are mainly aphanitic, rarely pillowed, with a color index of 40–60 in northern Wallace Lake. On the north shore of Siderock Lake the mafic volcanic rocks are fine-grained (<0.5 mm), mafic to intermediate flows with a color index of 20–30.

### *Siderock Lake Formation*

The eastern part of Siderock Lake preserves a south-facing panel of metasedimentary rocks. Siderock Lake Formation is made up of a succession, from base to top, of local felsic tuff, feldspathic wacke turbidite with A and E Bouma sequences, and a thick unit of polymictic conglomerate (clasts of chert, tonalite, dacite, iron-formation, basalt, and argillite in a volcanogenic matrix). There are also rare ultramafic lenses in this conglomerate (western part of Siderock Lake only). The conglomerate is overlain by felsic ash flow tuff, tuff, minor mafic flow, and wacke.

Contact relationships between the Big Island and Siderock Lake formations remain cryptic. At one outcrop (sector C, Fig. 1), a structural and lithological discordance occurs at the contact between sheared and folded mafic rocks and south-facing, feldspathic wacke turbidites. This may represent a fault, although there is no map-scale discordance between these formations.

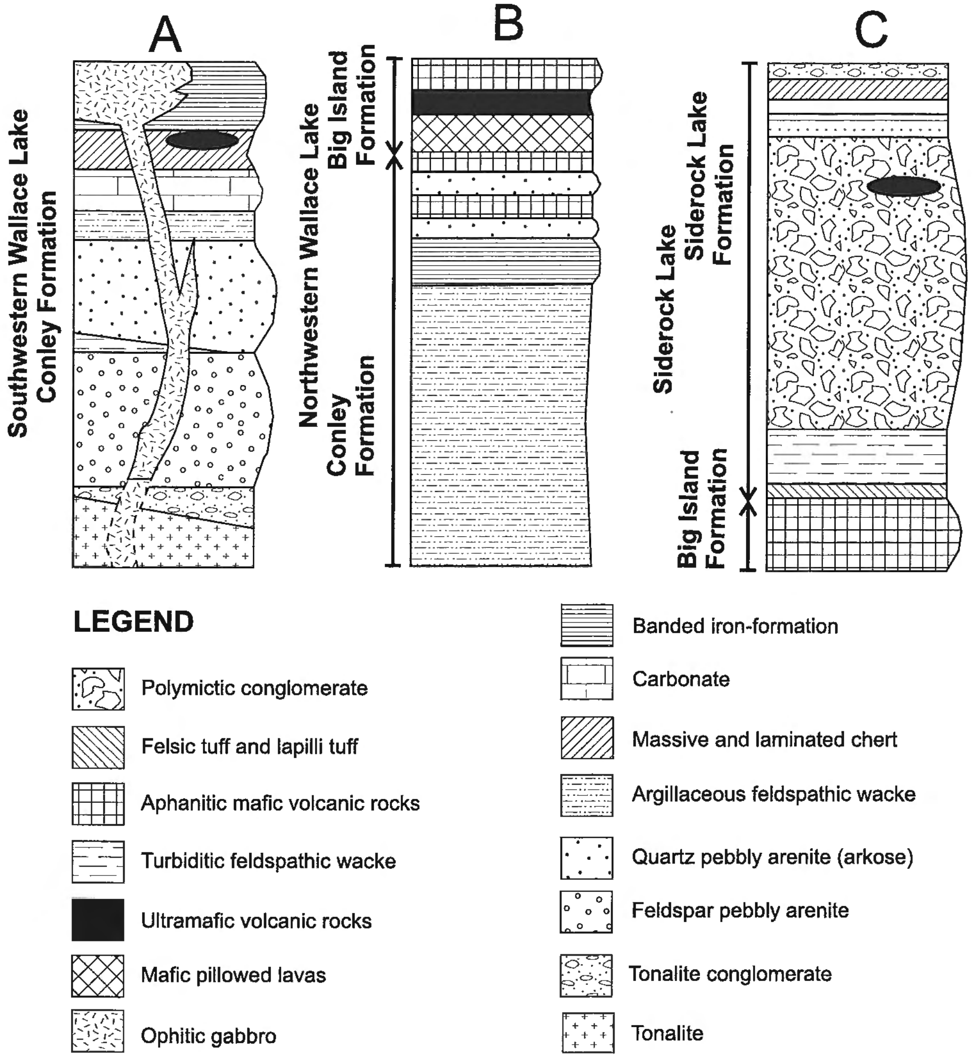


***Figure 2.** Schematic stratigraphic columns for the Wallace Lake belt. Column labels refer to locations in Figure 1.*

### *Wanipigow River quartz diorite suite*

Granite of the Wanipigow River plutonic complex, from the north shore of Wallace Lake has an age of 2730 Ma, equivalent to the main period of volcanism in the Rice Lake belt (Poulsen et al., 1994). This, together with the older plutonic tonalitic 'basement' predating the Conley Formation (cf. Turek and Weber, 1991; D. Davis, unpub. report, 1994) confirms that the Wanipigow River plutonic complex is a domain of rocks with diverse crystallization ages rather than a comagmatic plutonic 'suite' (Poulsen et al., 1994). The Wanipigow plutonic complex, as reported by McRitchie (1971), is a plutonic complex made up of a suite of biotite quartz diorite, hornblende quartz diorite, quartz diorite-migmatite complex, aplite-pegmatite, granodiorite, and quartz diorite. This plutonic complex surrounds the Wallace Lake belt and was interpreted as syntectonic by McRitchie (1971).

The tonalite (quartz diorite of McRitchie, 1971) east of Wallace Lake (Fig. 1) may preserve a ca. 3.0 Ga basement on which the Conley Formation was deposited. The southern contact of the Wallace Lake belt is in fault contact with the Wanipigow River plutonic complex. North of Wallace Lake, sediments of the Conley Formation and an ultramafic lens are cut by a 2730 Ma granodiorite pluton (Fig. 1; Poulsen et al., 1994).

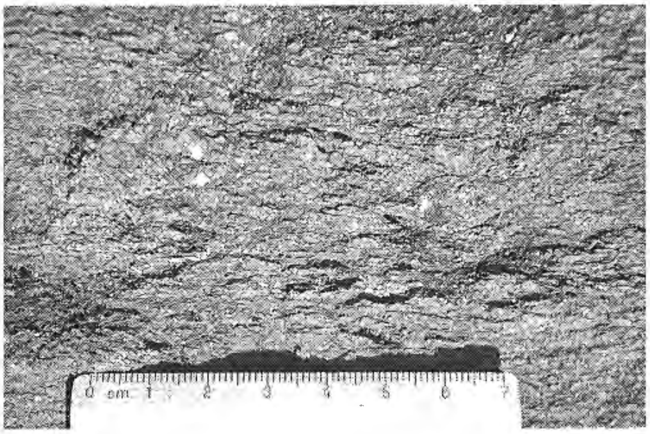


***Figure 3.** Ultramafic volcaniclastic rock, Twins Bay, Wallace Lake.*

***Figure 4.** Spinifex-texture komatiite, north shore of Siderock Lake.*

### *Ultramafic volcanic rocks of Wallace Lake belt*

McRitchie (1971) reported three ultramafic facies, tremolite-actinolite schist, pyroxenite, and serpentinite. Only two ultramafic occurrences have been reported in the Wallace Lake belt (K.H. Poulsen, W. Weber, R. Brommecker, and D. Seneshen, unpub. manuscript, 1998). One is a serpentinite (Scoates, 1971) and the other is described as a spinifex-textured ultramafic unit (Theyer, 1983), possibly a flow. No spinifex textures were observed by the authors at these ultramafic occurrences, but a distinctive texture was observed that may represent an ultramafic welded tuff. This observation, if confirmed by thin section analysis, indicates an episode of ultramafic volcanism prior to deposition of the iron-formation. Additional ultramafic units were recognized this summer about 100 m above the iron-formation in two semi-continuous horizons. One ultramafic volcaniclastic unit is exposed north of Wallace Lake at the mouth of the Blende River area (Fig. 3). The second outcrops on the north shore of Siderock Lake and extends east to the mouth of the Wanipigow River, where well preserved spinifex textures (Fig. 4) and associated pillow lavas are present. The detailed distributions of outcrops and facies is available in Sasseville et al. (in press). Two serpentinite outcrops were also noted in the Siderock Lake Formation in western Siderock Lake.

## STRUCTURE OF THE WALLACE LAKE BELT

The map-scale geometry of the Wallace Lake belt is dominated by an east-northeast-plunging, east-facing, $F_2$ anticline-syncline couplet. $S_1$ is preserved in southwestern Wallace Lake where it is folded by an $F_2$ east-trending anticline. $S_2$ is the dominant foliation and is axial planar to a northwest-trending $F_2$ syncline in northwestern Wallace Lake. The axial plane of the syncline is cut by a fault whose trend is parallel to the Gatlan fault. Local northwest-plunging and west-facing, $F_3$ folds produce map-scale interference patterns on Big Island. $F_4$ is gentle north-northwest-trending warps and kinkbands. The youngest structural event is faulting associated with the Wanipigow Lake–Wallace Lake fault.

An $S_1$ penetrative schistosity subparallel to bedding ($S_0$) is preserved in the arkose units of southwestern Wallace Lake and is associated with a mineral lineation, $L_1$. The $S_1$ schistosity is axial planar to rare, tight to isoclinal, steeply-plunging, $F_1$ 'S' folds ($F_1$).

In southwestern Wallace Lake, $S_1$ and $S_0$ are folded into an east-facing upright, easterly trending anticline plunging about 45° east. A millimetre-scale spaced cleavage ($S_2$) is axial planar to this fold, which corresponds to an antiform identified by McRitchie (1971). The fold axes of the $F_2$ minor folds are coaxial to the mineral lineation $L_1$. Figure 5 presents a stereographic projection of structural features associated with this $F_2$ fold.

The fold continues into the southeastern Siderock Lake area, where similar relationships are observed. $S_0$ and $S_1$ are folded into an east-facing, $F_2$ anticline that plunges moderately east-northeast. The minor 'Z' folds on the north limb and 'S' folds on the south have chevron forms, unlike the elliptical forms characteristic of southwestern Wallace Lake.

The map pattern in northwestern Wallace Lake is dominated by an $F_2$ syncline. McRitchie (1971) emphasized the continuity of the iron-formation in the Conley Formation, treating it as a good stratigraphic marker. Following this interpretation, Theyer (1983) used the broader chemical sedimentary units, made up of carbonate, chert, and iron-formation, as a marker, to define a belt-scale 'S' fold. The continuity with the southwestern Wallace Lake antiform is demonstrated on high-resolution geophysical maps of the Conley property (J.D. Busch, unpub. report, 1997), which define the extent of the iron-formation beneath the lake. The major $F_2$ syncline has a high strain zone in its axial region, defined by a penetrative $S_2$ schistosity and steeply northwest-plunging mineral lineation, $L_2$. The $S_2$ foliation overprints locally preserved $S_1$. $S_2$ is developed in the arkosic rocks to the south as a millimetre-scale spaced cleavage. The high-strain zone trends parallel to the Gatlan fault, which is locally sinistral and hosts the Gatlan gold showing (Gaba, 1987). To the north, a homoclinal structural panel isolated by the high-strain zone consists of south-facing (overturned) members of the Conley Formation. The panel extends eastward into the northern Siderock Lake area.

A third generation of folds, $F_3$, trends northwest and has associated $S_3$ axial planar foliation. Near Conley Bay, a northwest-trending, $F_3$ anticline folds the southern limb of the main east-trending, $F_2$ anticline. At the eastern end of Big Island, an $F_3$ syncline is defined by a west-facing fold in iron-formation, which lies on the northern limb of the east-facing, $F_2$ anticline. Figure 6 presents a stereographic projection of the $F_3$ folds. Figure 1 illustrates the interference patterns interpreted from the facing and the stratigraphic relationships. In the northern panel, $S_1$ and $S_2$ are deformed by a $F_3$ 'S' fold that plunges moderately northwest.

$F_4$ warps have regionally north-northwest-trending axial traces. Folds of this generation are evident in iron-formation on the north shore of Wallace Lake. The $F_4$ folds are associated with a locally developed, north-northwest-trending, 10 cm spaced cleavage, $S_4$. Where developed at the outcrop scale, $F_4$ folds are kinkbands. In areas of $F_4$ folding, $F_2$ and $F_3$ folds are tight to isoclinal.

Dextral motion of the Wanipigow Lake–Wallace Lake fault is the youngest structural event. The south shore of Siderock Lake is an abrupt topographic discontinuity marking the faulted contact between the Siderock Lake Formation and the Wanipigow River plutonic complex to the south. North of Siderock Lake, a linear magnetic anomaly (Hosain et al., 1993) associated with the northern panel terminates abruptly.

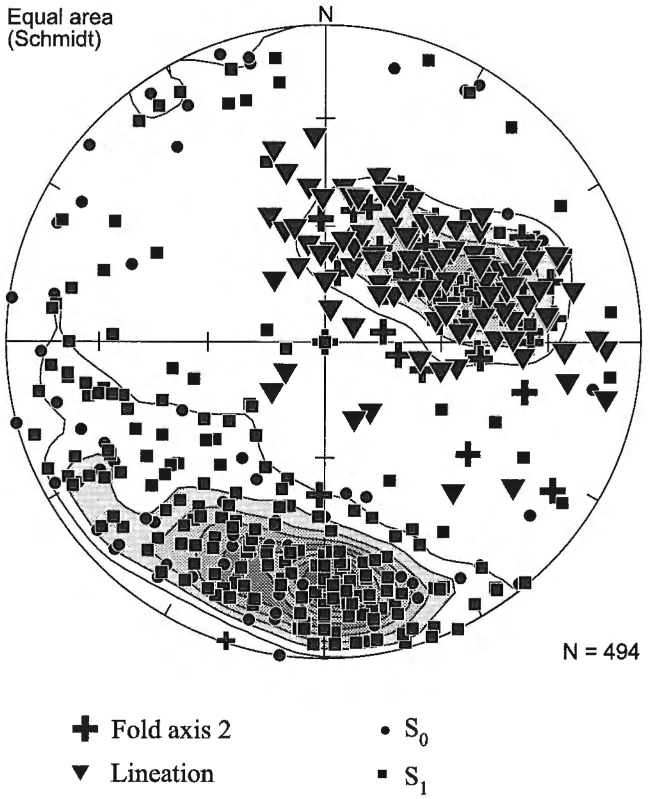


*Figure 5. Equal area, lower hemisphere stereographic projection of $D_2$ features in southwestern Wallace Lake.*

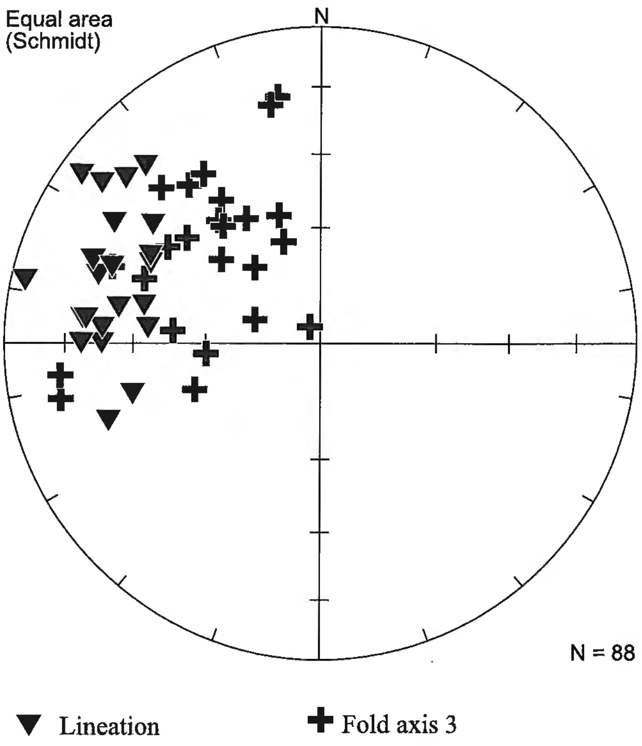


*Figure 6. Stereographic projection of $F_3$ features.*

A steeply-dipping, west-southwest-trending, high-strain zone was mapped on Siderock Lake, where it corresponds to the end of the magnetic anomaly. The high-strain zone is characterized by flattened clasts with aspect ratios up to 1:100, and the presence of grey phyllite, which are interpreted regionally as fault gouge (T. Corkery, pers. comm., 1998). This fault may be continuous with the topographic discontinuity separating mafic volcanic rocks of Big Island Formation from sedimentary rocks of the Siderock Lake Formation. Together, these three observations form the basis of the interpretation of this zone as the north Siderock Lake fault (Fig. 1). A locally developed, spaced cleavage, $S_5$, trending east-southeast and dipping moderately to the north-northwest, locally indicates dextral sense of shear. This structure is parallel to the north Siderock Lake fault and was previously related to the Wanipigow Lake–Wallace Lake fault (McRitchie, 1971).The angular relationship of the Wanipigow Lake–Wallace Lake fault to the north Siderock Lake fault is consistent with a Riedel shear model in which $S_5$ and the north Siderock Lake fault would be P shears related to the main Wanipigow Lake–Wallace Lake shear.

### *Structural control of the Gatlan gold occurrence*

Gaba (1987) demonstrated that the Gatlan gold occurrence is structurally controlled. Arsenopyrite and gold are disseminated along the $S_2$ foliation as well as within spaced cleavage $S_2$, apparently without accompanying mineral alteration. The presence of metallic minerals along foliation planes suggested precipitation from fluids that percolated along these surfaces. The auriferous fluids were later redirected along the $S_3$ crenulation cleavage as result of the prevailing dynamic stress regime (Gaba, 1987). The structural interpretation of Gaba (1987) differs in many aspects from our new observations. First, he interpreted the Gatlan fault as synsedimentary. Secondly, no $S_1$ foliation was reported from this area and Gaba's (1987) $S_2$ was everywhere parallel to the lithological layering. Thirdly, the $S_3$ crenulation cleavage is parallel to, and associated with, the Gatlan fault, rather than a feature of regional extent. This interpretation requires re-evaluation in light of the new observations.

## REGIONAL CORRELATIONS

Platformal sedimentary sequences and overlying komatiitic and tholeiitic volcanic rocks, dated at 3.0 to 2.9 Ga, occur in the North Caribou terrane and central Wabigoon region, where they have been suggested to represent widespread continental cover sequences (Thurston and Chivers, 1990) overlain by plume-generated rift deposits (Tomlinson et al., 1996; Tomlinson et al., in press). It has been suggested that the central Wabigoon region may have once been part of the North Caribou terrane and rifted from it during the Mesoarchean (Tomlinson et al., 1996). It is therefore an important component of this project to compare the stratigraphy of the Wallace Lake greenstone belt, and the geochemistry of the volcanic rocks, with those from other platformal-rift greenstone belts in the North Caribou terrane and central Wabigoon, to examine regional correlations and the early history of rifting of the western Superior Province.

There are many similarities between the Wallace Lake and Steep Rock greenstone belts. Each belt has approximately 1000 m of platformal sedimentary rocks at its base. Quartz-rich sedimentary rocks, limestone, and iron-formation are present within each belt, although proportions vary. In the basal quartz-rich sediments of the Wallace Lake belt four detrital zircons have been dated at 2999 Ma (K.H. Poulsen, R. Brommecker, W. Weber, and D.W. Davis, unpub. manuscript, 1998) and in the basal sediments of the Steep Rock belt, six detrital zircons have been dated at 2999 Ma (D. Davis, unpub. data, reported *in* Fralick and King, 1996). The Wallace Lake sedimentary sequence is cut by a 2920 Ma quartz-feldspar phyric dyke (K.H. Poulsen, R. Brommecker, W. Weber, and D.W. Davis, unpub. manuscript, 1998) whereas the Steep Rock sedimentary sequence has not been dated.

In both the Wallace Lake and Steep Rock belts, komatiitic and then mafic volcanic rocks overlie the sedimentary sequences. The mafic volcanics of the Steep Rock belt are correlated with 2932 Ma volcanic rocks in the neighboring Finlayson greenstone belt (Tomlinson, 1996; D. Davis, unpub. report, 1993) and hence the age of deposition of the Wallace Lake and Steep Rock sequences appears to be very similar. The komatiite units in each belt are unusual in that pyroclastic textures predominate. Pyroclastic komatiitic rocks are rare on a global scale but have been described from the Steep Rock belt (Schaefer and Morton, 1991) and the nearby Lumby Lake belt (Tomlinson et al., in press) of the central Wabigoon Subprovince. The welded tuff-like textures in komatiitic rocks at Wallace Lake may represent similar volcanological characteristics. In the Steep Rock and Wallace Lake belts the komatiitic rocks occupy the same stratigraphic position. The geochemistry of the pyroclastic komatiitic rocks from the Steep Rock and Lumby Lake belts is identical but also unusual and suggests a deep mantle plume source (involving majorite-garnet fractionation; Tomlinson et al., in press). Further studies will examine whether similar geochemical signatures characterize the pyroclastic komatiitic rocks of the Wallace Lake belt.

Geochronological and geological data suggest that the Wallace Lake and Steep Rock sequences formed upon a tonalitic basement that was identical in age. The occurrence of komatiite and basalt above the platformal sedimentary sequence at Wallace Lake suggests rifting, as in the Steep Rock belt. The similarity in the stratigraphy and age of these two greenstone belts suggests that they may have formed in close proximity. These correlations represent the strongest evidence to date for a rifting event that split apart the central Wabigoon Subprovince and the North Caribou terrane.

## CONCLUSIONS

Stratigraphic mapping has revealed numerous way-up indicators which demonstrate that the sediments of the Conley Formation are at the base of the Wallace Lake stratigraphy. Ultramafic volcanic rocks, primarily spinifex-textured komatiite, ultramafic tuff, and metamorphosed equivalents of these, occur in the upper Conley Formation just below and above the iron-formation. A conformable and transitional contact separates the Conley Formation from the mafic volcanic rocks of the overlying Big Island Formation. The contact relationship between the Big Island Formation and the south-facing Siderock Lake Formation remains cryptic.

Structural studies have defined a $D_1$ event, expressed primarily as a penetrative $S_1$ foliation. In light of the revised stratigraphic scheme, the map pattern appears to represent a $F_2$-$F_3$ fold interference pattern. A newly recognized fault, possibly associated with the Wanipigow Lake–Wallace Lake fault, has been mapped north of Siderock Lake. The revised stratigraphic sequence in the Wallace Lake belt suggests regional correlations with the Steep Rock Lake belt in the Wabigoon Subprovince.

## ACKNOWLEDGMENTS

Special thanks to Nicole Auty, whose field assistance was greatly appreciated. Thanks to Werner Weber and Tim Corkery for an introduction to the geology of the area. Bill Conley provided us with precious geological information and friendly hospitality, both of which were appreciated. Reviews by Andrew Hynes, Tim Corkery, and John Percival of an earlier version of the manuscript were extremely helpful. Thanks to the Ministry of Natural Resources, Manitoba and the Geological Survey of Canada for providing effective technical and field support.

## REFERENCES

**Brommecker, R., Scoates, R.F.J., and Poulsen, K.H.**
1993: Komatiites in the Garner Lake-Beresford Lake area: implications for tectonics and gold metallogeny of the Rice Lake greenstone belt, southeast Manitoba; *in* Current Research, Part C; Geological Survey of Canada, Paper 93-1C, p. 259–264.

**Fralick, P. and King, D.**
1996: Meso-Archean evolution of western Superior Province: evidence from metasedimentary sequences near Atikokan; *in* Western Superior Transect Second Annual Workshop (Oct. 1995), (ed.) R.M. Harrap and H. Helmstaedt; LITHOPROBE Report # 53, LITHOPROBE Secretariat, University of British Columbia, p. 29–35.

**Gaba, R.G.**
1987: The Archean turbidite-hosted Gatlan gold occurrence, southeastern Manitoba; M.Sc. thesis, University of Western Ontario, London, Ontario, 180 p., map, scale 1:500.

**Hosain, I.T., Weber, W., Fedikow, M.A.F.**
1993: Summary and evaluation of the geophysical data of the Rice Lake area, southeastern Manitoba; Manitoba Energy and Mines, Geological Services, Winnipeg, Open File OF93-2, p.1–10, map, scale 1:50 000.

**McRitchie,W.D.**
1971: Geology of the Wallace-Siderock Lake area: a reappraisal; *in* Geology and Geophysics of the Rice Lake Region Southeastern Manitoba (Project Pioneer), (ed.) W.D. McRitchie; Manitoba Department of Mines and Natural Resources, Winnipeg, p. 107–125.

**Poulsen, K.H., Weber, W., Garson, D.F., and Scoates, R.F.J.**
1994: New geological observations in the Rice Lake belt, southern Manitoba (NTS 52M/3,4 and 52L/14); *in* Manitoba Energy and Mines, Mineral Division, Report of Activities, 1994; p. 163–166.

**Poulsen, K.H., Weber, W., Brommecker, R., and Seneshen, D.**
1996: Lithostratigraphic assembly of the eastern Rice Lake greenstone belt and structural setting of gold mineralization at Bissett, Manitoba; Geological Association of Canada, Field Trip Guidebook, A4, 106 p.

**Sasseville, C., Tomlinson, K.Y., and Corkery, T.**
in press: Geology of Wallace Lake with 1:20000 map in pocket; *in* Report of Field Activities; Manitoba Department of Energy and Mines, Winnipeg.

**Schaefer, S.J. and Morton, P.**
1991: Two komatiitic pyroclastic units, Superior Province, northwestern Ontario: their geology, petrography, and correlation; Canadian Journal of Earth Sciences, v. 28, p. 1455–1470.

**Scoates, R.F.J.**
1971: Ultramafic rocks of the Rice Lake Greenstone Belt, *in* Geology and Geophysics of the Rice Lake Region Southeastern Manitoba (Project Pioneer), (ed.) W.D. McRitchie; Manitoba Department of Mines and Natural Resources, Winnipeg, p.189–201.

**Theyer, P.**
1983: Geology of gold environments in Bissett/Wallace Lake portion of the Rice Lake greenstone belt; *in* Report of Field Activities, Manitoba Department of Energy and Mines, Winnipeg, GS-17 p. 101–106.

**Thurston, P.C. and Chivers, K.M.**
1990: Secular variation in greenstone sequence development emphasizing Superior Province, Canada; Precambrian Research, v. 46, p. 21–58.

**Tomlinson, K.Y.**
1996: The geochemistry and tectonic setting of early Precambrian greenstone belts, northern Ontario, Canada; Ph.D. thesis, University of Portsmouth, England, 287 p.

**Tomlinson, K.Y., Thurston, P.C., Hughes, D.J., and Keays, R.R.**
1996: The central Wabigoon region: petrogenesis of mafic-ultramafic rocks in the Steep Rock, Lumby Lake and Obonga Lake greenstone belts (continental rifting and drifting in the Archean); *in* Western Superior Transect Second Annual Workshop (Oct. 20–21, 1995), (ed.) R.M. Harrap, and H. Helmstaedt; LITHOPROBE Report #53, LITHOPROBE Secretariat, University of British Columbia, p. 65–73.

**Tomlinson, K.Y., Hughes, D.J., Thurston, P.C., and Hall, R.P.**
in press: Plume magmatism and crustal growth at 2.9 to 3.0 Ga. in the Steep Rock and Lumby Lake area, western Superior Province; Precambrian Research.

**Turek, A. and Weber, W.**
1994: The 3 Ga. basement the Rice Lake supracrustal rocks, southeast Manitoba; *in* Report of Activities 1994; Energy and Mines, Mineral Division, p. 167–169.

Geological Survey of Canada Project 970014

# Recent advances in the geology and structure of the Confederation Lake region, northwestern Ontario[1]

N. Rogers, C.R. van Staal, and V. McNicoll
Continental Geoscience Division, Ottawa

*Rogers, N., van Staal, C.R., and McNicoll, V., 1999: Recent advances in the geology and structure of the Confederation Lake region, northwestern Ontario;* in *Current Research 1999-C; Geological Survey of Canada, p. 187–195.*

**Abstract:** The Uchi–Confederation greenstone belt consists of three distinct lithotectonic assemblages (Balmer, Woman, and Confederation) spanning at least 240 million years (2975–2735 Ma). At least two phases of deformation have affected the entire stratigraphic sequence. None of the assemblage boundaries are marked by high-strain zones, and no evidence for accretionary structures has been identified. Where assemblage boundaries are tectonic, the shear zones are narrow, sinistral, late syn- to post-$D_2$ structures with relatively minor motion. Uranium-lead dates of 2832 Ma for gabbro dykes demonstrate that the Woman assemblage was fed through the Balmer assemblage (2975 Ma). Hence, the Balmer–Woman assemblage boundary is a disconformity. The Woman–Confederation assemblage boundary partially occurs along the Rowe Lake shear zone. However, field evidence suggests that the original boundary is a disconformity marked by a sedimentary rock package. These relationships suggest that the assemblage concept needs critical reassessment within the Uchi Subprovince.

**Résumé :** La ceinture de roches vertes d'Uchi–Confederation englobe trois assemblages lithotectoniques distincts (Balmer, Woman et Confederation) s'échelonnant sur au moins 240 millions d'années (2975–2735 Ma). L'ensemble de la succession stratigraphique a subi au moins deux phases de déformation. Aucune des limites des assemblages n'est marquée par des zones de forte contrainte et aucune indication de structures d'accrétion n'a été observée. Lorsque les limites des assemblages sont de nature tectonique, les zones de cisaillement correspondent à des structures étroites, sénestres, contemporaines de la fin de la phase $D_2$ ou postérieure à cette phase, où le mouvement a été relativement mineur. L'âge U-Pb de 2832 Ma obtenu pour des dykes de gabbro indique que l'assemblage de Woman a été alimenté par l'assemblage de Balmer (2975 Ma). Ainsi, la limite entre les assemblages de Balmer et de Woman est une discordance. La limite entre les assemblages de Woman et de Confederation se rencontre en partie le long de la zone de cisaillement de Rowe Lake. Toutefois, les observations de terrain portent à croire que la limite originale correspondrait à une discordance marquée par un assemblage sédimentaire. Au vue de ces relations, la notion d'assemblage devrait être réexaminée attentivement à l'intérieur de la Sous-province d'Uchi.

[1] Contribution to the Western Superior NATMAP Project

## INTRODUCTION

This paper represents an interim report on the Confederation Lake region of the Uchi Subprovince, northwestern Ontario. Following a reconnaissance study (van Staal, 1998), a detailed geological mapping program of the Uchi–Confederation greenstone belt was undertaken during the 1998 field season. The intention of this project, which forms part of Western Superior NATMAP Project, is to better understand the nature and timing of interactions between the three distinct lithotectonic units that make up this greenstone belt.

The Uchi–Confederation greenstone belt was original described by Goodwin (1967) as comprising two mafic to felsic sequences, to which Pryslak (1971a, b) added a stratigraphically lower unit. Thurston (1985) interpreted these as three distinct cycles of volcanism (tholeiitic, pillow basalt, and andesite flows overlain by andesitic to rhyolitic pyroclastic deposits and minor flows), each of which represents a different stage of caldera development. Nunes and Thurston (1980) and Wallace et al. (1986) recognized the large time scale over which volcanism occurred, dating Cycle I at ca. 2959 Ma, Cycle II at 2840 Ma and Cycle III at ca. 2738 Ma. These cycles were interpreted to be folded into a north-trending syncline, with Cycle III occurring in the core of the fold (Thurston, 1980). However, additional U-Pb zircon determinations from the eastern margin of the greenstone belt (2739–2735 Ma; Noble, 1989) show that this simple synclinal geometry is not a viable model.

Stott and Corfu (1991) later reinterpreted the cycles as lithotectonic assemblages and correlated them to other similarly dated parts of the Uchi Subprovince. The Balmer and Woman assemblages are equivalent to the western portions of Cycle I and II respectively, with the Confederation assemblage accounting for the remaining portion of the greenstone belt.

## BALMER ASSEMBLAGE

The Balmer assemblage occurs to the east of, and is intruded by, the ca. 2838 Ma phase of the Trout Lake batholith (Noble, 1989) (Fig. 1). The Balmer assemblage consists mainly of pillowed to massive tholeiitic basalt interlayered with numerous diabase and gabbro sills and underlain by layered gabbro. Whilst no pillow facings have been identified in this area (Pryslak, 1971a, b; van Staal, 1998), younging directions from the minor volcaniclastic and sedimentary rocks indicates that the Balmer generally faces east, towards the Woman assemblage (Fig. 2).

A new U-Pb zircon age of 2975 ± 1 Ma (V. McNicoll, unpub. data, 1998) from a strongly foliated rhyolite on Spot Lake (VL97-14, Fig.2) confirms that the Balmer assemblage constitutes the oldest supracrustal rocks in the region. Together with a unit of felsic tuff at Narrow Lake, these felsic volcanic rocks locally mark the structural top of the Balmer assemblage. A small, quartz-feldspar-xenocrystic, felsic, lithic tuff unit occurs near the contact with the Trout Lake batholith on Narrow Lake (Fig. 1). This unit yielded a U-Pb zircon age of ca. 2959 Ma (Nunes and Thurston, 1980), which suggests that the internal structure of this assemblage is more complex than currently understood. As it has proven impossible to distinguish any macroscopic petrographic units within the basaltic volcanic rocks, it is hoped that a cryptic geochemical stratigraphy may help to outline the structure.

A relatively thick sequence of dominantly gabbroic (locally pegmatitic) to diabasic rocks, along with minor trondhjemite and plagiogranite dykes, occurs towards the structural base (i.e. adjacent to the Trout Lake batholith) of the Balmer assemblage. These basic plutonic rocks exhibit amphibolite-facies shear zones and highly ductile folding (Fig. 3) that is synchronous in part with basic and felsic magmatism. Such high-temperature deformation has been observed in the basal sections of recent ophiolites (Thayer, 1980; van Staal et al., 1988). Furthermore, as the oldest phase of the Trout Lake batholith appears to be petrographically related to the ca. 2959 Ma felsic tuff, there is no known continental basement to the Balmer assemblage. Although it is possible that the Balmer was erupted onto continental crust (that has since been detached or is represented by an unrecognized phase of the Trout Lake batholith), the lack of a known continental basement tends to suggest an oceanic setting for the Balmer assemblage. However, improved age constraints for the Trout Lake batholith along with detailed geochemical and isotopic data are required to constrain the tectonic environment.

## WOMAN ASSEMBLAGE

The Woman assemblage has previously been mapped as a single, generally eastward-facing, mafic to felsic sequence extending between Spot Lake and a stromatolitic marble which locally outcrops on the western side of the Woman Lake 'narrows' (Thurston, 1985; Stott and Corfu, 1991). However, geochemical evidence (K. Tomlinson, pers. comm., 1998) has indicated that Woman-type basaltic volcanism also occurs to the east of the 'narrows' (Fig.1 and 2). This corresponds with field evidence of macroscopically identical pillow basalts that are present on both sides of Woman Lake. These particular basalts are distinctive, even from other basalts in the Woman assemblage, due to their very light grey-green colour. The petrographic and geochemical evidence indicates that at least in the southern part of the map area, the Woman assemblage extends to the Rowe Lake shear zone (Fig.1, 2). The narrow zone of felsic tuffs that occurs adjacent to this shear zone is petrographically very similar to Thurston's (1985) Woman Lake tuff, which was interpreted as the final volcanic product of Cycle II (Thurston, 1985). Both units consist of tuff, lapilli tuff, and minor tuff breccia, with relatively common fiamme and felsic pumiceous lapilli. Together with the petrographic and chemical similarities of the tholeiitic pillow basalts, this evidence implies structural repetition by faulting and/or folding within the Woman assemblage rather than a second cycle of basic to felsic volcanism. However, as the Woman assemblage in the Meen–Dempster greenstone belt, eastern Uchi Subprovince, has a ca. 2825 Ma sequence paraconformably overlying the

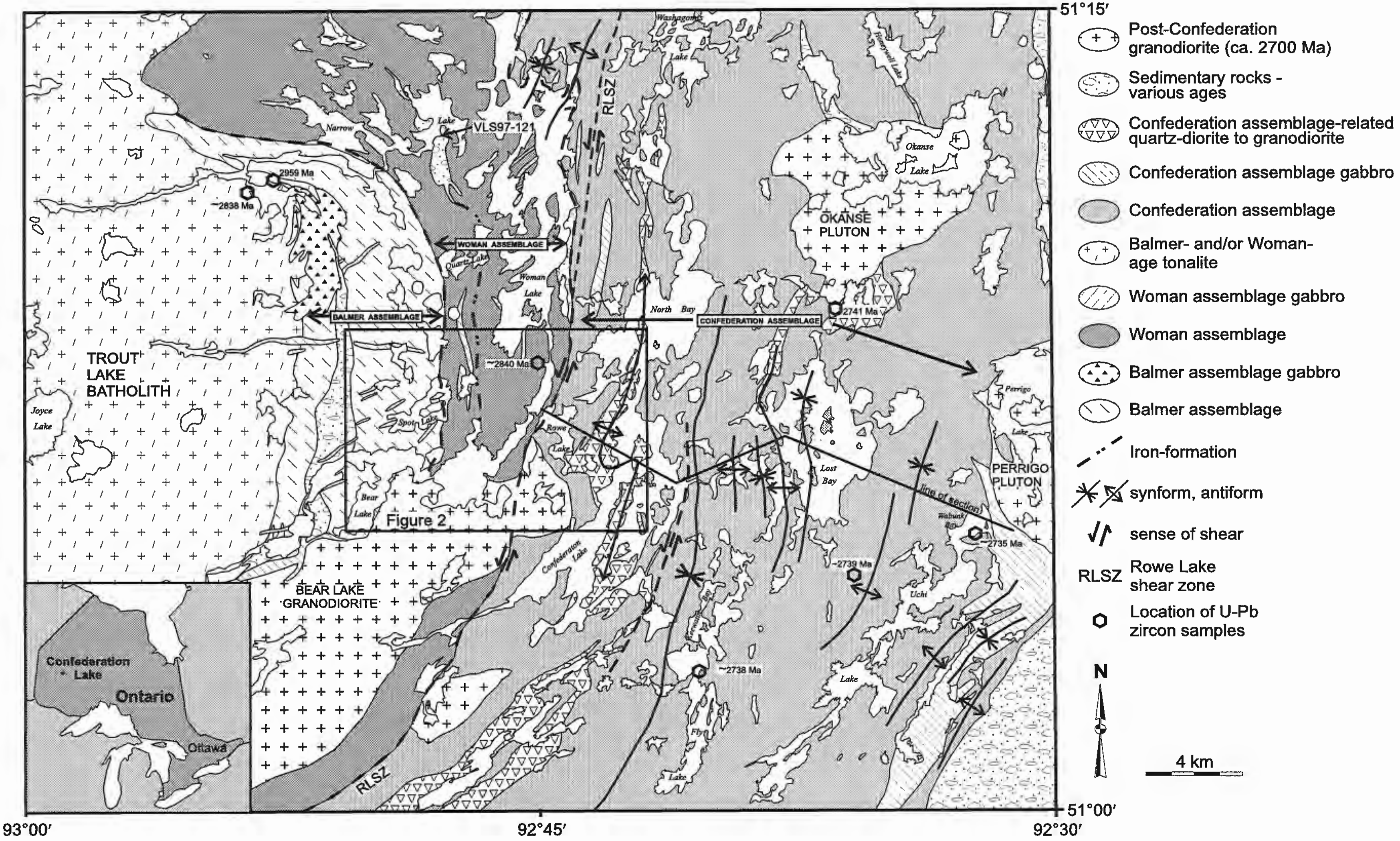


***Figure 1.*** *Geology of the Confederation Lake area (NTS 52 N/02).*

ca. 2840 Ma volcanic rocks (Stott and Corfu, 1991), additional geochronological data is required to constrain the stratigraphy.

It is proposed that the Woman assemblage be extended to include a suite of volcanic rocks to the south of a crosscutting granitoid (herein referred to as the Bear Lake granodiorite; Fig. 1). These rocks have been correlated primarily on the basis of the felsic volcanic field petrology. Several felsic tuff, lapilli tuff, and tuff breccia units that exhibit a marked similarity to the Woman Lake tuff have been observed within this section. However, of particular importance is a relatively narrow band of welded tuffs that contain very distinctive fiamme (Fig. 4). This pyroclastic, and therefore presumably regionally well distributed unit does not correlate with any strata within the Confederation assemblage. However, similar

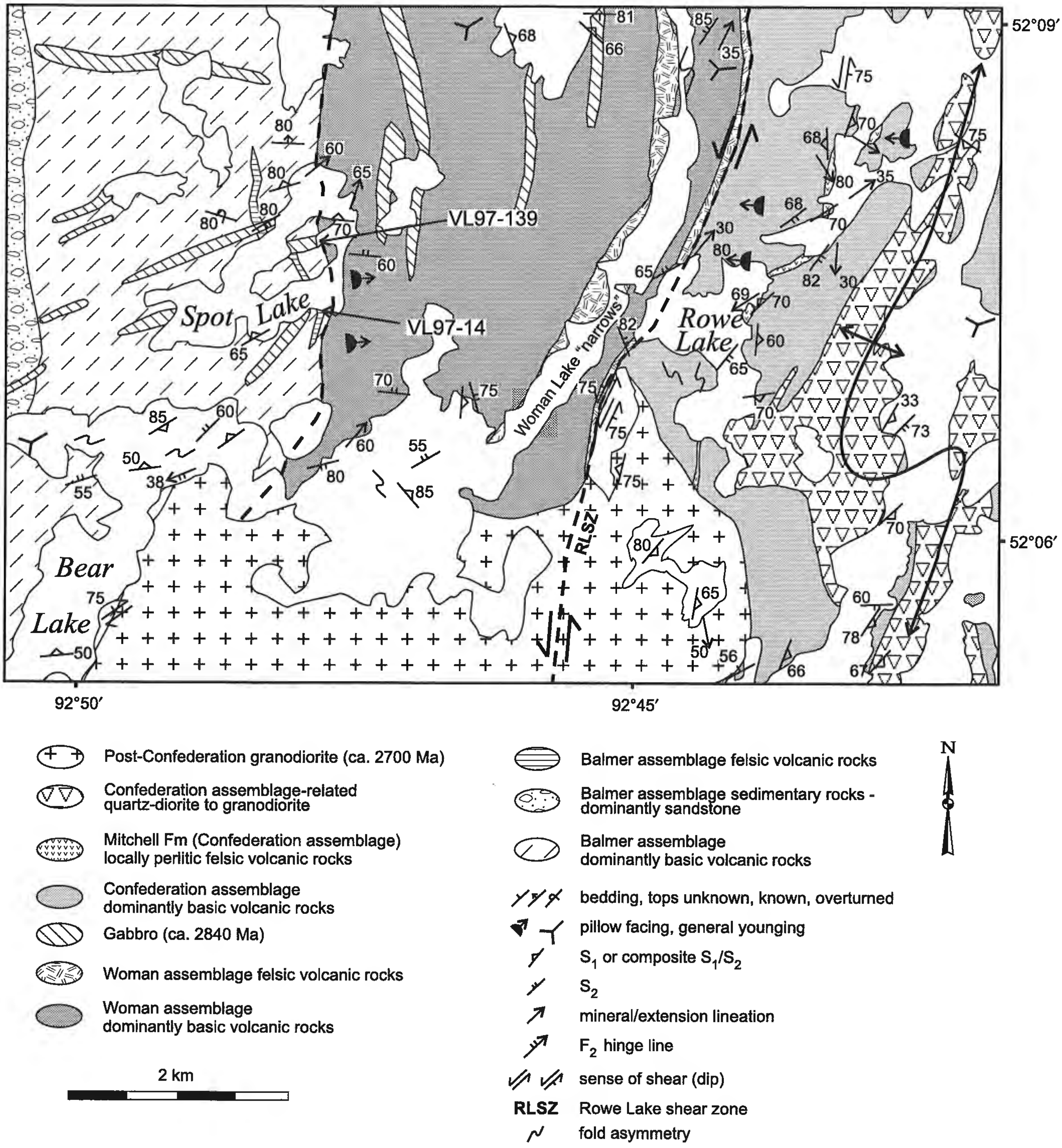


*Figure 2. Detailed geology of the Spot Lake to Rowe Lake region.*

rocks are well documented within the Woman Lake tuff (Thurston, 1985). As geological relationships between these rocks and those on Woman Lake are impossible to determine due to the crosscutting, younger granitoid unit, the true association of these rocks cannot be established until analytical data is available.

*Figure 3. Intensely high-temperature-type folded Balmer gabbro cut by trondhjemite veins.*

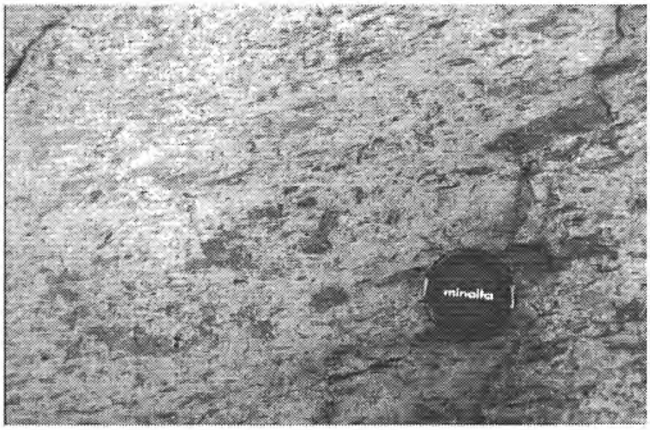


*Figure 4. Well preserved fiamme in Woman assemblage ignimbrite.*

New U-Pb zircon data from a sedimentary rock package in Narrow Lake (VLS97-121, Fig. 1; V. McNicoll, unpub data, 1998) suggest the possibility that the western side of the Woman assemblage should be correlated with an older suite of volcanic rocks. The youngest detrital zircons analyzed fall into the general range 2890 to 2873 Ma, and are accompanied by older grains at ca. 2985 Ma. Whilst the older zircons probably reflect sampling of Balmer volcanic rocks, the ca. 2880 Ma zircons are more intriguing. Volcanism of similar age is present elsewhere in the Uchi Subprovince, such as the Bruce Channel assemblage of the Red Lake greenstone belt (Stott and Corfu, 1991). Although petrographically the sedimentary rock package appears to be immature bedded sandstone consisting of primarily proximal, juvenile, volcanic detritus, further work is required to confirm whether the zircons are locally derived or reflect exotic material from adjacent belts. Assuming that the source is local, this indicates that the basaltic rocks structurally and stratigraphically underlying the sedimentary rock package should be correlated with pre-Woman volcanism. The southern extension of this sedimentary package is marked by a narrow band of iron-formation (Thurston, 1985), implying a regional cessation of volcanism occurred at this stratigraphic position. Interestingly, a unit of iron-formation also marks the top of the Bruce Channel assemblage in the Red Lake greenstone belt (Stott and Corfu, 1991).

## CONFEDERATION ASSEMBLAGE

The Confederation assemblage includes all the supracrustal rocks east of Rowe Lake (Fig. 1). As postulated by van Staal (1998), a simple mafic to felsic cycle cannot explain the distribution of volcanic rocks within the Confederation assemblage. It is evident from field relations that several distinct felsic volcanic units are stratigraphically separated by batches of tholeiitic (predominantly pillowed flows and/or pillow breccia) magmatism (Fig. 1, 2, 5).

Field petrology suggests that felsic volcanic rocks of the Confederation assemblage can be separated into at least three units, each of which consists of one or more beds. This discovery is significant as it enables the internal structure of the

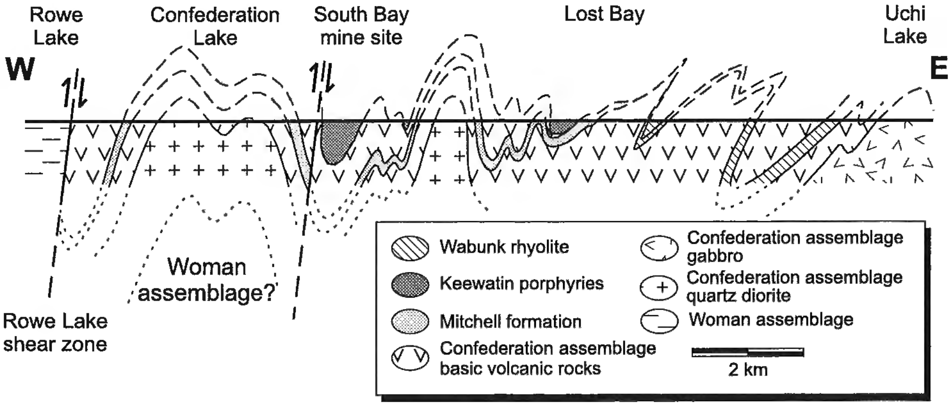


*Figure 5. Schematic cross-section through the Confederation assemblage (line of profile on Fig. 1).*

Confederation assemblage to be determined. Although subtle petrographic variations between the Confederation pillow basalts of Washagomis Lake, northeastern Lost Bay, and Uchi Lake have been noted, without geochemical support they are not distinct enough to constitute mappable units.

The suite of felsic volcanic rocks herein informally referred to as the Mitchell formation (Fig. 2, 5) is of particular interest as it includes rocks previously described as variolitic basalt (Thurston, 1985; van Staal, 1998). The Mitchell formation typically consists of dark grey to black, massive, dacite flows and associated welded and unwelded tuff units. The so-called variolitic basalt is in fact perlitic dacite (Fig. 6). The observations by van Staal (1998) of reverse grading of the varioles (perlite) relates to the tendency of perlite to concentrate at flow margins where interactions with external water sources enable hydration of the glassy rhyolite. A quenched texture is apparent in thin section, which supports the flow-margin model for these rocks. The dacitic nature of these rocks is clear from chemical analysis (K. Tomlinson, unpub. data, 1998), with silica contents between 62 and 72 weight per cent, relatively high concentrations of high-field-strength elements, and a flat rare-earth profile.

To the west of Lost Bay, the Mitchell formation acts as an effective structural marker. The distribution of this unit clearly traces out the Confederation Lake anticline proposed by van Staal (1998) as a north-south-trending, doubly plunging anticline. The fold axis approximately follows Confederation Lake, closing at the southern end of Washagomis Lake (Fig. 1, 5). A large sill-like body of metamorphosed quartz-diorite to granodiorite cores the anticline. These rocks appear to form the structural base of the Confederation assemblage, and as such are a useful structural marker. Geochemical analysis (Thurston and Fryer, 1983) and a poorly constrained U-Pb age of ca. 2737 Ma (Nunes and Thurston, 1980), both suggest that these granitoid bodies are genetically related to Confederation assemblage volcanic rocks. The distribution of the Confederation Lake quartz-diorite and $S_1/S_2$ foliations show that the large-scale north-south-trending fold is a $D_1$ structure, which has been refolded into an 'S' form by the northeast-trending $D_2$ (Fig. 2).

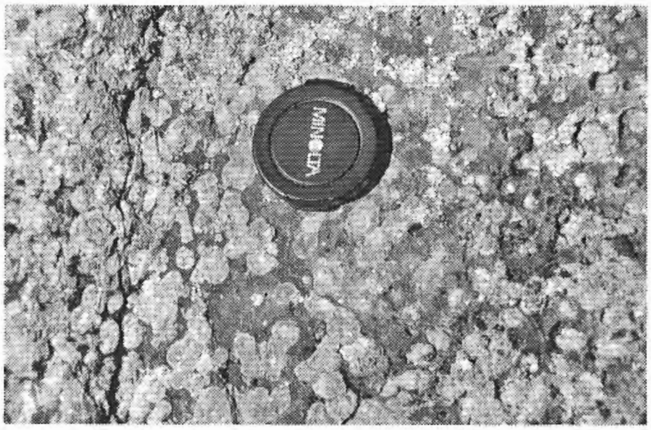

***Figure 6.*** *Perlitic dacite from the Mitchell formation, Confederation assemblage.*

Similarly, the Mitchell formation and the syn-Confederation granitoid body trace out another regional-scale, north-south-trending anticline along the western shore of Lost Bay. This structure can be traced north across the younger (post-$D_1$) Okanse pluton to at least Honeywell Lake.

The main structure between these anticlines is the South Bay syncline (van Staal, 1998), which is cored by a suite of quartz and quartz-feldspar porphyries, herein informally referred to as the Keewatin porphyries (Fig. 1, 5). These form a very distinctive suite of felsic welded to unwelded tuff and tuff breccia, with associated shallow-level hypabyssal equivalents. Typically these porphyry units contain 5–20% quartz phenocrysts up to 8 mm in diameter, commonly with a strong blue colouration. The commonly embayed and shattered form of the quartz phenocrysts is consistent with crystallization at depth, rather than in situ. The Keewatin porphyries trace out the core of the South Bay syncline along the western shore of Fly Lake.

The final suite of felsic volcanic rocks identified within the Confederation assemblage is a unit of light grey, aphyric rhyolite and ignimbrite flows centred in the east of the belt, and informally referred to herein as the Wabunk rhyolites (Fig. 1, 5). The few geochemical analyses available (Thurston and Fryer, 1983; Noble, 1989) indicate that these rhyolite flows are genetically unrelated to the Mitchell formation, as they have low concentrations of highly charged elements (such as Y, Zr, and Nb) and a steeply dipping rare-earth profile. As the Wabunk rhyolites and Mitchell formation are centred on either side of Lost Bay, determining their exact stratigraphic relations is problematic.

Overlapping error ranges for dates within the Confederation assemblage prevents the development of a consistent chronostratigraphy at present. However, the relative stratigraphic position of the rhyolites can be determined from the mass flow deposits of Lost Bay. Stix and Gorton (1988; 1989) conducted detailed studies of these deposits, including the separation and chemical analysis of individual rhyolitic clasts. They identified two chemically distinct groups of aphyric rhyolitic clasts that they were otherwise unable to separate. Analysis of these data clearly shows that Stix and Gorton's Group 2 clasts are from the Mitchell formation, whilst the Group 1 clasts are very probably Wabunk rhyolite. As both the Mitchell formation and Wabunk rhyolites appear to be supplying material for these epiclastic deposits, this implies that the two units are approximately contemporaneous. Stix and Gorton (1989) also noted the abrupt appearance of quartz-feldspar-phyric clasts within the stratigraphically higher beds of the Lost Bay mass flow deposits. Field observations appear to confirm that these clasts are derived from the Keewatin porphyries. It is possible that the source of these clasts was unroofing of subvolcanic intrusions and therefore does not hold any stratigraphic significance. However, this does not explain why the pyroclastic units of the Keewatin porphyries would be excluded from the earlier mass flow deposits. Consequently, the most likely scenario is that the Keewatin porphyries are in fact the final-stage felsic volcanism within the Confederation assemblage.

## TROUT LAKE BATHOLITH

The Trout Lake batholith occupies the western side of the map area and consists of at least two distinct phases of pre-$D_1$ tonalite, partially surrounded to the south by post- to syn-$D_2$, granodiorite (Bear Lake granodiorite). The oldest phase currently petrographically identified consists of schistose to gneissic tonalite that closely resembles the felsic tuff in the Balmer assemblage. Locally this phase is preserved as rafts within a younger, regionally more voluminous, foliated tonalite phase. There are also numerous pegmatitic veins and regions crowded by mafic xenoliths that may represent additional intrusive phases. The oldest phase currently dated is a ca. 2840 Ma (Noble, 1989) foliated tonalite close to the intrusive contact with the Balmer assemblage. The similarity in age between this phase and the Woman assemblage led Stott and Corfu (1991) to conclude that they are related. Additional dates are required to fully constrain the age of all the intrusive phases.

The Bear Lake granodiorite presumably represents a phase of the ca. 2700 Ma Walsh Lake pluton, which was defined east of the Red Lake greenstone belt (Noble, 1989). In addition to transecting $D_1$ folds, the Bear Lake granodiorite stitches both the Balmer–Woman and Woman–Confederation assemblage boundaries (Fig. 1).

## BALMER–WOMAN ASSEMBLAGE BOUNDARY

Based on age relations of the Trout Lake batholith, Stott and Corfu (1991) postulated that the Woman assemblage disconformably overlies the Balmer assemblage. This assessment is in agreement with structural data which clearly show that the boundary as defined by an aeromagnetic anomaly is in fact the enveloping surface to numerous small, tight, northeast- to east-northeast-trending $F_2$ folds. Furthermore, structural mapping has confirmed van Staal's (1998) assessment that the area lies within the hinge of a large, S-shaped, $F_2$ structure, and therefore could not have accommodated significant $D_2$ or later motion. No signs of high $D_1$ strain have been recognized along this boundary, indicating it was not a structural dislocation during $D_1$.

The most compelling evidence that the Woman assemblage developed over the Balmer, however, is from a new U-Pb baddeleyite age of 2832 ± 2 Ma (V. McNicoll, unpub. data, 1998) obtained from a pegmatitic gabbro on Spot Lake (VLS97-132; Fig. 2). This body is part of a swarm of gabbro sheets that transect the whole Balmer assemblage and the Balmer–Woman assemblage boundary (Pryslak, 1971a; van Staal, 1998). This age shows that the gabbro sheets are feeders to the Woman assemblage basalts and gabbro sills. Consequently, the Spot Lake gabbro stitches the Woman assemblage to the Balmer and makes their boundary a disconformity.

## WOMAN–CONFEDERATION ASSEMBLAGE BOUNDARY

As previously stated, geochemical and field petrographic evidence has indicated that in the southern part of the map sheet the Woman–Confederation assemblage boundary occurs to the east of the Woman Lake 'narrows' at the Rowe Lake shear zone.

At Rowe Lake, the shear zone is a narrow (approximately 10 m wide) mylonite zone, with shear bands and numerous Riedel shears that indicate mainly sinistral transcurrent, brittle-ductile shear, with a relatively small amount of west-side-up motion. The shear zone has a strong geophysical signature, both on aeromagnetic and particularly conductivity maps. These enable the shear zone to be traced north of the map area toward the dextral Swain Lake deformation zone (Pryslak 1973; 1974), with which it likely forms a conjugate set.

Although it is evident that the Rowe Lake shear zone at least locally forms the Woman–Confederation assemblage boundary, several lines of evidence indicate that it does not mark a major tectonic dislocation. Firstly, the Rowe Lake shear zone seems to have formed after the assemblages were together. From Rowe Lake the shear zone trends north-northeast towards Washagomis Lake, cutting across a regional-scale, S-shaped, $F_2$ fold (as is indicated by truncated aeromagnetic anomalies). As $D_2$ appears to have affected all of the assemblages, it follows that the Confederation and Woman assemblages were together before the Rowe Lake shear zone formed. Similarly, to the south, the Rowe Lake shear zone sinistrally offsets the margin of the Bear Lake granodiorite by approximately 2 km (Fig.1, 2). Within the granodiorite the deformation is recorded by a weak foliation and numerous pseudotachylite bands. As the Bear Lake granodiorite intrudes all of the assemblages, this relationship confirms that the Woman and Confederation assemblages were together prior to 2700 Ma, whereas the shear zone formed at a later (as yet undetermined) time.

Hence, if, as seems apparent from field relations, the north-northeast-trending Rowe Lake shear zone only locally accounts for the juxtaposition of Woman and Confederation assemblages, it follows that the nature of the original assemblage boundary remains to be identified. Field studies indicate that the original assemblage boundary might be exposed along the northeastern shore of Woman Lake (Fig. 1). In this region, a unit of sedimentary rocks can be traced north from where the Rowe Lake shear zone marks the assemblage boundary. Previously, this package of sedimentary rocks was interpreted as part of the Confederation assemblage (Stott and Corfu, 1991; van Staal, 1998). Tentatively, it is suggested that these sedimentary rocks represent the top of the Woman assemblage for the following reasons. Firstly, although several small-scale folds are apparent from younging reversals within the sedimentary package, it is evident from the internal stratigraphy and overall eastward younging, that this sedimentary package is not an infolded keel. From west to east (i.e. older to younger) the sediment types appear to reflect a deepening environment from a possible beach deposit (conglomerate with well rounded pebble-to boulder-size clasts) to distal turbiditic siltstone. Petrographically, the clasts appear to be derived from Woman volcanic rocks (samples of individual clasts have been taken to test this assessment). Currently no indications of a pre-Confederation folding event, depositional break, or angular unconformity between the underlying basalts and the sedimentary package have been observed, hence the sedimentation reflects localized erosion and subsidence of the Woman volcanic edifice(s).

Immediately to the west of (i.e. underlying) this sedimentary package are Woman pillow basalt and pillow breccia units, whilst to the east of it (i.e. overlying) are basaltic rocks that are petrographically similar to basalt of the Confederation assemblage. Whether the basaltic rocks between the sedimentary package and Rowe Lake shear zone are Woman or Confederation assemblage remains to be confirmed by geochemical analysis.

If this sedimentary package is shown to mark the Woman–Confederation assemblage boundary, then the presence of basaltic dykes crosscutting the sedimentary rocks (Fig. 7) proves that magmatism continued in this region after Woman volcanism ceased. Similar relations are apparent from the units previously defined as the top of the Woman assemblage. Numerous basaltic to gabbroic dykes cut the Woman felsic volcanic rocks of northern Woman Lake (Fig. 1), whilst a basalt dyke cuts rhyolite and overlying marble at the Woman Lake 'narrows'. Whereas gabbro dykes cut bedding at a high angle in the upper Woman assemblage, immediately east of the sedimentary package the gabbro bodies are sills. This suggests that the crosscutting gabbro units are feeders to the Confederation assemblage. Work is currently in progress to confirm that these two sets of basaltic rocks are, in fact, related. This situation is remarkably similar to the gabbros that stitch the Balmer–Woman assemblage described above. Hence, provisionally, the same conclusion is drawn, namely that the Confederation assemblage formed directly on the Woman assemblage.

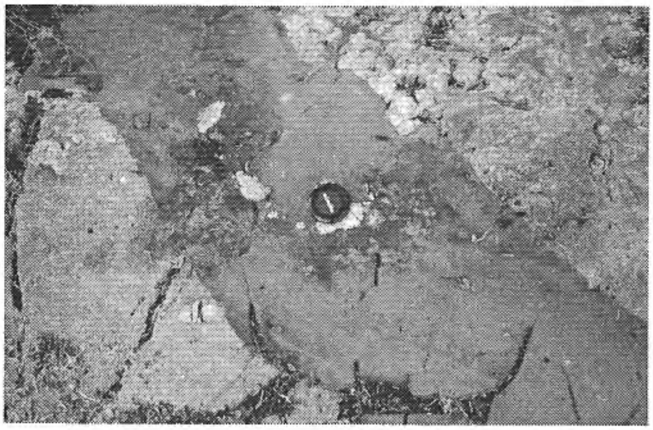

***Figure 7.*** *Possible Confederation basaltic feeder dyke cutting Woman assemblage breccia.*

## SUMMARY AND CONCLUSIONS

As this represents an interim report, most of the conclusions are provisional pending petrographic, geochemical, and geochronological analysis. Approximately 350 samples have been collected for petrographic and/or geochemical analysis, along with several units for U-Pb zircon geochronological analysis. Major questions that this work will attempt to resolve include the following:

- Is the Woman assemblage, as currently defined, a single, tectonically thickened group of ca. 2840 Ma volcanic rocks, or could it represent several distinct episodes of volcanism separated disconformably by significant time gaps (ca. 20 million years)? If the latter possibility is valid, it would argue for inclusion of the Bruce Channel assemblage and/or the younger phase of the Woman assemblage identified within the Meen–Dempster greenstone belt.
- What is the nature of the Woman–Confederation assemblage boundary and its position? Where this boundary is tectonic, the deformation clearly occurred after the Woman and Confederation assemblages were together, as the shear zone also transects a ca. 2700 Ma stitching pluton (Fig. 1, 2). Elsewhere, field evidence suggests that a sedimentary unit marks the boundary; however, it remains to be established whether the immediately overlying basaltic rocks belong to the Confederation assemblage, and if so, that the sedimentary rocks are not themselves part of the Confederation assemblage.
- Do the assemblages contain reliable chemical stratigraphic features that will enable their internal geometries to be constrained? This is particularly important for the Confederation assemblage where stratigraphic correlations between petrographically similar units require confirmation from geochemical analyses.

Structural studies and the new U-Pb dates appear to confirm earlier suggestions that the Balmer forms a basement to the Woman assemblage. No indications of a major tectonic dislocation are evident, and Woman-age gabbros (ca. 2832 Ma) clearly cut across the Balmer volcanic rocks (ca. 2975 Ma). The apparently large time gap (60–120 Ma) between these two assemblages without a major unconformity or fault is still enigmatic (c.f. Nunes and Thurston, 1980). Furthermore, considering that field evidence suggests that the Woman–Confederation assemblage boundary is also a disconformity covering a major stratigraphic break, and that up to two more disconformities could occur within the Woman assemblage, it follows that the assemblage concept requires critical reassessment within the Uchi–Confederation greenstone belt.

Given that the various assemblages formed in stratigraphic sequence, determining the tectonic setting of the Balmer volcanic rocks is critical to understanding the tectonic environment of the Uchi–Confederation greenstone belt as a whole. It is possible that the Balmer formed on continental crust or was obducted onto a continental margin prior to Woman volcanism and emplacement of the ca. 2840 Ma phase of the Trout Lake batholith. However, the lack of indications for a pre-Balmer continent (such as detrital zircons or old phases of the Trout Lake batholith) within this region, tentatively suggests that none of the volcanism occurred in a continental setting. Such a model would require that all three assemblages formed sequentially within an oceanic environment. Whilst the pulses of magmatism can be explained by a series of mantle plumes, basically as a modified version of Thurston's (1985) cyclical volcanism model, this setting has no modern analogue. Hence, the tectonic setting and evolution of the Uchi–Confederation greenstone belt formed remain to be determined.

## ACKNOWLEDGMENTS

The authors would like to acknowledge the support of the Western Superior NATMAP Project that made this research possible, and are indebted to J.A. Percival, P.C. Thurston, and T. Skulski for their assistance in setting up this project. C. Blackburn and the staff of the Ontario Geological Survey, Red Lake office are thanked for their assistance, as is F. Schwerdtner. K. Tomlinson provided access to unpublished geochemical analyses. Kabeelo Lodge once again provided an excellent base camp and air service. Woman Lake, Woman River, South Bay and Uchi lodges are also thanked for their assistance during the field season. Finally, N. Rogers expresses many thanks to his excellent field assistants Allysson Lindsay, Sebastien Hogan, and Sheldon Thistle, without whom the field season would not have been so productive.

Critical reviews by J. Percival, T. Skulski, and S. Hanmer improved this paper.

## REFERENCES

**Goodwin, A.M.**
1967: Volcanic studies in the Birch–Uchi Lakes Area of Ontario; Ontario Department of Mines, Miscellaneous Paper 6, 96 p.

**Noble, S.R.**
1989: Geology, geochemistry and isotope geology of the Trout Lake Batholith and the Uchi-Confederation Lakes greenstone belt, northwestern Ontario, Canada; Ph.D. thesis, University of Toronto, Toronto, Ontario, 288 p.

**Nunes, P.D. and Thurston, P.C.**
1980: Two hundred and twenty million years of Archean evolution: a zircon U-Pb age stratigraphic study of the Uchi–Confederation lakes greenstone belt; Canadian Journal of Earth Sciences, v. 17, p. 710–721.

**Pryslak, A.P.**
1971a: Corless Township, District of Kenora (Patricia Portion); Ontario Department of Mines and Northern Affairs, Preliminary Map P. 634, scale 1:15 840 .
1971b: Knott Township, District of Kenora (Patricia Portion); Ontario Department of Mines and Northern Affairs, Preliminary Map P. 635, scale 1:15 840.
1973: Shabumeni River–Narrow Lake area (northeastern part), District of Kenora (Patricia Portion); Ontario Department of Mines and Northern Affairs, Preliminary Map P. 901, scale 1:15 840.
1974: Shabumeni River–Narrow Lake area (northwestern part), District of Kenora (Patricia Portion); Ontario Department of Mines and Northern Affairs, Preliminary Map P. 973, scale 1:15 840.

**Stix, J. and Gorton, M.P.**
1988: Physical and chemical processes of Archean subaqueous pyroclastic rocks; *in* Geoscience Research Grant Program, Summary of Research 1987–1988, Ontario Geological Survey, Miscellaneous Paper 140, p. 231–238.
1989: Subaqueous volcaniclastic rocks of the Confederation Lake area, northwestern Ontario: discrimination between pyroclastic and epiclastic emplacement; *in* Geoscience Research Grant Program, Summary of Research 1988–1989, Ontario Geological Survey, Miscellaneous Paper 143, p. 83–93.

**Stott, G.M. and Corfu, F.**
1991: Uchi Subprovince; *in* Geology of Ontario, Ontario Geological Survey, Special Volume 4, part 1, p. 145–238.

**Thayer, T.P.**
1980: Syncrystallization and subsolidus deformation in ophiolitic peridotite and gabbro; American Journal of Science, v. 280-A, p. 269–283.

**Thurston, P.C.**
1980: Subaerial volcanism in the Archean Uchi–Confederation volcanic belt; Precambrian Research, v. 12, p. 79–98.
1985: Physical volcanology and stratigraphy on the Confederation Lake area, District of Kenora (Patricia Portion); Ontario Geological Survey, Report 236, 117 p.

**Thurston, P.C. and Fryer, B.J.**
1983: The geochemistry of repetitive cyclical volcanism from basalt through rhyolite in the Uchi–Confederation greenstone belt; Contributions to Mineralogy and Petrology, v. 83, p. 204–226.

**van Staal, C.R.**
1998: Some notes on the assemblage boundaries and internal structure of the Uchi–Confederation greenstone belt, northwestern Ontario; *in* Current Research 1998-C, Geological Survey of Canada, p. 107–114.

**van Staal, C.R., Langton, J.P., and Sullivan, R.W.**
1988: A U-Pb zircon age for the ophiolitic Deveraux Formation, Elmtree Terrane, northeastern New Brunswick; *in* Radiogenic Age and Isotopic Studies: Report 1, Geological Survey of Canada, Paper 88-2, p. 37–40.

**Wallace, H., Thurston, P.C., and Corfu, F.**
1986: Developments in stratigraphic correlation: western Uchi Subprovince; *in* Volcanology and Mineral Deposits, Ontario Geological Survey, Miscellaneous Paper 129, p. 88–102.

Geological Survey of Canada Project 970014

# Geology of the central Wabigoon region in the Sturgeon Lake–Obonga Lake corridor, Ontario[1]

J.A. Percival, S. Castonguay[2], J.B. Whalen, J.L. Brown[3], V. McNicoll, and J.R. Harris
Continental Geoscience Division, Ottawa

*Percival, J.A., Castonguay, S., Whalen, J.B., Brown, J.L., McNicoll, V., and Harris, J.R., 1999: Geology of the central Wabigoon region in the Sturgeon Lake–Obonga Lake corridor, Ontario;* in *Current Research 1999-C; Geological Survey of Canada, p. 197–208.*

**Abstract:** Plutonic rocks, older gneiss units, and supracrustal remnants occur as kilometre-scale sheets in the northern part of the Sturgeon–Obonga corridor and are separated from large, homogeneous tonalite and granodiorite plutons to the south by the Gunter Lake and Brightsand River shear zones. A common structural chronology characterizes both areas; $S_1$ gneissosity and $F_2$ folds (>2.715 Ga) occur in tonalite gneiss units; penetrative $S_3$ foliation, equivalent to $S_1$ in adjacent greenstone belts, is carried by most plutonic units and is folded into tight, upright, gently east-plunging $F_4$ folds. Complexly deformed tonalitic gneiss units occur in the vicinity of quartz-rich sedimentary rocks of the Sturgeon belt margin and could represent depositional basement. Geochemically, most plutonic units have tonalite-trondhjemite-granodiorite affinities, with pronounced negative Nb and Ti anomalies, suggesting derivation in an island- or continental-arc setting.

**Résumé :** Des roches plutoniques, des unités gneissiques plus anciennes et des lambeaux supracrustaux se rencontrent sous forme de nappes kilométriques dans la partie septentrionale du corridor de Sturgeon–Obonga. Vers le sud, ces roches sont séparées de gros plutons homogènes de tonalite et de granodiorite par les zones de cisaillement de Gunter Lake et de Brightsand River. Ces deux régions se caractérisent par une chronologie structurale commune; une structure gneissique $S_1$ et des plis $F_2$ ( >2,715 Ga) sont présents dans des unités de gneiss tonalitique, alors qu'une schistosité pénétrative $S_3$, équivalente à $S_1$ dans des ceintures de roches vertes adjacentes, se rencontre dans la plupart des unités plutoniques et est déformée en plis $F_4$ droits et serrés qui plongent doucement vers l'est. Des unités de gneiss tonalitique à déformation complexe sont présentes à proximité de roches sédimentaires quartzeuses de la bordure de la ceinture de Sturgeon et pourraient représenter un socle primaire. D'un point de vue géochimique, la plupart des unités plutoniques montrent des affinités tonalitiques-trondhjémitiques-granodioritiques, avec des anomalies négatives marquées en Nb et Ti, ce qui indiquerait qu'elles sont issues d'un milieu d'arc insulaire ou continental.

[1] Contribution to the Western Superior NATMAP Project
[2] INRS-Géoressources, Sainte Foy
[3] Department of Earth Sciences, University of Ottawa, 365 Nicholas Street, Ottawa, Ontario K1N 6N5

## INTRODUCTION

The Western Superior NATMAP project was formulated to address outstanding questions concerning the Archean tectonic evolution of the Superior Province of western Ontario and eastern Manitoba, through co-ordinated activities of the Geological Survey of Canada, Ontario Geological Survey, Manitoba Geological Services Branch, and the Western Superior LITHOPROBE transect. Recent syntheses (Williams et al., 1992; Card and Poulsen, 1998) have regarded the linear volcanic-plutonic subprovinces of the western Superior Province as intra-oceanic island arc terranes, juxtaposed during ca. 2.7 Ga collisional events. However, these models do not adequately account for either the presence or age similarity of ca. 3.0 Ga crustal blocks within the Wabigoon and Uchi subprovinces and North Caribou terrane. Resolving whether the sialic relics represent depositional basement to Neoarchean greenstone sequences, or are unrelated microcontinental terranes, is a principal goal of the NATMAP project.

A transverse corridor containing vestiges of 3.07–2.93 Ga crust divides the Wabigoon Subprovince into eastern and western parts. Its eastern part contains mixed volcanic and plutonic rocks, of both Meso- and Neoarchean age (Stott et al., 1998), whereas the western Wabigoon Subprovince consists mainly of juvenile Neoarchean greenstone belts and granite units (Blackburn et al., 1991; Henry et al., 1998). A telescoped continent-ocean transition zone is interpreted within the Sturgeon–Savant greenstone belt (Sanborn-Barrie and Skulski, 1999).

A project was initiated in 1997 to map the dominantly granitoid rocks in the central Wabigoon region between Sturgeon and Obonga lakes, with the following goals: 1) to distinguish structurally complex, potentially older granitoid units from postvolcanic intrusive bodies, through establishment of relative and absolute structural-intrusive chronologies; 2) to examine boundaries between potentially 'old' granitoid units and supracrustal rocks and determine their contact relationships (i.e. unconformable, tectonic); and 3) to establish correlations between regional structures in the granitoid complex and those in the adjacent supracrustal belts. This report summarizes the results of 1998 fieldwork, directed toward production of a 1:100 000 map, as well as ongoing geochemical and geochronological studies.

## REGIONAL GEOLOGICAL SETTING

The study area encompasses the central Wabigoon region, postulated to be basement to bordering Neoarchean greenstone belts (Fig. 1; Thurston and Davis, 1985). Dominated by granitoid rock types (Sage et al., 1974), the region houses a complex record of intrusive and structural events of regional extent (Percival, 1998). Tonalitic gneiss units of unknown antiquity are characterized by early ($D_1$, $D_2$) fabrics, whereas younger rocks carry a regional $S_3$ foliation, folded into upright, east-trending, $F_4$ folds. Amphibolite-facies metamorphism accompanied both $D_3$ and $D_4$ events.

To the west, a volcanic-dominated continental margin succession (<2.9 Ga Jutten Group; Davis and Moore, 1991) forms the eastern edge of the Sturgeon–Savant belt (Sanborn-Barrie et al., 1998), and is juxtaposed with a 2.775–2.718 Ga volcanic terrane consisting of tholeiitic and volcanogenic massive sulphide-bearing (ca. 2.735 Ga), calc-alkaline volcanic sequences. These are overlain by a sedimentary overlap sequence of conglomerate and wacke less than ca. 2.704 Ga (Post Lake sediments, Quest Lake sediments; Skulski et al., 1998). All units were affected by greenschist- to amphibolite-facies metamorphism and two phases of ductile deformation that produced steep, north-trending, $D_1$ folds and foliations, and east-trending, $D_2$ structures (Sanborn-Barrie and Skulski, 1999; equivalent to $D_3$ and $D_4$ regionally). In the Obonga belt to the east, calc-alkaline volcanic rocks are of similar age (ca. 2.73 Ga) to those of the Sturgeon belt (Tomlinson et al., 1996). Metamorphic grade is also similar, although $D_4$ strain is more pronounced in the Obonga belt.

## LITHOTECTONIC MAP UNITS

A first-order subdivision of the central Wabigoon region can be made into generally foliated, homogeneous granitoid rocks and relatively rare gneiss units (Fig. 2). Crosscutting relationships demonstrate that the gneiss units are generally older than the foliated granitoid rocks. However, several ages of foliated rocks may be present; some bodies older than 2.9 Ga (e.g. Caribou Lake pluton (Davis et al., 1988); southern Obonga tonalite (Tomlinson et al., 1996)) are foliated rather than gneissic and are indistinguishable in the field from younger tonalite units. Screens of amphibolite-grade supracrustal rocks enclosed by granitoid units may be correlative with strata in the adjacent greenstone sequences.

### *Tonalitic rocks*

Tonalitic gneiss occurs as lenses and sheets up to tens of kilometres long, and as smaller xenoliths within younger plutonic units. They are fine- to medium-grained, biotite-plagioclase-quartz rocks with up to 20% leucosome layers that form millimetre-scale layering parallel to a grain-scale foliation ($S_1$). Isoclinal $F_2$ folds are recognized to form complex interference patterns where they are overprinted by younger generations of structures.

Homogeneous tonalite borders the Obonga Lake greenstone belt on the south. In one locality Cortis et al. (1988) interpreted the medium- to coarse-grained, foliated biotite tonalite, dated at ca. 2.931 Ga (Fig. 2; Davis and Moore, 1991), as basement to a tholeiitic volcanic sequence based on the presence of mafic dykes and regolithic alteration. Elsewhere the contact is tectonic.

Foliated to gneissic, coarse-grained, biotite±hornblende tonalite occurs as 1–5 m scale homogeneous sheets within tonalite gneiss. One body east of Harmon Lake contains igneous zircons of 2.774±0.002 Ga and metamorphic grains of 2.697±0.002 Ga (D. Davis, unpub. report, 1989).

### *Supracrustal rocks (ca. 2.775–2.70 Ga)*

Screens of supracrustal rock occur in the western map area (Rogers, 1964), separated from the Sturgeon Lake greenstone belt by granitoid units (Fig. 2). Their structural position and character suggest that they may represent displaced units of the Sturgeon belt margin.

Steeply dipping, thick-bedded wacke, up to 3 km wide, occurs in the western Seseganaga Lake area (Fig. 2, locality A). These white-weathering rocks consist mainly of biotite, quartz, and plagioclase, with sporadic muscovite, garnet, and sillimanite (Fig. 3). They are bordered by medium-grained amphibolite, 20–40 m wide, to the west and locally to the east, and cut by tonalite and granodiorite. Detrital zircons from this unit yielded a range of ages from ca. 2.890–2.709 Ga (V. McNicoll, unpub. data, 1998).

Between Mountairy and Harmon lakes, kilometre-thick screens of amphibolite-facies supracrustal rock alternate with a variety of plutonic and gneissic units (Rogers, 1964). One of these occurs along the eastern tail of the Sturgeon Lake belt (Fig. 2, locality B), which includes conglomerate units that may be correlative with the Post Lake sediments (<2.700 Ga; Skulski et al., 1998). To the east, the mafic rocks are plagioclase-porphyritic andesite and amphibolite with epidote-quartz layers. This screen is separated by tonalite and granodiorite sills from the structurally overlying screen to the north (Fig. 2, locality C), which consists mainly of garnet amphibolite derived from volcanic and gabbroic protoliths, and minor greywacke. Like the main Sturgeon Lake belt (Sanborn-Barrie and Skulski, 1999), these supracrustal rocks have two generations of variably developed penetrative structures, a bedding-parallel foliation-layering ($S_3$) affected

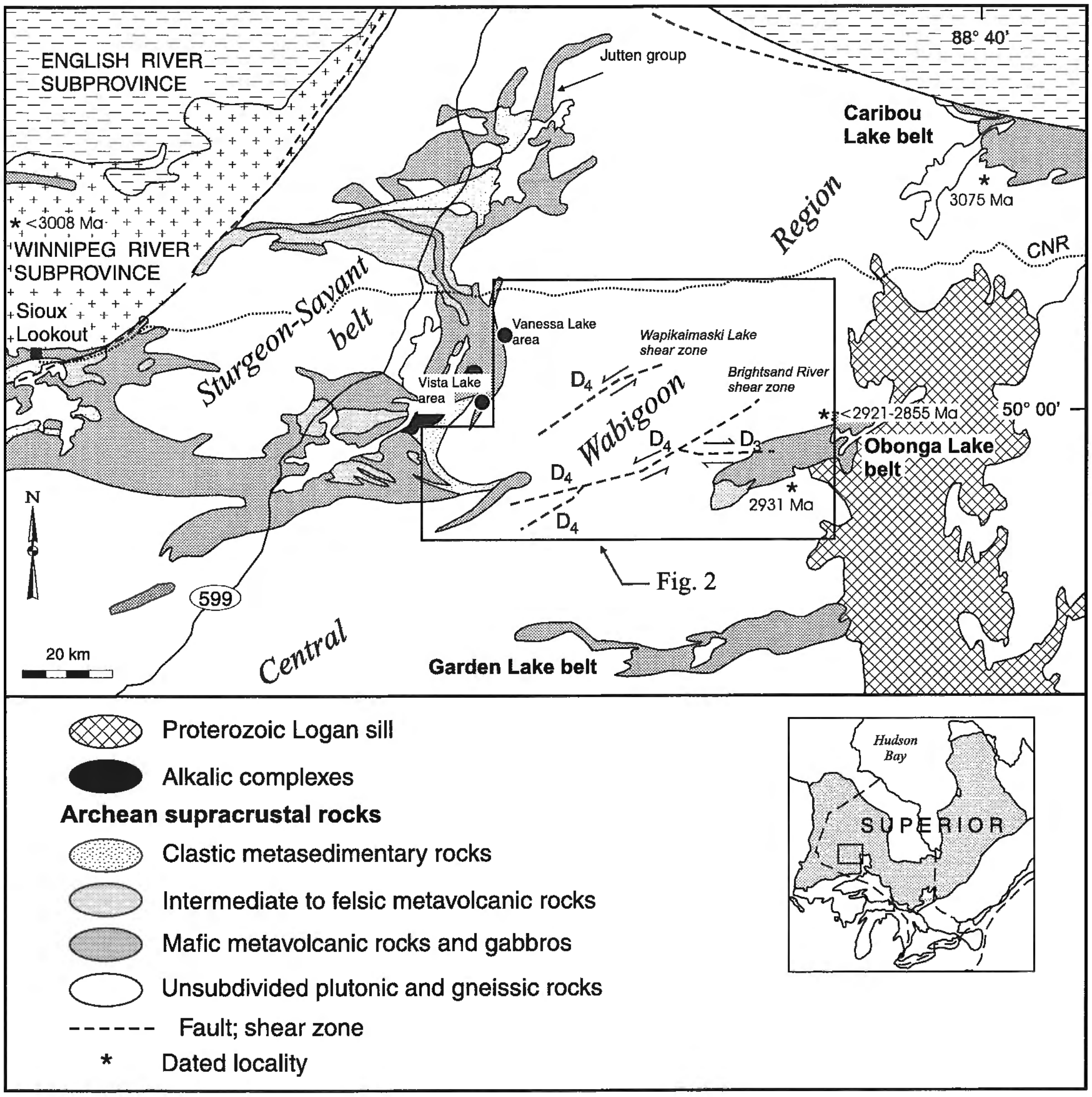


***Figure 1.** Location map showing the central Wabigoon region and flanking greenstone belts (after Sanborn-Barrie and Skulski, 1999).*

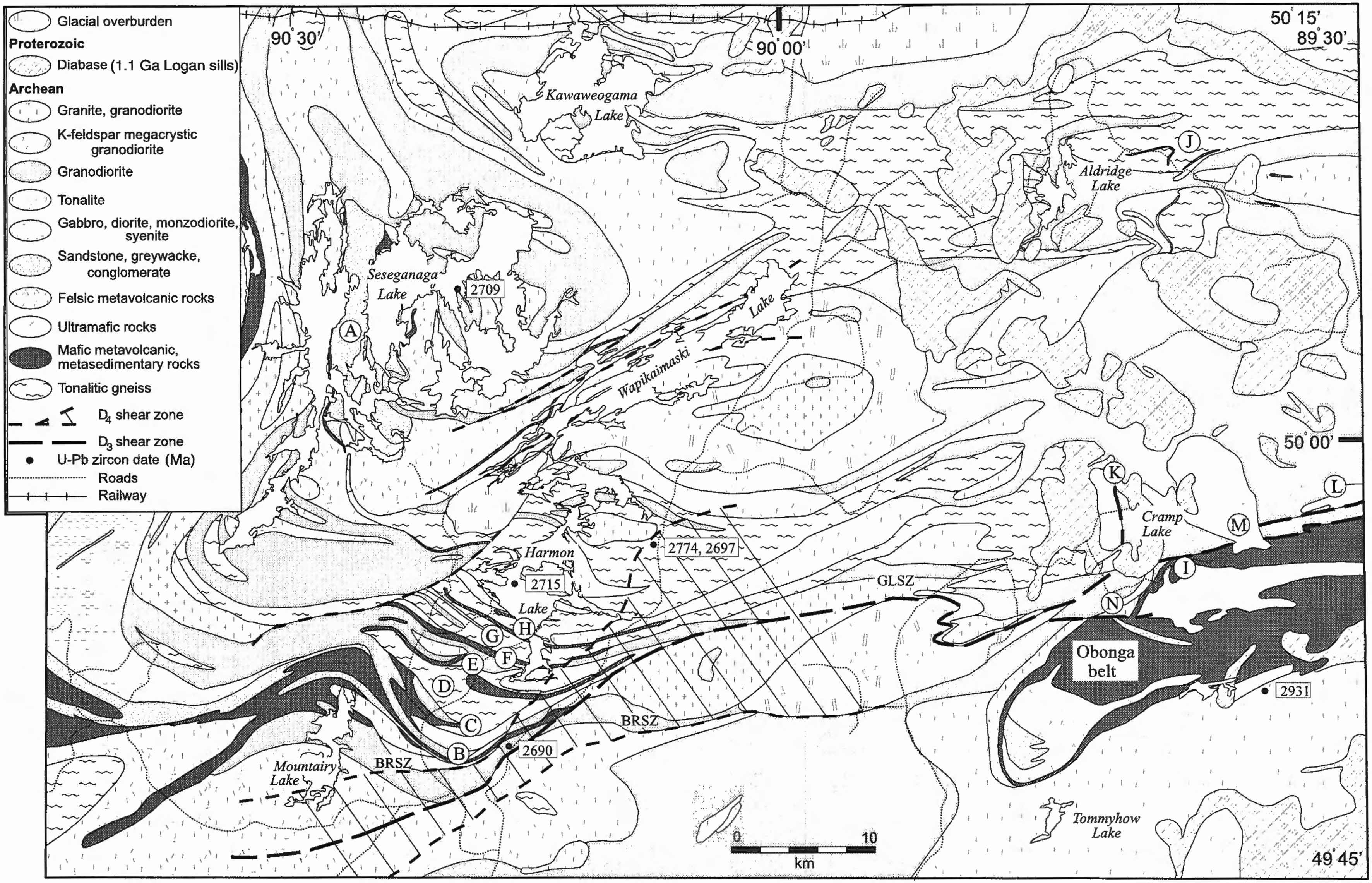


*__Figure 2.__ Sketch map showing the geology of the central Wabigoon region in the Sturgeon–Obonga corridor. BRSZ: Brightsand River shear zone; GLSZ: Gunter Lake shear zone.*

*Figure 3. Bedded wacke in sandstone, western Seseganaga Lake. Note minor leucosome development.*

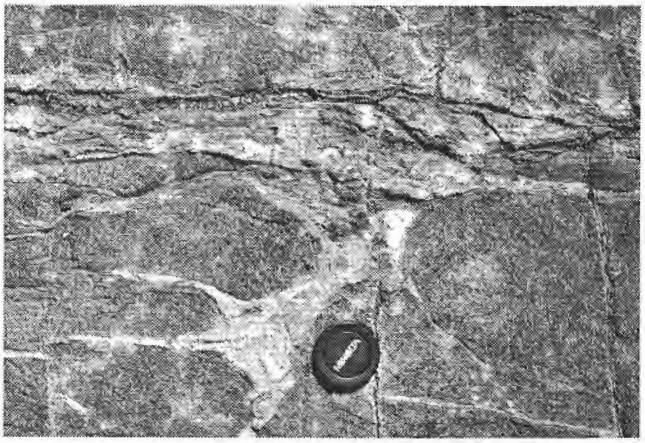

*Figure 4. Deformation-alteration relationships in gabbro, northern Obonga belt. Early shears are replaced by epidote-albite-tourmaline veins, suggesting seafloor deformation and alteration. Lens cap is 5 cm in diameter.*

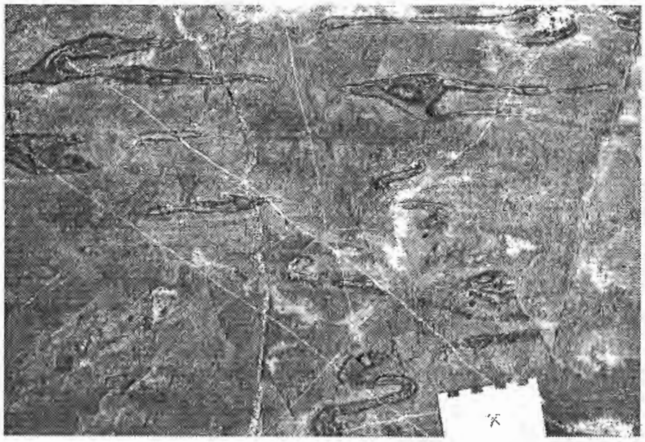

*Figure 5. Attenuated pillow selvages in epidote amphibolite east of Aldridge Lake. The stratigraphic affinity of these isolated metavolcanic screens is unknown.*

by younger folds ($F_4$) with axial planar foliation. A sedimentary unit at the northern margin of the screen includes quartz-rich sandstone and is in a structurally similar position to quartzose wacke units of the Vista–Vanessa lakes area (Fig. 1) that yielded detrital zircon ages greater than 2.9 Ga (Skulski et al., 1998) and have been correlated with the Jutten Group sedimentary sequence (Sanborn-Barrie and Skulski, 1999). Geochemical studies and geochronology will determine whether volcanic-sedimentary screen 'C' correlates with the Jutten Group. A few tens of metres north of the quartz-rich metasedimentary rocks is a unit of tonalitic gneiss (Fig. 2, locality D), with a complex, polyphase intrusive-structural character (*see* Fig. 3 of Percival, 1998). Although this gneiss could represent depositional basement to less complexly deformed supracrustal rocks, the contact is obscured by late pegmatite dykes and glacial cover. North of this, a screen of amphibolite of unknown stratigraphic affinity (Fig. 2, locality E) consists of alternating epidote-quartz- and hornblende-rich decimetre-scale layers and plagioclase-porphyritic andesite, cut by deformed biotite diorite dykes. This screen is separated by granodiorite and tonalite sills from a supracrustal unit including garnet amphibolite derived from volcanic and gabbroic precursors, greywacke, and pelite (Fig. 2, locality F). In one locality this screen is in ductile fault contact with tonalite gneiss to the north (Fig. 2, locality G) which exhibits complex structural chronology relative to the adjacent supracrustal units. The gneiss units are bounded to the north by a thin band of amphibolite with epidote-quartz layers (Fig. 2, locality H). Farther north, supracrustal remnants become progressively smaller and less continuous. The southeastern Sturgeon belt margin appears to be made up of a repeated sequence (Fig. 2, D-C-B; G-F-E) consisting of tonalite gneiss (possibly basement), garnet amphibolite-greywacke strata (possibly Jutten Group equivalents), tonalite-granodiorite sills, and epidote-amphibolite supracrustal rocks (possibly South Sturgeon equivalents).

Supracrustal rocks of the Obonga belt include variably preserved mafic, felsic, and sedimentary rock units. Near the northwestern belt margin (Fig. 2, locality I), a sequence of quartz-rich sandstone and iron formation occurs within a sequence of pillow basalt, gabbro, and peridotite-pyroxenite sills. Although the sedimentary rocks have locally well preserved primary structures, it is difficult to derive stratigraphic facing information owing to complex fold interference and generally high levels of strain.

Small-scale shear zones, which constitute the dominant tectonic fabric in gabbro units, are cut by epidote-albite± tourmaline alteration zones (Fig. 4). Nearby basalt units have similar alteration assemblages in pillow selvages and flow-top breccia matrices, suggesting hydrothermal seafloor alteration. The altered shear zones in gabbro suggests that the deformation occurred early, possibly on the seafloor.

Narrow screens of mafic metavolcanic rock, 30–50 m wide, occur in tonalitic gneiss units east of Aldridge Lake (Fig. 2, locality J). They have rarely preserved pillow selvages (Fig. 5) and amphibolite-facies assemblages that include garnet, clinopyroxene, or epidote.

### *Tonalite (postdates 2.774 Ga)*

Homogeneous, foliated, medium- to coarse-grained tonalite occurs as kilometre-scale sheets throughout the region. It has consistent mafic contents ranging from 15–20% biotite, with only local hornblende-bearing phases. The tonalite cuts supracrustal units, and carries the regional $S_3$ foliation, which varies in intensity from weak grain alignment to gneissic layering.

### *Granodiorite (2.709 Ga)*

Homogeneous, foliated, medium-grained granodiorite underlies large parts of the area. It can be divided into biotite (10–20% biotite), and hornblende-biotite types. The latter generally has higher mafic content and is transitional to more mafic compositions (quartz diorite, diorite, monzodiorite, gabbro). Although mainly homogeneous, granodiorite may be gneissic and migmatitic, locally with clinopyroxene-bearing leucosome. The hornblende-bearing rocks are commonly K-feldspar porphyritic to megacrystic and are significantly more magnetic than other granitoid units. Biotite granodiorite from central Seseganaga Lake yielded a zircon age of 2.709±0.004 Ga (V. McNicoll, unpub. data, 1998).

### *Granite*

Late, massive to weakly foliated granitic rocks are common. Dykes and sills at less than map scale are ubiquitous throughout the area; only the larger bodies are illustrated in Figure 2. This group of leucocratic (<5% biotite) rocks includes pegmatite and aplite which range in composition from true granite to trondhjemite. In some areas, such as west of Harmon Lake, massive pegmatite makes up close to half of the exposed bedrock, with only relict older units.

Granite is also abundant in $D_3$ and $D_4$ ductile shear zones (Fig. 2), where several generations occur in variable deformation states. Parts of the shear zones consist entirely of multiple generations of syntectonic granite.

## STRUCTURAL GEOLOGY

Several generations of ductile strain are recorded in the region. The earlier deformation phases ($D_1$, $D_2$) are preserved only sporadically in tonalite gneiss units, having been largely overprinted by later strain (mainly $D_3$), whereas $D_3$ and $D_4$ are recorded in all units. In general, $D_1$ and $D_3$ resulted in penetrative fabrics, whereas $D_2$ and $D_4$ produced megascopic to map-scale folds.

$D_1$ structures include grain-scale biotite alignment and concordant migmatitic leucosome ($S_1$) in tonalitic gneiss. The millimetre-scale leucosome layers constitute 10–20% of these rocks, which are characteristically folded by later deformation events; $S_1$ may have been largely transposed during $D_3$.

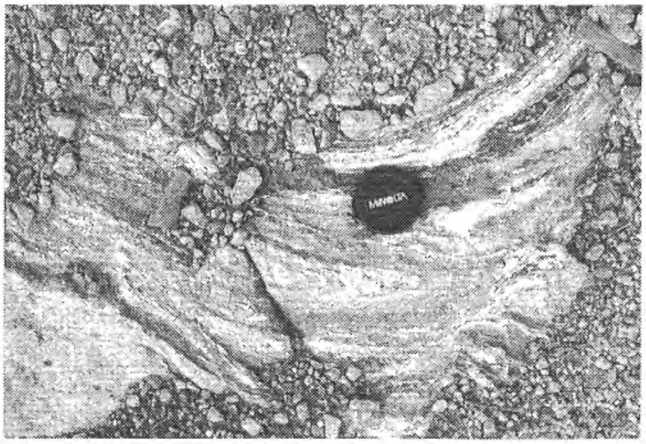

***Figure 6.*** *Isoclinal $F_3$ fold of $S_1$ layering in tonalitic gneiss east of Aldridge Lake. Curvature of the $F_3$ hinge line is the result of refolding by an upright $F_4$ synform.*

$F_2$ folds are identified within type 1 and type 3 small-scale interference structures at a few localities, where they affect $S_1$ layering and are refolded by $F_3$ folds. However, most outcrops have only one generation of folds which are indistinguishable as $F_2$ or $F_3$. On an island in Harmon Lake, a well defined $F_2$ fold is transected by a weakly foliated tonalite dyke (Percival, 1998; Fig. 6) that gave a preliminary U-Pb zircon age of ca. 2.715 Ga (V. McNicoll, unpub. data, 1998).

The $D_3$ event affected most of the rock types in the area, imposing a penetrative foliation on previously undeformed units, folding heterogeneous rocks, and producing discrete ductile shear zones. The $S_3$ foliation is a synmetamorphic, grain-scale, biotite alignment, accompanied in some areas by development of migmatitic layering. It is axial planar to tight to isoclinal, upright to reclined $F_3$ folds, which are generally well preserved in $F_4$ fold hinges (Fig. 6). $L_3$ lineations appear regionally preserved in the northwestern Seseganaga Lake area (Fig. 2, 7). Based on the low dips of $S_3$ foliation in this area, and shallow plunges of $F_4$ folds regionally, Percival (1998) inferred that $D_3$ structures formed in subhorizontal attitudes.

Correlation between structural fabrics in supracrustal and plutonic rocks is evident along the steeply dipping eastern margin of the Sturgeon–Savant belt. In supracrustal rocks, a penetrative, grain-scale $S_1$ foliation (Sanborn-Barrie and Skulski, 1999) is concordant to the regional penetrative $S_3$ foliation in granitoid rocks to the east.

The kilometre-wide, east-trending, $D_3$ Gunter Lake shear zone (Fig. 2) separates gneissic units to the northwest from homogeneous granodiorite to the southeast. From the north, $S_1$ layering and $F_2$ folds become progressively transposed into a steep $S_3$ shear fabric, itself refolded into steeply plunging, $F_{3b}$ 'Z' folds. The central portion of the 800 m wide shear zone is occupied by several generations of variably foliated syntectonic granite carrying enclaves of more intensely foliated and folded units, including gabbro, diorite, and garnet-clinopyroxene-bearing mafic gneiss. Some of the later, more homogeneous units are cut by mylonitic seams with dextral shear bands. In homogeneous rocks to the south, shear strain is evident as dextral C-S fabrics, shear bands, and discrete, narrow, ultramylonitic seams (Fig. 8). The eastern end of the shear zone, as well as older fabrics, swing to the north in the Cramp Lake area (Fig. 2, locality K). There, the shear zone represents a break in metamorphic grade, from pyroxene-bearing migmatite on the west, to homogeneous granitoid rocks and muscovite-andalusite-grade rocks of the Obonga belt to the east. The bend may reflect transfer of motion from dextral strike-slip to west-over-east reverse sense.

The most common $D_4$ structures are megascopic to map-scale, tight, upright, gently east-plunging folds. At the outcrop scale, fold asymmetry can be related to map-scale structures (Percival, 1998). Fold hinges are marked by prominent subhorizontal rodding lineations, $L_4$, whereas in steep limbs, older fabric elements are transposed without development of a new ($S_4$) foliation or lineation. A compilation of mainly $D_4$ linear structures through the eastern part of the area (Fig. 7) shows a narrow azimuthal range (070–110°; average 090°), with plunges averaging 15°E.

Two east-northeast-trending shear zones have characteristics linking them to $D_4$ structures. The 2–10 km wide Brightsand River shear zone extends from the southwestern corner of the map area toward the Obonga belt. It represents the southeastern limit of supracrustal screens and the boundary between a northern domain made up of kilometre-scale sheets of gneiss and homogeneous plutonic rocks, and a southern domain consisting of large homogeneous plutons (Fig. 2). The shear zone consists of a northwestern part, 1–4 km wide, characterized by flattening strain, and a southeastern zone, 1–6 km wide, characterized by L>S fabrics, developed mainly in homogeneous granitoid rocks. Strain intensity appears to decrease and become sporadic to the northeast as the shear zone broadens to its maximum width. Lineations in both parts of the zone have consistent 075° trends and 0–10° plunges. Narrow seams of ultramylonite occur near the northern boundary of the northern zone. Shear-sense indicators yield variable or no displacement senses in the north, despite locally intensely sheared appearance, possibly because the dextral Gunter Lake zone has been reworked in the Brightsand zone (Fig. 2). In the southern zone, abundant shear bands in subhorizontally lineated rocks yield a consistent sinistral sense (Fig. 9). Map-scale sinistral deflection of supracrustal screens into the Brightsand zone (Fig. 2) are consistent with macroscopic shear-sense criteria.

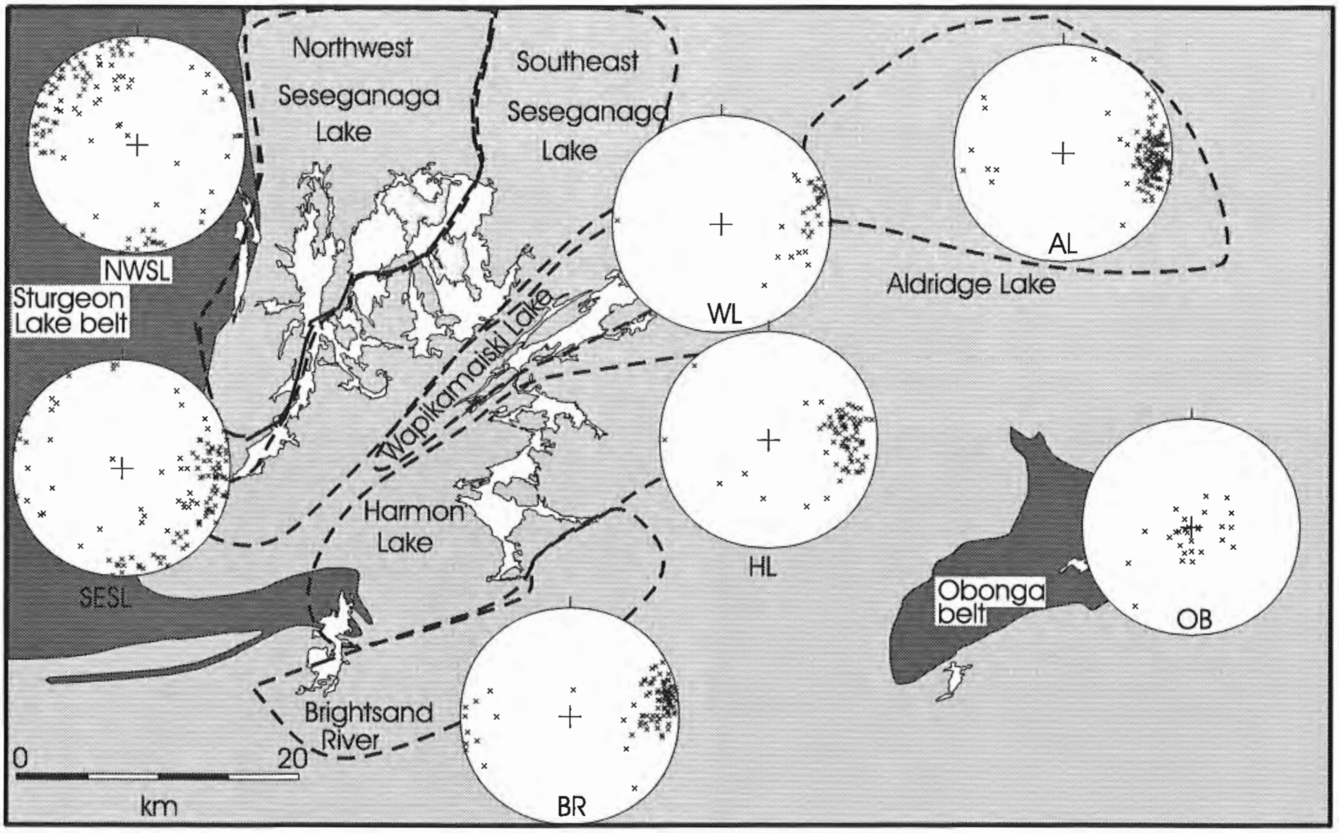


*Figure 7. Equal area, lower hemisphere stereographic projections showing the orientation of mainly $L_4$ linear structures through the region. Regional $L_4$ structures have similar, although more dispersed orientations to stretching lineations in the Brightsand and Wapikamaiski shear zones. Lineations in the northwestern Seseganaga Lake area are probably $L_3$.*

Multiple generations of variably deformed syntectonic granite occupy large parts of both northern and southern zones. The youngest syntectonic granite dykes carry only a weak lineation suggesting that the linear fabric elements developed late in the evolution of the zone. Existing geochronology supports this inference; a strongly foliated tonalite from the northern strand yielded metamorphic zircons of 2.697±0.002 Ga (D. Davis, unpub. report, 1989), whereas a lineated tonalite from the south has an igneous age of 2.690±0.002 Ga (D. Davis, pers. comm., 1997). Further geochronology is underway to constrain the age of movement. The Wapikaimaski Lake shear zone to the north (Fig. 2) has similar characteristics to the Brightsand zone, including subhorizontal, east-northeast-trending stretching lineations and sinistral shear-sense indicators. In addition, it contains mylonite zones, 5–20 m wide, with strike lengths of at least several kilometres.

Several shear zones of unknown age or affinity have been observed in different parts of the area. In the northern Obonga belt, a mylonite zone up to 200 m wide separates the Puddy Lake serpentinite to the north (Fig. 2, locality L; Fig. 10) from felsic units to the south. This shear zone, which cuts tonalite and sandstone, has a moderately west-plunging stretching lineation and well developed dextral shear bands. Anastamosing shear zones in this area dissect tonalite into lozenges forming a false conglomeratic appearance (Fig. 10). The shear zone is truncated to the west by the Awkward Lake gabbro pluton (Fig. 2, locality M). A fault bounding the sedimentary unit against mafic rocks to the south is a narrow zone of brittle gouge.

The northwestern margin of the Obonga belt is defined by a complex brittle-ductile fault zone (Fig. 2, locality N). Conglomerate at the belt margin has ductile fabrics, including a steep down-dip stretching lineation defined by clast elongation, overprinted by dextral shear bands and late quartz-filled

***Figure 8.*** *K-feldspar megacrystic granodiorite in the dextral Gunter Lake shear zone. Kinematic indicators include shear bands and ultramylonite seams. Hammer handle is 30 cm long.*

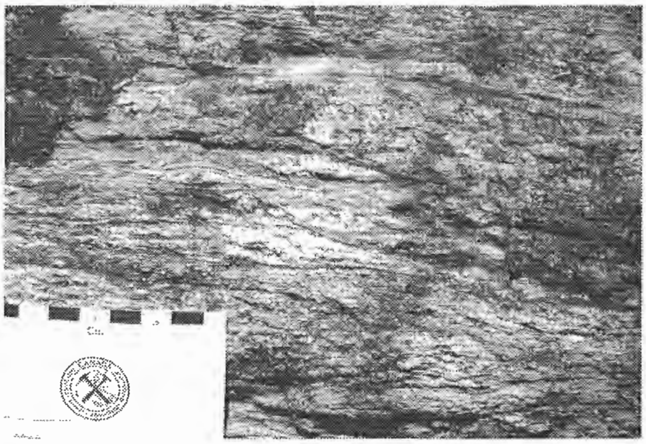

***Figure 10.*** *Sheared tonalite south of Puddy Lake in the Obonga belt. Anastamosing dextral shears produce a false conglomeratic appearance.*

***Figure 9.*** *Tonalitic gneiss in the sinistral Brightsand River shear zone. Note small syntectonic pegmatite pods.*

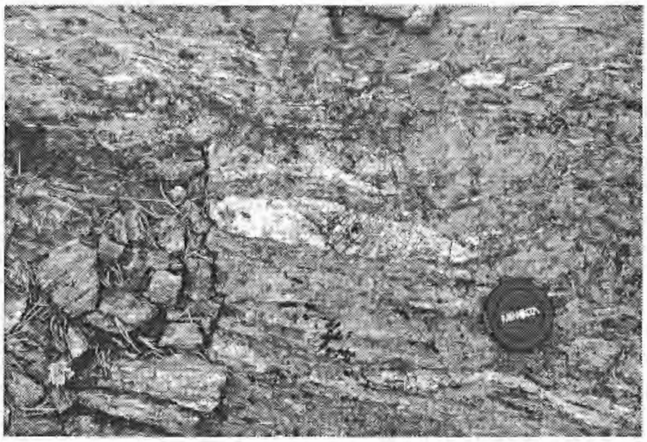

***Figure 11.*** *Stretched-pebble conglomerate, northwestern Obonga belt. Clasts are stretched subvertically and cut by quartz-filled tension gashes related to late brittle movement.*

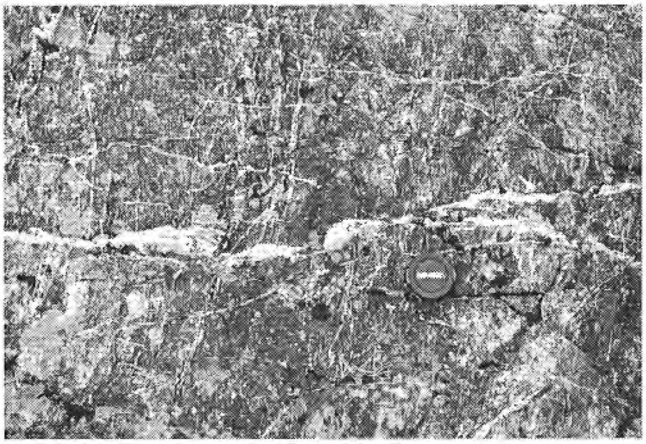

*Figure 12. Quartz vein-riddled cataclasite developed in granite, northwestern Obonga belt.*

tension gashes (Fig. 11). These rocks are separated by a 2 m wide zone of cataclasite from cataclastic granite to the north, itself riddled with quartz veins within 20 m of the contact (Fig. 12). The juxtaposition of brittle and ductile fault structures suggests north-side-down normal displacement and unroofing to produce a brittle overprint on ductile structures.

Other late cataclastic zones are apparent in a few localities. East of Aldridge Lake, linear, east-southeast-trending valleys are occupied by chloritic cataclastic zones up to 100 m wide and locally include fault breccias with chloritic matrix. A strong subhorizontal lineation suggests transcurrent motion.

## GEOCHEMISTRY

Analyses of 1997 samples indicate mainly granodiorite, tonalite, and trondhjemite lithologies (Fig. 13). On a $K_2O$-$SiO_2$ diagram (Fig. 14A), granite samples split into high-, medium-, and low-K groups; only a few are true granite samples (Fig. 13). Based on an AFM plot (not shown) the granitoid samples are calc-alkaline and metaluminous to slightly peraluminous.

A La-$SiO_2$ plot highlights large variations in LREE contents within the plutonic rocks (Fig. 14B). Granodiorite samples fall into low-, medium-, and high-La groups, along with tonalite and tonalite gneiss (Fig.14B). Examination of various X-Y and extended element-normalized diagrams indicates internal consistency within units, which are averaged in Figure 15.

The extended-element-normalized pattern for a single gabbro sample (Fig. 15A) exhibits a moderate negative Nb anomaly and positive Ti anomaly (possibly cumulate Fe-Ti oxides). Overall, its pattern resembles that of the low-La granodiorite samples and it plots on the low-La granodiorite trend (Fig. 14B). Six tonalite gneiss samples cluster tightly in their major elements and in most trace elements, suggesting that leucosome developed in situ rather than by noncogenetic injections. Medium- and high-La tonalite gneiss subgroups exhibit similar patterns to the granodiorite subgroups with which they plot on the La-$SiO_2$ diagram. The low-La tonalite subgroup has the lowest HREE content and a marked positive Sr anomaly. All three tonalite subgroups exhibit pronounced negative Nb anomalies and lack Eu anomalies.

Mafic monzodiorites plot on the low-silica extension of the medium-La granodiorite trend (Fig. 14B). Their normalized pattern is more enriched but subparallel to those of the medium-La granodiorite and tonalite samples, with similar pronounced negative Nb and Ti anomalies. Overall, the K-feldspar megacrystic granodiorite pattern resembles that of the monzodiorite, except that it is more LREE-enriched and HREE-depleted (higher La/Yb), similar to the high-La granodiorite subgroup. In Figure 14B, these samples plot above the high-La granodiorite trend. Based on field observations, a cogenetic relationship was inferred between K-feldspar megacrystic granodiorite, the high-La granodiorite subgroup, and the monzodiorite samples; the preliminary geochemistry is compatible with this interpretation.

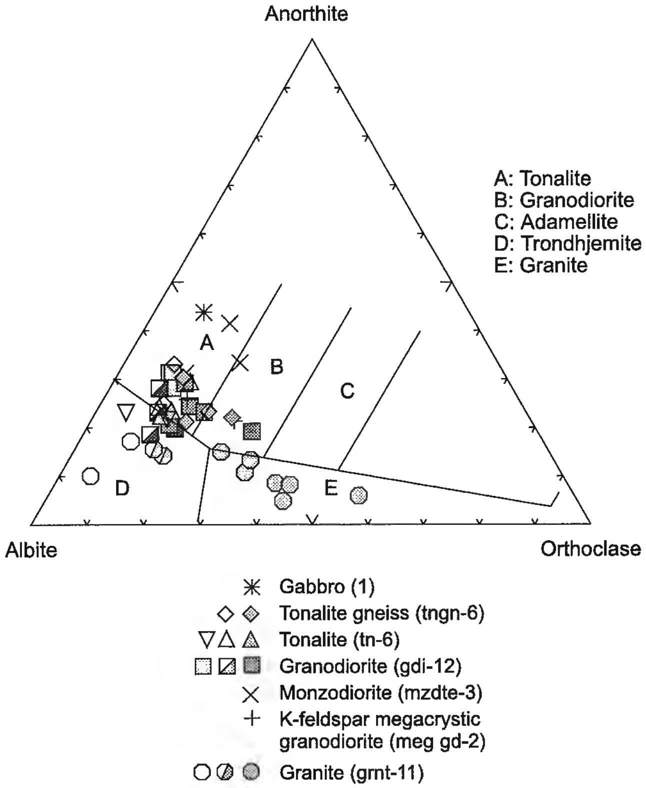


*Figure 13. Granitoid compositions plotted in the CIPW normative albite-anorthite-orthoclase diagram (after Barker, 1979). In the symbol legend, multiple symbols for field-based rock units refer to subgroups defined by $K_2O$ and La contents (see Fig. 14 and text); abbreviations and number of samples plotted for each unit are given in parentheses. tngn=tonalitic gneiss; tn=tonalite; gdi=granodiorite; mzdte=monzodiorite; meg gd=megacrystic granodiorite; grnt=granite.*

The medium- and high-La granodiorite subgroups exhibit overlapping to subparallel normalized REE and extended-element patterns, whereas the low-La subgroup is less HREE depleted such that its pattern crosses over other granodiorite patterns. This feature may reflect different petrogenesis for the low-La subgroup.

Extended-element-normalized patterns for two trondhjemites included one with positive Eu and Sr anomalies and no Nb anomaly (possibly a plagioclase cumulate) and one with HREE>LREE, with major negative Eu and Sr anomalies (possibly a product of extreme plagioclase removal). Patterns of medium- and high-K granite samples overlap; both groups include samples with and without negative Eu anomalies, all are moderately to strongly HREE depleted and exhibit negative Nb anomalies. The low- and medium-K granite samples fall on the low- and medium-La granodiorite trends, respectively, whereas high-K granite samples plot mainly above the high-La trend.

The calc-alkaline character of the plutonic units, their pronounced negative Nb anomalies (Fig. 15), and the fact that they plot exclusively within the volcanic-arc granite field in tectonomagmatic classification diagrams (Pearce et al., 1984; not shown) suggest they were formed in a destructive margin setting or from a crustal source that was itself derived from arc crust.

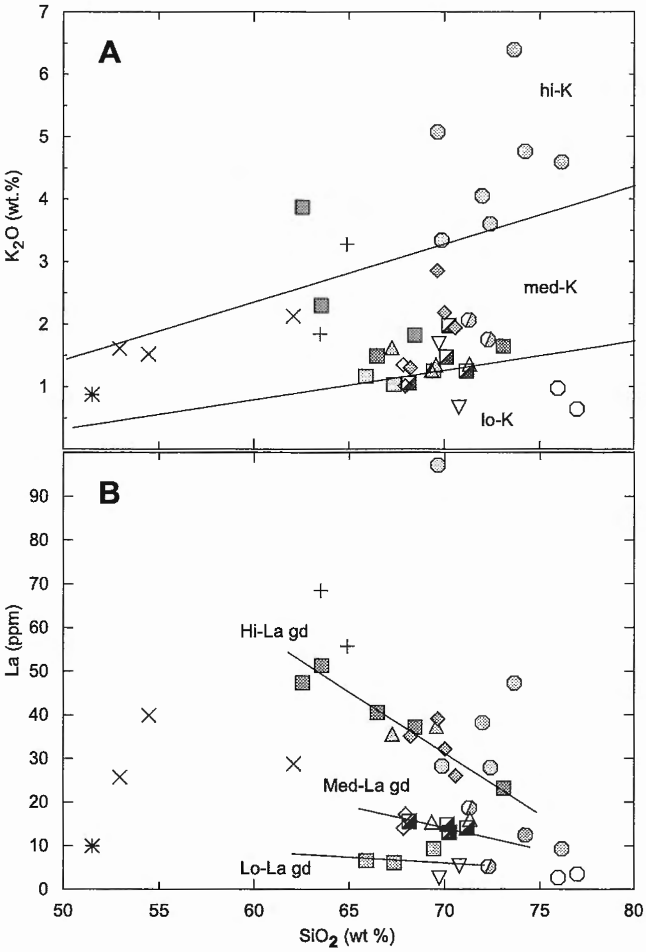


***Figure 14.*** *Plot of $SiO_2$ versus A) $K_2O$, and B) La (an immobile, incompatible element) for the various plutonic units (symbols as in Fig. 13, 15). Subdivisions of igneous suites based on $K_2O$ content in A) into Hi-, Med-, and Lo-K (high-, medium-, and low-K) suites are from LeMaitre (1989) and in* ***B****) granodiorites (gd) are subdivided based on $SiO_2$-La trends into Hi-, Med-, and Lo-La (high-, medium-, and low-La) subgroups.*

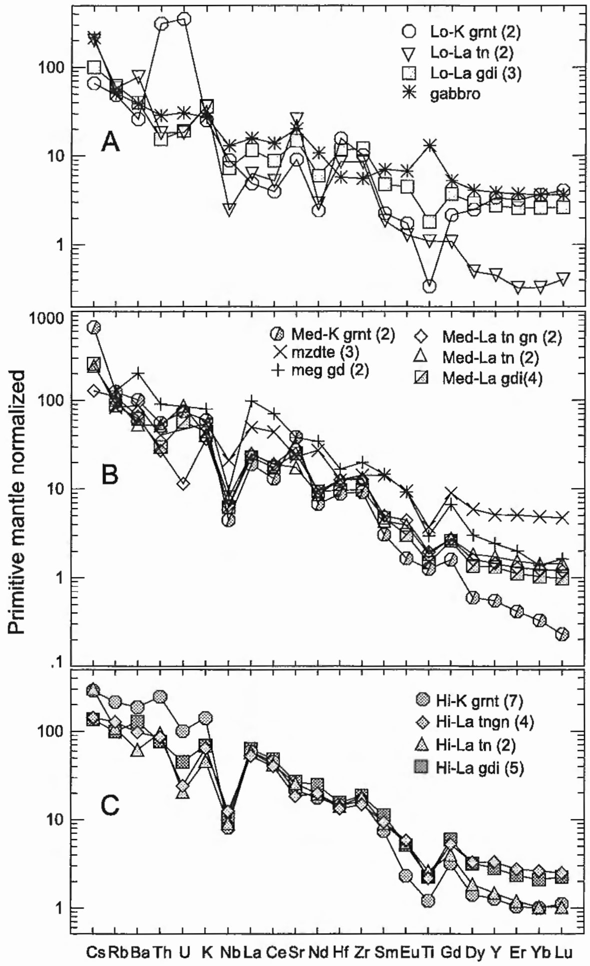


***Figure 15.*** *Primitive-mantle-normalized extended-element plots for averages of various plutonic units, as well as La- and $K_2O$-based subdivisions. Numbers in parentheses indicate the number of samples averaged. Normalizing values are from Taylor and McLennan (1985). tngn=tonalitic gneiss; tn=tonalite; gdi=granodiorite; mzdte=monzodiorite; meg gd=megacrystic granodiorite; grnt=granite; Hi=high; Med=medium, Lo=low.*

## DISCUSSION

Contact relationships between screens of supracrustal rock and various granitoid units require further examination. In the Mountairy Lake–Harmon Lake area, structural panels include tonalitic gneiss, highly attenuated volcanic and sedimentary units (possible equivalents of the Jutten Group and South Sturgeon Lake sequences), together with intrusive sills. Repetition of the sequence may be due to thrust or transcurrent faults, or folds. The geochemistry and nature of relationships among units within these panels, as well as between adjacent panels, is being investigated in an M.Sc. project by J. Brown (University of Ottawa).

The intersection between the dextral, $D_3$ Gunter Lake shear zone and sinistral, $D_4$ Brightsand River shear zone is complicated by the presence of abundant syntectonic granite and late pegmatite (Fig. 2). Although these shears mark the boundary between a northern domain with sheet-like intrusive geometry and gneissic units, and a southern domain characterized by large homogeneous plutonic bodies, common lithological units occur in the two domains, and the $D_3$-$D_4$ structural styles are consistent to the north and south. The shear zones may have utilized a pre-existing lithological domain boundary.

The northwestern Seseganaga Lake area appears to represent a $D_4$ strain shadow in which original orientations of $D_3$ structures are preserved. Over a 10 km wide transition zone from Vanessa Lake (Fig. 1) to central Seseganaga Lake, $S_3$ foliation changes from steep (70°W) attitudes to subhorizontal. This $D_3$ feature could be analogous to the subgreenstone belt transition from steep to flat structures observed on many seismic reflection profiles (e.g. Ludden et al., 1993; D. White, pers. comm., 1998). Outside of the $D_4$ strain shadow, east-trending, steeply plunging, $F_2$ folds in the Savant and northern Sturgeon belts have geometrical equivalents in the $F_4$ folds of the central Wabigoon region. In greenstones, hinges are steep, whereas in granitoid rocks they are gentle, suggesting that the steep-to-flat foliation transition separates large structural domains.

## ACKNOWLEDGMENTS

Field assistance by Y. Beaudoin and J.P. Rioux is gratefully acknowledged. Visits and discussions with K. Benn, K. Tomlinson, and the Western Superior NATMAP team are appreciated. D. Davis shared unpublished geochronological information. West Caribou Air Services (Savant Lake) provided safe and efficient fixed-wing support. C. Hemmingway helped with figure preparation. Simon Hanmer, Sally Pehrsson, and Mary Sanborn-Barrie provided thoughtful and thorough critical reviews.

## REFERENCES

**Barker, F.**
1979: Trondhjemite: definition, environment and hypotheses of origin; *in* Trondhjemites, Dacites, and Related Rocks, (ed.) F. Barker; Elsevier, New York, p. 1–12.

**Blackburn, C.E., John, G.W., Ayer, J., and Davis, D.W.**
1991: Wabigoon Subprovince; *in* Geology of Ontario; Ontario Geological Survey, Special Volume 4, pt. 1, p. 303–381.

**Card, K.D. and Poulsen, K.H.**
1998: Geology and mineral deposits of the Superior Province of the Canadian Shield; Chapter 2 *in* Geology of the Precambrian superior and Grenville Provinces and Precambrian Fossils in North America, (co-ord.) S.B. Lucas and M.R. St-Onge (*also* Geological Society of America, The Geology of North America, v. C-1).

**Cortis, A.L., Stott, G.M., Osmani, I.A., Atkinson, B., and Thurston, P.C.**
1988: A geological re-evaluation of northwestern greenstone belts; *in* Summary of Field Work and Other Activities 1988; Ontario Geological Survey, Miscellaneous Paper 141, p. 25–52.

**Davis, D.W. and Moore, M.**
1991: Geochronology in the western Superior province, summary report. Unpublished Ontario Geological Survey Report, 22 p.

**Davis, D.W., Sutcliffe, R.H., and Trowell, N.F.**
1988: Geochronological constraints on the tectonic evolution of a late Archean greenstone belt, Wabigoon subprovince, northwest Ontario; Precambrian Research, v. 39, p. 171–191.

**Henry, P., Stevenson, R., and Gariepy, C.**
1998: Late Archean mantle composition and crustal growth in the western Superior Province of Canada: neodymium and lead isotopic evidence from the Wawa, Quetico, and Wabigoon subprovinces; Geochimica et Cosmochimica Acta, v. 62, p. 143–157.

**Le Maitre, R.W.**
1989: A Classification of Igneous Rocks and Glossary of Terms; Blackwell, Oxford, 193 p.

**Ludden, J.N., Hubert, C., Barnes, A.E., Milkereit, B., and Sawyer, E.W.**
1993: A three dimensional perspective on the evolution of Archean crust: LITHOPROBE seismic reflection images in the southwestern Superior Province; Lithos, v. 30, p. 357–372.

**Pearce, J.A., Harris, N.B.W., and Tindle, A.G.**
1984: Trace element discrimination diagrams for the tectonic interpretation of granitic rocks; Journal of Petrology, v. 25, p. 956–983.

**Percival, J.A.**
1998: Structural transect of the central Wabigoon subprovince between the Sturgeon Lake and Obonga Lake greenstone belts; *in* Current Research 1998-C; Geological Survey of Canada, p. 127–136.

**Rogers, D.P.**
1964: Metionga Lake area; Ontario Department of Mines, Geological Report 24, 53 p.

**Sage, R.P., Breaks, F.W., Stott, G.M., McWilliams, G.M., and Robertson, D.**
1974: Operation Ignace-Armstrong; Obonga Lake-Lac des Iles sheet, District of Thunder Bay; Ontario Division of Mines, Preliminary Map P.963, scale 1 inch to 2 miles.

**Sanborn-Barrie, M. and Skulski, T.**
1999: Tectonic assembly of continental margin and oceanic terranes at 2.7 Ga in the Savant Lake–Sturgeon Lake greenstone belt, Ontario; *in* Current Research 1999-C; Geological Survey of Canada.

**Sanborn-Barrie, M., Skulski, T., and Whalen, J.B.**
1998: Tectonostratigraphy of central Sturgeon Lake, Ontario: deposition and deformation of submarine tholeiites and emergent calc-alkaline volcano-sedimentary sequences; *in* Current Research 1998-C; Geological Survey of Canada, p. 115–126.

**Skulski, T., Sanborn-Barrie, M., and Stern, R.A.**
1998: Did the Sturgeon Lake supracrustal belt form near a continental margin? *in* Western Superior LITHOPROBE Transect Fourth Annual Workshop, March 23-24, 1998, (ed.) R.M. Harrap, and H.H. Helmstaedt; LITHOPROBE Report #65, LITHOPROBE Secretariat, University of British Columbia, p. 87–89.

**Stott, G.M., Davis, D.W., and Parker, J.R.**
1998: Observations on the Tectonic Framework of the Eastern Wabigoon Subprovince; *in* Western Superior LITHOPROBE Transect Fourth Annual Workshop, March 23-24, 1998, (ed.) R.M. Harrap, and H.H. Helmstaedt; LITHOPROBE Report #65, LITHOPROBE Secretariat, University of British Columbia, p. 74–76.

**Taylor, S.R. and McLennan, S.M.**
1985: The Continental Crust: its Composition and Evolution; Blackwell, Oxford, United Kingdom, 312 p.

**Thurston, P.C. and Davis, D.W.**
1985: The Wabigoon diapiric axis as a basement complex; *in* Summary of Field Work and Other Activities 1985; Ontario Geological Survey, Miscellaneous Paper 126, p. 138–141.

**Tomlinson, K.Y., Thurston, P.C., Hughes, D.J., and Keays, R.R.**
1996: The central Wabigoon region: petrogenesis of mafic-ultramafic rocks in the Steep Rock, Lumby Lake and Obonga Lake greenstone belts (continental rifting and drifting in the Archean); *in* Western Superior Transect Second Annual Workshop, (ed.) R.M. Harrap and H. Helmstaedt; LITHOPROBE Report 53, p. 65–73.

**Williams, H.R., Stott, G.M., Thurston, P.C., Sutcliffe, R.H., Bennett, G., Easton, R.M., and Armstrong, D.K.**
1992: Tectonic evolution of Ontario: Summary and synthesis, in Geology of Ontario, (ed.) P.C. Thurston, H.R. Williams, R.H. Sutcliffe, and G.M. Stott; Ontario Geological Survey, Special Volume 4, pt. 2, p. 1255–1332.

---

Geological Survey of Canada Project 970014

# Tectonic assembly of continental margin and oceanic terranes at 2.7 Ga in the Savant Lake–Sturgeon Lake greenstone belt, Ontario[1]

M. Sanborn-Barrie and T. Skulski
Continental Geoscience Division, Ottawa

*Sanborn-Barrie, M. and Skulski, T., 1999: Tectonic assembly of continental margin and oceanic terranes at 2.7 Ga in the Savant Lake–Sturgeon Lake greenstone belt, Ontario;* in *Current Research 1999-C; Geological Survey of Canada, p. 209–220.*

**Abstract:** The Savant Lake–Sturgeon Lake greenstone belt formed between continental crust, represented by granitoid rocks to the east within which vestiges of ca. 3.0 Ga basement and Mesoarchean cover sequences occur, and oceanic crust, represented by Neoarchean greenstone belts of the western Wabigoon Subprovince to the west. The belt can be subdivided into three major components, 1) a <2.9 Ga volcanic rift margin dominated by tholeiitic basalt with basal quartz-rich clastic rocks; 2) diverse oceanic crust comprising a conformable sequence of 2.775 Ga basaltic basement, 2.745–2.704 Ga island arc crust, and 2.718 Ga arc rift deposits; and 3) a <2.704 Ga turbiditic succession (foredeep) that rests unconformably on the rift margin but conformably on oceanic rocks. Penetrative, ductile deformation after ca. 2.703 Ga, but before ca. 2.68 Ga, is interpreted to record collision between the volcanic rift margin and the diverse oceanic terrane following 2.71 Ga continental arc magmatism.

**Résumé :** La ceinture de roches vertes du lac Savant–lac Sturgeon s'est formée entre la croûte continentale, représentée à l'est par des roches granitoïdes dans lesquelles se rencontrent des vestiges de socle d'environ 3,0 Ga et des successions de couverture mésoarchéennes, et la croûte océanique, représentée à l'ouest par des ceintures de roches vertes néoarchéenes de la partie occidentale de la Sous-province de Wabigoon. La ceinture se subdivise en trois composantes majeure : 1) une marge de rift volcanique de <2,9 Ga où dominent des basaltes tholéiitiques accompagnés de roches clastiques quartzeuses de base; 2) une croûte océanique variée comprenant une succession concordante de socle basaltique de 2,775 Ga, une croûte d'arc insulaire de 2,745 à 2,704 Ga et des dépôts de rift d'arc de 2,718 Ga; et 3) une succession turbiditique (avant-fosse) de <2,704 Ga qui repose en discordance sur la marge de rift et en concordance sur des roches océaniques. Une déformation ductile pénétrative, postérieure à environ 2,703 Ga mais antérieure à environ 2,68 Ga, témoignerait d'une collision entre la marge de rift volcanique et le terrane océanique varié survenue après le magmatisme d'arc continental de 2,71 Ga.

[1] Contribution to the Western Superior NATMAP Project

## INTRODUCTION

The Savant Lake–Sturgeon Lake granite-greenstone belt occupies a unique position in the Wabigoon Subprovince of the western Superior Province. It occurs along an arcuate, 120 km long, north-striking interface between a granite-gneiss complex to the east (Percival et al., 1999), which contains vestiges of ca. 3.0 Ga crust, and younger than 2.77 Ga oceanic crust to the west, represented by greenstone belts of the western Wabigoon Subprovince (Fig. 1). Along its eastern margin, quartz-rich clastic rocks with detrital zircons older than 2.9 Ga, conformably underlie the volcanic pile and provide an early link with Mesoarchean continental basement to the east. The south-central parts of the belt represent long-lived volcanic activity in an oceanic setting (*see* below) from 2.775–2.704 Ga.

As part of the Western Superior NATMAP program, this study is aimed at understanding the nature of this ancient continental-oceanic interface, and its influence on patterns of volcanism, sedimentation, and deformation. Ongoing tectonic studies compliment Western Superior LITHOPROBE activities, and provide a richer awareness of an area that, until recently, was an important source of Cu-Pb-Zn minerals.

Field- and laboratory-based results (*see also* Sanborn-Barrie et al. 1998; Sanborn-Barrie and Skulski, 1998) show that the northern and eastern parts of the Savant Lake–Sturgeon Lake greenstone belt likely have continental margin affinities, whereas its south-central part has stratigraphic and chemical characteristics of a diverse oceanic terrane (Skulski et al., 1998). The early history of these continental and oceanic domains is reconstructed here, as is the history of later sedimentation and deformation accompanying their amalgamation.

## CONTINENTAL MARGIN SEQUENCE

The northern and eastern parts of the Savant Lake–Sturgeon Lake greenstone belt are dominated by tholeiitic basalt that overlies a thin but contiguous sequence of quartz-rich clastic rocks of Mesoarchean provenance (Jutten group; Fig. 1, 2). Proximity of these to granitoid complexes, within which Mesoarchean rocks occur (Fig. 1), reveals the close spatial relationship between ancient continental crust and early greenstone belt sequences in this area. Lithological, structural, and geochemical evidence presented below collectively support an interpretation of the Jutten group as a continental margin sequence.

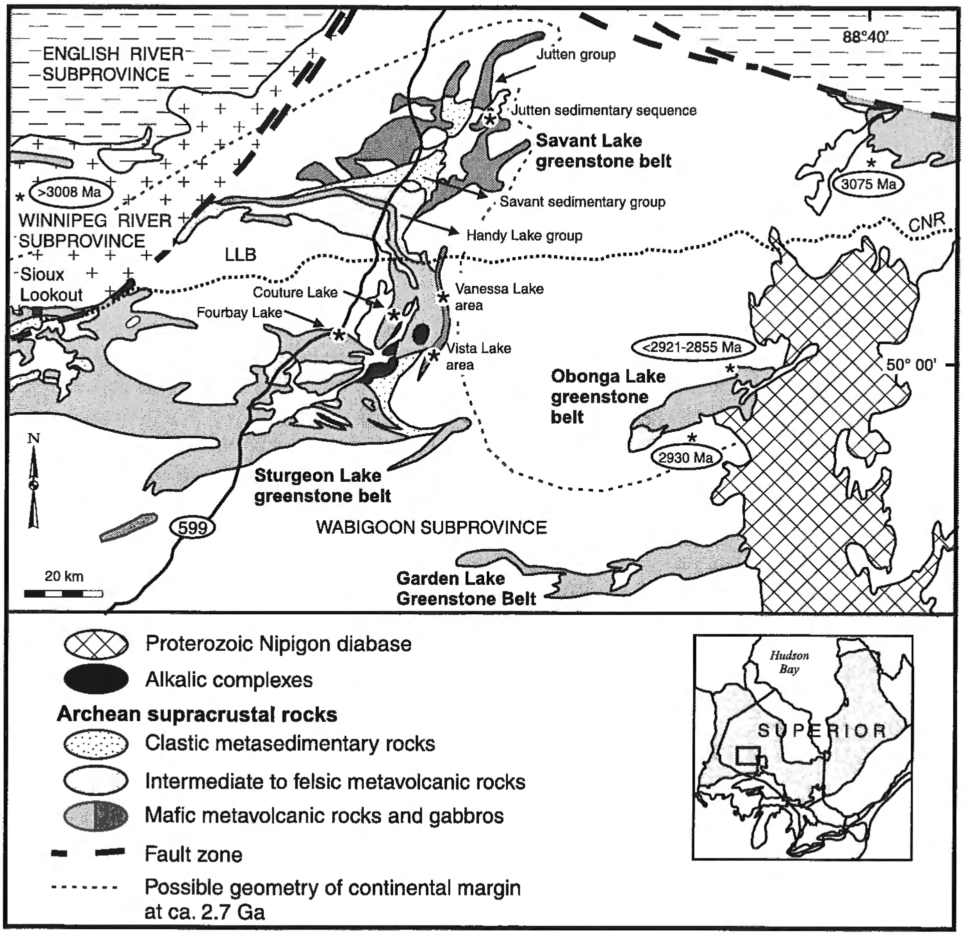


***Figure 1.*** *Regional geology of the central Wabigoon Subprovince, western Superior Province with location of Mesoarchean crust. LLB – Lewis Lake batholith.*

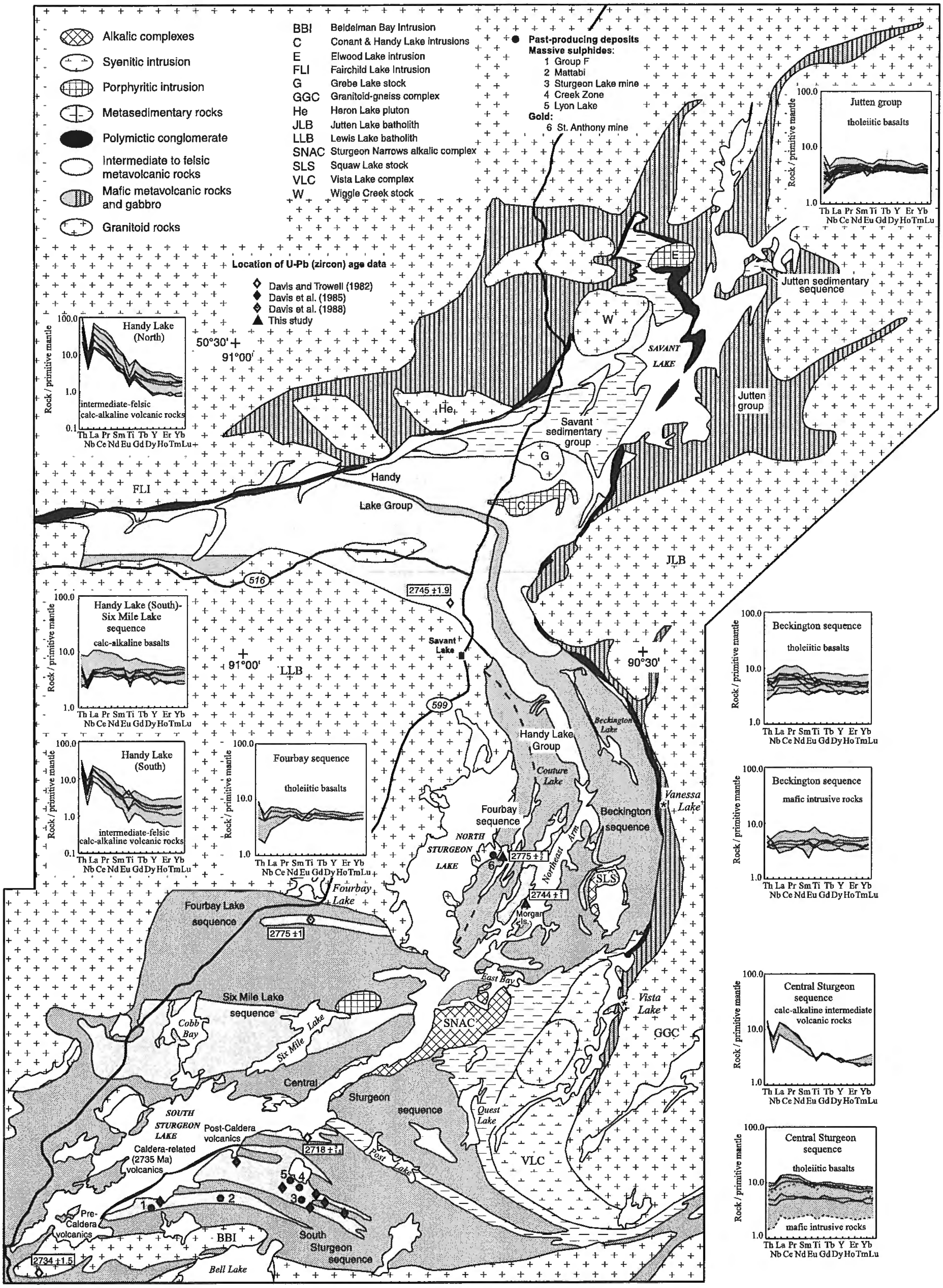


*Figure 2. Geology of the Savant Lake–Sturgeon Lake greenstone belt modified from Trowell (1983 and references therein) and Bond (1977, 1980). Trace element profiles for the major volcanic sequences are normalized to primitive mantle values of Sun and McDonough (1989).*

### *Quartz-rich metasedimentary rocks*

A distinctive sequence of quartzose wacke and quartz-rich conglomerate forms the basal unit of the basalt-dominated Jutten group in northern and eastern parts of the Savant Lake–Sturgeon Lake greenstone belt. These rocks, unique to the Wabigoon Subprovince, were originally identified in northeast Savant Lake area (Fig. 1, 2) where they are designated the Jutten sedimentary sequence (Cortis et al., 1988; Sanborn-Barrie, 1989). Here, the 1–2 km thick sequence consists of 1) conglomerate with a feldspathic wacke matrix supporting clasts of granodiorite, ultramafic rock, and vein quartz; 2) carbonatized angular quartz grit containing previously deformed, boulder- to pebble-size clasts of trondhjemite, iron carbonate, and possible wacke (Fig. 3); and 3) quartzose wacke and conglomerate with clasts of ultramafic rock, fuchsitite, sericite schist, and vein quartz. A sample of quartzose wacke from the upper part of the sequence yielded detrital zircons with concordant ages of 2948 ± 3 Ma and 3199 ± 3 Ma, and discordant $^{207}Pb/^{206}Pb$ ages of 3258 ± 3 Ma and 3297 ± 6 Ma (D.W. Davis and M. Moore, unpub. report, 1991). These ages indicate a Mesoarchean source for these metasedimentary rocks and provide a maximum depositional age of ca. 2950 Ma.

Quartz-rich clastic rocks are now known to extend south into the Sturgeon Lake area. Quartzose wacke from Vista Lake (Fig. 1, 2) described by Sanborn-Barrie et al. (1998) yielded detrital zircon ages of 2.95 to 2.91 Ga (n=20; GSC SHRIMP II, T. Skulski, unpub. data, 1998). Similar rocks on Vanessa Lake (Fig. 1, 2), contiguous with the Vista Lake locality, are represented by a less than 150 m wide panel of quartzose wacke (Fig. 4) ±lithic wacke that extends for a strike length of 20 km. These contain 45–65% quartz, commonly with 20% muscovite, 10–20% feldspar, 2–3% garnet, and trace sillimanite. On central Vanessa Lake, quartzose wacke is conformable with dacite lapilli tuff (Fig. 5), whose age will better constrain the depositional age of these clastic rocks.

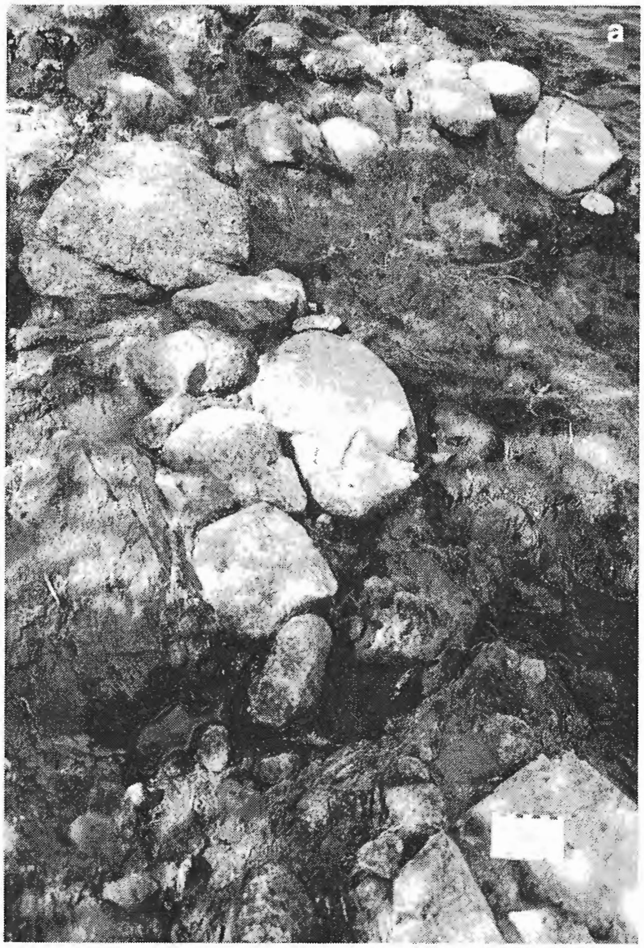



***Figure 3.*** *Conglomerate facies of the Jutten sedimentary sequence.* ***a)*** *in situ boulder-size clasts of trondhjemite with iron-carbonatized quartz grit matrix;* ***b)*** *detail of a) showing previously deformed cobble (possibly wacke) adjacent to white-weathering trondhjemite clast (left).*

***Figure 4.*** *Strongly foliated to gneissic ($S_1$) quartzose wacke from northern Vanessa Lake, eastern Sturgeon Lake belt.*

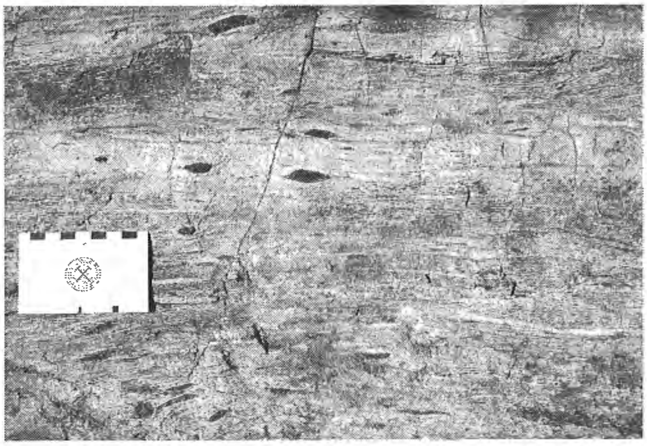

*Figure 5. Rhyodacite tuff from northern Vanessa Lake. Dark lenses, 1–2 cm long, are dismembered smokey quartz veins.*

Underlying the Jutten sedimentary sequence on northeast Savant Lake are newly recognized supracrustal rocks. These form an approximately 100 m thick sequence comprising, from base to top, ultramafic schist (Fig. 6a), rhyodacitic lapilli tuff (Fig.6b), and fuchsitic siltstone±chert, capped by ultramafic-derived siltstone-ash (Fig. 6c). The uppermost layered rocks are in contact with basal conglomerate of the Jutten sedimentary sequence (Fig. 6d) which, at this locality, has a higher proportion of original silt and clay than stratigraphically higher conglomerate units. An unconformable relationship between the substrate and the Jutten sedimentary sequence is indicated by the presence of clasts of all substrate units within the latter. An angular unconformity is suggested by the presence of previously deformed clasts of substrate units within conglomerates of the Jutten sedimentary sequence (Fig. 3b, 6d).

### *Jutten group*

Overlying the Jutten sedimentary sequence in the northern and eastern parts of the belt are tholeiitic basalt units of the Jutten group (Fig. 1, 2). These are pillowed to massive, greenschist-facies flows that attain amphibolite facies in proximity to intrusive granitoid batholiths. Pillowed flows are dominant, constituting up to 85%. Massive flows are locally plagioclase phyric with 20% or less euhedral phenocrysts, 3 mm long. Intermediate to felsic metavolcanic rocks

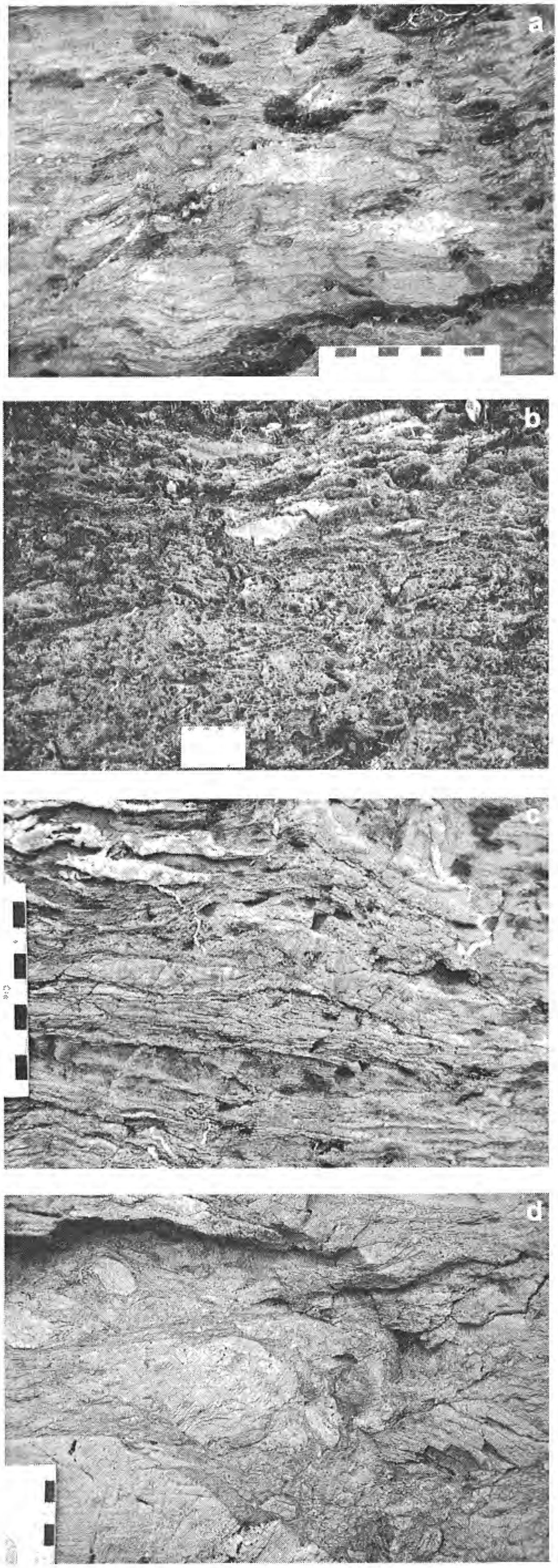


*Figure 6. Rocks of northeast Savant Lake. **a)** ultramafic schist; **b)** rhyodacitic lapilli tuff; **c)** layered, fine-grained fuchsitic rocks interpreted as ultramafic-derived siltstone-ash±chert; **d)** basal conglomerate of the Jutten sedimentary sequence with previously deformed clasts of c).*

of restricted extent are spatially associated with tholeiitic basalt units of the Jutten group at isolated localities and are the subject of an ongoing U-Pb dating program.

Tholeiitic basalt flows of the Jutten group are characterized by modest enrichment in Fe and low $TiO_2$ contents (<1.1 wt.% $TiO_2$, n=72; this study and Trowell (1986)). The majority of basalts analyzed represent evolved liquids, however a high MgO (13.6 wt.%) basalt may represent a primary magma composition. Jutten basalt samples have flat to slightly light rare-earth element (LREE) -depleted primitive mantle-normalized profiles (Fig. 2), and most are enriched in Th and La relative to Nb. Enrichment in immobile large ion lithophile elements (LILE) such as Th, and depletion in Ti, are characteristic of chemically-evolved sialic crust. Accordingly, the observed increase in Th-Ti with increasing differentiation, above that expected for Fe-Ti enrichment in tholeiitic basalt, is qualitatively consistent with crustal contamination. Several analyzed basalt samples, in contrast, are depleted in Th (Fig. 2) and may represent depleted mantle-derived magmas that escaped interaction with continental crust. Preliminary neodymium isotopic data on two Jutten basalt samples yielded $\varepsilon_{Nd}$ values of +0.6 and +1.7 (at 2.85 Ga, *see* 'Discussion and summary').

Linking the submarine Jutten volcanic pile to underlying continentally derived clastic rocks are gabbro and leucogabbro that cut the clastic rocks and are potential feeder dykes and sills to the stratigraphically overlying mafic pile. Two additional lines of evidence point to a conformable relationship between these sequences. Facing relationships between them are consistent with conformable deposition; in northeast Savant Lake, Jutten group basalt flows face west to southwest, away from southwest-facing quartzose clastic rocks, while in the Vanessa–Vista lakes corridor both sequences appear to young away from an anticlinal axis. Lastly, both clastic and volcanic rocks preserve fabric evidence of the same two penetrative deformation events.

## SOUTH-CENTRAL OCEANIC TERRANE

The south-central Savant Lake–Sturgeon Lake belt preserves a conformable, ca. 70 Ma sequence of episodic volcanism. In contrast to the Jutten group, this diverse volcanic terrane does not require interaction with continental crust. As such it is interpreted as oceanic, typical of other greenstone belt rocks of the western Wabigoon Subprovince.

The base of the exposed pile is represented by a 1 km thick sequence of massive to pillowed basalt (Fig. 7), which may be strongly foliated to gneissic with centimetre-scale banding. This is capped by 2775 ± 1 Ma felsic tuffs near Fourbay Lake (Davis et al., 1988), and 2775 +5/-2 Ma dacite lapilli tuff (T. Skulski, unpub. data, 1998) on Couture Lake (Fig. 2). These geochronological constraints support correlation between volcanic rocks exposed south of Fourbay Lake (Fourbay Cycle of Trowell (1983); Fig. 2) and those at Couture Lake (North Arm cycle of Trowell (1983)), collectively referred to here as the Fourbay sequence.

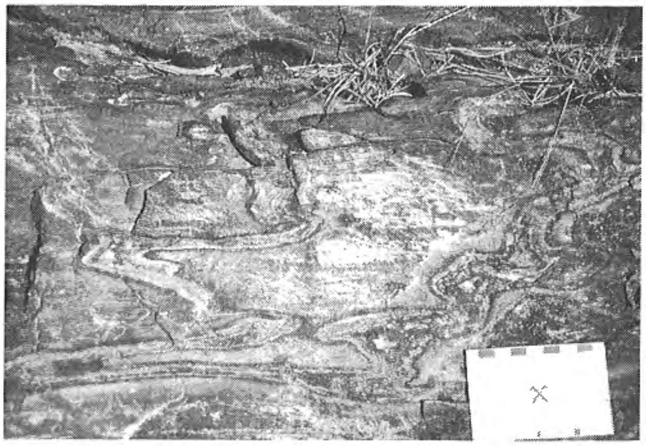

*Figure 7. Pillowed flow of the tholeiitic Fourbay sequence.*

Basalts of the Fourbay sequence are tholeiitic, with modest Fe enrichment and $TiO_2$ contents <1.5 wt.% (n=23; Beggs (1975); Trowell (1983) and this study) that represent chemically evolved liquid compositions (<9 wt.% MgO). They have primitive mantle-normalized LREE abundances that are flat to LREE depleted, and are variably enriched in Th and La relative to Nb (Fig. 2). Dacite lapilli tuff that caps the mafic part of the sequence at Couture Lake exhibits simple U-Pb systematics that show no indication of inherited Pb. This rock is enriched in Th>La>>Nb, with a primitive mantle-normalized La/Yb value of 4. Neodymium isotopic data on the Fourbay sequence yield positive $\varepsilon_{Nd}$ values of +2.6 (at 2.775 Ga) for basalt and +2.2 for 2.775 Ga dacite lapilli tuff. Positive initial Nd isotopic values, simple zircon U-Pb systematics, and lack of intercalated terrigenous sediment are consistent with formation of this submarine sequence in an oceanic setting, unlike the chemically similar Jutten group basalt flows.

The Fourbay sequence is conformably overlain by south- and east-facing, calc-alkaline pillow basalts and minor massive tholeiitic basalt flows (lower Six Mile Lake cycle of Robinson (1992); Beckington West cycle of Trowell (1983)) which, in turn, are conformably overlain by calc-alkalic intermediate pyroclastic rocks (Fig. 8). New geochronological, chemical, and Nd isotopic data confirm earlier field-based correlations between these intermediate pyroclastic rocks, now dated at 2744 +2/-1 Ma (T. Skulski, unpub. data, 1998), and the lower Handy Lake Group in the Savant Lake area (Fig. 2), dated at 2745 ± 1.9 Ma (Davis and Trowell, 1982). Ongoing U-Pb dating will test whether the Six Mile Lake sequence to the southwest (Fig. 2) is of similar age. Volcanic activity between ca. 2745–2730 Ma is represented also by volcanic strata of south Sturgeon Lake, dated at 2735 Ma (Davis et al., 1985), which are host to volcanogenic massive sulphide mineralization (Morten et al., 1991), and hypabyssal intrusions, dated at 2733 ± 1 Ma (Davis, 1996), that cut the Handy Lake pile (Conant and Handy Lake intrusions indicated by C in Fig. 2).

*Figure 8. View to south of south-facing, graded pyroclastic breccia overlying ungraded tuff, Six Mile Lake calc-alkaline sequence, Cobb Bay.*

Calc-alkaline basalt samples of the lower Handy Lake–Six Mile sequence have flat to LREE-enriched trace element profiles (Fig. 2) and are relatively depleted in Nb relative to Th and La, and in Ti relative to middle REEs. Overlying intermediate to felsic volcanic rocks are enriched in LREE relative to HREE (normalized La/Yb 8–34) and are enriched in Th>La>>Nb (Fig. 2). Epsilon Nd values of basalt, dacite, and rhyolite are similar within error (±0.5 epsilon units) and fall in the range +1.0 to +1.7. Similar positive $\varepsilon_{Nd}$ values of rocks with widely different major element composition, and simple zircon U-Pb systematics of 2744 Ma rhyolite and 2745 Ma dacite tuff, indicate that Handy Lake–Six Mile magmas were not contaminated by ancient continental crust. Hence, the enrichment in LILE relative to LREE and high field-strength elements (i.e. Nb, Ti) in these basalt flows likely reflects mantle source characteristics.

Conformably overlying the Six Mile Lake calc-alkaline pyroclastic succession is a basalt-dominated sequence capped by 2718 +2.7/-1.5 Ma felsic pyroclastic rocks (Davis and Trowell, 1982). These rocks, designated the Central Sturgeon Lake sequence (Central Sturgeon Lake cycle of Trowell (1983)), are a mixed tholeiitic and calc-alkaline group. Some tholeiitic basalt samples are notable for their high Fe and $TiO_2$ abundances (up to 2.5 wt.%; Trowell (1983); this study, *see also* Sanborn-Barrie et al. (1998)). Samples of high Fe and Ti basalt east of Post Lake are enriched in LREE but depleted in Nb and Th (Fig. 2). Gabbroic rocks that cut the Handy Lake Group are tholeiitic, with similar trace element profiles as Central Sturgeon Lake basalt (Fig. 2). This supports a genetic link between the two and a conformable relationship between the Six Mile and Central Sturgeon Lake sequences. In contrast, calc-alkaline intermediate volcanic rocks from this sequence show greater enrichment in LREE, are depleted in Nb relative to Th and La, and are depleted in Ti relative to heavy REEs (Fig. 2). Samples of calc-alkaline basalt and high-Fe tholeiitic basalt have similar $\varepsilon_{Nd}$ values of +2.2 and +1.6, respectively.

A basalt-dominated sequence, possibly correlative with the Central Sturgeon Lake sequence, lies east of the Northeast Arm of Sturgeon Lake (Fig. 2). These rocks (the Beckington East cycle of Trowell (1983) and Sanborn-Barrie et al. (1998)) have a maximum age of 2745 Ma, the age of the underlying rhyolite (Fig. 2). This mafic sequence contains approximately equal amounts of calc-alkaline and tholeiitic basalt flows with $TiO_2$ in the latter up to 1.8 wt.%, and MgO contents <9.5 wt.% (Trowell, 1983; this study). Both tholeiitic basalt and mafic intrusive rocks have flat to slightly LREE-enriched profiles, and the majority are depleted in Nb and Th relative to La (Fig. 2). A tholeiitic basalt has an $\varepsilon_{Nd}$ value of +1.9 (at 2745 Ma) reflecting derivation from a depleted mantle source.

### *Summary*

The 2775 Ma Fourbay sequence, the oldest volcanic rocks presently dated in the western Wabigoon Subprovince, is interpreted as oceanic basement to overlying calc-alkaline rocks. These calc-alkaline rocks include intermediate to felsic fragmental rocks of the Handy Lake–Six Mile sequence, which show a distinctive pattern of trace element enrichment (Th>La>>Nb) similar to modern island arc sequences. The conformable nature of the Fourbay–Handy Lake contact and upward-shoaling of the Handy Lake Group (Sanborn-Barrie et al., 1998) are consistent with a model in which an emergent Handy Lake–Six Mile arc was built on oceanic basement. Eruption of submarine, tholeiitic basalt flows with depleted LILE and LREE contents in both the Central Sturgeon and Beckington sequences on calc-alkaline volcanic rocks of the Handy Lake–Six Mile sequence may reflect subsidence and rifting of arc crust prior to 2718 Ma.

## OVERLAPPING CLASTIC SUCCESSION

Late- to postvolcanic clastic rocks of the Savant Lake–Sturgeon Lake belt everywhere separate rocks of the continental margin sequence from those of the oceanic terrane. This clastic succession is interpreted to have formed in a foredeep setting prior to arc-continent collision.

Turbiditic wacke and oxide-facies ironstone of the Savant sedimentary group (Fig. 2) have a maximum age of 2704 Ma (Davis, 1996), and wacke±argillite of southeast Sturgeon Lake has a preliminary maximum age of 2700 ± 14 Ma (T. Skulski, unpub. GSC SHRIMP II data, 1998). Where the Savant sedimentary group is in contact with Jutten group basalt it rests with angular unconformity, its contact marked by a regionally extensive polymictic conglomerate of local derivation (Fig. 2). This unit, designated the Savant Narrows formation (Trowell, 1986), has a maximum depositional age of 2704±1 Ma (Davis et al., 1988), the age of a granitoid clast. Polymictic conglomerate (Fig. 9) has now been traced south into the eastern Sturgeon Lake belt (Fig. 2) where it separates tholeiitic basalt and quartz-rich clastic rocks of the continental margin sequence from all other components of the greenstone belt (Fig. 10). In contrast, turbiditic wacke and volcanic rocks of the south-central oceanic terrane are generally observed to be conformable. They take the form of interbedded, same-facing, turbiditic wacke-magnetite ironstone with dacite lapilli tuff on central Savant Lake, and intercalated tuff and epiclastic rocks on central Sturgeon Lake.

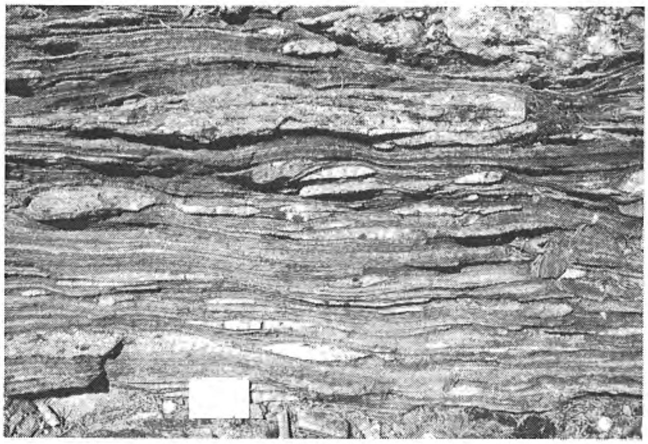

*Figure 9. Polymictic conglomerate of the less than 2704 Ma Savant Narrows formation, west shore of northern Vanessa Lake.*

Preliminary data suggest that two main facies of clastic rocks of the basin have characteristic source terrains. Basinal facies turbiditic wacke from Savant Lake and Quest Lake contain detrital zircons that range in age from 3275 Ma to 2704 Ma (Davis, 1996; T. Skulski unpub. data, 1998). Apparent age clusters at ca. 3060 Ma, ca. 2950–2920 Ma, ca. 2830 Ma, and ca. 2790–2770 Ma (Davis, 1996) reflect their diverse source region. In contrast, crossbedded sandstones from Post Lake (Fig. 2) that were proximal to the oceanic terrane show a restricted range of detrital zircon ages from 2769 Ma to 2716 ± 14 Ma (16 grains, GSC SHRIMP II, T. Skulski, unpub. data, 1998). These data reflect a one to one correspondence with known ages of volcanic rocks of the oceanic terrane.

## DEFORMATION

Two main episodes of ductile deformation have affected all rocks within the belt to varying degrees. These are interpreted to record collision and convergence between the continental margin sequence and the diverse oceanic terrane. In the Savant Lake area, earliest penetrative deformation, $D_1$, involved north- to northwest-trending, shallow-plunging, $F_1$ folds and development of an associated axial planar cleavage ($S_1$) (Fig. 11a). This is overprinted by 050–070°-trending, steeply plunging, $F_2$ folds with an associated axial planar foliation, $S_2$ (Fig. 11b). Zones of localized $D_2$ strain include the 070°-trending Kashaweogama Lake shear zone and Stillar Bay shear zone, and narrow, east-striking shear zones that transect the Handy Lake volcanic group (Fig. 11b).

In the Sturgeon Lake area, the dominant fabric (Fig. 4, 5, 9, 10) is a northerly-striking, steeply dipping penetrative ductile fabric which correlates with $S_1$ (Fig. 11a). This fabric is axial planar to tight, moderate north-plunging folds, similar in style to $F_1$ to the north. It is recognized to extend east of the supracrustal belt where it is moderately to strongly developed


***Figure 10.***

*View to south of quartzose wacke (left); garnet-bearing, amphibolite-facies basalt (centre); and polymictic conglomerate (right); northeast Vanessa Lake.*

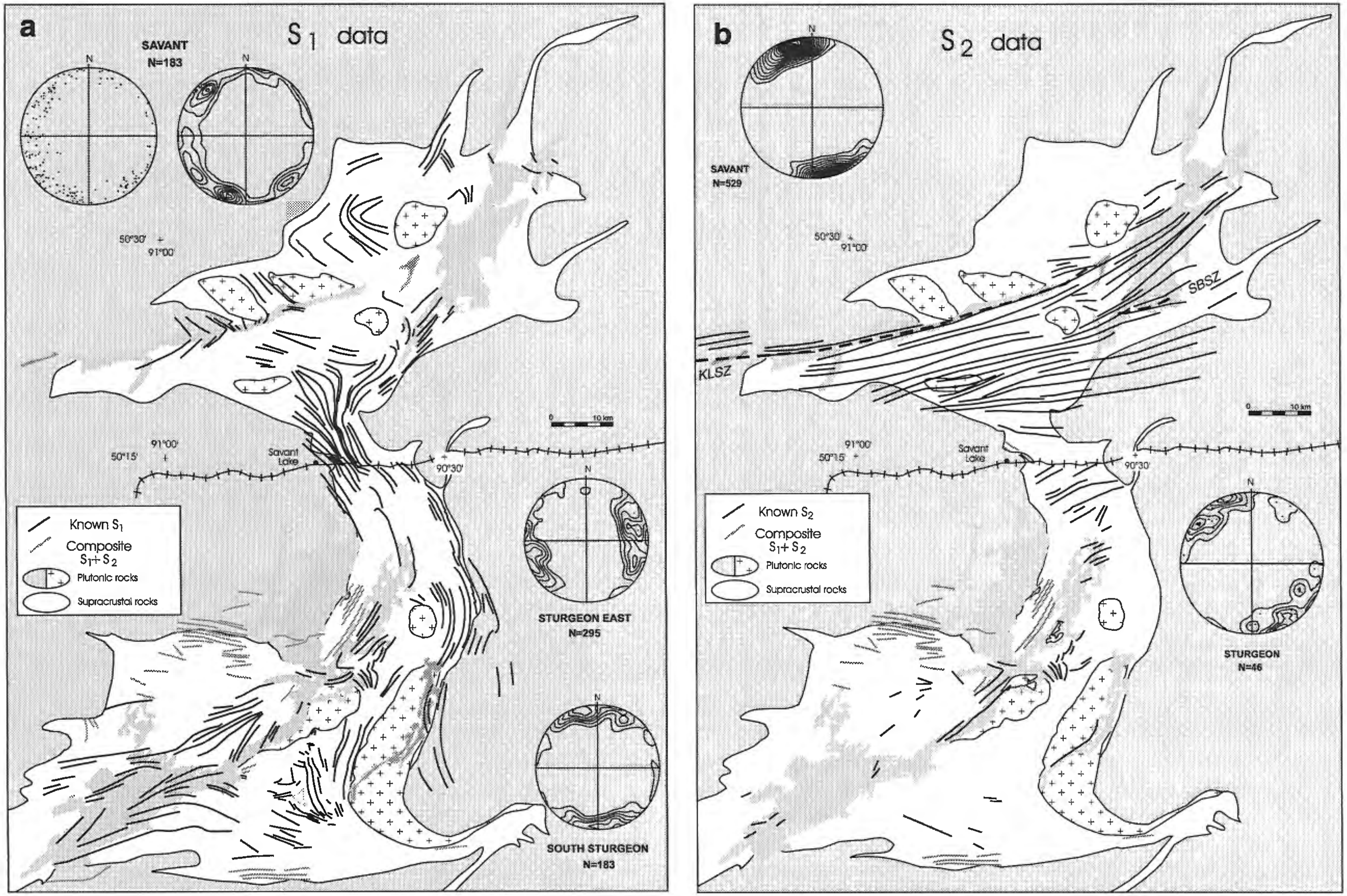


*Figure 11. Planar tectonic fabric trends for the Savant Lake–Sturgeon Lake greenstone belt. **a**) first generation foliation, $S_1$, showing poles to planes, uncontoured and contoured and trajectories of $S_1$ which are axial planar to $F_1$ (not shown). A triple point (open grey triangle) is defined by discordance between $D_1$ structures in the south and east parts of the Sturgeon Lake belt. **b**) second generation foliation, $S_2$, showing contoured poles to planes and trajectories of $S_2$ which are axial planar to $F_2$ (not shown). KLSZ – Kashaweogama Lake shear zone, SBSZ – Stillar Bay shear zone.*

within ca. 2710 Ma (V. McNicoll and J. Percival, unpub. data, 1998) granitoid rocks (Fig. 12; *see also* Percival et al., 1999). Along the eastern margin of the Sturgeon Lake belt, shear band structures (Fig. 9) and asymmetrically Z-folded $S_1$ foliation (Fig. 11a) indicate dextral vorticity during $D_1$. Fabric elements of south Sturgeon Lake, in contrast, comprise southwest- to southeast-trending folds ($F_1$) and fabrics ($S_1$) which are at a high angle to those described above. Overprinting $D_2$ structures, geometrically consistent with those in the Savant Lake area, penetratively affect rocks in the northern Sturgeon Lake area (Fig. 11b), but are only locally developed throughout much of the Sturgeon Lake belt.

### *Pre-$D_1$ deformation*

Both areas show evidence of nonpenetrative structures interpreted to predate $D_1$. In the Savant Lake area, this is a tilting event, manifested by the angular unconformity between the Jutten group and overlying polymictic conglomerate. In the central Sturgeon Lake area, structures which predate $D_1$ are open, upright, east- to southeast-trending, shallow-plunging folds. These are manifested mainly by opposing structural facing directions across the central Sturgeon Lake area (Sanborn-Barrie et al., 1998), however, spaced fractures axial planar to pre-$D_1$ folds and folded by $S_1$ are recognized at several localities. Structures which predate $D_1$ are interpreted as pre collisional to early collisional structures in both cases, however, they did not develop contemporaneously. Tilting (during uplift) in the Savant Lake area prior to turbiditic sedimentation predated open folding of metavolcanic and turbiditic metasedimentary rocks in the Sturgeon Lake area.

Ductile deformation prior to $D_1$ is recorded in granitoid clasts, possible sedimentary clasts (Fig. 3b), and rare felsic volcanic clasts that occur within conglomeratic facies of the Jutten sedimentary sequence. These fabrics may be equivalent to the oldest fabric recognized in the granitoid gneiss complex to the east ($S_1$ of Percival et al., 1999). The presence of previously foliated substrate clasts in the Jutten sedimentary sequence suggests that the supracrustal substrate unconformably below the Jutten sedimentary sequence was penetratively affected by a strain event prior to $D_1$ and/or $D_2$.

***Figure 12.*** *$S_1$ in monzogranite, Seseganaga Lake.*

## DISCUSSION AND SUMMARY

The Jutten sedimentary and volcanic group of the northeastern Savant Lake–Sturgeon Lake greenstone belt is interpreted to record rifting of continental crust older than 2.9 Ga. This volcanic rift margin consists of compositionally mature, texturally immature, quartzose rocks of Mesoarchean provenance which form a clastic veneer upon which voluminous mafic flows erupted (Fig. 13). The thin nature of these clastic rocks, in contrast to the thick succession of overlying submarine tholeiitic basalt flows is characteristic of rapid extension in volcanic-dominated rift margins (White and McKenzie, 1989). If active rifting was driven by a mantle plume, the erupted products analyzed to date reflect melting of depleted mantle to produce high-MgO basaltic primary magmas. The Ti-depleted, Th-enriched character of evolved basalt units may be a signature of their contamination by thinned continental crust through which they erupted.

Volcanic rocks that do not require interaction with continental crust are represented by the diverse oceanic rocks of the south-central part of the greenstone belt. The 2775 Ma Fourbay sequence may represent oceanic basement whose high La/Nb and Th/Nb values may indicate that these basalts formed in a supra-subduction environment, and could represent island-arc tholeiites. Alternatively, they could represent a relict oceanic plateau, as some modern examples (e.g. Naturaliste Plateau, Indian Ocean) have high normalized La/Nb values that reflect recycling of continental lithospheric mantle or crust (Kent et al., 1996). Chemical similarity of the Jutten and Fourbay basalt units allow that they formed in a similar setting, a possibility that will be tested by U-Pb dating of Jutten group gabbro and rhyodacite tuff. At present, our best estimate of the age of the Jutten group is ca. 2.85 Ga. This is based on the lack of 2.85–2.82 Ga detrital zircons in the quartz-rich clastic rocks, a population contained in other clastic rocks in the area. If the Jutten group is ca. 2775 Ma, the Fourbay Lake sequence may represent a vestige of the volcanic rift margin which then evolved separately in an oceanic setting for ca. 70 Ma, prior to amalgamation.

Island arc magmatism represented by early Handy Lake volcanism between 2745–2733 Ma, and the likely correlative Six Mile Lake sequence, culminated in the construction of volcanic centres conformable on the Fourbay Lake sequence. The contrasting pattern of LILE enrichment and lower $\varepsilon_{Nd}$

values of Handy Lake volcanic rocks, relative to the underlying Fourbay sequence, may reflect subduction-related recycling of continental crust postdating 2775 Ma in the mantle wedge (c.f. Henry et al., 1998). Eruption of submarine tholeiitic basalt flows of the Beckington and Central Sturgeon Lake sequences, which lack enrichment of Th relative to Nb (Fig. 2), is interpreted to reflect upwelling and melting of asthenospheric mantle in an intra-arc setting between 2745 Ma and 2718 Ma. Our preliminary data do not require a continental crustal component to Fourbay, overlying Handy Lake–Six Mile, and Central Sturgeon–Beckington magmatism. This is consistent with both the primitive isotopic compositions and simple U-Pb zircon systematics of volcanic and intrusive rocks of the western Wabigoon Subprovince, in general (e.g. Henry et al. 1998; Davis et al., 1988).

Intrusion of 2710 Ma calc-alkaline, tonalitic to granodioritic plutons along the eastern margin of the greenstone belt and farther east (*see* Percival et al., 1999), record east-dipping (present co-ordinates) continental arc magmatism during collision of the oceanic terrane and the continental margin sequence (Fig. 13). Tilting of the Jutten volcanic margin, required by the angular unconformity which everywhere separates the continental margin sequence from the oceanic terrane, and unroofing of 2704 Ma or older plutonic rocks, which occur as clasts in conglomerate, likely took place just prior to, or coeval with, coarse clastic deposition of conglomerate later than 2704 Ma. Tilting of a thinned continental margin may have been driven by attempted subduction of buoyant (e.g. anomalously thick) oceanic crust, the vestiges of which are represented by the Fourbay sequence.

Deposition of turbiditic sediments in both the Savant Lake (Savant sedimentary group) and Sturgeon Lake (Quest Lake sedimentary rocks) areas on alluvial conglomerate derived mainly from the continental margin sequence reflects subsidence in a foredeep basin (Fig. 13). This basin separated 2775–2704 Ma oceanic rocks from a tilted ca. 2710 Ma continental arc built, in part, on a less than 2900 Ma volcanic rift margin in the north and east. Fundamental to this interpretation is the fact that this turbiditic succession is everywhere unconformable on the continental margin but conformable with volcanic and epiclastic rocks of the oceanic terrane. Minor felsic volcanism (Handy volcanism) at ca. 2704 Ma, early in the depositional history of the Savant sedimentary group, suggests that arc magmatism was waning during foredeep sedimentation.

Terminal collision between the continental margin sequence and the diverse oceanic terrane is recorded by penetrative ductile deformation that affected all rocks of the Savant Lake–Sturgeon Lake greenstone belt and some adjacent granitoid rocks. The geometry of the continental margin at ca. 2.7 Ga and the local boundary conditions imposed by it appear to had a strong influence on the developing structures. Our interpretation of the accumulation of a quartz-rich clastic veneer and overlying volcanic sequence on thinned Mesoarchean continental crust, together with the presence of Mesoarchean plutonic rocks northeast and northwest of the belt, suggest the ca. 2.7 Ga margin may have been an irregular, concave margin (dashed line in Fig. 1), not dissimilar to the geometry of the present-day Winnipeg River subprovince boundary. Northeast-directed shortening during collisional convergence is attributed to the development of $D_1$ structures in south Sturgeon Lake (Fig. 11a), far removed from the continental margin. In the central part of the belt, the switch to north-trending $D_1$ structures is interpreted to record an influence of the (north-trending) continental margin during northeasterly convergence. In the north, penetrative refolding of $D_1$ structures and localization of $D_2$ strain may reflect the increasing influence of a northeast-trending segment of the continental margin at a late stage in the evolution of structures in this collisional regime.

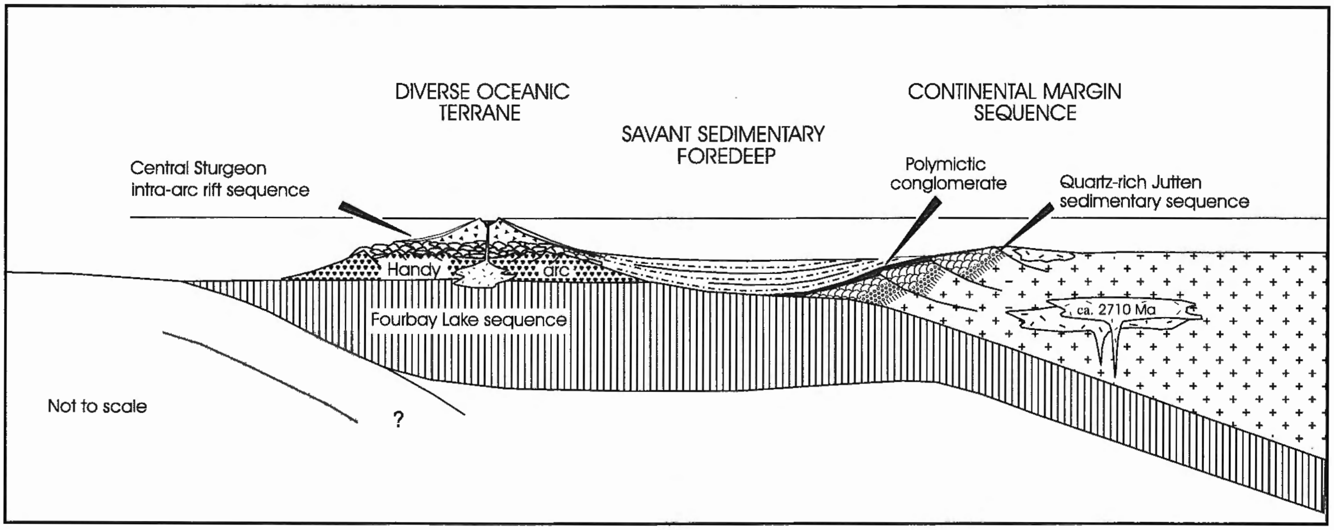


***Figure 13.*** *Schematic section showing proposed tectonic setting of the Savant Lake–Sturgeon Lake area at ca. 2710–2701 Ma. Subduction of buoyant 2775 Ma oceanic plateau crust beneath the continental margin sequence may account for uplift, erosion, and deposition of orogenic sediments concurrent with arc magmatism.*

## ACKNOWLEDGMENTS

We thank Chris Hemmingway and Marianne Mader for their reliable, cheerful assistance during fieldwork. Chris Hemmingway is also thanked for independent mapping. The Ministry of Natural Resources, Fire Centre is thanked for the use of the Silvaculture Camp facilities. Al Smith provided an introduction to the geology of Noranda's Mattabi mine property to which access was facilitated by both Al and Ron Kennedy. Excellent air service was provided by West Caribou Air. Informal discussion in the field with participants of the western Superior NATMAP–LITHOPROBE Field Workshop is appreciated. Geochemical analyses used in this paper were obtained from McGill University, Memorial University, and the Geochemistry Laboratories of the Geological Survey of Canada. Uranium-lead geochronology on detrital zircons was carried out on the Geological Survey of Canada's SHRIMP II with Richard Stern. Preparation of this manuscript was assisted by Chris Hemmingway, and reviews by Wouter Bleeker, Simon Hanmer, John Percival, and Cees van Staal improved it.

## REFERENCES

**Beggs, D.G.**
1975: Petrology and geochemistry of Archean volcanic rocks north of Sturgeon Lake; M.Sc. thesis, University of Toronto, Toronto, Ontario, 151 p.

**Bond, W.D.**
1977: Geology of McCubbin, Poisson, and McGillis townships (Savant Lake area), District of Thunder Bay; Ontario Division of Mines, Geoscience Report 160, 78 p.
1980: Geology of the Houghton-Hough lakes area (Savant Lake area), District of Thunder Bay; Ontario Geological Survey, Report 195, 112 p.

**Cortis, A.L., Stott, G.M., Osmani, I.A., Atkinson, B., and Thurston, P.C.**
1988: A geological re-evaluation of northwestern greenstone belts; *in* Summary of Field Work and Other Activities 1988; Ontario Geological Survey, Miscellaneous Paper 141, p. 28–52.

**Davis, D.W.**
1996: Provenance and depositional age constraints on sedimentation in the westernSuperior transect area from U-Pb ages of zircons; LITHOPROBE Report 53, p. 18–23.

**Davis, D.W. and Trowell, N.F.**
1982: U-Pb zircon ages from the eastern Savant Lake-Crow Lake metavolcanic-metasedimentary belt, northwest Ontario; Canadian Journal of Earth Sciences, v. 19, p. 868–877.

**Davis, D.W., Krogh, T.E., Hinzer, J., and Nakamura, E.**
1985: Zircon dating of polycyclic volcanism at Sturgeon Lake and implications for base metal mineralization; Economic Geology, v. 80, p. 1942–1952.

**Davis, D.W., Sutcliffe, R.H., and Trowell, N.F.**
1988: Geochronological constraints on the tectonic evolution of a Late Archean greenstone belt, Wabigoon Subprovince, Northwest Ontario, Canada; Precambrian Research, v. 39, p. 171–191.

**Henry, P., Stevenson, R.K., and Gareipy, C.**
1998: Late Archean mantle composition and crustal growth in the Western Superior Province of Canada: Neodymium and lead isotopic evidence from the Wawa, Quetico and Wabigoon subprovinces; Geochimica et Cosmochimica Acta, v. 62, p. 143–157.

**Kent, R.W., Hardarson, B.S., Saunders, A.D., and Storey, M.**
1996: Plateaux ancient and modern: geochemical and sedimentological perspectives on Archean oceanic magmatism; Lithos, v. 37, p. 129–142.

**Morton, R.L., Walker, J.S., Hudak, G.J., and Franklin, J.M.**
1991: The early development of an Archean submarine caldera complex with emphasis on the Mattabi ash-flow tuff and its relationship to the Mattabi massive sulphide deposit; Economic Geology, v. 86, p. 1002–1011.

**Percival, J.A., Castonguay, S., Whalen, J.B., Brown, J.L., McNicoll, V., and Harris, J.R.**
1999: Geology of the central Wabigoon region in the Sturgeon Lake–Obonga Lake corridor, Ontario; *in* Current Research 1999-C; Geological Survey of Canada.

**Robinson, D.J.**
1992: Geology of the Six Mile Lake area; Ontario Geological Survey, Open File Report 5838, 93 p.

**Sanborn-Barrie, M.**
1989: Geology of the Savant Lake area; *in* Summary of Field Work and Other Activities 1989; Ontario Geological Survey, Miscellaneous Paper 146, p. 54–62.

**Sanborn-Barrie, M. and Skulski, T.**
1998: Structural geology, central Sturgeon Lake area, Ontario; Geological Survey of Canada, Open File 3641, scale 1:50 000.

**Sanborn-Barrie, M., Skulski, T., and Whalen, J.B.**
1998: Tectonostratigraphy of central Sturgeon Lake, Ontario: deposition and deformation of submarine tholeiites and emergent calc-alkaline volcano-sedimentary sequences; *in* Current Research, Part C; Geological Survey of Canada, Paper 98-1C, p. 115–126.

**Skulski, T, Sanborn-Barrie, M., and Stern, R.**
1998: Did the Sturgeon Lake supracrustal belt form near a continental margin? *in* LITHOPROBE Transect Fourth Annual Workshop, March 23-24, 1998, (ed.) R.M. Harrap and H.H. Helmstaedt; LITHOPROBE Report #65, p. 87–98.

**Sun, S.-S. and McDonough, W.F.**
1989: Chemical and isotopic systematics of oceanic basalts: implications for mantle composition and processes; *in* Magmatism in the Ocean Basins, (ed.) A.D. Saunders and M.J. Norry; Geological Society of London, Special Publication 42, p. 313–345.

**Trowell, N.F.**
1983: Geology of the Sturgeon Lake area; Ontario Geological Survey, Report 221, 97 p.
1986: Geology of the Savant Lake area, districts of Kenora and Thunder Bay; Ontario Geological Survey, Open File Report 5606, 181 p.

**White, R. and McKenzie, D.**
1989: Magmatism at rift zones: the generation of volcanic continental margins and flood basalts; Journal of Geophysical Research, v. 94, p. 7685–7729.

Geological Survey of Canada Project 970014

# Archean carbonate-bearing alkaline igneous complexes of the western Quetico metasedimentary belt, Superior Province, Ontario

Kéiko Hattori[1] and John A. Percival
Continental Geoscience Division, Ottawa

*Hattori, K. and Percival, J.A., 1999: Archean carbonate-bearing alkaline igneous complexes of the western Quetico metasedimentary belt, Superior Province, Ontario;* in *Current Research 1999-C; Geological Survey of Canada, p. 221–231.*

**Abstract:** Archean carbonate-bearing alkalic igneous complexes are under study in the Harnett Lake, Beaverhouse Lake, and Whalen Lake complexes of the western Quetico metasedimentary belt. Isotopic compositions of calcite indicate a high-temperature origin and are similar to those of carbonatites of all geological ages. The alkaline intrusions are cut by peraluminous granite dykes of 2.67–2.65 Ga. The Archean ages of the intrusions are further supported by low measured values of $^{87}Sr/^{86}Sr$ for apatite and titanite: initial $^{87}Sr/^{86}Sr$ values of 0.701094 and 0.701323 indicate mildly depleted to bulk-earth-like signatures. Bulk-rock compositions show high concentrations of large-ion-lithophile elements (LILE) with negative anomalies for high-field-strength elements. High concentrations of LILE in cumulus clinopyroxenites support an intrinsically alkaline nature for the parental magmas. Combined with low $^{87}Sr/^{86}Sr$, the data are consistent with derivation of the parental magmas from a depleted mantle wedge which had undergone metasomatism not long before the igneous activity.

**Résumé :** Des complexes archéens de roches ignées alcalines à carbonates sont en cours d'étude dans les complexes de Harnett Lake, de Beaverhouse Lake et de Whalen Lake, dans la partie occidentale de la ceinture de roches métasédimentaires de Quetico. Les compositions isotopiques de la calcite sont semblables à celles des carbonatites de tous les âges géologiques et indiquent une formation à haute température. Des dykes de granite hyperalumineux de 2,67 à 2,65 Ga recoupent les intrusions alcalines. Les basses valeurs de $^{87}Sr/^{86}Sr$ mesurées pour les apatites et les titanites corroborent les âges archéens des intrusions. Les valeurs initiales de $^{87}Sr/^{86}Sr$ de 0,701094 et de 0,701323 indiquent des signatures allant de légèrement appauvries au type terrestre globale. Les compositions globales de la roche montrent de fortes concentrations d'éléments lithophiles à grand rayon ionique avec des anomalies négatives pour des éléments à intensité de champ élevé. Les fortes concentrations d'éléments lithophiles à grand rayon ionique dans les clinopyroxénites à cumulus témoignent de la nature intrinsèquement alcaline des magmas parentaux. Ces données, alliées aux basses valeurs de $^{87}Sr/^{86}Sr$, portent à croire que les magmas parentaux sont dérivés d'un biseau mantellique appauvri qui a subi un métasomatisme peu avant que ne débute l'activité ignée.

[1] Department of Earth Sciences, University of Ottawa, Ottawa, Ontario K1N 6N5

# INTRODUCTION

Alkaline igneous rocks are rare in Archean sequences and reported occurrences are almost exclusively from metavolcanic terranes (e.g. Brooks et al., 1982; Ben Othman et al., 1990; Laflèche et al., 1991; Cavell et al., 1992; Blichert-Toft et al., 1996) possibly because assimilation of metasedimentary rocks easily modifies alkaline melt compositions. The Quetico metasedimentary belt of the Superior Province contains alkaline plutons which may be used as probes of mantle sources distinct from those that produced greenstone-granite terranes. Furthermore, the syn- to late tectonic timing of emplacement of the alkaline bodies may provide clues to processes that resulted in final cratonization of the Superior Province.

Carbonate-bearing alkaline rocks are extremely rare in the Archean rock record (e.g. Sage, 1991), and small carbonatite dykes have only recently been reported from the Superior Province (Bédard and Chown, 1992; Skulski et al., 1997). This report documents three calcite-bearing alkaline complexes of the western Quetico metasedimentary belt of the southern Superior Province in Ontario. The intrusions display bird's-eye aeromagnetic anomalies that had previously been interpreted as alkaline complexes (Pye and Fenwick, 1984); however, no published descriptions were available, and this is the first report of magmatic carbonate from these rocks. The Beaverhouse, Harnett, and Whalen Lake complexes are variably exposed along the shores and islands of these lakes. A fourth complex, at Samuels Lake, was reported to contain pyroxenite and hornblendite with significant PGE contents (Blackburn et al., 1988).

## *Geological setting*

The Quetico metasedimentary belt consists primarily of turbiditic greywackes and their metamorphosed equivalents (Fig. 1). Paragneiss, migmatites, and peraluminous granites appear to have been derived from greywackes. Detrital zircons from greywackes in the northern Quetico indicate provenance ages ranging from ca. 3.0 Ga to 2698 Ma and the sedimentation is narrowly constrained to be younger than the youngest zircon (2698 Ma) and older than a tonalitic intrusion (2696 Ma; Davis et al., 1990; Davis and Corfu, 1995). Younger depositional ages are evident from the southern Quetico metasedimentary belt, where detrital zircons as young as 2.690 Ga have been reported (Zaleski et al., 1997).

The belt was deformed shortly after the sedimentation as the principal deformation event is ca. 2.69 Ga, bracketed by the youngest deformed rocks and oldest undeformed plutons. The sedimentary rocks were intruded by early tonalite, a suite of mafic-ultramafic rocks, several alkaline igneous bodies, and two or more generations of granite and pegmatite. One of the best studied igneous bodies is the Poohbah complex with a K/Ar age of ca. 2706 Ma (Mitchell, 1976) and a Pb-Pb isochron age of 2667 Ma (Tilton and Kwon, 1990). The former old age may be due to the presence of excess Ar, common in many alkaline rocks.

Metamorphic grade increases through a low-pressure (2–3 kb), high-temperature facies series from greenschist grade near the belt margins to migmatite grade toward the axis of the belt, which contains voluminous peraluminous granite with ages ranging from 2.67 to 2.65 Ga (Percival and Sullivan, 1988; Percival, 1989; Southwick, 1991). The Quetico metasedimentary belt in the study area contains abundant pegmatitic dykes of peraluminous (two-mica) granite and biotite granite. The Harnett and Whalen Lake complexes intrude staurolite-grade metasedimentary rocks near the northern margin of the belt, whereas the country rocks of the Beaverhouse Lake complex in the central portion of the belt are sillimanite-grade schists.

## *Relationship with the host sedimentary rocks and age of complexes*

Metasedimentary rocks close to the intrusive complexes and in the xenoliths are foliated, equigranular, biotite-quartz-plagioclase+hornblende schists with foliation defined by the preferred orientation of biotite and hornblende. Metamorphic aureoles are not evident around the complexes, but the host metasedimentary rocks underwent alkali metasomatism as is evident from the occurrence of blue alkali amphibole.

Regional deformation effects appear to be confined to the margins of the intrusions. The interiors of the igneous complexes retain their primary igneous textures and minerals, and foliations are not evident even under the microscope. The margins of the complexes, especially apophyses within the host metasedimentary rocks, are foliated and folded. The style of deformation observed in the margins is similar in fold style and intensity to that in the host rocks, suggesting that the complexes intruded before or during the regional deformation. This observation is consistent with the presence of peraluminous granite dykes that cut the complexes, thereby providing a minimum age for the alkaline intrusions of 2.65 Ga.

## *Alkaline intrusive complexes*

The Beaverhouse Lake, Whalen Lake, and Harnett Lake complexes are northeasterly elongate oval plutons. They have syenitic phases with common appearance, but there are substantial differences in the composition of associated rock types and in internal textures. Most rock units, except for local quartz-bearing varieties, contain calcite that reacts with 10% HCl solution. Melanocratic units contain generally high calcite contents. The prefixes 'mela' and 'leuco' are used for rocks with mafic mineral contents greater than 35% and less than 10%, respectively.

The Beaverhouse Lake complex is a 5 by 3 km body made up predominantly of medium-grained augite-hornblende-biotite syenite. It encloses cognate xenoliths of coarse melanocratic clinopyroxene-biotite syenite containing some calcite. The relative proportion of intrusive phases is not known. An approximately 50 m wide, 500 m long dyke extends northward from the main body into country-rock migmatitic paragneiss. The dyke consists of subhorizontal compositional layers on a 10–100 cm scale, K-feldspar-megacrystic syenite

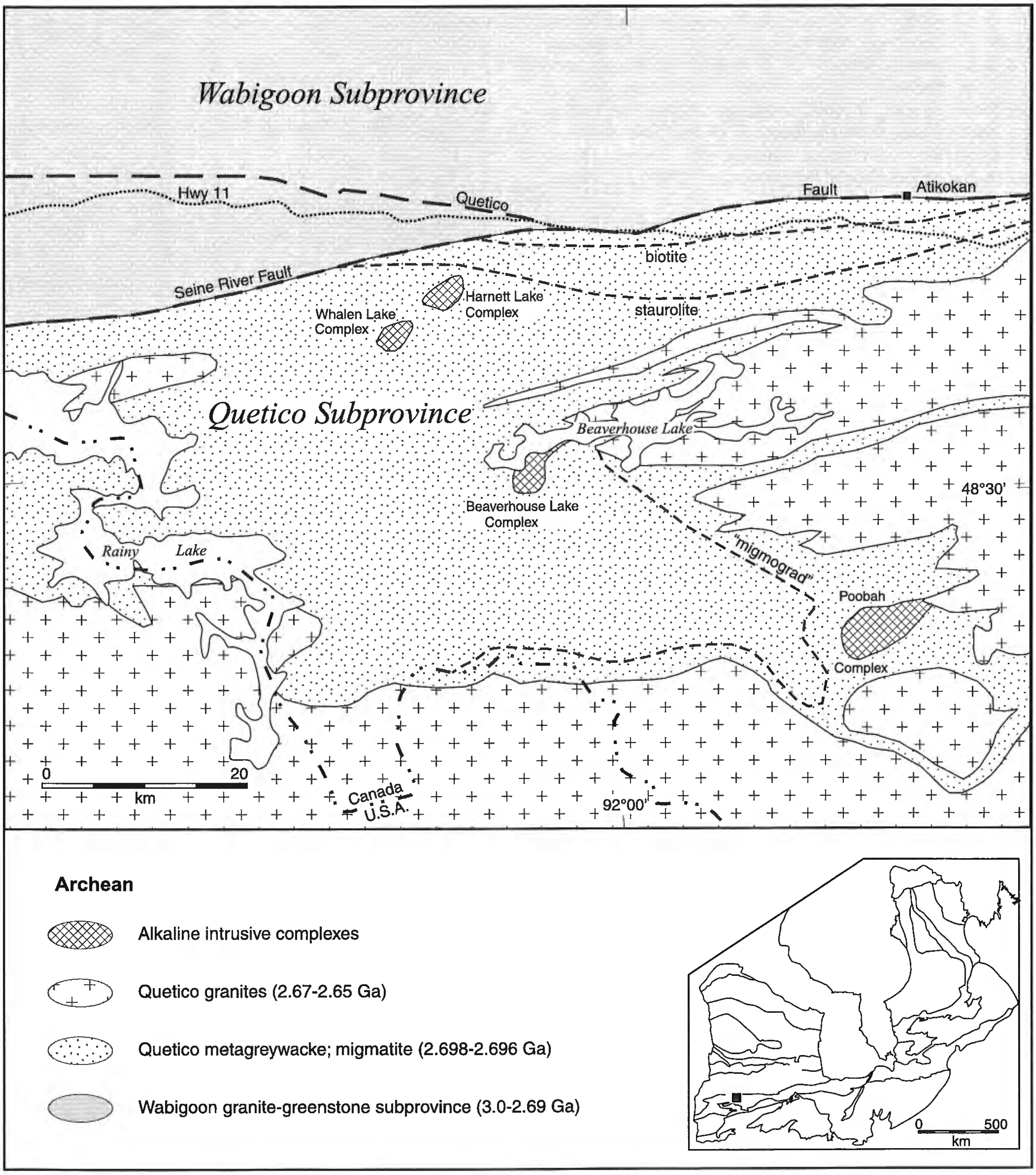


***Figure 1.*** *Location map showing the Beaverhouse, Harnett, Whalen, and Poohbah igneous complexes of the western Quetico belt (modified after Percival, 1988a, b). Inset map shows location of study area in the western Superior Province.*

(Fig. 2) and various coarse-grained, calcite-rich (up to 50%) silicocarbonatite phases. The latter rocks contain variable proportions of biotite, perthitic K-feldspar, aegirine augite, titanite, and apatite in addition to calcite (Fig. 3). Other less-common minerals include alkali amphibole, allanite, and eudialite (tentative identification). Strongly aligned K-feldspar megacrysts form a trachytic texture, suggesting that the magmas were emplaced as crystal-laden mushes. This body of the Beaverhouse Lake complex appears to be the most silica undersaturated, with abundant evidence of nepheline pseudomorphs.

Fine-grained gabbro-basalt occurs in an isolated outcrop on the western shore of the lake. Judging from its location and the general absence of any mafic extrusive rocks in the Quetico metasedimentary belt, it appears to be a part of the intrusive complex. However, the fine-grained massive unit with its smooth-weathering surface is different from other intrusive phases in its lack of calcite and abundant euhedral epidote. Field relationships with other intrusive phases or the metasedimentary rocks were not established.

The alkaline complexes to the northwest intrude lower-grade metasedimentary schists. The Whalen Lake complex is a heterogeneous 2 by 4 km pluton. It consists of relatively mafic (25–30% combined hornblende and biotite) medium-grained syenite, commonly with metasedimentary and cognate monzodiorite xenoliths. Some enclaves have ovoid shapes and thin chill margins, suggestive of magma mingling processes, as are thin monzodiorite dykes with cuspate margins. More-mafic enclaves (coarse-grained hornblende clinopyroxenite, hornblendite) are interpreted as cumulates. Coarse-grained melasyenite, possibly a marginal phase of the pluton, consists of clinopyroxene and K-feldspar, with accessory calcite, titanite, and epidote.

The 3 by 5 km Harnett Lake pluton cuts amphibolite-facies metagreywacke. It consists mainly of medium-grained, leucocratic hornblende-biotite+clinopyroxene syenite, with accessory magnetite, titanite, calcite, and epidote. Compared to the other two complexes, these rocks are more leucocratic and have undergone more hydrous alteration. Minor quartz grains are present in the most leucocratic phases. Coarse epidote is present and augite is commonly altered to epidote and hornblende. Hornblende grains have a mottled colour with uneven extinction, common for hornblende that has undergone hydrothermal alteration. Biotite is variably replaced by chlorite. Mafic phases occur in faintly layered poikilitic melasyenite whose K-feldspar oikocrysts enclose clinopyroxene, hornblende, biotite, and calcite (Fig. 4). Aggregates of euhedral alkali amphibole were noted in fractures. Leucocratic syenite contains up to 5% quartz in addition to minor calcite which is likely of hydrothermal origin.

Calcite in all of the intrusions is commonly coarsely crystalline and in some rocks, is enclosed in aegirine augite (Fig. 5), apatite, and perthite bearing fine lamellae without evidence of low-temperature alteration. Weathered surfaces are commonly irregularly mottled due to erosion of carbonates and probable nepheline. Although the presence of nepheline has not been confirmed, angular aggregates of fine mica

***Figure 2.*** *Trachytic texture in K-feldspar-megacrystic nepheline syenite, Beaverhouse Lake complex. Hammer handle is 30 cm long.*

***Figure 3.*** *Layered silicocarbonatite in the Beaverhouse Lake complex. Colour variations result from differences in proportions of calcite, biotite, and aegerine-augite.*

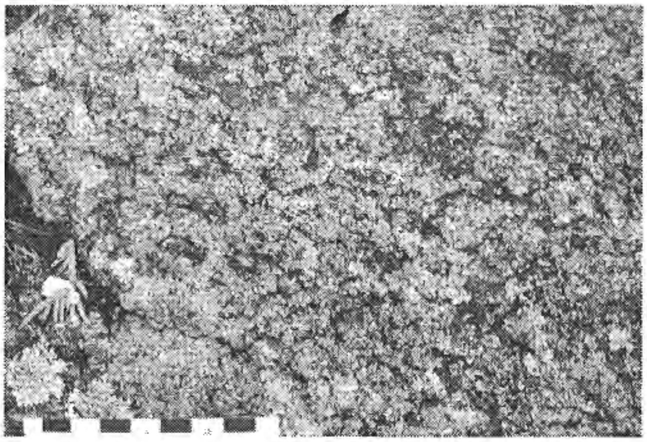

***Figure 4.*** *Poikilitic melasyenite, Harnett Lake complex. Perthite oikocrysts enclose biotite, hornblende, and pyroxene inclusions. Scale bar in centimetres.*

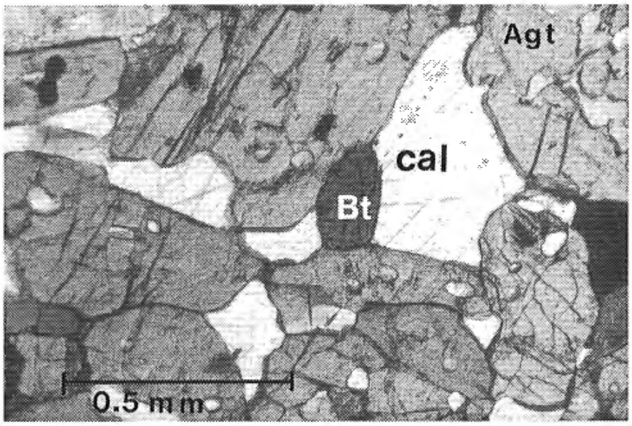


*Figure 5. Calcite enclosed in aegirine augite in melasyenite of Beaverhouse Lake Complex. Bt = biotite, cal = calcite, Agt = augite.*

and clay minerals are likely pseudomorphs after nepheline phenocrysts. They are most abundant in rocks with high amounts of calcite and augite. None was observed in leucocratic rocks nor hornblende-bearing rocks. Hornblende occurs as a late-stage magmatic phase mantling clinopyroxene, and as an alteration product after augite. Blue decussate alkali-amphibole grains up to 10 cm long are present along joints and fractures in several locations.

The Poohbah complex (Mitchell and Platt, 1979; Sage, 1988) is only 30–40 km southeast of the studied intrusions, but the mineralogy is significantly different. Garnet and nepheline are significant phases at Poohbah; garnet has not been recognized in the study area. Conversely, primary calcite has not been reported at Poohbah, but is volumetrically significant in the Beaverhouse, Harnett, and Whalen Lake complexes.

### *Bulk chemical compositions*

Syenitic phases contain coarse minerals with highly variable abundances, making it difficult to obtain representative bulk compositions. Furthermore, rocks commonly display centimetre-scale melanocratic layers. These characteristics produce large variations in the absolute abundance of elements (Table 1). However, it is clear that the rocks are alkaline, except for quartz-bearing leucocratic syenite. Melanocratic syenites contain high amounts of total alkalis ($Na_2O$ + $K_2O$) ranging from 4.7 weight per cent at 35.3 weight per cent $SiO_2$ to 8.9 weight per cent at 52.4 weight per cent $SiO_2$, and they all plot in the alkaline rock field on an alkali-silica diagram (Irvine and Baragar, 1971). An alkaline nature for the intrusions is consistent with the occurrence of aegirine augite and phlogopitic biotite (Table 2).

The intrusions also contain variable abundances of accessory minerals such as apatite, allanite, and titanite. These minerals contain high concentrations of trace elements such as REEs and Y, and their presence strongly influences bulk compositions. Primitive-mantle-normalized patterns are surprisingly similar among samples (Fig. 6). Many samples show negative Nb, P, and Ti anomalies. In the absence of data for heavy rare-earth elements, it is difficult to identify the negative Ti anomaly; however, its consistently low normalized values with respect to Y support this inference.

Clinopyroxenite has high MgO, Cr, and Ni contents (Table 2), reflecting the cumulate nature of the rock, yet it also has very high concentrations of large-ion lithophile elements (LILE) including light rare earth elements (LREE). This confirms the intrinsically alkaline nature of the intrusions.

Normalized trace-element patterns are characterized by negative anomalies for Nb and Ti with high LILE. High ratios of LILE/HFSE (high field-strength elements) are generally considered to be 'arc' signatures. The parental magmas likely originated in a mantle-wedge environment that had undergone metasomatic enrichment in LILE during the subduction process. Among the HFSE, Zr does not show negative

**Table 1.** Representative composition of bulk rocks.

| sample no. | 98627-3 | 98627-8 | 98626-3 | 98625-3 |
|---|---|---|---|---|
| $SiO_2$ | 35.33 | 64.72 | 47.2 | 47.03 |
| $TiO_2$ | 0.85 | 0.31 | 0.89 | 1.65 |
| $Al_2O_3$ | 11.32 | 16.2 | 10.68 | 15.7 |
| $Fe_2O_3$(total) | 11.21 | 2.23 | 10.58 | 12.04 |
| MnO | 0.24 | 0.05 | 0.38 | 0.15 |
| MgO | 4.44 | 0.73 | 10.70 | 4.24 |
| CaO | 17.88 | 1.91 | 12.29 | 9.06 |
| $Na_2O$ | 1.66 | 5.6 | 1.27 | 4.28 |
| $K_2O$ | 2.69 | 4.65 | 2.04 | 1.68 |
| $P_2O_5$ | 3.10 | 0.15 | 0.76 | 1.58 |
| LOI | 9.0 | 2.9 | 2.0 | 1.7 |
| V | 139 | 28 | 148 | 214 |
| Cr | 8 | 20 | 723 | 16 |
| Co | 21 | 4 | 42 | 29 |
| Ni | 10 | 3 | 232 | 13 |
| Zn | 140 | 58 | 186 | 153 |
| Rb | 27 | 141 | 67 | 41 |
| Sr | 2989 | 611 | 1121 | 1771 |
| Y | 52 | 14 | 24 | 35 |
| Zr | 34 | 274 | 113 | 108 |
| Nb | 13 | 24 | 56 | 18 |
| Ba | 1983 | 889 | 435 | 767 |
| La | 231 | 42 | 88 | 93 |
| Ce | 462 | 65 | 179 | 200 |
| Nd | 304 | 31 | 103 | 134 |
| Pb | 4 | 10 | 4 | 12 |
| Th | 1.89 | 6.9 | 7.63 | 4.1 |
| U | 2.8 | <1.0 | <1.0 | <1.0 |
| Ga | 18.8 | 22.4 | 15.6 | 20.2 |

Note: The composition was determined by a X-ray fluorescent spectrometer, PW 2400, after the fusion of samples with a mixture of $Li_2B_4O_7$ and $Li_2CO_3$

98627-3: Calcite-augite-hornblende melasyenite from Harnett Lake complex
98627-8: Hornblende-quartz syenite, central Harnett Lake
98626-3: Calcite-biotite-hornblende melasyenite from the Beaverhouse Lake complex
98625-3: Biotite-hornblende syenite from the Whalen Lake complex

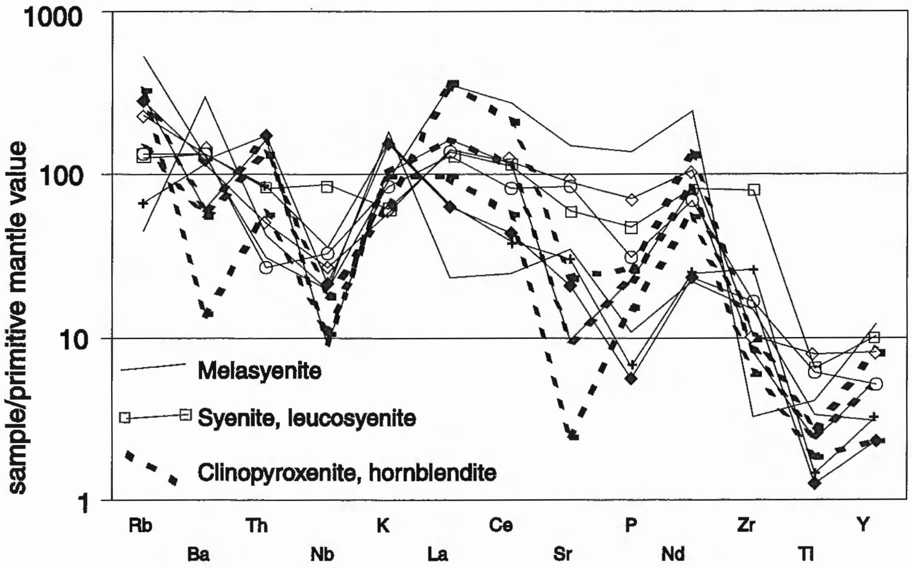


*Figure 6.*

*Primitive mantle-normalized trace-element pattern for minor and trace elements. Normalization factors from McDonough and Sun (1995).*

**Table 2a.** Representative clinopyroxene compositions.

| sample no. | 6-18fpc | 6-18epc |
|---|---|---|
| $SiO_2$ | 53.56 | 54.97 |
| $TiO_2$ | 0.42 | 0.00 |
| $Al_2O_3$ | 1.37 | 1.18 |
| $Fe_2O_3$ | 8.69 | 8.76 |
| FeO | 6.92 | 7.67 |
| MnO | 0.30 | 0.45 |
| MgO | 8.60 | 8.12 |
| CaO | 16.34 | 15.36 |
| $Na_2O$ | 4.51 | 5.06 |
| Total | 100.74 | 101.57 |
| $Si^{4+}$ | 3.998 | 4.067 |
| $Al^{3+}$(IV) | 0.002 | 0.000 |
| | 4.000 | 4.067 |
| $Al^{3+}$(VI) | 0.119 | 0.103 |
| $Fe^{3+}$ | 0.448 | 0.488 |
| $Ti^{4+}$ | 0.024 | 0.000 |
| $Fe^{2+}$ | 0.410 | 0.474 |
| $Mn^{2+}$ | 0.000 | 0.028 |
| $Mg^{2+}$ | 0.957 | 0.896 |
| | 2.000 | 1.989 |
| $Fe^{2+}$ | 0.022 | 0.000 |
| $Mn^{2+}$ | 0.019 | 0.000 |
| $Ca^{2+}$ | 1.307 | 1.218 |
| $Na^{+}$ | 0.653 | 0.726 |
| | 2.001 | 1.944 |
| Wo | 33.80 | 32.86 |
| En | 22.70 | 20.24 |
| Fs | 10.46 | 14.07 |
| Jd | 5.63 | 5.75 |
| Ae | 26.38 | 31.16 |
| Ka | 0.98 | 0.00 |

**Table 2b.** Representative compositions of biotite.

| sample no. | 7-5GBC | 5-3bbc |
|---|---|---|
| $SiO_2$ | 35.79 | 36.70 |
| $TiO_2$ | 0.42 | 1.33 |
| $Al_2O_3$ | 14.19 | 14.56 |
| $Fe_2O_3$ | 4.43 | 6.28 |
| FeO | 16.39 | 13.94 |
| MnO | 0.44 | 0.25 |
| MgO | 10.88 | 12.34 |
| $Na_2O$ | 0.02 | 0.08 |
| $K_2O$ | 9.65 | 9.04 |
| SrO | 0.23 | 0.11 |
| BaO | 0.02 | 0.73 |
| F | 0.44 | 0.01 |
| Cl | 0.03 | 0.00 |
| Total | 94.13 | 95.50 |
| $Si^{4+}$ | 5.601 | 5.591 |
| $Al^{3+}$(IV) | 0.399 | 0.409 |
| | 6.000 | 6.000 |
| $Al^{3+}$(VI) | 2.000 | 2.000 |
| $Fe^{3+}$ | 0.000 | 0.000 |
| | 2.000 | 2.000 |
| Ti | 0.188 | 0.153 |
| $Fe^{2+}$ | 2.145 | 1.776 |
| Mn | 0.059 | 0.032 |
| Mg | 2.537 | 2.802 |
| | 6.072 | 6.098 |
| $Na^{+}$ | 0.007 | 0.024 |
| $K^{+}$ | 1.926 | 1.758 |
| $Sr^{2+}$ | 0.0226 | 0.020 |
| $Ba^{2+}$ | 0.007 | 0.045 |
| | 1.9626 | 1.856 |
| F | 0.217 | 0.04 |
| Cl | 0.008 | 0.00 |
| | 0.225 | 0.004 |

anomalies. Variable normalized ratios of Zr/Nd are common in many rocks, including subduction-related rocks (e.g. Hattori et al., 1996).

A gabbro sample from the Beaverhouse Lake complex has a very primitive geochemical character with high MgO (>10 %) and Cr (723 ppm), yet it also contains high LILE. Its LREE content is over 300 times chondritic values. The trace-element pattern is significantly different from the syenite patterns. It is similar to typical patterns for oceanic-island basalts. Unfortunately, the sample is highly altered with abundant epidote (10 %) and pyrite (~ 3 %). In addition, the relationship with other intrusive phases and metasedimentary rocks is not understood. The significance of this gabbro will be evaluated after obtaining a full spectrum of trace-element data from less-altered samples collected in subsequent fieldwork.

### *Stable isotopic compositions of carbonates*

Calcite shows isotopic compositions between $\delta^{13}C$ = -2.91 to - 10.09 ‰ and $\delta^{18}O$ = +8.2 to 11.2 ‰ (Table 3; Fig. 7). Carbon-isotope values for calcite from the least altered samples are clustered around ~ - 4 ‰. The data are comparable to those for mantle-derived carbon and unaltered carbonatites of all ages, which are considered to range from - 4 to - 8 ‰ (Kyser, 1986; Deines, 1989; Reid and Cooper, 1992; Veizer et al., 1989).

Oxygen-isotope data support a high-temperature origin for calcite. Calcite formed at low temperatures would have much higher $^{18}O$ because of large isotopic fractionation factors between calcite and water. Recrystallization of calcite during the cooling of the intrusions would raise the values of $\delta^{18}O$. The values for primary carbonatite range from + 6 to + 10 ‰ (Reid and Cooper, 1992). Deines (1989) shows a positive correlation between $\delta^{13}C$ and $\delta^{18}O$ for calcite from carbonatites. The observed isotopic compositions from the studied igneous rocks fit well with the values for the majority of primary carbonatites compiled by Deines (1989).

Relatively high $\delta^{18}O$ and low $\delta^{13}C$ values for calcite in a sample taken from rock adjacent to a pegmatite dyke suggests that the calcite underwent re-equilibration with carbon with low $^{13}C$, possibly derived from peraluminous granite.

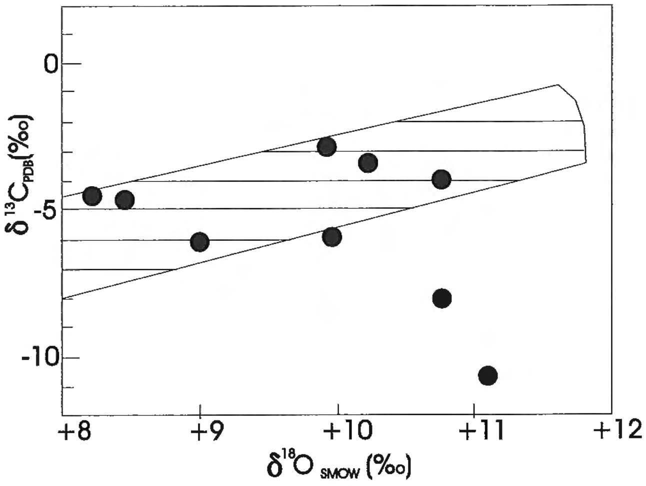


*Figure 7.* *$\delta^{13}C_{PDB}$ and $\delta^{18}O_{SMOW}$ for calcite. SMOW = standard mean ocean water, PDB = Peedee belemnite. The field of carbonatites is shown as a striped area (after Deines, 1989; Reid and Cooper, 1992).*

**Table 3.** Isotopic compositions of calcite.

| sample no. | Rock Type* | $\delta^{13}C_{PDB}$ (‰) | $\delta^{18}O_{SMOW}$ (‰) |
|---|---|---|---|
| 98625-10 | Hbl melasyenite, WHL | -7.26 | +10.06 |
| 98626-6 | Cal-Ap band in melasyenite, BHL | -4.36 | +8.29 |
| 98626-6B | Cal-rich portion of melasyenite, BHL | -4.46 | +8.51 |
| 98626-9 | Bt syenite, BHL | -3.97 | +10.57 |
| 98626-10 | Bt-Cpx melasyenite, BHL | -2.91 | +9.75 |
| 98626-11 | Bt-Cpx melasyenite, least altered in the BHL | -3.20 | +10.06 |
| 98627-12 | Bt-Cpx melasyenite least altered specimen in the HNL | -6.1 | +9.24 |
| 98626-16 | altered lamprophyre in BHL | -8.03 | +9.04 |
| 98625-11 | adjacent to granite pegmatite, WHL | -10.09 | +11.10 |

Note: Isotopic measurement was carried out with a Sira 12 mass spectrometer on $CO_2$ gas extracted from bulk rock samples after the reaction with 100% $H_3PO_4$ at 25°C (McCrea, 1950). The use of bulk rock samples is a well established analytical procedure for isotopic composition of calcite disseminated in silicate rocks (e.g., Lattanzi et al, 1980; Hattori and Sakai, 1980; Hattori and Muehlenbachs, 1982; Stakes and O'Neil, 1982).

* Abbreviations:
Ap = apatite
BHL = Beaverhouse Lake Complex
Cal = calcite
Cpx = augite
HNL = Harnett Lake Complex
WHL = Whalen Lake Complex
Hbl = hornblende
Bt = biotite

**Table 4.** Strontium isotopic compositions of mineral separates.

| sample no. | mineral | Rb (ppm)* | Sr (ppm) | $^{87}Sr/^{86}Sr$ measured* | $^{87}Rb/^{86}Sr$ | $^{87}Sr/^{86}Sr$ (2680Ma)** | εSr*** (2680Ma) |
|---|---|---|---|---|---|---|---|
| 98625-3 | Titanite | 0.080 | 60.75 | 0.701247 ± 21 | 0.00524 | 0.701094 | -2.8 |
| 98626-6 | Apatite | 0.420 | 360.5 | 0.701454 ± 11 | 0.00337 | 0.701323 | +0.4 |

Note: 98625-3 = hornblende-biotite melasyenite, Whalen Lake Complex
98626-6 = apatite-rich band in silicocarbonatite, Beaverhouse Lake Complex
* Isotopic compositions were measured in static mode with a six-collector thermal-ionization mass spectrometer (Finnigan MAT 261), and the ratios were normalized to $^{86}Sr/^{88}Sr$ of 0.1940. NBS987 yielded $^{87}Sr/^{86}Sr$ of 0.710252 ± 16. Concentrations of Sr and Rb were determined by isotopic dilution technique using a mixed spike of $^{84}Sr/^{87}Rb$ to a quarter of the digested samples. Errors reported are 2 σ values.
** Initial ratios were calculated at 2680 Ma. Uncertainty of the age, ~ 20 Ma, would not result in any difference in the calculation of initial $^{87}Sr/^{86}Sr$.
*** Bulk Earth parameters used for the calculation are $^{87}Sr/^{86}Sr$ = 0.704755 and $^{87}Rb/^{86}Sr$ = 0.08923 (Allègre et al, 1983).

### *Strontium isotopic compositions of mineral separates*

Pure mineral separates of titanite and apatite yielded low measured $^{87}Sr/^{86}Sr$ values, 0.701247 ± 21 and 0.701454 ± 11, and confirm an Archean age for the intrusions (Table 4). Very low Rb/Sr ratios of the minerals made it possible to obtain precise initial $^{87}Sr/^{86}Sr$ at 2.68 Ga, 0.70109 and 0.70132. Uncertainties on the order of 20 Ma in the age of the intrusions would not change the calculated initial ratio. The values are similar to those from Archean alkaline rocks of the Abitibi greenstone belt (0.70155; Laflèche et al., 1991; 0.7008–0.7016; Hattori et al., 1996).

The values suggest that the parental magmas originated from a slightly depleted to a bulk-earth-like mantle. The bulk-earth-like value could have been obtained through minor contamination by sedimentary rocks, either during ascent or through a subducted component in the mantle wedge. Considering the depletion in HFSE and low $SiO_2$ contents, it is more likely that the parental magmas acquired their $^{87}Sr$ from slabs. This hypothesis will be tested with Nd isotope data of these samples.

## DISCUSSION

### *Origin of calcite*

The origin of carbonate in alkaline rocks has been controversial, as demonstrated in discussions on recent carbonate-bearing alkaline volcanic rocks in central Italy (e.g. Stoppa and Woolley, 1997; Stoppa and Cundari, 1998; Peccerillo, 1998). In the Quetico alkaline intrusive complexes, the occurrence of calcite and apatite inclusions within aegirine augite (Fig. 5) suggests that the calcite crystallized at magmatic temperatures, together with the silicate minerals. This inference is supported by the low $\delta^{18}O$ values, as described above (Table 3). This in turn implies that the parental magmas had high carbonate contents. Considering the lack of carbonates in the host metagreywackes, the carbonate must have been derived either from the mantle source or from the deep crust. Limestone in the deep crust or in subducted carbonates could have contributed to the parental magmas of the studied igneous rocks. Marine limestone generally has higher $^{87}Sr/^{86}Sr$ than the contemporaneous mantle, although Archean limestones have relatively low $^{87}Sr/^{86}Sr$ (e.g. Veizer et al., 1989). For example, $^{87}Sr/^{86}Sr$ values for the Steep Rock Lake limestone (ca.3.0 Ga) near Atikokan are mostly around 0.7022 (Veizer, 1971) and those for Hammersley basin of Australia (ca. 2.7Ga) are over 0.705. Limestone carbonates generally contain high Sr contents (normally several thousand parts per million) and significant contributions of marine carbonate would raise $^{87}Sr/^{86}Sr$ of silicate melts. Furthermore, clastic sediments associated with limestones would likely also contribute their radiogenic Sr to the melt. If sedimentary carbonates had contributed significantly to the parental magmas, the $^{87}Sr/^{86}Sr$ isotopic compositions would be much higher than those observed, which are less than 0.7015.

Limestone has high $\delta^{18}O$ values, greater than +30 ‰. Assimilation of marine limestone would increase $d^{18}O$ of the melt, and resultant minerals. As described above, the observed $\delta^{18}O$ values are similar to those of many mantle-derived carbonates. This supports the hypothesis that calcite in the studied samples is indeed magmatic, not derived from limestone.

Evidence commonly used to identify calcite of carbonatitic affiliation includes high concentration of LILE in the host rocks, $\delta^{13}$ values near – 5 ‰, low $^{87}Sr/^{86}Sr$, high Sr and Ba contents in calcite, and the existence of other unusual minerals in the host rocks (e.g. Barker, 1996). Unfortunately, none of these characteristics is unique for carbonatitic calcite. For example, calcite with similar carbon isotopic compositions may occur in marble or hydrothermal veins. High Sr and Ba contents are also common in hydrothermal calcite. Nevertheless, the studied samples display all of these criteria.

Carbonatites generally contain high Nb and Ta contents, unlike the studied samples which have relatively low Nb (Table 1). Several Italian carbonatites have low Nb, thought to reflect mantle source characteristics (e.g. Stoppa and Cundari, 1998). In summary, the evidence presented above strongly supports the interpretation that the carbonates in the studied rocks are magmatic and mantle derived.

### *Significance of carbonate-bearing intrusions in Quetico metasedimentary belt*

The Quetico belt contains several alkaline intrusions. The largest is the Poohbah complex (Mitchell and Platt, 1979; Sage, 1988). Other intrusions include a small aegirine augite–bearing syenite stock near the northern boundary adjacent to the Wabigoon metavolcanic belt (Kresz and Zayachivsky, 1988) and minor nephelinitic rocks in the vicinity of the southern boundary of the Quetico belt to the west in Minnesota (Boerboom, 1994). Defining the spatial distribution of alkaline intrusions and comparison of their characteristics will further constrain the tectonic setting and evolution of the Quetico belt.

The arc-like geochemical signature and occurrence of magmatic carbonate in the alkaline rocks may provide useful constraints on the tectonic setting of the Quetico belt during the intrusive activity. Crosscutting 2.67–2.65 Ga granites suggest that the alkaline magmatism took place shortly after sedimentation. Thus the studied intrusions provide information relevant to the tectonic regime during the 25–45 Ma period between sedimentation and granitic magmatism.

The Quetico metasedimentary belt has been variably interpreted as an accretionary prism (Percival and Williams, 1989; Devaney and Williams, 1989; Fralick et al., 1992) or collisional forearc basin, based on detrital zircon populations (Davis, 1997). It shares many characteristics with the Paleoproterozoic Kisseynew belt, interpreted as a back-arc basin (Ansdell et al., 1995). Alkaline rocks are reported in active forearc basins (e.g., Stein et al, 1996), but there appears to be no modern analogue for silica-undersaturated carbonate-bearing alkaline magmatism in this setting. If the alkaline rocks intruded a forearc basin shortly after or during sediment deposition, the mantle-derived magmatism would have occurred in an anomalously near-trench setting. Magmas of asthenospheric derivation have been inferred to have penetrated the slab in zones of hinge faulting, along subducting fracture zones in active forearc regions (DeLong et al., 1975). A 'slab window' for the ascent of asthenosphere-derived magmas can be formed by ridge-trench collisions (e.g. Hole et al., 1994). However, the arc-like signatures of the alkaline rocks mitigate against interpretations involving asthenosphere-derived magmas through thin oceanic crust. Shallow levels of magma generation in forearc settings are unlikely in light of the presence of magmatic carbonate in the alkaline rocks.

Conversely, if the Quetico metasedimentary rocks formed in a back-arc setting, the sedimentation and magmatism would be related to subduction an unspecified distance to the south. A back-arc basin the size of the Quetico would require an extensional regime for a significant length of time, and magmatism in the belt should reflect such a setting. If the alkaline rocks are the product of an extensional setting, far from a trench, the magmatic activity could have started early and lasted throughout much of the sedimentation period. However, rifting in a back arc generally results in higher degrees of partial melting than those required to produce alkaline magmas, predicting that basaltic-gabbroic magmatism should have followed the emplacement of alkaline rocks. Good examples are found in the Japan Sea back-arc basin, where alkaline rocks occur along the margin of the basin and mafic igneous rocks underlie the sediment-filled basin. Mafic rocks are a very minor component of the Quetico belt and a negative gravity anomaly over the belt does not support the presence of large quantities of mafic igneous rocks at depth. Thus, the occurrence of carbonate-bearing alkaline rocks is not consistent with intrusion in a back-arc setting. The tectonic setting may have changed between the time of sedimentation and that of alkaline magmatism.

The time span between sedimentation and alkaline activity is currently bracketed at 25–45 Ma, a sufficiently long time to accommodate major changes in tectonic regime. For example, in the Kirkland Lake area in the Abitibi belt of the eastern Superior Province, a major change took place in less than 10 Ma, involving a transition from subduction-related dioritic rocks to post-subduction syenitic rocks (Legault and Hattori, 1994a). In conjunction, earlier subduction-related turbidites were tectonically juxtaposed with later collision-related turbidites (Legault and Hattori, 1994b). Thorough evaluation of the significance of the alkaline rocks will require precise age data for the intrusions, constraints on the timing of deformation of the host sedimentary rocks, and emplacement ages for spatially related igneous rocks.

## ACKNOWLEDGEMENTS

We thank Monika Wilk for collecting mineral separates and cation separation, Ron Hartree for XRF analysis, Wendy Palmer for stable isotope analysis, and John Stirling for the electron microprobe analysis. The project was supported by a LITHOPROBE grant. K. Hattori's field expenses are covered by a NSERC research grant. Bruce Kjarsgaard is thanked for helpful review comments.

## REFERENCES

**Allègre, C.J., Hart, S.R., and Minster, J.F.**
1983: Chemical structure and evolution of the mantle and continents determined by inversion of Nd and Sr isotopic data. II. numerical experiments and discussion; Earth and Planetary Science Letters, v. 66, p. 191–213.

**Ansdell, K.M., Lucas, S.B., Connors, K., and Stern, R.A.**
1995: Kisseynew metasedimentary gneiss belt, Trans-Hudson orogen (Canada): back-arc origin and collisional inversion. Geology, v. 23, p. 1039–1043.

**Barker, D.S.**
1996: Carbonatite volcanism; *in* Undersaturated Alkaline Rocks: Mineralogy, Petrogenesis and Economic Potential. (ed.) R.H. Mitchell; Mineralogical Association of Canada, Short Course v. 24, p. 45–61.

**Bédard, L.P. and Chown, E.H.**
1992: The Dolodau dykes, Canada: an example of an Archean carbonatite; Mineralogy and Petrology, v. 46, p. 109–121.

**Ben Othman, D., Arndt, N.T., White, W.M., and Jochum, K.P.**
1990: Geochemistry and age of Timiskaming alkali volcanics and the Otto syenite stock, Abitibi, Ontario; Canadian Journal of Earth Sciences, v. 27, p. 1304–1311.

**Blackburn, C.E., Hailstone, M.R., Parker, J.R, and Storey, C.C.**
1988: Kenora Resident Geologist's district — 1988; *in* Report of Activities, 1988, Resident Geologists, Ontario Geological Survey, Miscellaneous Paper 142, p. 3–40.

**Blichert-Toft, J., Arndt, N.T., and Ludden, J.N.**
1996: Precambrian alkaline magmatism, Lithos, v. 37, p. 97–111.

**Boerboom, T.J.**
1994: Alkalic plutons of northeastern Minnesota; *in* Minnesota Geological Survey, Report of Investigations, p. 20–38

**Brooks, C., Ludden, J., Pigeon, Y., and Hubregtse, J.J.M.W.**
1982: Volcanism of shoshonite to high-K andesite affinity in an Archean arc environment, Oxford Lake, Manitoba; Canadian Journal of Earth Sciences, v. 19, p. 55–67.

**Cavell, P.A., Sijbrans, J.R., and Baardsgaard, H.**
1992: Archean magmatism in the Kaminak Lake area, District of Keewatin, Northwest Territories: ages of the carbonatite-bearing alkaline complex and some host granitoid rocks; Canadian Journal of Earth Sciences, v. 29, p. 896–908

**Davis, D.W.**
1997: Accretion of the Superior Province by collapse of an arc/back-arc/continent margin system: evidence from comparison of U-Pb ages in the Western Superior and Abitibi Lithoprobe transects; *in* Western Superior Transect Second Annual Workshop, (ed.) R.M. Harrap and H. Helmstaedt; Lithoprobe Report 63, p. 92–94.

**Davis, D.W. and Corfu, F.**
1995: Correlations and contrasts among Superior Province terranes from U-Pb geochronology and Hf isotopes; Precambrian '95 Program and Abstracts, Université de Québec à Montréal, p. 34.

**Davis, D.W., Pezzutto, F., and Ojakangas, R.W.**
1990: The age and provenance of metasedimentary rocks in the Quetico Subprovince, Ontario, from single zircon analyses: implications for Archean sedimentation and tectonics in the Superior Province; Earth and Planetary Science Letters, v. 99, p. 195–205.

**Deines, P.**
1989: Stable isotope variations in carbonatites; *in* Carbonatites, Unwin Hyman, London, United Kingdom, p. 301–359.

**DeLong, S.E., Hodges, F.N., and Arculus, R.J.**
1975: Ultramafic and mafic inclusions, Kanaga Island, Alaska, and the occurrence of alkaline rocks in island arcs; Journal of Geology, v. 83, p.721–736.

**Devaney, J.R. and Williams, H.R.**
1989: Evolution of an Archean subprovince boundary: a sedimentological and structural study of part of the Wabigoon–Quetico boundary in northern Ontario; Canadian Journal of Earth Sciences, v. 26, p. 1013–1026

**Fralick, P., Wu, J., and Williams, H.R.**
1992: Trench and slope basin deposits in an Archean metasedimentary belt, Superior Province, Canadian Shield; Canadian Journal of Earth Sciences, v. 29, p. 2551–2557.

**Hattori, K. and Muehlenbachs, K.**
1982: Oxygen isotope ratios of the Icelandic crust; Journal of Geophysical Research, v. 87, p. 6559–6565.

**Hattori, K. and Sakai, H.**
1980: Meteoric hydrothermal origin of calcite in submarine "Green Tuff" formations, Miocene age, Japan; Contributions to Mineralogy and Petrology, v. 73, p. 145–150.

**Hattori, K., Hart, S.R., and Shimizu, N.**
1996: Melt and source mantle compositions in the late Archaean: a study of strontium and neodymium isotope and trace elements in clinopyroxenes from shoshonitic alkaline rocks; Geochimica et Cosmochimica Acta, v. 60, p. 4551–4562.

**Hole, M.J., Sauders, A.D., Rogers, G., and Sykes, M.A.**
1994: The relatioship between alkaline magmatism, lithospheric extension and slab window formation along continental destructive plate margins; Geological Society Special Publication, v. 81, p. 265–285.

**Irvine, T.N. and Barager, W.R.A.**
1971: A guide to the chemical classification of the common volcanic rocks; Canadian Journal of Earth Sciences, v. 8, p. 523–548

**Kyser, K.T.**
1986: Stable isotope variations in the mantle; Reviews in Mineralogy, v. 16, p.141–164

**Kresz, D.U. and Zayachivsky, B.**
1988: Seagram Lake area, District of Thunder Bay, Ontario Geological Survey, Miscellaneous Paper 141, p.173–178.

**Laflèche, M.R., Dupuy, C., and Dostal, J.**
1991: Archaean orogenic ultrapotassic magmatism: an example from the southern Abitibi greenstone belt; Precambrian Research, v. 52, p. 71–96.

**Lattanzi, P., Rye, D.M., and Rice, J.M.**
1980: Behavior of $^{13}C$ and $^{18}O$ in carbonates during contact metamorphism at Marysville, Montana: implications for isotope systematics in impure dolomitic limestone; American Journal of Science, v. 280, p. 890–906.

**Legault, M.I. and Hattori, K.**
1994a: Provenance of igneous clasts in conglomerates of the Archaean Timiskaming Group, Kirkland Lake area, Abitibi greenstone belt, Canada; Canadian Journal of Earth Sciences, v. 31, p. 1749–1762.

**Legault, M.I. and Hattori, K.**
1994b: Late Archaean geological development recorded in the Timiskaming Group sedimentary rocks, Kirkland Lake area, Abitibi greenstone belt, Canada; Precambrian Research, v. 68, p. 23–42.

**McCrea, J.M.**
1950: The isotopic chemistry of carbonates and a paleotemperature scale; Journal of Physical Chemistry, v. 18, p. 849–857.

**McDonough, W.F. and Sun, S.S.**
1995: The composition of the Earth; Chemical Geology, v. 120, p. 223–253.

**Mitchell, R.H.**
1976: Potassium-argon geochronology of the Poohbah Lake alkaline complex, northwestern Ontario; Canadian Journal of Earth Sciences, v. 13, p. 1456–1459.

**Mitchell, R.H. and Platt, R.G.**
1979: Nepheline-bearing rocks from the Poohbah Lake Complex, Ontario; Malignites and malignites; Contributions to Mineralogy and Petrology, v. 69, p. 255–264.

**Peccerillo, A.**
1998: Relationships between ultrapotassic and carbonate-rich volcanic rocks in central Italy: petrogenetic and geodynamic implications; Lithos, v. 43, p. 267–279.

**Percival, J.A.**
1988a: Geology, Quetico, Ontario–United States; Geological Survey of Canada, Map 1682A, scale 1:250 000.
1988b: Geology, International Falls (52A); Geological Survey of Canada, Open File 1479, scale 1:250 000.
1989: A regional perspective of the Quetico belt, Superior Province, Canada; Canadian Journal of Earth Sciences, v. 26, p. 677–693.

**Percival, J.A. and Sullivan, R.W.**
1988: Age constraints on the origin of the Quetico belt, Superior Province, Ontario; *in* Radiogenic and Isotopic Studies: Report 2, Geological Survey of Canada, Paper 88-2, p. 97–107.

**Percival, J.A. and Williams, H.R.**
1989: Late Archean Quetico accretionary complex, Superior Province, Canada; Geology, v. 17, p. 23–25.

**Pye, E.G. and Fenwick, K.G.**
1984: Atikokan–Lakehead sheet; Ontario Department of Mines, Map 2065, scale 1:253 440.

**Reid, D.L. and Cooper, A.F.**
1992: Oxygen and carbon isotope patterns in the Dicker Willem carbonatite complex, Southern Namibia; Chemical Geology, v. 94, p. 293–305

**Sage, R.P.**
1988: Geology of carbonatite-alkalic rock complexes in Ontario: Poohbah Lake alkalic rock complex, District of Rainy River; Ontario Geological Survey, Study 48, 67p.
1991: Alkalic rock, carbonatite and kimberlite complexes of Ontario, Superior Province; *in* Geology of Ontario; Ontario Geological Survey, Special Volume 4, Part 1, p. 683–709.

**Skulski, T., Orr, P., and Taylor, B.**
1997: Archean carbonatite in the Minto block, NE Superior Province; Geological Association of Canada Abstracts, v. 22, p. A138.

**Southwick, D.L.**
1991: On the genesis of Archean granite through two-stage melting of the Quetico accretionary prism at a transpressional plate boundary; Geological Society of America Bulletin, v. 103, p. 1385–1394

**Stakes, D.S. and O'Neil, J.R.**
1982: Mineralogy and stable isotope geochemistry of hydrothermally altered oceanic rocks. Earth and Planet; Science Letters, v. 57, p. 285–304.

**Stein, G., Lapierre, H., and Charvet, J.**
1996: The Miocene Ashizuri Complex (SW Japan) — source and magma differentiation of an alkaline plutonic assemblage in an island arc environment; Bulletin de la Societé Géologique de France vol 167, no. 1, p. 125–139

**Stoppa, F. and Cundari, A.**
1998: Origin and multiple crystallization of the Kamafugite-carbonatite association- the San-Venanzo Pian-Di-Celle occurrence (Umbria, Italy). Mineralogical Magazine, v. 62, p. 273-289.

**Stoppa, F. and Woolley, A.R.**
1997: The Italian carbonatites: field occurrence, petrology and regional significance; Mineralogy and Petrology, v. 59, p. 43–67

**Tilton, G.R. and Kwon, S.T.**
1990: Isotopic evidence for crust-mantle evolution with emphasis on the Canadian Shield; Chemical Geology, v. 83, p. 149–163.

**Veizer, J., Hoefs, J., Lowe, D.R., and Thurston, P.C.**
1989: Geochemistry of Precambrian carbonates: II. Archean greenstone belts and Archean sea water; Geochimica et Cosmochimica Acta, v. 53, p. 859–871.

**Veizer, J.**
1971: Chemical and strontium isotopic evolution of sedimentary carbonate rocks in geologic history; Ph.D. thesis, Australian National University, Canberra, Australia, 151 p.

**Zaleski, E., van Breemen, O., Peterson, V.L., and Fralick, P.**
1997: Provenance and depositional age of Manitouwadge and Quetico greywackes— volcaniclastic input from monzodiorites; Geological Association of Canada, Abstracts, v. 22, p. A162.

Geological Survey of Canada Project 970014

# Mineralogical investigation of sediments from a mercury-contaminated lake in northwestern Ontario

Jeanne B. Percival, Isabelle Drouin-Brisebois[1], and W. Lyle Lockhart[2]
Mineral Resources Division, Ottawa

*Percival, J.B., Drouin-Brisebois, I., and Lockhart, W.L., 1999: Mineralogical investigation of sediments from a mercury-contaminated lake in northwestern Ontario;* in *Current Research 1999-C; Geological Survey of Canada, p. 233–240.*

---

**Abstract:** The form of inorganic mercury in a highly contaminated river-lake system in northwestern Ontario was investigated using routine X-ray powder diffraction analyses and scanning electron microscopy. Evidence for the occurrence of authigenic cinnabar in the peak contaminated zone is shown. The presence of a mercuric sulphide mineral indicates anoxic conditions with depth, limits methylation of mercury in the lake sediment, and accounts for the progressive burial history of contaminated sediments.

**Résumé :** La composition du mercure inorganique dans un système fluviolacustre très contaminé du nord-ouest de l'Ontario a été étudiée au moyen d'analyses systématiques de diffractométrie aux rayons X et de microscopie électronique à balayage. On a relevé des indices de cinabre authigène dans la zone la plus contaminée. La présence d'un minéral de sulfure de mercure témoigne de conditions anoxiques en profondeur et limite la méthylation du mercure dans les sédiments lacustres; elle explique en outre l'histoire d'enfouissement progressif des sédiments contaminés.

---

[1] Department of Earth Sciences, University of Windsor, Windsor, Ontario N9B 3P4
[2] Department of Fisheries and Oceans, 501 University Crescent, Winnipeg, Manitoba R3T 2N6

## INTRODUCTION

Between 1962 and 1970, a chlor-alkali plant in Dryden, Ontario, discharged about 10 t of inorganic mercury into the Wabigoon River system. The chlor-alkali plant was part of the pulp and paper mill complex in Dryden that manufactured caustic soda and chlorine gas by means of a mercury (as electrode) cell through electrolytic decomposition of a brine. In 1970, industry was encouraged by the Federal Environment Minister to voluntarily reduce mercury losses. At this time the discharges from the Dryden plant dropped from 105 g Hg per tonne chlorine (0.21 lb Hg per ton chlorine) produced, to about 3.5 g/t (0.007 pounds per ton), giving a total input of just over 100 g Hg per day (Armstrong and Hamilton, 1973). In 1972, chlor-alkali mercury regulations were introduced by Environment Canada under the Fisheries Act, and in 1975, the chlor-alkali plant was closed (Sherbin, 1979). In addition to uncontrolled mercury discharges in the 1960s, organic wastes from the paper mill had been discharged to the Wabigoon River since 1913 (German, 1969).

The highly contaminated Wabigoon–English River system has been studied extensively since 1970, when it became apparent that biota in the area were highly contaminated (e.g. Vermeer et al., 1973; Armstrong and Hamilton, 1973; Scott, 1974; Parks, 1976). In 1978, a joint federal-provincial study began to examine the biogeochemistry and pathways of mercury, and assess the sources, distribution, and migration of methyl and other forms of mercury in the entire system (Jackson et al., 1980). The results of this two-year study were reported in Jackson (1980) and Allan et al. (1984). In 1995, the site was revisited to determine if mercury peak levels are being buried under cleaner, more recently deposited sediments, and to assess whether the sediment profile accurately records the history of anthropogenic mercury contamination using independent $^{137}Cs$ and $^{210}Pb$ dating techniques. It is hoped that knowledge concerning the form of mercury in these sediments may give insight into its potential mobility.

The objectives of this mineralogical study are 1) to determine the bulk mineralogy of sediments from Clay Lake using routine X-ray diffraction (XRD) methods; 2) identify the form of (inorganic) mercury by XRD and SEM techniques; and 3) evaluate the potential for mobility of mercury within the sediment column based upon results from 1) and 2). This paper reports some preliminary findings and forms the basis of a B.Sc. mineralogical investigation at the University of Windsor.

## STUDY AREA

Clay Lake is located 80 km northwest of Dryden, Ontario along the Wabigoon–English River system (Fig. 1). It occurs in an area of low relief and is covered by boreal forest. Clay Lake occurs in the Winnipeg River Subprovince, a major subdivision of the Archean Superior Province, and is underlain by plagioclase-quartz-biotite gneiss (Twilight gneiss) (Westerman, 1977; Beakhouse, 1991). The Precambrian basement is overlain by Pleistocene glaciolacustrine clay and sandy till deposited in the proglacial Lake Agassiz, forming a regional clay plain (Jackson et al., 1980; Nielson, 1989; Sharpe et al., 1992). Clay Lake is 3000 ha in area, has a maximum depth of 24 m, and an average depth of 8 m. It can be subdivided into two main basins: the western basin is dimictic and thermally stratifies during the summer, whereas the eastern basin is isothermal (Parks and Hamilton, 1987). Sedimentation rate for the lake has been determined to be between 0.6 and 1.0 mm per year (Armstrong and Hamilton, 1973).

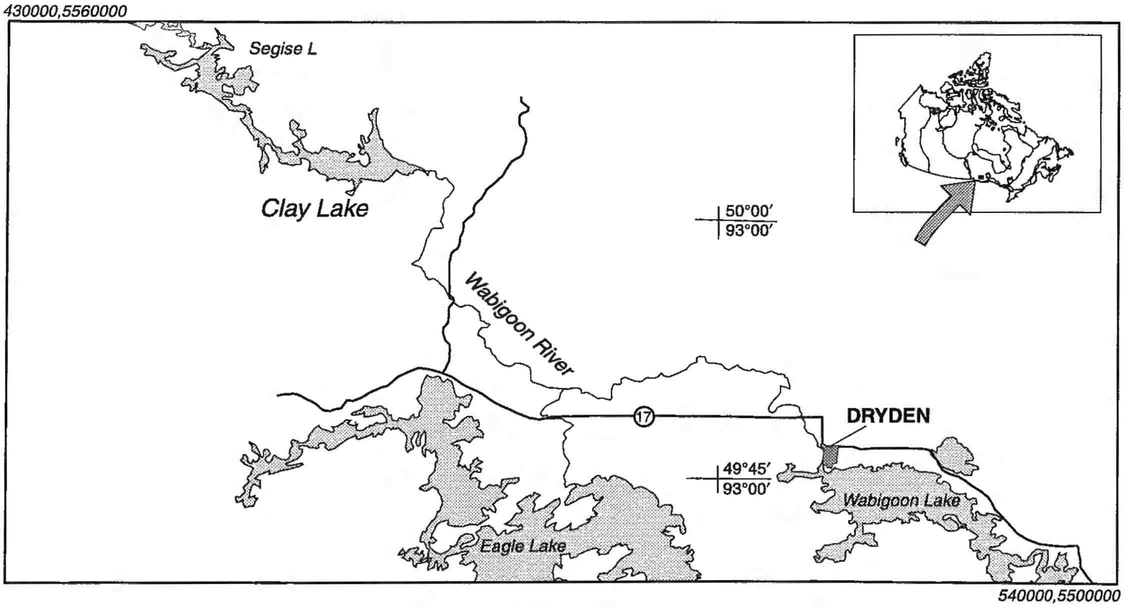


*Figure 1. Location of Clay Lake situated along the Wabigoon–English River system in northwestern Ontario.*

## MATERIALS AND METHODS

In 1995, three cores were taken from Clay Lake using a 10 cm KB corer fitted with a plastic tube; locations were determined using a hand-held GPS and were aligned with previous coring sites (Fig. 2). The cores were extruded in the field and 0.5 cm slices were bagged and returned to the laboratory where they were freeze-dried. Splits from these slices were sent to the GSC for Pb isotopic analyses (Outridge, pers. comm., 1998). Splits from 35 samples from core 3 were provided to the X-ray laboratory for detailed mineralogical analyses.

A subsample of freeze-dried material from each slice was counted on a gamma spectrometer using a hyper-pure germanium crystal to determine $^{7}Be$, $^{137}Cs$, and $^{134}Cs$. Then, 1–2 g aliquots were analyzed for $^{210}Pb$ and $^{226}Ra$. The samples were leached at 80°C with nitric and hydrochloric acids with a known amount of $^{209}Po$ present as a tracer. Polonium was then autoplated onto a silver disc from 1.5 N HCl (Flynn, 1968). The disc was counted on an alpha spectrometer using a silicon surface barrier detector and $^{210}Pb$ was determined as the activity of its daughter, $^{210}Po$. The remaining solution was placed in a sealed radon bubbling bottle and analyzed for $^{226}Ra$ by the radon de-emanation method (Mathieu, 1977; Lockhart et al., 1995).

Mercury in sediment was analyzed by boiling 0.1–0.5 g of sediment with 8 mL of aqua regia and bringing the volume to 50 mL with distilled water, followed by flameless atomic absorption (Hendzel and Jamieson, 1976).

The mineralogy of the samples was determined by X-ray powder diffraction analysis (XRD). A 40 mg suspension (in water) of each sample was pipetted onto glass slides and air-dried overnight to produce oriented mounts. X-ray patterns of the air-dried samples were digitally recorded using a Philips PW1710 automated powder diffractometer equipped with a graphite monochromator, Co K$\alpha$ radiation set at 40 kV and 30 mA. The samples were also X-rayed following saturation with ethylene glycol and heat treatment (550°C). Data was processed using a PC-based program, JADE® (Materials Data, Inc.) which enables manipulation of the X-ray pattern for optimization (e.g. correction for background, instrument error) in identification of mineral species and calculation of abundances. Semiquantitative analyses are possible through comparison with a set of reference standards using a predetermined reference intensity ratio (RIR). The RIRs available from the International Centre for Diffraction Data database are based on a weighted factor of a mineral relative to corundum. The weighted factors or RIRs used at the GSC laboratory have been, in many cases, recalculated using quartz as the internal standard.

Grain mounts were prepared for scanning electron microscopy (SEM) by pipetting a very dilute (<10–20 ppm) suspension onto a carbon-coated planchette, followed by carbon-coating before examination. A Leica Cambridge Stereoscan S360 SEM was used. The SEM was equipped with an Oxford/Link eXL-II energy-dispersion X-ray analyzer, Oxford/Link Pentafet Be window/light-element detector, and an Oxford/Link Tetra backscattered-electron detector. The SEM is operated at an accelerating voltage of 20kV. The SEM images are captured at 768 x 576 x 256 greyscale and digitally stored for further processing.

## PREVIOUS STUDIES

In 1971, sediment core and grab samples were taken along 27 transects in Clay Lake. Armstrong and Hamilton (1973) estimated that the sediment contained about 2000 kg of Hg in the top 6 cm, based on a mean concentration of 3 $\mu g \cdot g^{-1}$. They

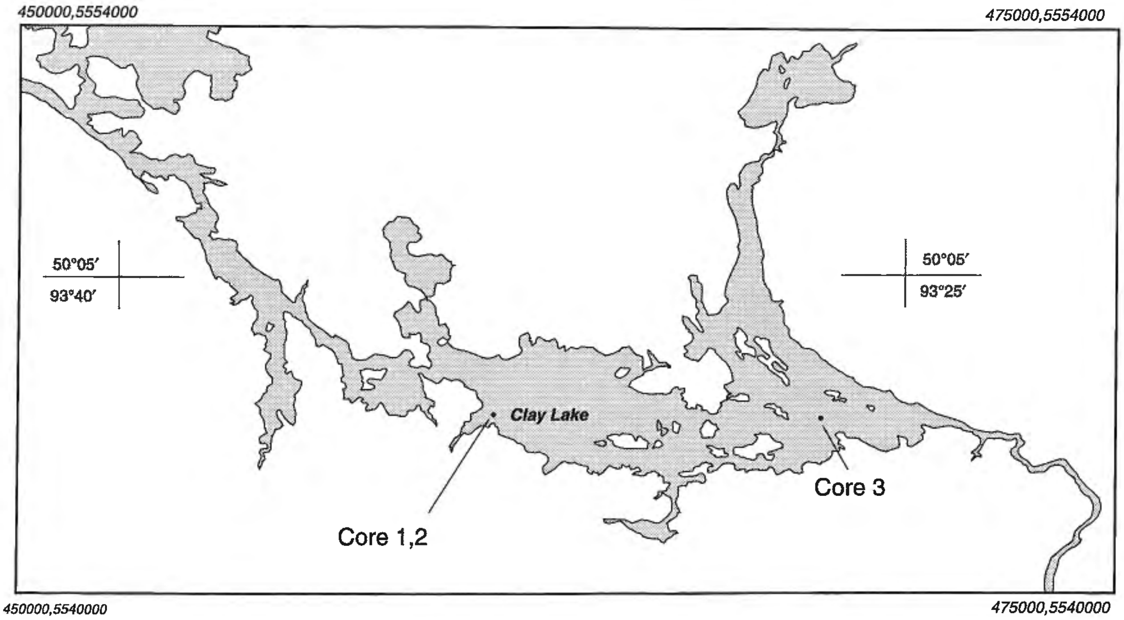


*Figure 2. Detailed map of Clay Lake showing location of cores taken in 1995 study.*

indicated that bioturbation was the main factor in mixing the mercury discharged in the 1960s to a depth that was 10 times deeper than expected from sedimentation rates alone. They suggested that it was not possible to predict if these mercury-rich layers would deepen with time.

A series of bottom-sediment grab samples were collected in 1978 between Dryden and Ball Lake (Jackson and Woychuk, 1980a). The sediments from Clay Lake, consisting of grey-brown to grey clay-rich mud, contained, on average, about 12 $ng \cdot g^{-1}$ $CH_3Hg^+$ in both the east and west basins, and about 7.8 $\mu g \cdot g^{-1}$ and 3.1 $\mu g \cdot g^{-1}$ total Hg in the east and west basins, respectively. Jackson and Woychuk (1980a) estimated that about 2700 kg of total mercury resided in the Clay Lake sediments and found no relation between total mercury and methyl-mercury content. Although iron and manganese nodules were not observed in Clay Lake, total mercury was associated with total iron and manganese for the east basin (group 1 samples which are anomalously rich in methyl-mercury) and strongly correlated with interstitial $Cl^-$. However, the group 2 (lower concentrations of methyl-mercury) samples from the east basin, and the west-basin samples were correlated with $S^{2-}$. Jackson and Woychuk (1980a) suggested that precipitation of HgS or organic sulphide complexes could occur in Clay Lake. Jackson (1979a) suggested that when $S^{2-}$ is plotted against either organic carbon or nitrogen, a steeper trend results for Clay Lake relative to Ball Lake (further downstream). He argued that this resulted from an enrichment in oxygen-consuming, biodegradable, organic matter which produced biogenic $H_2S$. In the study of suspended particulates collected by continuous-flow centrifugation in 1979, Jackson et al. (1982) found that methyl-mercury correlated significantly with $S^{2-}$ content for all samples in the Wabigoon River system, but total mercury did not correlate. They believe that methyl-mercury and inorganic mercury differ in their affinities for binding sites. Usually, inorganic $Hg^{2+}$ has a stronger affinity for sulphides than methyl-mercury thus binding by biogenic organic sulphides may be the cause of this observed difference.

Parks and Hamilton (1987) believe that sedimentation is the main natural restorative mechanism operating in the Wabigoon system. The most contaminated sediment is buried below the sediment-water interface and not available for uptake in the ecosystem (Rudd et al., 1980; Parks et al., 1984; Parks and Hamilton, 1987). In Figure 3, total mercury in sediment cores determined in 1995 is compared to data from 1971 and 1978 (Lockhart, unpub. data, 1995). Note that the mercury-rich layer has become progressively buried with time. Independent dating of the 1995 samples by $^{137}Cs$ and $^{210}Pb$ is shown along the trend line. The decline in $^{210}Pb$ with depth gave a good approximation of exponential decay, suggesting a relatively consistent sedimentation rate over time; the slope was used to calculate a sedimentation rate of 1530 $g \cdot m^{-2} \cdot a^{-1}$ (e.g. ~0.58 $mm \cdot a^{-1}$). There was little apparent focusing of sediment to the core site because the $^{210}Pb$ flux was calculated to be 139 $Bq \cdot m^{-2} \cdot a^{-1}$, in good agreement with a flux to soil of 175 $Bq \cdot m^{-2} \cdot a^{-1}$ measured nearby at the Experimental Lakes Area (Lockhart et al., 1998). An estimate of the flux of mercury can be obtained from the product of the sedimentation rate and the concentration of mercury in each

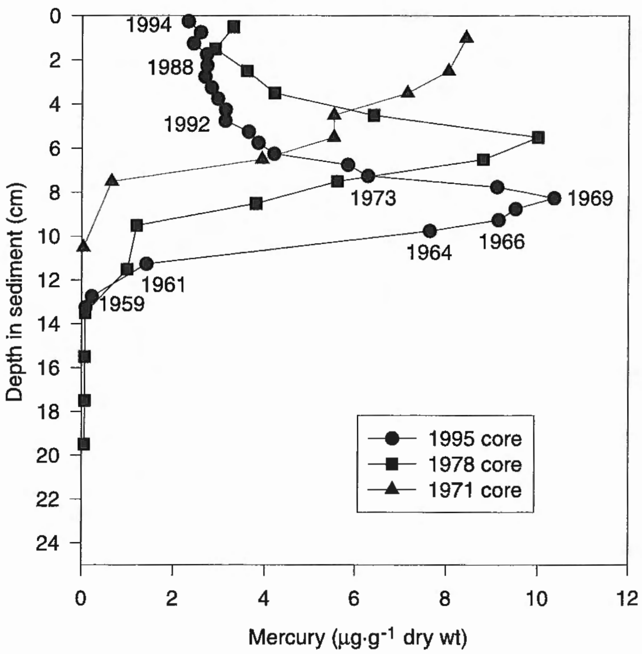


*Figure 3. Total mercury vs. depth for sediment cores taken in 1971 (Armstrong and Hamilton, 1973), 1978 (Rudd et al., 1980) and 1995. Dates are based on $^{137}Cs$ and $^{210}Pb$ isotopic measurements.*

slice on the assumption that the mercury is associated with particles. For example, the concentration of mercury in the top slice was 2.32 $\mu g \cdot g^{-1}$ whereas the peak concentration in the 17th slice was 10.4 $\mu g \cdot g^{-1}$. Combining these concentrations with the sedimentation rate gives an estimated flux for the top slice and the 17th slice as 3.6 and 15.6 $mg \cdot m^{-2} \cdot a^{-1}$, respectively. These are extremely high fluxes. Lockhart et al. (1998) made similar flux calculations for some other lakes in northwestern Ontario and reported values of about 17 $\mu g \cdot m^{-2}$ $a^{-1}$, or about three orders of magnitude lower than the maximum flux in Clay Lake. The highest flux they reported was for the south basin of Lake Winnipeg — only 114 $\mu g \cdot m^{-2} \cdot a^{-1}$. Hence, although the situation has improved in Clay Lake relative to the period when the chlor-alkali plant was operating, even the most recent flux to Clay Lake of 3.6 $mg \cdot m^{-2} \cdot a^{-1}$ is about 200-fold higher than expected, based on the other lakes in the area (Lockhart et al., 1998), and in other relatively remote Alaskan and Minnesotan lakes (Engstrom and Swain, 1997). The bottom slice in the core had a Hg concentration of 86 $ng \cdot g^{-1}$, which can be combined with the sedimentation rate to indicate a flux of 131 $\mu g \cdot m^{-2} \cdot a^{-1}$, still a very high value. This flux rate is only slightly lower than those measured in urban Minnesota lakes after 1980 (approximately 110–220 $\mu g \cdot m^{-2} \cdot a^{-1}$; Engstrom and Swain, 1997).

## RESULTS AND DISCUSSION

Preliminary XRD results show that all samples in core 3 are mineralogically similar. Semiquantitative analyses in progress are not reported here. The samples are dominated by quartz and plagioclase, with minor K-feldspar, chlorite, and

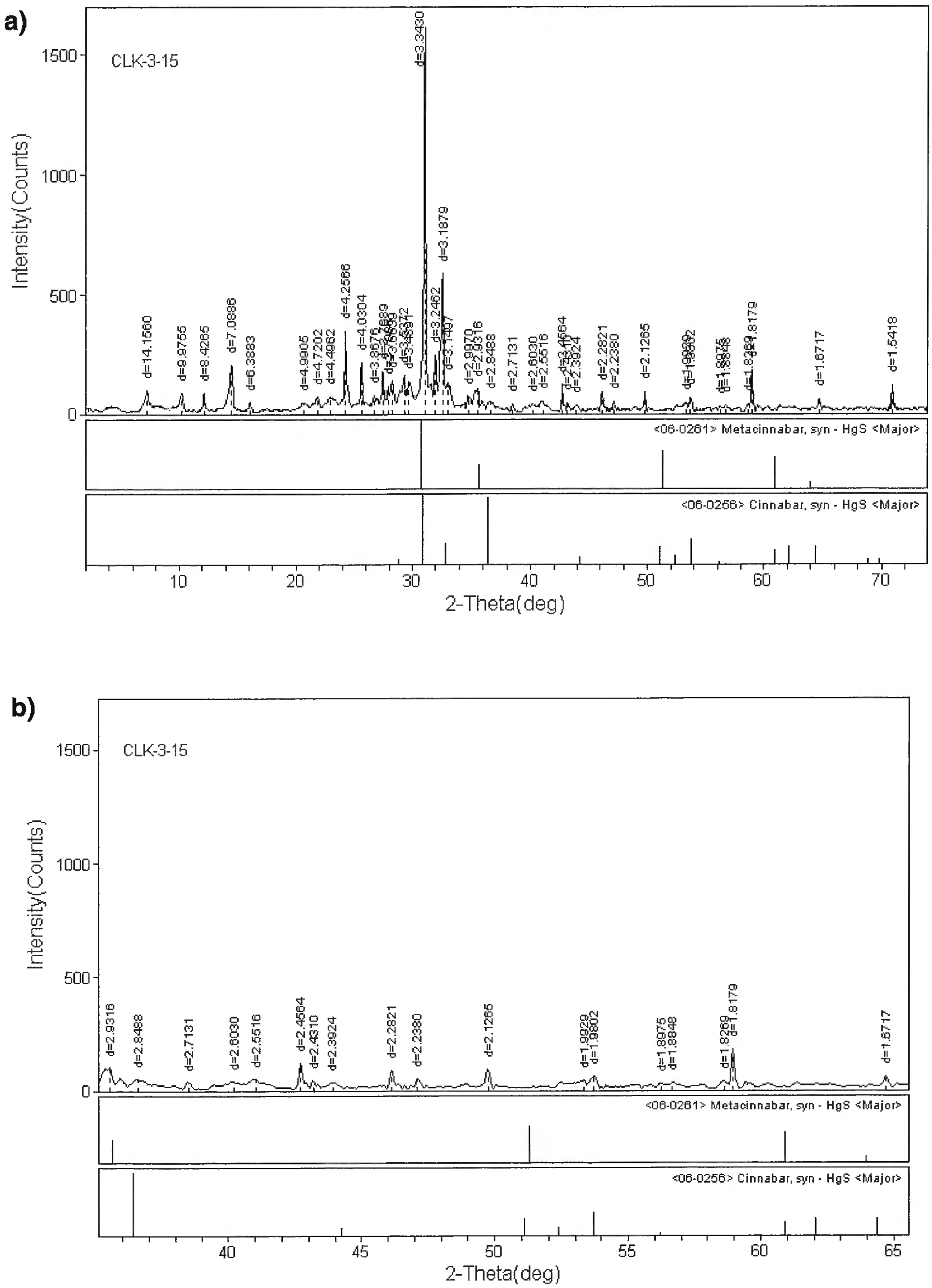


***Figure 4. a**) XRD chart of sample CLK-3-15 as compared to reference minerals meta-cinnabar and cinnabar (stick underlays). **b**) Expansion of XRD chart between 35 and 65°2θ (Co tube).*

**Table 1.** List of trace minerals and other particulates observed under the SEM.

| Sample No. | Minerals Observed | Other Particulates | Sample No. | Minerals Observed | Other Particulates |
|---|---|---|---|---|---|
| CLK-3-10 | titanite (Si, Ti, Ca, O, Al)<br>ilmenite (Fe, Ti, O)<br>Fe oxide (Fe, O)<br>cinnabar (Hg, S) | Si, Fe, Ni, V, Ti, Cr<br>Si, Fe, O<br>Fe, Cr<br>Si, Cu, Zn, Pb, Cl, Si, C, Al | CLK-3-15 | ilmenite<br>Fe oxide<br>rutile<br>titanite<br>monazite (Ce, P, O)<br>cinnabar | Si, Fe, Ni, V, Ti |
| CLK-3-11 | Fe oxide<br>pyrite ( Fe, S) | Si<br>Fe, Cr<br>Si, Fe, Ni, V<br>Ti<br>Si, Fe, Ti<br>W | CLK-3-16 | native Cu<br>chalcopyrite (Cu, S)<br>Fe oxide<br>titanite<br>cinnabar<br>apatite (Ca, P)<br>pyrite | Si<br>Si, Fe, Ni<br>Fe, Cr<br>Si, Fe |
| CLK-3-12 | cinnabar<br>molybdenite (Mo, S)<br>titanite<br>ilmenite<br>Fe oxide | Si<br>Si, Ca<br>Fe, Cr, Ni<br>Fe, S, O, Pb<br>Si, Fe, Cr, Ni | CLK-3-17 | ilmenite<br>rutile<br>pyrite<br>cinnabar | Si, Fe, V, Ni<br>Si<br>Fe, Cr |
| CLK-3-13 | argentite? (Ag, S)<br>titanite<br>Fe oxide<br>cinnabar<br>galena (Pb, S) | Si<br>Si, Fe, Ni<br>Si, Fe, Cr<br>Si, Fe, Cr, Mn<br>Cu, Zn, S, Cl | CLK-3-18 | ilmenite<br>titanite<br>Fe oxide | Si<br>Fe, Cr<br>Bi<br>Si, Ti, V |
| CLK-3-14 | rutile (Ti, O)<br>pyrite (Fe, S)<br>Fe oxide (Fe, O)<br>cinnabar (Hg, S) | Fe<br>Si, C, O<br>Fe, O, Si, Al<br>Fe, Cr<br>Ti, Si, O<br>Ti, Si, Cr, Fe<br>Ti, Si, W<br>Si, Fe, V, Ti, Ni | CLK-3-19 | monazite<br>pyrite<br>ilmenite<br>cassiterite<br>sphalerite<br>chalcopyrite<br>cinnabar | Fe, V, Ni<br>Si<br>Fe<br>Si, Fe, V |

amphibole, and minor to trace amounts of pyroxene, possible epidote, and rare hematite. Smectite and mixed-layer clay minerals (e.g. chlorite/smectite or illite/smectite) occur in trace amounts in many of the samples. In particular, the samples were examined for trace amounts of cinnabar or meta-cinnabar, because of the known high concentration of total mercury (*see* Fig. 3). Samples 3-14 to 3-19 appear to contain trace amounts of cinnabar. Figure 4a shows a typical XRD pattern for these samples, as processed using JADE® software, compared to meta-cinnabar and cinnabar reference minerals (stick underlays). It appears that some of the XRD peaks for cinnabar do match the whole sediment pattern (Figure 4b). However, the main cinnabar peaks shown in Figure 4a near 30°2θ is coincident with the main X-ray peak of quartz. The low intensity of the higher angle peaks and the slight broadening are related to the small grain size and nominal detection limit (~1–3%) of XRD.

Samples 3-10 to 3-19 were examined under the SEM for their trace-mineral components. Examination was made using backscatter mode with extreme contrast (darkened screen) to ensure visibility of the heavier minerals relative to the silicates. Silicates such as quartz, feldspar, amphibole, pyroxene, epidote, and micas were observed in most samples. Trace minerals included a variety of oxides (Fe oxide, rutile, titanite, ilmenite), sulphides (cinnabar, pyrite, sphalerite, galena, molybdenite, argentite) and phosphates (monazite, apatite) (Table 1). Examples of the cinnabar (e.g. HgS) grains are shown in Figures 5a and b. Other particulates found probably include stainless steel and a variety of other alloys or mixtures containing Fe, Cr, Ni, and V, and possibly silicon carbide (Si), are probably anthropogenic in origin. Many of the grains occur in clusters and individual grains are not readily analyzed. The anthropogenic particulates may result from original discharges from the plant, or may be due to contamination introduced during processing of the cores.

Jackson (1998), in his review paper on mercury in aquatic systems, notes that inorganic mercury tends to be less strongly sorbed to clays, oxides, and silt than organic matter and sulphides. If mercury is associated with clays and oxides it may be more available for methylation (Jackson, 1998); however, Jackson and Woychuk (1980b) reported that, at least in the west basin of Clay Lake, methylation is probably limited by the presence of sulphides. Jackson (1979b) indicated that Clay Lake was richer in sulphide and organic matter than the next downstream lake, Ball Lake, and therefore was a more efficient sink for mercury. As noted above,

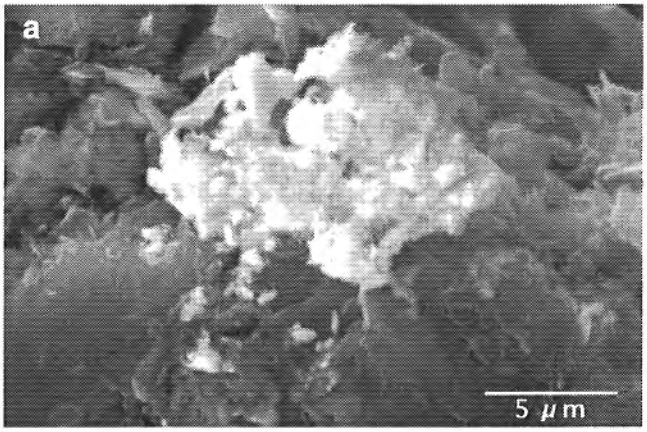


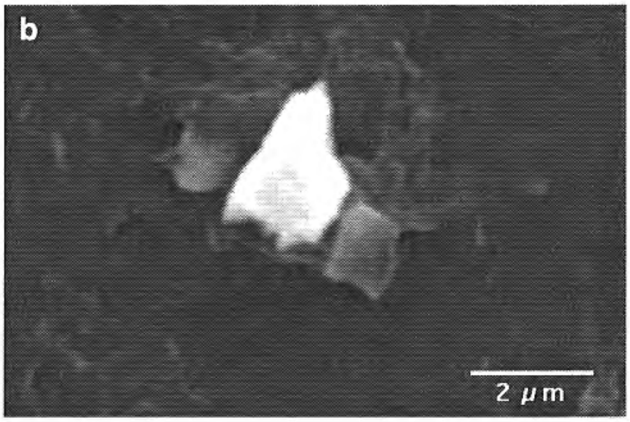


***Figure 5.*** ***a****) SEM photomicrograph of a backscatter image (BSI) of a cluster of mercury- and sulphur-bearing mineral in sample CLK-3-15.* ***b****) BSI of mercury and sulphur mineral in sample CLK-3-12.*

Jackson and Woychuk (1980a) predicted that formation of HgS or organic sulphide complexes could occur in Clay Lake. In a study of floodplain soils and sediment contaminated by about 100 t of Hg discharged into the East Fork Poplar Creek in Oak Ridge, Tennessee, during the 1950s, the presence of meta-cinnabar was confirmed through XRD and microbeam studies (Barnett et al., 1995). Barnett et al. (1995) believed this to be the first evidence for the formation of authigenic mercuric sulphide in soils. Based on the preliminary results from this study, it is clear that authigenic HgS has formed under ambient reducing conditions in Clay Lake and accounts for the fact that the peak contamination is now buried.

## FUTURE RESEARCH

Detailed mineralogical analyses of these sediments are in progress. If sufficient material is available, a clay-size separation will be undertaken to attempt to concentrate the clay minerals and other fine-grained particulates. In addition, heavy-mineral separation may be used for some selected samples to clearly identify if the HgS mineral is the more stable mineral cinnabar as opposed to meta-cinnabar, or if there is a mixture of these two minerals.

## ACKNOWLEDGMENTS

The authors would like to thank P.M. Outridge for suggestion of the topic and discussions throughout the summer. We are grateful to J.W. Parks and T.A. Jackson for references and useful discussions concerning past studies and the current results, and to P.E. Rasmussen, P.J. Henderson, and A. Plouffe for discussions about mercury. Thanks to P. Hunt for SEM analyses, E. Hillary for digitizing and computer drafting of maps, and R. Lacroix for final preparation of the SEM photomicrographs. Reviews by P.M. Outridge and P.E. Rasmussen were helpful.

## REFERENCES

**Allan, R.J., Brydges, T.G., Dodge, D.P., Hamilton, R.D., Jeffs, D.N., and Shikaze, K.**
1984: Mercury pollution in the Wabigoon–English River system of northwestern Ontario and possible remedial measures; Final Report of Steering Committee, 1 and 2; Environment Canada and Ontario Ministry of Environment, 570 p.

**Armstrong, F.A.J. and Hamilton, A.L.**
1973: Pathways of mercury in a polluted northwestern Ontario lake; *in* Metals and Metal-Organic Interactions in Natural Waters, (ed.) P.C. Singer; Ann Arbor Science Publ. Inc., Ann Arbor, Michigan, p. 131–156.

**Barnett, M.O., Harris, L.A., Turner, R.R., Henson, T.J., Melton, R.E., and Stevenson, R.J.**
1995: Characterization of mercury species in contaminated floodplain soils; Water, Air, and Soil Pollution; v. 80, p. 1105–1108.

**Beakhouse, G.P.**
1991: Winnipeg River subprovince; *in* Geology of Ontario, (ed.) P.C. Thurston, H.R. Williams, R.H. Sutcliffe, and G.M. Stott; Ontario Geological Survey, Special Volume 4, Part 1, p. 279–301.

**Engstrom, D.R. and Swain, E.B.**
1997: Recent declines in atmospheric mercury deposition in the Upper Midwest; Environmental Science and Technology, v. 31, p. 960–967.

**Flynn, W.W.**
1968: The determination of low levels of Po-210 in environmental materials; Analytica Chimica Acta, v. 43, p. 221–227.

**German, M.J.**
1969: A water pollution survey of the Wabigoon River; Report of the Ontario Water Resources Commission (predecessor of the Ontario Ministry of the Environment), 24 p.

**Hendzel M.R. and Jamieson D.M.**
1976: Determination of mercury in fish; Analytical Chemistry, v. 48, p. 926–928.

**Jackson, T.A.**
1979a: Sources of heavy metal contamination in a river-lake system; Environmental Pollution, v. 18, p. 131–138.
1979b: Relationships between the properties of heavy metals and their biogeochemical behaviour in lakes and river-lake systems; *in* Proceedings of the International Conference on Management and Controls of Heavy Metals in the Environment, London, September, 1979, CEP Consultants, Edinburgh, Scotland, p. 457–460.
1998: Mercury in aquatic systems; *in* Metal Metabolism in Aquatic Environments, (ed.) W.J. Langston and M.J. Bebianno; Chapman & Hall, London, New York, p. 77–158.

**Jackson, T.A. (ed.)**
1980: Mercury pollution in the Wabigoon–English River system of northwestern Ontario, and possible remedial measures: a progress report; Environment Canada and Ontario Ministry of the Environment, 139 p.

**Jackson T.A. and Woychuk, R.N.**
1980a: The geochemistry and distribution of mercury in the Wabigoon River system; *in* Mercury Pollution in the Wabigoon–English River System of Northwestern Ontario, and Possible Remedial Measures: a Progress Report, (ed.) T.A. Jackson; Environment Canada and Ontario Ministry of the Environment, 28 p.
1980b: Mercury speciation and distribution in a polluted river-lake system as related to the problem of lake restoration; *in* Restoration of Lakes and Inland Waters (Proceedings of an International Symposium on Inland Waters and Lake Restoration, Portland, Maine, September 8–12, 1980); U.S. Environmental Protection Agency, Washington, D.C., p. 93–101.

**Jackson, T.A., Parks, J.W., Jones, P.D., Woychuk, R.N., Sutton, J.A., and Hollinger, J.D.**
1982: Dissolved and suspended mercury species in the Wabigoon River (Ontario, Canada): seasonal and regional variations; Hydrobiologia, v. 92, p. 473–487.

**Jackson, T.A., Parks, J.W., and Rudd, J.W.M.**
1980: Introduction: the problem of mercury pollution in the Wabigoon–English River system; *in* Mercury Pollution in the Wabigoon–English River System of Northwestern Ontario, and Possible Remedial Measures: a Progress Report, (ed.) T.A. Jackson; Environment Canada and Ontario Ministry of the Environment, 6 p.

**Lockhart , W.L., Wilkinson, P., Billeck, B.N., Danell, R.A., Hunt, R.V., Brunskill, G.J., Delaronde, J., and St. Louis, V.**
1998: Fluxes of mercury to lake sediments in central and northern Canada inferred from dated sediment cores; Biogeochemistry v. 40, p. 163–173.

**Lockhart, W.L., Wilkinson, P., Billeck, B.N., Hunt, R.V., Wagemann, R., and Brunskill, G.J.**
1995: Current and historical inputs of mercury to high-latitude lakes in Canada and to Hudson Bay; Water, Air and Soil Pollution, v. 80, p. 603–610.

**Mathieu, G.G.**
1977: Rn-222 - Ra-226 technique of analysis; Annual Technical Report C00-2185-0, Lamont-Doherty Geological Observatory, Palisades, New York, 29 p.

**Nielson, J.M.**
1989: Northern Ontario engineering geology terrain study, Perrault Lake, data base map; Ontario Geological Survey, Map 5109, scale 1:100 000.

**Parks, J.W.**
1976: Mercury in sediments and waters in the Wabigoon–English River system, 1970–1975; Ontario Ministry of the Environment, Technical Report, 28 p.

**Parks, J.W. and Hamilton, A.L.**
1987: Accelerating recovery of the mercury-contaminated Wabigoon/English River system; Hydrobiologia, v. 149, p. 159–188.

**Parks, J.W., Sutton, J.A., and Hollinger, J.D.**
1984: Mercury contamination of the Wabigoon–English–Winnipeg River system. Causes, effects and possible remedial measures; *in* Mercury Pollution in the Wabigoon–English River system of northwestern Ontario and possible remedial measures, (eds.) R.J. Allan, T.G. Brydges, D.P. Dodge, R.D. Hamilton, D.N. Jeffs, and K. Shikaze, Final Report of Steering Committee, 1 and 2, Environment Canada and Ontario Ministry of Environment, p. 1–352.

**Rudd, J.W.M., Turner, M.A., Townsend, B.E., Swick, A., and Furutani, A.**
1980: Mechanisms of movement of mercury into aquatic biota and a preliminary examination of some amelioration procedures; *in* Mercury Pollution in the Wabigoon–English River System of Northwestern Ontario, and Possible Remedial Measures: a Progress Report, (ed.) T.A. Jackson; Environment Canada and Ontario Ministry of the Environment, 41 p.

**Scott, D.P.**
1974: Mercury concentration of white muscle in relation to age, growth and condition in four species of fish from Clay Lake; Canadian Journal of Fisheries and Aquatic Sciences, v. 31, p. 1723–1729.

**Sharpe, D.R., Pullan, S.E. and Warman, T.A.**
1992: A basin analysis of the Wabigoon area of Lake Agassiz, a Quaternary clay basin in northwestern Ontario; Géographie physique et Quaternaire, v. 46, p. 295–309.

**Sherbin, I.G.**
1979: Mercury in the Canadian environment; Environmental Protection Service, Environment Canada, Economic and Technical Review Report EPS 3-EC-79-6, 359 p.

**Vermeer, K., Armstrong, F.A.J. and Hatch, D.R.M.**
1973: Mercury in aquatic birds at Clay Lake, western Ontario; Journal Wildlife Management, v. 37, p. 58–61.

**Westerman, C.**
1977: Tectonic evolution of a part of the English River Subprovince, northwestern Ontario; Ph.D. thesis, McMaster University, Hamilton, Ontario, 292 p.

Geological Survey of Canada Project 680023ZC

# A note on the occurrence of nepheline syenite in Calvin Township, District of Nipissing, Ontario

K.L. Currie

Continental Geoscience Division, Ottawa

*Currie, K.L., 1999: A note on the occurrence of nepheline syenite in Calvin Township, District of Nipissing, Ontario;* in *Current Research 1999-C; Geological Survey of Canada, p. 241–246.*

**Abstract:** Nepheline syenite occurs about 20 km southwest of Mattawa, Ontario, as an elliptical mass about 1 km by 1.5 km in size within an east-southeast-trending belt of metagabbro and mafic gneiss. Nepheline-free syenite extends 2 km farther to the east as a belt less than 100 m wide. The nepheline syenite is zoned from sodium-rich margins to a potassic core, but is bisected by a layer of amphibolitic gneiss similar to the surroundings. The syenite shows some mineralogical similarities to a huge massif of monzonitic rocks of granulitic affinity which lies a few kilometres to the west. All rocks have been strongly affected by two or more periods of deformation, but the nepheline syenite shows no obvious relation to this deformation. It appears to have been emplaced as a pluton subsequent to initial deformation, but prior to final assembly of the Grenville Province.

**Résumé :** Une masse elliptique de syénite néphélinique mesurant 1 km sur 1,5 km se rencontre environ 20 km au sud-ouest de Mattawa, Ontario, dans une ceinture de métagabbro et de gneiss mafique à orientation est-sud-est. Une zone de moins de 100 m de largeur de syénite sans néphéline se prolonge 2 km plus loin vers l'est. La syénite néphélinique présente une zonation, les marges riches en sodium passant à un noyau potassique; elle est divisée en deux par une couche de gneiss amphibolitique qui ressemble aux roches environnantes. La minéralogie de la syénite ressemble à certains égards à celle d'un énorme massif de roches monzonitique d'affinité granulitique qui se trouve à quelques kilomètres à l'ouest. Toutes les roches ont été fortement perturbées par au moins deux périodes de déformation, mais la syénite néphélinique ne montre aucun lien évident avec cette déformation. Elle aurait été mise en place sous la forme d'un pluton après la déformation initiale, mais avant l'assemblage final de la Province de Grenville.

## INTRODUCTION

Nepheline syenite is a minor, but widely disseminated, component of the Grenville Province of the Precambrian shield. Most occurrences lie within the Central metasedimentary belt, forming a northeast-trending chain extending from west of Bancroft across the Ottawa River into western Quebec, but nepheline syenite also occurs sparsely in the Central gneiss belt to the north of the Central metasedimentary belt. Currie and van Breemen (1996) and Currie (1998) recently concluded that two occurrences of nepheline syenite in the Central gneiss belt exhibit major metasomatism associated with large-scale structural dislocations. Lumbers (1976) mapped nepheline syenite in the Central gneiss belt in Calvin Township, about 2 km southwest of the hamlet of Eau Claire near Mattawa, Ontario, but little is known about the structure or petrography of this occurrence. These rocks were reexamined this year in order to assess the role of structurally controlled metasomatism in their formation.

## GEOLOGICAL SETTING

Calvin Township (Fig. 1) lies within the Algonquin Terrane of the Central gneiss belt (Easton, 1992, p. 720). Domain terminology within this region is not well defined (cf. Easton, 1992), but the area shown in Figure 1 appears to straddle the boundary between the Opeongo and Powassan domains, and to lie near the northeastern tip of the Kiosk domain. Both Opeongo and Powassan domains are largely underlain by large monzonitic plutons separated by screens of paragneiss and quartzofeldspathic gneiss of ambiguous origin (Easton, 1992, p. 772).

Glacial and glaciofluvial deposits, ranging from clay through boulder clay to stratified sand and gravel, cover low-lying parts of the mapped area to depths of several metres. Low, rounded hills project through this cover, and locally expose bedrock, most commonly on the northeast side. Much of the low-lying ground has been cleared for agriculture, but the hills are covered with thick second-growth forest, making discovery of the sparse outcrop difficult. However a network of secondary roads and tracks permits easy access to all parts of the area, and provides much of the outcrop in roadcuts and excavations.

## DESCRIPTION OF UNITS

Lumbers (1976) divided the bedrock into 18 units, of which two are Paleozoic sedimentary strata. For the present purpose it was found sufficient to divide the plutonic and igneous rocks into six units (cf. Fig. 1), listed in order of apparent decreasing age; 1) thinly foliated, microcline-rich granitic gneiss with schliers and screens of biotite gneiss and minor paragneiss; 2) foliated and lineated granitic augen gneiss; 3) lineated, olive-grey, garnet-amphibole-pyroxene monzonite of granulitic aspect; 4) mafic rocks, varying from leucocratic metagabbro to foliated amphibolite; 5) a syenite complex, including white, amphibole-biotite nepheline syenite; buff to pink hydronepheline syenite; and garnetiferous, nepheline-free syenite; and 6) lamprophyre dykes.

The oldest rocks, thinly foliated, microcline-rich granitic gneiss, form a narrow screen in the northwest corner of Figure 1 and a broad, southeast-trending belt enclosing the metagabbro and syenite. In both cases a fine- to medium-grained, granoblastic, buff to pink, quartz-biotite-feldspar gneiss with a colour index (CI) less than 15 predominates. The rock commonly exhibits a millimetre-scale foliation with low dips forming open folds about a prominent lineation plunging 5–20° toward the southeast. In many exposures, sharply defined, decimetre-scale, layers of biotite-rich material (CI~50) form 5–10% of the outcrop. Pronounced mineral segregation layering is relatively rare, but most outcrops contain nebulous, schlier-like masses of coarser grained, more leucocratic granitoid segregations. In thin section these gneiss units are dominated by small, rounded grains of grid-twinned microcline. The only mafic mineral present in most specimens is biotite, but several contain traces of fine-grained, rounded garnet (not observed in hand specimen), and one section has a few grains of muscovite. The seriate, rounded mosaic texture, combined with the strong foliation suggests mylonitic material recrystallized by annealing subsequent to deformation. Lumbers (1976) considered schliers and enclaves in this unit to be paragneiss units of various origins, but a sedimentary origin is only obvious for a screen of coarse to pegmatitic marble along Pimisi Bay in the northwest corner of the area.

A belt of granitic augen gneiss separates the metagabbro-amphibolite complex to the northeast from a monzonite massif to the southwest. Strongly foliated augen gneiss is well exposed on roads west of the Amable du Fond River forming a distinctive rock with sinuous lenses of fine-grained biotite and minor amphibole wrapped around ovoid, monocrystalline or polycrystalline quartz augen up to 2 cm in diameter. The matrix consists of a fine-grained mosaic of microcline and oligoclase. One specimen contains scattered garnet. Lumbers (1976) grouped these rocks with his 'garnet-ferrohastingsite monzonitic rocks'. However the strong foliation and high contents of microcline and quartz more closely resemble the granitic gneiss to the east. Occurrence of quartz augen in a granitic augen gneiss is anomalous, unless the augen represent remnants of disrupted quartz veins.

A very large and homogeneous mass of garnet-amphibole monzonite underlies the western edge of the map area and extends for many kilometres to the south and west (Bonfield batholith of Lumbers (1976)). These rocks are massive to L-tectonite units characterized by the greasy grey to buff weathering typical of granulitic rocks. On fresh surfaces they are pale grey or greenish grey. The mafic minerals commonly form spindle-shaped aggregates, mainly amphibole and deep red garnet, which impart a southeast-plunging lineation to the rock. In general the colour index of the rocks is 15–20, but locally there are gradual transitions to more mafic varieties. Along the east side of the massif, nebulous metre-scale areas are pink and have a stronger foliation, but otherwise appear to be mineralogically identical to the more massive varieties. Metre-scale schlieren of granoblastic amphibolitic material, which resemble the mafic gneiss to the east, accompany this pink phase. At the southern edge of the map area on Highway 630 (grid reference NTS 31 L/2; UTM 660950, 5115850) there is an inclusion 5 m across of massive, fine-grained, granoblastic, greenish-black, garnet-clinopyroxene-amphibole rock with about 40% garnet (retrograded eclogite).

Mineralogically, the mafic rocks contain a low tenor of quartz, commonly 5–15%. Oligoclase is typically the only feldspar. Pale green clinopyroxene (salite), surrounded and dotted by opaque dust, occurs in mafic clusters with dominant unoriented amphibole euhedra to subhedra. The strongly absorbing, buff to olive, pleochroic scheme of the amphibole resembles that of amphibole in the nepheline syenite. Garnet forms rounded grains, moderately poikilitic, with tiny quartz and plagioclase inclusions. Biotite is consistently present in minor amounts as small prisms oriented along the lineation. Zircon forms large but sparse euhedra.

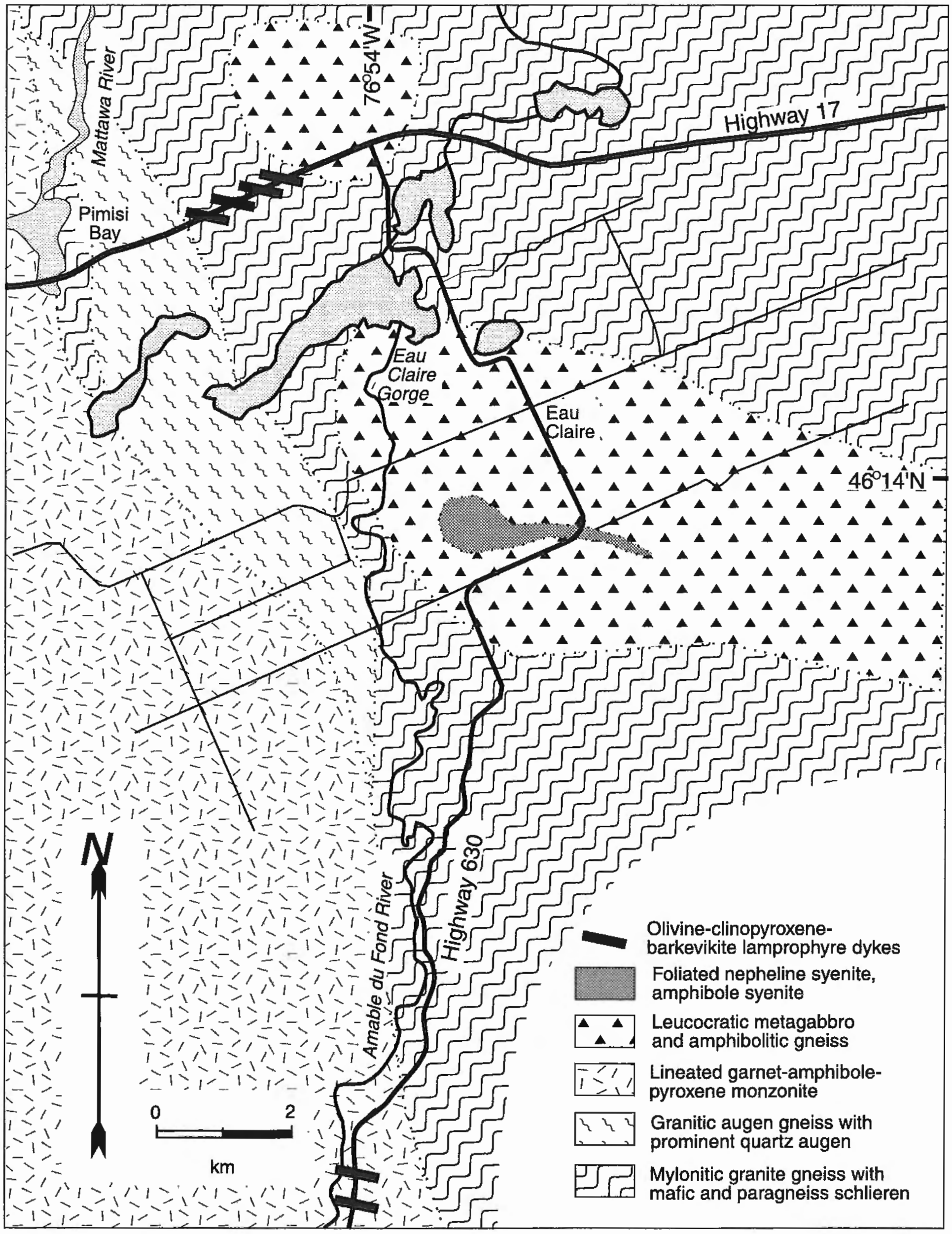


***Figure 1.*** *Geological sketch of the Calvin Township nepheline syenite occurrence and surrounding rocks (modified after Lumbers, 1976).*

Lumbers (1976) mapped a lens of anorthosite and mafic rocks extending from Eau Claire gorge east and southeast beyond the area of Figure 1 (Eau Claire anorthosite). No true anorthosite (CI<10) was observed during this year's mapping, although many outcrops are leucocratic (CI~15–25). Along Highway 630 south of Eau Claire, and in the Eau Claire gorge of the Amable du Fond River, some coarse-grained rocks appear to preserve relict igneous texture (metagabbro), although the primary pyroxene is entirely converted to amphibole and weakly aligned parallel to the pervasive southeast-plunging tectonic lineation. In thin section many of these rocks are spectacularly coronitic with thin, continuous shells of garnet around amphibole. Finer grained and more mafic (CI~60) rocks occur along the southwestern side of the belt, well exposed on the west side of the Amable du Fond River. These rocks consist of fine-grained amphibole and plagioclase with minor biotite, titanite, and apatite. Foliation and lineation, although commonly present, are not prominent. Similar or identical rocks form metre-scale boudins within the more leucocratic varieties in Eau Claire gorge and south of the syenite along Highway 630.

Mafic, amphibole-biotite gneiss occurs along Highway 17 as granoblastic, relatively massive and fine-grained rocks. A granitoid component is consistently present in the form of unoriented schlier-like masses of coarse, leucocratic pink granite, commonly less than 10 cm by 100 cm, although a few amphibole granite pegmatite masses reach 5 m by 50 m in size. A weak foliation appears erratically in these rocks, trending either southeast or east-northeast and dipping gently. This region of mafic rocks is not connected to the mafic rocks further south.

Despite the mafic or anorthositic appearence of many of these rocks, optical determination of plagioclase compositions consistently fall in a narrow range from $An_{22-30}$, which is essentially identical to plagioclase compositions in both the granitic gneiss and nepheline syenite.

Nepheline syenite outcrops within an elliptical area approximately 1.5 km long and 1 km wide, elongated in an east-west direction, and situated on top of a large hill just north of the Calvin Township dump. A representative collection of rock types from the nepheline syenite can be examined in large boulders unearthed by excavation for the dump, and good outcrop can readily be accessed from an ATV track passing a few tens of metres east of the dump. Two major variants of nepheline-bearing rocks occur. One is a coarse-grained, weakly foliated, grey rock, distinguished by large poikilitic amphibole crystals. The other is a coarse to pegmatitic, massive, brownish-pink rock containing large amounts of red 'hydronepheline' (a fine-grained alteration product of nepheline consisting of natrolite and other zeolites, sericite, clay minerals, and sufficient hematite dust to colour the mixture). The grey syenite contains large equant grains of nepheline (up to 2 mm across) dispersed in a finer grained feldspar matrix. The character of the feldspar varies with distance from the enclosing metagabbro. Close to the (unexposed) contact, the feldspar is exclusively oligoclase. The proportion of microcline rapidly increases toward the core of the nepheline syenite, and the central parts contain plagioclase only as an exsolved phase from alkali feldspar. The predominant mafic mineral is amphibole, pleochroic in almost opaque greens, but greenish-brown biotite is consistently present. Some biotite grains have a symplectic rim against plagioclase. Amphibole may form individual subhedra, or clump into spindles. In either case the mineral is intensely poikilitic with small subhedral plagioclase crystals. A few of the marginal specimens contain small amounts of garnet, but the core area does not. Large euhedral crystals of titanite and zircon are common. Small amounts of cancrinite and scapolite occur in two specimens, but no 'exotic' alkaline minerals were identified.

The red phase of the nepheline syenite forms pods and lenses within the grey phase, with dimensions reaching 5 m by 10 m. Contacts are abruptly gradational across a few centimetres. The rock consists of subhedral feldspar and amphibole surrounded by a continuous net of hydronepheline. Like the grey phase, the proportion of microcline perthite increases towards the core of the nepheline syenite, but the red phase has a consistently higher content of plagioclase ($An_{22-25}$) than the grey phase. Much of the amphibole exhibits the strongly absorbent, deep green pleochroism characteristic of the grey phase, but some grains have a weaker blue or violet pleochroism suggestive of arfvedsonite. Minor amounts of fine-grained, disseminated biotite are consistently present. The red phase contains carbonate, both dispersed and as tiny, boudined veinlets. Minor amounts of scapolite and cancrinite occur along the margins of these veins. One specimen contains garnet forming a symplectic intergrowth with amphibole.

The main body of nepheline syenite is split by a screen of gneissic amphibolite about 20 m wide. These rocks appear to be identical to amphibolite within the mafic complex which hosts the syenite. Contacts with the syenite are sharp, but completely conformable on both sides, and there are no obvious crosscutting or reaction relations between the differing rocks.

Small amounts of nepheline-free syenite occur east of the main body, apparently forming a thin 'tail' extending eastward more than a kilometre. Most of this material resembles the main body except for the absence of nepheline, and lower optical absorption of the amphibole. One outcrop (near grid reference NTS 31 L/2, UTM 663300, 5121900) is unique in containing spindles of colourless pargasitic amphibole coated by a thin shell of garnet.

Lamprophyre dykes occur mainly on the northern and southern edges of the area. As recognized by Lumbers (1976), dykes of more than one age are present, although they are shown on Figure 1 by a single symbol. The older dykes exhibit a crude fracture cleavage, and have clearly been deformed, although apparently not metamorphosed. They consist of coarse, unoriented olivine, salitic clinopyroxene, and barkevikitic amphibole, in that order of abundance, with plentiful accessory apatite. The texture is typically coarse grained, nonporphyritic, and lacks the several generations of phenocrysts typical of lamprophyre. Some of these older dykes appear to be more than 5 m thick. Younger dykes trend about 110°, dip almost vertically, and commonly are less than 1 m thick. Their mineralogy resembles that of the older dykes, but ocelli of carbonate and zeolite are present, and the rocks exhibit several generations of zoned pyroxene and amphibole. Olivine is commonly completely serpentinized and concentrated in central zones, giving outcrops a pitted appearence. The dykes themselves are typically polyphase, with as many as ten zones separated by chilled margins. Overall density of dykes is difficult to estimate due to lack of exposure, but one roadcut of almost 1 km along Highway 17 contains four dykes. These dykes form part of a regional swarm of Cambrian or Neoproterozoic age associated with central alkaline complexes to the west (cf. Ferguson and Currie (1978)).

## STRUCTURE

As noted in the introduction, the structural pattern in this region is dominated by large, equant, almost massive, monzonitic massifs separated by strongly foliated supracrustal and plutonic rocks. The complex structure between the massifs is not well understood. Observations on strongly foliated units in the mapped area show that outcrop-scale isoclinal recumbent folds with differing vergence but a common, gentle, southeasterly plunge are present. These folds are in turn folded by the kilometre-scale, relatively open folds identified by Lumbers (1976) which also have low southeasterly plunges. Some late, northeast- to east-northeast-trending isoclinal folds and shearing are also present. These relations resemble those in the Kipawa region, 50 km to the north, which Currie and van Breemen (1996) ascribed to persistent, southeast-over-northwest thrusting. In this model, the diverse vergence of the recumbent isoclinal folds results from stretching of original northeast-trending folds during further thrusting, producing sheath-like geometry. Late, open folds trend northwesterly due to constriction between large competent massifs. The persistent lineation parallel to fold plunge within these massifs suggests that they have also been deformed by thrusting, but in a relatively homogeneous manner.

In the Kipawa region, these phenomena are accompanied by the presence of several tectonic slices. Similar slices may occur in the Calvin Township area, but none were definitely identified during this year's mapping. The northeastern margin of the granulitic monzonite may be faulted, as suggested by the presence of strongly deformed augen gneiss along its border, and the presence of eclogitic boudins within its border. Indares and Dunning (1997) noted the latter as indicators of large tectonic breaks in the Kipawa region.

## DISCUSSION

Nepheline syenite in Calvin Township forms a discrete body, only slightly elongated along tectonic strike, which shows a distinct zonation from sodic rim to potassic core. The margins appear to be reasonably well defined, although on a small scale there is some gradation toward the lithology of the host. Although locally foliated, the nepheline syenite is relatively undeformed. All of these features are compatible with emplacement as a late, discrete pluton. Although geochronology is not available for the Calvin Township area, the almost massive character of the nepheline syenite, metagabbro, and granulitic monzonite would be consistent with emplacement subsequent to deformation of the quartzofeldspathic gneiss and augen granite gneiss, but prior to deformation associated with final assembly of the Grenville Province. Comparing these deductions with the regional studies of Easton (1992), the older rocks may be correlative to 1800–1600 Ma gneiss units of the Powassan, Opeongo, and Kiosk domains, while the monzonitic rocks form part of a widespread ca. 1450 Ma suite. Easton (1992) considered that the Eau Claire 'anorthosite', and possibly the nepheline syenite, were emplaced significantly later at ca. 1250 Ma. There is no direct evidence for the age of the nepheline syenite, which must be considered uncertain. Similarly the age of latest metamorphism and deformation remains uncertain, although extrapolation from the data compiled by Easton (1992) suggest an age of about 1050 Ma.

The septum of normal amphibolitic gneiss within the nepheline syenite could be explained in at least three ways; 1) as a dyke-like body, indicating that the host mafic complex overlapped in age with emplacement of the nepheline syenite; 2) as a fault slice, with susequent annealing and metamorphism disguising the suture(s); or 3) as a roof pendant, indicating that the host mafic complex is older than the nepheline syenite. Due to the complex structural and metamorphic history, none of these scenarios can be completely excluded, but 1) and 3) seem more probable.

The spatial association of nepheline syenite with the mafic complex, and less intimately with quartz-poor monzonitic rocks of alkaline affinity, suggests a genetic connection among these three igneous rock types, but the character and extent, if any, of such a connection remains unknown. If the age assignments are correct, the monzonite could serve as a potential source for syenitic rocks, but could not be directly genetically related.

## ACKNOWLEDGMENT

I wish to acknowledge a careful and constructive review by my colleague Tony Davidson which significantly improved the manuscript.

## REFERENCES

**Currie, K.L.**
1998: New observations on the French River alkaline syenite complex, Bigwood Township,Ontario; *in* Current Research 1998-C; Geological Survey of Canada, p. 137–143.

**Currie, K.L. and van Breemen, O.**
1996: The origin of rare minerals in the Kipawa alkaline complex, western Quebec; Canadian Mineralogist, v. 34, p. 435–451.

**Easton, R.L.**
1992: The Grenville Province and the Proterozoic history of central and southern Ontario; *in* Geology of Ontario; Ontario Geological Survey, Special Volume 4, pt. 2, p. 714–904

**Ferguson, J. and Currie, K.L.**
1978: Evidence of liquid immiscibility in alkaline basic dikes from Callander Bay, Ontario Journal of Petrology, v.12, p. 561–585.

**Indares, A. and Dunning, G.**
1997: Coronitic metagabbro and eclogite from the Grenville Province of western Quebec: interpretation of U-Pb geochronology and metamorphism; Canadian Journal of Earth Sciences, v. 34, p. 891–901.

**Lumbers, S.B.**
1976: Mattawa-Deep River area (western half), District of Nippissing; Ontario Division of Mines Preliminary Map 1196, Geological Series, scale 1:1 000 000.

Geological Survey of Canada Project 680071

# Preliminary observations on the Oso Pluton, Frontenac suite, Grenville Province, Ontario

Olga Ijewliw
Continental Geoscience Division, Ottawa

*Ijewliw, O., 1999: Preliminary observations on the Oso Pluton, Frontenac suite, Grenville Province, Ontario;* in *Current Research 1999-C; Geological Survey of Canada, p. 247–251.*

**Abstract:** The undeformed Oso pluton lies between two shear zones in the Central Metasedimentary Belt of the Grenville Province and intrudes deformed supracrustal rocks previously metamorphosed to lower amphibolite facies. This polyphase intrusion, ranging in composition from the oldest gabbro to the youngest syenite units, provides evidence for multistage intrusion, and magma commingling and mixing. Quartz tourmaline veins are found on the margins and periphery.

**Résumé :** Le pluton non déformé d'Oso est situé entre deux zones de cisaillement de la ceinture de roches métasédimentaires centrale; il recoupe des roches supracrustales déformées, antérieurement métamorphisées au sous-faciès inférieur des amphibolites. Cette intrusion polyphasée, dont la composition passe des gabbros les plus anciens aux syénites les plus récentes, présente des indices de phases multiples d'intrusion et de mélange de magma. Des filons de tourmaline et quartz se rencontrent sur les bordures et en périphérie.

## INTRODUCTION

The Oso pluton is located north of Sharbot Lake in central Ontario (NTS 31 C/15). It is one of several contemporaneous plutons referred to as the Frontenac suite which are distributed across two tectonic terranes (Fig. 1) in the Central Metasedimentary Belt of the Grenville Province. Previous regional mapping, Wolff (1985), identified the presence of several phases within the eastern part of the Oso pluton. This project was designed, as part of a larger study, to map the whole pluton in detail, and to document its complexity and its apparent lithological, chemical, and chronological affinities with other plutons in the Frontenac suite.

The Oso pluton is located within the Sharbot Lake terrane (Moore, 1982) of the Central Metasedimentary Belt (Fig. 1). To the northwest, the terrane is bounded by the Robertson Lake shear zone which is interpreted to be extensional (Busch et al., 1994). The rocks within the shear zone comprise a series of mylonites derived from marble, gabbroic, and felsic rocks that dip gently to moderately southeast. The extensional shearing event has been estimated to have occurred over a period of about 100 Ma from 1018–911 Ma (Busch et al., 1994) and overlaps with time estimates of the youngest regional metamorphic event (1030–980 Ma) within the Mazinaw (Corfu and Easton, 1994). The Maberly shear zone delimits the boundary between the Sharbot Lake terrane and the Frontenac terrane overthrust from the southeast (Davidson and Ketchum, 1993). The shear zone units comprise high-strain gneiss, tectonites of anorthositic gabbro, and marble (Easton and Davidson, 1994). The episode of shearing is estimated to have taken place at about 1150 Ma (Davidson, 1996).

## LITHOLOGY

### *Country rocks*

The Sharbot Lake terrane rocks in the map area comprise foliated, greenschist-amphibolite-facies metasedimentary rocks. The rock types are marble, two-mica schist, quartzofeldspathic gneiss, amphibolite, and gossans. The fabric is generally east dipping all around the pluton with some local variation.

The marble is either all white or all grey or can have centimetre-scale lamination. It is convolute in its folding patterns. Laminated dolomite is also locally present. Where the marble is in contact with syenite or fine- to medium-grained mafic dykes, there is a coarse-grained reaction assemblage of pink calcite, green amphibole, and biotite. The areas of marble found within the pluton are interpreted as rafts. There are also marble septa separating the different episodes of intrusion. The two-mica schist (muscovite > biotite) schist is fine grained and thinly laminated. The quartzofeldspathic gneiss is a banded rock ranging in composition from siliceous to ferromagnesian. In places, these rocks grade into silicified metasedimentary rocks. The amphibolite is an amphibole- and biotite-rich rock with alternating bands of feldspar and quartz several millimetres thick. Gossans are found in restricted locations on the periphery of the pluton. There is a wide band of gossaned rocks extending almost 1 km beyond the eastern boundary and a narrow 10–20 m band to the south and southwest. They are fine-grained micaceous or highly silicified rocks containing sulphides and severely weathered.

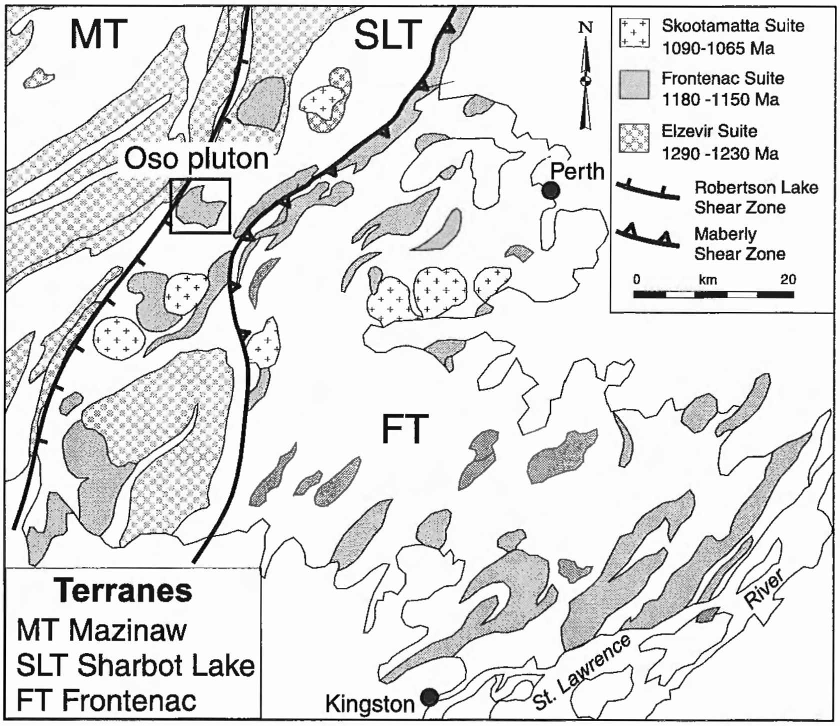


***Figure 1.***

*Location of the Oso pluton with respect to the terranes and their boundaries in the vicinity of Sharbot Lake, southeastern Ontario (modified after Davidson. 1996).*

## *The Oso Pluton*

The Oso pluton is an irregularly shaped lobate body about 6.5 by 5.0 km in size (Fig. 2). Preliminary dating indicates an emplacement age of 1153 Ma (Davidson, pers. com., 1998) similar to some of the other Frontenac suite plutons. There is local evidence of foliation in the western part of the pluton, parallel to the foliation noted in the Robertson Lake shear zone. Otherwise the pluton is undeformed and is in discordant contact with the host rocks. Abundant jointing and veining is observed, though not apparently in any preferred orientation. The rock types range from gabbro to syenite, from coarse grained to fine grained, and show compositional gradation, as well as magma commingling and mixing features. Contact-aureole effects are noted in the eastern part of the pluton where the marble forms an embayment. The marble grain size increases, calcite is pink rather than white, with accompanying green amphibole and coarse-grained biotite.

Porphyritic gabbro contains coarse-grained biotite or amphibole phenocrysts within a fine-grained matrix. It is found in the east-central portion of the pluton with a subsidiary lens near the western margin. Fine-grained gabbro occurs as angular or rounded, cuspate inclusions within a dioritic, medium-grained matrix (Fig. 3, 4). A less hydrous gabbro with coarse plagioclase laths in a fine-grained matrix also occurs in smaller bodies.

The diorite is generally medium to coarse grained with plagioclase, amphibole, and minor biotite±magnetite. It occurs in large lobate bodies either in the centre or periphery

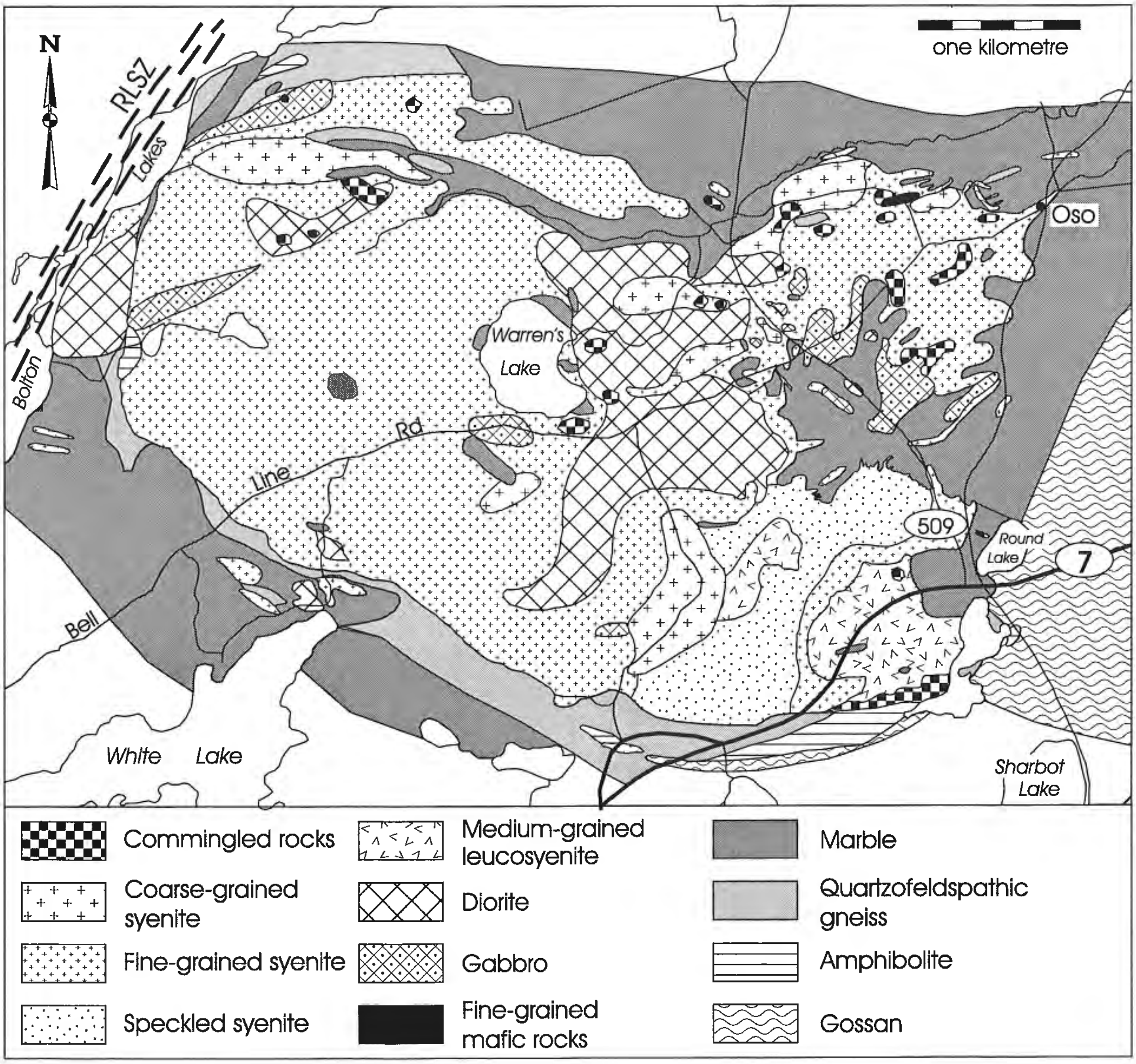


***Figure 2.*** *Preliminary geological map of the Oso pluton.*

of the pluton. This diorite is cut by coarse- and fine-grained syenite veins or dykes up to 20 cm wide. It is possible that there is a gradation from the gabbro to the diorite.

The syenite ranges from coarse to fine grained, and has a variable colour index. Mafic minerals consist of hornblende and biotite, and their relative abundance varies locally. Medium-grained leucosyenite is particularly devoid of mafic minerals. The coarse-grained syenite forms large blocks within the pluton. Coarsening is also seen as gradational from the margin inwards.

The particular variety 'speckled syenite' is medium grained, and equigranular with the relative abundance of mafic and felsic minerals giving it a 'speckled' appearance. Boundaries between the coarse- and fine-grained syenite phases tend to be gradational. However, the boundaries between some of the syenite phases, such as the speckled and medium-grained leucosyenite are sharply defined. The mafic minerals are usually amphibole with subordinate biotite and magnetite. Titanite may constitute up to 5% by volume. The felsic component is mainly pink K-feldspar, with accessory quartz. Some of the syenite phases are denoted on the preliminary map (Fig. 2).

Mafic dykes are found near the eastern and southeastern margin and periphery of the pluton intruding coarse-grained pink syenite and marble. These mafic rocks have fine-grained matrix with centimetre-sized plagioclase phenocrysts. Where the dykes intrude syenite, there is also syenitic material in fractures perpendicular to the dyke walls. Syenitic to granitic, coarse- and fine-grained dykes or veins are present throughout the pluton area in random orientations.

Small, elongate satellites of gabbro, diorite, fine-grained syenite, and commingled rocks occur in the host rock surrounding the main pluton body. They are generally oriented subparallel to the contacts of the pluton.

Quartz-tourmaline veins ranging from fine (Fig. 5) to coarse (Fig. 6) grained are present in the syenite portions of the pluton near its margins, peripherally in proximity to the gabbro body in the east-central portion of the pluton and in the

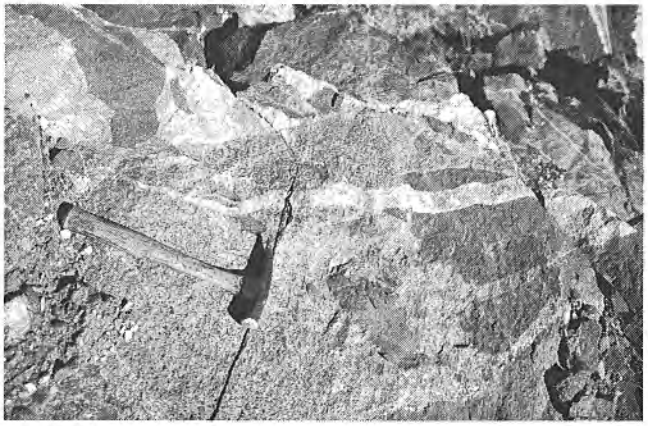

***Figure 3.*** *Inclusion and commingling texture with blocks of mafic biotite gabbro within diorite all crosscut by late-phase, fine-grained, pink syenite. Hammer (33 cm) for scale.*

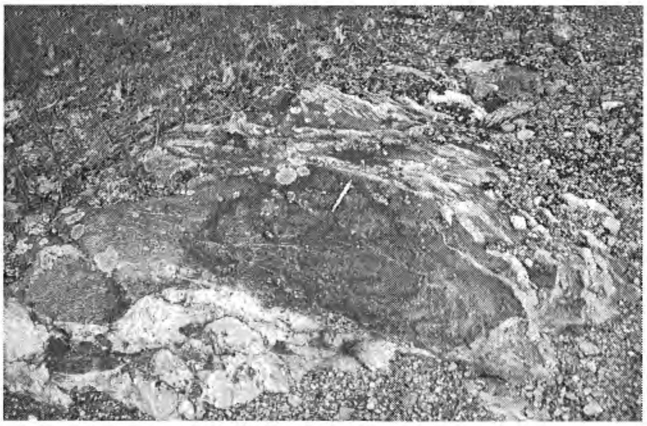

***Figure 4.*** *Mixing-commingling texture with rounded inclusions of mafic gabbro in a dioritic matrix and cut by late-phase, coarse- and fine-grained, pink syenite veins. Pen (14 cm) for scale.*

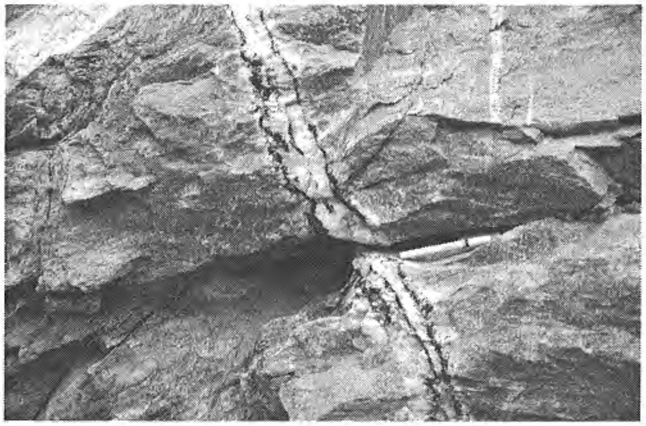

***Figure 5.*** *Quartz (white) tourmaline (black selvage) vein in a biotite-muscovite schist on the periphery of the Oso pluton. Pen (14 cm) for scale.*

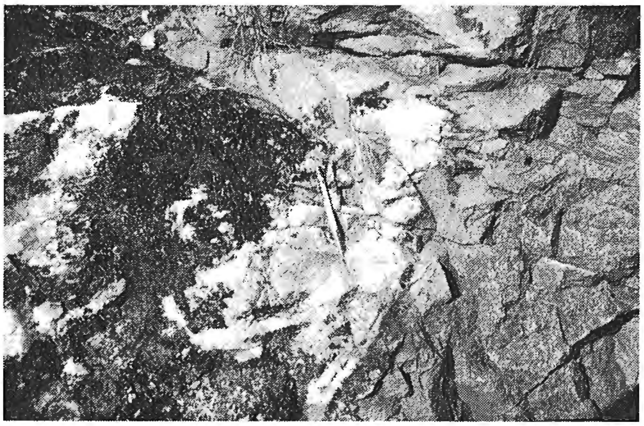

***Figure 6.*** *Quartz (white) tourmaline (black) and sulphide segregation within the syenitic phase of the Oso pluton near its margin. Pen (14 cm) for scale.*

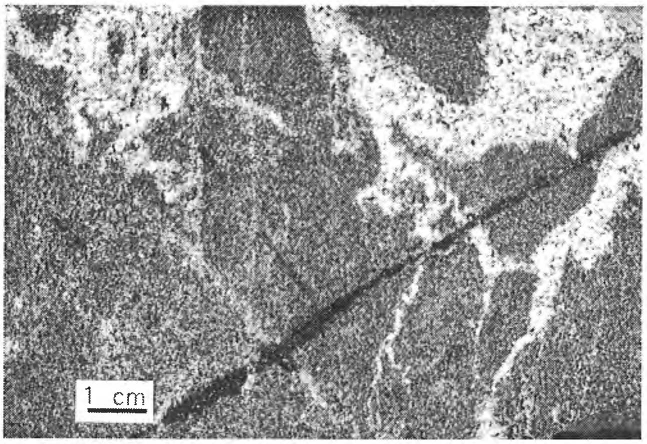


*Figure 7. Commingling texture with rounded, cuspate inclusion of fine-grained mafic magma component chilled against the cooler syenite.*

country rocks. They were not noted in the central or peripheral diorite bodies. The quartz-tourmaline veins are probably a syn-emplacement dilation-and-fill phenomenon, and may be the result of chemical interaction with the host rocks.

### *Inclusions, commingling and mixing textures*

The different igneous phases of the Oso pluton exhibit a variety of relationships. Inclusions, commingling, and mixing are inferred to have occurred from textural and mineralogical observations. Inclusions are angular to subangular fragments within a groundmass of different composition and/or grain size (Fig. 3). Coarse, angular syenite fragments occur locally in finer grained syenite. Commingling is evidenced by round, cuspate, fine-grained mafic blobs in a coarser grained, more felsic matrix (Fig. 4, 7). Mixing would be inferred from an unusual mineralogy which could be the product of chemically diverse magmas. For example, the unusual combination of coarse-grained biotite within a gabbro could be the product of mixing with another more potassic (syenitic) magma batch.

Figure 5 also illustrates a complex of mafic phases with a fine-grained mafic matrix, a subangular, medium-grained dioritic component, and a medium-grained biotite-bearing, irregularly shaped component. Their interrelationship is not yet clear.

### *Age and Space Relationships*

Crosscutting relationships and map distributions suggest a general sequence of age relationships from the oldest, coarse-grained, mafic rocks through the intermediate rocks to the youngest, fine-grained, felsic rocks. The biotite gabbro, locally grading into the more extensive bodies of coarse-grained diorite is considered to have been emplaced first. This is crosscut by dykes or veins of coarse- and fine-grained syenite. Most of the Oso pluton consists of a range of syenites with the fine-grained variety predominating at the margins and as abundant dykes crosscutting the coarser grained syenite. The oldest mafic rocks are found within the eastern embayed region of the body. The intermediate diorite occurs as extensive bodies in the central and peripheral regions and may have constituted one body prior to the influx of syenite. The final episodes of emplacement of coarse- and fine-grained syenite surround the older rocks which remain as rafts.

## ACKNOWLEDGMENTS

Much is owed to Anthony Davidson at the Geological Survey of Canada whose many years experience in the Grenville Province and expertise in the field, and whose active and tireless participation has been of invaluable assistance on this project.

## REFERENCES

**Busch, J.P., van der Pluijm, B.A., and Essene, E.J.**
1994: Late orogenic extension in the Grenville: evidence from the plastic to brittle Robertson Lake shear zone; Geological Association of Canada, Program with Abstracts, v. 19, p. A16.

**Corfu, F. and Easton, R.M.**
1994: U-Pb geochronology of the Mazinaw Terrane, Central Metasedimentary Belt, Grenville Province, Ontario; Geological Association of Canada, Program with Abstracts, v. 19, p. A22.

**Davidson, A.**
1996: Post-collisional A-type plutonism, southwest Grenville Province: evidence for a compressional setting; Geological Society of America, Abstracts with Programs, v. 28 No.7, p. A440.

**Davidson, A. and Ketchum, J.W.F.**
1993: Observations on the Maberly shear zone, a terrane boundary within the Central Metasedimentary Belt, Grenville Province, Ontario; *in* Current Research, Part C, Geological Survey of Canada, Paper 93-1C, p. 265–269.

**Easton,, R.M. and Davidson, A.**
1994: Terrane boundaries and lithotectonic assemblages within the Grenville Province, eastern Ontario, Field Trip A1: Guidebook, Geological Association of Canada–Mineralogical Association of Canada Joint Annual Meeting, 1994, Waterloo, Ontario, Canada, p. 89.

**Moore, J.M.**
1982: Stratigraphy and tectonics of the Grenville Orogen in eastern Ontario; 1982 Grenville Workshop, Rideau Ferry, Abstracts, p. 7.

**Wolff, J.M.**
1985: Sharbot Lake; Ontario Geological Survey, Map 2471, scale 1: 31 680.

Geological Survey of Canada Project 76006

# AUTHOR INDEX

## NOTE TO CONTRIBUTORS

Submissions to the Discussion section of Current Research are welcome from both the staff of the Geological Survey of Canada and from the public. Discussions are limited to six double-spaced typewritten pages (about 1500 words) and are subject to review by the Managing Editor. Discussions are restricted to the scientific content of Geological Survey reports. General discussions concerning sector or government policy will not be accepted. All manuscripts must be computer word-processed on an IBM compatible system and must be submitted with a diskette using WordPerfect. Illustrations will be accepted only if, in the opinion of the editor, they are considered essential. In any case no redrafting will be undertaken and reproducible copy must accompany the original submissions. Discussion is limited to recent reports (not more than two years old) and may be in either English or French. Every effort is made to include both Discussion and Reply in the same issue. Current Research is published in January and July. Submissions should be sent to the Managing Editor, Geological Survey of Canada, 601 Booth Street, Ottawa K1A 0E8.

## AVIS AUX AUTEURS D'ARTICLES

Nous encourageons tant le personnel de la Commission géologique que le grand public à nous faire parvenir des articles destinés à la section discussion de la publication Recherches en cours. Le texte doit comprendre au plus six pages dactylographiées à double interligne (environ 1500 mots), texte qui peut faire l'objet d'un réexamen par la rédactrice en chef administrative. Les discussions doivent se limiter au contenu scientifique des rapports de la Commission géologique. Les discussions générales sur le Secteur ou les politiques gouvernementales ne seront pas acceptées. Le texte doit être soumis à un traitement de texte informatisé par un système IBM compatible et enregistré sur disquette WordPerfect. Les illustrations ne seront acceptées que dans la mesure où, selon l'opinion du rédacteur, elles seront considérées comme essentielles. Aucune retouche ne sera faite aux illustrations et dans tous les cas, une copie qui puisse être reproduite doit accompagner le texte original. Les discussions en français ou en anglais doivent se limiter aux rapports récents (au plus de deux ans). On s'efforcera de faire coïncider les articles destinés aux rubriques discussions et réponses dans le même numéro. La publication Recherches en cours paraît en janvier et en juillet. Les articles doivent être envoyés à la rédactrice en chef administrative, Commission géologique du Canada, 601, rue Booth, Ottawa K1A 0E8.

Geological Survey of Canada Current Research, is released twice a year, in January and July. The four parts published in January 1999 (Current Research 1999-A to D) are listed below.

Recherches en cours, une publication de la Commission géologique du Canada, est publiée deux fois par année, en janvier et en juillet. Les quatre parties publiées en janvier 1999 (Recherches en cours 1999-A à D) sont énumérées ci-dessous.

Part A: Cordillera and Pacific Margin
Partie A: Cordillère et marge du Pacifique

Part B: Interior Plains and Arctic Canada
Partie B: Plaines intérieures et région arctique du Canada

Part C: Canadian Shield
Partie C: Bouclier canadien

Part D: Eastern Canada and national and general programs
Partie D: Est du Canada et programmes nationaux et généraux